

University of Southampton Research Repository ePrints Soton

Copyright © and Moral Rights for this thesis are retained by the author and/or other copyright owners. A copy can be downloaded for personal non-commercial research or study, without prior permission or charge. This thesis cannot be reproduced or quoted extensively from without first obtaining permission in writing from the copyright holder/s. The content must not be changed in any way or sold commercially in any format or medium without the formal permission of the copyright holders.

When referring to this work, full bibliographic details including the author, title, awarding institution and date of the thesis must be given e.g.

AUTHOR (year of submission) "Full thesis title", University of Southampton, name of the University School or Department, PhD Thesis, pagination



Faculty of Engineering, Science and Mathematics
School of Civil Engineering and the Environment
University of Southampton

**The Use of Joint Probability Analysis to Predict Flood Frequency in
Estuaries and Tidal Rivers**

by

Christopher John White

Thesis submitted in candidacy for the degree of Doctor of Philosophy

November 2007

UNIVERSITY OF SOUTHAMPTON

ABSTRACT

FACULTY OF ENGINEERING, SCIENCE & MATHEMATICS
SCHOOL OF CIVIL ENGINEERING & THE ENVIRONMENT

Doctor of Philosophy

THE USE OF JOINT PROBABILITY ANALYSIS TO PREDICT FLOOD
FREQUENCY IN ESTUARIES AND TIDAL RIVERS

by Christopher John White

This thesis investigates the combined influence of river flow, tide and surge on the frequency of extreme water levels in tidal rivers and estuaries. The estimation of flood risk may depend on extreme combinations of these variables rather than individual extreme events, but these relationships are complex and difficult to quantify. A probabilistic approach traditionally involves an assumption of independence between these primary hydrological variables, which can lead to the underestimation of the level of risk where river flow and tidal surge are often linked to the same low pressure weather system. This research develops a new methodology which combines traditional flood risk modelling techniques with statistical dependence to define the relationship between the hydrological variables. Dependence between river flow, tide and surge is assessed for a case study area of Lewes, East Sussex, UK, a town which is prone to both tidal and fluvial flooding. Bivariate and trivariate daily and extreme joint exceedance methods are developed and used in conjunction with a one-dimensional hydraulic model to analyse the interaction of river flow, tide and surge to predict the joint probability of potential flood events occurring in Lewes. The approach is validated using existing historical water levels observed in Lewes. The results demonstrate that the joint exceedance approach can be successfully employed to model the frequency of flood events caused by tide and river flow. The incorporation of a third variable of surge refines the approach further, and identifies the zone where the interaction of the variables has the greatest impact on resultant flood water levels.

CONTENTS

Abstract	ii
Contents	iii
List of Figures	vii
List of Tables.....	x
Declaration of Authorship.....	xii
Acknowledgements	xiii
Notation.....	xiv
1 INTRODUCTION	1
1.1 Background	1
1.2 Aims & Objectives.....	2
2 REVIEW OF JOINT PROBABILITY FOR FLOOD RISK ESTIMATION.....	4
2.1 The Joint Probability Approach	4
2.1.1 Introduction to Joint Probability	4
2.1.2 Applications of Joint Probability Methods to Flood Risk Analyses.....	4
2.2 Dependence in Joint Probability Problems	8
2.2.1 Introduction to Dependence	8
2.2.2 Dependence Theory	9
2.2.2.1 The Dependence Measure χ	9
2.2.2.2 Threshold Selection.....	13
2.2.2.3 Positive & Negative χ Values	14
2.2.3 Applications of Dependence Theory in Flood Risk Analyses	14
2.2.3.1 Dependence between River Flow & Sea level.....	14
2.2.3.2 Dependence between River Flow & Surge	16
2.2.3.3 Dependence between Precipitation & Surge.....	17
2.3 Interpretation of the Dependence Measure χ	18
2.4 Structure Functions	22
2.4.1 Structure Functions & Matrices	22
2.4.2 Hydraulic Modelling	23
2.5 Non-Probabilistic Flood Risk Methods.....	23
2.5.1 Direct Analysis.....	23
2.5.2 Continuous Simulation.....	24
2.5.3 Historical Emulation	24
2.6 Flood Risk Studies in the River Ouse Catchment.....	25
2.6.1 General Flood Risk & Joint Probability Investigations	25
2.6.2 Dependence Studies	26
2.7 Conclusions	28
3 METHODS	31
3.1 Introduction	31
3.2 Methods for Flood Frequency Analysis	32
3.2.1 Event Definition	32
3.2.2 Annual Maxima (AMAX) Series	32
3.2.3 Peaks-Over-Threshold Series.....	33
3.2.4 Distribution Selection & Return Period Estimation.....	34
3.2.5 Correlation.....	35
3.3 Methods for the Calculation of Dependence.....	35
3.3.1 Dependence Modelling	35

3.3.2	Threshold Selection.....	37
3.3.3	Significance Testing.....	37
3.3.4	Confidence Intervals	38
3.4	Extreme Joint Return Period Methods	39
3.4.1	Extreme Bivariate Approach.....	39
3.4.2	Extreme Trivariate Approach.....	43
3.5	Daily POT Joint Probability Methods.....	45
3.5.1	Daily POT Bivariate Approach.....	45
3.5.2	Daily POT Trivariate Approach.....	48
4	PRELIMINARY ANALYSIS.....	50
4.1	Introduction	50
4.2	Selection of the Case Study Area.....	50
4.3	The Ouse Catchment, East Sussex	51
4.3.1	Overview	51
4.3.2	Sub-Catchment Divisions	52
4.3.2.1	Upper Ouse Sub-Catchment.....	52
4.3.2.2	Uck Sub-Catchment	53
4.3.2.3	Middle Ouse Sub-Catchment	54
4.3.2.4	Lower Ouse Sub-Catchment	55
4.4	Flooding in the Ouse Catchment.....	56
4.5	Hydrology	58
4.5.1	Data Sourcing.....	58
4.5.2	River Flow.....	59
4.5.3	River Stage.....	60
4.5.4	Sea Levels	62
4.5.4.1	Sea Level Observations.....	62
4.5.4.2	Tidal Effects on the Ouse Catchment.....	63
4.5.4.3	Local Chart to Ordnance Datum Conversion.....	65
4.5.5	Surge	67
4.5.5.1	Definition of Surge.....	67
4.5.5.2	Surge Observations	68
4.5.6	Precipitation	68
4.6	Preliminary Assessment.....	68
5	GENERAL METHODS FOR THE MODELLING & SIMULATION OF EXTREME WATER LEVELS.....	70
5.1	Introduction	70
5.2	Hydraulic Model	70
5.2.1	Modelling Philosophy & Sequence.....	70
5.2.2	Model Extent.....	70
5.2.3	Software	71
5.2.4	Cross-Section Topographical Data	71
5.2.5	Hydraulic Structures.....	73
5.2.6	Model Construction.....	73
5.2.7	Inflows at the Model Boundaries	73
5.2.7.1	Upstream Synthesised Barcombe Mills Series	73
5.2.7.2	Downstream Recorded Newhaven Sea Level.....	77
5.2.8	Model Trials & Testing.....	77
5.2.8.1	Test Data	77
5.2.8.2	Selected Test Events	77
5.2.8.3	Results & Discussion	78

5.2.8.4	Correlation.....	81
5.3	Continuous Simulation.....	82
5.4	Structure Function Simulation	84
5.4.1	Structure Function Overview	84
5.4.2	Representative Hydrographs	84
5.4.3	Structure Function Matrix	85
5.4.4	Structure Function Contours	88
5.4.5	Historical Emulation Calibration	89
5.5	Discussion	90
6	EXTREME VALUE ANALYSIS & FLOOD FREQUENCY ESTIMATION.....	92
6.1	Introduction	92
6.2	Annual Maxima (AMAX) Extraction & Return Periods	93
6.2.1	Upper Ouse & Uck Fluvial AMAX Series	93
6.2.1.1	Return Periods	93
6.2.2	Middle Ouse Fluvial AMAX Series.....	94
6.2.2.1	Extending the Barcombe Mills AMAX Series.....	94
6.2.2.2	Return Periods	97
6.2.3	Lower Ouse Stage & Newhaven Sea Level AMAX Series	98
6.2.3.1	Extending the Lewes Corporation Yard AMAX Series.....	98
6.2.3.2	Extending the Newhaven AMAX Series	99
6.2.3.3	Return Periods	100
6.2.4	Newhaven Surge AMAX Series	103
6.2.4.1	Return Periods	103
6.3	Independent Peaks-Over-Threshold (POT) Selection.....	105
6.3.1	Threshold Selection.....	105
6.3.2	Threshold Magnitudes.....	105
6.3.3	Seasonality Effects	106
6.4	Multivariate Extreme Value Analysis.....	108
6.4.1	Joint AMAX Occurrences.....	108
6.4.2	Joint POT Exceedances	111
6.5	Discussion	115
7	STATISTICAL DEPENDENCE	117
7.1	Introduction	117
7.2	Dependence between Barcombe Mills & Newhaven.....	117
7.2.1	Data Preparation	117
7.2.2	Threshold Values	119
7.2.3	Time-Lagged Analysis	121
7.2.4	Dependence Values	124
7.3	Dependence at Lewes.....	125
7.3.1	The Combined Effects of Flow, Sea level & Surge at Lewes.....	125
7.3.2	Dependence Values	131
7.4	Dependence at Newhaven	132
7.4.1	The Combined Effects of Tide & Surge at Newhaven	132
7.4.2	Dependence Values	133
7.5	Discussion	134
8	JOINT PROBABILITY	136
8.1	Introduction	136
8.2	Extreme Joint Return Period Results at Lewes	137

8.2.1	Fully-Independent & Partially-Dependent Bivariate & Trivariate Extreme Joint Return Periods	137
8.2.2	Interpretation of Results	140
8.3	Daily Joint Probability Results at Lewes	144
8.3.1	Fully-Independent & Partially-Dependent Bivariate & Trivariate Daily Joint Probabilities.....	144
8.3.2	Interpretation of Results.....	147
8.4	Annual Exceedance Curves for Extreme Return Periods	151
8.5	Discussion	152
9	GENERAL DISCUSSION & CONCLUSIONS	154
9.1	General Discussion.....	154
9.2	Summary of General Conclusions	157
9.3	Recommendations for Further Research.....	158
	References	160
	APPENDICES A-G	165
	Appendix Contents.....	166
	List of Appendix Figures	169
	List of Appendix Tables.....	176

LIST OF FIGURES

Figure 2.1 Example of joint extreme values of surges & waves (reproduced with the permission of J. Tawn).....	10
Figure 3.1 Methods flow diagram.....	31
Figure 3.2 Daily probability of recorded sea level threshold exceedance at Newhaven (1982-2006).....	47
Figure 4.1 River Ouse catchment topography	51
Figure 4.2 River Ouse catchment and sub-catchment divisions	53
Figure 4.3 Lewes town centre under flood, 12th October 2000	56
Figure 4.4 Location of Lewes stage gauges.	62
Figure 4.5 Highest predicted astronomical spring tidal range (7.08m) at Newhaven (10 th March 1997).....	65
Figure 4.6 Admiralty Local Chart Datum to Ordnance Datum transformation differentials at the Proudman & EA Newhaven sea level gauges (October 2002)	66
Figure 5.1 Extent of the Lower Ouse model (Barcombe Mills to Newhaven).	71
Figure 5.2 Time-series plots of synthesised daily mean flow at Barcombe Mills with a. HYSIM simulated daily mean flow, & b. recorded daily mean flow, (2002).....	76
Figure 5.3 Plots of modelled and recorded stage at Lewes Corporation Yard (event no.'s 1 to 8)	80
Figure 5.4 Plots of modelled and recorded stage at Southease Bridge (event no.'s 1 to 6)	81
Figure 5.5 Comparison of continuously simulated & recorded daily maxima observations at Lewes Corporation Yard (Dec 2005 - May 2006)	83
Figure 5.6 Example range of maximum water levels simulated at Lewes Corporation Yard from the 90m ³ /s Barcombe Mills flow hydrograph with all increments of 1.20mAOD to 4.80mAOD Newhaven tide hydrographs for the production of the structure function matrix	86
Figure 5.7 3-dimensional matrix plot of Lewes Corporation Yard stage (Barcombe Mills flow & Newhaven tide hydrographs).....	87
Figure 5.8 3-dimensional matrix plot of Lewes Gas Works stage (Barcombe Mills flow & Newhaven tide hydrographs)	87
Figure 5.9 Structure function stage contour curves (mAOD) at Lewes Corporation Yard with simultaneous daily maxima observations of Barcombe Mills flow and Newhaven sea level (1982-2006).....	88
Figure 5.10 Structure function stage contour curves (mAOD) at Lewes Gas Works with simultaneous daily maxima observations of Barcombe Mills flow and Newhaven sea level (1982-2006).....	89
Figure 6.1 Rating Curve of Barcombe Mills AMAX stage & recorded/synthesised flow series observed on the same day (1957-1968; 1981-2000).....	96
Figure 6.2 Rating Curve of Barcombe Mills stage & extended flow AMAX series (1952-2000)	96
Figure 6.3 Extended Barcombe Mills flow AMAX series (1952-2005).....	97
Figure 6.4 Rating curve of annual maxima recorded & simulated stage at Lewes Corporation Yard (1982-2005)	99
Figure 6.5 Extended Newhaven AMAX series (1913-2006).....	100
Figure 6.6 Ranked AMAX stage at Lewes Corporation Yard & Lewes Gas Works (1952-2005)	102
Figure 6.7 Ranked AMAX sea level at Newhaven (1913-2005).....	103
Figure 6.8 Ranked AMAX maximum surge & surge at high tide at Newhaven (1981-2005)	104

Figure 6.9 Seasonality of 99th, 98th & 95th percentile POT river flow exceedances per calendar month at Barcombe Mills	107
Figure 6.10 Seasonality of 99th, 98th & 95th percentile POT stage exceedances per calendar month at Lewes Corporation Yard	107
Figure 6.11 Seasonality of 99th, 98th & 95th percentile POT sea level exceedances per calendar month at Newhaven	108
Figure 7.1 Scatter plots of a. daily maxima flow at Barcombe Mills versus daily maxima sea level at Newhaven, & b. daily maxima flow at Barcombe Mills versus daily maxima surge at Newhaven	118
Figure 7.2 Variation of dependence between daily maxima sea level at Newhaven & daily maxima flow at Barcombe Mills with POT percentile threshold selection ...	119
Figure 7.3 Variation of dependence between daily maxima surge at Newhaven & daily maxima flow at Barcombe Mills with POT percentile threshold selection	120
Figure 7.4 ± 1 day lagged dependence between daily maxima sea level at Newhaven & daily maxima flow at Barcombe Mills with POT percentile threshold selection ...	120
Figure 7.5 ± 1 day lagged dependence between daily maxima surge at Newhaven & daily maxima flow at Barcombe Mills with POT percentile threshold selection	121
Figure 7.6 Lagged dependence between daily maxima flow at Barcombe Mills with lagged sea level at Newhaven in 15-minute increments (98% threshold)	122
Figure 7.7 Lagged dependence between daily maxima sea level at Newhaven with lagged flow at Barcombe Mills in 15-Minute increments (98% threshold)	122
Figure 7.8 Lagged dependence between daily maxima surge at Newhaven with lagged flow at Barcombe Mills in 15-Minute increments (98% threshold)	123
Figure 7.9 Scatter plots of a. daily maxima stage at Lewes Corporation Yard versus daily maxima flow at Barcombe Mills, b. daily maxima stage at Lewes Corporation Yard versus daily maxima sea level at Newhaven, & c. daily maxima stage at Lewes Corporation Yard versus daily maxima surge at Newhaven.....	126
Figure 7.10 Dependence at Lewes Corporation Yard with daily maxima flow, sea level & surge, with POT percentile threshold selection.....	127
Figure 7.11 Scatter plots of a. daily maxima stage at Lewes Gas Works versus daily maxima flow at Barcombe Mills, b. daily maxima stage at Lewes Gas Works versus daily maxima sea level at Newhaven, & c. daily maxima stage at Lewes Gas Works versus daily maxima surge at Newhaven	128
Figure 7.12 Dependence at Lewes Gas Works with daily maxima flow, sea level & surge, with POT percentile threshold selection	129
Figure 7.13 Comparison of dependence at Lewes Corporation Yard and Lewes Gas Works gauges with a. daily maxima flow at Barcombe Mills, b. daily maxima sea level at Newhaven, & c. daily maxima surge at Newhaven, with POT percentile threshold selection.....	130
Figure 7.14 Scatter plots of a. daily maxima observed sea level versus daily maxima surge at Newhaven, & b. daily maxima predicted tide versus daily maxima surge at Newhaven.....	133
Figure 8.1 Comparison of resultant stage magnitudes for bivariate (flow & sea level) & trivariate (flow, predicted tide & surge) partially-dependent extreme joint return periods with recorded extreme return periods at a. Lewes Corporation Yard, & b. Lewes Gas Works	141
Figure 8.2 Relationship between bivariate & trivariate stage magnitudes with recorded stage magnitudes at Lewes Corporation Yard	142
Figure 8.3 Relationship between bivariate & trivariate stage magnitudes with recorded stage magnitudes at Lewes Gas Works.....	142
Figure 8.4 Comparison of resultant stage magnitudes at Lewes Corporation Yard from a. bivariate (flow & sea level) daily joint probabilities with recorded stage magnitudes,	

& b. trivariate (flow, predicted tide & surge) daily joint probabilities with recorded stage magnitudes	148
Figure 8.5 Relationship between extreme (top 2%) bivariate (flow & sea level) fully-independent, bivariate (flow & sea level) & trivariate (flow, predicted tide & surge) partially-dependent daily joint probabilities at Lewes Corporation Yard.....	149
Figure 8.6 Relationship between extreme (top 2%) bivariate (flow & sea level) fully-independent, bivariate (flow & sea level) & trivariate (flow, predicted tide & surge) partially-dependent daily joint probabilities at Lewes Gas Works	150
Figure 8.7 Bivariate partially-dependent (Barcombe Mills flow and Newhaven sea level) extreme joint return period curves at Lewes Corporation Yard with structure function stage contours (mAOD)	151
Figure 8.8 Bivariate partially-dependent (Barcombe Mills flow and Newhaven sea level) extreme joint return period curves at Lewes Gas Works with structure function stage contours (mAOD).....	152

LIST OF TABLES

Table 3.1 Joint return periods $T_{X,Y}$ (shaded area) for partially-dependent ($\chi=0.045$) variables X (Barcombe Mills flow, m^3/s) and Y (Newhaven sea level, mOD) with return periods T_x and T_y . Corresponding sea level and flow magnitudes are shown in italics.	41
Table 3.2 Structure function matrix for resultant water levels at Lewes Corporation Yard (mAOD) (shaded area) from combinations of variables X (Barcombe Mills flow, m^3/s) and Y (Newhaven sea level, mOD). Return periods T_x and T_y corresponding to sea level / flow magnitudes are shown in italics.	42
Table 3.3 Stage at Lewes Corporation Yard for combined Barcombe Mills flow and Newhaven sea level events equating to the 1:2 year ($T_{X,Y} = 2$) joint return periods. Highest stage at Lewes Corporation Yard (shaded area) selected as the maximum 1:2 year combined flow / sea level event.	43
Table 4.1 Ouse sub-catchments.....	52
Table 4.2 Number of properties in Lewes at risk from flooding	57
Table 4.3 Ouse catchment river flow gauges	60
Table 4.4 Ouse catchment river stage gauges	61
Table 4.5 Ouse catchment / south coast sea level gauges	63
Table 4.6 Newhaven sea level predictions (1996-2015).....	64
Table 4.7 South coast surge gauges	68
Table 5.1 Distances and times-of-travel values for upper catchment flow gauges to d/s Barcombe Mills.....	74
Table 5.2 Calibration of the synthesised flow series with the HYSIM simulated series and the recorded series at Barcombe Mills (2002)	75
Table 5.3 Model input events with peak hydrograph magnitudes at Barcombe Mills & Newhaven.....	78
Table 5.4 Model results and linear correlations of modelled and recorded stage at Lewes Corporation Yard and Southease Bridge.....	82
Table 5.5 Calibration of continuous daily maxima simulated stage with recorded daily maxima stage at Lewes Corporation Yard	83
Table 5.6 Maximum and minimum simulated water levels observed at Lewes from optimum time-delayed hydrographs at Barcombe Mills and Newhaven.....	85
Table 5.7 Calibration of daily maxima emulated stage with simulated / recorded daily maxima stage at Lewes Corporation Yard	90
Table 6.1 Estimated fluvial flow return period magnitudes for the Upper Ouse and Uck sub-catchments.....	94
Table 6.2 Estimated fluvial stage & flow return period magnitudes for the Middle Ouse sub-catchment	98
Table 6.3 Estimated stage & sea level return period magnitudes for the Lower Ouse sub-catchment & Newhaven	101
Table 6.4 Estimated surge & surge at high tide return period magnitudes for Newhaven	104
Table 6.5 Joint AMAX observations at station pairs throughout the Ouse Catchment ..	109
Table 6.6 Joint POT exceedances at Barcombe Mills & Lewes Corporation Yard (1982-2005)	111
Table 6.7 Joint POT exceedances at Barcombe Mills & Newhaven (sea level) (1982-2005)	112
Table 6.8 Joint POT exceedances at Barcombe Mills & Newhaven (surge) (1982-2005)	113

Table 6.9 Joint POT exceedances at Lewes Corporation Yard & Newhaven (sea level) (1982-2005).....	114
Table 6.10 Joint POT exceedances at Lewes Corporation Yard & Newhaven (surge) (1982-2005).....	115
Table 7.1 Dependence χ between Barcombe Mills & Newhaven, values of χ corresponding to the 5% significance level, and the lower and upper confidence intervals	124
Table 7.2 Dependence χ between Lewes Corporation Yard, Barcombe Mills & Newhaven, values of χ corresponding to the 5% significance level, and the lower and upper confidence intervals.....	131
Table 7.3 Dependence χ between Lewes Gas Works, Barcombe Mills & Newhaven, values of χ corresponding to the 5% significance level, and the lower and upper confidence intervals	132
Table 7.4 Dependence χ between Newhaven sea level and surge, values of χ corresponding to the 5% significance level, and the lower and upper confidence intervals	134
Table 8.1 Part I. Single, bivariate & trivariate extreme joint return periods (in bold) for independent & partially-dependent flow, sea level and surge with identical resultant stage at Lewes Corporation Yard. Shaded areas highlight the significant interaction zones between the variables on the joint return periods at Lewes Corporation Yard.	138
Table 8.2 Part I. Single, bivariate & trivariate extreme joint return periods (in bold) for independent & partially-dependent flow, sea level and surge with identical resultant stage at Lewes Gas Works. Shaded areas highlight the significant interaction zones between the variables on the joint return periods at Lewes Gas Works.	139
Table 8.3 Marginal, bivariate & trivariate daily joint probabilities (in bold) for independent & partially-dependent flow, sea level and surge at Lewes Corporation Yard. Shaded areas highlight the significant interaction zones between the variables on resultant stage levels at Lewes Corporation Yard.....	145
Table 8.4 Marginal, bivariate & trivariate daily joint probabilities (in bold) for independent & partially-dependent flow, sea level and surge at Lewes Gas Works. Shaded areas highlight the significant interaction zones between the variables on resultant stage levels at Lewes Gas Works.	146

DECLARATION OF AUTHORSHIP

I, CHRISTOPHER JOHN WHITE, declare that the thesis entitled THE USE OF JOINT PROBABILITY ANALYSIS TO PREDICT FLOOD FREQUENCY IN ESTUARIES AND TIDAL RIVERS and the work presented in the thesis are both my own, and have been generated by me as the result of my own original research. I confirm that:

- this work was done wholly or mainly while in candidature for a research degree at the University of Southampton;
- where any part of this thesis has previously been submitted for a degree or any other qualification at this University or any other institution, this has been clearly stated;
- where I have consulted the published work of others, this is always clearly attributed;
- where I have quoted from the work of others, the source is always given. With the exception of such quotations, this thesis is entirely my own work;
- I have acknowledged all main sources of help;
- where the thesis is based on work done jointly with others, I have made clear exactly what was done by others and what I have contributed myself;
- none of this work has been published before submission.

Signed:

Date:

ACKNOWLEDGEMENTS

I would like to thank the following people who have, in one form or another, provided invaluable help, support and advice over the last three and a half years.

The staff at the Environment Agency in Worthing for their responses to my numerous requests for information and data, in particular Nigel Baker, Russell Long and Dr. Chris Manning.

The members of the ASCCUE project for their support and provision of an environment where my ideas and thoughts were tried out and listened to.

Dr. Cecilia Svensson and Dr. David Jones of CEH Wallingford, Dr. Peter Hawkes of HR Wallingford and Prof. Jon Tawn of the University of Lancaster for their insight and generosity in helping me get to grips with the world of statistical dependence.

All of the staff of the School of Civil Engineering and the Environment at the University of Southampton who have helped me reach the end of this journey, especially Barbara Hudson, who has very kindly kept me solvent throughout my PhD.

My friends and family for their continual support and encouragement, who have all probably assumed by now that I have completely vanished judging by my mysterious disappearance over the last few years. I owe them all an awful lot.

Dr. Paul Tosswell for his unfailing help, guidance and general beat-me-round-the-head moments over the last few years, without which I wouldn't be writing this now.

My great thanks to my supervisor Prof. Trevor Tanton for everything over the last three and a half years. Thank you for keeping me on the straight and narrow and for putting up with me for so long. I said I would get there!

And finally, to my girlfriend Caroline Whalley, who has given me so much, not least a good a square meal every day.

NOTATION

χ	chi (dependence measure)
cm	centimetre
d/s	downstream
AOD	Above Ordnance Datum
DEM	Digital Elevation Map
DGPS	Differential Global Positioning System
EA	Environment Agency, UK
CD	Admiralty Local Chart Datum
HAT	Highest Astronomical Tide
LAT	Lowest Astronomical Tide
LOND	Ordnance Survey GPS Active Station at London, UK
m	metre
m ³ /s	cubic metres per second
MHWN	Mean High Water Neaps
MHWS	Mean High Water Springs
MLWN	Mean Low Water Neaps
MLWS	Mean Low Water Springs
MNR	Mean Neap Range
MSR	Mean Spring Range
mb	millibar
NFO1	Ordnance Survey GPS Active Station at North Foreland, Dover, UK
OS	Ordnance Survey, Southampton, UK
OSGM-02	Ordnance Survey Geoid Model, 2002
OSHQ	Ordnance Survey GPS Active Station at Southampton, UK
OSTN-02	Ordnance Survey National Grid Datum Transformation, 2002
STW	Sewage Treatment Works
u/s	upstream
WGS-84	World Geodetic System, 1984 (GPS Ellipsoid)

1 INTRODUCTION

1.1 Background

In recent years, widespread flooding has affected many parts of the United Kingdom. On 12th October 2000, the historic town of Lewes on the River Ouse in East Sussex was hit by serious floods, devastating the town centre and causing millions of pounds of damage. Towns such as Lewes are in a particularly difficult situation due to their position on tidal rivers and estuaries, which means they are at risk from the combination of both fluvial and tidal flooding. Expected rises in sea levels and increased precipitation resulting from climate change, coupled with pressure for increased urbanisation of low-lying areas, is expected to create major flood risk problems for many coastal and estuarine towns.

In the lower tidal reaches of rivers, the probability of the occurrence of extreme high water levels is a result of the interaction between river discharge, astronomical tide and surge. Extreme flood events in estuaries do not necessarily follow the largest or longest-duration storms, but are likely to be caused by a combination of factors which occur at vulnerable times and locations. There is however a lack of stochastic knowledge about the interaction between sea levels and river flows in estuarine environments as the risk of flooding posed by the interaction of river flow and sea levels is hard to quantify due to the dynamic nature of the hydrological variables and the complex interaction of catchment and tidal processes.

Conventional flood risk studies have therefore focused on statistical probabilistic-based methodologies for the determination of extreme water levels in estuaries and rivers at a specific point of interest. Statistics is a science of description, based on mathematical principles which identify the variation in a set of observations of a process. This brings attention on the observations at the site of interest rather than the systems which have caused them, disguising the remaining uncertainty of the dynamic fluvial and tidal interaction. By recognising that estuaries and tidal rivers are dynamic systems, probabilistic methods, when used in conjunction with a greater understanding of the physical processes that produce the resultant water levels, can then provide a meaningful answer. Existing techniques such as numerical hydraulic modelling, structure function generation and simulation methods can provide this.

As such, there has been a growth in the requirement for joint probability theory to be incorporated into flood risk analyses involving two or more hydrological variables, such

as sea level and river flow. Typical joint probability approaches however assume independence between these source variables, which can be inadequate when calculating the level of flood risk. Therefore, to accurately quantify the probability of extreme water levels produced by the combination of hydrological variables, the relationship between the primary variables has to be established. As such, a level of statistical dependence between the variables is required to determine the true probability of two potentially non-random events occurring together. This can be calculated by utilising a dependence measure, allowing a level of dependence to be found between the variables, based on two observed variables of interest (such as river flow and sea level) simultaneously exceeding a certain extreme levels.

The recent development of such statistical dependence methods for the quantification of simultaneously occurring extreme variables has enabled the calculation of realistic joint occurrences of extreme hydrological values as part of a flood risk study. However, although individual methods exist, there has been limited research into the combined use of dependence theory in conjunction with joint probability and modelling approaches to produce a comprehensive methodology.

1.2 Aims & Objectives

This aim of this research is to determine extreme water levels return periods at a series of locations upstream and downstream of Lewes in East Sussex, UK. The research will analyse both the physical and statistical relationship between the hydrological variables which may combine to produce extreme water levels in tidal rivers and estuaries, such as river flow, tide and surge, so as to determine the joint probability of their occurrence, producing a quantified level of flood risk.

The stated objectives of the research are:

- To determine the relationship between observed hydrological series through the use of hydraulic modelling and the production of structure functions based on the historical observations from the case study area of the River Ouse estuary at Lewes in East Sussex, UK.
- To determine the level of statistical dependence between the hydrological variables of river flow, tide and surge, which may combine to produce extreme water levels.

- To compare existing joint probability methods, encompassing both traditional single-variable probabilistic analyses and the multi-variable joint probability analyses.
- To determine a new joint probabilistic risk assessment methodology, combining extreme joint probability statistics in conjunction with statistical dependence and modelling methods.
- To apply the joint probability theory to the hydrological series in the case study area to analyse the risk of flooding from the interaction of hydrological variables in estuarine and tidal riverine environments.
- To enable the probability of flooding to be established from upstream flow data and downstream sea level data at an intermediate point of interest, in combination with the hydraulic model to convert probabilities to resultant water levels, calibrated against historical stage gauge data.
- To determine the significance of the joint probability approach against the more conventional methods for the assessment of flood risk.

2 REVIEW OF JOINT PROBABILITY FOR FLOOD RISK ESTIMATION

2.1 The Joint Probability Approach

2.1.1 Introduction to Joint Probability

Joint probability determines the chance of two (or more) conditions occurring simultaneously which may combine to produce a critical outcome of interest.

The method for the estimation of the probability of extreme values (e.g. extreme sea levels or river flow) occurring at a given location from a single variable (e.g. stage) is well understood. Such probabilities are usually expressed in the form of a return period. Similarly, the joint probability of two variables producing high or extreme values together, if they are assumed to be fully independent from each other, is also relatively straight forward (Hawkes, 2003).

Where two (or more) extreme variables are not totally independent but may be partially dependent, probabilistic approaches are limited in their reliability and scope. In tidal and estuarine environments, the assessment of the probability of flooding from the combined occurrence of both a high river flow and sea level is not straight forward, as high river flow and surge tides tend to be related to the same low pressure weather system, thus independence cannot be assumed. An assumption of independence would lead to under design of river defences, whereas an assumption of total dependence would be far too conservative.

The basis of joint probability theory is to identify extreme data within each of the variables to statistically correlate them to explore their linkage and risk of simultaneous occurrence. Understanding such risks, created by the combination of extreme events is crucial for the design of adequate and cost effective river and coastal defences and for the true estimate of flood risk.

2.1.2 Applications of Joint Probability Methods to Flood Risk Analyses

Prior to the 1980's, the use of joint probability theory was almost non-existent in the calculation of flood risk. Although studies of how a single hydrological variable (such as tide) affects two (or more) sites have been undertaken, research into how the combination of two differing variables affects an intermediate site where stage is effected by the

interaction of sea level and river flow have been more limited. Early published research focused on the comparison of historical records and the frequency of combined water levels (e.g. Weston, 1979; Vongvisessomjai and Rojanakamthorn, 1989). Weston (1979) quantified the magnitude of river flow and sea level that combine to produce observed water levels in the River Dee in North Wales. No frequency of joint probability estimates were made, but the author does comment on how much influence river flow has on the resultant water levels in the tidal reach of the river.

Vongvisessomjai and Rojanakamthorn (1989) found that historical records of stage in estuaries and tidal rivers in the United States show that an increase in the riverine discharge has a dampening effect on incoming tides, reducing the tidal propagation speed, which ultimately results in the raising of water levels.

Prandle and Wolf (1978) examined the interaction of surge and tide in the North Sea, and Walden *et al.* (1982) similarly looked at the interaction of surge and tide on the south coast of England by assessing the level of tide and surge interaction from historical observations. More detailed examples of published joint probability research on tidal water levels has been carried out at Proudman Oceanographic Laboratory, UK and developed in Dixon and Tawn (1994) and Coles and Tawn (1994), which assessed the interaction of extreme surges and wave heights and included a measure of dependence (section 2.2) between the input variables.

Dwyer (1995) reports on several different approaches to joint probability problems with a focus on river confluences. Although no research was undertaken, the author summaries and comments on some of the early work involved in joint probability problems, including Acreman (1994) and Coles and Tawn (1994). Various approaches are discussed, including simple grid and matrix methods which focused on extremes of the output variable, and more detailed dependence (section 2.2) and structure functions (section 2.4) methods examining extremes of the input variables.

Reed (1999) discussed joint probability problems involving tidal and fluvial input variables for the determination of water levels. The importance of the correct input variables in a joint probability analysis was identified, as well as the adoption of a time-blocking approach which selected one value per high tide or per day. Event definition (i.e. what defines an independent extreme event) was also discussed, and recommended that a POT (peaks-over-threshold) extreme value analysis approach should be used rather

than an AMAX (annual maxima) approach where the input variables may come from non-concurrent events.

Reed included a summary of a joint probability approach, based on structure functions and the double matrix method (see section 2.4). The assumption of inter-variable independence was also discussed, although no methods were provided for non-independent variables.

Environment Agency (2000) carried out a joint probability analysis at Brockenhurst, Hampshire, UK, following a flood in December 1999 caused by simultaneous high river flow and high tide events. The study used a limited historical data series to establish the joint probability of high tides and river flows occurring together, producing joint return periods of the input variables. A degree of dependence between the input variables was used, although no details are provided in the study. It concluded that although successful, the output produced the probability of the particular combination of input circumstances, rather than the likelihood of a specific water level.

In recent years, there has been a move by Defra, UK (originally MAFF) to fund R&D research programmes into how joint probability theory could be utilised for environmental applications, such as flood risk. Statistical methodologies for the analysis of flood risk, developed by several UK institutions, primarily focused on the application of joint probability theory to particular variable pairs. These included waves and sea levels, wind and sea swell (both at HR Wallingford, UK), tides and surges (developed at the Proudman Oceanographic Laboratory, UK), rainfall and surge, and surge and river flow (both at CEH Wallingford, UK). Although joint probability methods have been applied by the institutions involved, there has been limited dissemination or published information on its appropriate use. Consequently, take-up within the Civil Engineering and Hydrology communities has been limited.

Hawkes and Tawn (2000), as part of the Defra funded R&D joint probability programme, commented that methods for predicting single extremes of either tidal water levels or waves at a single location were in common use, but assessment of the joint probability of the two was more difficult. The project culminated in the production of a joint probability software package called JOIN-SEA, developed by HR Wallingford, UK and the University of Lancaster, UK (Hawkes and Tawn, 2000).

JOIN-SEA was primarily designed to calculate the joint probability between waves and still water levels at the same location by extrapolating the original source variables to extreme values. The statistical processes involved the fitting of statistical models to the variables. An extreme distribution was fitted to the top few percent of each variable, and a statistical correlation model applied to the datasets. A large sample of synthetic records was then simulated using a Monte Carlo method, based on the same fitted distributions as the input data. Joint exceedance extreme values were then extracted from the simulated dataset using a simple count-back procedure. Hawkes and Tawn (2000) concluded that although a degree of correlation (or dependence; see section 2.2) would be expected between waves and surges as both are related to local weather conditions, the degree of correlation varies from one site to another. It was also noted that the correlation was best determined from observed data series. A further conclusion was that the calculations led to multiple combinations of waves and water levels each with the same joint probability of occurrence at each location, only one of which produced the worst case for design.

HR Wallingford has undertaken joint probability studies in estuaries around the UK using various methods since the early 1990's, though there has been limited dissemination of the methods and results. Hawkes (2003) provided some example applications of the various joint probability methods employed, including the Severn Estuary, the River Thames, Cardiff Bay and the Clyde. Smaller studies listed included Truro and Whitby. Although the published output was brief, some conclusions can be drawn from the studies.

The Severn Estuary study produced extreme water levels at Minsterworth via continuous simulation (section 2.5.2) and JOIN-SEA simulation methods using simultaneous flow and sea level observations from Haw Bridge and Avonmouth respectively. Both simulated extreme value datasets were in close agreement with independently recorded data from the Minsterworth gauge, concluding that joint probability theory can be successfully implemented into a flood study. The other studies used various combinations of univariate (single variable), JOIN-SEA, simulation and correlation approaches, with the general conclusion that each flood risk study required some degree of a joint probability approach, even if to simply highlight a single key variable for the risk of flooding.

Hawkes (2003) stated that some estuaries may dictate that waves or surge may be further significant variables (other than upstream river flows and downstream tidal levels) which

need to be considered in a joint probability analysis. In some estuaries, surges and waves may have a substantial effect on water levels, which may necessitate at least a three-variable (i.e. trivariate) joint probability approach. It concludes that the introduction of a third variable of this type would make probability calculations extremely complex. To the author's knowledge, no trivariate joint probability flood risk examples currently exist.

Defra, in collaboration with HR Wallingford, CEH Wallingford and Proudman, produced a generic guide to joint probability usage in the flooding sector (Hawkes, 2004; Svensson and Jones, 2003; Hawkes and Svensson, 2003). Although no new developments were made during the programme, the aim was to pool previously unpublished research and methods from the three institutions to provide an 'official' Defra methodology. Each institution reported its joint probability results in terms of its preferred methodology however, resulting in a slightly compromised and limited exercise.

Hawkes (2004) detailed two methods for joint probability analysis. The first, labelled as the 'Simplified Approach', developed a desk study methodology aimed at non-specialist users. It produced a basic extreme joint exceedance output in annual return periods, for use when original time-series of the input variable pairs were not available. The method was reliant on the successful estimation of the correlation between the variable pairs from pre-calculated colour-coded small scale maps of the UK. There are inherent problems with the precision of the maps which, by the author's own admission, led to some of the mapping ideas being dropped. What is left is an unclear set of maps and broad-scale correlation values. It is questionable whether a non-specialist user would be able to appreciate the implications of some of the assumptions and methods used.

The second method, named the 'Applied Approach' was a revisit of the JOIN-SEA analysis. Unfortunately, the JOIN-SEA package was not made available to the reader, although the method can be applied without it by using Hawkes & Tawn (2000).

2.2 Dependence in Joint Probability Problems

2.2.1 Introduction to Dependence

Dependence determines the extent to which an observation of one variable is reliant on a value of another variable and is an essential part of any joint probability calculation.

Dependence indicates the likelihood of two (or more) variables, (such as tide, surge and river flow in the context of flood risk calculation), potentially producing high or extreme

values at the same time. To assess the probability of flooding (and therefore level of risk), dependence between these source variables needs to be identified. It is an essential part of an accurate joint probability analysis, yet quantification of dependence can be difficult and extreme values hard to define.

Dependence occurs when different processes have a behaviour that is linked for example to common meteorological conditions. It may also arise when the same (single) process is studied at different spatial locations or over different time periods (Coles *et al.*, 2000). In an estuarine or tidal environment, an example would be a storm event which may produce low atmospheric pressure, high winds and precipitation. These in turn is likely to create high river flows and surge conditions, which then interact with each other in an estuary or tidal river increasing the risk of flooding. A value of dependence between the variables of high river flow, tide and surge can determine the probability of a particular water level occurring in the estuary caused by this type of event.

2.2.2 Dependence Theory

2.2.2.1 The Dependence Measure χ

A method for the calculation of dependence measure was developed in the early-1990's to establish the probability of simultaneous occurrences of extreme hydrological values (e.g. Tawn, 1992; Coles and Tawn, 1992, 1994; Dixon and Tawn, 1994).

The theory of the dependence measure χ is based on two (or more) simultaneously observed variables of interest (such as river flow and sea level), known as observational pairs. If one variable exceeds a certain (extreme) threshold, then χ is the risk of the other variable will also exceed an extreme threshold. Coles *et al.* (2000) states that for an observational pair, if the all of the extreme observations of two variables exceed a given threshold at the same time, this indicates total dependence ($\chi = 1$). If the extreme observations of one variable exceed a given threshold but the second variable does not, this indicates total independence ($\chi = 0$). Similarly, if the extreme observations of one variable exceed a given threshold but the other variable produces lower observations than would normally be expected, this indicates negative dependence ($\chi = -1$). Hydrological analyses using real data often lead to the estimation of complete independence, which can lead to the under-estimation of the probability of simultaneously occurring extreme

events. Similarly, the assumption of complete dependence can lead to the over-estimation of probabilities.

For two variables X and Y with identical marginal distributions (where a marginal distribution is the probability distribution of a single variable, i.e. X , ignoring the information about the distribution of another variable, i.e. Y), Coles *et al.* (2000) states that the χ value is a measure of the likelihood of one variable being extreme provided that the other variable is extreme, such that:

$$\chi = \lim_{z \rightarrow z^*} P(Y > z \mid X > z) \quad (2.1)$$

where z^* is the upper limit of the observations of the common marginal distribution.

The calculation of χ is demonstrated in Figure 2.1 where values of simultaneously occurring surge and wave heights are plotted on opposite axis (Coles and Tawn, 1994). Extreme values are determined by the selection of an extremal threshold for each variable, producing a dataset of values which satisfy both extreme criteria.

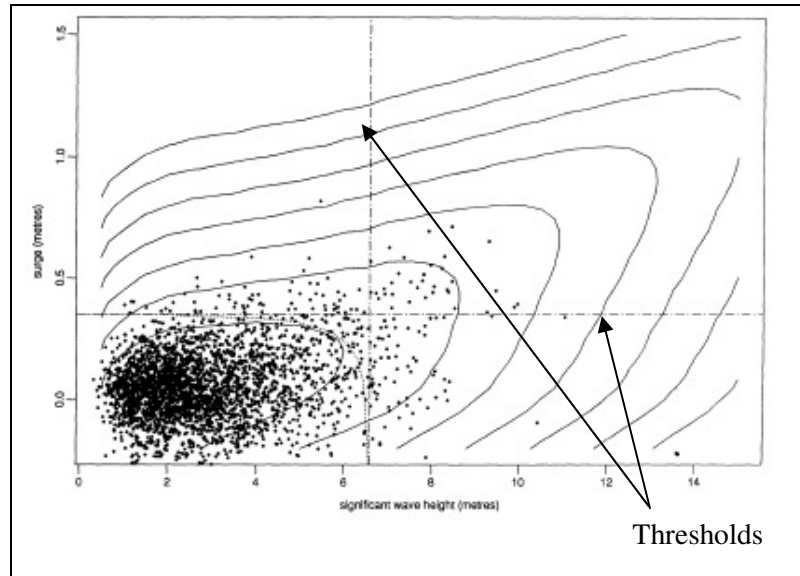


Figure 2.1 Example of joint extreme values of surges & waves (reproduced with the permission of J. Tawn)

As each of the variables approach extreme values, the observations located in the upper right-hand section of the chart exceed *both* of the selected thresholds and thus enable the calculation of dependence measure χ .

For the calculation of χ , the threshold values can be chosen through a peaks-over-threshold (POT) approach, which Coles *et al.* (2000) identified as a more accurate estimate of the probability distribution than using only the annual maximum series. The dependence measure χ may then be estimated for any pair of variables using any threshold.

Reed (1999) termed dependence in the Flood Estimation Handbook as the tendency for potentially critical values of the input variables to occur together more frequently than by chance alone, and highlighted some simple methods for determining inter-variable dependence, including scatter-plots of the input variables and correlation coefficients (e.g. R^2 values). Reed however noted that these methods were more likely to lead to crude and underestimated extreme values, and concluded that the more formal statistical multivariate extreme methods as suggested by Coles and Tawn (1994) are a considerable extension to the Flood Estimation Handbook approach, although they are highly specialised. Reed also noted that the degree of dependence can only be calculated from the analysis of simultaneous records, which typically have a much shorter duration than the required target return periods for flood estimation, concluding that results may be highly sensitive to a few extreme events in the relatively short input series.

Coles (2001) commented that the identification of the phenomenon of simultaneously occurring dependent extreme events in a multivariate extreme value model is likely to be important as the impact of such an event may be much greater than if extremes of either component occur in isolation. Coles concluded that an approximation of the dependence between variables at extreme levels as well as the extreme behaviour of each individual series is necessary for accurate extreme multivariate models.

The marginal distributions of the two primary variables (e.g. river flow and sea level) may not necessarily be identical however. Coles *et al.* (2000) states that to enable the dependence function to successfully calculate a value of dependence, the two primary variables required identical marginal distributions and thus have to be transformed to become so. This can be achieved using their empirical distributions. A simple estimate of this is to rank each set of observations separately and divide each rank with the total number of observations in each dataset which transforms the two datasets to a joint distribution with uniform $[0,1]$ margins. Coles and Tawn (1994) cite this method as having an advantage of using transformed distributions for the two input variables when

compared to single variable approaches, where the output variable is understood to reflect a combination of input factors (Reed, 1999).

However, instead of estimating χ from the general case, Svensson and Jones (2000) recommend that the calculation be approached in a different way. Instead of estimating the identical marginal distributions by ranking the datasets, a joint distribution function can be used which transforms pairs of simultaneously observed variables, producing a joint distribution. The influence of the non-identical marginal distributions can be removed using the function C such that:

$$F(x, y) = C\{F_x(x), F_y(y)\} \quad (2.2)$$

where F_x and F_y are (any) marginal distributions, and the function C is a multivariate distribution function called a Copula, such that the marginal distributions of the variables are uniform with $[0,1]$ margins. Svensson and Jones (2000) state that the Copula is unique as it contains complete information about the nature of the joint distribution (and therefore dependence) between the two simultaneously observed pairs of variables, which can be provided without the information on the marginal distributions. In other words, the Copula can be described as the joint distribution function of the two variables X and Y after transformation to variables U and V via $(U, V) = \{F_x(X), F_y(Y)\}$.

It follows that for two variables U and V with uniform distributions and $[0,1]$ margins with a given identical threshold u :

$$P(V > u | U > u) = \frac{P(U > u, V > u)}{P(U > u)} \quad (2.3)$$

As $u \rightarrow 1$, the following relation can then be used:

$$\begin{aligned} P(V > u | U > u) &= \frac{P(U > u, V > u)}{P(U > u)} = \frac{1 - 2u + C(u, u)}{1 - u} = 2 - \frac{1 - C(u, u)}{1 - u} \\ &\approx 2 - \frac{\ln C(u, u)}{\ln u} \end{aligned} \quad (2.4)$$

which is related to the general case of χ by:

$$\chi = \lim_{u \rightarrow 1} \chi(u) = \lim_{u \rightarrow 1} P(U > u \mid V > u) \quad (2.5)$$

The dependence measure χ is then defined, for a given threshold u , as:

$$\chi(u) = 2 - \frac{\ln C(u, u)}{\ln u} \quad (2.6)$$

Substituting for two variables U and V with transformed uniform $[0,1]$ margins, for a given threshold u with limits $0 \leq u \leq 1$:

$$\chi(u) = 2 - \frac{\ln P(U \leq u, V \leq u)}{\ln P(U \leq u)} \text{ for } 0 \leq u \leq 1 \quad (2.7)$$

Whilst this approach may be suitable for pairs of variables which are observed simultaneously and retained as pairs throughout the calculation (e.g. $X_1, Y_1; X_2, Y_2; \dots X_n, Y_n$) with similar (albeit non-identical) distributions, there may be limitations in its applicability with variables with either different marginal distributions or non-paired variables due to the lack of formal transformation (e.g. Coles *et al.*, 2000), and is not explored by Svensson and Jones.

2.2.2.2 Threshold Selection

The basis of Svensson and Jones (2000) approach for the calculation of χ (from here on used as shorthand for $\chi(u)$) is the probability of exceedance by two variables of an identical threshold level u . In practice however, the threshold Svensson and Jones state that u may not be identical for each variable, thus u corresponds to the threshold levels (x^*, y^*) for the two observed series (X, Y) .

Extreme values located in the upper right-hand quadrant of Figure 2.1 simultaneously exceed *both* of the selected x^* and y^* thresholds, and thus satisfy the extreme criteria required to calculate the dependence measure χ . The level of dependence however can be calculated from the simultaneous non-exceedance of the extreme thresholds of both variables, as well as the non-exceedance of the extreme thresholds for *each* variable. This can be achieved by counting the observational pairs of (X, Y) where *only one* variable does not exceed its threshold level x^* or y^* (and vice-versa), and where *neither* variable simultaneously exceeds their threshold levels. Svensson and Jones state that this may then be substituted for equation 2.7, thus:

$$P(U \leq u, V \leq u) = \frac{\text{Number of } (X, Y) \text{ such that } X \leq x^* \text{ and } Y \leq y^*}{\text{Total number of } (X, Y)} \quad (2.8)$$

and:

$$\ln P(U \leq u) = \frac{1}{2} \ln \left[\frac{\text{Number of } X \leq x}{\text{Total number of } X} \cdot \frac{\text{Number of } Y \leq y^*}{\text{Total number of } Y} \right] \quad (2.9)$$

To calculate $P(U \leq u, V \leq u)$ from equation 2.8, the total number of (X, Y) observation pairs may be counted together with the number of pairs of (X, Y) that satisfy *both* $X \leq x^*$ and $Y \leq y^*$. The other possible combination pairs of $X \geq x^*$ and $Y \geq y^*$, $X \leq x^*$ and $Y \geq y^*$, and $X \geq x^*$ and $Y \leq y^*$ are *not* counted.

Similarly, to calculate $\ln P(U \leq u)$ from equation 2.9, the total number observational pairs (X, Y) may be counted which satisfy either $X \leq x^*$ or $Y \leq y^*$ independently from the other variable. The resultant values can then substituted into the general equation 2.7 for the calculation of χ .

2.2.2.3 Positive & Negative χ Values

Dependence values can also be classified as either negatively or positively dependent. If two variables are said to be positively dependent, then if one variable has a high value, the other dependent value is likely to have a higher value than would normally be expected. Similarly, if two variables are found to be negatively dependent, then when one variable has a high value, the other dependent value is likely to have a lower value than would normally be expected.

An example of two positively dependent variables would be high offshore winds and high waves which are likely to occur simultaneously. These high observations are known as extremes values, as their occurrence is rare for the particular location of interest (Coles and Tawn, 1994).

2.2.3 Applications of Dependence Theory in Flood Risk Analyses

2.2.3.1 Dependence between River Flow & Sea level

River estuaries are at risk of flooding from either high river flow or sea levels, or as a combination of both. Dependence studies in estuarine environments however have been

limited. Calculations of this nature have also been suggested to be laborious and time consuming (Hawkes, 2003).

Van der Made (1969) investigated dependence river flow in the Rhine and water levels on the North Sea coastline of the Netherlands by comparing the frequency of river flows occurring simultaneously with extreme surges. No significant difference was found between the frequencies of the variables, and it was therefore concluded that no dependence existed.

Loganathan *et al.* (1987) found that there was dependence between river flow in the Rappahannock River and water levels in Chesapeake Bay on the east coast of the United States. Here, lines of probability of exceedance were simply plotted on a chart of water level versus river flow which concluded that high flows tended to occur simultaneously to high water levels in the Bay.

An investigation carried out by Samuels and Burt (2002) identified dependence between peak river flows on the Taff at Pontypridd and sea levels at Cardiff in South Wales. The research utilised the JOIN-SEA software package, developed by HR Wallingford and the University of Lancaster (section 2.1.2). The investigation assessed the frequency of occurrence of designed water levels in Cardiff Bay, following the recent installation of a tidal barrage. The barrage was designed to substantially eliminate the probability of tidal flooding of the Cardiff Bay waterfront from surge tides. The study was designed to analyse the ability of the bay to cope with storage of the river flow during periods of high surges. The twenty highest peak river flows were extracted and paired with the corresponding nearest high water levels. It was concluded that there was no correlation between the series, and that the corresponding sea levels were not unusually high (which would have suggested that there might be dependence). The analysis was repeated using a 9-hour time-lag between the series, finding positive dependence, suggesting that both river flow and sea level respond to certain weather conditions.

A dependence analysis for the same area was also undertaken by Svensson and Jones (2003), where significant dependence was found between daily mean river flow at Pontypridd and surge at Avonmouth. The differing datasets (river flow and sea level v river flow and surge) and resolutions (annual maxima v daily mean) may have been the contributing factor to the varying results between the two studies. Samuels and Burt (2002) do remark that some heavy-duty conservative assumptions were used in the

assessment, including the use of total sea level data rather than surge. The meteorological component of the tidal levels is more directly related to the weather causing both river flow (via precipitation) and surge, whereas the variation in total sea level arises mainly from the variation in astronomical tide, which is unrelated to the weather driving extreme events.

2.2.3.2 Dependence between River Flow & Surge

Surge is the change in sea level due to meteorological effects, caused by the tractive force of the wind and the effect of atmospheric pressure differences on the water surface (Svensson and Jones, 2004b). Studies of dependence between surge (observed sea level minus the predicted astronomical tide) and river flow may be expected to show more dependence than observed sea levels and river flow, due to the common link with meteorological storm systems simultaneously producing low atmospheric pressure, surges, high winds and precipitation.

Few publications exist which explore the relationship between surge and river flow on the south coast of Britain. However, studies of dependence between surge and river flow have been carried out on some of the tidal reaches and estuaries around the UK. Early cases include the River Trent (Granger, 1959) and the River Ancholme (Thompson and Law, 1983), both in North Lincolnshire. Both found surge and river flow to be independent, or were approximated to be so.

Mantz and Wakeling (1979) compared the predicted return period for a joint surge and river flow event assuming independence, with the return periods calculated from historical observations, for three rivers in the Yare catchment in Norfolk. It was noted that little difference existed between the predicted and historical return periods, concluding that surge and flow were independently occurring events. However, the results do suggest that there may be weak dependence which increased as the variables become more extreme, which was not analysed.

Van der Boogaard and Stive (1990) correlated extreme surge and river flow on the River Medway, UK, but found little evidence of a relationship, and assumed independence between the variables. Acreman (1994) noted however that any assessment of the joint probability of fluvial and tidal events involving the fitting of statistical distributions requires the correlation of the input data to be determined, suggesting that if high river flows and surge tides occur together as a result of meteorological conditions, they cannot

be considered to be independent. No statistical dependence value was however calculated in the study.

A study by Svensson and Jones (2000) focused on the joint probability of a single-variable extreme event (in this case, high river flow) occurring at more than one site at the same time, at pairs of flow gauges around the UK. Svensson and Jones stated that dependence analyses could be carried out using surge (or storm surges in extreme cases), either in addition to or instead of total sea level, which may express a purer indication of meteorological dependence. It was concluded that this may reduce any potential influence of tides and surge interaction on a dependence analysis.

Recent investigations calculated the dependence between surge and river flow on the east coast of Britain (Svensson and Jones, 2002), and on the south and west coasts of Britain (Svensson and Jones, 2004a). It was found that dependence between surge and river flow in estuaries and tidal rivers occur mainly in catchments with slopes exposed to south-westerly winds, where high river flow and surge events may occur simultaneously and combine to produce high water levels in an estuary on the same day. The authors also noted that dependence between surge and flow can vary over short distances due to the differing catchment characteristics of each river system, suggesting that a localised site-specific approach is required for successful dependence estimation. In southern England, the western part of the south coast was found to display the highest dependence.

Svensson and Jones (2002, 2003, 2004a) incorporated seasonal and time-lagged calculations into the same-variable (i.e. pairs of surge gauges) dependence analyses. A distance function was also utilised, although the results do not indicate whether any spatial factors were taken into consideration, such as the distance between each of the station pairs. Similarly, there was a lack of specific time-lagged values with no direct comparison with corresponding dependence results between different variable pairs (i.e. surge and flow). The seasonality analyses provided examples of differing dependence values between the summer and winter periods. No time-lagged analysis was undertaken between differing variable pairs.

2.2.3.3 Dependence between Precipitation & Surge

Early approaches to obtaining a summary measure of statistical dependence between extremes of different variables include Buishand (1984, 1991) which introduced a dependence function between pairs of precipitation gauges. Here, dependence was

preferred to the traditional correlation coefficient because it indicated how the distribution of a maxima in a sequence of paired observations was influenced by dependence. Coles and Tawn (1994) discuss some of the practical issues involved in the use of multivariate (multiple variable) extreme value techniques. Dixon and Tawn (1994) reviewed some of the statistical methods of multivariate extreme value modelling with environmental variables.

Bruun and Tawn (1998) produced a comparison of multivariate and structure function approaches to coastal hydrological variables, and Coles *et al.* (2000) showed dependence between different hydrological variables including surges and precipitation.

Svensson and Jones (2000) stated if a surge and river flow dependence analysis reveals low dependence, then a surge and precipitation dependence study could be undertaken which may avoid any possible catchment processes affecting the level of dependence. Svensson and Jones (2000, 2003) calculated dependence between surge and precipitation where surge and river flow dependence analyses revealed low dependence. It was concluded that precipitation assisted in the interpretation of why surge and river flow dependence occurs in some areas and not in others, and could be regarded as a tool to aid the dependence analysis process in conjunction with seasonality and time lagged analyses.

2.3 Interpretation of the Dependence Measure χ

Reed (1999) defines dependence as the tendency for critical values to occur together, and increases the frequency of a given (extreme) magnitude of the output variable. This means that dependence can therefore increase the magnitude of the output variable for a given rarity such as an annual return period. Even a small amount of dependence between the extremes of river flow and sea levels can have a significant impact on the resultant water levels in an estuary (Svensson & Jones, 2004b).

Examples of analyses which use the dependence measure χ however have mainly focused on the determination of an accurate value of χ (e.g. Svensson & Jones, 2000, 2004a etc.) rather than its use in a joint probability exercise. For example, Svensson and Jones (2003) show where extreme river flows and surges could occur simultaneously. The actual water levels (involving the third variable of astronomical tide) in the estuaries

and whether they may occur simultaneously were not analysed. Similarly, no time-lagged analysis was carried out between surges and extreme river flows in an attempt to model the catchment processes and associated spatial and temporal lags between the flow and sea level gauges.

Svensson and Jones (2000) proposed a method for the interpretation of χ using daily and annual return periods. Svensson and Jones detailed that equation 2.8 may be rearranged to obtain the following expression for the probability of non-exceedance of the threshold u by two variables U and V with identical probabilities of non-exceedance and dependence χ :

$$P(U \leq u, V \leq u) = P(U \leq u)^{2-\chi} \quad (2.10)$$

Thus:

$$P(U \leq u) = P(V \leq u) \quad (2.11)$$

Svensson and Jones (2000) stated that the probability of non-exceedance of threshold u could be expressed in terms of a return period T for identical probabilities, thus:

$$P(U \leq u) = P(V \leq u) = 1 - \frac{1}{T} \quad (2.12)$$

Given T , the marginal probability of exceedance could then be expressed as:

$$P(U > u) = P(V > u) = \frac{1}{T} \quad (2.13)$$

To calculate the probability of the exceedance of the threshold u by variables with identical probabilities, Svensson and Jones stated that the joint probability could be directly rewritten in terms of the identical return period T and dependence χ :

$$\begin{aligned} P(U > u, V > u) &= 1 - 2P(U \leq u) + P(U \leq u, V \leq u) \\ &= 1 - 2\left(1 - \frac{1}{T}\right) + \left(1 - \frac{1}{T}\right)^{2-\chi} \\ &= \left(1 - \frac{1}{T}\right)^{2-\chi} + \left(\frac{2}{T}\right) - 1 \end{aligned} \quad (2.14)$$

This was rearranged to obtain an expression to for the joint return period $T_{X,Y}$ of two variables (X,Y) with uniform marginal distributions and a calculated dependence measure χ , exceeding an identical threshold u with identical return periods:

$$T_{X,Y} = \frac{1}{\left(1 - \frac{1}{T}\right)^{2-\chi} + \left(\frac{2}{T}\right) - 1} \quad (2.15)$$

Analysis of the method by Svensson and Jones compared generalised strengths of dependence between 0 and 1 against predefined return periods, and found that the inclusion of a dependence measure in a joint probability calculation had a substantial impact on the resultant joint return period when compared to results calculated assuming independence, both in days and years. The study concluded that neglecting dependence in a joint probability analysis would likely underestimate estimated maximum water levels for a given frequency. However, although the approach appears to be robust, no analysis was undertaken to explore the application of this method on variables with non-identical return periods. This suggests that the approach is limited to variables with similar marginal distributions and identical return periods.

Svensson and Jones (2000) also noted that different parts of a study area (i.e. water level in a river estuary) will be influenced to varying degrees by the input variables (i.e. river flow and sea level), therefore the calculated joint return period of the combined events will not indicate the true return period of the resulting water level. Svensson and Jones recommend a structure function approach (see section 2.4) for the estimation of intermediate water levels, which contains a detailed description of how the input variables combine to influence the critical output variable.

Hawkes (2004) and Meadowcroft *et al.* (2004) used a more simplistic joint variable exceedance method which used dependence correlation factors including χ . Hawkes (2004) state that to obtain the of joint return period $T_{X,Y}$ of the exceedance of threshold u , for variables with identical return periods T and dependence χ , $T_{X,Y}$ could be expressed thus:

$$T_{X,Y} = \frac{T}{\chi} \quad (2.16)$$

The approach assumed the marginal distributions to be identical and did not require transformation to become so. This is a clear limitation of the approach. Hawkes (2004) developed a spreadsheet approach as part of the ‘Simplified Approach’ for the Defra R&D joint probability project (section 2.1.2), which generated graphical curves of joint exceedance based on an a predetermined value of χ , relating to four levels of correlation (low, moderate, high and super) between the input variable pairs.

Here, as in many cases, the return periods of the two primary variables were not always identical. Unlike Svensson and Jones however, Hawkes (2004) and Meadowcroft *et al.* (2004) derived equation 2.16 to obtain the joint probability $T_{x,y}$ of threshold levels (x^*, y^*) (which corresponded to the threshold u) with non-identical return periods (T_x, T_y) for variables (X, Y) and dependence measure χ , using the average of the two return periods, thus:

$$T_{x,y} = \sqrt{\frac{T_x \cdot T_y}{\chi^2}} \quad (2.17)$$

where it was assumed that the return periods were not required to be identical for the calculation of the joint return period. Hawkes (2004) and *pers comm.* used the assumption that when using non-identical return periods (i.e. T_x, T_y), a number of combined probabilities would equal the same joint return period (i.e. for a 1:100 year joint return period, this could be created by a combination of events such as a 1:10 & 1:10, 1:20 & 1:5, 1:50 & 1:2, 1:100 & 1:1 etc.). Hawkes concluded that the approach taken may underestimate the magnitude for a given joint return period, and recommended that a factor or around 2 may be required for the χ value.

Trials of equations 2.15 and 2.17 with identical marginal return periods and levels of dependence ranging from 0 (signifying complete independence) to 1 (signifying complete dependence), produced similar joint return period magnitudes for the highest levels of dependence and marginal return periods (Appendix G.2). However, equation 2.17 was found to underestimate the joint return period magnitudes for lower levels of dependence and marginal return periods when compared to equation 2.15, and was unable to calculate joint return periods with 0 level of dependence (i.e. fully independent). It was concluded that this was due to the limited expression used in equation 2.17.

To the author's knowledge, there have been no published studies or further research into the use of either method other than the general dissemination of the two approaches detailed here. No examples or case studies of use of the dependence measure χ in a joint probability analysis for the calculation of flood risk or extreme water levels exist.

2.4 Structure Functions

2.4.1 Structure Functions & Matrices

A structure function is a 'process' which relates an output variable (i.e. a water level at a point of interest) to two input variables (i.e. sea level and flow) described by e.g. Ibidapo-Obe and Beran (1988), Dwyer (1995), Jones (1998) and Reed (1999). There are two direct methods of calculating water levels (the intermediate structure function) in estuaries and tidal rivers. The first simulates water levels through the use of a numerical hydraulic model (section 2.4.2), and the second utilises a simplified formula, usually derived through a regression analysis (Hawkes, 2003).

The formulaic approach generates an equation derived from historical simultaneous datasets through which intermediate water-levels can be generated from input values of sea level and flow. The approach is limited by the duration of the historical datasets as the equation may differ under high flow / sea level events which are not contained in the historical data series.

Jones (1998) carried out an extensive structure function analysis of the tidal reaches of the River Thames, UK, in combination with a historical emulation exercise (section 2.5.3). Jones evaluated the hydraulic modelling and formula-based structure function approaches and recommended the modelling process as the most accurate method for determination of overall water levels as it has the ability to evaluate intermediate water-levels at the point of interest for all combinations of the input variables, including the most extreme loading conditions (i.e. every conceivable combination of sea level and river flow).

Reed (1999) suggested the best most reliable structure function method is to use matrices. For a two-variable (bivariate) analysis, two matrices are required, which Reed termed as the 'double matrix method'. The first matrix is a table of output variables generated from a series of hydraulic model runs, with input values on opposing axes and

the generated output ‘structure’ values at the point of interest corresponding to the input pair. The second is a joint density function matrix of probabilities for the same input variable pairs as the structure value matrix, calculated by the density functions of the two input variables. Using the matrices, peak water levels at a tidal river site can be estimated from peak sea levels and peak river flows for a selected probability, such as a return period.

Hawkes (2003) however noted that it would be impractical to generate hydraulic model output data for each possible pairing as there could be many thousands of combinations, and recommends that a look-up table could be used which interpolates between the data points. Similarly, as with any joint probability approach (e.g. Hawkes and Tawn, 2000), there may be multiple combinations of the input variables which display the same joint probability of occurrence at the point of interest, only one of which may produce the worst case for design (i.e. the highest water level).

2.4.2 Hydraulic Modelling

Historically, physical fluid flow models have been constructed at great expense of time and money. In recent years, the computerised numerical modelling of the hydraulic flows and sea levels has emerged as an integral part of flood frequency estimation, enabling complex calculations involved in fluid flow to be undertaken for an entire systems with relative ease and accuracy. Uses include the simulation of specified events or continuous (real-time) modelling, and the generation of structure functions, based on two (or more) input data records. Various examples exist of the use of one-dimensional hydraulic numerical models for estuaries and tidal rivers e.g. Acreman (1994), Jones (1998), Environment Agency (2000, 2001a, 2000), Hawkes (2003) etc. Typical models available for hydraulic simulation of water levels include HEC-RAS, Mike 21 and iSIS.

2.5 Non-Probabilistic Flood Risk Methods

2.5.1 Direct Analysis

Many studies (e.g. Reed, 1999; Hawkes, 2003) refer to a direct (univariate) analysis at (or close to) the point of interest using historical data, thus avoiding the need for a potentially complex joint probability study. In practise, this is not always possible due to either ungauged sites or poor historical records.

2.5.2 Continuous Simulation

A continuous simulation is a direct numerical hydraulic model simulation (section 2.4.2), typically using simultaneously recorded input river flow and sea level observations at the extremities of the model (i.e. the ‘cause’), producing a corresponding modelled output time series at an intermediate point of interest within the length of the hydraulic model (i.e. the ‘effect’) (Jones, 1998).

Jones (1998) discussed the methodology for continuous simulation modelling, concluding that it may be undertaken as a long-term or event-based exercise. The resultant dataset is a derived time series at each modelled cross-section for the same time period as the input variables, providing a real-time output to enable extraction of extreme value series (i.e. daily or annual maximas) or specific hydrological events at an intermediate point of interest within the model as though it had been historically observed (Reed, 1999).

Reed (1999) notes however that, although a continuous simulation is a way of avoiding a potentially complex joint probability problem, a successful continuous simulation requires both long simultaneous input variable record lengths and an accurately performing hydraulic model. Reed also suggests that the ideal input variables, for the modelling of a tidal river or estuary, would be records of sea level at the lower limit of the model and river flow at the higher limit above the tidal reach to avoid any interference.

Hawkes (2003) also comments on the use of a continuous simulation of water levels, stating that the approach benefits from not needing to know the nature of the dependence between the input variables, and that the output can be generated for any point in the hydraulic model. However, Hawkes notes that the approach is time consuming and is limited by the length of input records.

2.5.3 Historical Emulation

Unlike the continuous simulation approach which requires two simultaneous historical data series (i.e. sea level and river flow) to simulate a continuous output variable, the historical emulation approach uses the input data series to select, via a structure function matrix, corresponding values at the point of interest. Reed (1999) recommended that the structure function is derived through extensive trials and model runs (as per section 2.4),

and is then applied to potential flood events drawn from the historical records, creating a series of extreme output values. Reed concluded that the method is relatively straightforward to apply, assuming a well-defined structure function and hydraulic model exist or can be generated.

Acreman (1994) uses a ‘historical reconstruction’ method on the River Roding (a tributary to the River Thames, UK) involving the fitting of statistical distributions to the input variables and the use of a one-dimensional hydraulic model to reconstruct water levels from historical records of river flow and sea level through structure functions. The author found that although conceptually simple, the estimated water level for a specified return period in the estuary was found to rely heavily on extrapolated input data. The typically short duration of the historical input variables may not contain the rarest coincidences of extreme sea levels and river flows, resulting in a large extrapolation of the output data. Acreman concluded that the approach is however both flexible and adaptable through careful use of a sensitivity tests, and produced satisfactory results for the case study.

Jones (1998) detailed the methodology for a historical emulation exercise and provides examples of its use on tributaries of the River Thames, UK. Jones concluded that the approach is simple to apply when compared to a joint probability analysis, although it is limited to the duration of the record length.

2.6 Flood Risk Studies in the River Ouse Catchment

2.6.1 General Flood Risk & Joint Probability Investigations

The River Ouse catchment in East Sussex, UK, suffered severe flooding on the 12th October 2000. Environment Agency (2001a) modelled river flow and sea level in the Ouse catchment as part of the Section 105 study, using flood hydrographs and standard Flood Estimation Handbook rainfall-runoff methods (see Robson and Reed, 1999). No attempt was made to analyse the relationship or joint probability between extreme fluvial flows and high tides or surges.

Following the 12th October 2000 flood in Lewes and Uckfield, Environment Agency (2001c) produced a detailed account of the event. The interaction of sea level and river flow was analysed for the immediate period before and during the peak of the flood. The

causes of the flood were investigated, concluding that the event was primarily fluvially driven, caused by three successive extreme rainfall events in the upper catchment. No probability analysis or long-term flood prediction calculations were undertaken during the study.

Environment Agency (2002, 2004) produced a detailed River Ouse flood management strategy, comprising of probabilities and an iSIS hydraulic flood model. It comments that flooding at Lewes is a complex problem due to the interaction of sea level and river flow, offstream floodplain storage and narrow topography and river channel (including Cliffe Bridge) through the centre of the town. It was concluded that sea level (including surge) alone could not cause flooding in Lewes with the existing defence levels, although the interaction of flow and sea level was not discussed. The impact of fluvial flows was therefore the main focus of the study, and as such, no joint probability analysis was undertaken between sea level and river flow, with sea level was taken as a constant during the modelling exercise.

Environment Agency (2004) commented that sea level rise associated with climate change will increase the importance of extreme sea levels for flood levels in Lewes, particularly downstream of Cliffe Bridge. A brief analysis of the potential impact suggested any increase in the predicted extreme sea levels at Newhaven would require a joint probability analysis of the combined impact of sea level and fluvial events.

MacDonald (2004) derived flood estimates for the Uck sub-catchment (in the upper Ouse catchment), also using standard methods recommended in the Flood Estimation Handbook. The results updated Environment Agency (2002, 2004), and disseminated general recommendations for extreme river flow analyses. No specific impacts or implications were noted for flood risk calculation in the Ouse catchment.

A recent scoping report for the Ouse catchment flood management plan (Environment Agency, 2006) highlighted the current flood risk in the catchment, using findings from the flood risk management strategy. There was no discussion on the interaction of sea level and river flow at Lewes.

2.6.2 Dependence Studies

The Defra R&D funded joint probability project (e.g. Svensson and Jones, 2003; Hawkes, 2004) calculated dependence values for the Ouse catchment area. Dependence

between two tidal level gauges using a single variable of surge was investigated. The results indicated where surges could occur simultaneously along different stretches of the south coast of England at various tidal gauges, including Newhaven.

Svensson and Jones (2003) calculated that for surge, dependence between the same-variable pairs was weaker in the eastern half of the south coast of England than in the western half. From west to east, similarly distanced station pairs showed decreasing dependence; $\chi = 0.42$ for Newlyn and Weymouth, $\chi = 0.25$ for Weymouth and Newhaven and $\chi = 0.08$ for Portsmouth and Dover. It was suggested that the decreasing dependence values may be related to the incursion of North Sea surges into the English Channel from the east.

Svensson and Jones (2002, 2004a) also investigated dependence between daily maxima surge and daily mean river flow for station pairs around the UK, including the tidal reach of the River Ouse. Three UK regions displayed significant surge and river flow dependence which generally exceeded $\chi = 0.1$ as the western part of the English south coast, southern Wales, and around the Solway Firth.

Svensson and Jones (2004a) calculated dependence between pairs of daily maximum surge and river flow gauges on the southern coast of Britain. Dependence was often found to be strongest when surge and flow occur on the same day in catchments along the south coast. Dependence between Barcombe Mills river flow and Newhaven surge in the Ouse catchment was calculated as $\chi = 0.05$ at the 5% significance level. Higher dependence (i.e. $\chi > 0.1$) was generally found in hilly catchments with a southerly to westerly aspect.

It was suggested by the authors that this low value of dependence in the Ouse may be related to the catchments along this part of the coast comprising of a generally permeable (predominantly chalk) underlying geology, which respond slowly to rainfall, and therefore runoff (and subsequent high river flow) may not form on the same day as a surge occurs. Environment Agency (2002) however categorises the Ouse catchment as being ‘quickly responding’ and ‘flashy’ in nature, raising some doubts about this conclusion.

Seasonal and time-lagged (in days) dependence calculations were carried out for the three UK regions where significance was found to be generally high, but they did not

cover the Ouse catchment as dependence was not found to be significant here for the non-lagged analyses.

With the eastern part of the south coast of England producing low dependence between surge and high river flow, Svensson and Jones (2003) analysed dependence between surge and precipitation in an attempt to avoid any interference from any catchment processes and topography. Precipitation data was used from the Wye precipitation gauge, 40 miles to the east of the Ouse catchment and paired with Newhaven surge. Although the report only draws general conclusions, it found that on the south coast of England, dependence between precipitation and surge was widespread, including a significant level of dependence for the Ouse catchment, although the χ value was not given.

Dependence was found to be strongest when high surge and precipitation occur on the same day, but also remains strong for when river flows are lagged one day after the surge. The authors proposed that this was confirmation that the lack of dependence between surges and high river flows was related to catchment processes rather than any other factors.

Svensson and Jones (2002, 2003, 2004a) all utilised the Barcombe Mills river flow dataset for the dependence analyses in the Ouse catchment area, which has been confirmed as being of poor data quality and reliability (e.g. Environment Agency, 2001b, 2002 and *pers comm.*). The use of the Barcombe Mills dataset may have had a significant impact on the accurate determination of dependence values, and may explain the differing findings from the dependence analyses between surges and high river flows, against surges and precipitation.

2.7 Conclusions

Non-probabilistic approaches for the determination of (extreme) water levels in estuaries and rivers from the interaction of sea level and river flow are well established, including numerical hydraulic modelling, structure function generation, simulation and emulation methods. Similarly, univariate (single variable) probabilistic methods have been in use for flood risk estimation for many years. The recent development of statistical dependence methods for the quantification of simultaneously occurring extreme variables (e.g. Coles and Tawn, 1994; Coles et al., 2000) has enabled users to incorporate realistic joint occurrences of hydrological variables into flood risk studies. Coupled with this,

there has also been a growth in the requirement for joint probability to be incorporated into flood risk analyses (e.g. Hawkes and Svensson, 2003; Hawkes 2004). However, many of the existing joint probability analyses have aimed to simplify the procedures for the calculation of joint probability values, often for non-specialist users (e.g. Hawkes, 2004). In contrast, the majority of the existing statistical dependence studies focus on obtaining a highly accurate value of dependence for a given location or variable pair.

The existing body of research has identified several existing approaches to the joint probability problem. The use of statistical dependence with hydrological variables (e.g. Svensson and Jones, 2002) has been a clear success, especially between surge and river flow, as have the more traditional modelling and structure function approaches (e.g. Jones, 1998; Hawkes, 2003). There has however been limited research into whether these techniques can successfully be employed together to form a coherent methodology for the calculation of extreme joint probabilistic flood magnitudes from two (or more) variables. To the author's knowledge, Svensson and Jones did not apply this method to a complete joint probability scenario, nor have any further publications of its use been made.

The existing methods have led to several assumptions and limitations being identified. The approach for the determination of joint probabilities using the dependence measure χ suggested by Svensson and Jones (2000) appears robust, but there are immediate limitations due to the need for the marginal distributions to be similar and the assumption that the return periods of the single variables are required to be identical. In comparison, the Hawkes' approach is clearly limited by the lack of transformation of the marginal distributions, but does allow for the inclusion of non-identical return periods as well as providing methods for direct conversion of to extreme water level magnitudes. However, it can be hypothesised that both methods present viable solutions when used within their limitations provided they are presented accordingly. There is also clearly scope to develop these two approaches further in such as way as to take the more robust Svensson and Jones approach and derive it to accept non-identical return periods and probabilities as suggested by the Hawkes approach.

At present, there are few direct examples which demonstrate the use of sophisticated joint probability exercises for the determination of extreme values based on the occurrence of two (or more) input variables, largely due to the complexity and the site-specific nature of each problem. In estuaries and tidal rivers, the problem is compounded

by the different locations of the input variables (i.e. sea level occurring at one limit of the estuary and river flow at the other).

Svensson and Jones (2002, 2004b) show where extreme river flows and surges may occur simultaneously around the UK. How the dependent river flow and surge variables combine with astronomical tide to produce a resultant water level in an estuary has not been analysed. A dependence analysis between the source variables therefore needs to be undertaken alongside an investigation into the physical processes which exist to cause flooding, including the interaction of river flow, surge and astronomical tide, catchment processes, seasonality and time-lags, through the use of hydraulic simulation and structure function methods. These factors may either directly or indirectly affect the ultimate flood levels which a dependence value does not model.

More specific to the River Ouse catchment, the conclusion by Svensson and Jones (2003) that dependence between surge and high river flow breaks down on the eastern part of the south coast because of slowly responding catchments may be slightly too generalised. The fact that surge and precipitation conversely show high dependence for the same area implies that there could be dependence there. There may be a number of other possible factors which may contribute to the low level of dependence rather than one single factor such as a slowly responding catchment, such as the use of the unreliable Barcombe Mills dataset or the time-lag between surge and river flow events. Similarly, as the 12th October 2000 River Ouse flood event demonstrated, given the right combinations of meteorological events, the catchment can be flashy in nature and respond quickly to storm events, challenging Svensson and Jones conclusion.

This research aims to combine the existing probabilistic and non-probabilistic methods with a statistical dependence analysis to determine the probability of extreme flood events being caused by more than one hydrological variable on a site-specific study area of Lewes in East Sussex, UK. The approach will identify three methods involving single, bivariate and trivariate approaches, producing directly comparable joint probability values, and will address any limitations in the existing dependence and joint probability methods.

3 METHODS

3.1 Introduction

A flow diagram of the methods identified for the following research are shown below.

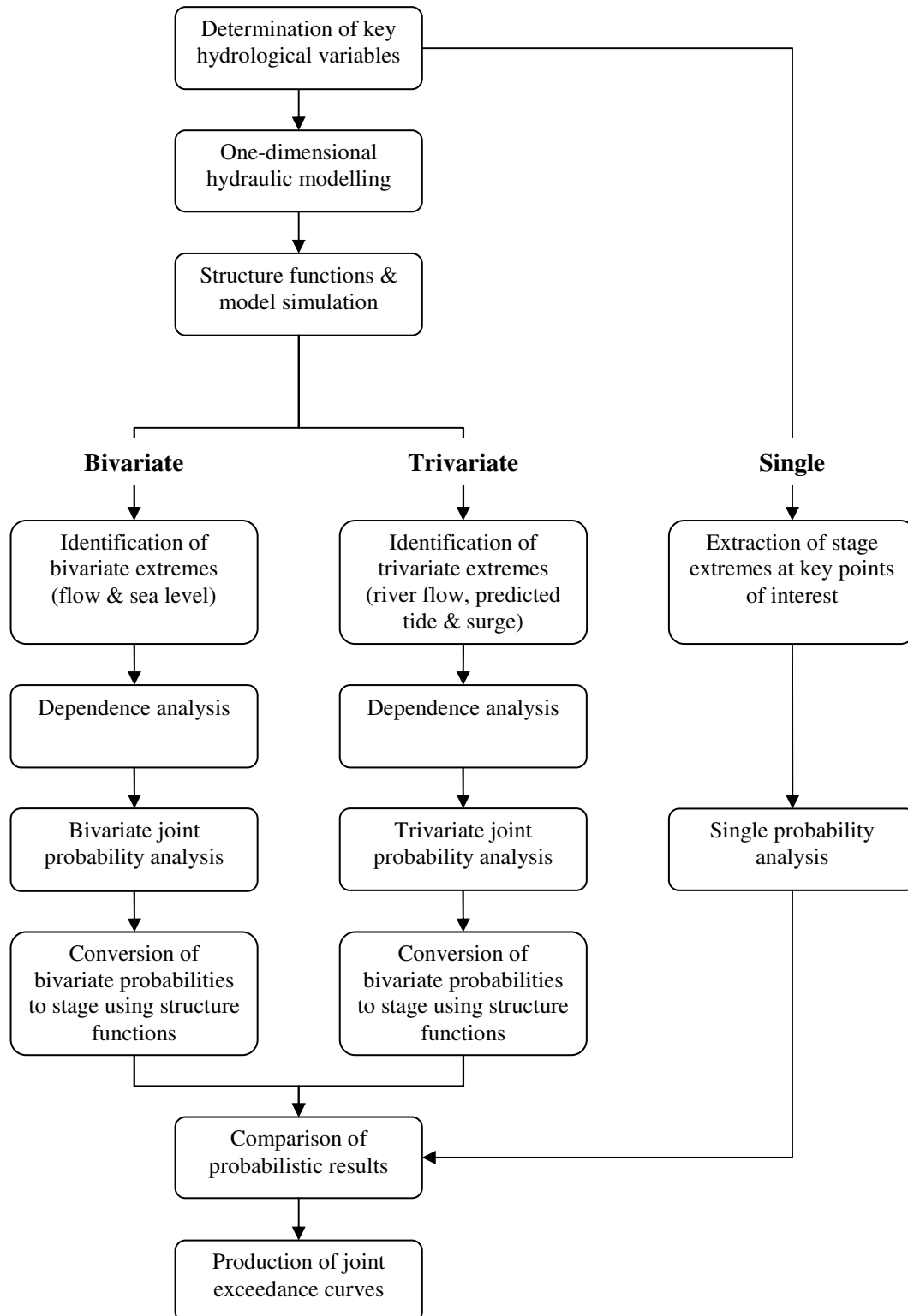


Figure 3.1 Methods flow diagram

3.2 Methods for Flood Frequency Analysis

3.2.1 Event Definition

Following the collation, checking and preliminary analysis of the collated datasets, extraction of extreme values and event definition was required. Independent extreme events were determined relative to each variable type. For sea levels, an independent event was defined as occurring at each successive tide. For river flow above the tidal reach, an event was determined as the duration of high flow period, typically around 48-hours, although many flow events extended over several days due to successive rainfall events maintaining high groundwater levels.

For the point of interest (Lewes), event definition was more complex due to the differing interactions of tide, surge and river flow during different events. An event analysis was undertaken to explore historical extreme high water levels at Lewes corresponding to simultaneous sea level and flow observations to establish the dependency on high tides and river flows.

3.2.2 Annual Maxima (AMAX) Series

Extreme values are produced rarely as their occurrence is unusual for the point of interest. Annual (water-year) maximas were extracted from the daily maxima series, from October 1st to September 31st, creating an annual maxima (AMAX) extreme value series for each variable. The process incorporated complete winter and summer seasons for each annual maxima value, allowing for seasonality effects to be identified.

Due to the variable nature of hydrologic data recording, the vast majority of water-years contained some period of null values. To assess whether any missing periods in each series may have included other high (and possibly the highest) annual value, each data series was cross-checked with neighbouring recorded series for the same period to see if high values were likely. Seasonality was also taken into account, with winter months most likely to contain the maxima values from each meteorologically driven series. The maxima value was extracted on a year-by-year basis, and the percentage of missing data from each annual maxima series was calculated and included with the maxima values to display their relative accuracy (Appendix A.1).

The annual maxima (AMAX) series at Barcombe Mills, Lewes Corporation Yard, Lewes Gas Works and Newhaven were identified as the four primary hydrological series for the

flood frequency analysis, due to their locations at the fluvial and tidal limits of the lower Ouse (Barcombe Mills and Newhaven), and at intermediate points of interest (Lewes Corporation Yard and Lewes Gas Works). Each AMAX series was extracted and extended (where possible) to provide a long series of AMAX observation at each location.

3.2.3 Peaks-Over-Threshold Series

Where an AMAX series only extracts the largest event from each calendar or water-year (possibly disguising the true historical pattern and rarity of events as any given year may contain more than one significant or extreme event), a peaks-over-threshold (POT) series uses a threshold exceedance approach to select peak values for each significant event in each series.

A POT approach was applied to each series which selected independent peak events that exceeded generic (i.e. percentile) threshold levels to each dataset. The process eliminated the non-extreme peaks (i.e. the everyday tidal peaks) and produced a series of the highest values uniformly across each dataset, independent from the calendar or water year.

Five POT series were calculated for each variable using threshold values selected as:

- 95th, 98th and 99th percentiles,
- an average of 5 POT exceedances per year based on the whole dataset, and
- selecting the lowest AMAX value as the threshold level.

The lowest AMAX value threshold level for each series was selected so as not to ignore observations from years when the peaks values were relatively low. This produced at least one peak value per water-year with many years containing numerous extreme values. To ensure the identification of independent POT events, exceedances were selected on the same day and within 3 day window (± 1 day from the day of the highest POT event) where only the peak value during this period was selected. Although it was not possible to take other factors into account, such as high groundwater levels from a previous POT event, the process enabled the POT series to represent extremal nature of flooding events as accurately as possible.

3.2.4 Distribution Selection & Return Period Estimation

Extreme value analysis is used to make inferences about the size and frequency of extreme events. The frequency of occurrence of the extreme hydrological observations was analysed using statistical probability distributions fitted to the annual maxima sequence of observation. The annual extreme hydrological observations are located in the extreme tail of the parent probability distribution. As such, a distribution which fits the complete duration series would not be suitable for the extreme values. A suitable distribution for extreme values is the Generalized Extreme Value (GEV) distribution, which merges the type I, II and III extreme value family of distribution (commonly known as Gumbel, Fréchet and Weibull) to allow for a continuous range. The extreme value distributions have been found to be ideal for describing annual series of extreme values from UK hydrological data (e.g. Chow *et al.*, 1988; Environment Agency, 2002) and were recommended for extreme distribution fitting in the Flood Estimation Handbook (Robson and Reed, 1999).

The GEV distribution has three parameters of location μ , scale α and shape k . The GEV probability distribution function for $-\infty \leq x \leq \infty$ is then given as:

$$F(x; \mu, \alpha, k) = \exp \left\{ - \left[1 + k \left(- \frac{x - \mu}{\alpha} \right) \right]^{-1/k} \right\} \quad (3.1)$$

When $k < 0$, the GEV distribution is equivalent to the type III (Weibull) extreme value distribution. Similarly, when $k > 0$, the GEV distribution is equivalent to the type II (Fréchet) extreme value distribution. As k approaches the limit of 0, the GEV becomes the type I (Gumbel) extreme value distribution.

An extreme value analysis was undertaken for each hydrological data series. The GEV distribution's suitability was mathematically checked by calculating the Goodness of Fit of each dataset using the Anderson Darling test and by estimating the coefficient of skew. The GEV distribution was fitted to each annual maxima extreme series using the Flood Estimation Handbook (Reed, 1999) software package WINFAP-FEH. The fitted probability distributions for each hydrological variable were extrapolated to extreme values to estimate the relative return periods beyond the duration of the series. Each of the distributions was extrapolated up to a maximum of the 1:200 year return period.

However, the majority of the data series extended to approximately 50 years, therefore return periods and estimated magnitudes were treated with caution above this level.

3.2.5 Statistical Correlation

Each hydrological POT series was cross-correlated with relevant corresponding POT series to provide an indication of the relationship and possible dependence (or independence) between each pair, and to establish the primary variables in the production of extreme water levels at the point of interest. Each hydrological pair of variables was statistically correlated to indicate the relationship between the series. P values were obtained using ANOVA multiple regression analysis. Significant results were taken where $P < 0.05$. Percentages of simultaneous and independent occurrences were also calculated to further assess the relationship. Time-lags of 1 and 2 days were also introduced to establish if correlation differed over longer time periods.

3.3 Methods for the Calculation of Dependence

3.3.1 Dependence Modelling

A model was produced which calculated dependence χ between the various pairs of hydrological variables in the Ouse catchment using daily maxima records X and Y based on equation 2.7 derived from Svensson and Jones (2000). The variables were independently observed but were paired through time (in this case one 24-hour water-day period). For example, the daily maxima X_1 was observed on the same water-day as the daily maxima Y_1 , X_2 was observed on the same water-day as Y_2 , and so forth. These pairs were retained throughout the dependence calculation such that the dependence calculation was calculated using pairs of X_1 and Y_1 , X_2 and $Y_2 \dots X_n$ and Y_n . As per Svensson and Jones (2000, 2002) the marginal distributions were assumed to be similar and were not transformed.

By using observed pairs taken at a daily resolution however, the dependence results may only be indicative of where extreme values occur simultaneously within any single temporal period (e.g. one water-day). The daily maxima values from each of the pairs of X and Y may therefore have occurred up to 24-hours apart. For quickly responding catchments such as the Ouse (Environment Agency, 2002), a 24-hour period may be too

long to ascertain whether the peaks of the two variables can actually occur simultaneously, which is important for the estimation of water levels in a joint probability analysis. Svensson and Jones (2003) however stated that if there was no dependence calculated from data at a daily resolution, dependence would not exist at a higher resolution, such as hourly observations. To explore this problem, the dependence model was extended to include the complete recorded 15-minute datasets of the two variables of interest, allowing a dependence value to be calculated from real-time simultaneously-recorded pairs of X and Y to compare to the dependence value χ calculated using daily maxima values. As with the daily maxima datasets, the pairs of 15-minute variables X_1 and Y_1 , X_2 and $Y_2 \dots X_n$ and Y_n were observed simultaneously and were kept intact as pairs throughout the dependence calculation.

It was understood that the topography and hydrodynamics of a tidal river system may affect the temporal relationship (and therefore dependence) between sea level and river flow. If both sea level and river flow peaks were to occur at the same point in time, the physical time-lag between both sites (in this case Newhaven and Barcombe) would mean the peaks would not arrive at the point of interest (in this case Lewes) at the same time. For example, it takes 55-minutes for the tidal peak to propagate upriver from Newhaven to Lewes, and approximately 1-hour for the peak of the river flow to travel downriver to Lewes from Barcombe. Therefore, observed river flow and sea level records could not be utilised at the same time at both boundary sites when using the real-time (e.g. 15-minute) datasets.

A time-lag algorithm was therefore incorporated into the dependence model, which inserted a lag between the river flow and sea level observations, rather than to rely on a fixed time period to calculate a dependence value. The process initially selected the daily maxima values from the first dataset, including the actual time they occurred. The model then automatically selected the corresponding value from the second dataset recorded at the same time. For example, for a variable pair of sea level X and river flow Y , if a tide were to peak at 07:15 on any given day (e.g. X_1), the model selected the corresponding flow value (e.g. Y_1) which was also recorded at 07:15 and calculated a value of dependence. The process was then repeated with negative and positive time-lags (in ± 15 -minutes increments) introduced to recreate the hydrodynamic lag between the two variables. A dependence value was then calculated for each lag increment, up to ± 1 -day.

3.3.2 Threshold Selection

The dependence measure χ can be estimated from any threshold level. The selection of x^* and y^* for this analysis was determined by two requirements: firstly to have enough data points above the threshold to be able to determine dependence, and secondly for the threshold to be high enough to regard the values as extreme (Svensson and Jones, 2002). For example, setting the threshold value above the maximum value in the series would produce a zero dependence value, where as setting the threshold to select only the extreme values would provide enough points to successfully calculate a value of dependence. The threshold values were also selected for each variable independently from each other.

To calculate a value of dependence, the selection of threshold values was determined using a POT approach, which selected extreme values for each dataset independently based on a series of percentile threshold levels (i.e. 95%, 98% etc). The independence criterion was that any two POTs must not occur on consecutive days, but be separated by at least one day (e.g. Svensson and Jones, 2000). The process eliminated the non-extreme peaks (i.e. the everyday maximum values), and produced sets of the most extreme peaks.

3.3.3 Significance Testing

Significance testing of the χ values was carried out using a permutation method (e.g. described by Svensson and Jones, 2003), which used generated datasets to test for where independence would hold (i.e. a hypothesis of null dependence). The process estimated values of χ corresponding to the 5% significance level.

Permutation is a random generation method, which tests for results which were above the 5% limit. If true (i.e. above the 5% limit), then the value is significant and the dependence value is null. However, if the results were below the 5% limit, then they could be labelled as insignificant and therefore the dependence value accepted. In other words, if the calculated χ value from the original dataset was significantly different to the calculated χ from the generated values, then it may be concluded that the original records are not independent, and that the dependence value would therefore be correct.

The method selected the complete daily maxima data series for the two variables. Each series was then divided into complete years blocks (using the water-year September to August), meaning that the daily maxima data within each year block was not altered so as

to preserve the seasonality. Each year block was labelled $1, 2, \dots, n$, in order of occurrence (i.e. $1 = 1982$, $2 = 1983$, etc) for each variable. The first series was kept unchanged and in sequence, whilst the second record was permuted by randomly shuffling the complete year blocks (i.e. $4, 7, \dots, n$). This created a random resample of observations from two records, so that each set equalled the same number of years as the original dataset, allowing for a new χ value to be calculated. For each resample, the full dataset was used, but each water-year block was used only once.

The permutation test was repeated 199 times, each time keeping the first dataset in sequence and reshuffling the second dataset. A new χ value was calculated for each resample. The 199 calculated values of χ were ranked in descending order, and the 10th largest value taken as corresponding to the 5% significance level. The original χ value was then compared to the resampled χ ; if it was found to be above the resampled χ , then the dependence between the variables could be considered genuine and the original χ value accepted.

3.3.4 Confidence Intervals

Confidence intervals may be calculated to provide an indication of the range where the true dependence value would be expected to lie. The process used a resampling method called bootstrapping, which was based on the generation of new datasets. Unlike the test for significance, the estimation of the confidence intervals looked for dependence rather than independence by generating data with the same level of dependence found between the original data series.

As with the significance test, to calculate the confidence intervals, both daily maxima series were kept intact within year-long blocks throughout the recalculation of χ . The year blocks (containing simultaneously recorded observations of both datasets) were then chosen randomly with replacement, meaning that each year block could be used infinitely within each recalculation of χ . The generated resample dataset was kept to the same size as the original dataset and a new value of χ calculated.

The process was then repeated 199 times, each time resampling the year blocks of the variables at random, generating a large number of χ values. Each simulation produced either a higher or lower dependence value than the original one as some years contained

higher levels of dependence than others, and others less. For example, for a given year which produced a high level of dependence and was randomly selected (i.e. 3 times) within a resampled dataset, it would be expected that the resultant χ value would be high. Similarly, a randomly resampled dataset which only contained years which displayed low levels of dependence, would produce a low value resampled value of χ .

The 199 calculated values of χ were then ranked in descending order, and the 10th and 190th largest value taken as representing the 95% and 5% confidence intervals respectively. The confidence intervals are displayed besides the calculated values of χ for each variable pairing.

3.4 Extreme Joint Return Period Methods

3.4.1 Extreme Bivariate Approach

The extreme bivariate approach used the return periods for Barcombe Mills flow (X) and Newhaven sea level (Y) (containing both the predicted tide and observed surge components) as primary variables for the estimation of the joint return periods and resultant water levels at Lewes. The return periods for sea level and flow however were not always identical. Hawkes (2004) suggested that the return periods were not required to be identical, thus it was hypothesised that equation 2.15 taken from Svensson and Jones (2000) could be transformed to calculate the joint return period $T_{X,Y}$ of non-identical return periods (T_x, T_y) for variables (X, Y) as the threshold u corresponded to the non-identical threshold levels (x^*, y^*) for the two observed series (X, Y) . Therefore, the return period T_x of the exceedance of threshold x^* for the variable X could then be expressed as $P(U > u) = P(X > x^*) = 1/T_x$, and the return period T_y of the exceedance of threshold y^* for the variable Y may be expressed as $P(V > u) = P(Y > y^*) = 1/T_y$, thus:

$$T_{X,Y} = \frac{1}{\left(1 - \frac{1}{\sqrt{T_x \cdot T_y}}\right)^{2-\chi} + \left(\frac{2}{\sqrt{T_x \cdot T_y}}\right) - 1} \quad (3.2)$$

Although some limitations have been identified to this method (see section 2.3), such as the assumption that the marginal distributions do not require transformation and are therefore assumed to be identical (or nearly identical), the process provided a reliable method for the estimation of joint return periods from variables with non-identical return periods.

To calculate return periods for the extreme joint exceedance of the primary bivariate variables of Barcombe Mills flow (X) and Newhaven sea level (Y), a probability table was constructed with the bivariate return periods (T_x, T_y) of 2, 5, 10, 25, 50, 100 & 200 years on opposing axes. Using equation 3.2, joint return periods $T_{x,y}$ were calculated for each pair for the exceedance of some assumed threshold u with dependence measure χ . The results were tabulated to form a grid containing every combination of the return periods. From the joint probability table, the effect of different levels of dependence χ on the calculation of bivariate joint return periods (e.g. of river flow and sea level) was assessed using levels of dependence ranging from 0 to 1 in 0.1 increments. The calculations showed a substantial difference between the results for return periods calculated for joint exceedances where the variables are assumed to be fully-independent (i.e. $\chi = 0$) and return periods calculated for variables where partial-dependence exists, even for dependence values as low as 0.1.

The probability table was expanded using logarithmic interpolations to incorporate each increment of sea level and flow. The calculated dependence value of χ between the bivariate variables of Barcombe Mills flow and Newhaven sea level was used to calculate the joint return periods for all combinations of the return periods, producing 63,300 possible joint return periods. The process was also repeated where full independence ($\chi = 0$) was assumed between the sea level and flow variables. An example of a partially-dependent matrix is shown in Table 3.1, displaying the results of the joint return periods $T_{x,y}$ for the return periods of 2, 5, 10, 25, 50, 100 & 200 years.

The joint return periods $T_{x,y}$ of the variables (X, Y) , representing Barcombe Mills flow and Newhaven sea level, do not however indicate the return periods of the resultant water levels at intermediate locations in the estuary (in this case Lewes Corporation Yard and Lewes Gas Works). Different combinations of flow and sea level produce varying water levels at these locations but which may have the same joint return period. For example,

using the joint probability tables for the return periods at Barcombe Mills and Newhaven defines a joint return period $T_{x,y}$ for a 1:1 year flow event at Barcombe Mills and a 1:28 year sea level at Newhaven as 1:25 years. Using the estimated marginal distributions, the 1:1 year flow event at Barcombe Mills and 1:28 year sea level at Newhaven equated to a $50\text{m}^3/\text{s}$ flow and a 4.27mAOD sea level. From the structure function matrix generated at Lewes Corporation Yard, a $50\text{m}^3/\text{s}$ flow and a 4.27mAOD sea level produced a resultant water level of 4.21mOD. A second event for the same variables, using the same required joint return period of $T_{x,y} = 1:25$ years, may conversely be formed by a 1:28 year flow event at Barcombe Mills and a 1:1 year sea level at Newhaven. However, these return periods equate to a $180\text{m}^3/\text{s}$ flow and a 4.04mAOD sea level event which, when converted to resultant water levels at Lewes Corporation Yard using the structure function matrix, produced a water level of 4.50mOD, 0.29m above the previous event with the same joint return period of 1:25 years.

Table 3.1 Joint return periods $T_{x,y}$ (shaded area) for partially-dependent ($\chi = 0.045$) variables X (Barcombe Mills flow, m^3/s) and Y (Newhaven sea level, mOD) with return periods T_x and T_y . Corresponding sea level and flow magnitudes are shown in italics.

Variable X (Barcombe Mills Flow) Return Periods T_x (years) & Flow Magnitudes (m^3/s)		Variable Y (Newhaven Sea level) Return Periods T_y (years) & Sea Levels (mAOD)							
		1	2	5	10	25	50	100	200
		<i>3.86</i>	<i>3.97</i>	<i>4.12</i>	<i>4.20</i>	<i>4.27</i>	<i>4.32</i>	<i>4.35</i>	<i>4.38</i>
1	<i>50.00</i>	1.00	1.98	4.80	9.25	21.52	39.88	72.20	127.31
2	<i>81.68</i>	1.98	3.88	9.25	17.57	39.88	72.20	127.31	218.08
5	<i>116.02</i>	4.80	9.25	21.52	39.88	86.93	151.89	257.68	424.27
10	<i>140.86</i>	9.25	17.57	39.88	72.20	151.89	257.68	424.27	678.82
25	<i>174.86</i>	21.52	39.88	86.93	151.89	303.53	495.07	785.23	1214.86
50	<i>202.13</i>	39.88	72.20	151.89	257.68	495.07	785.23	1214.86	1840.38
100	<i>231.04</i>	72.20	127.31	257.68	424.27	785.23	1214.86	1840.38	2740.64
200	<i>261.80</i>	127.31	218.08	424.27	678.82	1214.86	1840.38	2740.64	4026.74

To overcome this problem, the probability table was used in conjunction with structure function matrices to convert each joint return period to resultant stage at the two locations of Lewes Corporation Yard and Lewes Gas Works. The extreme marginal distributions which estimated the 2, 5, 10, 25, 50, 100 & 200 year return periods were then used to estimate the flow and sea level return periods for each magnitude increment

of the structure function matrices (peak river flow 1m³/s to 300m³/s, in increments of 1m³/s; sea level 0.60m AOD to 4.8mOD, in increments of 0.2mOD). Table 3.2 shows an example of a structure function matrix at Lewes Corporation Yard which demonstrates the linking of the structure function matrices with the joint probability table.

Table 3.2 Structure function matrix for resultant water levels at Lewes Corporation Yard (mAOD) (shaded area) from combinations of variables *X* (Barcombe Mills flow, m³/s) and *Y* (Newhaven sea level, mOD). Return periods *T_x* and *T_y* corresponding to sea level / flow magnitudes are shown in italics.

Variable <i>X</i> (Barcombe Mills Flow) Return Periods <i>T_x</i> (years) & Flow Magnitudes (m ³ /s)		Variable <i>Y</i> (Newhaven Sea level) Return Periods <i>T_y</i> (years) & Sea Levels (mAOD)							
		<i>1</i>	<i>2</i>	<i>5</i>	<i>10</i>	<i>25</i>	<i>50</i>	<i>100</i>	<i>200</i>
		3.86	3.97	4.12	4.20	4.27	4.32	4.35	4.38
<i>1</i>	50.00	3.89	3.97	4.09	4.15	4.19	4.24	4.25	4.28
<i>2</i>	81.68	4.00	4.08	4.20	4.27	4.31	4.36	4.38	4.41
<i>5</i>	116.02	4.09	4.17	4.30	4.37	4.42	4.47	4.48	4.52
<i>10</i>	140.86	4.21	4.28	4.41	4.47	4.52	4.56	4.57	4.60
<i>25</i>	174.86	4.46	4.52	4.61	4.66	4.70	4.73	4.75	4.77
<i>50</i>	202.13	4.74	4.78	4.85	4.88	4.91	4.93	4.94	4.96
<i>100</i>	231.04	5.03	5.05	5.10	5.13	5.15	5.17	5.18	5.19
<i>200</i>	261.80	5.36	5.38	5.42	5.43	5.45	5.47	5.48	5.49

A two-stage ‘look-up’ algorithm was created which firstly selected pairs of flow and sea level which satisfied a desired joint return period from the probability table, followed by the selection of the corresponding resultant stage from the structure function matrix for that pair. The results were tabulated and the highest stage generated at the response location (Lewes Corporation Yard or Lewes Gas Works) was then assumed to represent the maximum (i.e. the worst case) joint return period for the pair. Table 3.3 shows an example of the 1:2 year joint return period for combinations of the pairs of Barcombe Mills flow and Newhaven sea level with resultant stage at Lewes Corporation Yard. The highest stage at Lewes (in this instance 4.01mOD, shown in the greyed out areas) was produced by three different pairs of flow / sea level magnitudes which may be selected to represent the 1:2 year return period at Lewes Corporation Yard. The process was repeated for the 2, 5, 10, 25, 50, 100 & 200 year return periods at both Lewes Corporation Yard and Lewes Gas Works.

Table 3.3 Stage at Lewes Corporation Yard for combined Barcombe Mills flow and Newhaven sea level events equating to the 1:2 year ($T_{X,Y} = 2$) joint return periods. Highest stage at Lewes Corporation Yard (shaded area) selected as the maximum 1:2 year combined flow / sea level event.

Barc. Mills Flow (m ³ /s)	Newh'n Sea level (mAOD)	Lewes Corp. Yard Stage (mAOD)	Barc. Mills Flow (m ³ /s)	Newh'n Sea level (mAOD)	Lewes Corp. Yard. Stage (mAOD)	Barc. Mills Flow (m ³ /s)	Newh'n Sea level (mAOD)	Lewes Corp. Yard. Stage (mAOD)
50	3.96	3.97	61	3.94	4.00	72	3.90	4.00
51	3.96	3.97	62	3.94	4.01	73	3.90	4.00
52	3.96	3.98	63	3.92	3.99	74	3.90	4.01
53	3.96	3.98	64	3.92	4.00	75	3.88	3.99
54	3.96	3.99	65	3.92	4.00	76	3.88	4.00
55	3.94	3.98	66	3.92	4.00	77	3.88	4.00
56	3.94	3.98	67	3.92	4.00	78	3.88	4.00
57	3.94	3.99	68	3.92	4.01	79	3.86	3.99
58	3.94	3.99	69	3.90	3.99	80	3.86	3.99
59	3.94	4.00	70	3.90	4.00	81	3.86	3.99
60	3.94	4.00	71	3.90	4.00	82	3.86	4.00

To assess the relative accuracy of the fully-independent and partially-dependent bivariate joint return period magnitudes, the return period magnitudes assessed from the observed series at Lewes Corporation Yard and Lewes Gas Works were used to validate the joint return periods outputs.

3.4.2 Extreme Trivariate Approach

Whereas the extreme bivariate approach used observed sea level as a primary variable containing both the predicted tide and observed surge components, it was hypothesised that the interaction of river flow and surge may produce the most extreme water levels due to both being driven by meteorological events. This process was however confused by the need to incorporate the harmonics of the astronomical tide in the estimation of resultant water levels. Therefore, to assess the relative importance of surge (observed sea level minus predicted astronomical tide) on resultant water levels at Lewes, the bivariate approach was extended to form a trivariate joint probability approach which separated the three primary variables of river flow, predicted tide and surge to explore their relationships and influence on resultant water levels further.

The joint return period of the two partially dependent variables of river flow and surge was estimated using equation 3.2 derived from Svensson and Jones (2000) with an calculated level of dependence χ . This provided the joint return period of the two partially-dependent meteorologically-driven variables which could then be represented

by one single return period. The approach could then be extended to a double bivariate (or trivariate) return period by incorporating a third variable of predicted tide. It was hypothesised that predicted tide was statistically independent from both river flow and surge, therefore the joint return period of all three occurring could then be calculated using a repeat of the initial bivariate joint return period calculation, utilising the joint return period for river flow and surge as X and predicted tide as Y.

Two probability tables were constructed to calculate the joint return periods for Barcombe Mills flow, Newhaven predicted tide and Newhaven surge. The first produced a grid of joint return periods for the partially-dependent flow and surge variables using the estimated dependence value of χ . The second table produced a similar grid of joint return periods for the third variable of fully-independent predicted tide. The use of the partial dependence which exists between flow and surge in the first probability table enabled the second probability table to be developed based on the assumption that river flow and surge were both fully-independent from the predicted astronomically-driven tide, meaning that two rather than three probability tables could be used to calculate the trivariate joint return periods, as the variable pairings of river flow and predicted tide, and surge and predicted tide could be grouped together. The multiplication of any two joint exceedance values from each probability table (i.e. a partially-dependent flow and surge event from the first probability table with an independent predicted tide from the second) would produce a trivariate joint return period.

Unlike the extreme bivariate approach which used a two-stage 'look-up' algorithm to select pairs of river flow and sea level with corresponding resultant stage at Lewes for a given joint return period, the trivariate approach further developed the method to incorporate the complexities of the three hydrological variables at two locations. As two of the variables of predicted astronomical tide and surge were at the same location of Newhaven, it was assumed that the magnitudes were additive, and could be used to produce total sea levels. However, this meant that any single sea level at Newhaven could potentially be made up of hundreds of possible combinations of predicted astronomical tide and surge, any of which could coincide with any flow magnitude at Barcombe Mills. The algorithm was therefore extended to select a pair of river flow and surge from the first probability table together with a third variable of predicted tide from the second table which collectively satisfied a desired joint return period when multiplied together. The corresponding river flow and sea level (predicted tide plus surge)

magnitudes were then used to select the resultant stage from the structure function matrices for that pair. Due to their size, simplified extreme trivariate probability tables are shown in Appendix G.5 and structure function matrices for the estimation of resultant stage at Lewes Corporation Yard and Lewes Gas Works are shown in Appendix G.6.

As before, the results were then tabulated with the highest (worst case) stage generated at the response locations assumed to represent the joint return period for the trivariate grouping. The process was repeated to represent the 2, 5, 10, 25, 50, 100 & 200 year return periods at both the Lewes Corporation Yard and Lewes Gas Works locations.

3.5 Daily POT Joint Probability Methods

3.5.1 Daily POT Bivariate Approach

The previous section showed a bivariate joint probability method which calculated joint return periods for the most extreme combinations of Barcombe Mills flow and Newhaven sea level using return periods estimated from the annual maxima distributions. To test the accuracy of the approach and to further define the full range of interaction of river flow and sea level in the lower River Ouse, the method was developed to calculate daily maxima POT joint probabilities for the primary bivariate variables of Barcombe Mills flow (X) and Newhaven sea level (Y) using the complete observed daily maxima series.

Therefore, to calculate the joint probability of exceedance of the threshold u by variables (U, V) with similar marginal distributions and identical probabilities and dependence χ , equation 2.14 was rewritten and applied directly, thus:

$$\begin{aligned}
 P(U > u, V > u) &= 1 - 2P(U \leq u) + P(U \leq u, V \leq u) \\
 &= 1 - 2[1 - P(U > u)] + [1 - P(U > u)]^{2-\chi} \\
 &= [1 - P(U > u)]^{2-\chi} + 2[P(U > u)] - 1
 \end{aligned} \tag{3.3}$$

As with the bivariate extreme joint return period approach, the probabilities were not always identical as the threshold u corresponded to the non-identical threshold levels (x^*, y^*) for the two observed series (X, Y) . Therefore, the probability of exceedance of threshold x^* for the variable X may be expressed as $P(U > u) = P(X > x^*)$ and the

probability of exceedance of threshold y^* for the variable Y expressed as $P(V > u) = P(Y > y^*)$.

It was then assumed that the probabilities were not required to be identical (e.g. Hawkes, 2004) for the calculation of the joint probability. For example, a joint probability of 0.5 (i.e. 50%) could be produced by different combinations of probabilities, such as 0.5 & 1.0; 0.707 & 0.707; 1.0 & 0.5 etc. Therefore, equation 3.3 could be transformed to calculate the joint probability $P(U > u, V > u)$ of non-identical probabilities for variables (X, Y) with thresholds (x^*, y^*) and dependence measure χ , thus:

$$P(U > u, V > u) = \left[1 - \sqrt{P(X > x^*) \cdot P(Y > y^*)} \right]^{2-\chi} + 2 \left[\sqrt{P(X > x^*) \cdot P(Y > y^*)} \right] - 1 \quad (3.4)$$

Unlike the bivariate extreme joint return period approach, probabilities were instead calculated for the daily exceedance of predetermined threshold levels (x^*, y^*) . For the variable of Barcombe Mills flow, the threshold levels (x^*) were set in increments of $1\text{m}^3/\text{s}$, ranging from $1\text{m}^3/\text{s}$ to $300\text{m}^3/\text{s}$ to represent the minimum and maximum flow magnitudes from the synthesised series (1981-2006). Similarly, for the second variable of Newhaven sea level, the threshold levels (y^*) were set in increments of 0.02m , ranging from 1.1mAOD to 4.4mAOD to represent the minimum and maximum recorded sea level magnitudes from the observed series (1982-2006). Daily exceedance probabilities were then calculated by counting the number of observations that exceeded each threshold, divided by the total number of observations in the series. The output was a probability curve of exceedance between 0 and 1 for the complete observed tidal range at Newhaven and flow range at Barcombe Mills. Figure 3.2 shows an example probability curve for the daily probability of exceedance of the threshold levels at Newhaven. Appendix G.1 contains the daily joint probability curves.

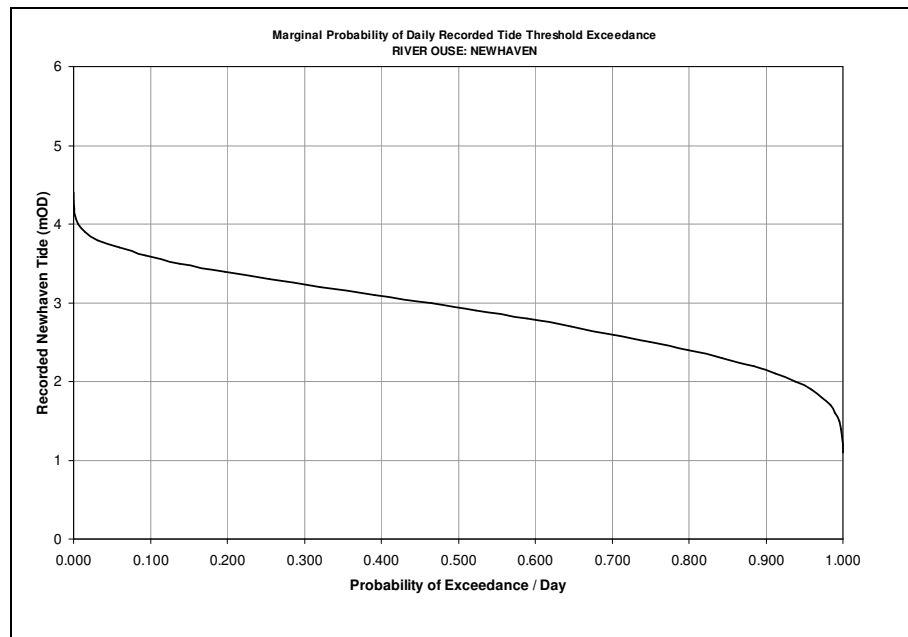


Figure 3.2 Daily probability of recorded sea level threshold exceedance at Newhaven (1982-2006)

A probability table was constructed with the bivariate daily probabilities for Barcombe Mills flow and Newhaven sea level on opposing axes, incorporating each increment of sea level and flow. Using equation 3.4, daily joint probabilities were calculated for each pair with the calculated dependence measure of χ forming a grid containing every combination of the probabilities. The process was also repeated where full independence ($\chi = 0$) was assumed between the sea level and flow variables. A simplified version of the probability matrix is shown in Appendix G.4 for selected magnitudes.

The ‘look-up’ algorithm developed for the bivariate joint return period approach was amended to firstly select pairs of flow and sea level which satisfied a desired daily joint probability from the probability table, then to select the corresponding resultant stage from the structure function matrix (Appendix G.6) for that pair. The results were tabulated and the highest stage generated by any pair at the response location (Lewes Corporation Yard or Lewes Gas Works) was then assumed to represent the true joint probability.

To assess the accuracy of the fully-independent and partially-dependent bivariate daily joint probability approaches, daily probabilities were calculated using the daily maxima simulated stage magnitudes at the intermediate locations of interest at Lewes Corporation Yard and Lewes Gas Works. For both Lewes locations, the threshold levels were set in

increments of 0.02mOD, ranging from 1.0mAOD to 5.0mOD* to represent the minimum and maximum observed stage magnitudes from the continuously simulated series (1982-2006). The daily exceedance probability curves were used as a comparison with the daily joint probabilities calculated for Barcombe Mills flow and Newhaven sea level.

3.5.2 Daily POT Trivariate Approach

As with section 3.4, the daily bivariate joint probability approach was extended to separate the third primary variable of surge at Newhaven from observed sea level. This enabled the exploration of the relationship between river flow and surge and their combined effects on the joint probability calculations and resultant water levels at Lewes when combined with predicted tide. Daily exceedance probabilities were calculated for Newhaven surge and predicted tide, with the threshold levels set in increments of 0.02m, ranging from -0.3m to 1.3m for surge and 1.0mAOD to 4.0mAOD for predicted tide, to represent the minimum and maximum recorded magnitudes from the observed series (1982-2006).

The daily trivariate joint exceedance approach extended the two probability tables required to calculate the joint probabilities for Barcombe Mills flow, Newhaven predicted tide and Newhaven surge using equation 3.4. Similar to before, the first table produced a grid of joint probabilities for the partially-dependent flow and surge variables using an estimated dependence value χ , and the second table produced a grid of joint probabilities for the fully-independent predicted tide. The 'look-up' algorithm was then extended to select a pair of values of river flow and surge from the first probability table, which then selected a value of predicted tide from the second table which collectively satisfied a desired joint probability when multiplied together. The corresponding river flow and sea level magnitudes (predicted tide plus surge) were then used to select the resultant stage from the structure function matrices. Again, due to their size, simplified daily trivariate probability tables are shown in Appendix G.5, and structure function matrices for the estimation of resultant stage at Lewes Corporation Yard and Lewes Gas Works are shown in Appendix G.6. The performance of the daily trivariate approach was tested against the daily maxima simulated stage magnitudes at the intermediate locations of interest at Lewes Corporation Yard and Lewes Gas Works.

* Maximum simulated stage at Lewes Corporation Yard was 5.74mAOD which was almost 1.5m above the second highest value of 4.28mOD, therefore daily exceedance probabilities were identical above 4.28mAOD as only one observation exceeded this threshold. The maximum threshold was capped at 5.0mAOD to match the threshold selection at Lewes Gas Works.

The daily trivariate results were tabulated with the highest (worst case) stage generated at the response locations assumed to represent the daily joint probability for the trivariate grouping, which was repeated to for each stage increment at Lewes Corporation Yard and Lewes Gas Works.

4 PRELIMINARY ANALYSIS

4.1 Introduction

The objective of this chapter is to define an estuarine case study area which will be used for the duration of this research. The primary hydrological variables which produce extreme water levels within the case study area are identified through the sourcing, collation, checking and analysis of historically recorded hydrological datasets.

4.2 Selection of the Case Study Area

On the 12th October 2000, many parts of the UK suffered severe flooding. Lewes in East Sussex was one of the worst affected. It was selected as the research case study area to explore the interaction between sea levels and river flows in an established flood risk zone. Although the event was primarily fluvial, the joint probability of sea level and river flow on the magnitude of water levels in tidal rivers is poorly defined. The location of sea level and river flow gauges around Lewes also made it potentially ideal for a joint probability study, with sea levels recorded at Newhaven, river flow at Barcombe Mills (above the tidal reach) and three intermediate stage gauges at Lewes Corporation Yard, Lewes Gas Works and Southease Bridge, recording the varying interaction of river stage and sea level.

Lewes was also selected as a case study area for the Adaptation Strategies for Climate Change in the Urban Environment (ASCCUE) project as part of the (EPSRC/UKCIP) Building Knowledge for a Changing Climate (BKCC) programme, which worked closely alongside many aspects of this research. Lewes formed a direct comparison to a large urban conurbation in the northern half of the country (selected as Manchester) to represent an extreme scenario of flooding and the future effects of climate change.

Through the ASCCUE project, the Environment Agency (EA) and the local authority of Lewes District Council (LDC) both recommended Lewes as a case study area due to the relevance of the recent flood. The EA was involved in design and implementation of flood alleviation works for Lewes during the period of this research.

4.3 The Ouse Catchment, East Sussex

4.3.1 Overview

The River Ouse catchment drains an area of 668km², the second largest in Sussex, reaching 40km inland from the English Channel with the main river course having a total length of 56km. The catchment is predominantly rural but contains several conurbations including the towns of Haywards Heath, Uckfield, Lewes and Newhaven, as well as numerous small villages (Figure 4.1).

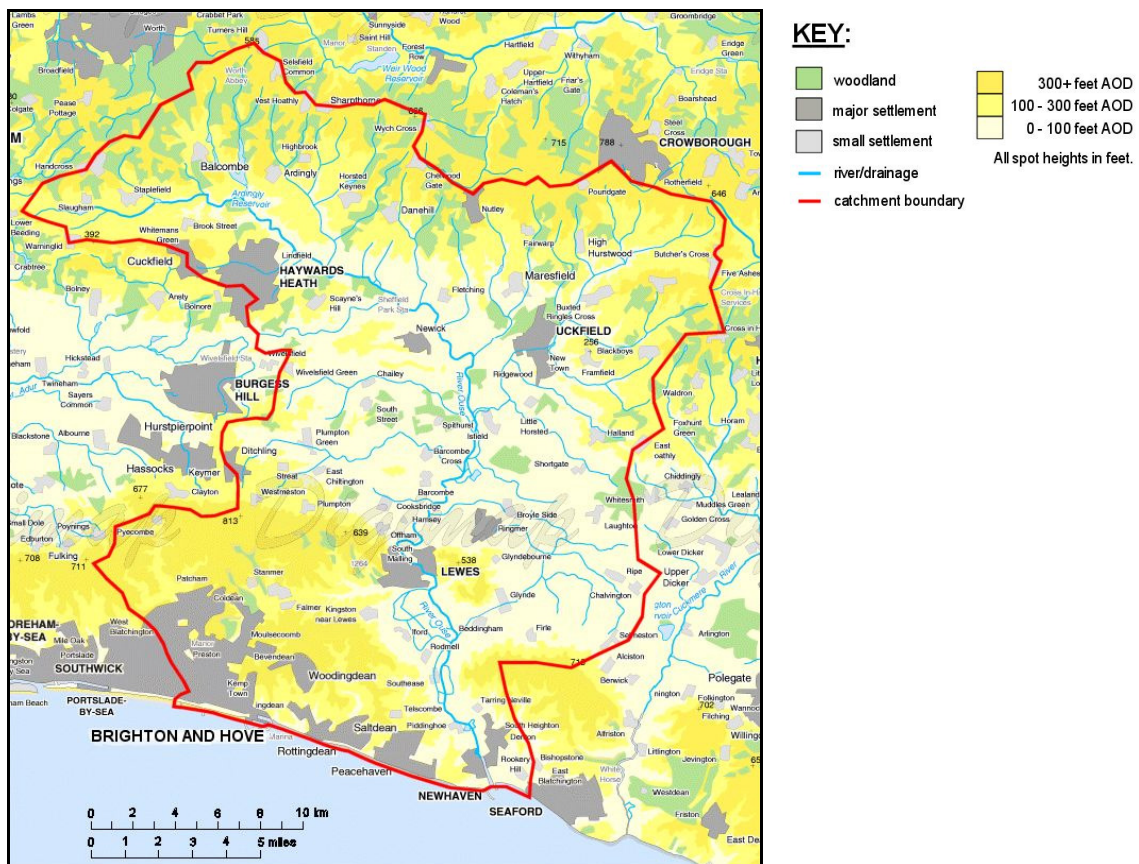


Figure 4.1 River Ouse catchment topography

Map based on Digimap supplied data, © Crown Copyright Ordnance Survey. An EDINA Digimap / JISC supplied service under licence.

The catchment is divided into four distinct sub-catchments of the Upper Ouse, Uck, Middle Ouse and Lower Ouse (Table 4.1). The River Ouse's source is in the High Wealden hills and flows down into the Low Weald flats through the chalk ridge of the South Downs before reaching the sea at Newhaven. The Lower Ouse stretch is within the tidal reach where water levels are governed by the interaction between fluvial flow from the upper catchment and sea level from Newhaven.

Table 4.1 Ouse sub-catchments

Sub-catchment	Area (km ²)	River Section Length (km)	Notes
Upper Ouse	234	29	Slaugham to Sutton Hall Weir
Uck	87	16	Huggats Furnace to Isfield Weir
Middle Ouse	79	5	Isfield Weir to Barcombe Mills
Lower Ouse	267	22	Barcombe Mills to Newhaven (inc. Winterbourne Stream)
Total	668	56	(River Ouse only)

Source: Environment Agency (2001, 2004)

4.3.2 Sub-Catchment Divisions

4.3.2.1 Upper Ouse Sub-Catchment

The predominantly rural Upper Ouse sub-catchment covers an area of 234km² and includes the town of Haywards Heath (Figure 4.2). The River Ouse falls from an elevation of 70m Above Ordnance Datum (AOD) at its source at Slaugham millpond to approximately 9mAOD just north of the confluence with the River Uck near Isfield. With a channel length of 29km, this produces an average gradient of 0.21%, or 1:475.

A series of small tributary streams drain into the main Ouse channel within the sub-catchment, including the Cockheise Stream, Haywards Drain, Pellingford Brook and Barts Bridge Stream.

The topography varies from gently undulating hills of Mid-Sussex's High Weald in the north to the flatter and lower Low Weald further south (Figure 4.1). The land coverage consists of woodland, arable and grazing land. The sub-catchment also includes Ardingly Reservoir, a major source of drinking water abstraction for the Mid-Sussex area. The outflow from the reservoir is controlled and regulates the low baseflow in the River Ouse. The High Weald has elevations ranging from 50m to 230mOD, and comprises of semi-permeable strata (Ashdown Beds and Wadhurst Clays), overlain by silty, loamy and clayey topsoils which become easily waterlogged during wet periods.

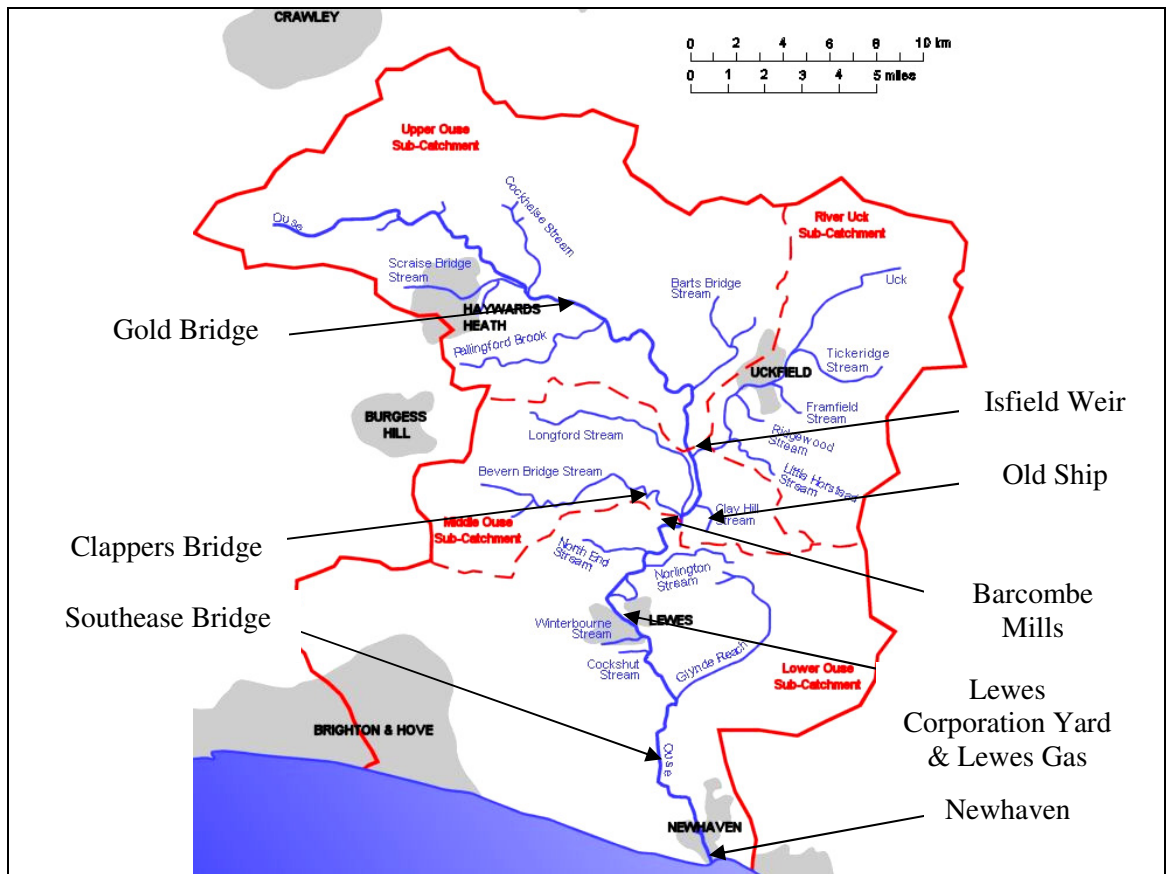


Figure 4.2 River Ouse catchment and sub-catchment divisions

Map based on Digimap supplied data, © Crown Copyright Ordnance Survey. An EDINA Digimap / JISC supplied service under licence.

The Low Weald, in the central and southern parts of the sub-catchment, is flatter and lower with elevations from 10m to 50mOD. The geology consists of permeable Tunbridge Sands and Greensands, with the most southerly part underlain by impermeable Gault and Weald Clays with clayey topsoils. As a consequence, this area is prone to waterlogging.

The relatively steep gradient combined with the mixture of semi-permeable and impermeable soils, means that the sub-catchment is characterised by rapid runoff.

4.3.2.2 Uck Sub-Catchment

The Middle Ouse sub-catchment covers an area of 104km². The River Uck, a main tributary to the Ouse, has its source at Huggats Furnace at a height of 50mAOD in the High Weald, and flows a distance of 16km through the town of Uckfield to Isfield Weir where it confluences with the River Ouse at an elevation of 11mAOD (Figure 4.2). This produces an average gradient of 0.24%, or 1:410, the steepest in the Ouse Catchment.

The majority of the sub-catchment is in the High Wealden hills, which has elevations up to 240mAOD (Figure 4.1). Unlike the wider Upper Ouse sub-catchment, the Uck valley is narrow with steep terrain and has several tributary streams and natural springs which cause a high natural base flow. The topography forms an almost circular-like catchment above the town of Uckfield, with the town centre situated at a particularly narrow point on the valley floor. The topography and stream network means that the peaks of high flows caused by the same rainfall event are likely to arrive in Uckfield around the same time.

The underlying geological properties of the Uck sub-catchment are similar to that of the Upper Ouse, with semi-permeable layers in the north and almost impermeable layers in the south. The valley floor is often in a semi-waterlogged state during winter months. The sub-catchment is also predominantly rural with the only significant settlement being the town of Uckfield. The remainder of the land is either woodland, or used as arable and grazing farmland. The narrowness of the valley floor limits any defined floodplain.

The steep circular terrain, relatively impermeable soil, high base flow, narrow valley floor and location of Uckfield means the town is susceptible to flooding from this flashy sub-catchment.

4.3.2.3 Middle Ouse Sub-Catchment

The Middle Ouse sub-catchment contains a short 5km section of the main River Ouse main channel but covers an area of 79km², categorising it as short but wide (up to 18km at its widest point). The channel of the River Ouse, from Hall Weir near Isfield (11mOD) to Barcombe Mills (7.5mOD), falls by 3.5m, producing a gradient of 0.07 %, or 1:1429, markedly shallower than the Upper Ouse and Uck sub-catchments (Figure 4.2).

The sub-catchment is within the impermeable section of the Low Weald, with clayey topsoils underlain by Weald Clay. In contrast to the Upper Ouse and Uck sub-catchments, the Middle Ouse catchment is low lying and flat, so runoff generated in the sub-catchment is slower than the Upper Ouse and Uck sub-catchments due to the small gradients. It is also the most rural sub-catchment of those within the Ouse Catchment. It contains no major settlements, with the only habitations being small villages (including Barcombe Cross and Plumpton Green), various hamlets and isolated properties. The land is primarily used for agricultural pasture and arable farming with some woodland.

There are a number of streams that confluence with the Ouse in the sub-catchment, including the River Uck in the north, Longford Stream, Bevern Stream and Clay Hill Stream. The low lying valley floor is generally 300-800m wide which narrows to approximately 100m where tributaries join the main river channel.

The semi-impermeable nature of the underlying geology means it liable to saturation, which can produce large runoff volumes. When combined with high runoff and channel flows from further up the catchment, a serious risk of flooding occurs.

4.3.2.4 Lower Ouse Sub-Catchment

The largest sub-catchment of the Ouse, the Lower Ouse sub-catchment covers an area of 267km², from Barcombe Mills village in the north to the mouth of the river at Newhaven on the English Channel (Figure 4.2). The northern boundary of the sub-catchment at Barcombe Mills also marks the limit of the tidal reach, meaning that water levels along the remaining 22km stretch of the Ouse to Newhaven are governed by the interaction of sea levels and river flows. The sub-catchment includes the urban centres of Lewes, Newhaven, Ringmer and western reaches of Brighton. However, only a small amount of runoff from Newhaven and Brighton enters the Ouse system, with the majority draining directly to the sea.

The Lower Ouse sub-catchment begins on the edge of the Low Weald, with underlying impermeable Green Sand and Gault Clay and overlying clayey soils. The majority of the sub-catchment though is in the permeable Chalk hills of the South Downs, with elevations of between 120m to 240mOD. The River Ouse initially flows through a complex of weirs, sluices and abandoned lock gates at Barcombe Mills, then enters into a wide valley of predominantly soft, clayey alluvial deposits. In the northern half of the sub-catchment, the low valley floor ranges from between 300m and 600m wide. The river meets the South Downs at the town of Lewes, and squeezes through a narrow valley bottom before widening to 2,500m at The Rodmell Levels. From here, the valley narrows back to between 700m and 1200m for the remainder of the course to Newhaven.

Aside from the urban areas, the land is almost exclusively arable farmland. Below Lewes, large low lying areas are drained by a network of levees controlled by the EA. Throughout the sub-catchment, the river is artificially embanked, with little naturally functioning floodplain remaining. However, the section between Barcombe and Lewes does see overtopping of the embankments during peak events.

The most significant tributaries are the Winterbourne Stream, which flows into the Ouse in the southern part of Lewes town centre, the Cockshut Stream, North End Stream, Norlington Stream and Glynde Reach, all of which have been artificially closed with controlled outfalls. The Winterbourne Stream is predominantly dry but responds quickly to runoff from The South Downs and rising groundwater levels.

4.4 Flooding in the Ouse Catchment

The location, topography and geology of the Ouse catchment mean that it is prone to periodic flooding, with the most recent and devastating flood occurring in October 2000 (Figure 4.3). Environment Agency (2002, 2004) commented that flooding at Lewes is a complex problem due to the interaction of sea level and river flow, offstream floodplain storage and narrow topography and river channel (including Cliffe Bridge) through the centre of the town. Appendix E.1 details recorded flood events in the catchment.



Figure 4.3 Lewes town centre under flood, 12th October 2000

Although the lower sections of the catchment are underlain by free-flowing chalk, the upper and middle sub-catchments consist of relatively impermeable geology with clayey topsoils which quickly become saturated during heavy rainfalls, causing quick and substantial runoff resulting in high fluvial flows. Between Barcombe and Lewes, the embankments of the River Ouse are susceptible to overtopping during extreme flow events. Once off-stream soil moisture deficits in the floodplain have been filled, river flow can increase in potentially substantial volumes.

The narrowing topography close to Lewes constricts any potential floodplain areas as the Ouse approaches the South Downs and Lewes town centre. The undulating hills containing Hamsey and Malling, and the railway embankments to the north of Lewes confine river flows to the narrow valley centre, which can cause floodwater levels to rise significantly during out of bank events.

River defences completed after the December 1960 flood saw pressure grow for the expansion of the town onto the floodplain areas. This trend increased the amount and rate of surface runoff and reduced the surface area available for flood storage and conveyance. By the time of the October 2000 flood, extensive urbanisation of the low lying areas had produced a significant impact on the flooding risk in Lewes where there were more properties and businesses at risk from flooding than ever before. Using historical maps, Environment Agency (2001) estimated the number of properties susceptible to flooding (Table 4.2) during the most extreme flood events recorded in Lewes.

Table 4.2 Number of properties in Lewes at risk from flooding

Year	Number of Properties Flooded in Lewes
1824	~200
1960	550-600
2000	836

Until very recently, the river defences in Lewes had seen little change since the 1960 flood. Although they protected the town from the smaller and more frequent high fluvial

flows and sea levels, extreme events such as the October 2000 flood saw magnitudes which exceeded the channel capacity and dramatically overtopped the defences, causing rapid and devastating flooding. Since the start of this research, the plan of defences improvement has been started (Environment Agency, 2004), with the aim of protecting the town against similarly severe flood events.

4.5 Hydrology

4.5.1 Data Sourcing

This analysis was reliant on historical observations (including extreme events) to enable accurate simulation and extreme probability analysis of the variables within the case study area. Hydrological datasets recorded at various locations within the Ouse catchment were sourced, including precipitation, fluvial river flows, river stage, tide and surge.

Data checking and correction was undertaken at the start of the analysis to incorporate high data quality rather than allow unseen errors to become apparent at a later more crucial stage in the analysis. A large-scale regional approach was adopted for the verification of the reliability of the data series, through the correlation between records from surrounding locations rather than reliance on any single gauge. This process aided the analysis of gaps in data, bad recordings and inherent bad positioning of some recording stations, as well as highlighting inconsistency between datasets. The differing resolutions of the various datasets required identification and correction prior to any further analysis. Scrutiny of the hydrological datasets included the following checks and exercises:

- Data source reliability – Data source verification including the organisation responsible and the gauge / recorder; identification of the gauge's history and limitations and problems of gauge and its location.
- Raw data series – Checking of compatible units and resolutions; identification of trends, any data shifts and changes in patterns; comparison of mean values and peak values throughout the datasets.

- Cleaned data series – Identification of pre-calculated and edited values by the data recording / collating organisation; examination of data reliability and comparison with raw data where available.
- Missing sections – Checking for missing data; determination of patterns and trends (i.e. times of year, during the peaks of floods, random gaps etc); checking the data either side of missing sections for sudden shifts in the data series.
- Comparison with other data series – Examination of the data for unusual values such as abnormally dry or wet spells or null values; correlation of the data with other gauges recording the same event (i.e. upstream / downstream or neighbouring sites).
- Data correction and deletion – Compilation of incorrect, error coded and flagged data; correction or editing of the unreliable series sections; calculation of the percentage of missing data in total series.

4.5.2 River Flow

The Uck and Upper Ouse sub-catchment gauges of Gold Bridge, Isfield Weir, Clapper Bridge and Old Ship provided daily and annual maxima historical flow series on the major tributaries and channels of the upper sub-catchments (Table 4.3). Time-to-peak (T_p) values were calculated using the 12th October 2000 flood event. This event provided an ideal opportunity to examine how the catchment behaves during a catchment-wide extreme event that simultaneously affected each gauge due to the already saturated ground leading up to the flood event. Clappers Bridge and Old Ship show the shortest T_p values due to their locations on tributary streams rather than the main river channel, which was found to be typical of other historical events monitored across the catchment.

At the southern boundary of the Middle Ouse sub-catchment is Barcombe Mills. Barcombe is at a pivotal location in the river system at the border between the upper sub-catchments and the end of the tidal reach from the Lower Ouse sub-catchment. The locations of Barcombe Mills u/s flow and ultrasonic gauges are ideal position for the measurement of cumulative flow from the Uck, Upper Ouse and Middle Ouse sub-catchments.

Table 4.3 Ouse catchment river flow gauges

Gauge	River	Catchment Area (km ²)	Time-to-Peak (mins)*	Mean Daily Max. Values (m ³ /s)	Series Completion	
Gold Bridge	Ouse	180.9	555	2.98	46 years (100%)	11703 days (98.6%)
Isfield Weir	Uck	87.8	540	2.00	41 years (100%)	12033 days (99.8%)
Clappers Bridge	Bevern Stream	34.6	495	0.86	35 years (97.2%)	11780 days (99.2%)
Old Ship	Clay Hill Stream	7.1	460	0.17	36 years (100%)	11872 days (100%)
Barcombe Mills u/s Flow / Ultrasonic	Ouse	395.7	680	6.53	49 years (100%)	10916 days (91.9%)

Source: Environment Agency (2005a)

*Time-to-Peak values calculated using historical data from the 12th October 2000 event

The Barcombe Mills site includes an additional 85.3km² of the upper catchment which is ungauged by the four upstream flow stations. Although there have been chart and telemetry recording stations in operation at Barcombe Mills since 1956, there is however a long history of inaccurate flow and level recordings at the site. There is no discernable main channel through Barcombe with numerous side streams and channels. The regular opening and closing of sluice gates as a response to river flow conditions drastically affects gauge readings, with extreme flows from the upper sub-catchments often overwhelming or bypassing the gauges completely. A new ultrasonic gauge was installed just upstream of Barcombe Mills in 2003 to address the problem, but this also has been poorly located and is found to still produce unreliable flow measurements. Appendix A highlights problems with location, recording and performance of each gauge under normal operational and extreme conditions.

4.5.3 River Stage

Barcombe marks the start of the wider and flatter Lower Ouse valley, which would once have formed part of a natural floodplain prior to the placing embankments within the river system. Today, the river between Barcombe and Newhaven has been fully embanked, with an estimated channel capacity of 85m³/s (Environment Agency, 2001). At Lewes, the embankments are susceptible to overtopping during high flows, which inundate the low lying fields in the area.

The gauging of river stage in the middle and lower Ouse catchment has a poor history. The gauge at Barcombe Mills Weir, downstream from the flow and ultrasonic gauges (4.5.2) is frequently bypassed by upstream flows. Environment Agency (2002) derived an AMAX series for the gauge based on upstream flows (Table 4.4). No daily stage series was obtainable.

A fairly consistent chart recorded AMAX stage series existed downstream at Lewes Corporation Yard (Figure 4.4). However, the reliability of the data was questioned due to the gauge's original design for the use of monitoring water levels for water management purposes during periods of low flow, making it unsuitable for extreme level recording. Environment Agency, *pers comm.* (2003) concluded that the recorded Corporation Yard chart dataset was reasonably complete and accurate up to 1988 when the original chart gauge was replaced with a telemetry gauge to form part of the EA regional telemetry system. After the installation of the new gauge, the reliability and accuracy dropped with datum shifts and mechanical failures creating significant periods of missing or unreliable data. Reliable 15-minute data has only become available at Lewes Corporation Yard from November 2005 onwards following the installation of a new gauge at the site.

The gauge at Lewes Gas Works (Figure 4.4) provided a limited data series due to unobtainable charts. It was possible to extract an AMAX stage series and the period covering the October 2000 flood event was digitised.

Table 4.4 Ouse catchment river stage gauges

Gauge	River	Catchment Area (km ²)	Mean Daily Max. Values (mAOD)	Series Completion	
				AMAX	Daily
Barcombe Mills Weir	Ouse	395.7	-	45 years (91.8%)	-
Lewes Corporation Yard	Ouse	-	2.63	45 years (91.8%)	1384 days (67.8%)
Lewes Gas Works	Ouse	-	-	44 years (89.8%)	-
Southease Bridge	Ouse	-	2.70	5 years (100%)	1583 days (99.4%)

Source: Environment Agency (2005a)

The main channel is lined with defensive walls throughout the urbanised areas of Lewes. Two structures affect river behaviour through the town centre which has a critical impact

on the recording of water levels during a flood event. The first, Phoenix Causeway, comprising of a bridge and high embankments built in the mid-1970s, splits the town in two across the urban valley floor, running east-west (Environment Agency, 2001). During a flood event, the Phoenix Causeway has been found to act like a dam across the town, stopping any floodwaters outside of the main channel conveying along the floodplain to the other half of the town. The second structure is the historic Cliffe Bridge, 150m further south, which is the main constriction across the river. The bridge has a calculated maximum capacity of $210\text{m}^3/\text{s}$ which seriously impedes extreme flows during flood events, most noticeably in October 2000.

The Southease (telemetry) gauge provided a reliable 15-minute stage gauge midway between Lewes and Newhaven. Data existed for the period of 1999-2003 only, covering the duration of an EA project, after which time the gauge was decommissioned.

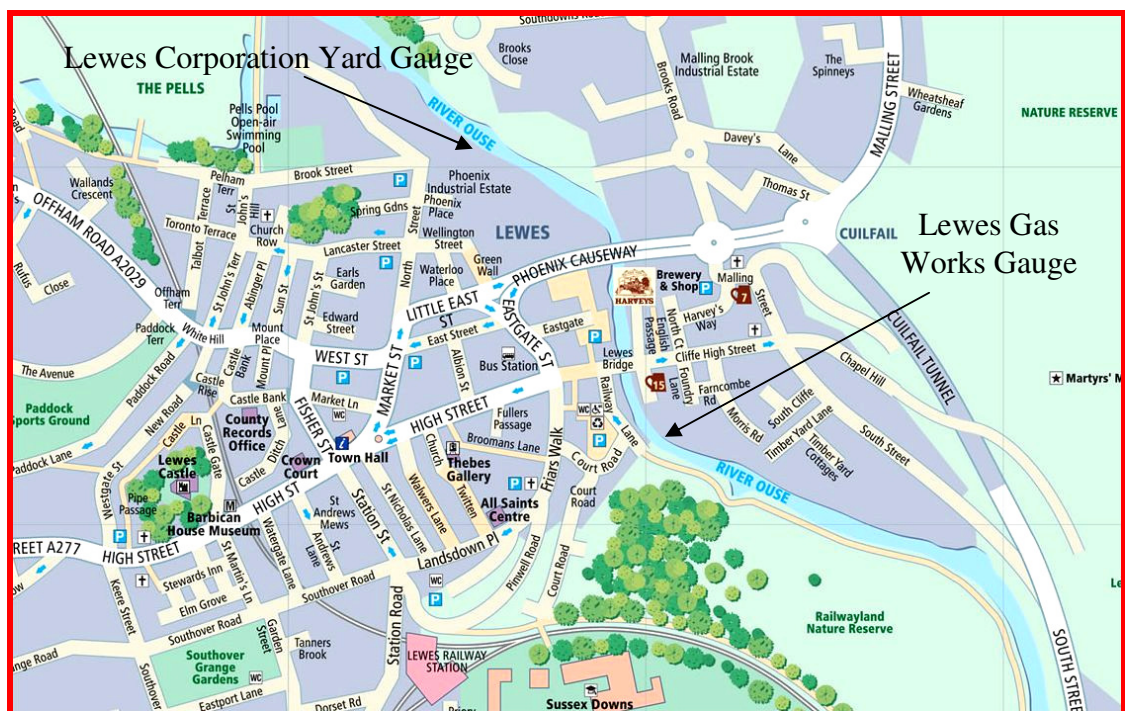


Figure 4.4 Location of Lewes stage gauges.
Map supplied by Lewes District Council.

4.5.4 Sea Levels

4.5.4.1 Sea Level Observations

The A-class Proudman tidal telemetry station at Newhaven provides an almost constant tidal record relative to Admiralty Local Chart Datum (CD), from 1991 to 2006 and a five

year dataset from the mid-1980's totalling 20 years (Table 4.5). A comparison of extreme upstream fluvial events with simultaneous downstream tidal records showed no influence of fluvial flows on the recorded tidal stage at Newhaven. The location of the Newhaven gauge at the river mouth was therefore deemed suitable for the extraction of a total tidal stage record, independent from any fluvial influences.

Table 4.5 Ouse catchment / south coast sea level gauges

Gauge	River	Catchment Area (km ²)	Mean Daily Max. Values (mAOD)	Series Completion	
				AMAX	Daily
Newhaven (EA)	Ouse / English Ch.	-	2.84	83 years (89.2%)	3884 days (74.5%)
Newhaven (Proudman)	Ouse / English Ch.	-	2.89	21 years (84%)	6022 days (69.9%)

Source: Environment Agency (2005a); Proudman (2006)

The EA tidal recording station, in close proximity to the Proudman station, in contrast has a poor history of tidal data recording since the installation of a telemetry gauge in 1990 (Table 4.5). Records show prolonged periods when data was either inaccurately recorded or was not recorded at all. As a consequence, observations from 1990 onwards were not utilised from the EA station.

4.5.4.2 Tidal Effects on the Ouse Catchment

Newhaven harbour is situated at the mouth of the River Ouse on the South Coast. The entrance to the harbour is between two piers, protected from the prevailing winds by a large breakwater to the west of the port. The harbour entrance is routinely dredged to a depth of 5.5m below CD to enable vessels to berth. The upstream end of the harbour (up to 1km inland) is reached via a swing bridge, with operation depending on tidal conditions and the size of vessel. Sea level predictions for Newhaven issued by the Admiralty are values based on historical recordings with known astronomical gravitation and tide generating forces, which produce tables of predicted sea levels and associated times for any given location for years ahead. Table 4.6 details predicted astronomical tide for Newhaven from Admiralty Tide Tables (Proudman, 2006). All levels are relative to CD.

The Mean Spring Range (MSR), the difference between Mean High Water Springs (MHWS) and Mean Low Water Springs (MLWS) at Newhaven, was calculated to be 5.97m for the period 1996-2015 (Proudman, 2006). The maximum predicted astronomical spring range for the same period was calculated to be 7.08m on the 10th March 1997 (Figure 4.5), and the minimum predicted astronomical neap range was 1.90m on the 19th March 2005 (Proudman, 2006).

Table 4.6 Newhaven sea level predictions (1996-2015)

Newhaven Sea Level Predictions	Values (mCD)
HAT	7.30
LAT	0.16
MHWS	6.69
MLWS	0.77
MHWN	5.22
MLWN	2.10
MSR	5.97
MNR	3.13

Source: Proudman (2006)

During low river flows, the tidal range at Lewes is approximately 0.0mAOD to 3.0mAOD on a spring tide, which drops to -0.2mAOD to 0.9mAOD on a neap tide. In the summer months, river flows in the Ouse can be very low, therefore at low tide river stage can drop to around zero Ordnance Datum.

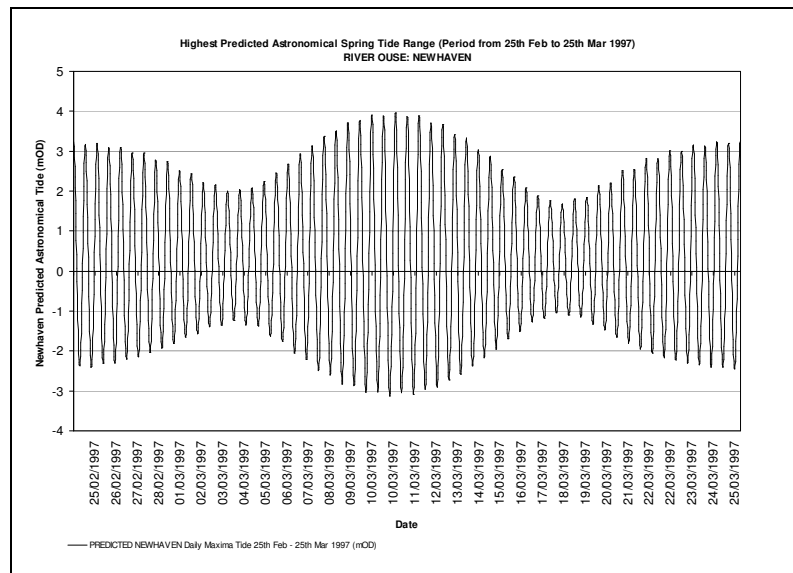


Figure 4.5 Highest predicted astronomical spring tidal range (7.08m) at Newhaven (10th March 1997)

The tidal limit in the River Ouse is Barcombe Mills, approximately 14km inland from the river's mouth at Newhaven. The majority of high tides do not actually reach the full tidal limit however, but stop around Hamsey, some 3km downstream from Barcombe Mills (Environment Agency, 2002). The distance a tide travels is dependent not only on the height of the tide at Newhaven, but also its range. The range of a tide determines how much power it has, which is directly applicable to the tidal limit; a spring tide will have the greatest range, thus it will cause the tidal limit to move further upstream. In estuaries, the tidal limit may also be affected by upstream fluvial flows dampening the tidal range. A surge does not have the same affect however, as it will simply add a higher level to the range of the tide (Pugh, 1987). Therefore, a surge which does not occur on a spring tide may not alter the tidal limit.

4.5.4.3 Local Chart to Ordnance Datum Conversion

It was necessary to convert the Proudman Newhaven tidal records from Admiralty Local Chart Datum to Ordnance Datum to allow comparison with the remainder of the hydrological data series in the Ouse catchment. However, datum inconsistencies were found between the Proudman recorded levels at Newhaven relative to Admiralty Local Chart Datum and other EA levels throughout the catchment which were relative to Ordnance Datum, including the EA Newhaven sea level gauge. Environment Agency (2002) noted a $\pm 0.25\text{m}$ error between the EA and Proudman gauges at Newhaven.

Although this problem was discounted by the exclusion of the EA Newhaven dataset, no attempt was made to clarify the potential Admiralty to Ordnance datum error.

Proudman (2006) identified the conversion of sea levels at Newhaven from Admiralty Local Chart Datum to Ordnance Datum as being -3.52m. Analysis of an example year of recorded Proudman Newhaven data (2002) was converted from Local Chart to Ordnance Datum using this value. When compared to the recorded EA series at Newhaven, the converted Proudman values revealed significant inconsistencies between the corresponding Ordnance Datum values, displaying an average 0.23m datum error. Figure 4.6 shows an example of the Ordnance Datum differential between the EA Newhaven series minus the converted Proudman Newhaven series for a one month period (October 2002). The results showed the error to be fairly constant throughout the tidal range, although the differential was greatest at low tide. The periods of increased datum differential are due to the inconsistencies with the EA sea level gauge noted in section 4.5.4.1.

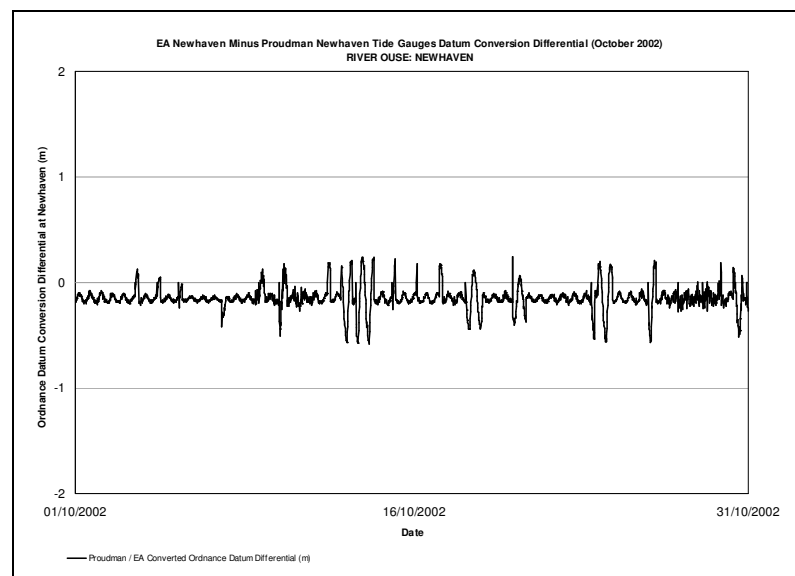


Figure 4.6 Admiralty Local Chart Datum to Ordnance Datum transformation differentials at the Proudman & EA Newhaven sea level gauges (October 2002)

Further analysis compared the 2002 predicted astronomical tide at Newhaven extracted from Admiralty Tide Tables (Proudman, 2006) with simultaneous predicted tide extracted from the Admiralty software package TotalTide (Admiralty, 2005). The results confirmed the Local Chart to Ordnance Datum conversion differential with an almost

identical error. As such, the Proudman Newhaven dataset was transformed from Local Chart Datum to Ordnance Datum using an additional 0.23m conversion.

4.5.5 Surge

4.5.5.1 Definition of Surge

Predicted sea levels are calculated for average meteorological conditions at specific times. The effect of wind and atmospheric pressure adds or subtracts a meteorologically-driven component to the predicted astronomical sea levels. This is known as a surge. It is categorised as the difference between the total observed sea level and the predicted astronomical tide. It can also be referred to as the ‘meteorological residual’ or the ‘weather effect’ (Pugh, 1987).

A reduction in pressure of 1mb corresponds to an approximate rise in the water level of about 1cm (Svensson and Jones, 2004). Similarly, the effect of wind, although most important in shallow waters, results in the water being dragged in a similar direction to the wind. However, in the northern hemisphere, this dragging effect is deflected to the right due to the Coriolis effect (Hunt, 1972).

This natural variance from the predicted sea levels occurs continuously, and it is rare for tidal levels to be exactly the same as predicted. The difference between predicted and recorded will usually be small, maybe a few centimetres. At Newhaven, the mean surge taken from daily maxima surge values was calculated to be around 0.15m.

Occasionally however, meteorological components combine to cause extreme sea levels way above or below the predicted levels. These are commonly known as storm surges and can occur under certain meteorological conditions such as low atmospheric pressure and high winds, which can occur during severe storms. Storm surges in the English Channel, including the port of Newhaven, are smaller than those encountered on the east and west coasts of Britain, with a maximum recorded surge of 1.5m. These may be generated locally in the English Channel, or enter it from the west or from the North Sea to the east (Heaps, 1983).

Surges are hard to model, and even harder to predict. Svensson and Jones (2004a) found that storm tracks associated with both high surge and high river flow on the south coast of Britain have a predominant north-easterly direction, which generally occur when depressions are located either near or over the British Isles. Wind is particularly hard to

quantify as it can either push or hold back the tide, creating positive and negative affects on overall sea levels. Svensson and Jones found the highest risk of flooding occurred as a consequence of a combination of high spring tide, strong onshore wind and very low barometric pressure.

4.5.5.2 Surge Observations

Surge was extracted from the sea levels observed at the Proudman tidal telemetry station at Newhaven, by calculating the difference between the total observed sea level and the predicted astronomical tide (Proudman, 2006). This provided a surge dataset for the same duration and completion as the Newhaven sea level series (Table 4.7). Surge data from the neighbouring A-class tidal stations of Dover and Portsmouth was obtained to cross-reference surge events along the English south coast.

Table 4.7 South coast surge gauges

Gauge	River / Location	Catchment Area (km ²)	Mean Daily Max. Values (m)	Series Completion	
				AMAX	Daily
Newhaven	Ouse / English Ch.	-	0.17	21 years (84%)	6022 days (69.9%)
Dover	English Ch.	-	0.22	-	365 days (100%)
Portsmouth	English Ch.	-	0.23	-	365 days (100%)

Source: Proudman (2006)

4.5.6 Precipitation

Data from four daily rain gauges (Plumpton, Barcombe CAM, Uckfield & Newick) and four hourly rain gauges (Plumpton, Barcombe CAM, Ardingly & Popeswood) for the Uck, Upper Ouse and Middle Ouse sub-catchments were obtained for the period of the October 2000 flood event.

4.6 Preliminary Assessment

The obtained hydrological variables of river flow, river stage, tide and surge were reviewed from 20 gauges in the upper, middle and lower Ouse catchments. Direct

comparison of the hydrological time-series was not immediately possible due to varying resolutions and recorded time periods of the various data series. Where available, the data was divided into both 15-minute and hourly complete duration series, providing simultaneous datasets for all hydrological variables from across the catchment with 35,040 15-minute observations and 8,760 1-hour observations for each (non-leap) calendar year.

Daily series were derived for 24-hour water-days from 09:00 to 09:00 GMT, to avoid limiting an event to any particular calendar day. Daily maxima and mean values were extracted for each series, extending the data series of each variable to include early records which only consisted of water-day maxima values. The percentage of missing data from each series was calculated and correlated with the times of year of the missing sections and included with the maxima / mean values to display their relative accuracy.

Although daily mean values are indicative of the peak flow magnitude throughout the duration of the water day, it was possible that by using mean rather than peak values, information could be lost or disguised. Mean values do not accurately display the peak of an event which occurred over a short period, such as in quickly responding catchments, thus the use of mean values is only suitable for slowly responding catchments so the peak value does not become defused or hidden. The Ouse catchment however is regarded as being quickly responding and ‘flashy’ in nature (Environment Agency, 2002), therefore daily mean values were not used as a variable to calculate or analyse peak values, but only used where comparisons with existing historical analysis which utilised daily mean values was necessary and to display the average magnitude for each gauge.

5 GENERAL METHODS FOR THE MODELLING & SIMULATION OF EXTREME WATER LEVELS

5.1 Introduction

This section identifies the methods used for the modelling and simulation of water levels in the Lower Ouse, including the development of a one-dimensional hydraulic model and structure function curves using historical hydrological datasets. Barcombe Mills (river flow) and Newhaven (sea level) were selected as the upstream and downstream model limits. The creation of the model is described below.

5.2 Hydraulic Model

5.2.1 Modelling Philosophy & Sequence

The process of constructing a one-dimensional flow model of the Lower Ouse began with the formation of the catchment drainage pattern, consisting of the main river channel and major tributaries. A series of cross sections were placed along the river's course, representing the geometry of the main channel, banks, levees and floodplain. Each cross-section contains data referring the distance between cross sections which may then be used to calculate conveyance areas and wetted perimeters. During a model simulation involving upstream river flow and downstream sea level, the completed geometry can then be used to calculate energy losses due to friction and from contraction and expansion. These were then used as inputs into the continuity and momentum equations, the laws that govern water flow in rivers. The output from an unsteady flow simulation was a set of water surface profiles for the extent of the river at each cross-section for every time-step in the simulation. The aim for the model was that the shape and progression of these profiles accurately replicated the behaviour of the historically recorded river stage to allow for calibration simulations and analysis.

5.2.2 Model Extent

The model covered the Lower Ouse from Newhaven 22km to the tidal range limit at Barcombe Mills, with the aim of accurately replicating the hydrodynamic behaviour of flows in the main channel. This would also allow for the complex relationship between river flow and sea level to be defined and their relative effect on the flooding problem in

Lewes to be explored. The model also included the floodplain and other low-lying areas up to 8mOD. The extent of the model is shown in Figure 5.1.

5.2.3 Software

The computer package HEC-RAS, version 3.1.2, was chosen to model the Lower Ouse, a programme written by the US Army Corps of Engineers (2004) and recognised by the engineering industry as a suitable package for performing analysis of steady and unsteady flow. It was primarily selected due to the capabilities of the one-dimensional unsteady state functionality for the modelling of in-bank flows.

5.2.4 Cross-Section Topographical Data

The construction of model was to some extent dictated by available data and previous studies in the Ouse catchment. Comprehensive and accurate topographical data was required to match reality as closely as possible.

The topography was divided into four descriptive types, comprising of the main channel, banks and levees, flood plain and key structures, including bridges and weirs. Main channel geometric data was obtained from a hydrographic survey undertaken by Longdin & Browning in June 2001 (Environment Agency, 2001d). The data was provided as lateral cross-sectional bed depth readings taken at 0.3m to 0.5m spacings, up to approximately high tide mark, suggesting the majority of survey was carried out by boat within a few hours of high tide. The sections were generally spaced at 200m intervals,

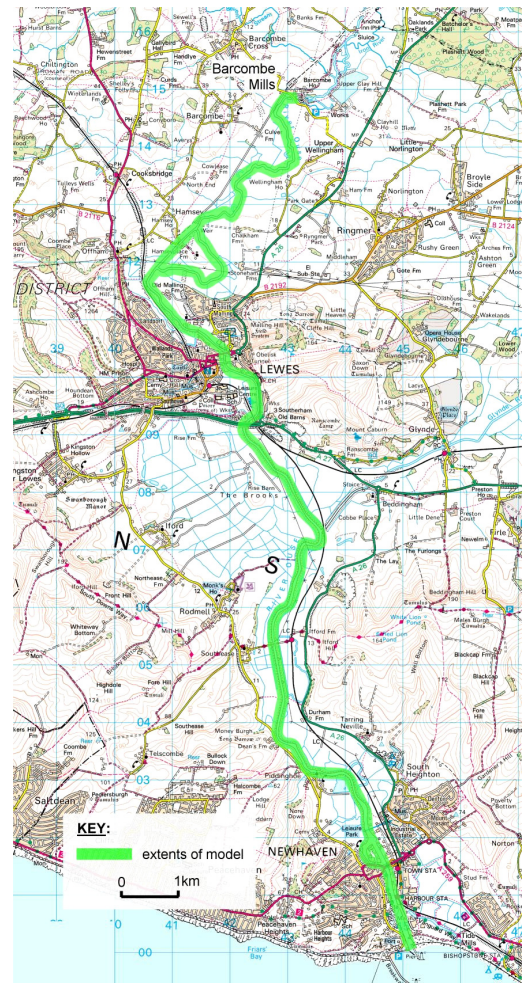


Figure 5.1 Extent of the Lower Ouse model (Barcombe Mills to Newhaven).
Based on Digimap supplied map, © Crown Copyright, Ordnance Survey. An EDINA Digimap / JISC supplied service.

except through the centre of Lewes and around bridge structures where more detail was provided. The cross-sections dictated the location of the main cross sections used in the HEC-RAS model. The majority of the data appeared to be accurate and checks with other data sources confirmed the reliability.

Except at key structures and bridges, no topographical data was provided for the river banks, levees and floodplain surface elevations above the high water mark. It was understood that the levees play a significant role in the behaviour of the river and the protection of Lewes during flood events. It was noted that it was not uncommon for flow downstream of Lewes to be contained within the levees (Environment Agency, *pers comm.*, 2003), at a higher level than the surrounding floodplain surface elevations.

The survey was conducted using a Trimble 5700 Differential Global Positioning System (DGPS). A static survey of a local network of base stations was post-processed using the Trimble Geomatics Office software and adjusted to the Ordnance Survey Active GPS Network. The topographical survey was conducted on both banks to record positions and elevations at each cross-section to relate the main channel depths to top of bank and floodplain elevations. The result of the survey defined the precise dimensions and over-topping heights of the banks and levees along the majority of the river course from Barcombe Mills to Newhaven. The elevation data was attached to the existing channel bed survey data, extending the cross sections beyond the levees to the start of the floodplains.

It was physically impractical to continue the DGPS survey beyond the limits of the river banks. As such, photogrammetry data (Environment Agency, 2001b) was used to extend the cross-sections to the extents of the floodplain and low lying areas. A three-dimensional image of the ground was used to create a contour map of the lower Ouse, and was presented as a Digital Elevation Map (DEM) in ESRI ArcView format. The accuracy of the photogrammetry was assessed by comparing contour levels with elevations taken at 144 points along the banks of the Lower Ouse during the DGPS survey. The contours were spaced at 0.25m, dictating that the two values at each location should be within this tolerance limit. Of the 144 samples, 91% were within the limit with the largest error as 0.38m. The results were deemed to be within acceptable limits. The details of the samples are shown in Appendix B.2. Due to the high level of accuracy of the photogrammetry data, it was further used to infill gaps in the DGPS river bank data caused by inaccessible areas or loss of satellite or differential radio link. The

photogrammetry ArcView shapefiles were converted into AutoDesk AutoCAD format. The channel cross-sections were overlain onto the photogrammetry map of the lower catchment and extended to the limits of the floodplains. Elevations and chainage values were then extracted along the extended cross-sections.

5.2.5 Hydraulic Structures

Several bridges and flood defence structures were observed to constrict flow during the October 2000 flood event and had a major role in the hydrodynamics in and around Lewes. Bridge decks, piers, abutments and defence structures of Cliffe Bridge, Phoenix Causeway and other flood defences in Lewes were surveyed within practical limitations and compared to existing geometric data for all the bridges in the Lower Ouse (Environment Agency, 2001d).

5.2.6 Model Construction

A total of 154 cross-sections were used to construct the model, incorporating the data from the main river channel bed survey, the DGPS survey of the banks and levees, and the photogrammetry data of the surrounding floodplains and low lying areas. During the construction phase of the model, each cross-section was set an initial value of Manning's n roughness coefficient of 0.030. Although a simplification, the Manning's n value of 0.030 was selected on the basis that the Lower Ouse was an example of a relatively clean, straight and smooth river (Chow, 1959). The Manning's n value was altered during the model calibration phase.

Initial test runs produced visually stable observations which closely replicated the true hydrodynamic behaviour of flows in the Lower Ouse. Of particular note was the interaction of river flow with the rising and falling tides and their combined effect on resultant water levels. A three-dimensional schematic of the completed model is illustrated in Appendix B.2.

5.2.7 Inflows at the Model Boundaries

5.2.7.1 Upstream Synthesised Barcombe Mills Series

The extraction of a consistent and reliable series of river flows recorded at Barcombe Mills for the generation of an upstream model input series proved impossible due to the poor history of data recording at the site. It was concluded that due to the geographical importance of the site at the limit of the tidal reach, the recorded Barcombe Mills dataset

was unsuitable for the requirements of this research and a new dataset be synthesised based upon cumulative observations from the more reliable upper catchment gauges.

The location of the Barcombe Mills gauge records flows from the entire upper catchment, covering an area of 395.7 km². The four upper catchment gauges of Gold Bridge, Isfield Weir, Clappers Bridge and Old Ship record flows from a total catchment area of 310.4km², leaving an ungauged catchment area of 85.3km², largely contained in the Longford Stream. The cumulative flows from the upper sub-catchments therefore required an additional component of approximately 21% to synthesise a flow series at Barcombe Mills. Similarly, peak flow events recorded at the four upper-catchment gauges do not arrive at Barcombe Mills simultaneously due to varying distances and catchment topography. Associated times of travel were estimated using the recorded upper catchment hydrographs, averaged flow velocities and simplified channel geometries which, where possible, were cross-referenced with the recorded Barcombe Mills flow series (Table 5.1).

Although the exercise generalised the true nature of the times of travel from the upper catchment to Barcombe Mills (i.e. increased flow velocities and out-of-bank events may, in reality, affect the times associated with each gauge), the process enabled a flow series to be synthesised for the Barcombe Mills site. The four upper-catchment gauges provided almost complete 15-min resolution series from 1981 to 2006. These were used together with an additional estimated 21% to account for the ungauged portion of the upper-catchment and the estimated times of travel to produce a synthesised series at Barcombe Mills.

Table 5.1 Distances and times-of-travel values for upper catchment flow gauges to d/s Barcombe Mills

Gauge	Distance to d/s Barcombe Mills (km)	Times-of-Travel to d/s Barcombe Mills (mins)
Old Ship	1	31
Clappers Bridge	2	66
Isfield Weir	3.5	158
Gold Bridge	8	255

Two existing series were obtained to calibrate the synthesised Barcombe Mills flow series. The first was a HYSIM simulated series (Environment Agency, 1998) generated for the modelling of flows at Barcombe Mills for water abstraction estimates, including 2002. Although the HYSIM model was limited to simulating flows up to $40\text{m}^3/\text{s}$, and was only available in daily mean flow format, it was regarded as being highly accurate below this level (Environment Agency, *pers comm.*, 2003). The second calibration used the recorded series extracted at Barcombe Mills weir. As previously noted (section 4.5.2), the gauge was known to underestimate flow magnitudes for the entire flow range and becomes overtopped by flows above $20\text{m}^3/\text{s}$. However, the timings of the peak flow events were understood to be accurate and could be compared to the synthesised flow series. For continuity with the HYSIM data series, the 2002 recorded Barcombe Mills series was extracted and converted to daily mean flow format. Two checks were carried out for each series; the complete 2002 series, and up to the limit of each of the range of each of the calibration series ($40\text{m}^3/\text{s}$ for HYSIM and $20\text{m}^3/\text{s}$ for recorded series). The resultant coefficients are shown in Table 5.2 and in graphically in Appendix B.1.

Table 5.2 Calibration of the synthesised flow series with the HYSIM simulated series and the recorded series at Barcombe Mills (2002)

Calibration Pair at Barcombe Mills	Calibration Period	Sample Size (days)	Maximum Flow Magnitude (m^3/s)	R^2
Synthesised & HYSIM	Jan 2002 - Dec 2002	357 (98%)	all	0.9205 ($P<0.01$)
			<40	0.9787 ($P=0.0196$)
Synthesised & Recorded	Jan 2002 - Dec 2002	365 (100%)	all	0.6967 ($P=0.7318$)
			<20	0.8816 ($P=0.0188$)

The results for the calibration of the synthesised series with the HYSIM simulated series (also see Figure 5.2a) showed a high correlation for magnitudes below $40\text{m}^3/\text{s}$, confirming the times of travel and the synthesised series were accurate for the lower flow estimates. The results for the calibration of the synthesised series with the recorded series below $20\text{m}^3/\text{s}$ also showed significant levels of correlation ($P<0.05$), and Figure 5.2b shows that the timings of the peak flow events were consistent. Calibration of the more extreme flow events (i.e. $>40\text{m}^3/\text{s}$) was limited by the lack of available data. Evidence from extreme events such as the 2000 flood however suggested that the synthesised peak

flow estimates closely matched previous estimates at Barcombe Mills. Environment Agency (2001c) estimated that flow values peaked well in excess of $250\text{m}^3/\text{s}$, which directly comparable with the synthesised magnitude of $292\text{m}^3/\text{s}$. Comparison with the timings of peak stage recorded at the downstream Lewes Corporation Yard gauge also showed significant commonalities. Following calibration with the HYSIM series, recorded Barcombe Mills series and noted extreme observations, a 15-minute resolution flow series was successfully synthesised at Barcombe Mills, with a duration of 23.7 years and series completion of 95.9%.

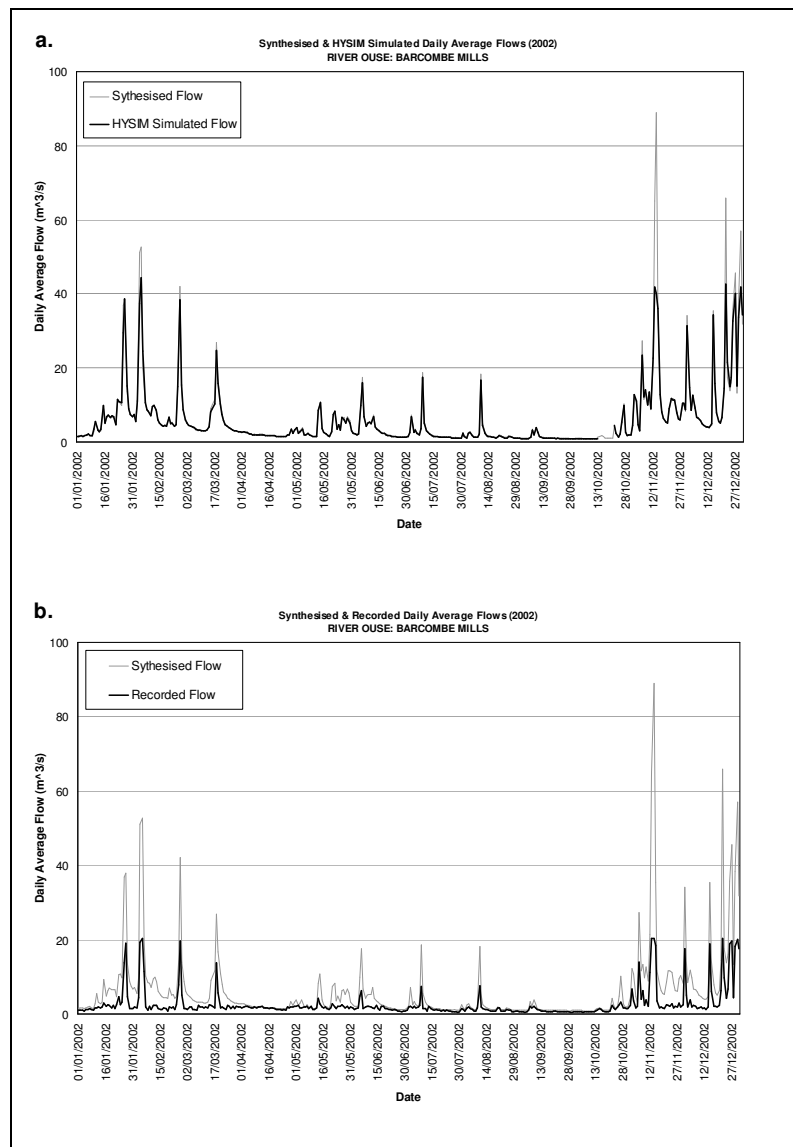


Figure 5.2 Time-series plots of synthesised daily mean flow at Barcombe Mills with **a.** HYSIM simulated daily mean flow, & **b.** recorded daily mean flow, (2002)

5.2.7.2 Downstream Recorded Newhaven Sea Level

The downstream boundary of the model is at the mouth of the Ouse at Newhaven. The model datum was relative to Ordnance Datum. Data obtained from the Proudman gauge at Newhaven was corrected from local Admiralty Local Chart Datum to Ordnance Datum and used to represent the tidal stage-time hydrographs for calibration events.

5.2.8 Model Trials & Testing

5.2.8.1 Test Data

The performance of the hydraulic model between Barcombe Mills and Newhaven was tested using historically recorded series at Lewes Corporation Yard and Southease Bridge stage gauges. Limited observations were also extracted from the Lewes Gas Works gauge to assist in the exercise through Lewes where available.

Telemetry data from Lewes Corporation Yard was available in 15-min intervals from June 2000 to May 2006. Due to the known poor quality and reliability of the Lewes series (see section 4.5.3), the most reliable periods of data recording were identified and extracted. Two significant periods from January to December 2002 and from December 2005 to May 2006 were selected as being generally suitable for testing purposes. The first test period of 2002, provided a constant recording, but contained several baseline shifts caused by a sticking float gauge. This was manually corrected to the known baseline for the period (Environment Agency, *pers comm.*, 2003). Following recent gauge improvements, the second test period of 2005/6 provided the most reliable series at Lewes. The period immediately surrounding the October 2000 flood event was also selected for testing due to the large amount of gathered documentation and hydrological data series for the event, as well as being the most significant flood event in the modern history of Lewes.

In comparison, in the predominantly tidally-influenced lower section of the model midway between Lewes and Newhaven, Southease Bridge provided a consistent (99.4% completion) and fairly reliable 15-min telemetry stage series from July 1999 to November 2003.

5.2.8.2 Selected Test Events

The event selection was determined by the periods of reliable test data at the intermediate stage gauges (see above). The events were selected on the basis of varying intensity,

ranging between low, moderate, medium, high and extreme. Each event contained input and test data for a 96-hour period, except for events 7 and 8 where recorded data for Southease Bridge was not available. The test events are summarised in Table 5.3 and shown in detail in Appendix B.2.

Table 5.3 Model input events with peak hydrograph magnitudes at Barcombe Mills & Newhaven

Event No.	Test Event Period	Maximum Barcombe Mills Flow Magnitude (m ³ /s)	Maximum Newhaven Sea level Magnitude (mAOD)	Event Category
1	09/10/00 - 13/10/00	291	3.24	Extreme
2	03/02/02 - 07/02/02	80	3.08	Moderate
3	25/02/02 - 01/03/02	68	3.73	Moderate
4	08/07/02 - 12/07/02	29	2.93	Low
5	30/11/02 - 04/12/02	54	3.34	Moderate
6	21/12/02 - 25/12/02	100	3.08	High
7	13/02/06 - 17/02/06	26	3.26	Low
8	29/03/06 - 02/04/06	30	3.85	Low

5.2.8.3 Results & Discussion

Simulated stage data was extracted at cross-sections 40 and 91, which represented the gauges at Southease Bridge and Lewes Corporation Yard respectively. Initial model runs showed the in-bank flows were fairly well represented at both gauges, with the tidal behaviour at Southease Bridge particularly good. To improve the performance further upstream, the sensitivity of the model to the initially selected Manning's n value of 0.030 for the main channel and banks was tested. Trials showed an improvement in the performance with the lowering of Manning's n . Final values of Manning's n for the main channel were selected as 0.023 from Barcombe to Lewes, increasing to 0.026 from Lewes to Newhaven. The effect was improved in-bank performance in the upper half of the model, with both peaks and the rising / falling limbs of the hydrographs accurately matched with recorded data at Lewes Corporation Yard. However, a significant head loss was identified between Lewes Corporation Yard and Lewes Gas Works gauge at model cross-section 80 during high flow events, which was believed to be created by the

hydraulic characteristics of Cliffe Bridge which is situated between the gauges. The modelled head drop closely matched with stage observed during the extreme October 2000 event, therefore it was decided no further action was required.

The low to moderate events were found to be suited to the test exercise due to the gauges recording accurate observations at Lewes Corporation Yard and Southease Bridge. Not surprisingly, the extent of the most extreme flows, in particular modelled by the October 12th flood event, could not simulated accurately and showed a disparity with the recorded stage. Tests highlighted the limitations of one-dimensional modelling of extreme events involving the overtopping of river banks, lateral floodplain flows and offstream storage. It was decided to increase the heights of the river banks with artificial infinite walls along the length of the model. The result was a dramatic improvement of stage at Lewes during extreme flow events, although the peaks of the flow hydrographs arrived in the town centre approximately 3 hours earlier than recorded, which was thought to be representative of the floodplains being filled, both within the extend of the model and upstream of Barcombe which also affected the synthesised dataset.

Figure 5.3 and Figure 5.4 illustrate the final modelled and recorded data outputs for the selected events at the Lewes Corporation Yard and Southease Bridge gauges. Note, on some charts a horizontal baseline can be seen in the recorded series at the Lewes Corporation Yard gauge due to observed water levels being below the range of the gauge compared to the model output which shows the full range of water levels.

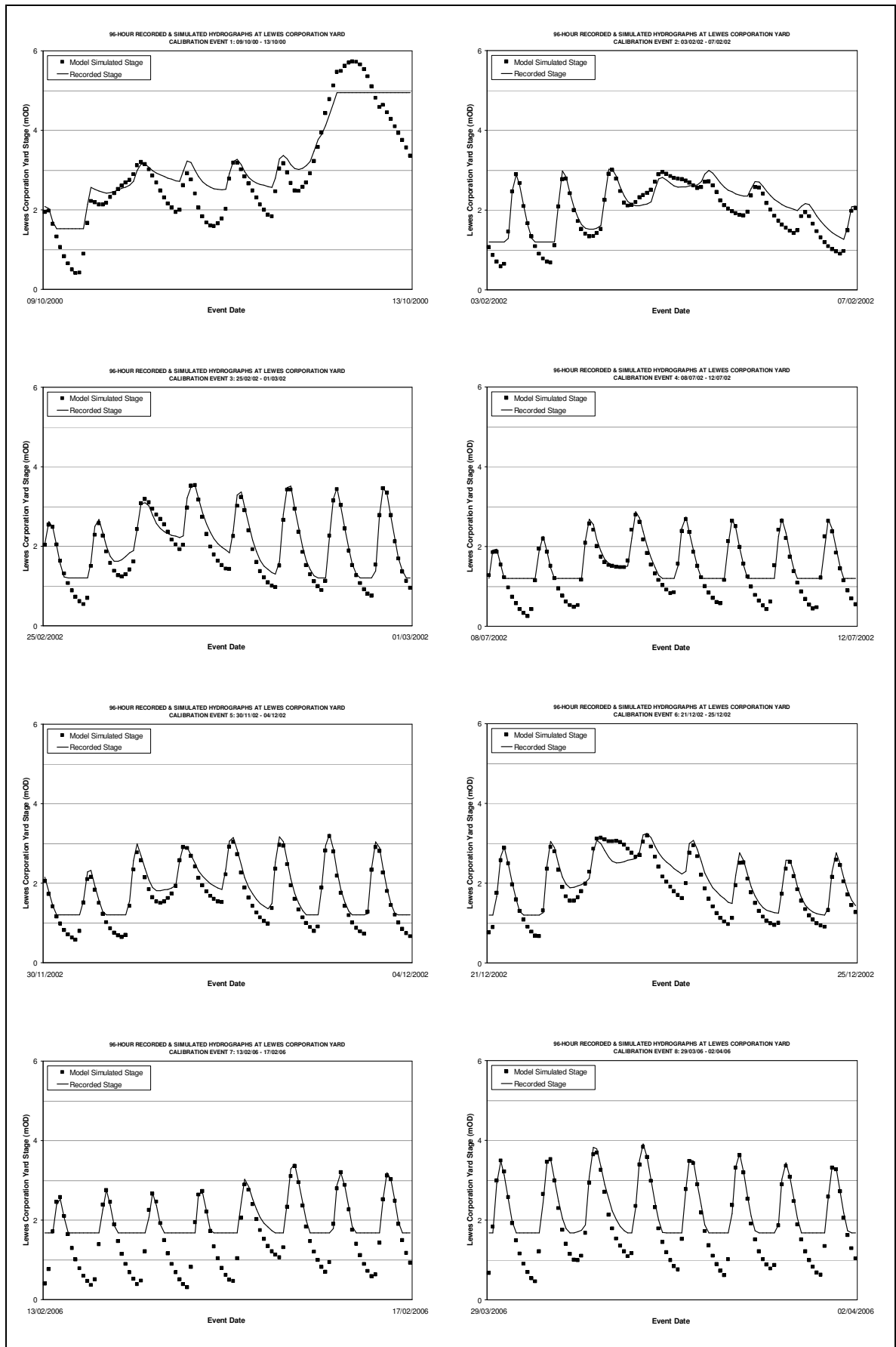


Figure 5.3 Plots of modelled and recorded stage at Lewes Corporation Yard (event no.'s 1 to 8)

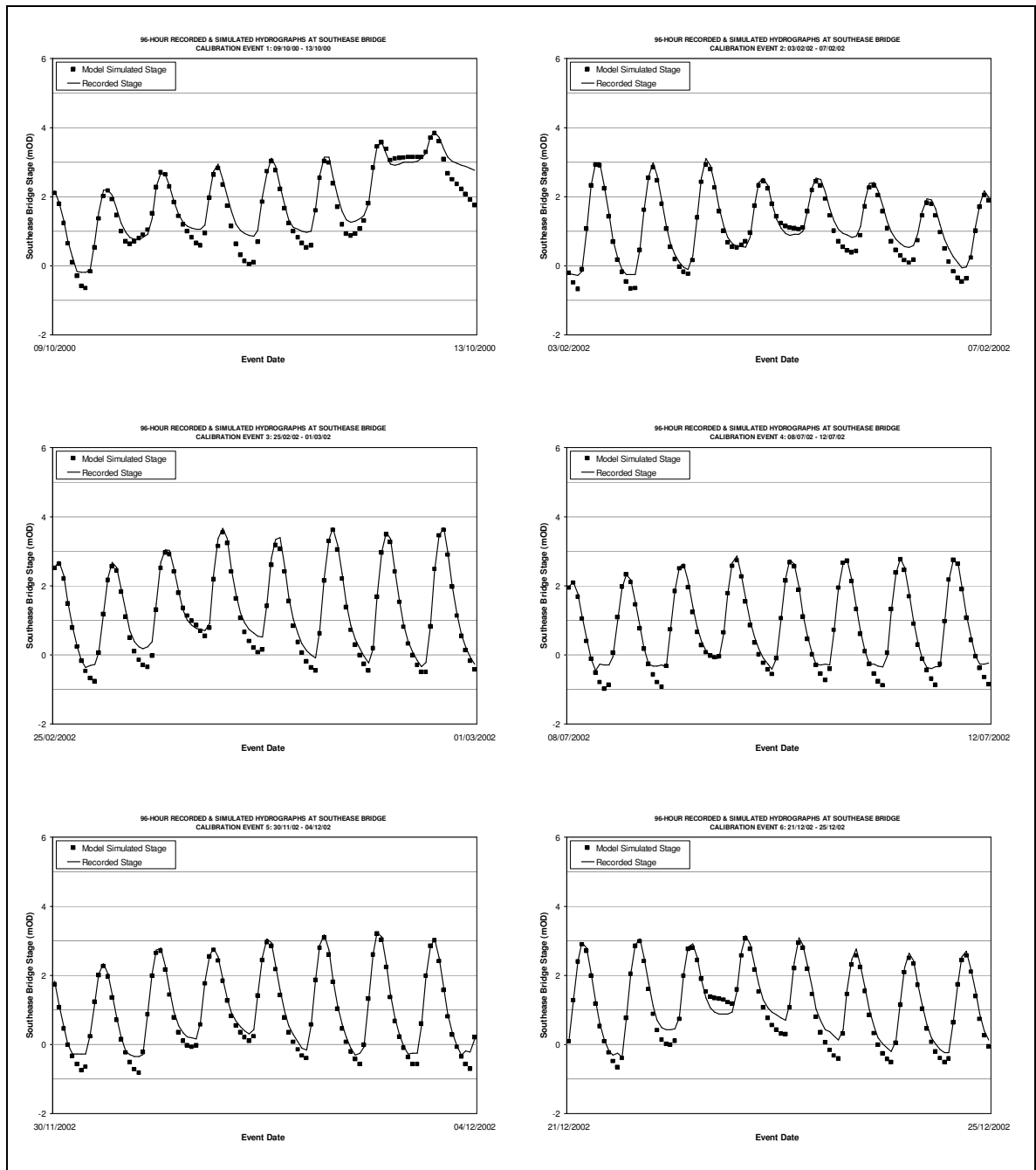


Figure 5.4 Plots of modelled and recorded stage at Southease Bridge (event no.'s 1 to 6)
Note: no recorded test data available for event no.'s 7 & 8

5.2.8.4 Correlation

A linear statistical correlation was undertaken for each event at Lewes Corporation Yard and Southease Bridge. Simulated data below the baseline limit of the Lewes Corporation Yard gauge was not included in the correlation exercise. Table 5.4 details the correlation results for each event, showing a high level of correlation between the recorded series and simulated model outputs.

Table 5.4 Model results and linear correlations of modelled and recorded stage at Lewes Corporation Yard and Southease Bridge

Event No.	Lewes Corporation Yard				Southease Bridge			
	Rec. Stage (mAOD)	Model Stage (mAOD)	Mean Diff. (m)	R ²	Rec. Stage (mAOD)	Model Stage (mAOD)	Mean Diff. (m)	R ²
1	4.95*	5.74	0.19	0.9680 (<i>P</i> <0.01)	3.86	3.84	0.20	0.9726 (<i>P</i> <0.01)
2	3.03	3.01	0.14	0.8843 (<i>P</i> <0.01)	3.10	2.99	0.14	0.9870 (<i>P</i> <0.01)
3	3.53	3.54	0.13	0.9742 (<i>P</i> <0.01)	3.67	3.64	0.14	0.9950 (<i>P</i> <0.01)
4	2.87	2.80	0.04	0.9799 (<i>P</i> <0.01)	2.87	2.77	0.11	0.9907 (<i>P</i> <0.01)
5	3.23	3.18	0.16	0.9846 (<i>P</i> <0.01)	3.24	3.20	0.12	0.9960 (<i>P</i> <0.01)
6	3.25	3.19	0.15	0.9335 (<i>P</i> <0.01)	3.15	3.07	0.13	0.9854 (<i>P</i> <0.01)
7	3.40	3.36	0.07	0.9534 (<i>P</i> <0.01)		n/a**		
8	3.91	3.83	0.13	0.9790 (<i>P</i> <0.01)		n/a**		

*Event 1 recorded stage overtopped gauge; peak estimated to be 5.8mAOD (Environment Agency, 2001c)

** Events 7 & 8 recorded stage not available for test period

If just the peak values were plotted rather than the complete series, the R² values would have all been close to 1. From the observed correlation coefficients and *P* values, it was concluded that the model was accurately test and further calibration could proceed, which is detailed in the following sections.

5.3 Continuous Simulation

The simultaneously observed synthesised Barcombe Mills flow and recorded Newhaven tide 15-min series (1982 to 2006) at the upstream and downstream boundaries of the hydraulic model were used as input variables for the production of a corresponding real-time continuous simulation of intermediate stage at Lewes. The resultant dataset was a modelled time series at the two key model cross-sections of 91 and 80, corresponding to the locations of Lewes Corporation Yard and Lewes Gas Works gauges. This created two series with the same time period as the input flow and sea level series as though they had been historically recorded. The process provided an extended time series at Lewes for calibration, later extraction of extreme values and further event analyses.

The reliability of the simulation was calibrated against the recorded dataset at Lewes Corporation Yard. The recorded series was however limited in duration (June 2000 to May 2006) and contained numerous missing and unreliable sections (see section 4.5.3). The most reliable period extending from November 2005 onwards. The calibration consisted of two recorded periods; the full June 2000 to May 2006 series and the more reliable December 2005 to May 2006 series. Correlation coefficients and differentials between simulated and recorded daily maxima series are shown in Table 5.5.

Table 5.5 Calibration of continuous daily maxima simulated stage with recorded daily maxima stage at Lewes Corporation Yard

Calibration Period	Sample Size (days)	Average Diff. (m)	Max. Diff. (m)	Min. Diff. (m)	R ²
Jun 2000 - May 2006	1455 (67%)	0.02	1.44	-0.68	0.9201 ($P=0.0444$)
Dec 2005 - May 2006	175 (100%)	0.03	0.30	-0.07	0.9901 ($P<0.01$)

The second calibration period showed the highest level of correlation with an R² coefficient of 0.9901 ($P<0.01$), which was reflective of the quality of the recorded calibration data (Figure 5.5). The high correlation deemed the continuous simulated data series at Lewes Corporation Yard and Lewes Gas Works suitable for further use.

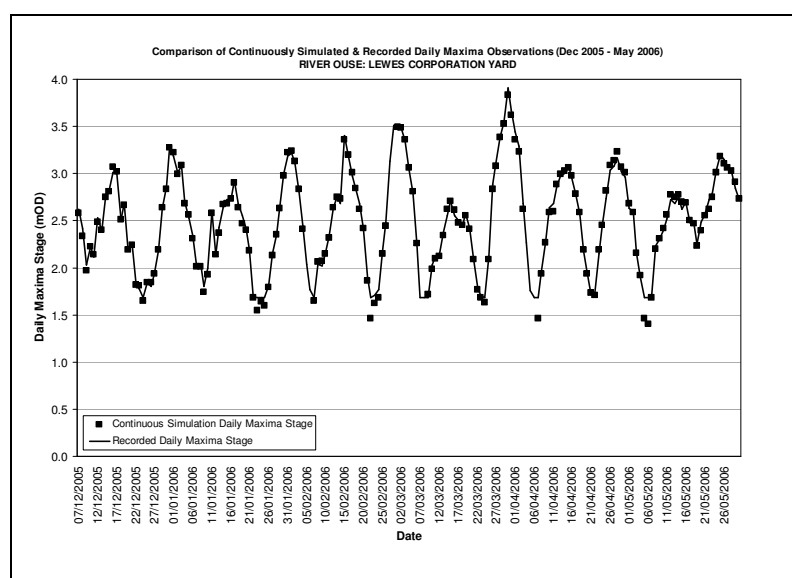


Figure 5.5 Comparison of continuously simulated & recorded daily maxima observations at Lewes Corporation Yard (Dec 2005 - May 2006)

Appendix B.3 contains continuous simulation graphical and calibration plots with the recorded series at Lewes Corporation Yard.

5.4 Structure Function Simulation

5.4.1 Structure Function Overview

In estuarine environments such as the lower River Ouse, a structure function is a process which relates two variables, (i.e. the ‘cause’, typically upstream river flow and downstream sea level), to an output value of interest, (i.e. the ‘effect’, such as stage at some intermediate location). Here, the structural response was created to estimate the maximum stage at Lewes Corporation Yard and Lewes Gas Works for all possible combinations of peak Barcombe Mills river flow and Newhaven sea level observations.

5.4.2 Representative Hydrographs

Tidal and fluvial hydrographs were required to represent a range of sea level and flow events. From the Barcombe Mills flow series, 15 events were selected which characterised a range of flow events from $20\text{m}^3/\text{s}$ to $300\text{m}^3/\text{s}$. Each hydrograph was adjusted relative to the maximum value to give relative flow values between 0 and 1 and plotted on the same axis. An average hydrograph was extrapolated and scaled to produce representative flow hydrographs ranging from $1\text{m}^3/\text{s}$ to $300\text{m}^3/\text{s}$ in increments of $30\text{m}^3/\text{s}$. A tidal hydrograph was similarly extracted from the recorded Newhaven series which had a tidal range that matched the mean spring range (MSR) and was then scaled around mean sea level (MSL) to produce representative sea level hydrographs ranging from 0.60mAOD to 4.80mAOD in increments of 0.30m. The hydrographs are shown graphically in Appendix B.4.

The scaled hydrographs were time-delayed to enable the maximum stage possible to be produced at Lewes. Environment Agency (2001c) reported that under normal conditions, the time of travel between high tide at Newhaven and high tide at Lewes is approximately 60 minutes, with a stage difference of 0.28m. Initial trial runs confirmed this to be accurate and constant for all magnitudes of tide. The time of travel of a peak flow observation at Barcombe Mills to a peak stage at Lewes however was found to increase with the magnitude of flow event. A range of flow hydrographs (30, 90, 150, 210 and $300\text{m}^3/\text{s}$) with identical 3mAOD peak tide curves were used to estimate the time

of travel using the hydraulic model, initially in increments of 1-hour, then reduced to 15-min. The flow and tide times of travel were then combined to produce typical delays required to produce maximum water levels at Lewes. The results of the analysis are shown in Table 5.6 and shown graphically in Appendix B.4, with the maximum and minimum stage simulated from the optimum and worst delayed hydrographs.

Table 5.6 Maximum and minimum simulated water levels observed at Lewes from optimum time-delayed hydrographs at Barcombe Mills and Newhaven

Hydrograph Pair	Times of Travel Barcombe Mills to Lewes (mins)	Times of Travel Newh'n to Lewes (mins)	Delay for Max. Water Level at Lewes* (mins)	Max. Water Stage at Lewes (mAOD)	Min. Water Stage at Lewes (mAOD)	Stage Diff. (m)
30m³/s Peak Flow v 3mAOD Peak Tide	90	60	30	3.10	2.98	0.12
90m³/s Peak Flow v 3mAOD Peak Tide	105	60	45	3.40	3.18	0.22
150m³/s Peak Flow v 3mAOD Peak Tide	120	60	60	3.92	3.73	0.19
210m³/s Peak Flow v 3mAOD Peak Tide	150	60	90	4.58	4.49	0.09
300m³/s Peak Flow v 3mAOD Peak Tide	180	60	120	5.81	5.77	0.04

*Delay measured as differential between tide and flow times of travel to Lewes

5.4.3 Structure Function Matrix

The hydraulic model was used to simulate the output stage at two key locations in Lewes at Corporation Yard and Gas Works. The locations were selected for their relative positions upstream and downstream of Cliffe Bridge in the centre of Lewes, which is known to impede flows during extreme flood events (e.g. Environment Agency, 2001c), enabling the differing effects of river flow and sea level to be identified.

It was impractical to simulate maximum output stage at Lewes for every conceivable combination of river flow and sea level due to the many thousands of hydraulic model runs that would be required. The problem was overcome through the use of look-up tables. Structure responses (stage) were generated from a range of input values of peak river flow at Barcombe Mills and maximum sea level at Newhaven, corresponding to each combination of tidal cycle curves and river flow hydrographs. The exercise required

a total of 176 hydraulic model runs, each with a 96-hour duration in 15-minute increments, generating optimum time-lagged peak stage at for each combination of flow and sea level. Figure 5.6 shows an example plot of maximum stage generated at Lewes Corporation Yard for all tidal hydrograph increments at Newhaven combined with the $90\text{m}^3/\text{s}$ flow hydrograph at Barcombe Mills and the maximum simulated water levels extracted. The process was repeated for each flow hydrograph with all tidal increments.

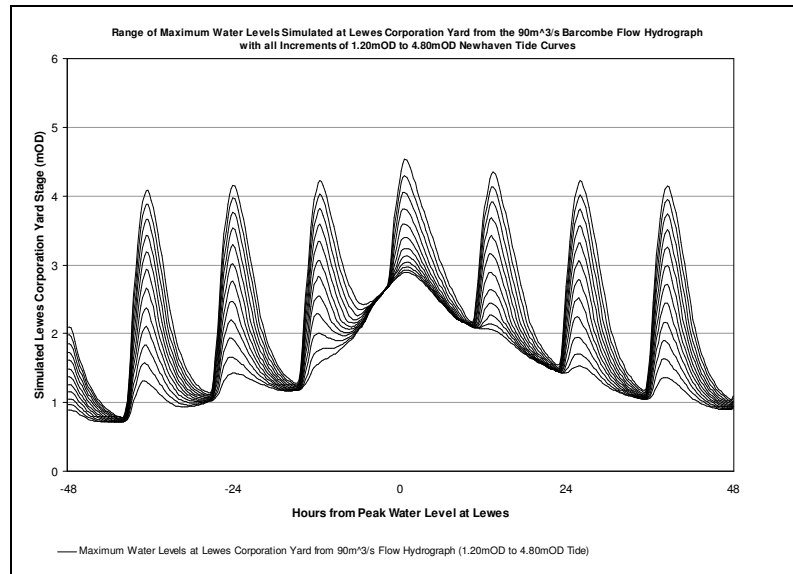


Figure 5.6 Example range of maximum water levels simulated at Lewes Corporation Yard from the $90\text{m}^3/\text{s}$ Barcombe Mills flow hydrograph with all increments of 1.20mOD to 4.80mOD Newhaven tide hydrographs for the production of the structure function matrix

The complete range of peak river flow ($1\text{m}^3/\text{s}$ to $300\text{m}^3/\text{s}$, in increments of $1\text{m}^3/\text{s}$) and sea level (0.60mOD to 4.8mOD, in increments of 0.2mOD) were tabulated on opposing axes in the look-up tables. The 176 generated peak stage at each of the Lewes sites, corresponding to each combination of river flow and sea level, were entered into the tables (see Appendix B.5) and the intervening values interpolated using a polynomial curve fitting procedure. The resulting 211 peak sea levels and 300 peak flow magnitudes produced matrices (termed as the 'structure function') consisting of 63,300 possible flow / sea level combinations, each with corresponding stage at Lewes Corporation Yard and Lewes Gas Works.

Figure 5.7 and Figure 5.8 show 3-dimensional plots of the resultant stage at Lewes Corporation Yard and Lewes Gas Works respectively, with corresponding input pairings of flow at Barcombe Mills and sea level at Newhaven. Longitudinal sections of the entire

model for all 176 modelled flow / sea level pairing are also shown in Appendix B.6. Both graphical plots display an increasing dependence on high fluvial flows for the generation of the most extreme stage upstream of Cliffe Bridge in the centre of Lewes. Downstream of Cliffe Bridge, the rapid head loss previously noted in section 5.2.8.3 is again clearly evident during the most extreme modelled events.

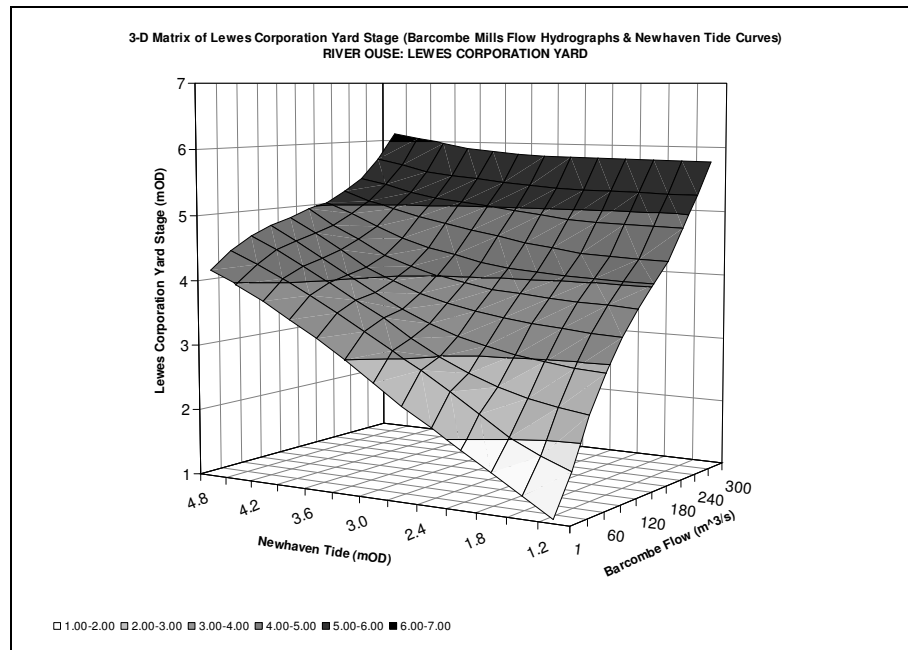


Figure 5.7 3-dimensional matrix plot of Lewes Corporation Yard stage (Barcombe Mills flow & Newhaven tide hydrographs)

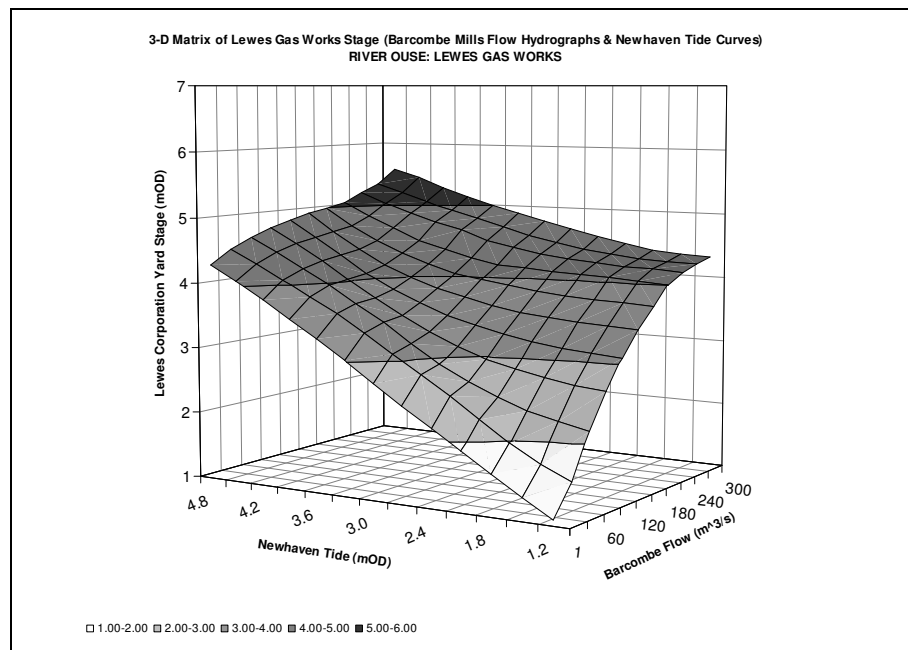


Figure 5.8 3-dimensional matrix plot of Lewes Gas Works stage (Barcombe Mills flow & Newhaven tide hydrographs)

5.4.4 Structure Function Contours

Structure function stage contours (Hawkes, 2004 and Meadowcroft *et al.*, 2004) were generated from the structure function matrices, providing a simplified graphical method of relating river flow and sea level to resultant stage (mAOD). Figure 5.9 and Figure 5.10 show the generated structure function stage contours at Lewes Corporation Yard and Lewes Gas Works, each also containing scatter plots of simultaneously recorded observations at Barcombe Mills and Newhaven (1982 to 2006) to demonstrate the range of typical combinations of river flow and sea level, together with intermediate stage at the two Lewes sites.

The contrast of the structure function stage contours at Lewes Corporation Yard and Lewes Gas Works demonstrates the relative affects of sea level and river flow on stage at different locations. Despite their close proximity (approx 0.5km), the contours show that river flow has a greater impact on resultant extreme water levels at Lewes Corporation Yard than at the downstream Lewes Gas Works location due to the increased flood magnitudes.

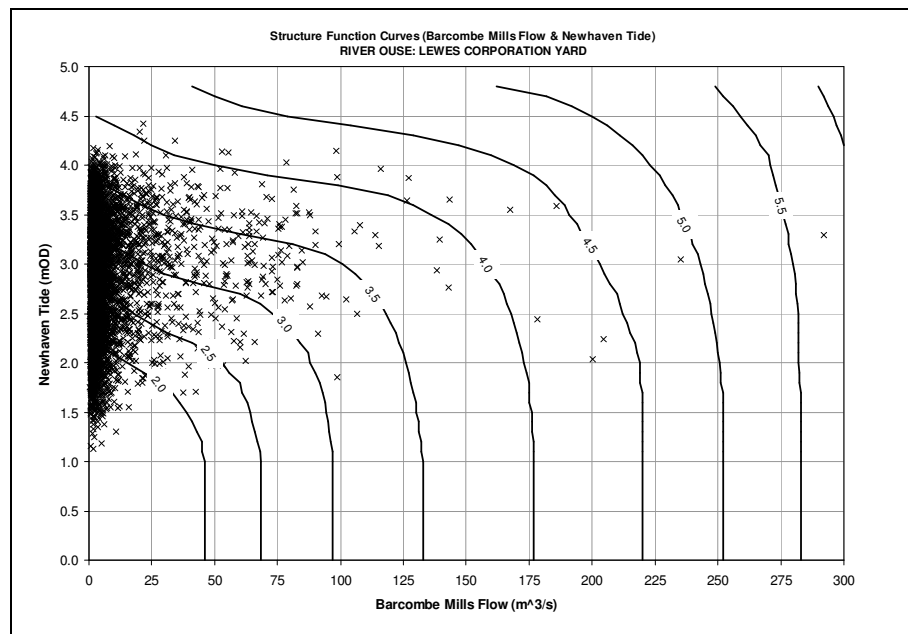


Figure 5.9 Structure function stage contour curves (mAOD) at Lewes Corporation Yard with simultaneous daily maxima observations of Barcombe Mills flow and Newhaven sea level (1982-2006)

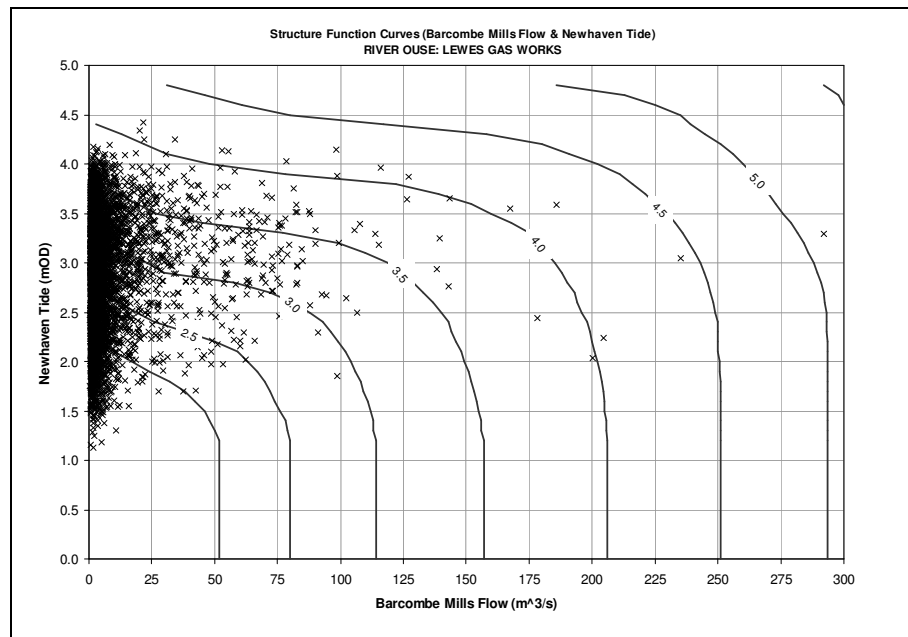


Figure 5.10 Structure function stage contour curves (mAOD) at Lewes Gas Works with simultaneous daily maxima observations of Barcombe Mills flow and Newhaven sea level (1982-2006)

5.4.5 Historical Emulation Calibration

The structure function matrices and contours were used to generate a historically emulated series to calibrate the structure function method (e.g. Jones, 1998). The historical emulation approach used simultaneous Barcombe Mills daily maxima flow and Newhaven sea level series (1982 to 2006) to select, via the structure functions matrices, corresponding daily maxima values at Lewes Corporation Yard and Lewes Gas Works - thus termed emulation rather than simulation.

Although the emulated time series may be regarded as a simplification of the continuous simulation technique (section 5.3), the extracted values at Lewes were still simultaneously and historically tied to the river flow and sea levels observed at Barcombe Mills and Newhaven. These were produced without the need for further time-consuming hydraulic model simulations. The emulation achieved a high level of correlation of 0.9721 with the December 2005 to May 2006 recorded series at Lewes Corporation Yard (see Table 5.7). The differentials showed that, in comparison with the continuously simulated time series at Lewes Corporation Yard, the emulation series slightly over-estimated the resultant stage by approximately 0.04m. This was expected as the emulation technique assumed that the observed daily maxima flow and sea level

values occur simultaneously to produce the worst-case resultant stage, which is somewhat conservative. In reality, the daily maxima values may occur up to 24-hours apart.

Table 5.7 Calibration of daily maxima emulated stage with simulated / recorded daily maxima stage at Lewes Corporation Yard

Calibration Period	Sample Size (days)	Average Diff. (m)	Max. Diff. (m)	Min. Diff. (m)	R ²
Jun 1982 - May 2006*	5919 (68%)	0.02	0.60	-0.50	0.9757 ($P < 0.01$)
Jun 2000 - May 2006	1455 (67%)	-0.02	1.36	-1.05	0.9040 ($P = 0.0645$)
Dec 2005 - May 2006	175 (100%)	-0.02	0.36	-0.34	0.9721 ($P = 0.0454$)

*Calibration between emulated and continuously simulated series

The successful calibration of the structure function approach provided a tested method by which peak stage at the point of interest (Lewes) could be obtained for *any* combination of river flow and sea level, without the need for simultaneously observed time series.

5.5 Discussion

The continuous simulation exercise provided an accurate and consistent time-series at Lewes when calibrated with the recorded series at Lewes Corporation Yard and Lewes Gas Works. The process was limited however by the duration of the two simultaneous input flow and sea level data series.

The structure function methods also provided a viable means of calculating extreme water levels at the primary case study locations of Lewes Corporation Yard and Lewes Gas Works for any combination of river flow and sea level at Barcombe Mills and Newhaven, without the limitations of simultaneous datasets. Jones (1998) however commented that such approaches involve considerable simplifications of the statistical and physical aspects of the real-world. Whilst this was true to some degree, the errors were minimised as far as possible and correlation with historical datasets at Lewes was undertaken at each stage.

The lack of a long reliable historical data series at Lewes however meant that calibration of the model and the subsequent calibrations was a continual problem. A further limitation was that the available calibration periods only contained a few historical extreme events. It was assumed therefore that the river response at the point of interest (Lewes) was similar for extreme events as it is for the more everyday occurring sea level and flow combinations.

The shape of the representative hydrographs and the estimation of water level at Lewes generated for any flow / sea level pair also involved considerable simplifications, although the introduction of the optimum input hydrographs was selected so as to produce the maximum water level possible. This provided slightly conservative values which compensated for any underestimation in the hydrographs and peak levels.

6 EXTREME VALUE ANALYSIS & FLOOD FREQUENCY ESTIMATION

6.1 Introduction

The Ouse catchment has historically been subjected to several extreme flood events, the most recent occurring in October 2000. Since 1830, there have been 45 calendar years during which a flood event has been reported in Lewes, which equates to a frequency of a flood occurring almost once in every three years. However, despite the long history of flooding in the catchment, information is remarkably scant with only the 1960 (Lewes), 1975 (Lewes) and 2000 (Uckfield and Lewes) floods well documented. Much of the historical information is brief, without the magnitude, duration, extent or number of properties flooded recorded, leaving an accurate frequency analysis of flood events a complex task.

Terms such as “the biggest tide since records began” or “the highest river flow since 1960” are frequently used to describe extreme flood events in Lewes, but they do not accurately describe their relative magnitude or rarity. An accurate determination of an extreme event is one which occurs outside of the normal expected parameters with the severity categorised by its magnitude, either through observed water levels or flow measurements. The frequency of such events relates the magnitude of the observation to how likely it is to occur. For any single hydrologic variable, calculation of the frequency of extreme levels through the use of historical records (such as annual maxima values) and probability distributions is a straightforward exercise.

The frequency of extreme water levels within the tidal riverine environments of rivers is however more difficult to categorise due to the combination of two (or more) variables including sea level and fluvial flow. Tides are generated by astronomical forces that can be predicted through the harmonic analysis of recorded sea levels. But in rivers directly connected to the sea, such as the River Ouse at Lewes, the variation of observed stage along the rivers depends on sea levels at the river mouth and upstream fluvial discharges. The interaction between sea levels and fluvial flows ultimately results in the raising of the mean water levels within the tidal reach. When a high tide coincides with a high fluvial discharge, the risk of flooding is increased (Vongvisessomjai and Rojanakamthorn, 1989).

The interaction of tides and river flows in the tidal reach of the Ouse is currently poorly defined due to the complex nature of the dynamic multivariate system and limited historical records. Defining the frequencies, timings and interactions between the hydrologic variables can establish how they combine to produce extreme flood events before probabilities of occurrence can be determined.

To better understand the interaction of tides and river flows within the tidal reach of the Ouse, this chapter uses historical, synthesised and simulated data to develop and quantitatively describe an appropriate approach. AMAX and POT series were extracted from the higher resolution datasets to estimate return periods and peak magnitudes. A joint exceedance analysis was performed comparing simultaneous extreme observations across the catchment and probabilities calculated of their joint occurrence.

6.2 Annual Maxima (AMAX) Extraction & Return Periods

6.2.1 Upper Ouse & Uck Fluvial AMAX Series

6.2.1.1 Return Periods

AMAX values were extracted from the Gold Bridge, Isfield Weir, Clappers Bridge and Old Ship historical records and return periods (Table 6.1) estimated using a General Extreme Value (GEV) distribution. Full results of the AMAX, distribution fitting and return period estimates can be found in Appendix C.1.

The duration of the four recorded AMAX series ranged from 35 to 46 years, with Gold Bridge and Isfield Weir providing both the longest duration and greatest total proportion of gauged flow from the upper sub-catchments. All four series provided reliable return period estimates up to 50 years, but higher return periods in the upper portion of the flood frequency curve displayed increased statistical uncertainty due to the inclusion of the 12th October 2000 extreme flood event record.

MacDonald (2004) undertook a fluvial flood analysis of Isfield Weir on the River Uck for flood defence design for Uckfield, a town in the upper catchment which saw extensive flooding during the 12th October 2000 flood event. Using AMAX data up to 2002, the 100 year return was estimated as 131m³/s for Isfield Weir using a General Logistic distribution. This is close to the estimated magnitude of 120m³/s calculated in

Table 6.1. The difference can be accounted for by the selection of a different distribution (the GEV distribution displayed a more accurate goodness-of-fit parameter than General Logistic distribution using Anderson Darling) and the three additional years added to the AMAX series since the 2004 study.

Table 6.1 Estimated fluvial flow return period magnitudes for the Upper Ouse and Uck sub-catchments

		GOLD BRIDGE 1959-2005		ISFIELD WEIR 1964-2005		CLAPPERS BRIDGE 1969-2005		OLD SHIP 1969-2005	
		Flow (m³/s)	S_E	Flow (m³/s)	S_E	Flow (m³/s)	S_E	Flow (m³/s)	S_E
Return Period (years) & Estimated Fluvial Flow (m³/s) Magnitude	2	31.87	±2.53	36.69	±2.44	14.70	±0.72	3.59	±0.42
	5	48.63	±4.01	54.35	±4.85	18.02	±0.81	5.55	±0.66
	10	61.69	±6.50	67.69	±8.72	19.72	±1.02	6.99	±0.91
	25	80.84	±11.96	86.69	±16.18	21.43	±1.37	8.98	±1.61
	50	97.23	±18.06	102.51	±24.46	22.44	±1.64	10.60	±2.43
	100	115.61	±26.62	119.85	±34.61	23.28	±1.96	12.34	±3.40
	200	136.28	±37.77	138.90	±47.44	23.96	±2.31	14.22	±4.91

6.2.2 Middle Ouse Fluvial AMAX Series

6.2.2.1 Extending the Barcombe Mills AMAX Series

An AMAX series was extracted from the synthesised Barcombe Mills flow (1981-2005) dataset (section 5.2.7.1). It was found to be statistically unsuitable for estimating magnitudes for high annual return periods due to its limited duration of 25 years and the inclusion of the extreme 2000 flood event. To estimate higher return periods accurately, the synthesised AMAX series was required to be extended using other existing data sources from Barcombe Mills and the upstream upper catchment gauges.

Close examination of the historical flow series at Barcombe selected a reliable set of monthly maxima flow observations from Barcombe Mills Weir (1957-1968), prior to channel alterations at the Barcombe site which subsequently affected gauging performance. An additional 12 AMAX observations were extracted and cross-referenced

with simultaneous upstream gauge observations and were added to the Barcombe Mills synthesised AMAX series, producing a partial series from 1957-1968 and 1981-2005.

Environment Agency (2002) studied the Barcombe Mills series to produce flood hydrographs with associated return periods as part of the Sussex Ouse Flood Management Strategy. An AMAX stage series (1952-2000) was also derived using the partial flow series at Barcombe Mills, total 24-Hour runoff magnitude estimates for the upper catchment, the reliable upstream flow series from the Gold Bridge gauge and rating curves for the Barcombe Mills complex which converted flow to stage.

Environment Agency (2002) derived AMAX stage series for Barcombe Mills was statistically correlated with the recorded flow observations (1957-1968) and part of the synthesised (1981-2000) flow observations taken on the same water-day to produce a rating curve. The two series displayed a near-linear relationship with an R^2 value of 0.8641 and a P value <0.05 . The exercise identified a single outlier where stage and synthesised flow did not correlate (28/05/2000 with an estimated stage of 6.10m and synthesised flow of $178.31\text{m}^3/\text{s}$). The stage magnitude was cross-checked with flow observations from the upper gauges and downstream stage at Lewes Corporation Yard and was found to be unrepresentative of the other observations for that event. Historical records also noted the event as localised flooding was reported in parts of the catchment. It was concluded that the stage estimate was too low and the outlying observational pair deleted. The regression analysis was repeated without the 28/05/2000 event (Figure 6.1), producing an improved rating curve with an R^2 of 0.9351 and a significant P value <0.01 .

The equation of $y = 137.6x - 740.36$ from the stage and flow series was used to infill and extend the Barcombe Mills AMAX flow series for the remaining duration of the stage series (Figure 6.2). The rating curve of stage and flow produced a final R^2 of 0.9442 and a significant P value <0.01 for the period of 1952-2000. The AMAX flow series was then completed using synthesised data up to 2005, producing a complete series of 53 AMAX values (Figure 6.3).

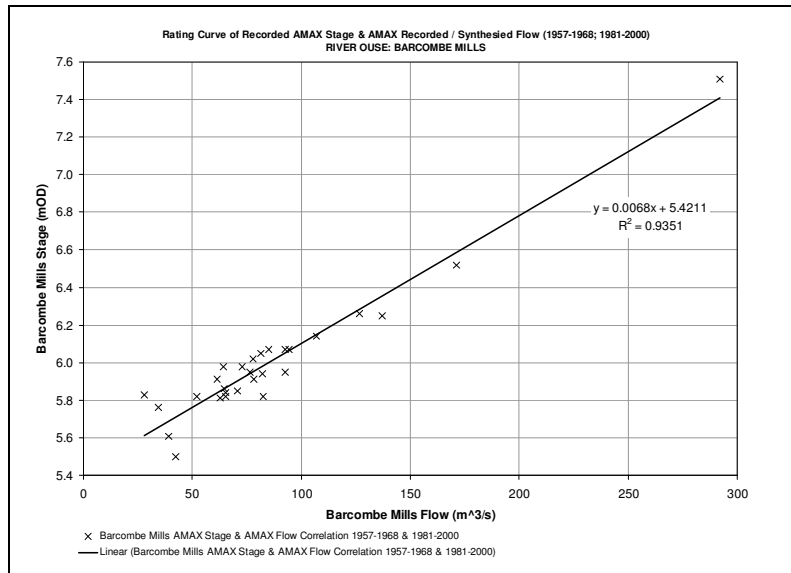


Figure 6.1 Rating Curve of Barcombe Mills AMAX stage & recorded/synthesised flow series observed on the same day (1957-1968; 1981-2000)

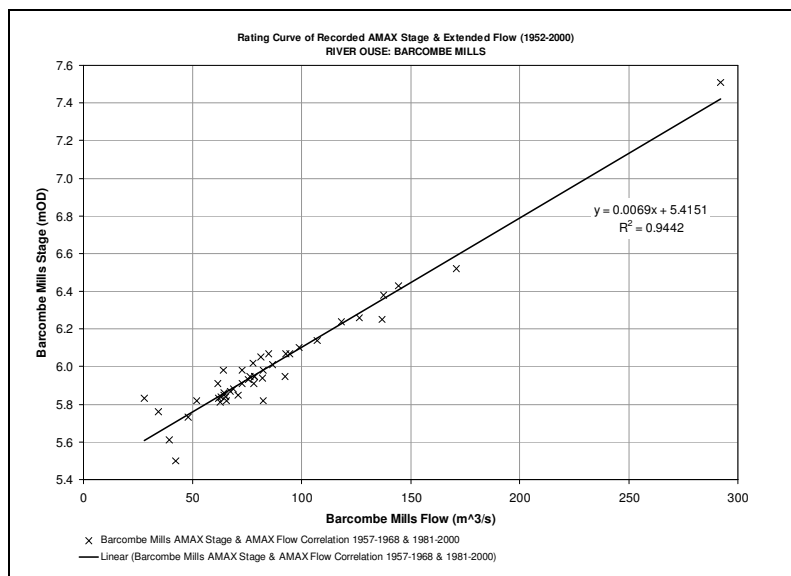


Figure 6.2 Rating Curve of Barcombe Mills stage & extended flow AMAX series (1952-2000)

The recorded / extended portion of the Barcombe Mills AMAX flow series (1952-1980) was cross-referenced with corresponding maxima values observed at the four upstream fluvial flow gauges (see Appendix C.2). In nearly all cases, the AMAX observations at Barcombe Mills correlated with a significant (and in many cases an AMAX) flow observation at the four upstream gauges. Gold Bridge displayed the highest correlation with 70% of AMAX values recorded at Gold Bridge coinciding with an AMAX observation at Barcombe Mills.

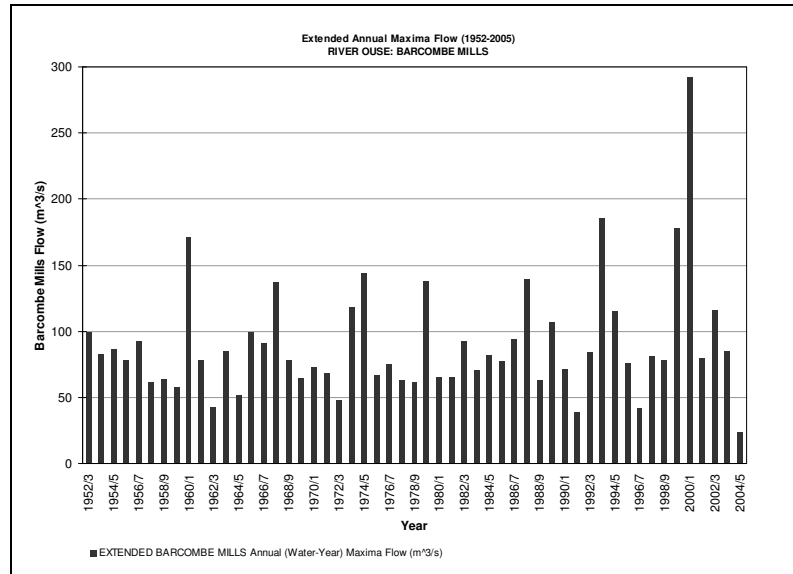


Figure 6.3 Extended Barcombe Mills flow AMAX series (1952-2005)

6.2.2.2 Return Periods

AMAX values were used from the synthesised and extended Barcombe Mills AMAX flow series to calculate return periods using a GEV distribution. The flow magnitude estimates for the synthesised and extended Barcombe Mills flow series produced differing levels of statistical accuracy (Table 6.2). The additional 29 years of AMAX values in the extended flow series (see section 6.2.2.1) increased the statistical viability of the flood frequency curve and return periods.

The original synthesised AMAX flow series (1981-2005) produced high flow magnitudes with significant standard errors for the high return period estimates, suggesting statistical uncertainty over the validity of the results. The standard errors were reduced by more than 50% by the extended Barcombe Mills AMAX flow series (1952-2005) with flow magnitudes also reducing markedly. Full results of the annual maxima extraction, distribution fitting and return period estimates can be found in Appendix C.2.

Table 6.2 Estimated fluvial stage & flow return period magnitudes for the Middle Ouse sub-catchment

		SYNTHESISED BARCOMBE MILLS Flow 1981-2005		EXTENDED BARCOMBE MILLS Flow 1952-2005	
		Flow (m³/s)	S_E	Flow (m³/s)	S_E
Return Period (years) & Estimated Fluvial Stage (mAOD) & Flow (m³/s) Magnitude	2	84.84	±7.60	81.68	±4.17
	5	127.16	±13.80	116.02	±7.95
	10	158.50	±24.56	140.86	±13.26
	25	202.33	±46.60	174.86	±21.94
	50	238.21	±66.78	202.13	±32.24
	100	276.94	±100.5	231.04	±46.44
	200	318.87	±139.1	261.80	±62.79

6.2.3 Lower Ouse Stage & Newhaven Sea Level AMAX Series

6.2.3.1 Extending the Lewes Corporation Yard AMAX Series

Unlike Barcombe Mills, a fairly consistent recorded AMAX stage series exists for the Lewes Corporation Yard gauge. However, as section 4.5.3 noted, the reliability of data recorded at Lewes Corporation Yard gauge was questionable. Environment Agency, (*pers. comm.*, 2003) concluded that the recorded Corporation Yard chart dataset was reasonably complete and accurate from 1953-1988 when the chart gauge was replaced with a telemetry gauge. After the installation of the new gauge, the reliability and accuracy dropped with datum shifts and mechanical failures creating significant periods of missing or unreliable data, leading to the latter portion of the recorded dataset being infilled with a simulated stage dataset where necessary. A rating curve of the recorded AMAX stage series at Lewes Corporation Yard (1982-2005) and an AMAX stage series extracted from the continuous simulation of stage at Lewes Corporation Yard generated using the HEC-RAS model for the same period (see section 5.3) however showed a significant 1:1 correlation (Figure 6.4) with an R^2 of 0.9575 and a P value <0.01

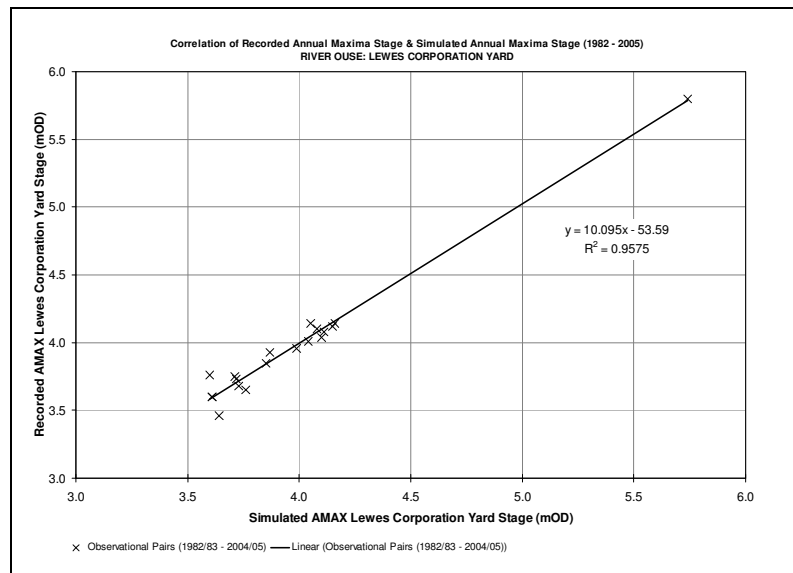


Figure 6.4 Rating curve of annual maxima recorded & simulated stage at Lewes Corporation Yard (1982-2005)

Several of the AMAX stage observations between 1982-2005 were noted as differing in magnitude. The recorded AMAX stage series was found to be 0.04m lower than the simulated AMAX stage series on average, with a range of 0.24m for the 24 AMAX observations. Each of the recorded AMAX readings was cross-checked with tidal and fluvial observations at Barcombe Mills and Newhaven respectively to assess their reliability. Any recorded stage values that were inconsistent with the simultaneous sea level / flow observations were removed from the recorded AMAX stage series and infilled with simulated AMAX stage. This created a complete AMAX stage series at Lewes Corporation Yard from 1953-2005 (Appendix C.3).

6.2.3.2 Extending the Newhaven AMAX Series

AMAX observations were extracted from chart data records observed at the EA Newhaven gauge for the period 1913-1990. Due to a poor history of tidal observations at the EA Newhaven gauge since 1990 (see section 4.5.4.1), no data was utilised after this date. AMAX observations from the Proudman Newhaven telemetry gauge from 1991 onwards were added to the EA annual maxima series to create an annual maxima series dating from 1913 to 2006 (Figure 6.5 and Appendix C.3).

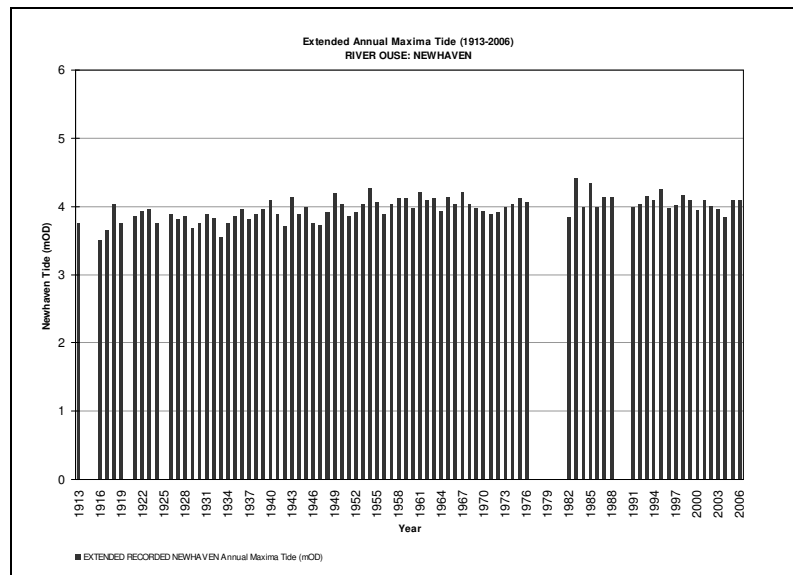


Figure 6.5 Extended Newhaven AMAX series (1913-2006)

Appendix C.3 shows the probability of exceedance of the highest astronomical tide (HAT), estimated to be 4.03m AOD at Newhaven, to be 39% in any given year, calculated from the extended AMAX observations (1913-2006).

6.2.3.3 Return Periods

AMAX observations were used from the simulated and extended stage series for Lewes Corporation Yard, together with the historical Lewes Gas Works and Newhaven AMAX series to estimate return periods using the GEV distributions. As with the Barcombe Mills AMAX analysis, the stage magnitude estimates for the simulated and extended Lewes Corporation yard series produced differing levels of statistical accuracy (Table 6.3). The additional 29 years of AMAX values from the recorded stage series at Lewes dramatically increased the statistical results of the flood frequency curve and return period estimate approach.

The simulated AMAX stage series for Lewes Corporation Yard (1982-2005) produced high stage magnitudes with significant standard errors for longest return periods (up to 3.8m for the 1:200 year return period), suggesting statistical uncertainty over the validity of the results. These standard errors were reduced by approximately 70% with the inclusion of the recorded AMAX flow series creating the 1953-2005 series. The standard errors were however still significant ($\pm 1.15\text{m}$ for the 1:200 year return period), providing a degree of unreliability in the stage magnitudes at Lewes. However, the 1:50 year return period which produce a stage magnitude around the critical river defence overtopping

height (typically 5mAOD in Lewes) produced a lower standard error of ± 0.46 which would have far less impact on any errors created by the relatively short AMAX series.

Table 6.3 Estimated stage & sea level return period magnitudes for the Lower Ouse sub-catchment & Newhaven

		SIMULATED LEWES CORP YARD Stage 1982-2005		EXTENDED LEWES CORP YARD Stage 1953-2005		LEWES GAS WORKS Stage 1953-2000		NEWHAVEN Sea level 1913-2005	
		Stage mAOD	S _E	Stage mAOD	S _E	Stage mAOD	S _E	Stage mAOD	S _E
Return Period (years) & Estimated Stage & Sea level (mAOD) Magnitude	2	3.83	± 0.09	3.79	± 0.03	3.83	± 0.03	3.97	± 0.02
	5	4.15	± 0.14	4.00	± 0.07	4.01	± 0.05	4.12	± 0.02
	10	4.48	± 0.44	4.21	± 0.13	4.15	± 0.08	4.20	± 0.02
	25	5.09	± 1.20	4.57	± 0.27	4.34	± 0.17	4.27	± 0.03
	50	5.76	± 1.84	4.93	± 0.46	4.51	± 0.26	4.32	± 0.04
	100	6.67	± 2.64	5.40	± 0.75	4.75	± 0.36	4.35	± 0.05
	200	7.93	± 3.80	6.01	± 1.15	4.99	± 0.49	4.38	± 0.06

This effect is reduced however for the observed AMAX series at Lewes Gas Works gauge further downstream. This is emphasised by the estimated stage differential between the highest return periods at the two Lewes gauges, with Corporation Yard experiencing higher (extreme) stage estimates than Gas Works due to their relative positions upstream and downstream of Cliffe Bridge (Figure 6.6). Corporation Yard experiences the full magnitude of a fluvial flood event, whereas Gas Works is partially protected by Cliffe Bridge which historically holds back flood waters and pushes flows out of bank prior to them reaching Gas Works. This demonstrated the affect of the complex system hydrodynamics (especially the constriction of Cliffe Bridge) and the interaction between sea levels and fluvial flows at Lewes. It also illustrates the sensitivity of the distributions to the extreme observations from the 2000 flood which affected the Corporation Yard gauge more significantly than Gas Works.

The estimated stage magnitudes for the short return periods (2 and 5 years) are marginally lower at Lewes than at the Newhaven gauge at the mouth of the Rover Ouse. This can be accounted for by the modelled sea level drop of 0.27m from Newhaven to

the upstream gauges at Lewes. With longer return periods, the estimated stage magnitudes were noticeably higher at both Lewes gauges than at Newhaven. This indicates the increasing importance of fluvial flows as the predominant cause of extreme level estimates at Lewes for longer return periods.

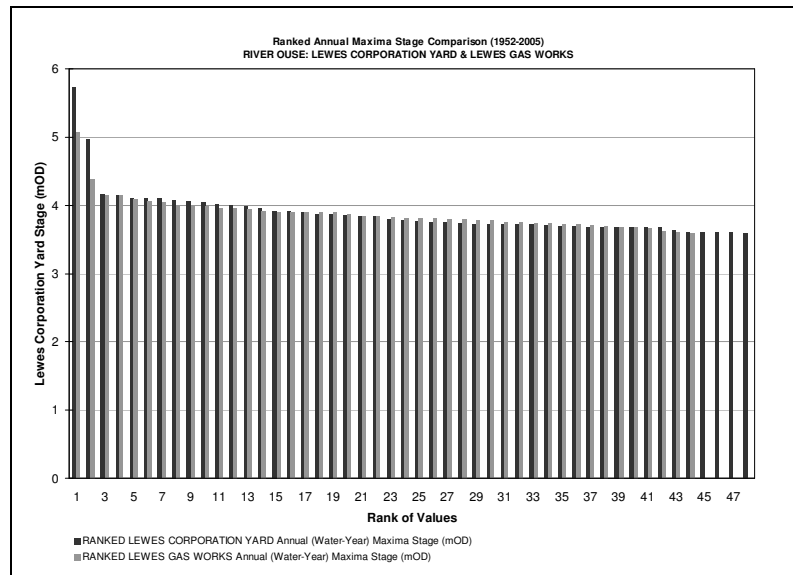


Figure 6.6 Ranked AMAX stage at Lewes Corporation Yard & Lewes Gas Works (1952-2005)

The Newhaven sea level AMAX series itself provided a more consistent and reliable AMAX series than the two Lewes series, containing 83 AMAX observations dating back to 1913. Environment Agency (2004) quality checked the Newhaven AMAX series and found it to be complete and accurate (Appendix C.3.). The long AMAX series also identified trends in the sea level observations (Figure 6.7). There is an increase in observed sea levels observed at Newhaven since 1913 which highlights rising sea levels and possibly changes in instrumentation and datums. For example, the two most extreme observations occur just after an upgrade of the tidal instruments at Newhaven in 1982. This is believed to reflect the more accurate observations using the new equipment, although with rising sea levels this may simply be coincidental.

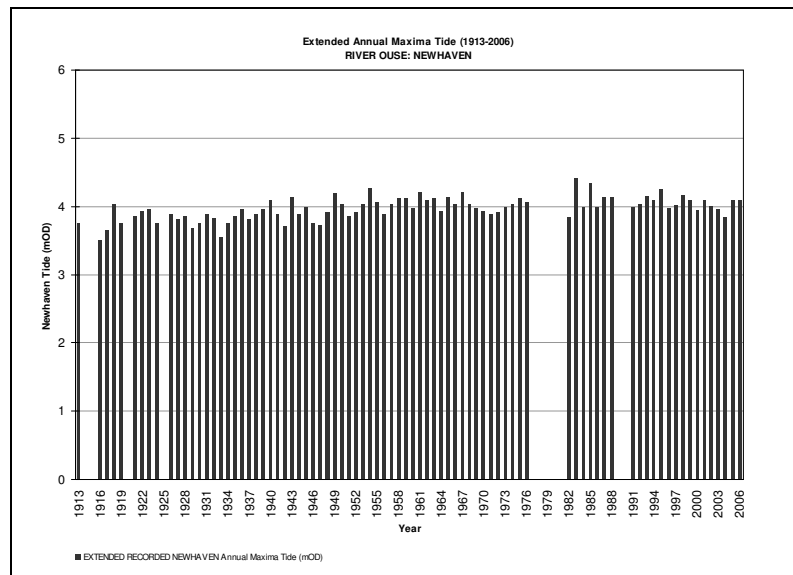


Figure 6.7 Ranked AMAX sea level at Newhaven (1913-2005)

6.2.4 Newhaven Surge AMAX Series

6.2.4.1 Return Periods

An AMAX series was extracted from the Newhaven sea level gauge series of surge (the maximum differential between recorded and predicted tidal observations). A similar AMAX series was also extracted of the surge at high tide (the observed difference between recorded and predicted tidal observations at high tide) using the 15-Min resolution Newhaven dataset (1981-2005). Digitised records at this temporal resolution do not exist prior to this date.

Return periods were estimated for both surge datasets using the GEV distribution method (Table 6.4). The surge values display similar magnitudes for the same return periods with almost identical statistical standard errors.

These results highlight the independent nature of the surge from the predicted astronomical tide. Figure 6.8 however illustrates the limited difference between the daily maximum surge and daily surge at high tide datasets, producing an average 0.1m differential. For short return periods (up to 25 years), this trend is mirrored between the two AMAX series, with surge at high tide producing slightly lower magnitudes than the daily maximum surge series. At higher return periods (greater than 25 years), the trend is reversed with the surge at high tide series producing magnitudes higher than the daily maximum surge series.

Table 6.4 Estimated surge & surge at high tide return period magnitudes for Newhaven

		NEWHAVEN Daily Maximum Surge 1981-2005		NEWHAVEN Surge at High Tide 1981-2005	
		Surge (m)	S_E	Surge (m)	S_E
Return Period (years) & Estimated Surge (m) Magnitude	2	0.75	± 0.05	0.61	± 0.05
	5	0.92	± 0.06	0.78	± 0.07
	10	1.03	± 0.07	0.91	± 0.09
	25	1.18	± 0.19	1.09	± 0.18
	50	1.30	± 0.28	1.24	± 0.28
	100	1.42	± 0.39	1.41	± 0.42
	200	1.55	± 0.50	1.60	± 0.58

It was concluded that surge magnitudes beyond a 25 year return period need to be treated with caution. For the purposed of this research, the daily maximum surge dataset was utilised throughout due to its close relationship with surge at high tide. Full results of the annual maxima extraction, distribution fitting and return period estimates can be found in Appendix C.4.

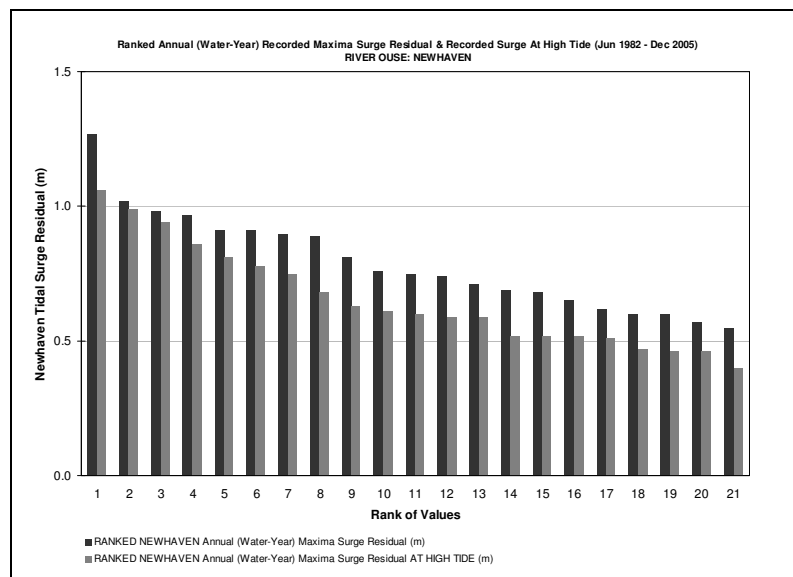


Figure 6.8 Ranked AMAX maximum surge & surge at high tide at Newhaven (1981-2005)

6.3 Independent Peaks-Over-Threshold (POT) Selection

6.3.1 Threshold Selection

The daily maxima data series for Barcombe Mills flow, Lewes Corporation Yard stage, Newhaven recorded sea level and Newhaven surge and were analysed for peaks-over-threshold (POT) exceedances (Appendix D.1). Five POT series were calculated for each location using threshold values selected as:

- 95th, 98th and 99th percentiles,
- an average of 5 POT exceedances per year based on the whole dataset, and
- selecting the lowest AMAX value as the threshold level.

To ensure the identification of independent POT events, exceedances were selected on the same day and within 3 day window (± 1 day from the day of the highest POT event) where only the peak value during this period was selected. Although it was not possible to take other factors into account, such as high groundwater levels from a previous POT event, the process enabled the POT series to represent extremal nature of flooding events as accurately as possible.

6.3.2 Threshold Magnitudes

The independent POT exceedance selection process calculated five POT series for each data series through the use of different threshold levels (Appendix D.1). The percentile approach (99%, 98% and 95%) and 5 exceedances per year threshold approach selected values at Barcombe Mills ranging from 23.73m³/s at the 95th percentile to 74.84m³/s at the 99th percentile, demonstrating the wide spread of extreme flow values historically recorded at the site. The location of Barcombe Mills at the boundary between the upper catchment and the tidal reach of the Ouse determined the nature of extreme river flows without the influence of sea level which is felt further downstream at Lewes. At Lewes Corporation Yard, the range of the stage was 3.43mAOD calculated at the 95th percentile threshold value up to 3.74mAOD for the 99th percentile.

At Newhaven, the range of the sea level was close to Lewes but as expected displayed higher values with 3.74mAOD calculated at the 95th percentile threshold value up to 3.95mAOD for the 99th percentile, reflecting the tidal head loss of 0.27m from Newhaven to Lewes.

The results of the threshold selection which used the lowest AMAX value as the threshold value produced inconsistent results. The number of calculated exceedances per year varied between each dataset due to the differing affects of meteorological events. The POT series calculated from the lowest AMAX were particularly affected by unusually dry winter seasons (such as 1999 and 2005) which produced an unrealistically low AMAX value, creating an overly large and non-extreme POT series.

6.3.3 Seasonality Effects

Bayliss and Jones (1993) analysed over 800 UK POT flood records, including the four upper Ouse catchment gauges Gold Bridge, Isfield Weir, Clappers Bridge and Old Ship, to assess the affects of seasonality on POT exceedances. Using an average of 5 POT exceedance events per year, the results indicated that for medium to large catchments to the south and east England, including the Ouse, the occurrence of floods was highest between November and January, because a large percentage of the catchment needs to be at or near field capacity before high runoff and flooding can take place. Typically, the result was a mid-winter onset and a short flood season. An updated analysis of the same gauges using identical threshold selections and corrected historical POT records extended up to 2005 produced more accurate results with the highest occurrence of floods in December or January across the four gauges (Appendix D.1).

Barcombe Mills displayed similar strong seasonality affects as the upper catchment gauges (Figure 6.9), with January being the modal month of POT river flow exceedance. October to March contained the majority of POT events, with the summer months containing few POT exceedances. At Lewes Corporation Yard, the affects of seasonality were still evident in the higher number of POT stage exceedances in the winter months (Figure 6.10). However, the interaction with sea level widened the spread of POT stage exceedances from September through to April and reduced the percentages of exceedance in each month.

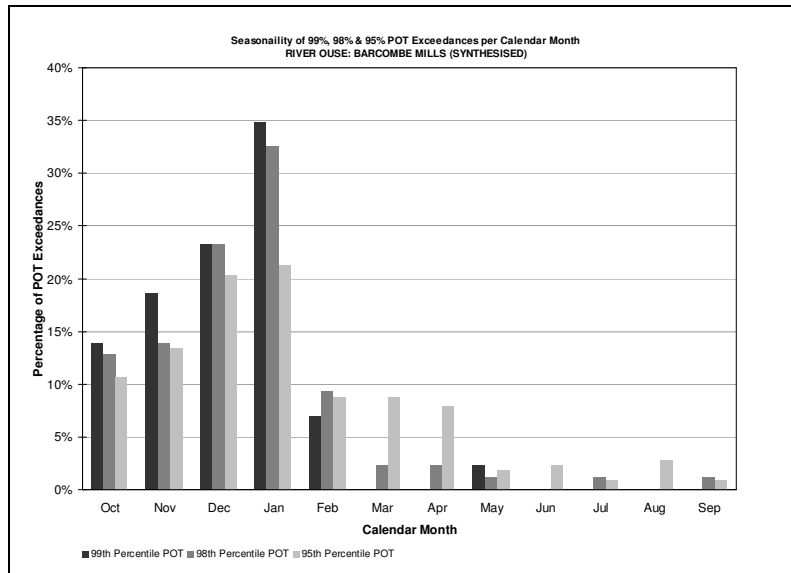


Figure 6.9 Seasonality of 99th, 98th & 95th percentile POT river flow exceedances per calendar month at Barcombe Mills

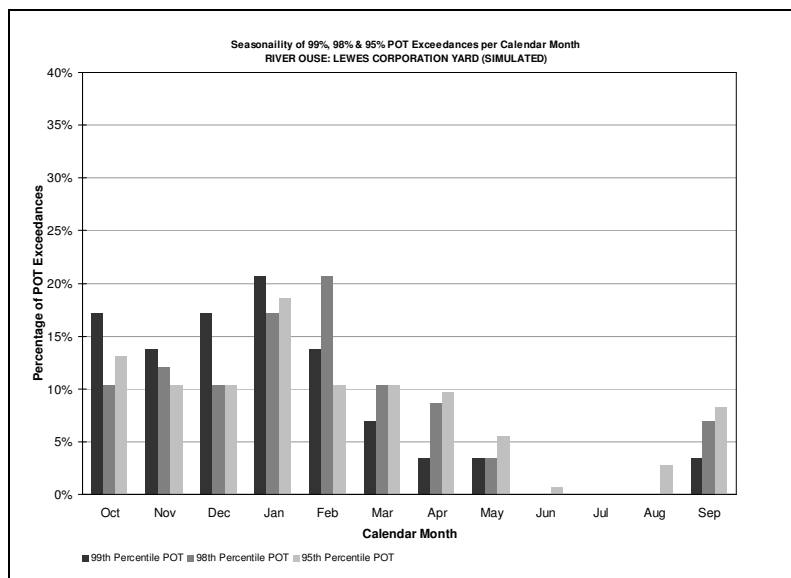


Figure 6.10 Seasonality of 99th, 98th & 95th percentile POT stage exceedances per calendar month at Lewes Corporation Yard

The same analysis at Newhaven reflected the semidiurnal nature of the astronomically driven tide rather than the seasonal and meteorological effects driving rainfall and river flows (Figure 6.11). The highest percentage of POT spring tides occurred in March and September/October. This may strongly affect any statistical dependence between predicted tide and river flow, with expectedly higher river flows occurring in Autumn and Spring at the same time as the predicted March and September spring tides. Surge

also displayed strong seasonality with exceedances closely following the river flow results shown at Barcombe Mills, with peak POT exceedance occurrences in January.

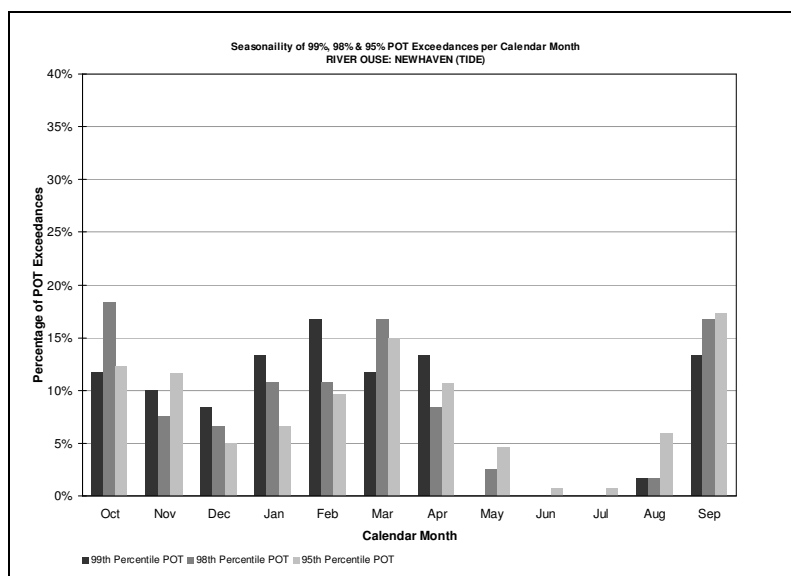


Figure 6.11 Seasonality of 99th, 98th & 95th percentile POT sea level exceedances per calendar month at Newhaven

6.4 Multivariate Extreme Value Analysis

6.4.1 Joint AMAX Occurrences

A joint AMAX occurrence analysis was undertaken to assess if historical AMAX observations occurred simultaneously between selected pairs (or groups) of gauges in the Ouse catchment (Table 6.5).

Although the AMAX series selected one observation to represent each water-year, the results illustrate the number of times the most extreme values per year (e.g. an AMAX value) occurred simultaneously at more than one location. Due to the size of the catchment, a meteorological event can produce peak values at different locations outside of a single fixed 24-hour period of a water-day. A low pressure weather system can cause increased sea levels and rainfall simultaneously, but different parts of the catchment may react slower than others to rainfall due to varying groundwater conditions, causing river levels to peak at different times (or days) than sea levels. This can be confused further by time-lags experienced in the river channel. Similarly, a flood magnitude may be observed at one location at the end of one water-day but which may be observed at the start of the

following water-day at another location; both are within the same 24-hour period but not the same 09:00 to 09:00 water-day. As such, the AMAX analysis compared observations which occurred both simultaneously within the same day and within a 3 day (± 1 day) window. The latter produced results which covered the true nature of extreme observations throughout the catchment.

Table 6.5 Joint AMAX observations at station pairs throughout the Ouse Catchment

Gauge Grouping	Joint AMAX Observations (years)	Same Day Joint AMAX Observations		± 1 Day Joint AMAX Observations	
		(days)	(%)	(days)	(%)
Gold Br., Isfield, Clappers Br. & Old Ship	35	6	17%	14	40%
Gold Br., Isfield, Clappers Br., Old Ship & Barcombe	35	6	17%	14	40%
Barcombe Mills & Lewes Corporation Yard	48	14	29%	16	33%
Barcombe Mills & Lewes Gas Works	44	6	14%	6	14%
Barcombe Mills & Newhaven (Sea Level)	22	0	0%	0	0%
Barcombe Mills & Newhaven (Surge)	21	0	0%	1	5%
Lewes Corporation Yard & Lewes Gas Works	44	18	41%	23	52%
Lewes Corporation Yard & Newhaven (Sea level)	19	6	32%	7	37%
Lewes Corporation Yard & Newhaven (Surge)	19	4	21%	4	21%
Lewes Gas Works & Newhaven (Sea level)	15	2	13%	5	33%
Lewes Gas Works & Newhaven (Surge)	15	1	7%	2	13%
Newhaven (Sea level) & (Predicted Sea level)	19	3	16%	4	21%
Newhaven (Sea level) & (Surge)	21	3	14%	3	14%

The upper catchment gauges of Gold Bridge, Isfield Weir, Clappers Bridge and Old Ship display an expectedly high percentage of AMAX observations occurring simultaneously,

with 40% of AMAX values observed simultaneously at all four gauges using a three day window. This same percentage was found when the Barcombe Mills gauge is added to the grouping, clearly showing the response of flow magnitudes at Barcombe Mills to extreme large scale (i.e. catchment-wide) rainfall events.

This affect is felt downstream into the tidal reaches of the lower Ouse at Lewes where 33% of AMAX values observed at Barcombe Mills coincide with AMAX values observed at Lewes Corporation Yard. A similar percentage of simultaneous AMAX observations at Newhaven and Lewes Corporation Yard were also found, with 37% of AMAX values observed at Newhaven coinciding with AMAX values observed at Lewes Corporation Yard, demonstrating that extreme stage at Lewes Corporation Yard are caused by both sea level and fluvial flows. Appendix C.4 shows the simultaneous AMAX occurrences between Lewes Corporation Yard, Barcombe Mills and Newhaven.

The average return period of Lewes Corporation Yard AMAX levels, occurring at the same time at Barcombe Mills AMAX flows is 1:25 years, compared to 1:6 years for Lewes Corporation Yard and Newhaven. There are no recorded instances where AMAX values occur simultaneously at all three locations.

Approximately 0.7km downstream from Lewes Corporation Yard, the number of AMAX values observed simultaneously at Lewes Gas Works and Barcombe Mills drops significantly, where only 14% of AMAX values observed at Barcombe Mills coincide with AMAX values observed here. This can be accounted for by the constriction of Cliffe Bridge 175m upstream from the Gas Works gauge which seriously impedes fluvial flows through the town centre, creating a head loss downstream. This is justified by the higher percentage of AMAX values observed simultaneously at Newhaven and at Lewes Gas Works, with 33% of AMAX values observed simultaneously at both gauges. This suggests that extreme stage at Lewes Gas Works are caused predominantly by tidal flows from Newhaven rather than fluvial flows from Barcombe Mills.

When viewed together, the results for Lewes Corporation Yard and Lewes Gas Works show the highest percentage of simultaneous AMAX observations with 52% occurring at the same time at the two Lewes locations, although this was below what may have been expected when considering their close proximity. This demonstrates how the effects of sea level and river flow alter at different locations, which is caused predominantly by varied channel geometry and river structures such as Cliffe Bridge.

At Newhaven, only 21% of recorded AMAX sea levels actually occur at the same time as the predicted AMAX tides due to the variability caused by meteorologically-driven surge conditions.

6.4.2 Joint POT Exceedances

An extreme event analysis was undertaken to assess if joint POT exceedances observations occurred simultaneously at more than one location. The likelihood of joint occurrences and their relative impacts on water levels at the point of interest of Lewes was then calculated. Pairs of POT series, calculated using thresholds at the 95th, 98th and 99th percentiles (Appendix D.1) were selected, and the number of joint POT occurrences calculated both on the same day and within a 3 day (± 1 day) window. The resultant observational pairs were statistically correlated to assess the relationship between the relative magnitudes of the observational pairs and the likelihood of joint POT exceedance. Barcombe Mills flow and downstream Lewes Corporation Yard stage produced significant percentages of joint POT exceedance across the three threshold percentiles with results being fairly constant (Table 6.6). Between 20.3% and 25.7% of Barcombe POT exceedances occurred on the same day as Lewes POT exceedances, with a similar range of 22.4% to 31.0% of Lewes POT exceedances occurring on the same day as Barcombe POT exceedances. The percentages increased with the 3 day window where 29.3% to 37.9% of Lewes POT exceedances occurred within the same period as Barcombe POT exceedances.

Table 6.6 Joint POT exceedances at Barcombe Mills & Lewes Corporation Yard (1982-2005)

Gauge Grouping	Threshold Selection		Same Day Joint POT Exceedances		± 1 Day Joint POT Exceedances		R^2
	(%)	(value)	(days)	(%)	(days)	(%)	
Barcombe Mills Lewes Corp Yard	99%	74.84 m ³ /s	9	25.7%	11	31.4%	0.90 ($P=0.0323$)
		3.96 mOD		31.0%		37.9%	
Barcombe Mills Lewes Corp Yard	98%	52.14 m ³ /s	13	20.3%	17	26.6%	0.81 ($P=0.0454$)
		3.72 mOD		22.4%		29.3%	
Barcombe Mills Lewes Corp Yard	95%	23.73 m ³ /s	38	24.4%	53	34.0%	0.64 ($P=0.1760$)
		3.44 mOD		26.2%		36.6%	

The correlation analysis of the observational pairs revealed a close relationship between the magnitudes of the POT exceedances. At the 95th percentile, an R^2 value of 0.64 was calculated between Barcombe and Lewes POT series, which increased to 0.90 at the 99th percentile. Statistical correlation also improved with P values ranging from $P < 0.05$ to $P < 0.01$. This confirmed that stage magnitudes at Lewes are highly correlated with fluvial flows at Barcombe Mills, which increases as the observations become more extreme.

The same analysis between the pairs of Barcombe Mills flow and recorded sea level at Newhaven produced low percentages of joint POT exceedance (Table 6.7). The joint exceedance percentages were found to reduce as the threshold increased, with between 5.7% and 12.1% of Barcombe POT exceedances occurring on the same day as Newhaven sea level POT exceedances. The percentages increased marginally using the three day window, ranging from 5.7% to 15.3 % of Barcombe POT exceedances occurring within the same period as Newhaven sea level POT exceedances. The correlation exercise revealed no statistical relationship between the magnitudes of the POT exceedances, confirming that fluvial flows at Barcombe Mills are poorly correlated with sea levels at Newhaven, which is largely due to the predominantly astronomically driven tides and meteorologically (and seasonally) driven river flows.

Table 6.7 Joint POT exceedances at Barcombe Mills & Newhaven (sea level) (1982-2005)

Gauge Grouping	Threshold Selection		Same Day Joint POT Exceedances		±1 Day Joint POT Exceedances		R^2
	(%)	(value)	(days)	(%)	(days)	(%)	
Barcombe Mills Newhaven (Sea level)	99%	74.84 m ³ /s 3.95 mOD	2	5.7%	2	5.7%	N/A
Barcombe Mills Newhaven (Sea level)	98%	52.14 m ³ /s 3.87 mOD	5	7.7%	7	10.8%	0.02 ($P=0.1056$)
Barcombe Mills Newhaven (Sea level)	95%	23.73 m ³ /s 3.74 mOD	19	12.1%	24	15.3%	0.00 ($P=0.1619$)

Unlike flow and sea level, the results of the analysis between Barcombe Mills flow and surge recorded at Newhaven produced a significant percentage of joint POT exceedance

at the 95th percentile (Table 6.8), with up to 40.3% of Newhaven surge POT exceedances occurring in the same ± 1 day period as Barcombe Mills flow POT exceedances. The joint exceedance percentages reduced to 20.0% as the percentile threshold increased to the 98th and 99th percentiles repeatedly, which suggested that not all of most extreme surges occur simultaneously with fluvial flows. The correlation of the POT exceedances for the observed pairs of the three threshold levels produced a significant but small R^2 of between 0.11 and 0.14. This indicated that fluvial flows at Barcombe Mills are weakly correlated with surge, which is thought to be related to low pressure systems causing heavy precipitation with subsequent runoff at the same time as creating increased sea levels.

Table 6.8 Joint POT exceedances at Barcombe Mills & Newhaven (surge) (1982-2005)

Gauge Grouping	Threshold Selection		Same Day Joint POT Exceedances		± 1 Day Joint POT Exceedances		R^2
	(%)	(value)	(days)	(%)	(days)	(%)	
Barcombe Mills Newhaven (Surge)	99%	74.84 m^3/s 0.69 m	5	14.3% 17.2%	7	20.0% 24.1%	0.14 ($P=0.3201$)
Barcombe Mills Newhaven (Surge)	98%	52.14 m^3/s 0.61 m	12	18.5% 20.3%	20	30.8% 33.9%	0.11 ($P=0.4098$)
Barcombe Mills Newhaven (Surge)	95%	23.73 m^3/s 0.51 m	37	23.6% 24.8%	60	38.2% 40.3%	0.13 ($P=0.2642$)

The joint POT exceedance analysis between stage at Lewes Corporation Yard and recorded sea level at Newhaven produced the highest percentages of joint POT exceedance of any POT pair (Table 6.9). The percentage of Lewes POT exceedances occurring on the same day as Newhaven sea level POT exceedances ranged from 51.7% at the 99th percentile to 70.3% at the 95th percentile, with the ± 1 day period showing slightly higher values. As expected, the results suggested that high water levels at Lewes are highly influenced by the sea levels at Newhaven.

Table 6.9 Joint POT exceedances at Lewes Corporation Yard & Newhaven (sea level) (1982-2005)

Gauge Grouping	Threshold Selection		Same Day Joint POT Exceedances		±1 Day Joint POT Exceedances		R ²
	(%)	(value)	(days)	(%)	(days)	(%)	
Lewes Corp Yard Newhaven (Sea level)	99%	3.96 mOD 3.95 mOD	15	51.7% 25.4%	16	55.2% 27.1%	0.04 (<i>P</i> =0.0448)
Lewes Corp Yard Newhaven (Sea level)	98%	3.72 mOD 3.87 mOD	35	60.3% 30.7%	37	63.8% 32.5%	0.06 (<i>P</i> =0.0386)
Lewes Corp Yard Newhaven (Sea level)	95%	3.44 mOD 3.74 mOD	102	70.3% 35.1%	106	73.1% 36.4%	0.10 (<i>P</i> =0.0235)

The magnitudes of the POT exceedances displayed a conversely low but significant ($P < 0.05$ in all cases) statistical correlation however, which implied that although the astronomical tide directly influences the timing of the high water levels at Lewes, the eventual magnitude is only partially governed by the tide, with the interaction of river flow creating the variation in magnitudes between Lewes and Newhaven gauges.

The analysis of the POT series of Lewes Corporation Yard stage and Newhaven recorded surge produced significant percentages of simultaneous exceedances, with a relatively constant 20.7% to 27.1% of Lewes POT exceedances at the 95th to 99th percentile occurring on the same day as Newhaven surge POT exceedances (Table 6.10). The ±1 day period showed similar constant results regardless of threshold selection. Again however, the magnitudes of the POT exceedances displayed a low R² value of 0.06 which was less statistically significant. The results determined that the timing of high water levels at Lewes corresponds with surge, but the magnitude is more likely to be governed by the astronomical tide and its interaction with upstream fluvial flows than surge alone due to the small surge range at Newhaven.

Table 6.10 Joint POT exceedances at Lewes Corporation Yard & Newhaven (surge) (1982-2005)

Gauge Grouping	Threshold Selection		Same Day Joint POT Exceedances		±1 Day Joint POT Exceedances		R ²
	(%)	(value)	(days)	(%)	(days)	(%)	
Lewes Corp Yard Newhaven (Surge)	99%	3.96 mOD 0.69 m	6	20.7% 20.7%	6	20.7% 20.7%	0.00 (<i>P</i> =0.3201)
Lewes Corp Yard Newhaven (Surge)	98%	3.72 mOD 0.61 m	16	27.6% 27.1%	16	27.6% 27.1%	0.02 (<i>P</i> =0.2367)
Lewes Corp Yard Newhaven (Surge)	95%	3.44 mOD 0.51 m	32	22.1% 21.5%	39	26.9% 26.2%	0.06 (<i>P</i> =0.1014)

6.5 Discussion

Flood frequency estimates have been made at each of the key hydrological locations in the Ouse catchment, using AMAX series fitted to GEV distributions and POT exceedance series.

The joint AMAX and POT occurrences between the hydrological pairs showed high percentages of simultaneous occurrences between stage at Lewes Corporation Yard with fluvial flow at Barcombe Mills, and both astronomical tide and surge at Newhaven. Tide predominates, with a close relationship established between the occurrence of high tides at Newhaven and corresponding high stage at Lewes. Barcombe Mills flow and Newhaven surge joint POT exceedances also displayed a significant likelihood of occurring simultaneously due to their common link with meteorological weather systems.

This regression analysis results however, showed that although a high percentage of sea level at Newhaven and stage at Lewes occur simultaneously, stage magnitudes at Lewes are more highly correlated with fluvial flow at Barcombe Mills than sea level at Newhaven. This correlation increases as the observations become more extreme, linking the highest observations at Lewes to high fluvial flow. Similarly, the results determined that whilst there was a significant percentage of simultaneous POT exceedances between Lewes stage and Newhaven surge, surge alone had little direct affect on the stage

magnitudes at Lewes, due to the limited surge range at Newhaven and the overriding volume of the astronomically driven tides and fluvial flows.

The hydrodynamics of the catchment and river channel also have a significant affect on stage at Lewes. The constriction of Cliffe Bridge in the centre of Lewes directly affects the interaction of sea level and flow, which was demonstrated through the joint analysis of the Lewes Corporation Yard and Gas Works AMAX series and the extreme event analysis of the October 2000 flood.

The results demonstrate that although the astronomical tide directly influences the timing and magnitude of the Lewes stage, the actual magnitude is only partially governed by the tide. The interaction of river flow and the system dynamics create the variation in stage magnitudes at Lewes from the sea levels at Newhaven. This interaction is not clearly defined, with fluvial flow showing significant correlation with stage at Lewes but tide and surge difficult to differentiate because of the combined fluvial flow. As such, the multivariate relationship between Barcombe Mills fluvial flow, Lewes stage, Newhaven astronomical tide and Newhaven surge requires further analysis, using both modelling and statistical methodologies to categorise their interaction and dependency, and joint probabilities of occurrence determined.

7 STATISTICAL DEPENDENCE

7.1 Introduction

To quantify the probability of occurrence of extreme water levels in a tidal river, such as the lower River Ouse, the probability of a combination of sea level and river flow producing high or extreme values at the same time needs to be established.

Where two or more conditions are assumed to be either fully independent or dependent, the joint probability of their occurrence is relatively trivial to calculate (Meadowcroft *et al.*, 2004). However, an assumption of independence may lead to the under design of river defences, whereas an assumption of dependence may be far too conservative.

For a joint probability of occurrence to be determined successfully, a level of statistical dependence is required, which will lie somewhere between the independent and dependent cases. This may take the form of dependence between rainfall, extreme river flow and surge which are linked to meteorological systems.

The dependence measure χ is especially suited for estimating dependence between two simultaneously recorded variables as they reach their extremes (Coles *et al.*, 2000). This chapter explores the statistical dependence between the hydrological variables in the lower Ouse catchment, to quantify the combined causes of flooding.

7.2 Dependence between Barcombe Mills & Newhaven

7.2.1 Data Preparation

River flow observed above the tidal reach in the lower Ouse at Barcombe Mills and sea level observed at Newhaven at the mouth of the Ouse were categorised as the primary input variables into the lower Ouse tidal river system for the generation of water levels at Lewes, the intermediate site of interest. The relative locations of Barcombe Mills and Newhaven determined that the observations were both spatially and hydraulically independent from each other (i.e. one does not directly influence the other), and may only be linked by a meteorological system such as a low atmospheric pressure event causing high river flow and increased sea levels at the same time.

Daily maxima flow observed at Barcombe Mills was plotted against daily maxima sea level simultaneously observed at Newhaven for the period of June 1982 to May 2006 (Figure 7.1a). Daily maxima flow was also plotted against daily maxima surge simultaneously observed at Newhaven (Figure 7.1b). This removed the influence of the astronomically-driven tidal component, thereby leaving the surge component which may display a stronger ‘meteorological’ relationship with river flow. Both series contained 5804 simultaneous daily maxima observations (see section 4.5), providing a completion of 66.21%.

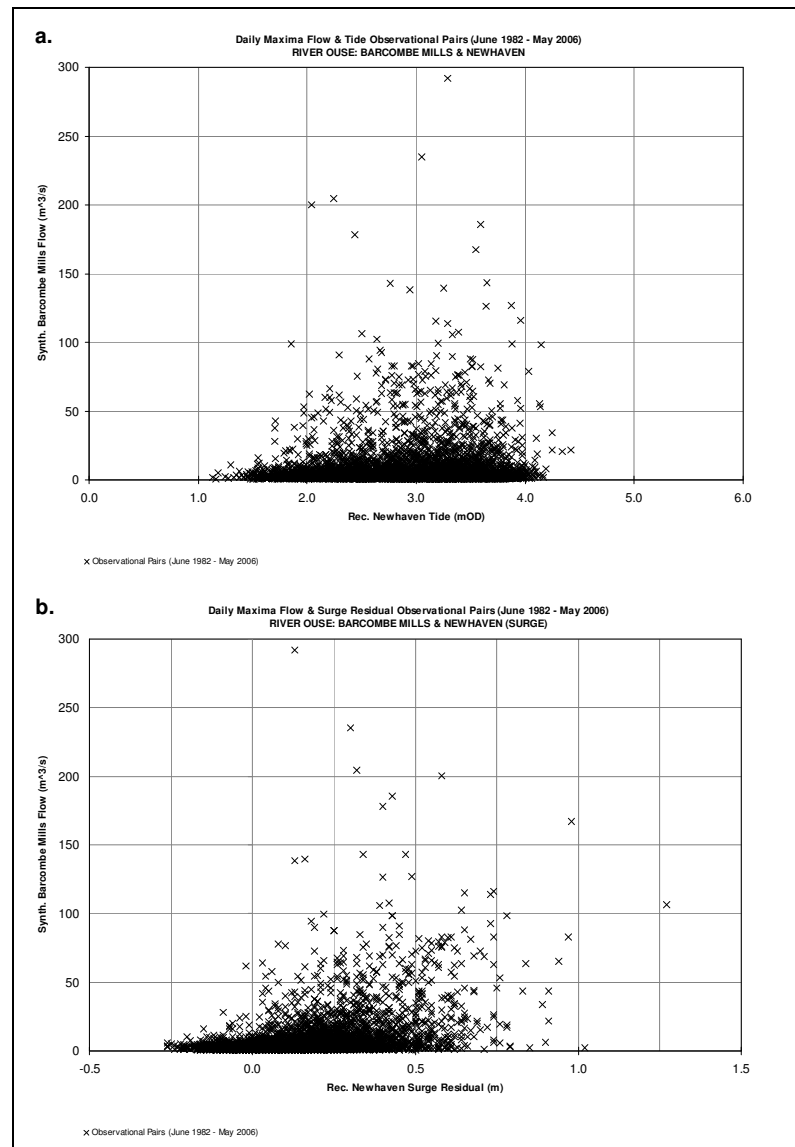


Figure 7.1 Scatter plots of **a.** daily maxima flow at Barcombe Mills versus daily maxima sea level at Newhaven, & **b.** daily maxima flow at Barcombe Mills versus daily maxima surge at Newhaven

Figure 7.1a shows the occurrence of the highest sea levels and river flows are well spread, although a slight tendency for the medium sea levels (i.e. around 3mOD) to cluster around the 50-100m³/s flow observations. Figure 7.1b however shows a greater trend towards simultaneously extreme observations, with the majority of the highest flows occurring when significant surge values were also recorded.

7.2.2 Threshold Values

Although the dependence value χ may be estimated for any threshold value, a sensitivity test was carried out to assess the variation of dependence corresponding with the threshold level. The thresholds were selected using a percentile POT approach taken from the daily maxima datasets, ranging from 80% to 99.5% (i.e. the 95% threshold corresponded to highest 5% of the independent POT events in the record). The results suggested that for both variable pairs (Barcombe Mills flow ν Newhaven sea level, and Barcombe Mills flow ν Newhaven surge), the χ value showed a fairly constant, slightly decreasing trend from the 80% to 98% threshold levels (Figure 7.2 and Figure 7.3). For the most extreme observations (i.e. above the 98% level), the χ value decreased towards 0 where none of the observational pairs exceeded both threshold simultaneously.

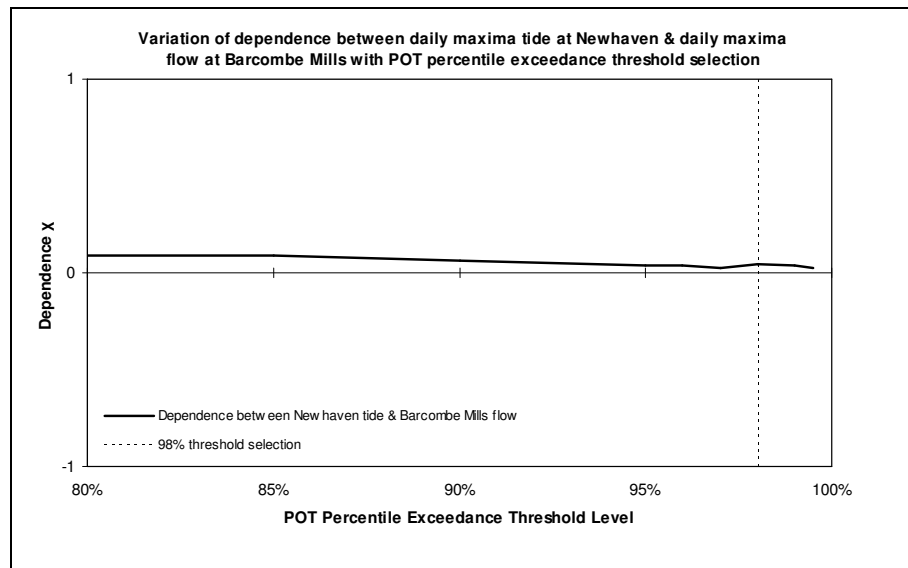


Figure 7.2 Variation of dependence between daily maxima sea level at Newhaven & daily maxima flow at Barcombe Mills with POT percentile threshold selection

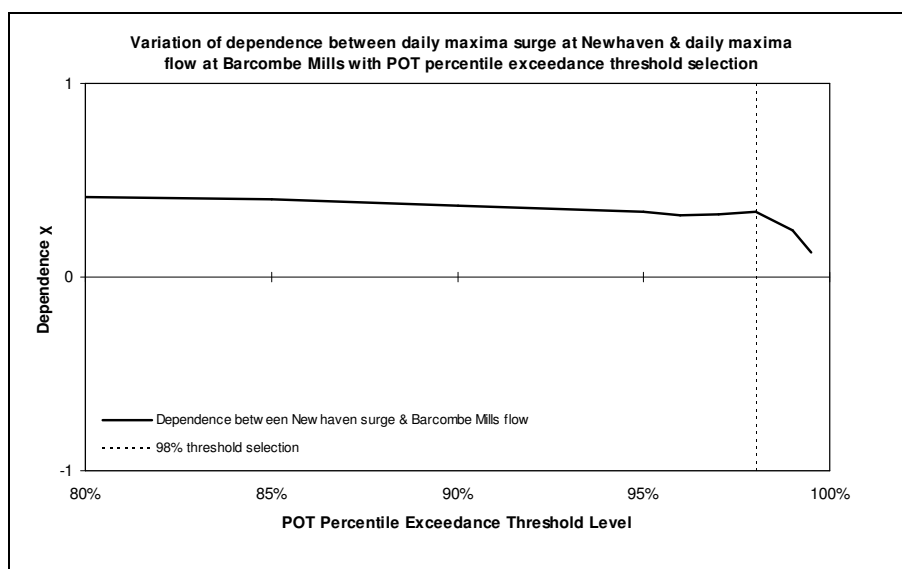


Figure 7.3 Variation of dependence between daily maxima surge at Newhaven & daily maxima flow at Barcombe Mills with POT percentile threshold selection

A lagged analysis was also undertaken to assess the variation of χ with a ± 1 day time lag for different threshold levels. As with the same day calculation, the χ values for both variable pairs of Barcombe Mills flow ν Newhaven sea level and Barcombe Mills flow ν Newhaven surge showed a constant, slightly decreasing trend at the lower threshold levels (Figure 7.4 and Figure 7.5). However, both lagged results showed a dramatic decreasing χ value as the percentile threshold levels became more extreme, producing negative dependence values for the most extreme observations.

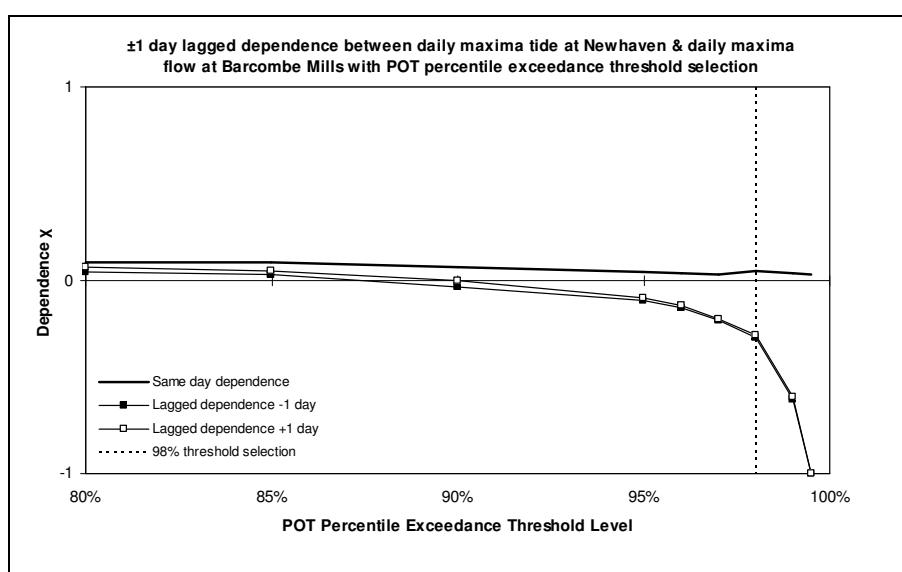


Figure 7.4 ± 1 day lagged dependence between daily maxima sea level at Newhaven & daily maxima flow at Barcombe Mills with POT percentile threshold selection

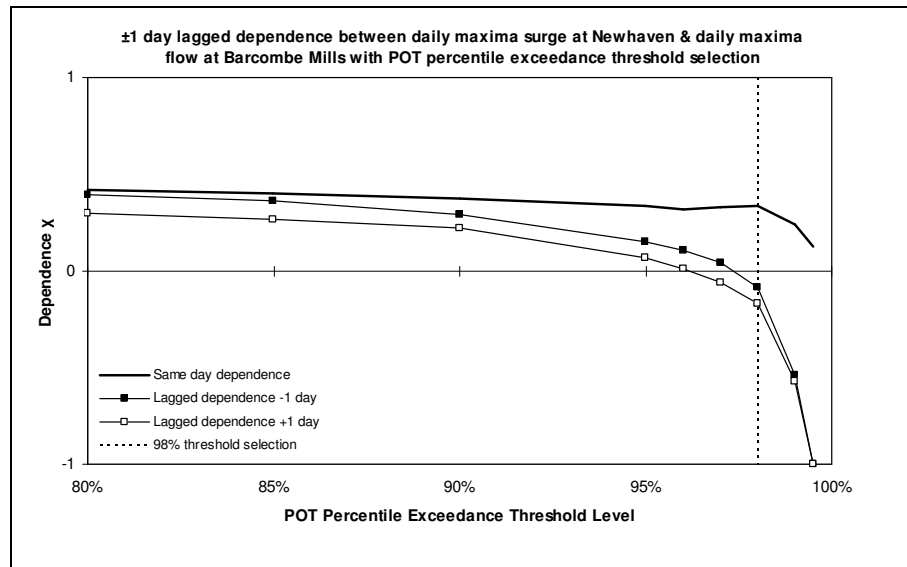


Figure 7.5 ±1 day lagged dependence between daily maxima surge at Newhaven & daily maxima flow at Barcombe Mills with POT percentile threshold selection

For both variable pairs, the results for the +1 day and -1 day lagged analyses displayed similar χ values, which were below the values calculated using daily maxima values on the same day. It was concluded that the dependence between both variable pairs of Barcombe Mills flow ν Newhaven sea level and Barcombe Mills flow ν Newhaven surge was stronger on the same day (i.e. within 24-hours) than on either the preceding or following days. This is consistent with the fact that the Ouse catchment responds quickly to the same meteorological event, creating higher river flow at Barcombe and surge at Newhaven (which ultimately affects the total sea level) within the same day, increasing the risk of extreme water levels at Lewes.

The 98% threshold was selected to calculate the χ value between flow ν sea level and between flow ν surge based on the results from the threshold and lagged analyses, producing a χ of 0.045 for flow ν sea level, and 0.338 for flow ν surge. The threshold level corresponded to approximately 3.7 independent POT events per year on average (see Appendix D.1). This upheld the principle of having enough observations above the threshold to be able to obtain a reliable value of dependence, whilst maintaining the extremal nature of the dependence calculation.

7.2.3 Time-Lagged Analysis

To test the hypothesis that a dependence value calculated at a daily maxima resolution would hold if a higher resolution was used, the dependence between Barcombe Mills

flow v Newhaven sea level was recalculated at the 98th percentile threshold using the full 15-minute observed series.

Figure 7.6 shows the lagged dependence between each daily maxima flow observation and the lagged corresponding sea level. Figure 7.7 shows the reverse, with lagged dependence between daily maxima sea level and the lagged corresponding flow. A new χ value was calculated for each 15-minute lag increment, up to ± 1 day.

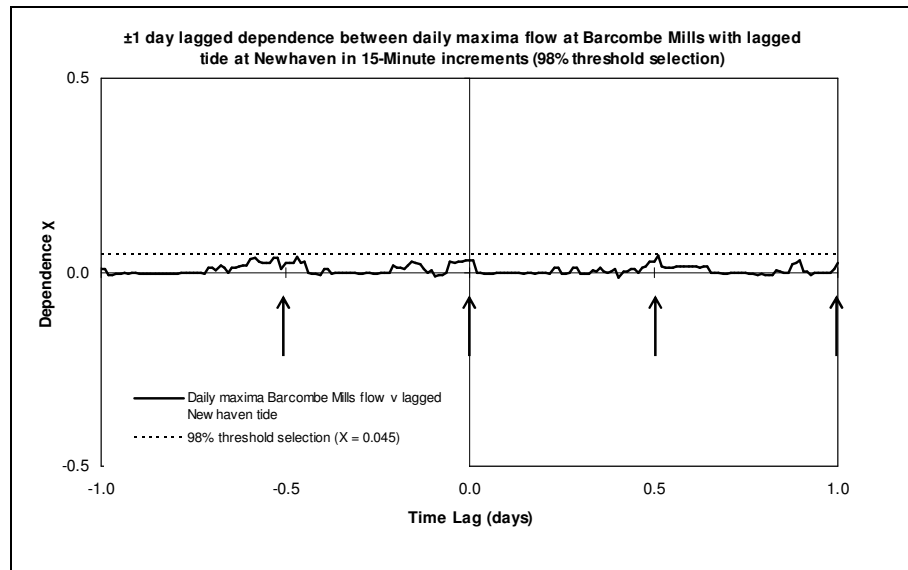


Figure 7.6 Lagged dependence between daily maxima flow at Barcombe Mills with lagged sea level at Newhaven in 15-minute increments (98% threshold)

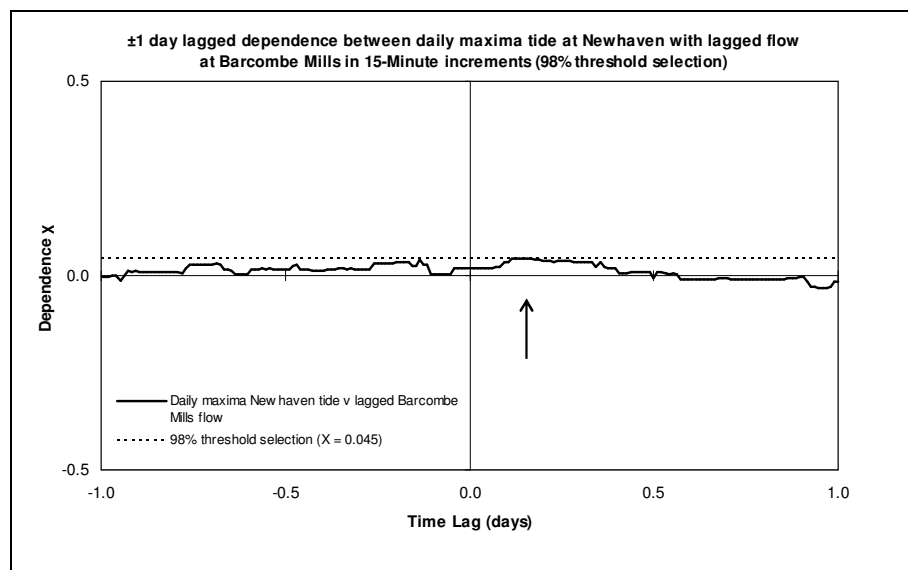


Figure 7.7 Lagged dependence between daily maxima sea level at Newhaven with lagged flow at Barcombe Mills in 15-Minute increments (98% threshold)

In both cases, the new χ values calculated for each time-lag increment of 15-minutes did not exceed the original χ of 0.045 calculated using the daily maxima flow v sea level records (shown on the charts; see section 7.2.2), concluding that a daily maxima resolution was acceptable for the accurate calculation of dependence. However, the lagged analysis produced some interesting results. The 15-minute analysis demonstrated the effect of the tidal astronomical cycle of the dependence value. The upward arrows on Figure 7.6 highlight the peak of each tide and the increasing / decreasing level of dependence with river flow either side, separated by approximately 12 hours (i.e. a peak-to-peak tidal cycle is 12.42 hours). Figure 7.7 shows the maximum dependence values between maximum sea level and river flow were calculated with an approximate 3 to 4 hour time-lag. This reflected the meteorological influence on sea levels (creating higher levels through surge) with corresponding high river flow 3-4 hours later.

The 15-minute lagged dependence analysis was repeated using Barcombe Mills flow v Newhaven surge at the 98th percentile threshold level. Figure 7.8 shows the lagged dependence between each daily maxima surge at Newhaven and lagged river flow at Barcombe Mills, with χ calculated for each 15-minute lag increment, up to ± 1 day.

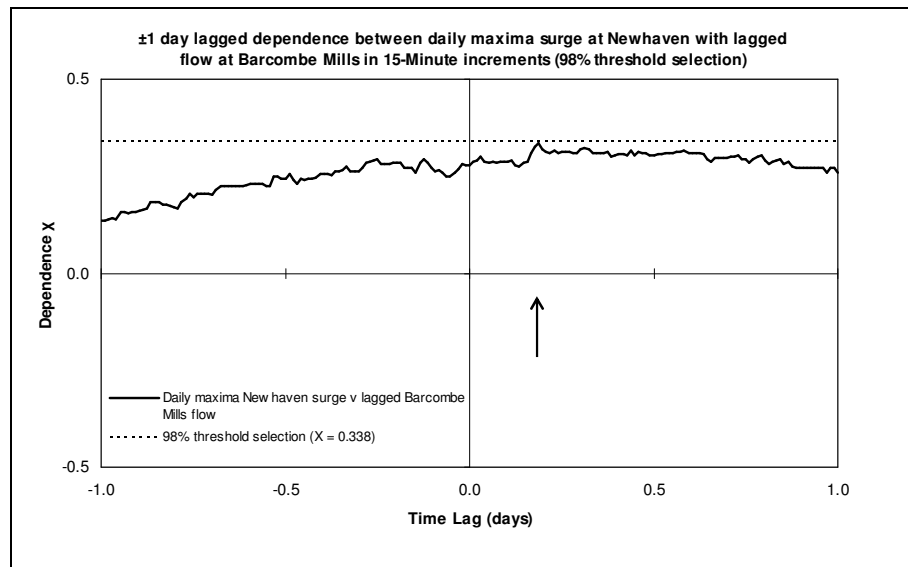


Figure 7.8 Lagged dependence between daily maxima surge at Newhaven with lagged flow at Barcombe Mills in 15-Minute increments (98% threshold)

As with the previous analysis, the new χ values calculated for each time-lag increment of 15-minutes did not exceed the original χ of 0.338, calculated using the daily maxima flow v surge records (see section 7.2.2). The maximum dependence value between the

peak surge and lagged river flow occurred when there was an average 4 hour time-lag between the occurrence of the peak surge and flow values, closely matching the optimum time-lag calculated when calculating dependence between flow and sea level (Figure 7.7). This confirmed the common meteorological link between high river flow and surge and defined the average time-lag experienced between the peaks of river flow and surge necessary for the generation of (extreme) intermediate water levels.

7.2.4 Dependence Values

Table 7.1 shows the dependence χ between Barcombe Mills daily maxima flow and Newhaven daily maxima sea level, daily maxima predicted tide and daily maxima surge. All values were calculated using the 98% independent POT exceedance threshold level. Table 7.1 also contains the values of χ relative to the 5% significance level, and the upper and lower confidence intervals.

Table 7.1 Dependence χ between Barcombe Mills & Newhaven, values of χ corresponding to the 5% significance level, and the lower and upper confidence intervals

Gauge / Station Pair	Threshold Selection		χ	5% Signif. Level	Confidence Intervals	
	(POT %)	(value)			Lower (5%)	Upper (95%)
Barcombe Mills (Peak Flow) Newhaven (Sea level)	98%	52.14 m ³ /s 3.87 mOD	0.045	0.029	-0.009	0.132
Barcombe Mills (Peak Flow) Newhaven (Predicted Tide)	98%	52.14 m ³ /s 3.80 mOD	-0.021	0.011	-0.023	0.054
Barcombe Mills (Peak Flow) Newhaven (Surge)	98%	52.14 m ³ /s 0.57 m	0.338	0.041	0.106	0.452

The dependence calculation for flow ν sea level produced a χ value of 0.045. This indicates that, on average, just under 5% of the highest tidal events at Newhaven will coincide with a high flow event at Barcombe Mills. The results for flow ν surge show a significant level of dependence, with a χ value of 0.338 at the 98% threshold level, highlighting the strong meteorological connection between river flow and surge in the

Ouse catchment. The inclusion of the predicted tide record at Newhaven was to measure the direct affect of the surge component on the χ value calculated for flow ν sea level. The results show a slightly negative χ of -0.021 for flow ν predicted tide, compared to the χ of 0.045 for flow ν sea level, demonstrating that the dependence between Barcombe Mills and Newhaven is determined by the meteorological components of surge and flow rather than the astronomically-driven tide.

7.3 Dependence at Lewes

7.3.1 The Combined Effects of Flow, Sea level & Surge at Lewes

Lewes Corporation Yard is the first gauge downstream of Barcombe Mills on the lower River Ouse, just upstream from the Phoenix Causeway and Cliffe Bridge, with Lewes Gas Works 150m downstream of Cliffe Bridge (often called Lewes Bridge); see Figure 4.4. The flow recorded at Barcombe Mills will ultimately pass through Lewes (except during the most extreme events where overtopping occurs), with a peak-to-peak time-lag estimated to approximately 1-hour. Similarly, tidal flows from Newhaven propagate upstream to Lewes, with an estimated 55-minute peak-to-peak time-lag. It was therefore expected that the observed stage at Lewes Corporation Yard would be partially dependent on both the flows recorded at the upstream Barcombe Mills gauge and sea level recorded downstream at Newhaven. The level of dependence therefore would be determined by the hydrological interaction of sea level and river flow in the lower Ouse.

Daily maxima stage simulated at Lewes Corporation Yard was plotted against daily maxima flow simultaneously observed at Barcombe Mills (Figure 7.9a), daily maxima sea level observed at Newhaven (Figure 7.9b) and daily maxima surge also observed at Newhaven (Figure 7.9c), for the period of June 1982 to May 2006. Figure 7.9a shows a clear trend for extreme flow and downstream high stage events to occur simultaneously. Figure 7.9b shows a strong correlation between sea level and upstream stage, although there are few extreme simultaneous observations. There is also an extremal relationship between surge and stage (Figure 7.9b), with a defined trend between the simultaneous occurrence of the highest surges and upstream stage.

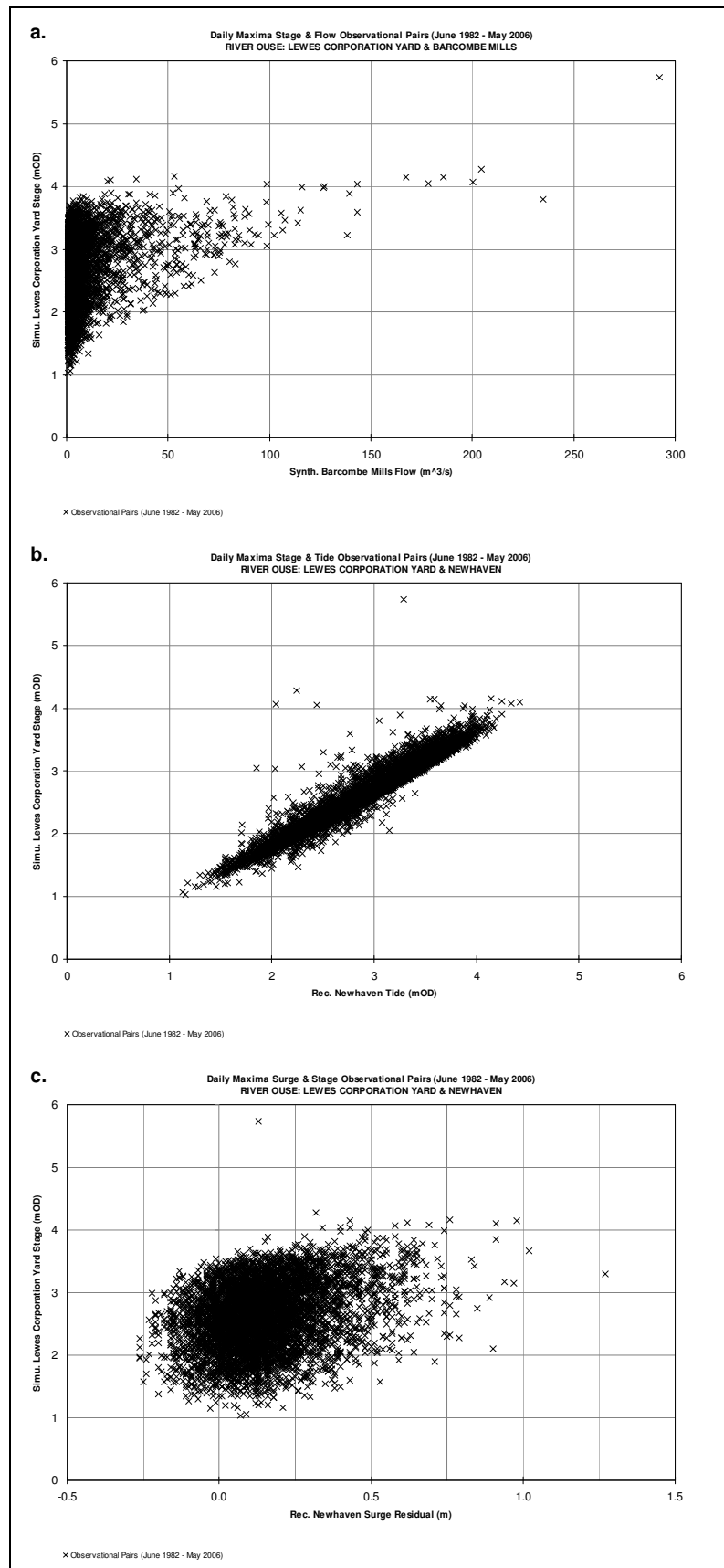


Figure 7.9 Scatter plots of **a.** daily maxima stage at Lewes Corporation Yard versus daily maxima flow at Barcombe Mills, **b.** daily maxima stage at Lewes Corporation Yard versus daily maxima sea level at Newhaven, & **c.** daily maxima stage at Lewes Corporation Yard versus daily maxima surge at Newhaven

Figure 7.10 shows the variation of dependence calculated between daily maxima stage at Lewes Corporation Yard, with daily maxima flow at Barcombe, daily maxima sea level and daily maxima surge at Newhaven, for threshold levels from 80% to 99% independent POT exceedance. The high level of dependence between stage at Lewes Corporation Yard and sea level at Newhaven up to the 95th percentile threshold signified the dominance of sea level on the lower (i.e. non-extreme) stage at Lewes. River flow and surge also showed a fairly constant significant level dependence across the threshold range. However, as the variables reached their extremes, the dependence between river stage at Lewes and sea level at Newhaven dropped dramatically, whilst dependence between stage and river flow at Barcombe Mills increased. This represents the altering relationship between stage at Lewes and the input variables of flow and sea level under extreme conditions, with flow determining the occurrence of the highest stage at Lewes Corporation Yard.

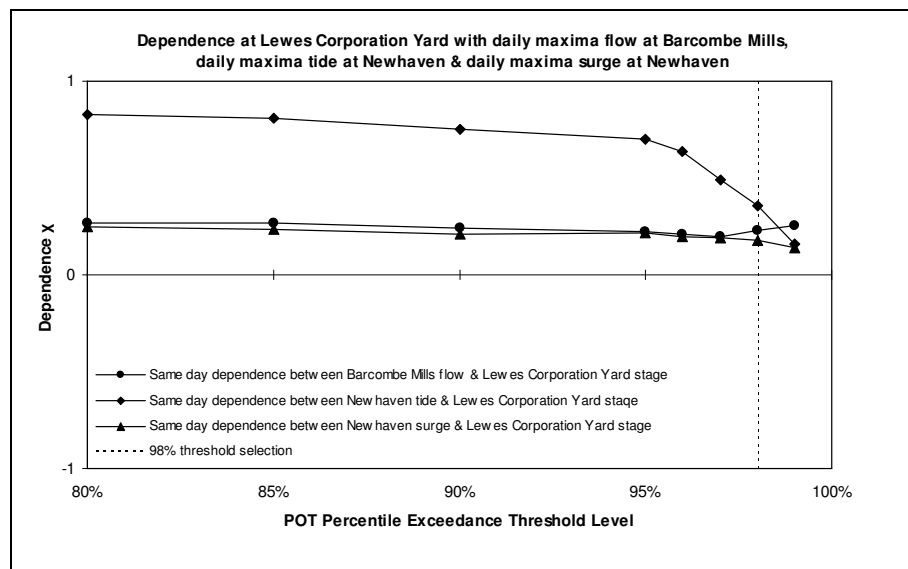


Figure 7.10 Dependence at Lewes Corporation Yard with daily maxima flow, sea level & surge, with POT percentile threshold selection

As with Lewes Corporation Yard, daily maxima stage simulated at the downstream Lewes Gas Works gauge was plotted against daily maxima flow observed at Barcombe Mills (Figure 7.11a), daily maxima sea level observed at Newhaven (Figure 7.11b) and daily maxima surge also observed at Newhaven (Figure 7.11c), for the period of June 1982 to May 2006. The results were visually similar, with Figure 7.11a showing a trend for extreme flow and downstream high stage events to occur simultaneously,

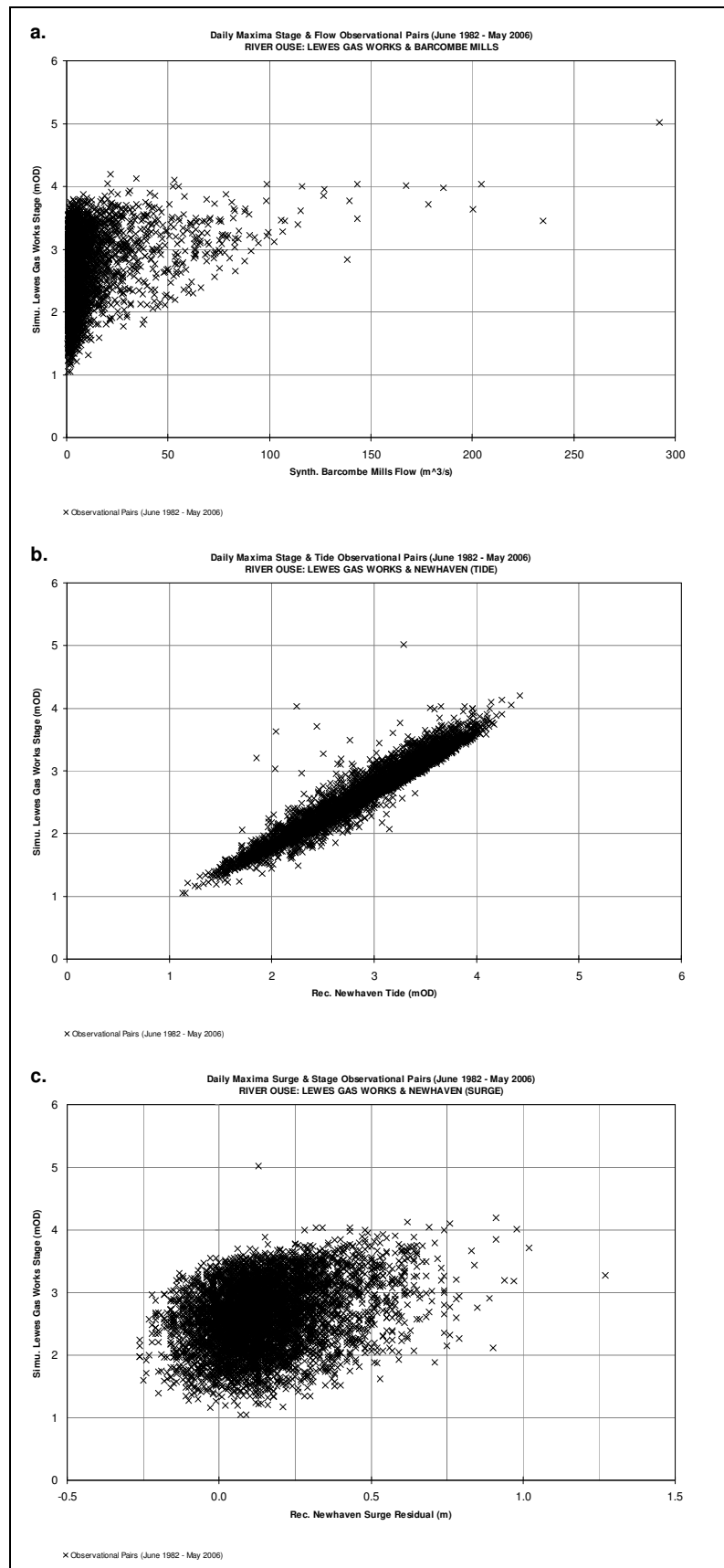


Figure 7.11 Scatter plots of **a.** daily maxima stage at Lewes Gas Works versus daily maxima flow at Barcombe Mills, **b.** daily maxima stage at Lewes Gas Works versus daily maxima sea level at Newhaven, & **c.** daily maxima stage at Lewes Gas Works versus daily maxima surge at Newhaven

Figure 7.11b showing a strong link between sea level and upstream stage, and Figure 7.11b defining a trend between the simultaneous occurrence of the highest surges and stage. A similar dependence pattern also emerged at Lewes Gas Works gauge. Figure 7.12 displays strong dependence between sea level and stage at Lewes, as well as significant dependence with flow and surge.

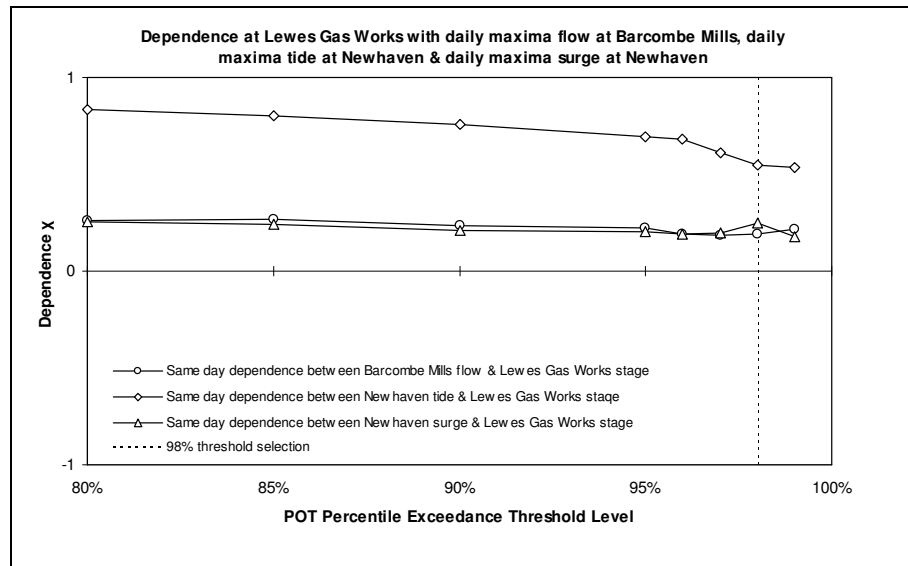


Figure 7.12 Dependence at Lewes Gas Works with daily maxima flow, sea level & surge, with POT percentile threshold selection

Figure 7.13 compares the individual effects of flow, sea level and surge on two Lewes gauges. The level of dependence χ between pairs of input variables and the two gauges at Lewes produced slightly different results under extreme conditions. Figure 7.13a shows that the dependence χ for flow ν stage at Lewes Corporation Yard was higher than at Lewes Gas Works, where as Figure 7.13b shows that for sea level ν stage at Lewes Corporation Yard, the dependence χ was significantly lower than at Lewes Gas Works for the most extreme threshold levels.

Despite the close proximity of the two Lewes gauges, the differing dependence results highlight the affect of the channel hydrodynamics on the resulting water levels in and around Lewes. During an extreme event, the narrow channel through the centre of Lewes at Cliffe Bridge alters the interaction of sea level and flow, resulting in the increased river flow dominance of the upstream Lewes Corporation Yard gauge and the increased tidal dominance of the downstream Lewes Gas Works gauge.

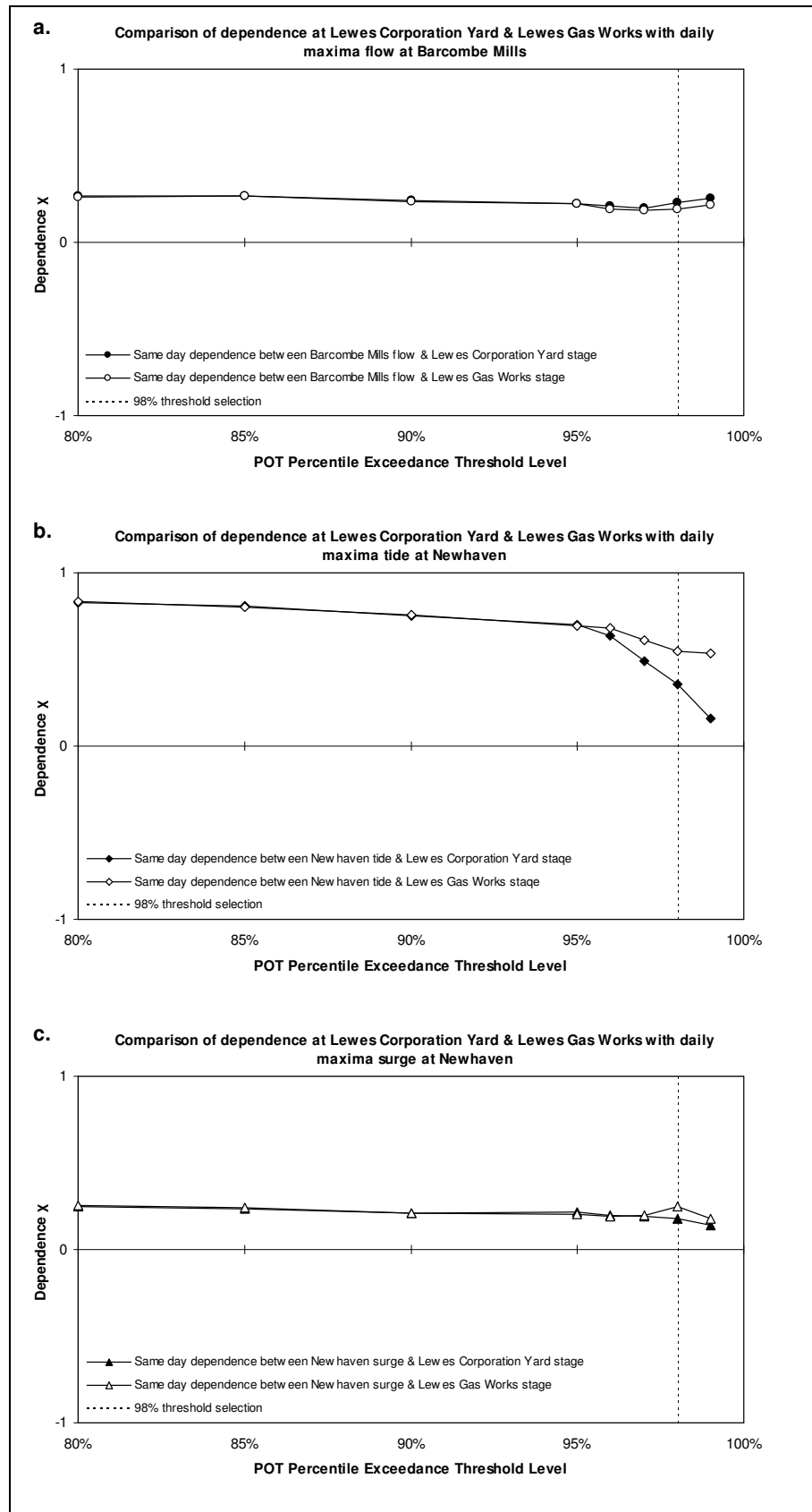


Figure 7.13 Comparison of dependence at Lewes Corporation Yard and Lewes Gas Works gauges with **a.** daily maxima flow at Barcombe Mills, **b.** daily maxima sea level at Newhaven, & **c.** daily maxima surge at Newhaven, with POT percentile threshold selection

7.3.2 Dependence Values

Table 7.2 shows the dependence χ calculated between Lewes Corporation Yard daily maxima stage, Barcombe Mills daily maxima flow and Newhaven daily maxima sea level and daily maxima surge. All values were calculated using the 98% independent POT exceedance threshold level, and show the values of χ relative to the 5% significance level with lower and upper confidence intervals. The results show significant levels of dependence, highlighting the interaction between river flow and sea level at Lewes. As the variables become more extreme, flow starts to dominate stage (see Figure 7.10), with dependence for sea level ν stage dropping to zero.

Table 7.2 Dependence χ between Lewes Corporation Yard, Barcombe Mills & Newhaven, values of χ corresponding to the 5% significance level, and the lower and upper confidence intervals

Gauge / Station Pair	Threshold Selection		χ	5% Signif. Level	Confidence Intervals	
	(POT %)	(value)			Lower (5%)	Upper (95%)
Lewes Corp. Yard (Stage) Barcombe Mills (Peak Flow)	98%	3.72 mOD 52.14 m ³ /s	0.230	0.054	0.131	0.332
Lewes Corp. Yard (Stage) Newhaven (Sea level)	98%	3.72 mOD 3.87 mOD	0.354	0.080	0.157	0.454
Lewes Corp. Yard (Stage) Newhaven (Surge)	98%	3.72 mOD 0.57 m	0.177	0.085	0.059	0.284

Table 7.3 shows the dependence χ between Lewes Gas Works daily maxima stage, Barcombe Mills daily maxima flow and Newhaven daily maxima sea level and daily maxima surge, again calculated using the 98% independent POT exceedance threshold level. As with Lewes Corporation Yard, the results show significant levels of dependence for all three pairings. However, unlike Lewes Corporation Yard, as the variables become more extreme, sea level continues to dominate stage (see Figure 7.12), with only the most extreme pairings of flow ν stage producing high levels of dependence.

Table 7.3 Dependence χ between Lewes Gas Works, Barcombe Mills & Newhaven, values of χ corresponding to the 5% significance level, and the lower and upper confidence intervals

Gauge / Station Pair	Threshold Selection		χ	5% Signif. Level	Confidence Intervals	
	(POT %)	(value)			Lower (5%)	Upper (95%)
Lewes Gas Works (Stage) Barcombe Mills (Peak Flow)	98%	3.60 mOD 52.14 m ³ /s	0.190	0.038	0.115	0.309
Lewes Gas Works (Stage) Newhaven (Sea level)	98%	3.60 mOD 3.87 mOD	0.550	0.089	0.169	0.701
Lewes Gas Works (Stage) Newhaven (Surge)	98%	3.60 mOD 0.57 m	0.249	0.067	0.083	0.317

7.4 Dependence at Newhaven

7.4.1 The Combined Effects of Tide & Surge at Newhaven

A further dependence analysis was undertaken at Newhaven to define the relationship between astronomical tide, surge and total sea levels using the 98% threshold level. Unlike the previous dependence calculations, tide and surge both occur at the same location, therefore levels are additive with no time-lags required.

Daily maxima observed sea level was plotted against daily maxima surge simultaneously observed at Newhaven (Figure 7.14a), for the period of June 1982 to May 2006. As was expected, there is a trend for the most extreme observed sea levels to occur simultaneously with high surge events. This was due to the inclusion of the surge in the total sea level record (e.g. predicted astronomical tide plus surge). Figure 7.14b shows a plot of daily maxima predicted tide against daily maxima surge at Newhaven, which displays no obvious trend when the variables are extreme, suggesting independence between the astronomically-driven tide and meteorologically driven surge components.

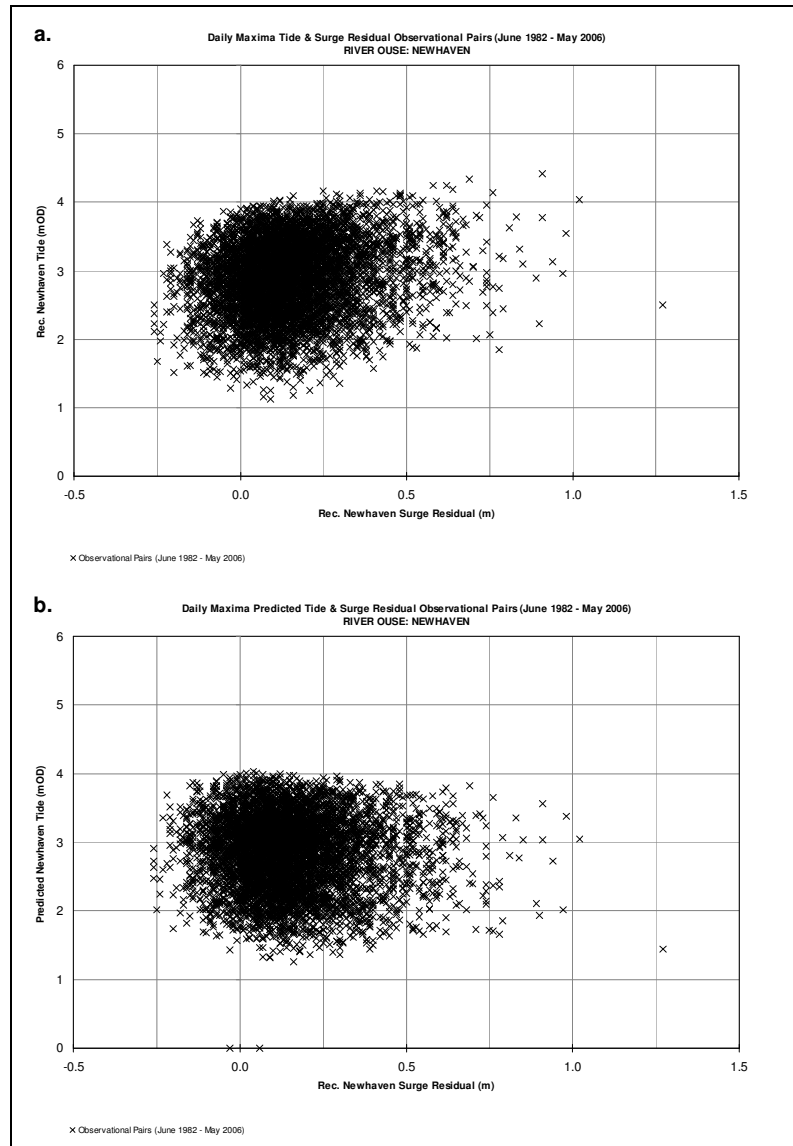


Figure 7.14 Scatter plots of **a.** daily maxima observed sea level versus daily maxima surge at Newhaven, & **b.** daily maxima predicted tide versus daily maxima surge at Newhaven

7.4.2 Dependence Values

Table 7.4 shows the dependence χ calculated between daily maxima sea levels and daily maxima surge at Newhaven. All values were calculated using the 98% independent POT exceedance threshold level, and show the values of χ relative to the 5% significance level with lower and upper confidence intervals. The results for observed sea level ν surge found a significant level of dependence, with just under 10% of the most extreme tidal events being influenced by surge at Newhaven. This was underlined by the slightly negative dependence value calculated for predicted tide ν surge, confirming the assumption of independence.

Table 7.4 Dependence χ between Newhaven sea level and surge, values of χ corresponding to the 5% significance level, and the lower and upper confidence intervals

Gauge / Station Pair	Threshold Selection		χ	5% Signif. Level	Confidence Intervals	
	(POT %)	(value)			Lower (5%)	Upper (95%)
Newhaven (Sea level) Newhaven (Surge)	98%	3.87 mOD 0.57 m	0.094	0.039	0.021	0.166
Newhaven (Predicted Tide) Newhaven (Surge)	98%	3.80 mOD 0.57 m	-0.011	0.008	-0.018	0.035

7.5 Discussion

The dependence modelling exercise utilising daily maxima hydrological datasets from the Ouse system demonstrates how levels of dependence can be successfully employed to categorise the likelihood of simultaneous extreme events and the relative importance of each variable on the production of estuary water levels. When compared to the more straightforward linear statistical correlation exercise in Chapter 5, the calculated R^2 and P values show little of the true extremal relationship which exists between the various hydrological pairs determined by the χ dependence measure.

The significant level of dependence calculated for flow ν surge at Barcombe Mills and Newhaven of $\chi = 0.338$ contrasts with the $\chi = 0.04$ level found by Svensson and Jones (2003, 2004a) for the same variable pair. The authors used the original Barcombe Mills flow record (Svensson and Jones, *pers comm.*) which was found to contain numerous errors, null values and the overtopping of the gauge for flows $> 20 \text{ m}^3/\text{s}$. To avoid this problem, the synthesised Barcombe Mills dataset was utilised for the dependence calculation in this research (section 5.2.6), which successfully modelled the upper catchment flows from the four upstream gauges. The use of the recorded Barcombe Mills dataset is likely to have led to the differing χ values.

Although the daily maxima dependence value accurately captured the maximum χ value within any 24-hour period, the likelihood of extreme values from two datasets occurring together required calculation at a finer resolution to allow for the meteorological and

hydrodynamic time-lags to be accurately obtained. The use of time-lag algorithms at a high resolution (e.g. 15-minute) for the calculation of the dependence measure χ has been shown to accurately model the hydrological time-lags inherent in the hydrodynamics of the river system, and determined the time-lag between common meteorological events producing surges and high river flows. The spatial qualities of the Ouse estuary system were found to affect the dependence between downstream sea level and upstream river flow. Unlike coastal sites where tide, waves and surge combine at the same location, the two source variables of river flow and sea level were at two separate locations; it therefore takes time for the peak tide to propagate up the river and river flow to travel down. The time-lag modelling detailed the temporal and spatial factors, enabling an accurate dependence value to be calculated between two variables at different locations.

It was found that the value of dependence also varied over relatively short distances. Dependence values calculated for two locations at close proximity in Lewes (Corporation Yard and Gas Works), produced differing levels of dependence with river flow and sea level, with extreme water levels at the upstream location influenced to a greater extent by extreme river flows, and the extreme water levels at the downstream location influenced predominantly by sea level. In this instance, it was found that this was due to the narrowing river channel and Cliffe Bridge structures in between the locations dramatically effecting the interaction of sea level and river flow during extreme events, altering the dependence χ values. Dependence values in any river system will therefore respond differently depending on the catchment characteristics and system hydrodynamics.

To be able to calculate an overall probability of specified extreme water levels occurring from the combination of two (or more) variables producing extreme values at the same time requires the further interpretation and use of the dependence values in a full joint probability analysis, combined with the hydraulic modelling and structure function methods developed in the preceding chapters.

8 JOINT PROBABILITY

8.1 Introduction

The term joint probability typically refers to two (or more) variables occurring simultaneously to produce a response of interest (Hawkes, 2003). For flood risk analysis in estuaries and tidal rivers, this may be a high river flow coinciding with an extreme sea level at the same time to produce an extreme flood event.

Section 7.2 demonstrated that a low but significant level of dependence existed between the variables of river flow and sea level in the River Ouse case study area, and that a much higher level of dependence existed between river flow and surge due to their common link to meteorological conditions. Both results suggested that an assumption of full independence between the primary variables of river flow, sea level and surge in a joint probability exercise, would be inaccurate. The pairing of river flow and sea level naturally lends itself to the generation of resultant water levels due to them representing all of the hydrological variables, including precipitation, river flow, astronomical tide and surge. However, to explore the strong dependence found between river flow and surge, a third primary variable of astronomical tide has to be introduced to produce resultant water levels.

This chapter develops two- and three-variable (bivariate and trivariate) joint probability methods for the calculation of joint return periods using both dependence and joint exceedance theories. Barcombe Mills flow and Newhaven sea level were selected as the primary bivariate partially-dependent variables, with Barcombe Mills flow, Newhaven predicted tide and Newhaven surge selected as the primary trivariate partially-dependent variables for the generation of extreme water levels at Lewes.

Probability is not however an exact science and needs to be used in conjunction with a sound physical and hydrological knowledge of the whole estuary system. Crucially, it needs to be understood whether any realistic combination of river flow, tide and surge *could* physically combine to cause extreme water levels, or whether this phenomenon is unrealistic for a specific location such as Lewes. The joint probability approach is therefore combined with the previously calculated structure functions to estimate the overall probability of extreme water levels being exceeded at Lewes through the combination of river flow, tide and surge.

8.2 Extreme Joint Return Period Results at Lewes

8.2.1 Fully-Independent & Partially-Dependent Bivariate & Trivariate Extreme Joint Return Periods

Table 8.1 and Table 8.2 show the extreme joint return periods with corresponding stage calculated at Lewes Corporation Yard and Lewes Gas Works. Each table is divided into extreme exceedance return periods estimated at the response locations from the recorded series, fully-independent bivariate (flow and sea level) joint return periods, partially-dependent bivariate (flow and sea level) joint return periods and partially-dependent trivariate (flow, predicted tide and surge) joint return periods.

The tables display the results in two formats. Part I shows the estimated joint return periods (independent bivariate, partially-dependent bivariate and partially-dependent trivariate) for identical resultant stage targets calculated from the return periods observed at the Lewes Corporation Yard and Lewes Gas Works gauges. For example, the 1:10 year stage magnitude estimated at Lewes Gas Works in Table 8.2 was 4.15mOD. The bivariate and trivariate joint return periods were then estimated for the same stage magnitude observed at Lewes, producing comparative joint return periods of 1:6, 1:5 and 1:4 years respectively. Part II shows the reverse, with estimated stage for identical joint return periods. Both formats allow for direct comparison with the return periods and resultant stage estimates at the response locations. In all cases, the extreme return periods have been rounded to the nearest whole year.

Beside each bivariate and trivariate joint return period / stage estimate, the magnitudes of the primary input variables are displayed (flow, predicted tide and surge), representing the most probable (worst case) pair or group which produced the resultant stage. The shaded areas define the most interactive bivariate and trivariate zones, where the combination of the primary variables produced the most probable response levels, rather than being singularly dominated. Using the same example of the 1:10 year stage magnitude estimated at Lewes Gas Works in Table 8.2, the primary variables all produced magnitudes greater than their 1:1 year estimates, suggesting that their interaction defined the resultant stage.

Table 8.1 Part I. Single, bivariate & trivariate extreme joint return periods (in bold) for independent & partially-dependent flow, sea level and surge with identical resultant stage at Lewes Corporation Yard. Shaded areas highlight the significant interaction zones between the variables on the joint return periods at Lewes Corporation Yard.

Stage Obs. at Lewes C. Yard	Return Periods at Lewes Corp. Yard	Fully-Independent Bivariate Extreme Joint Exceedance (Barcombe Mills Flow & Newhaven Sea Level): ($\chi = 0$)			Partially-Dependent Bivariate Extreme Joint Exceedance (Barcombe Mills Flow & Newhaven Sea Level): ($\chi = 0.045$)			Partially-Dependent Trivariate Extreme Joint Exceedance (Barcombe Mills Flow, Newhaven Predicted Tide & Newhaven Surge): (surge ν flow $\chi = 0.338$; flow/surge ν tide $\chi = 0$)			
<i>stage</i> (mAOD)	<i>return</i> <i>period</i>	<i>flow</i> (<i>m</i> ³ / <i>s</i>)	<i>sea level</i> (mAOD)	<i>return</i> <i>period</i>	<i>flow</i> (<i>m</i> ³ / <i>s</i>)	<i>sea level</i> (mAOD)	<i>return</i> <i>period</i>	<i>flow</i> (<i>m</i> ³ / <i>s</i>)	<i>pred. tide</i> (mAOD)	<i>surge</i> (<i>m</i>)	<i>return</i> <i>period</i>
3.79	1:2	28	3.90	<1:1	28	3.90	<1:1	26	3.88	0.04	<1:1
4.00	1:5	68	3.90	1:2	68	3.90	1:2	51	3.86	0.12	1:2
4.25	1:10	148	3.86	1:12	148	3.86	1:11	51	3.86	0.44	1:9
4.57	1:25	186	3.86	1:33	186	3.86	1:27	186	3.86	0.00	1:33
4.93	1:50	221	3.86	1:79	221	3.86	1:57	221	3.86	0.00	1:79
5.40	1:100	265	3.86	1:258	265	3.86	1:149	265	3.86	0.00	1:258
6.01	1:200	300	3.86	>1:500	300	3.86	>1:500	300	3.86	0.00	>1:500

Part II. Resultant stage (in bold) for independent & partially-dependent flow, sea level and surge with identical single, bivariate & trivariate extreme joint return periods at Lewes Corporation Yard. Shaded areas highlight the significant interaction zones between the variables on the resultant extreme stage at Lewes Corporation Yard.

Target Return Periods	Stage Obs. at Lewes Corp. Yard	Fully-Independent Bivariate Extreme Joint Exceedance (Barcombe Mills Flow & Newhaven Sea Level): ($\chi = 0$)				Partially-Dependent Bivariate Extreme Joint Exceedance (Barcombe Mills Flow & Newhaven Sea Level): ($\chi = 0.045$)				Partially-Dependent Trivariate Extreme Joint Exceedance (Barcombe Mills Flow, Newhaven Predicted Tide & Newhaven Surge): (surge ν flow $\chi = 0.338$; flow/surge ν tide $\chi = 0$)			
<i>return period</i>	<i>stage (mAOD)</i>	<i>flow (m³/s)</i>	<i>sea level (mAOD)</i>	<i>return period</i>	<i>flow (m³/s)</i>	<i>sea level (mAOD)</i>	<i>return period</i>	<i>flow (m³/s)</i>	<i>pred. tide (mAOD)</i>	<i>surge (m)</i>	<i>return period</i>		
1:2	3.79	68	3.92	4.01	68	3.92	4.01	50	3.88	0.14	4.03		
1:5	4.00	76	4.04	4.12	78	4.04	4.13	50	3.90	0.28	4.16		
1:10	4.25	140	3.86	4.21	144	3.86	4.23	50	3.86	0.48	4.27		
1:25	4.57	174	3.86	4.45	182	3.86	4.52	174	3.86	0.00	4.45		
1:50	4.93	202	3.86	4.74	214	3.86	4.87	202	3.86	0.00	4.74		
1:100	5.40	231	3.86	5.03	250	3.86	5.23	231	3.86	0.00	5.03		
1:200	6.01	261	3.86	5.35	292	3.86	5.78	261	3.86	0.00	5.35		

Table 8.2 Part I. Single, bivariate & trivariate extreme joint return periods (in bold) for independent & partially-dependent flow, sea level and surge with identical resultant stage at Lewes Gas Works. Shaded areas highlight the significant interaction zones between the variables on the joint return periods at Lewes Gas Works.

Stage Obs. at Lewes Gas Wks	Return Periods at Lewes Gas Works	Fully-Independent Bivariate Extreme Joint Exceedance (Barcombe Mills Flow & Newhaven Sea Level): ($\chi = 0$)			Partially-Dependent Bivariate Extreme Joint Exceedance (Barcombe Mills Flow & Newhaven Sea Level): ($\chi = 0.045$)			Partially-Dependent Trivariate Extreme Joint Exceedance (Barcombe Mills Flow, Newhaven Predicted Tide & Newhaven Surge): (surge ν flow $\chi = 0.338$; flow/surge ν tide $\chi = 0$)				
<i>stage</i> (mAOD)	<i>return</i> <i>period</i>	<i>flow</i> (m ³ /s)	<i>sea level</i> (mAOD)	<i>return</i> <i>period</i>	<i>flow</i> (m ³ /s)	<i>sea level</i> (mAOD)	<i>return</i> <i>period</i>	<i>flow</i> (m ³ /s)	<i>pred. tide</i> (mAOD)	<i>surge</i> (m)	<i>return</i> <i>period</i>	
3.83	1:2	29	3.90	<1:1	29	3.90	<1:1	29	3.90	0.00	<1:1	
4.01	1:5	63	3.92	1:2	63	3.92	1:2	51	3.86	0.12	1:2	
4.15	1:10	70	4.08	1:6	70	4.08	1:5	51	3.90	0.28	1:4	
4.34	1:25	188	3.86	1:35	188	3.86	1:29	50	3.92	0.52	1:15	
4.51	1:50	214	3.86	1:66	214	3.86	1:51	68	3.92	0.64	1:51	
4.75	1:100	243	3.86	1:131	243	3.86	1:90	243	3.86	0.00	1:131	
4.99	1:200	282	3.86	1:307	282	3.86	1:178	282	3.86	0.00	1:307	

Part II. Resultant stage (in bold) for independent & partially-dependent flow, sea level and surge with identical single, bivariate & trivariate extreme joint return periods at Lewes Gas Works. Shaded areas highlight the significant interaction zones between the variables on the resultant extreme stage at Lewes Gas Works.

Target Return Periods	Stage Obs. at Lewes Gas Works	Fully-Independent Bivariate Extreme Joint Exceedance (Barcombe Mills Flow & Newhaven Sea Level): ($\chi = 0$)			Partially-Dependent Bivariate Extreme Joint Exceedance (Barcombe Mills Flow & Newhaven Sea Level): ($\chi = 0.045$)			Partially-Dependent Trivariate Extreme Joint Exceedance (Barcombe Mills Flow, Newhaven Predicted Tide & Newhaven Surge): (surge ν flow $\chi = 0.338$; flow/surge ν tide $\chi = 0$)			
<i>return period</i>	<i>stage (mAOD)</i>	<i>flow (m³/s)</i>	<i>sea level (mAOD)</i>	<i>return period</i>	<i>flow (m³/s)</i>	<i>sea level (mAOD)</i>	<i>return period</i>	<i>flow (m³/s)</i>	<i>pred. tide (mAOD)</i>	<i>surge (m)</i>	<i>return period</i>
1:2	3.83	59	3.94	4.01	59	3.94	4.01	50	3.88	0.14	4.03
1:5	4.01	64	4.08	4.12	64	4.08	4.13	51	3.94	0.26	4.16
1:10	4.15	81	4.12	4.20	79	4.14	4.21	50	3.88	0.46	4.27
1:25	4.34	89	4.20	4.29	89	4.22	4.30	51	3.94	0.56	4.41
1:50	4.51	201	3.86	4.42	213	3.86	4.50	50	3.90	0.74	4.49
1:100	4.75	231	3.86	4.66	248	3.86	4.78	231	3.86	0.00	4.66
1:200	4.99	261	3.86	4.85	289	3.86	5.04	261	3.86	0.00	4.85

Above the shaded areas (i.e. the longest return periods), the variable of Barcombe Mills flow dominated the resultant stage at the response locations, whilst Newhaven sea level settled to the minimum 1:1 year level of 3.86mOD. Similarly, for the trivariate case, above the shaded areas the variable of Barcombe Mills flow again dominated, with the second variable of Newhaven predicted tide also settling to the minimum 1:1 year level and the third variable of Newhaven surge returning to zero. These results are discussed in detail below.

8.2.2 Interpretation of Results

Figure 8.1a shows the relationship between the estimated partially-dependent bivariate and trivariate stage and the stage recorded at the Lewes Corporation Yard gauge for the same extreme return periods. Figure 8.1b corresponds the equivalent stage estimates at Lewes Gas Works. In both the bivariate and trivariate extreme joint exceedance cases, the shortest return periods (i.e. 1:2 and 1:5 years) appear to overestimate the stage magnitudes compared to the estimates recorded at both Lewes gauges. For example, the target 1:5 year estimated stage magnitude from the recorded series at Lewes Corporation Yard was 4.0mOD, compared to 4.13mAOD and 4.16mAOD for the bivariate and trivariate joint exceedance cases. Similar results were observed at Lewes Gas Works. Examination of the complete simulated daily maxima series at Lewes Corporation Yard (from section 5.3) found that the 4.0mAOD stage was actually exceeded, on average, once in every 1.22 years, far below the estimated once in every 5 years taken from the extreme distribution of recorded AMAX values recorded at the Lewes Corporation Yard gauge (from section 6.2). Although the simulated series had a much shorter overall duration than the recorded AMAX series, this suggests that the joint exceedance approach may be more accurate than the approach for the estimation of the shorter return periods.

The estimated stage magnitudes for the longer bivariate and trivariate joint return periods showed a closer relationship with the target recorded stage estimates, although the trivariate approach notably underestimated the stage at Lewes Corporation Yard. The same trend was identified at Lewes Gas Works, although the effect was less defined. Correlation of the estimated bivariate and trivariate stage magnitudes with the recorded stage magnitudes at each of the Lewes response locations (Figure 8.2 and Figure 8.3) displayed significant R^2 values ($P < 0.01$), with the trivariate approach producing slightly higher correlation at both Lewes Corporation Yard and Lewes Gas Works than the

bivariate approach. However, the bivariate stage at both Lewes locations are in closer agreement with the 1:1 stage plot when compared to the trivariate approach.

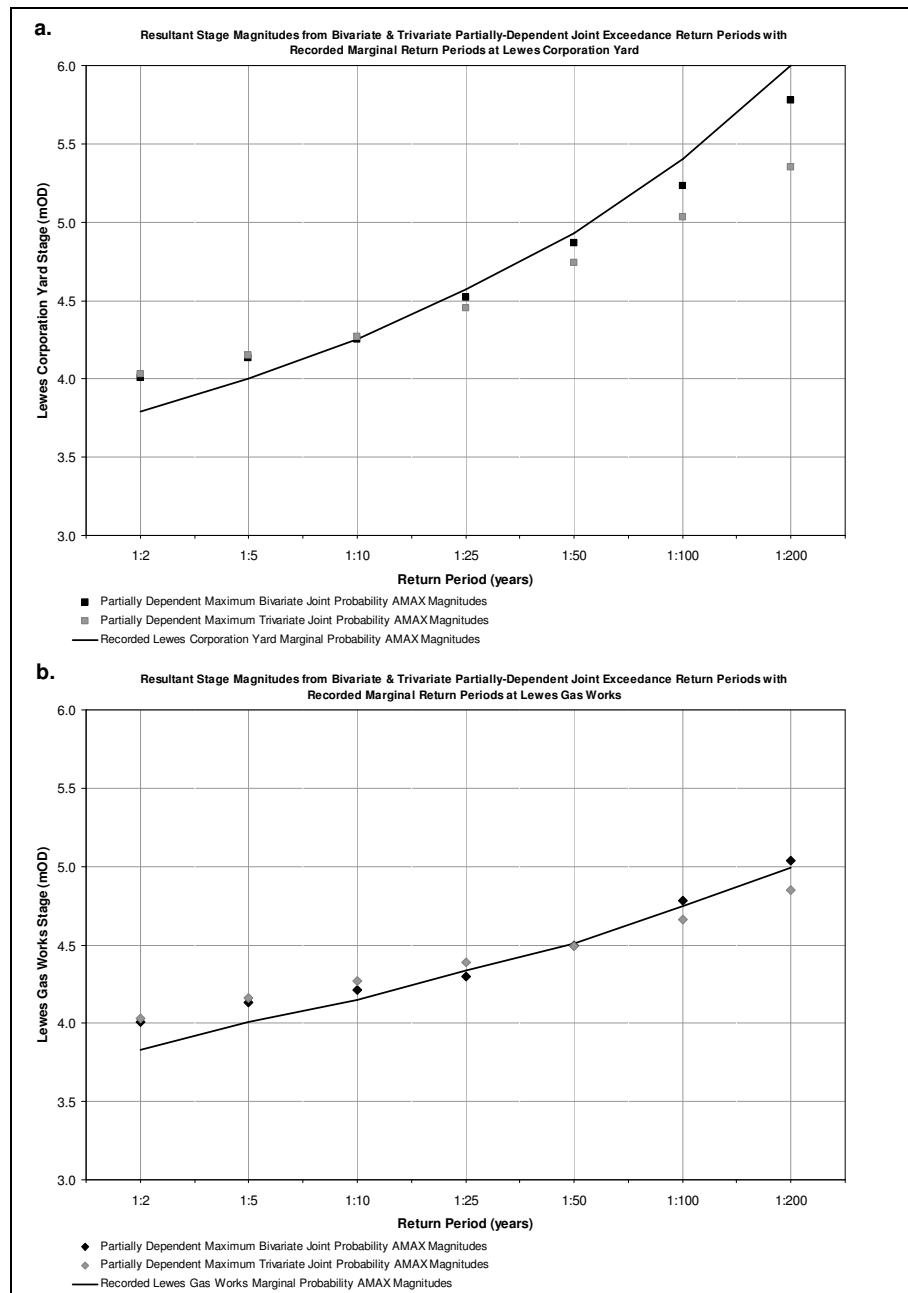


Figure 8.1 Comparison of resultant stage magnitudes for bivariate (flow & sea level) & trivariate (flow, predicted tide & surge) partially-dependent extreme joint return periods with recorded extreme return periods at **a.** Lewes Corporation Yard, & **b.** Lewes Gas Works

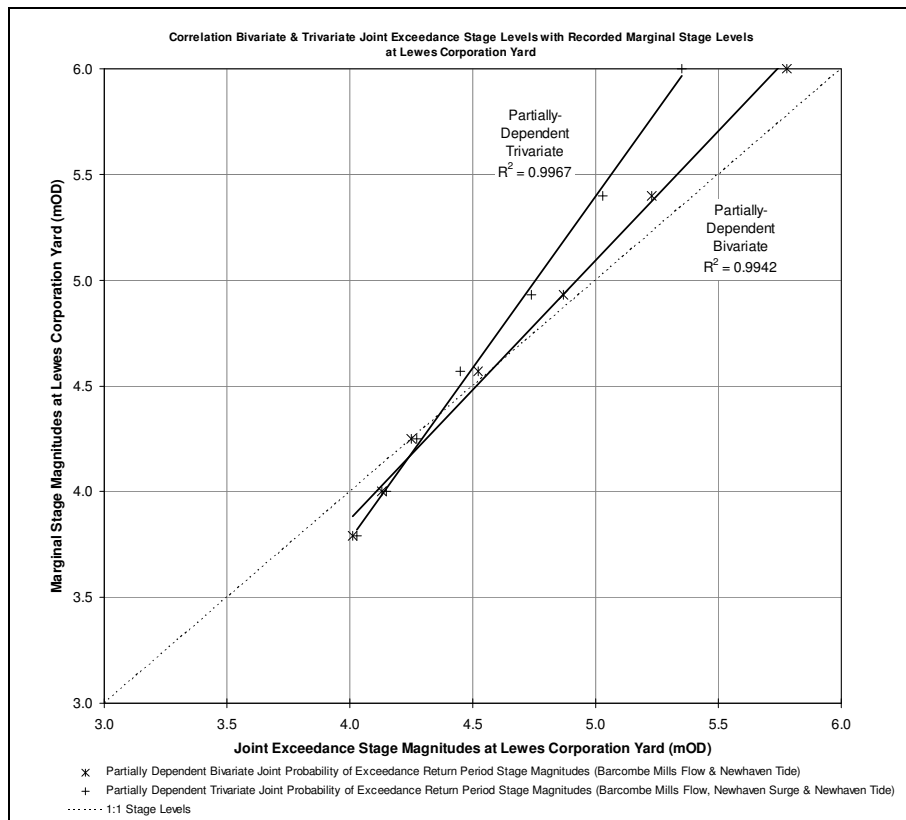


Figure 8.2 Relationship between bivariate & trivariate stage magnitudes with recorded stage magnitudes at Lewes Corporation Yard

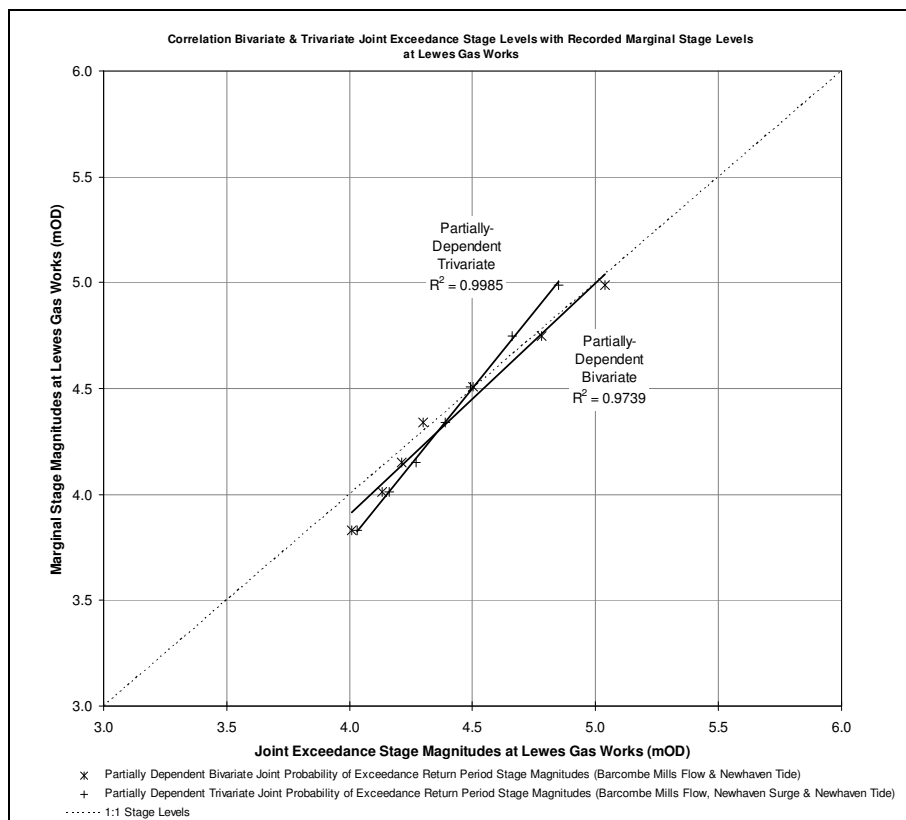


Figure 8.3 Relationship between bivariate & trivariate stage magnitudes with recorded stage magnitudes at Lewes Gas Works

Several reasons were identified as the cause of the underestimation of stage at the response locations, especially by the trivariate approach. Firstly, Table 8.1 and Table 8.2 demonstrated that above a certain level, one of the primary variables was found to dominate the resultant stage. At Lewes Corporation Yard, magnitudes above the 1:10 year joint return period were found to be controlled by river flow magnitudes from Barcombe Mills. Further downstream at Lewes Gas Works, the same river flow domination was evident above the 1:25 year return period. This signified the differing effects of flow and sea level at the two Lewes locations, which may have reduced the extreme joint exceedance stage magnitudes for the longest (i.e. 1:100 and 1:200 year) return periods. The bivariate case produced the nearest stage magnitudes to the target recorded stage magnitudes at both Lewes gauges, due to the same level of partial dependence existing throughout the flow and sea level ranges. In comparison, the trivariate case produced lower stage magnitudes for the longest return periods where full independence was assumed between river flow and predicted tide. This meant that once above a certain level, the domination of river flow reduced the impact of the partially-dependent flow and surge variables, causing the assumed full independence between river flow and predicted tide to underestimate the Lewes stage magnitudes.

Similarly, the sensitivity of both the Barcombe Mills and Lewes Corporation Yard distributions to the October 2000 flood event would have been carried over to the joint exceedance estimates and calibration with the return periods. This effect was not as apparent at Lewes Gas Works because of the lower stage observed during the flood event.

The extreme joint exceedance approach is also, to a significant degree, reliant on the accuracy of the two (or in the trivariate case, three) distributions. The inherent problems associated with the calculation of extreme distributions, such as the number of available AMAX values, meant that the standard errors for the calculated extreme return periods (e.g. from Table 6.2 and Table 6.3) would be compounded by the extreme joint exceedance approach. The effects of this were greater at Lewes Corporation Yard than Lewes Gas Works due to the high impact of the Barcombe Mills flow on the most extreme water levels upstream of Cliffe Bridge, which was demonstrated through the use of the structure functions (section 5.4). Downstream of Cliffe Bridge at Lewes Gas Works, the effect is less significant due to the reduced impact of the Barcombe Mills flow on the resultant stage, which meant the joint exceedance stage estimates were in closer agreement with the target recorded estimates.

Where the extreme joint exceedance approach was found to excel therefore was in the highly interactive zones where the primary variables combined to produce the most probable response stage magnitude, shown in the shaded areas of Table 8.1 and Table 8.2. The trivariate case identified surge as a primary variable in the production of resultant estuary water levels. Complete graphical plots and correlations are shown in full in Appendix G.7.

8.3 Daily Joint Probability Results at Lewes

8.3.1 Fully-Independent & Partially-Dependent Bivariate & Trivariate Daily Joint Probabilities

Table 8.3 and Table 8.4 show daily joint probabilities with corresponding stage at Lewes Corporation Yard and Lewes Gas Works. Each table is divided into daily exceedance probabilities estimated at the response locations. These comprise of fully-independent bivariate (flow and sea level) daily joint probabilities, partially-dependent bivariate (flow and sea level) daily joint probabilities and partially-dependent trivariate (flow, predicted tide and surge) daily joint probabilities. Unlike the previous section however, the tables are displayed in a single format. Each table shows selected stage at the response locations which have been reduced to increments of 0.1m, ranging from 2.7mAOD to 5.0mAOD due to reproductive limitations.

The exceedance probabilities and the joint probabilities (fully-independent and partially-dependent bivariate and partially-dependent trivariate) were then estimated for each increment of the target stage at Lewes Corporation Yard and Lewes Gas Works. For example, the 3.5mAOD stage magnitude at Lewes Gas Works in Table 8.4 had a daily exceedance probability of 0.0415 calculated using the simulated series (roughly equivalent to 15 days per year). The bivariate (fully-independent and partially-dependent) and trivariate daily joint probabilities were then estimated for the same target stage magnitude, producing comparative daily joint probabilities of 0.0287, 0.0352 and 0.0373 respectively. This format allowed for direct comparison of the daily joint probabilities with the probability estimates at the response locations in terms of response stage. It also enabled the different effects of flow, predicted tide and surge on the

Table 8.3 Marginal, bivariate & trivariate daily joint probabilities (in bold) for independent & partially-dependent flow, sea level and surge at Lewes Corporation Yard. Shaded areas highlight the significant interaction zones between the variables on resultant stage levels at Lewes Corporation Yard.

Stage at Lewes Corp. Yard	Daily Probability Observed at Lewes Corp. Yard	Fully-Independent Bivariate (Barcombe Mills Flow & Newhaven Sea Level) Daily Joint Probability: ($\chi = 0$)				Partially-Dependent Bivariate (Barcombe Mills Flow & Newhaven Sea Level) Daily Joint Probability: ($\chi = 0.045$)				Partially-Dependent Trivariate (Barcombe Mills Flow, Newhaven Predicted Tide & Newhaven Surge) Daily Joint Probability: (surge ν flow $\chi = 0.338$; flow/surge ν tide $\chi = 0$)					
$mAOD$	$prob./$ day	$%/day$	Bivariate Variables		Probability of Exceedance	Bivariate Variables		Probability of Exceedance	Bivariate Variables		Probability of Exceedance	Trivariate Variables			Probability of Exceedance
	$prob./$ day	$%/day$	$flow$ m^3/s	$sea\ level$ $mAOD$	$prob./$ day	$%/day$	$flow$ m^3/s	$sea\ level$ $mAOD$	$prob./$ day	$%/day$	$flow$ m^3/s	$sea\ level$ $mAOD$	$surge$ m	$prob./$ day	$%/day$
5.0	0.0002	0.0169	252	1.94	0.0001	0.0095	252	1.94	0.0006	0.0576	252	1.94	0.00	0.0001	0.0095
4.9	0.0002	0.0169	246	1.76	0.0001	0.0098	246	1.76	0.0006	0.0585	246	1.76	0.00	0.0001	0.0098
4.8	0.0002	0.0169	240	1.64	0.0001	0.0099	240	1.64	0.0006	0.0588	240	1.64	0.00	0.0001	0.0099
4.7	0.0002	0.0169	233	1.84	0.0001	0.0099	233	1.84	0.0006	0.0588	233	1.84	0.00	0.0001	0.0099
4.6	0.0002	0.0169	227	1.62	0.0001	0.0099	227	1.62	0.0006	0.0589	227	1.62	0.00	0.0001	0.0099
4.5	0.0002	0.0169	205	2.94	0.0001	0.0117	205	2.94	0.0007	0.0650	205	2.94	0.00	0.0001	0.0117
4.4	0.0002	0.0169	201	2.74	0.0002	0.0184	201	2.74	0.0008	0.0848	201	2.74	0.00	0.0002	0.0184
4.3	0.0002	0.0169	197	2.46	0.0003	0.0273	197	2.46	0.0011	0.1079	197	2.46	0.00	0.0003	0.0273
4.2	0.0003	0.0338	192	2.18	0.0004	0.0383	192	2.18	0.0013	0.1333	192	2.18	0.00	0.0004	0.0383
4.1	0.0012	0.1182	185	1.86	0.0005	0.0516	185	1.86	0.0016	0.1614	1	3.58	1.10	0.0007	0.0713
4.0	0.0022	0.2194	175	1.68	0.0007	0.0674	175	1.68	0.0019	0.1923	1	3.60	0.92	0.0011	0.1149
3.9	0.0030	0.3038	166	1.48	0.0008	0.0817	166	1.48	0.0022	0.2186	1	3.74	0.64	0.0028	0.2808
3.8	0.0052	0.5233	49	3.74	0.0012	0.1190	49	3.74	0.0028	0.2829	1	3.70	0.56	0.0052	0.5219
3.7	0.0095	0.9453	31	3.72	0.0025	0.2466	31	3.72	0.0048	0.4769	1	3.60	0.52	0.0094	0.9373
3.6	0.0194	1.9413	1	4.00	0.0076	0.7648	1	4.00	0.0115	1.1468	1	3.72	0.28	0.0174	1.7420
3.5	0.0395	3.9500	1	3.88	0.0222	2.2205	1	3.88	0.0281	2.8071	1	3.70	0.16	0.0347	3.4735
3.4	0.0667	6.6678	1	3.76	0.0485	4.8467	1	3.76	0.0560	5.6075	1	3.66	0.10	0.0561	5.6075
3.3	0.1055	10.5503	1	3.64	0.0867	8.6729	1	3.64	0.0955	9.5486	1	3.64	0.00	0.0867	8.6729
3.2	0.1526	15.2600	1	3.50	0.1380	13.7980	1	3.50	0.1473	14.7260	1	3.50	0.00	0.1380	13.7980
3.1	0.2081	20.8136	1	3.40	0.1961	19.6095	1	3.42	0.2053	20.5307	1	3.40	0.00	0.1961	19.6095
3.0	0.2655	26.5530	1	3.30	0.2552	25.5205	1	3.30	0.2640	26.3972	1	3.30	0.00	0.2552	25.5205
2.9	0.3249	32.4949	1	3.20	0.3203	32.0293	1	3.20	0.3283	32.8322	1	3.20	0.00	0.3203	32.0293
2.8	0.3903	39.0277	1	3.10	0.3912	39.1193	1	3.10	0.3983	39.8253	1	3.10	0.00	0.3912	39.1193
2.7	0.4661	46.6070	1	3.00	0.4651	46.5081	1	3.00	0.4710	47.1044	1	3.00	0.00	0.4651	46.5081

Table 8.4 Marginal, bivariate & trivariate daily joint probabilities (in bold) for independent & partially-dependent flow, sea level and surge at Lewes Gas Works. Shaded areas highlight the significant interaction zones between the variables on resultant stage levels at Lewes Gas Works.

Stage at Lewes Gas Works	Daily Probability Observed at Lewes Gas Works	Fully-Independent Bivariate (Barcombe Mills Flow & Newhaven Sea Level) Daily Joint Probability: ($\chi = 0$)				Partially-Dependent Bivariate (Barcombe Mills Flow & Newhaven Sea Level) Daily Joint Probability: ($\chi = 0.045$)				Partially-Dependent Trivariate (Barcombe Mills Flow, Newhaven Predicted Tide & Newhaven Surge) Daily Joint Probability: (surge ν flow $\chi = 0.338$; flow/surge ν tide $\chi = 0$)								
	Probability of Exceedance	$prob./$ day	$\%/day$	Bivariate Variables		Probability of Exceedance	$prob./$ day	$\%/day$	Bivariate Variables		Probability of Exceedance	$prob./$ day	$\%/day$	Trivariate Variables		Probability of Exceedance		
$mAOD$				$flow$ m^3/s	$sea\ level$ $mAOD$				$flow$ m^3/s	$sea\ level$ $mAOD$				$flow$ m^3/s	$sea\ level$ $mAOD$	$surge$ m		
5.0	0.0002	0.0169	0.0009	300	3.60	0.0000	0.0009	0.0146	300	3.60	0.0001	0.0146	0.0009	300	3.60	0.00	0.0000	0.0009
4.9	0.0002	0.0169	0.0023	300	3.34	0.0000	0.0023	0.0238	300	3.34	0.0002	0.0238	0.0023	300	3.34	0.00	0.0000	0.0023
4.8	0.0002	0.0169	0.0041	300	3.08	0.0000	0.0041	0.0325	300	3.08	0.0003	0.0325	0.0041	300	3.08	0.00	0.0000	0.0041
4.7	0.0002	0.0169	0.0059	300	2.80	0.0001	0.0059	0.0401	300	2.80	0.0004	0.0401	0.0059	300	2.80	0.00	0.0001	0.0059
4.6	0.0002	0.0169	0.0074	300	2.52	0.0001	0.0074	0.0456	300	2.52	0.0005	0.0456	0.0074	300	2.52	0.00	0.0001	0.0074
4.5	0.0002	0.0169	0.0088	300	2.22	0.0001	0.0088	0.0503	300	2.22	0.0005	0.0503	0.0088	300	2.22	0.00	0.0001	0.0088
4.4	0.0002	0.0169	0.0096	300	1.86	0.0001	0.0096	0.0532	300	1.86	0.0005	0.0532	0.0096	300	1.86	0.00	0.0001	0.0096
4.3	0.0002	0.0169	0.0100	295	1.20	0.0001	0.0100	0.0543	295	1.20	0.0005	0.0543	0.0100	295	1.20	0.00	0.0001	0.0100
4.2	0.0003	0.0338	0.0100	253	1.20	0.0001	0.0100	0.0543	253	1.20	0.0005	0.0543	0.0674	1	3.58	1.06	0.0007	0.0674
4.1	0.0007	0.0675	0.0152	205	2.70	0.0002	0.0152	0.0757	205	2.70	0.0008	0.0757	0.0965	1	3.66	0.88	0.0010	0.0965
4.0	0.0020	0.2026	0.0277	193	2.66	0.0003	0.0277	0.1008	193	2.66	0.0010	0.1008	0.1850	1	3.74	0.68	0.0019	0.1850
3.9	0.0030	0.3038	0.0531	51	3.84	0.0005	0.0531	0.1644	51	3.84	0.0016	0.1644	0.3691	1	3.74	0.56	0.0037	0.3691
3.8	0.0046	0.4558	0.1192	31	3.82	0.0012	0.1192	0.2831	31	3.82	0.0028	0.2831	0.6567	1	3.70	0.48	0.0066	0.6567
3.7	0.0106	1.0635	0.3553	1	4.06	0.0036	0.3553	0.6274	1	4.06	0.0063	0.6274	1.1476	1	3.70	0.36	0.0115	1.1476
3.6	0.0204	2.0425	1.1689	1	3.94	0.0117	1.1689	1.6253	1	3.94	0.0163	1.6253	2.0746	1	3.68	0.26	0.0207	2.0746
3.5	0.0415	4.1526	2.8730	1	3.82	0.0287	2.8730	3.5165	1	3.82	0.0352	3.5165	3.7328	1	3.68	0.14	0.0373	3.7328
3.4	0.0714	7.1404	5.9443	1	3.70	0.0594	5.9443	6.7489	1	3.70	0.0675	6.7489	5.9443	1	3.70	0.00	0.0594	5.9443
3.3	0.1060	10.6009	9.3647	1	3.60	0.0936	9.3647	10.2525	1	3.60	0.1025	10.2525	9.3647	1	3.60	0.00	0.0936	9.3647
3.2	0.1502	15.0236	14.9485	1	3.48	0.1495	14.9485	15.8793	1	3.48	0.1588	15.8793	14.9485	1	3.48	0.00	0.1495	14.9485
3.1	0.2068	20.6786	20.7720	1	3.38	0.2077	20.7720	21.5941	1	3.38	0.2159	21.5941	20.7720	1	3.38	0.00	0.2077	20.7720
3.0	0.2620	26.1985	26.8109	1	3.28	0.2681	26.8109	27.5868	1	3.28	0.2759	27.5868	26.8109	1	3.28	0.00	0.2681	26.8109
2.9	0.3229	32.2924	33.4288	1	3.18	0.3343	33.4288	34.1336	1	3.18	0.3413	34.1336	33.4288	1	3.18	0.00	0.3343	33.4288
2.8	0.3891	38.9095	40.5818	1	3.08	0.4058	40.5818	41.1965	1	3.08	0.4120	41.1965	40.5818	1	3.08	0.00	0.4058	40.5818
2.7	0.4649	46.4889	48.7938	1	2.96	0.4879	48.7938	49.2976	1	2.96	0.4930	49.2976	48.7938	1	2.96	0.00	0.4879	48.7938

resultant stage to be more accurately defined. The reverse format (estimated stage for predetermined probabilities) was found to produce an output which was too large due to the high number of possible probability increments used between 0 and 1.

Beside each bivariate and trivariate daily joint probability for each response stage, the magnitudes of the primary input variables are displayed (flow, predicted tide and surge), representing the most probable (worst case) pair (or group) which produced the daily joint probability. This meant the tables were able to demonstrate the different zones where one of the variables dominated (or in the case of Newhaven surge, strongly influenced) the resultant water levels at Lewes.

As with the extreme joint exceedance approach, the shaded areas define the most interactive bivariate and trivariate zones where the combination of the primary variables produced the most probable response level, rather than being dominated by just one variable. Below the shaded areas however (i.e. the highest probabilities), the variable of Newhaven sea level clearly dominates, with river flow (and surge in the trivariate case) reduced to minimum values. Above the shaded areas (i.e. the lowest probabilities), Barcombe Mills flow dominates the resultant stage at the response locations, whilst the impact of tide and surge levels is reduced. These results are discussed in detail below.

8.3.2 Interpretation of Results

Figure 8.4a shows an example comparison of bivariate joint probabilities with the stage values observed at Lewes Corporation Yard. Figure 8.4b shows the corresponding comparison of trivariate and probabilities at Lewes Corporation Yard. In both cases, the bivariate and trivariate daily joint exceedance cases produced probabilities which closely matched the simulated stage at Lewes Corporation Yard. Similar results were found at Lewes Gas Works.

Correlation of the bivariate and trivariate probabilities with the target probabilities (Figure 8.5 and Figure 8.6) observed at Lewes using all stage from 1.0mAOD to 5.0mAOD produced high R^2 values ($P < 0.01$). The bivariate case where full independence was assumed underestimated the stage magnitudes when compared to the estimates simulated at the Lewes gauges however, notably above the 0.020 probability level (equivalent to a 2% chance of joint occurrence per day). Correlation of the probabilities above the 2% level with corresponding probabilities produced

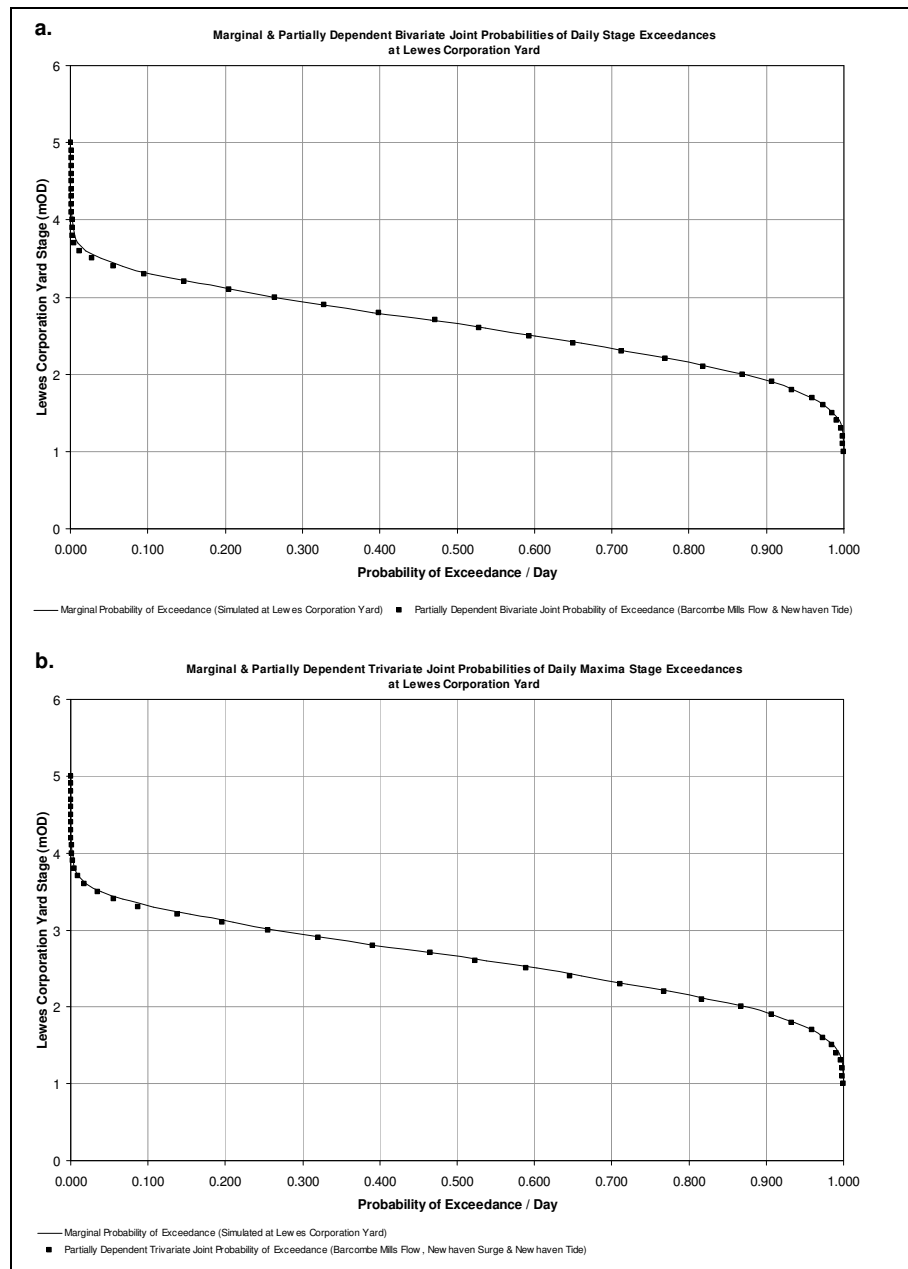


Figure 8.4 Comparison of resultant stage magnitudes at Lewes Corporation Yard from **a.** bivariate (flow & sea level) daily joint probabilities with recorded stage magnitudes, & **b.** trivariate (flow, predicted tide & surge) daily joint probabilities with recorded stage magnitudes

an R^2 value of 0.9643 ($P < 0.01$) at Lewes Corporation Yard and 0.9468 ($P < 0.01$) at Lewes Gas Works. The second bivariate case which used the calculated partial dependence value ($\chi = 0.045$) improved the joint probabilities with an R^2 value of 0.9827 ($P < 0.01$) at Lewes Corporation Yard and 0.9774 ($P < 0.01$) at Lewes Gas Works for the corresponding levels above 2%. The trivariate case which incorporated surge improved the joint probabilities further still, producing the closest correlation with the target probabilities, with an R^2 value of 0.9948 ($P < 0.01$) at Lewes Corporation Yard and 0.9913 ($P < 0.01$) at Lewes Gas Works above the 2% level.

Figure 8.5 and Figure 8.6 show that the highest probabilities (i.e. the top 2%) from the trivariate approach closely align with the 1:1 probability plots both at Lewes Corporation Yard and Lewes Gas Works, demonstrating the accuracy of the daily trivariate approach compared to the bivariate approaches. Full correlation plots are shown in Appendix G.8.

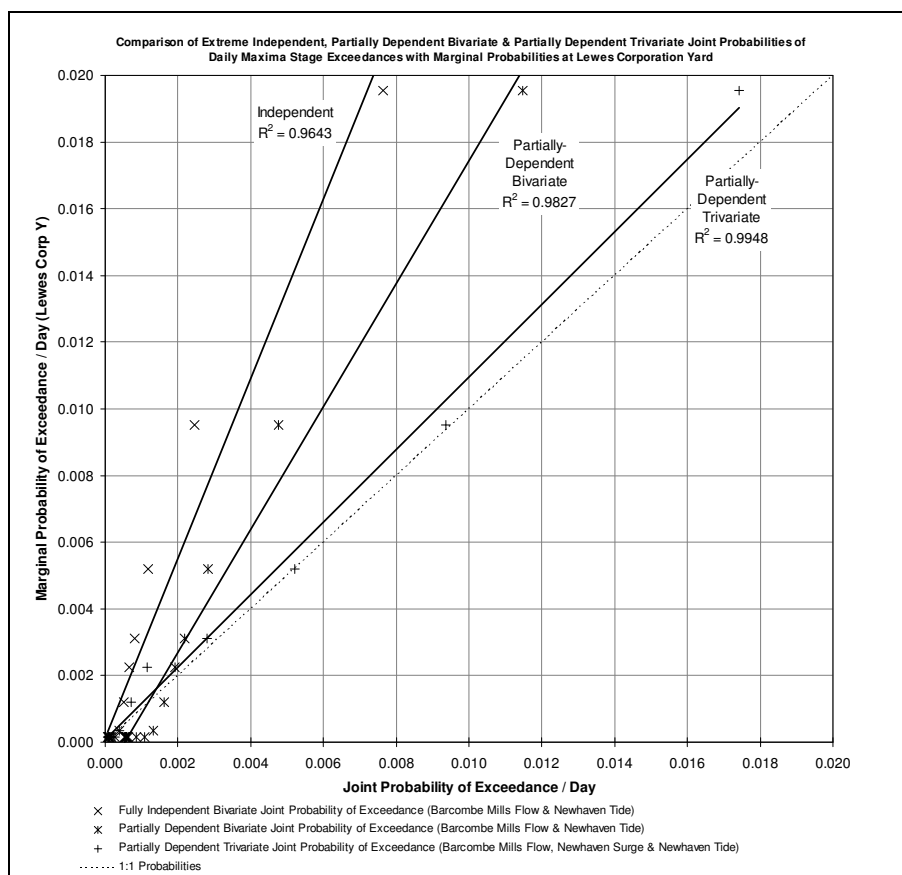


Figure 8.5 Relationship between extreme (top 2%) bivariate (flow & sea level) fully-independent, bivariate (flow & sea level) & trivariate (flow, predicted tide & surge) partially-dependent daily joint probabilities at Lewes Corporation Yard

Table 8.3 and Table 8.4 demonstrated that above a certain stage magnitude, the primary variable of Barcombe Mills flow dominated the resultant probabilities. However, unlike the extreme joint exceedance approach, the daily joint exceedance approach also demonstrated that *below* a certain stage magnitude, the primary variable of Newhaven sea level conversely dominated the resultant probabilities. The intermediate stage, shown as shaded areas in Table 8.3 and Table 8.4, categorise the highly interactive zones where the primary variables combine to produce the highest probabilities for the selected stage at Lewes. The trivariate case again showed the closest correlation with probabilities at the Lewes gauges, with surge identified as a primary variable in the production of resultant estuary water levels.

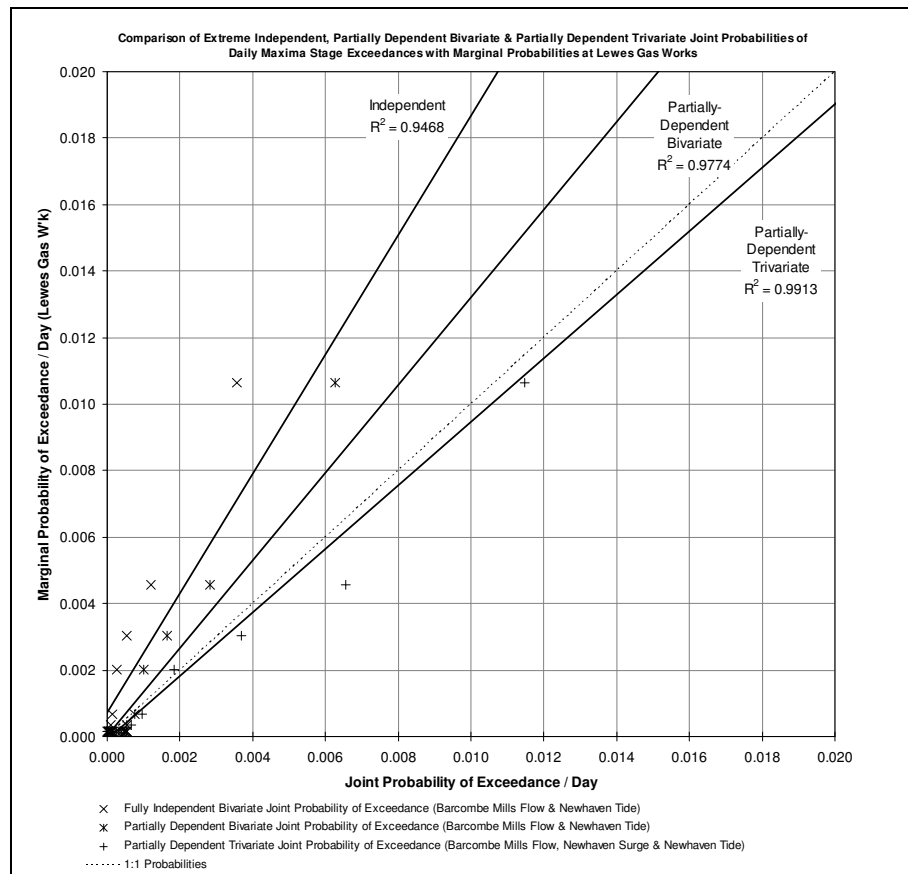


Figure 8.6 Relationship between extreme (top 2%) bivariate (flow & sea level) fully-independent, bivariate (flow & sea level) & trivariate (flow, predicted tide & surge) partially-dependent daily joint probabilities at Lewes Gas Works

Whereas the extreme joint exceedance approach is dependent on the accuracy of the distributions, the daily joint exceedance approach is reliant on the length of the two (or in the trivariate case, three) primary daily maxima series. In the case of River Ouse data, the series lengths were typically around 25 years which was found to be sufficient for the calculation of the vast majority of stage at Lewes. Beyond the duration of the series however, the primary Barcombe Mills flow, Newhaven predicted tide and surge series and the target Lewes stage series produced inaccurate daily probabilities of exceedance due to the limited number of true ‘extreme’ events contained within the daily maxima series. The daily probabilities can simply be converted to the more familiar return period format as used in the extreme joint exceedance approach, but trials with the bivariate and trivariate daily joint probabilities were found to drastically underestimate the more extreme return period magnitudes beyond the duration of the primary variables.

8.4 Annual Exceedance Curves for Extreme Return Periods

Perhaps the most important output for a joint probability analysis is to provide a method by which the relative risk the input variables pose at a particular point of interest. For the Lewes case study, this would be different combinations of the partially-dependent Barcombe Mills flow and Newhaven sea level variables which may interact to produce stage at Lewes.

Using the bivariate extreme joint return period estimates for stage at Lewes Corporation Yard and Lewes Gas Works, joint probability curves were generated for each pair of river flow and sea level which satisfied the chosen joint return periods of 2, 5, 10, 25, 50, 100 and 200 years. Figure 8.7 and Figure 8.8 show the joint exceedance curves at Lewes Corporation Yard and Lewes Gas Works. The joint exceedance curves are shown with the structure functions contours from section 5.4.4 to enable the probabilities to be converted to resultant stage at the response locations. Tables containing each flow and sea level pair for the extreme joint return periods are shown in full in Appendix G.9 for both Lewes Corporation Yard and Lewes Gas Works. Appendix G.10 shows detailed plots for each joint exceedance curve.

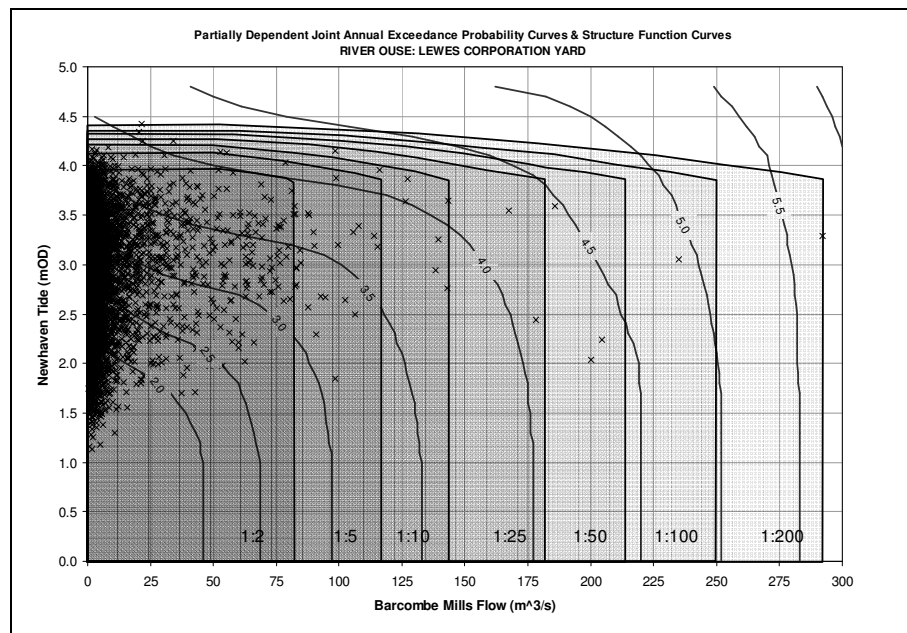


Figure 8.7 Bivariate partially-dependent (Barcombe Mills flow and Newhaven sea level) extreme joint return period curves at Lewes Corporation Yard with structure function stage contours (mAOD)

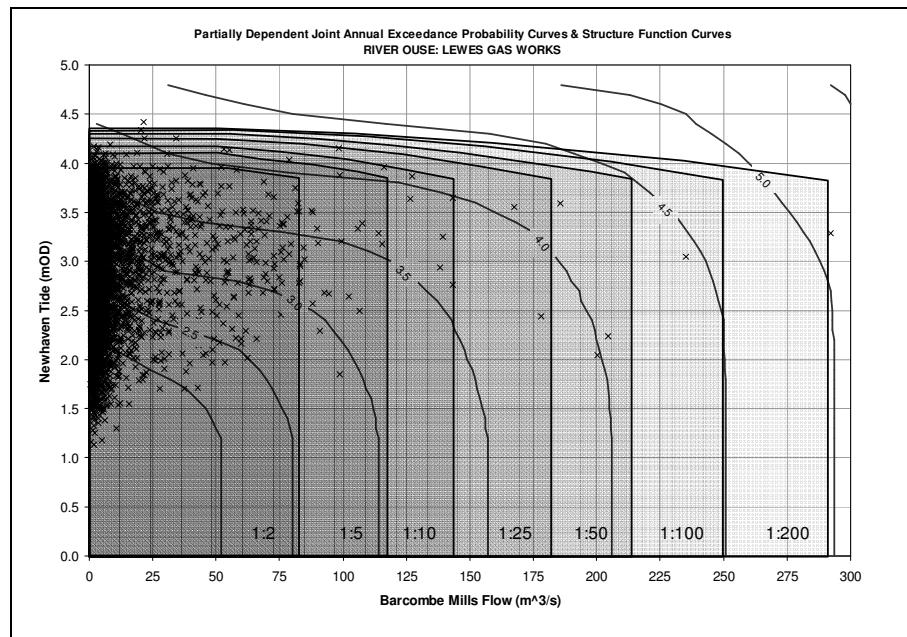


Figure 8.8 Bivariate partially-dependent (Barcombe Mills flow and Newhaven sea level) extreme joint return period curves at Lewes Gas Works with structure function stage contours (mAOD)

Although the joint exceedance curves are a simplified graphical output, they have the ability to accurately demonstrate the relative impacts of the flow and sea level magnitudes on resultant stage together with an estimate of the probability of simultaneous occurrence.

8.5 Discussion

This chapter has developed two joint exceedance approaches to estimate the probability of extreme water levels occurring in an estuarine environment caused by the interaction of partially-dependent river flow, predicted tide and surge. In both the extreme and daily joint exceedance approaches, the methodology has been shown to effectively assess the joint probabilities where dependence was found to exist between the variables.

The extreme joint return period approach however produced probabilities which, in most cases, were found to underestimate the resultant stage when compared to the values observed at the response locations. This was due to the inherent errors created in the extreme distribution and return period estimation being compounded by the joint exceedance approach. Coles (2001) comments that restricting an extreme value modelling exercise such as this to using AMAX (i.e. extreme) data is a wasteful approach

in a multivariate setting if complete data on each variable is available. This was confirmed by the development of the daily joint exceedance approach which, in comparison, has been shown to produce joint probabilities which matched the values more closely. The daily approach was also found to model the entire range of stage at the response locations, and which does not involve the fitting of statistical distributions to the variables. This approach is however limited by the duration of the daily maxima series, which may only contain a few extreme events, thus preventing the approach being extended to true extreme values. Similarly, the assumption that the partial-dependent measure χ would hold for the full range of flow, predicted tide and surge values is a simplification of the nature of dependence.

The interpretation of the dependence measure χ in a joint probability approach has identified a method by which the interaction of the variables can be accurately categorised. Svensson and Jones (2000) noted that the effect of neglecting dependence is likely to underestimate the maximum water levels for a given frequency, a finding which was confirmed by both the extreme and daily joint exceedance approaches.

The use of a third variable of surge to create a trivariate approach refined the joint exceedance methodology in the interaction zone of the variables. The examination of partial dependence between surge and river flow has been the focus of previous studies (e.g. Svensson and Jones, 2002), however the joint exceedance approach has shown that any joint probability exercise in an estuarine environment also has to incorporate astronomical tide to be able to convert probabilities to flood levels.

In the specific case of the River Ouse catchment however, it was found that the zone where the interaction of the variables had the greatest impact on the resultant stage was below the river defence overtopping heights at the response locations in Lewes. Above this level, river flow was found to dominate the most extreme flood water levels, with sea level (including surge) having a limited impact. This concluded that a bivariate approach involving river flow and sea level would be sufficient for the determination of extreme water levels at Lewes. In other estuarine systems where surge has a greater impact on the more extreme estuarine stage, such as the River Thames or River Severn, the trivariate joint exceedance approach would have clear benefits for the probabilistic determination of flood stage.

9 GENERAL DISCUSSION & CONCLUSIONS

9.1 General Discussion

Where extreme events may be created by partially-dependent variables, as was found to be the case at Lewes in East Sussex, UK, the use of bivariate joint probability methods between river flow and sea level to calculate the frequency of an extreme event provided a more reliable estimate of extreme water level frequency than more conventional approaches where statistical independence is assumed. Although the amount of daily gauged river flow and sea level data in the case study area was relatively limited, the predictions from the combined statistical and modelling approaches were in close agreement with the observed data, providing confidence that the method is sound for the estimation of joint probabilities. For more extreme values however, the bivariate daily joint exceedance probabilistic approach was found to underestimate probability values beyond the duration of the input series which may only contain a few extreme events, thus preventing the approach being extended to true extreme values. The generation of larger datasets could be utilised (e.g. Jones, 1998) to explore this further, which may produce more confident extreme joint probabilities from daily probabilities of exceedance.

Trivariate joint probability methods, which incorporated a third variable of surge in addition to river flow and sea level, achieved a greater level of accuracy than the independent and partially-dependent bivariate approaches for estimating joint probabilities and return periods in the mid-range interaction zone, where flow, predicted tide and surge combine to produce resultant water levels at the response locations of interest. However, it was found that the zone where the interaction of the variables had the greatest impact on the resultant stage was below the river defence overtopping heights at the response locations in Lewes, and that as the values reached critical extreme levels, river flow dominated the resultant stage. In other estuarine environments therefore, where surge has a greater impact on the more extreme estuarine stage, (e.g. the River Thames or River Severn), the trivariate joint exceedance approach would be clearly beneficial for flood frequency estimation.

The dependence measure χ was shown to successfully model the extremal relationship between the hydrological variables of river flow, predicted tide and surge, due to the identification of extreme values whilst maintaining complete datasets. The results were in

direct contrast to initial regression analyses performed on the most extreme annual maxima and peaks-over-threshold values which were found to misrepresent the true extremal relationship. Where calculated dependence between the variables was found to be high, this research has concluded that an accurately calculated χ dependence value can have a significant and positive effect on the estimation of resultant flood heights by successfully refining estimated joint probabilities.

Dependence between surge and river flow has been identified as having the strongest relationship due both being driven by meteorological storm systems (e.g. Svensson and Jones, 2002). However, the results of this research have demonstrated that a measure of dependence between surge and flow should be used in conjunction with further hydraulic modelling and joint probability analyses involving predicted tide to produce ultimate extreme water levels a point of interest. Apart from locations which have a highly interactive storm surge and flow zone above the range of the predicted tide, the most extreme flood levels are likely to be dominated by one of the variables of tide or river flow rather than surge alone.

Dependence χ was also found to differ over relatively short distances, enabling the interaction of river flow and sea level to be successfully quantified at different locations in the tidal river channel. The case study locations of Lewes Corporation Yard and Lewes Gas Works, sited approximately 0.5km apart, provided a good example of this. The upstream Lewes Corporation Yard site was shown to be more susceptible to fluvial flooding than Lewes Gas Works further downstream due to narrowing channel geometry between the gauges which reduced the tidal / fluvial interaction in upper reaches during extreme events. This lead to increased dependency between flow and stage at the upstream gauge, whilst reducing dependence between flow and stage at the downstream Lewes Gas Works gauge.

The presented joint probability methods could be further extended to investigate the frequency of potential future flood events incorporating the predicted effects of climate change. Due to the weakness of the supporting climate change data, no attempt was made to try to gain an understanding of the implications of either increased storm magnitude or changed storm frequency on dependence values or joint probabilities, although the methods have clearly demonstrated the sensitivity of flood levels to increasing levels of dependence and magnitude.

The purpose of any flood risk analysis is to determine how at risk a particular location is from flooding. Traditional approaches rely heavily on statistical methods to demonstrate both the cause and the effect of flooding, focusing attention on observations rather than the physical processes that may have caused them. However, risk analysis is not an exact science, a fact which is often overlooked especially when statisticians have provided good, but not flawless, methodologies to calculate probabilities and return periods of extreme events from single (and often short) observed data series. Statistics is a science of description, not causality, (Chow, *et al.*, 1988) which is based on mathematical principles that describe the variation of a set of observations of a process, such as water levels in an estuary, rather than the causes. In flood risk terms, this may provide a believable answer, but it is one that disguises a remaining uncertainty which cannot be quantified due to the often limited historical datasets, which may only contain a few extreme events. This research has shown that statistics can only provide a meaningful answer if it can be utilised with a greater insight into the processes behind it. Estuaries and tidal rivers are real dynamic systems rather than a statistical problem, comprising of numerous variables which can all contribute to flooding, including astronomically-driven tides, surges and river flows. Knowledge of how these variables interact with each other and with the other less-quantifiable catchment processes is essential for an accurate flood risk analysis. Take-up of existing dependence and joint probability methods for the analysis of flood risk has therefore been low however due to fragmented methods, lack of published research and perceived difficulty of joint probability analyses.

The aim of this research was to address these issues by combining the existing methods of hydraulic modelling, structure functions, single probability, statistical dependence and joint probability to produce a coherent and workable joint probability solution. This has been achieved by successfully testing the approach on a typical case study area of Lewes, where flooding may potentially be caused by the combination of more than one variable. Extreme joint probability statistics was found to be effective in estimating the bivariate and trivariate joint probabilities of river flow, sea level and surge, when used in conjunction with one-dimensional hydraulic modelling techniques and structure functions, which contain the physical processes to enable the direct prediction of both the frequency and magnitude of flood events at any locations within the river. Joint probability therefore has a clear role to play in flood risk analysis as a method for the interpretation of results from a physical analysis of the causes of flooding.

9.2 Summary of General Conclusions

- The combination of traditional flood risk methods of extreme value analysis, one-dimensional hydraulic modelling and structure function generation, when used with statistical dependence and multivariate joint probability approaches has been shown to produce more refined estimates of flood level exceedance probabilities caused by the combination of more than one hydrological variable than conventional probabilistic techniques.
- The bivariate extreme dependence and joint probability research has been shown to accurately categorise the probability of flooding in low lying floodplain zones by successfully quantifying the risk created by the complex interaction of sea level and river flow in tidal rivers and estuaries. The predictions from the combined statistical and modelling approaches was found to be comparable with observed data and probabilities, providing confidence that the approach was sound for predicting more extreme events.
- The trivariate joint probability approach, which incorporated a third variable of surge in addition to river flow and sea level, achieved a greater level of accuracy than the independent and partially-dependent bivariate approaches for the estimation of joint probabilities and return periods in the interaction zone where flow, tide and surge combine to produce resultant water levels at a point of interest.
- The multivariate joint probability methods were however limited by the quality and duration of the input variables. The research found that the calculation of extreme daily joint probabilities was affected by relatively short datasets which contained few observed extreme events. Similarly, it was concluded that the calculation of annual joint return periods magnified the inaccuracies of the input distributions and estimated return periods.
- The dependence measure χ was found to successfully categorise the extremal relationship between the hydrological variables of river flow, tide and surge to a higher accuracy than traditional statistical regression methods.
- The research noted that existing dependence theory which has focused on determining dependence between surge and river flow due to being commonly

linked to meteorological storm systems, can not be directly applied to a joint probability analysis for the conversion to design flood levels at a determined point of interest, necessitating a trivariate joint probability approach involving total sea level.

- It was concluded that although the joint probability approach has been shown to be complex and site specific in nature, the methodology was generic and could be applied to any location at risk of flooding from more than one source.

9.3 Recommendations for Further Research

- The bivariate and trivariate dependence and joint probability methods should be applied to further areas where the third variable of surge has a far greater impact on both the total sea levels and the resultant upstream stage.
- The effects of predicted climate change (either increased frequency or magnitudes) on the level of dependence between input variables and resultant joint probabilities should be analysed and compared to the results presented here.
- Methods for the improvement to the hydrological variables used in the daily joint exceedance approach, to allow for more extreme responses to estimated beyond the duration of the daily maxima series.
- The integration of different dependence values of χ calculated for various thresholds, to improve the simplification of applying the same χ value to the complete ranges used in the daily joint exceedance approach.
- The methodology of joint probability analysis should be made more available and readily usable to practicing engineers and hydrologists by providing clear guidelines for the complete process than currently exist. A robust, user friendly and more accessible process should be designed for the determination of multivariate joint probabilities, based on non-identical probabilities and return periods, using the dependence measure χ .
- Legislation and policy implications of the research in comparison to and in conjunction with existing methods should be explored, including any

ramifications of the joint probability methodology and the applicability to end users. This would link the science, method and application to policy.

- The use of extreme value theory in the field of financial mathematics could be explored, including the use of statistical dependence.

REFERENCES

- ACREMAN, M. C. (1994). Assessing the joint probability of fluvial and tidal floods in the River Roding. *J. IWEM*, **8**, 490-496.
- ADMIRALTY (2005). *Admiralty TotalTide World Tidal Prediction Software, version DP550, 2005*. Admiralty Charts and Publications, United Kingdom Hydrographic Office (UKHO).
- BAYLISS, A. C. and JONES, R. C. (1993). *Peaks-over-threshold flood database: Summary statistics and seasonality*. Report No. 121, Institute of Hydrology, Wallingford, UK.
- VAN DER BOOGAARD, H. F. P and STIVE, R. J. H. (1990). *A correlation of analysis of extreme River Medway discharges and Sheerness storm surges*. In Proc. Int. Conf. on River Flood Hydraulics, John Wiley & Sons, 1990.
- BRUUN, J. T. and TAWN, J. A. (1998). Comparison of approaches for estimating the probability of coastal flooding. *Appl. Statist.*, **47**, 405-423.
- BUISHAND, T. A. (1984). Bivariate extreme-value data and the station-year method. *J. Hydrol.*, **69**, 77-95.
- BUISHAND, T. A. (1991). Extreme rainfall estimation by combining data from several sites. *Hydrological Science Journal*, **36**, 345-365.
- COLES, S. G. (2001). *An introduction to statistical modelling of extreme values*. Springer-Verlag (Series in Statistics), London, UK.
- COLES, S. G., HEFFERNAN, J. and TAWN, J. A. (2000). Dependence measures for extreme value analyses. *Extremes*, **2**, 339-365.
- COLES, S. G. and TAWN, J. A. (1991). Modelling extreme multivariate events. *J. R. Statist. Soc.*, **B 53**, 377-392.
- COLES, S. G. and TAWN, J. A. (1994). Statistical methods for multivariate extremes: an application to structural design. *Appl. Statist.*, **43**, 1-48.
- CHOW, V. T. (1959). *Open Channel Hydraulics*. McGraw-Hill Kogakusha, Tokyo, Japan.
- CHOW, V. T., MAIDMENT, D. R. and MAYS, L. W. (1988). *Applied hydrology (international edition)*. McGraw-Hill (Series in Water Resources and Environmental Engineering), New York, U.S.A.
- DIXON, M. J. and TAWN, J. A. (1994). *Extreme sea-levels at the UK A-class sites: site-by-site analyses*. Internal Document No. 65, Proudman Oceanographic Laboratory, UK.
- DWYER, I. J. (1995). *Confluence flood joint probability*. Report to MAFF, project number FD0417. Institute of Hydrology, UK.
- ENVIRONMENT AGENCY (1998). *Simulation of Flow of Sussex Ouse: Data Collection & Simulation Using HYSIM (Hydrological Simulation Model, Oxford Science Software Ltd, UK), 1920-1996*. Report by Water Resource Associates for Environment Agency (Southern Region), UK, 1998.
- ENVIRONMENT AGENCY (2000). *Report on the Brockenhurst flood, 24th-25th December 1999*. Report by Environment Agency (Southern Region), No. R1274, UK, May 2000.
- ENVIRONMENT AGENCY (2001a). *River Ouse Section 105 Study: River Ouse Flood Risk Mapping Final Report*. Report by Atkins (AK2904) for Environment Agency (Southern Region), UK, 2001.

- ENVIRONMENT AGENCY (2001b). *Lower Ouse Section 105 Coastal Flood Plain Mapping B5826*. Report by BKS Surveys for Environment Agency (Southern Region), UK, 2001.
- ENVIRONMENT AGENCY (2001c). *Sussex Ouse 12th October 2000 Flood Report*. Report by Binnie Black & Veatch for Environment Agency (Southern Region), UK, March 2001.
- ENVIRONMENT AGENCY (2001d). *Survey of the Lower Ouse Channel*. Data produced by Longdin and Browning for Environment Agency (Southern Region), UK, 2001.
- ENVIRONMENT AGENCY (2002). *Sussex Ouse Flood Management Strategy*. Appraisal Report by Binnie Black & Veatch for Environment Agency (Southern Region), UK, May 2002.
- ENVIRONMENT AGENCY (2003). Personal communications with Russell Long & Chris Manning, 2003 to 2007. Hydrology and Water Resources dept., Environment Agency (Southern Region), UK.
- ENVIRONMENT AGENCY (2004). *Sussex Ouse Flood Management Strategy 2004 Update*. Report by Black & Veatch for Environment Agency (Southern Region), UK, May 2004.
- ENVIRONMENT AGENCY (2005a). HYDROLOG hydrometric database. Environment Agency, Sussex Area, UK.
- ENVIRONMENT AGENCY (2005b). RAINARK rainfall database. Environment Agency, Sussex Area, UK.
- ENVIRONMENT AGENCY (2006). *River Ouse Catchment Flood Management Plan (CFMP)*. Consultation Scoping Report by Environment Agency (Southern Region), UK, October 2006.
- GRANGER, C. W. J. (1959). Estimating the probability of flooding on a tidal river. *J. Instn. Water Engineers*, **13**, 165-174.
- HALCROW (2001). Southern Region Sussex & Kent Flooding 2000: 2240/2241 Lewes & Uckfield Flood survey undertaken for the Environment Agency, Southern Region.
- HAWKES, P. J. (2003). *Extreme water levels in estuaries and rivers: the combined influence of tides, river flows and waves*. R&D Technical Report FD0206/TR1 to Defra. HR Wallingford, UK.
- HAWKES, P. J. (2004). *Use of joint probability methods for flood & coastal defence: a guide to best practice*. R&D Interim Technical Report FD2308/TR2 to Defra. HR Wallingford, UK.
- HAWKES, P. J. & SVENSSON, C. (2003). *Joint probability: dependence mapping & best practice*. R&D Interim Technical Report FD2308/TR1 to Defra. HR Wallingford and CEH Wallingford, UK.
- HAWKES, P. J. & TAWN, J. A. (2000). *Joint probability of waves and water levels: JOIN-SEA: A rigorous but practical new approach*. Internal Document No. SR 537, HR Wallingford with Lancaster University, UK. (Originally dated Nov. 1998, re-issued with minor adjustments in final form May 2000).
- HEAPS, N. S. (1983). Storm surges, 1967-1982. *Geophys. J. Roy. Ast.*, **74**, 331-376.
- HUNT, R. D. (1972). North Sea storm surges. *Marine Observer*, **42**, 115-124.
- IBIDAPO-OBE, O. and BERAN, M. (1988). *Hydrological aspects of combined effects of storm surges and heavy rainfall on river flow*. Report No. 30 in the Operational Hydrology Series, WMO Report No. 704. World Meteorological Organisation, Geneva.

- JONES, D. A. (1998). *Joint probability fluvial-tidal analyses: structure functions and historical emulation*. Report to MAFF, project number FD0417. Institute of Hydrology, UK.
- LOGANATHAN, G. V., KUO, C. Y. and YANNACCONC, J. (1987). Joint probability distribution of streamflows and tides in estuaries. *Nord. Hydrol.*, **18**, 237-246.
- MACDONALD, D. (2004). *Derivation of design flood estimates for the River Uck near Uckfield – problems and solutions*. In Proceedings from the DEFRA 39th Flood & Coastal Management Conference, York, UK, July 2004, 5B.3.1- 5B.3.10.
- VAN DER MADE, J. W. (1969). *Design levels in the transition zone between the tidal reach and the river regime reach*. In Hydrology of Deltas, Vol. 2 of Proc. Bucharest Symposium, May 1969. 257-272.
- MANTZ, P. A. and WAKELING, H. L. (1979). Forecasting flood levels for joint events of rainfall and tidal surge flooding using extreme value statistics. *Proc. Inst. Civil Eng.*, **67**, 31-50.
- MEADOWCROFT, I., HAWKES, P. J. and SURENDRAN, S. (2004). *Joint probability best practice guide: practical approaches for assessing combined sources of risk for flood and coastal risk managers*. In Proceedings from the DEFRA 39th Flood & Coastal Management Conference, York, UK, July 2004, 6A.2.1- 6A.2.12.
- MET OFFICE (METEOROLOGICAL OFFICE) (2000). Meteorological Office Rainfall and Evaporation Calculating System (MORECS) data for squares 172 and 173 Meteorological Office.
- ODPM (OFFICE OF THE DEPUTY PRIME MINISTER) (2001). Planning Policy Guidance Note PPG25 – Development & Flood Risk. Committee report by Environment, Transport and Regional Affairs, 2000-01, HC64: Development on, or Affecting the Flood Plain for the Office of the Deputy Prime Minister (6th February 2001).
- PRANDLE, D. and WOLF, J. (1978). The interaction of surge and tide in the North Sea and River Thames. *Geophysical J. Royal Astronomical Soc.*, **55**, 203-216.
- PROUDMAN OCEANOGRAPHIC LABORATORY (2006). Newhaven Sea Level Predictions and Recordings, Admiralty Tide Tables. Proudman Oceanographic Laboratory.
- PUGH, D. T. (1987). *Tides, surges and mean sea-level*. Wiley, Chichester, UK.
- REED, D. W. (1999). *Flood Estimation Handbook, Vol. 1: Overview*. Institute of Hydrology, Wallingford, UK.
- ROBSON, A. and REED, D. W. (1999). *Flood Estimation Handbook, Vol. 3: Statistical procedures for flood frequency estimation*. Institute of Hydrology, Wallingford, UK.
- SOUTHERN WATER AUTHORITY (1975). Winterbourne Stream, Lewes: Flood Survey Report Southern Water Authority report into November 1974 flood (November 1975).
- SAMUELS, P. G. and BURT, N. (2002). A new joint probability appraisal of flood risk. *Proc. Inst. Civil Eng. – Water & Maritime Eng.*, **154**, 109-115.
- SVENSSON, C. and JONES, D. A. (2000). *Dependence between extreme sea surge, river flow and precipitation: a study in eastern Britain*. Report to MAFF, project number FD0206. CEH Wallingford, UK.
- SVENSSON, C. and JONES, D. A. (2002). Dependence between extreme sea surge, river flow and precipitation in eastern Britain. *Int. J. Climatol.*, **22** (10), 1149-1168.

- SVENSSON, C. and JONES, D. A. (2003). *Dependence between extreme sea surge, river flow & precipitation: a study in south & west Britain*. R&D Interim Technical Report FD2308/TR3 to Defra. CEH Wallingford, UK.
- SVENSSON, C. and JONES, D. A. (2004a). Dependence between sea surge, river flow & precipitation in south & west Britain. *Hydrol. Earth Sys. Sci.*, **8**, 973-992.
- SVENSSON, C. and JONES, D. A. (2004b). *Sensitivity to storm track of the dependence between extreme sea surges and river flows around Britain*. In Hydrology: Science and Practice for the 21st Century, Vol. 1. Proc. from the British Hydrological Society's international conference, London, UK, July 2004, 239a-245a (addendum).
- SVENSSON, C. and JONES, D. A. (2005). *Climate change impacts on the dependence between sea surge, precipitation and river flow around Britain*. In Proceedings from the DEFRA 40th Flood & Coastal Management Conference, York, UK, July 2005, 6A.3.1-6A.3.9.
- TAWN, J. A. (1992). Estimating probabilities of extreme sea-levels. *Appl. Statist.*, **41**, 77-93.
- THOMPSON, G. and LAW, F. M. (1983). *An assessment of the fluvial tidal flooding problem of the River Ancholme, UK*. In Proceedings from the IUGG Interdisciplinary Symposium on the Assessment of Natural Hazards, Hamburg, Germany, August 1983.
- TYAGI, A. C. & SAALMULLER, J. (2004). *Integrated flood management*. In Proceedings from the DEFRA 39th Flood & Coastal Management Conference, York, UK, July 2004, 7.1.1-7.1.5.
- U.S. ARMY CORPS OF ENGINEERS (2004). *Hydrologic Engineering Center – Rivers Analysis System (HEC-RAS), version 3.1.2, April 2004*. U.S. Army Corps of Engineers, U.S.A.
- VONGVISESSOMJAI, S. and ROJANAKAMTHORN, S. (1989). Interaction of tide and river flow. *J. Waterway Port Coastal Ocean Eng. (ASCE)*, **115**, 86-104.
- WALDEN, A. T., PRESCOTT, P. and WEBBER, N. B. (1982). The examination of surge-tide interaction at two ports on the central south coast of England. *Coastal Engineering*, **6**, 59-70.
- WESTON, A. E. (1979). The measurement of interactive freshwater and tidal flows in the River Dee, North Wales. *J. Inst. Water Eng. Sci.*, **33**, 69-79.
- WORTH, D. & HUNT, T. (2004). *Tides - a level of confidence*. In Proceedings from the DEFRA 39th Flood & Coastal Management Conference, York, UK, July 2004, 6A.4.1-6A.4.9.



APPENDICES A-G

APPENDIX CONTENTS

Appendix Contents.....	166
List of Appendix Figures	169
List of Appendix Tables.....	176
 APPENDIX A HYDROLOGICAL DATA.....	 181
A.1 Upper Ouse & Uck Sub-Catchment Gauges.....	182
A.2 Middle Ouse Sub-Catchment Gauges	183
A.3 Lower Ouse Sub-Catchment Gauges	184
A.4 Locations of the Ouse Catchment Gauges	186
 APPENDIX B MODELLING & SIMULATION.....	 187
B.1 Synthesised Barcombe Mills Flow Series.....	188
B.1.1 Calibration with HYSIM Simulated Series.....	188
B.1.2 Calibration with Barcombe Mills Recorded Series.....	189
B.2 Hydraulic Modelling of the Lower Ouse	190
B.2.1 DGPS Survey of the Lower Ouse	190
B.2.2 Model Calibration Input Event Hydrographs.....	193
B.2.3 HEC-RAS Model	194
B.3 Continuous Simulation.....	195
B.3.1 Simulated Stage at Lewes Corporation Yard & Lewes Gas Works.....	195
B.3.2 Calibration of Simulated Stage at Lewes Corporation Yard with 2000 - 2006 Recorded Series.....	196
B.3.3 Calibration of Simulated Series at Lewes Corporation Yard with 2005 - 2006 Recorded Series.....	197
B.4 Representative Hydrographs	198
B.4.1 Barcombe Mills Flow Representative Hydrographs.....	198
B.4.2 Newhaven Tide Representative Hydrographs.....	199
B.4.3 Time-Lagged Analysis	200
B.5 Structure Function Matrices.....	200
B.6 Simulated Longitudinal Sections	202
B.7 Historical Emulation	204
B.7.1 Calibration of Emulated Series at Lewes Corporation Yard with 1982 - 2006 Simulated Series.....	204
B.7.2 Calibration of Emulated Series at Lewes Corporation Yard with 2000 - 2006 Recorded Series.....	205
B.7.3 Calibration of Emulated Series at Lewes Corporation Yard with 2005 - 2006 Recorded Series.....	206
 APPENDIX C ANNUAL MAXIMA SERIES	 207
C.1 Upper Ouse & Uck Sub-Catchments	208
C.1.1 Gold Bridge AMAX.....	208
C.1.2 Isfield Weir AMAX	211
C.1.3 Clappers Bridge AMAX	214
C.1.4 Old Ship AMAX	217
C.2 Middle Ouse Sub-Catchment	220
C.2.1 Extending the Barcombe Mills Series.....	220
C.2.2 Barcombe Mills (Flow) AMAX.....	222
C.3 Lower Ouse Sub-Catchment	225
C.3.1 Extending the Lewes Corporation Yard Series.....	225
C.3.2 Lewes Corporation Yard AMAX.....	227

C.3.3	Lewes Gas Works AMAX	230
C.4	Tide	233
C.4.1	Extending the Newhaven (Tide) Series.....	233
C.4.2	Frequency of Tidal AMAX Events at Newhaven	233
C.4.3	Newhaven (Tide) AMAX	235
C.4.4	Newhaven (Surge) AMAX	239
C.4.5	Newhaven (Surge at High Tide) AMAX	242
C.5	Concurrent AMAX Events.....	245
C.5.1	Lewes Corporation Yard & Barcombe Mills	245
C.5.2	Lewes Corporation Yard & Newhaven (Tide).....	245
APPENDIX D	PEAKS-OVER-THRESHOLD SERIES	246
D.1	Independent POT Exceedance	247
D.1.1	Comparison of Threshold Selections	247
D.1.2	Upper Ouse Catchment POT Results Comparison	250
D.1.3	Seasonality	251
D.2	Joint Occurrence of POT Events.....	253
D.2.1	Barcombe Mills & Lewes Corporation Yard	253
D.2.2	Barcombe Mills & Newhaven (Tide).....	254
D.2.3	Barcombe Mills & Newhaven (Maximum Surge)	255
D.2.4	Lewes Corporation Yard & Newhaven (Tide).....	256
D.2.5	Lewes Corporation Yard & Newhaven (Maximum Surge)	257
D.2.6	Newhaven (Tide) & Newhaven (Maximum Surge).....	258
D.2.7	Newhaven (Maximum Surge) & Newhaven (Surge at High Tide).....	259
D.3	Joint POT Correlation	260
D.3.1	Barcombe Mills & Lewes Corporation Yard	260
D.3.2	Barcombe Mills & Newhaven (Tide).....	261
D.3.3	Barcombe Mills & Newhaven (Surge).....	262
D.3.4	Lewes Corporation Yard & Newhaven (Tide).....	263
D.3.5	Lewes Corporation Yard & Newhaven (Surge).....	264
APPENDIX E	HISTORICAL FLOOD EVENTS	265
E.1	Historical Flooding in the Ouse Catchment	266
E.2	Extreme Event Analysis of the 12 th October 2000 Flood	268
E.2.1	Flood Account.....	268
E.2.2	Peak Flood Magnitudes & Estimated Return Periods.....	270
E.2.3	Interaction of Fluvial Flow & Tide at Lewes.....	272
E.2.4	Calibration Hydrographs.....	274
E.2.5	Flood Hydrographs	275
E.2.5.1	Barcombe Mills	275
E.2.5.2	Lewes Corporation Yard	276
E.2.5.3	Southease Bridge.....	277
E.2.5.4	Newhaven (Tide).....	278
E.2.5.5	Newhaven (Surge).....	279
E.2.6	Hydrographs of Flow & Tide Interaction at Lewes	280
APPENDIX F	STATISTICAL DEPENDENCE	281
F.1	Dependence Worked Example.....	282
F.1.1	Data Preparation.....	282
F.1.2	Threshold Selection.....	282
F.1.3	Calculation of the Dependence Measure χ	284
F.1.4	Interpreting χ	288

F.2	Daily Maxima Dependence Datasets	289
APPENDIX G	JOINT PROBABILITY	291
G.1	Daily Exceedance Probabilities.....	292
G.2	Comparison of Joint Return Period Methods.....	294
G.3	Interpretation of the Dependence Measure	295
G.3.1	Calculation of Extreme Joint Return Periods using χ	295
G.3.2	Calculation of Daily Joint Probabilities using χ	299
G.4	Bivariate Joint Probability Tables.....	300
G.4.1	Bivariate Joint Return Periods	300
G.4.2	Bivariate Daily Joint Probabilities	300
G.5	Trivariate Joint Probability Tables.....	302
G.5.1	Trivariate Joint Return Periods	302
G.5.2	Trivariate Daily Joint Probabilities	302
G.6	Structure Function Tables	305
G.6.1	Structure Functions for Return Period Conversions	305
G.6.2	Structure Functions for Daily Probability Conversions.....	305
G.7	Extreme Joint Return Periods	308
G.7.1	Extreme Joint Return Periods at Lewes Corporation Yard.....	308
G.7.2	Extreme Joint Return Periods at Lewes Gas Works	311
G.8	Daily Joint Probabilities.....	314
G.8.1	Daily Joint Probabilities at Lewes Corporation Yard	314
G.8.2	Daily Joint Probabilities at Lewes Gas Works.....	317
G.9	Extreme Joint Return Periods & Resultant Water Levels.....	320
G.9.1	Joint Return Periods at Lewes Corporation Yard	320
G.9.2	Joint Return Periods at Lewes Gas Works	329
G.10	Joint Exceedance Curves for Extreme Return Periods	338
G.10.1	Joint Exceedance Curves at Lewes Corporation Yard.....	338
G.10.2	Joint Exceedance Curves at Lewes Gas Works	340

LIST OF APPENDIX FIGURES

Figure A.1 Map of river flow, stage and tide gauges in the Ouse catchment	186
Figure B.1 Time-series plot of synthesised daily mean flow with HYSIM simulated daily mean flow at Barcombe Mills (2002)	188
Figure B.2 Correlation of synthesised and HYSIM simulated daily mean flow magnitudes at Barcombe Mills (2002): complete series	188
Figure B.3 Correlation of synthesised and HYSIM simulated daily mean flow magnitudes at Barcombe Mills (2002): <40m ³ /s only	188
Figure B.4 Time-series plot of synthesised daily mean flow with recorded daily mean flow at Barcombe Mills (2002)	189
Figure B.5 Correlation of synthesised and recorded daily mean flow magnitudes at Barcombe Mills (2002): complete series	189
Figure B.6 Correlation of synthesised and recorded daily mean flow magnitudes at Barcombe Mills (2002): <20m ³ /s only	189
Figure B.7 Map of OS active GPS stations, UK	190
Figure B.8 Calibration input event hydrographs at Barcombe Mills & Newhaven (event no.'s 1 to 8)	193
Figure B.9 3-dimensional map of the Lower Ouse hydraulic HEC-RAS model	194
Figure B.10 Simulated stage at Lewes Corporation Yard (June 1982 - May 2006)	195
Figure B.11 Simulated stage at Lewes Gas Works (June 1982 - May 2006)	195
Figure B.12 Recorded minus model simulated stage differentials (Jun 2000 - May 2006)	196
Figure B.13 Correlation of recorded & model simulated stage (Jun 2000 - May 2006)	196
Figure B.14 Recorded minus model simulated stage differentials (Dec 2005 - May 2006)	197
Figure B.15 Correlation of recorded & model simulated stage (Dec 2005 - May 2006)	197
Figure B.16 Mean representative flow hydrograph at Barcombe Mills	198
Figure B.17 Scaled representative flow hydrographs at Barcombe Mills (30m ³ /s to 300m ³ /s, in 30m ³ /s increments)	198
Figure B.18 Mean representative tide hydrograph at Newhaven	199
Figure B.19 Scaled representative tide hydrographs at Newhaven (1.20mAOD to 4.80mOD, in 0.30m increments)	199
Figure B.20 Maximum water level at Lewes from time-lagged 90m ³ /s Barcombe Mills flow & 3mAOD Newhaven tide hydrographs (0-hour to 11-hour lags)	200
Figure B.21 Maximum water level at Lewes from time-lagged 90m ³ /s Barcombe Mills flow & 3mAOD Newhaven tide hydrographs (0-min to 120-min lags)	200
Figure B.22 Longitudinal sections of maximum water levels at for all combinations of flow and tide (1 to 300m ³ /s flow v 0.60 to 4.80mAOD tide)	202
Figure B.23 Recorded minus model simulated stage differentials (Jun 2000 - May 2006)	204
Figure B.24 Correlation of recorded & model simulated stage (Jun 2000 - May 2006)	204
Figure B.25 Recorded minus structure function emulated stage differentials (Jun 2000 - May 2006)	205
Figure B.26 Correlation of recorded & structure function emulated stage (Jun 2000 - May 2006)	205
Figure B.27 Recorded minus structure function emulated stage differentials (Dec 2005 - May 2006)	206
Figure B.28 Correlation of recorded & structure function emulated stage (Dec 2005 - May 2006)	206
Figure C.1 Daily maxima flow observations at Gold Bridge (1973-2005)	208
Figure C.2 Annual maxima flow observations at Gold Bridge (1973-2005)	208

Figure C.3 Extended annual maxima flow observations at Gold Bridge (1959-2005)...	208
Figure C.4 Ranked annual maxima flow observations at Gold Bridge (1959-2005)	209
Figure C.5 GEV distribution plot at Gold Bridge (1959-2005)	210
Figure C.6 Daily maxima flow observations at Isfield Weir (1972-2005)	211
Figure C.7 Annual maxima flow observations at Isfield Weir (1972-2005)	211
Figure C.8 Extended annual maxima flow observations at Isfield Weir (1964-2005) ...	211
Figure C.9 Ranked annual maxima flow observations at Isfield Weir (1964-2005)	212
Figure C.10 GEV distribution plot at Isfield Weir (1964-2005).....	213
Figure C.11 Daily maxima flow observations at Clappers Bridge (1973-2005)	214
Figure C.12 Annual maxima flow observations at Clappers Bridge (1973-2005)	214
Figure C.13 Extended annual maxima flow observations at Clappers Bridge (1969-2005)	214
Figure C.14 Ranked annual maxima flow observations at Clappers Bridge (1969-2005)	215
Figure C.15 GEV distribution plot at Clappers Bridge (1969-2005).....	216
Figure C.16 Daily maxima flow observations at Old Ship (1973-2005)	217
Figure C.17 Annual maxima flow observations at Old Ship (1973-2005)	217
Figure C.18 Extended annual maxima flow observations at Old Ship (1969-2005)	217
Figure C.19 Ranked annual maxima flow observations at Old Ship (1969-2005)	218
Figure C.20 GEV distribution plot at Old Ship (1969-2005)	219
Figure C.21 Daily maxima flow observations at Barcombe Mills (1981-2005).....	222
Figure C.22 Annual maxima flow observations at Barcombe Mills (1981-2005).....	222
Figure C.23 Extended annual maxima flow observations at Barcombe Mills (1952-2005)	222
Figure C.24 Ranked annual maxima flow observations at Barcombe Mills (1952-2005)	223
Figure C.25 GEV distribution plot at Barcombe Mills (Flow) (1952-2005)	224
Figure C.26 Annual maxima recorded & simulated stage at Lewes Corporation Yard (1982-2005).....	226
Figure C.27 Simulated daily maxima stage observations at Lewes Corporation Yard (1981-2005).....	227
Figure C.28 Simulated annual maxima stage observations at Lewes Corporation Yard (1981-2005).....	227
Figure C.29 Extended annual maxima stage observations at Lewes Corporation Yard (1953-2005).....	227
Figure C.30 Ranked annual maxima stage observations at Lewes Corporation Yard (1953-2005).....	228
Figure C.31 GEV distribution plot at Lewes Corporation Yard (1953-2005)	229
Figure C.32 Simulated daily maxima stage observations at Lewes Gas Works (1981- 2005)	230
Figure C.33 Extended annual maxima stage observations at Lewes Gas Works (1953- 2000)	230
Figure C.34 Ranked annual maxima stage observations at Lewes Gas Works (1953-2000)	231
Figure C.35 GEV distribution plot at Lewes Gas Works (1953-2000)	232
Figure C.36 Histogram of Newhaven recorded AMAX tide & probability of exceedance in any given year (1913-2006)	234
Figure C.37 Recorded daily maxima tide observations at Newhaven (1982-2005)	235
Figure C.38 Recorded annual maxima tide observations at Newhaven (1982-2005)....	235
Figure C.39 Ranked annual maxima tide observations at Newhaven (1913-2006).....	237
Figure C.40 GEV distribution plot at Newhaven (1913-2006).....	238
Figure C.41 Recorded daily maxima surge observations at Newhaven (1982-2005)....	239

Figure C.42 Recorded annual maxima surge observations at Newhaven (1982-2005) ..	239
Figure C.43 Ranked annual maxima surge observations at Newhaven (1982-2005)	240
Figure C.44 GEV distribution plot at Newhaven (1982-2005)	241
Figure C.45 Recorded daily surge at high tide observations at Newhaven (1982-2005)	242
Figure C.46 Recorded annual maxima surge at high tide observations at Newhaven (1982-2005)	242
Figure C.47 Ranked annual maxima surge at high tide observations at Newhaven (1982- 2005)	243
Figure C.48 GEV distribution plot at Newhaven (1982-2005)	244
Figure D.1 Seasonality of 99th, 98th & 95th percentile POT exceedances per calendar month at Barcombe Mills	251
Figure D.2 Seasonality of 99th, 98th & 95th percentile POT exceedances per calendar month at Lewes Corporation Yard	251
Figure D.3 Seasonality of 99th, 98th & 95th percentile POT exceedances per calendar month at Newhaven (recorded tide)	251
Figure D.4 Seasonality of 99th, 98th & 95th percentile POT exceedances per calendar month at Newhaven (predicted tide)	252
Figure D.5 Seasonality of 99th, 98th & 95th percentile POT exceedances per calendar month at Newhaven (maximum surge)	252
Figure D.6 Seasonality of 99th, 98th & 95th percentile POT exceedances per calendar month at Newhaven (surge at high tide)	252
Figure D.7 Correlation of 99th percentile joint POT exceedances at Barcombe Mills & Lewes Corporation Yard (1982-2005)	260
Figure D.8 Correlation of 98th percentile joint POT exceedances at Barcombe Mills & Lewes Corporation Yard (1982-2005)	260
Figure D.9 Correlation of 95th percentile joint POT exceedances at Barcombe Mills & Lewes Corporation Yard (1982-2005)	260
Figure D.10 Correlation of 99th percentile joint POT exceedances at Barcombe Mills & Newhaven (tide) (1982-2005)	261
Figure D.11 Correlation of 98th percentile joint POT exceedances at Barcombe Mills & Newhaven (tide) (1982-2005)	261
Figure D.12 Correlation of 95th percentile joint POT exceedances at Barcombe Mills & Newhaven (tide) (1982-2005)	261
Figure D.13 Correlation of 99th percentile joint POT exceedances at Barcombe Mills & Newhaven (maximum surge) (1982-2005)	262
Figure D.14 Correlation of 98th percentile joint POT exceedances at Barcombe Mills & Newhaven (maximum surge) (1982-2005)	262
Figure D.15 Correlation of 95th percentile joint POT exceedances at Barcombe Mills & Newhaven (maximum surge) (1982-2005)	262
Figure D.16 Correlation of 99th percentile joint POT exceedances at Lewes Corporation Yard & Newhaven (tide) (1982-2005)	263
Figure D.17 Correlation of 98th percentile joint POT exceedances at Lewes Corporation Yard & Newhaven (tide) (1982-2005)	263
Figure D.18 Correlation of 95th percentile joint POT exceedances at Lewes Corporation Yard & Newhaven (tide) (1982-2005)	263
Figure D.19 Correlation of 99th percentile joint POT exceedances at Lewes Corporation Yard & Newhaven (maximum surge) (1982-2005)	264
Figure D.20 Correlation of 98th percentile joint POT exceedances at Lewes Corporation Yard & Newhaven (maximum surge) (1982-2005)	264
Figure D.21 Correlation of 95th percentile joint POT exceedances at Lewes Corporation Yard & Newhaven (maximum surge) (1982-2005)	264

Figure E.1 15-Day recorded & simulated stage hydrographs (2nd – 16th October 2000) at Lewes Corporation Yard	274
Figure E.2 15-Day recorded & simulated stage hydrographs (2nd – 16th October 2000) at Southease Bridge.....	274
Figure E.3 15-Day flow hydrograph & daily rainfall (2nd – 16th October 2000) at Barcombe Mills	275
Figure E.4 4-Day flow hydrograph & hourly rainfall (9th - 13th October 2000) at Barcombe Mills	275
Figure E.5 15-Day stage hydrograph & daily rainfall (2nd – 16th October 2000) at Lewes Corporation Yard	276
Figure E.6 4-Day stage hydrograph & hourly rainfall (9th - 13th October 2000) at Lewes Corporation Yard	276
Figure E.7 15-Day stage hydrograph & daily rainfall (2nd – 16th October 2000) at Southease Bridge.....	277
Figure E.8 4-Day stage hydrograph & hourly rainfall (9th - 13th October 2000) at Southease Bridge.....	277
Figure E.9 15-Day tide hydrograph & daily rainfall (2nd – 16th October 2000) at Newhaven.....	278
Figure E.10 4-Day tide hydrograph & hourly rainfall (9th - 13th October 2000) at Newhaven.....	278
Figure E.11 15-Day surge hydrograph & daily rainfall (2nd – 16th October 2000) at Newhaven.....	279
Figure E.12 4-Day surge hydrograph & hourly rainfall (9th - 13th October 2000) at Newhaven.....	279
Figure E.13 15-Day stage hydrographs (2nd – 16th October 2000) at Barcombe Mills & Lewes Corporation Yard	280
Figure E.14 15-Day stage hydrographs (2nd – 16th October 2000) at Lewes Corporation Yard & Newhaven.....	280
Figure F.1 Scatter plot of example threshold levels for daily maxima flow at Barcombe Mills and daily maxima tide at Newhaven.....	284
Figure F.2 Synthesised daily maxima flow observations at Barcombe Mills (May 1982 - June 2006)	289
Figure F.3 Simulated daily maxima stage observations at Lewes Corporation Yard (May 1982 - June 2006).....	289
Figure F.4 Simulated daily maxima stage observations at Lewes Gas Works (May 1982 - June 2006)	289
Figure F.5 Recorded daily maxima tide observations at Newhaven (May 1982 - June 2006)	290
Figure F.6 Predicted daily maxima tide at Newhaven (May 1982 - June 2006)	290
Figure F.7 Recorded daily maxima surge observations at Newhaven (May 1982 - June 2006)	290
Figure G.1 Daily probability of synthesised flow threshold exceedance at Barcombe Mills (1981-2006)	292
Figure G.2 Daily probability of simulated stage threshold exceedance at Lewes Corporation Yard (1982-2006)	292
Figure G.3 Daily probability of simulated stage threshold exceedance at Lewes Gas Works (1982-2006)	292
Figure G.4 Daily probability of recorded tide threshold exceedance at Newhaven (1982-2006)	293
Figure G.5 Daily probability of predicted tide threshold exceedance at Newhaven (1982-2006)	293

Figure G.6 Daily probability of tidal surge threshold exceedance at Newhaven (1982-2006)	293
Figure G.7 Resultant stage magnitudes from bivariate (flow & tide) fully-independent joint return periods with recorded return periods at Lewes Corporation Yard.....	308
Figure G.8 Correlation of resultant stage magnitudes from bivariate (flow & tide) fully-independent joint return periods with recorded return periods at Lewes Corporation Yard.....	308
Figure G.9 Resultant stage magnitudes from bivariate (flow & tide) partially-dependent joint return periods with recorded return periods at Lewes Corporation Yard.....	309
Figure G.10 Correlation of resultant stage magnitudes from bivariate (flow & tide) partially-dependent joint return periods with recorded return periods at Lewes Corporation Yard	309
Figure G.11 Resultant stage magnitudes from trivariate (flow, tide & surge) partially-dependent joint return periods with recorded return periods at Lewes Corporation Yard.....	310
Figure G.12 Correlation of resultant stage magnitudes from trivariate (flow, tide & surge) partially-dependent joint return periods with recorded return periods at Lewes Corporation Yard	310
Figure G.13 Resultant stage magnitudes from bivariate (flow & tide) fully-independent joint return periods with recorded return periods at Lewes Gas Works	311
Figure G.14 Correlation of resultant stage magnitudes from bivariate (flow & tide) fully-independent joint return periods with recorded return periods at Lewes Gas Works	311
Figure G.15 Resultant stage magnitudes from bivariate (flow & tide) partially-dependent joint return periods with recorded return periods at Lewes Gas Works	312
Figure G.16 Correlation of resultant stage magnitudes from bivariate (flow & tide) partially-dependent joint return periods with recorded return periods at Lewes Gas Works	312
Figure G.17 Resultant stage magnitudes from trivariate (flow, tide & surge) partially-dependent joint return periods with recorded return periods at Lewes Gas Works	313
Figure G.18 Correlation of resultant stage magnitudes from trivariate (flow, tide & surge) partially-dependent joint return periods with recorded return periods at Lewes Gas Works	313
Figure G.19 & fully-independent bivariate (flow & tide) joint probabilities of daily maxima stage exceedances at Lewes Corporation Yard.....	314
Figure G.20 Correlation of single & fully-independent bivariate (flow & tide) joint probabilities of daily maxima stage exceedances at Lewes Corporation Yard: complete series	314
Figure G.21 Correlation of single & fully-independent bivariate (flow & tide) joint probabilities of daily maxima stage exceedances at Lewes Corporation Yard: extreme values (top 2%) only	314
Figure G.22 Single & partially-dependent bivariate (flow & tide) joint probabilities of daily maxima stage exceedances at Lewes Corporation Yard	315
Figure G.23 Correlation of single & partially-dependent bivariate (flow & tide) joint probabilities of daily maxima stage exceedances at Lewes Corporation Yard: complete series	315
Figure G.24 Correlation of single & partially-dependent bivariate (flow & tide) joint probabilities of daily maxima stage exceedances at Lewes Corporation Yard: extreme values (top 2%) only	315
Figure G.25 Single & partially-dependent trivariate (flow, tide & surge) joint probabilities of daily maxima stage exceedances at Lewes Corporation Yard.....	316

Figure G.26 Correlation of single & partially-dependent trivariate (flow, tide & surge) joint probabilities of daily maxima stage exceedances at Lewes Corporation Yard: complete series	316
Figure G.27 Correlation of single & partially- trivariate (flow, tide & surge) joint probabilities of daily maxima stage exceedances at Lewes Corporation Yard: extreme values (top 2%) only	316
Figure G.28 Single & fully-independent bivariate (flow & tide) joint probabilities of daily maxima stage exceedances at Lewes Gas Works	317
Figure G.29 Correlation of single & fully-independent bivariate (flow & tide) joint probabilities of daily maxima stage exceedances at Lewes Gas Works: complete series.....	317
Figure G.30 Correlation of single & fully-independent bivariate (flow & tide) joint probabilities of daily maxima stage exceedances at Lewes Gas Works: extreme values (top 2%) only	317
Figure G.31 Single & partially-dependent bivariate (flow & tide) joint probabilities of daily maxima stage exceedances at Lewes Gas Works	318
Figure G.32 Correlation of single & partially-dependent bivariate (flow & tide) joint probabilities of daily maxima stage exceedances at Lewes Gas Works: complete series.....	318
Figure G.33 Correlation of single & partially-dependent bivariate (flow & tide) joint probabilities of daily maxima stage exceedances at Lewes Gas Works: extreme values (top 2%) only	318
Figure G.34 Single & partially-dependent trivariate (flow, tide & surge) joint probabilities of daily maxima stage exceedances at Lewes Gas Works	319
Figure G.35 Correlation of single & partially-dependent trivariate (flow, tide & surge) joint probabilities of daily maxima stage exceedances at Lewes Gas Works: complete series	319
Figure G.36 Correlation of single & partially- trivariate (flow, tide & surge) joint probabilities of daily maxima stage exceedances at Lewes Gas Works: extreme values (top 2%) only	319
Figure G.37 Bivariate partially-dependent Barcombe Mills flow and Newhaven tide joint 1:2 year return period exceedance curve at Lewes Corporation Yard, with structure function curves and concurrent Barcombe Mills flow and Newhaven tide observations (1982 - 2005).....	338
Figure G.38 Bivariate partially-dependent Barcombe Mills flow and Newhaven tide joint 1:5 year return period exceedance curve at Lewes Corporation Yard, with structure function curves and concurrent Barcombe Mills flow and Newhaven tide observations (1982 - 2005).....	338
Figure G.39 Bivariate partially-dependent Barcombe Mills flow and Newhaven tide joint 1:10 year return period exceedance curve at Lewes Corporation Yard, with structure function curves and concurrent Barcombe Mills flow and Newhaven tide observations (1982 - 2005).....	338
Figure G.40 Bivariate partially-dependent Barcombe Mills flow and Newhaven tide joint 1:2 year return period exceedance curve at Lewes Corporation Yard, with structure function curves and concurrent Barcombe Mills flow and Newhaven tide observations (1982 - 2005).....	339
Figure G.41 Bivariate partially-dependent Barcombe Mills flow and Newhaven tide joint 1:50 year return period exceedance curve at Lewes Corporation Yard, with structure function curves and concurrent Barcombe Mills flow and Newhaven tide observations (1982 - 2005).....	339
Figure G.42 Bivariate partially-dependent Barcombe Mills flow and Newhaven tide joint 1:100 year return period exceedance curve at Lewes Corporation Yard, with	

structure function curves and concurrent Barcombe Mills flow and Newhaven tide observations (1982 - 2005).....	339
Figure G.43 Bivariate partially-dependent Barcombe Mills flow and Newhaven tide joint 1:200 year return period exceedance curve at Lewes Corporation Yard, with structure function curves and concurrent Barcombe Mills flow and Newhaven tide observations (1982 - 2005).....	340
Figure G.44 Bivariate partially-dependent Barcombe Mills flow and Newhaven tide joint 1:2 year return period exceedance curve at Lewes Gas Works, with structure function curves and concurrent Barcombe Mills flow and Newhaven tide observations (1982 - 2005).....	340
Figure G.45 Bivariate partially-dependent Barcombe Mills flow and Newhaven tide joint 1:5 year return period exceedance curve at Lewes Gas Works, with structure function curves and concurrent Barcombe Mills flow and Newhaven tide observations (1982 - 2005).....	340
Figure G.46 Bivariate partially-dependent Barcombe Mills flow and Newhaven tide joint 1:10 year return period exceedance curve at Lewes Gas Works, with structure function curves and concurrent Barcombe Mills flow and Newhaven tide observations (1982 - 2005).....	341
Figure G.47 Bivariate partially-dependent Barcombe Mills flow and Newhaven tide joint 1:25 year return period exceedance curve at Lewes Gas Works, with structure function curves and concurrent Barcombe Mills flow and Newhaven tide observations (1982 - 2005).....	341
Figure G.48 Bivariate partially-dependent Barcombe Mills flow and Newhaven tide joint 1:50 year return period exceedance curve at Lewes Gas Works, with structure function curves and concurrent Barcombe Mills flow and Newhaven tide observations (1982 - 2005).....	341
Figure G.49 Bivariate partially-dependent Barcombe Mills flow and Newhaven tide joint 1:100 year return period exceedance curve at Lewes Gas Works, with structure function curves and concurrent Barcombe Mills flow and Newhaven tide observations (1982 - 2005).....	342
Figure G.50 Bivariate partially-dependent Barcombe Mills flow and Newhaven tide joint 1:200 year return period exceedance curve at Lewes Gas Works, with structure function curves and concurrent Barcombe Mills flow and Newhaven tide observations (1982 - 2005).....	342

LIST OF APPENDIX TABLES

Table A.1 Gold Bridge river flow gauge, River Ouse	182
Table A.2 Isfield Weir river flow gauge, River Uck.....	182
Table A.3 Clappers Bridge river flow gauge, Bevern Stream	182
Table A.4 Old Ship river flow gauge, Clay Hill Stream.....	183
Table A.5 Barcombe Mills river flow gauge, River Ouse	183
Table A.6 Barcombe Mills river stage gauge, River Ouse	183
Table A.7 Lewes Corporation Yard river stage gauge, River Ouse.....	184
Table A.8 Lewes Gas Works river stage gauge, River Ouse	184
Table A.9 Southease Bridge river stage gauge, River Ouse	184
Table A.10 Newhaven (EA) tide gauge, River Ouse	185
Table A.11 Newhaven (Proudman) tide gauge, River Ouse.....	185
Table B.1 Structure function matrix for resultant simulated maximum water levels at Lewes Corporation Yard (mAOD) (shaded area) from the combinations of variables of Barcombe Mills flow (m^3/s) and Newhaven tide (mAOD).	201
Table B.2 Structure function matrix for resultant simulated maximum water levels at Lewes Gas Works (mAOD) (shaded area) from the combinations of variables of Barcombe Mills flow (m^3/s) and Newhaven tide (mAOD).	201
Table C.1 Annual maxima flow observations at Gold Bridge (1959-2005).....	209
Table C.2 Return periods & flow magnitude estimates at Gold Bridge	210
Table C.3 Annual maxima flow observations at Isfield Weir (1964-2005).....	212
Table C.4 Return periods & flow magnitude estimates at Isfield Weir	213
Table C.5 Annual maxima flow observations at Clappers Bridge (1969-2005).....	215
Table C.6 Return periods & flow magnitude estimates at Clappers Bridge	216
Table C.7 Annual maxima flow observations at Old Ship (1969-2005).....	218
Table C.8 Return periods & flow magnitude estimates at Old Ship.....	219
Table C.9 Linearly correlated Barcombe Mills total runoff, stage and flow AMAX series (1952-2000).....	220
Table C.10 Analysis of extended Barcombe Mills flow AMAX series with concurrent upper catchment observations (1952-1980).....	221
Table C.11 Annual maxima flow observations at Barcombe Mills (1952-2005).....	223
Table C.12 Return periods & flow magnitude estimates at Barcombe Mills	224
Table C.13 Concurrent recorded and simulated Lewes Corporation Yard stage AMAX series differential (1982-2005).....	225
Table C.14 Annual maxima stage observations at Lewes Corporation Yard (1953-2005)	228
Table C.15 Return periods & stage magnitude estimates at Lewes Corporation Yard...	229
Table C.16 Annual maxima stage observations at Lewes Gas Works (1953-2000).....	231
Table C.17 Return periods & stage magnitude estimates at Lewes Gas Works	232
Table C.18 Extended annual maxima flow observations at Newhaven (1913-2006)....	233
Table C.19 Annual maxima tide observations at Newhaven (1913-2006)	236
Table C.20 Return periods & tide magnitude estimates at Newhaven	238
Table C.21 Annual maxima surge observations at Newhaven (1982-2005)	240
Table C.22 Return periods & surge magnitude estimates at Newhaven.....	241
Table C.23 Annual maxima surge at high tide observations at Newhaven (1982-2005)	243
Table C.24 Return periods & surge at high tide magnitude estimates at Newhaven.....	244
Table C.25 Concurrent AMAX Lewes Corporation Yard stage & Barcombe Mills flow series with estimated return periods	245
Table C.26 Concurrent AMAX Lewes Corporation Yard stage & Newhaven tide series with estimated return periods	245

Table D.1 Synthesised flow POT exceedance occurrences at Barcombe Mills (1981-2005)	247
Table D.2 Simulated stage POT exceedance occurrences at Lewes Corporation Yard (1982-2005).....	247
Table D.3 Recorded tide POT exceedance occurrences at Newhaven (1982-2005)	248
Table D.4 Predicted tide POT exceedance occurrences at Newhaven (1982-2005).....	248
Table D.5 Recorded maximum surge POT exceedance occurrences at Newhaven (1982-2005)	249
Table D.6 Recorded surge at high tide POT exceedance occurrences at Newhaven (1982-2005)	249
Table D.7 POT exceedance occurrences at the upper Ouse catchment gauges (1993 & 2007 Study Comparison)	250
Table D.8 Joint POT exceedances at Barcombe Mills & Lewes Corporation Yard (1982-2005)	253
Table D.9 Joint POT exceedances at Barcombe Mills & Newhaven (tide) (1982-2005)	254
Table D.10 Joint POT exceedances at Barcombe Mills & Newhaven (maximum surge) (1982-2005).....	255
Table D.11 Joint POT exceedances at Lewes Corporation Yard & Newhaven (tide) (1982-2005).....	256
Table D.12 Joint POT exceedances at Lewes Corporation Yard & Newhaven (maximum surge) (1982-2005).....	257
Table D.13 Joint POT exceedances at Newhaven (tide) & Newhaven (maximum surge) (1982-2005).....	258
Table D.14 Joint POT exceedances at Newhaven (maximum surge) & Newhaven (surge at high tide) (1982-2005)	259
Table E.1 Record of flood events at Uckfield (River Uck) & Lewes (River Ouse)	266
Table E.2 Peak flood magnitudes for the 11th / 12th October 2000 Ouse catchment flood event & estimated return periods	270
Table E.3 Peak 12th October 2000 Lewes flood magnitudes at key river structures & corresponding overtopping levels	272
Table F.1 Example observational pairs of daily maxima Barcombe Mills flow and Newhaven tide.....	283
Table F.2 Example threshold exceedance of observational pairs	287
Table G.1 Joint return periods T (shaded area) for combined events with identical return periods T_u with different levels of dependence χ , calculated using equation 7.6..	294
Table G.2 Joint return periods T (shaded area) for combined events with identical return periods T_u with different levels of dependence χ , calculated using equation 7.7..	294
Table G.3 Joint return periods T (shaded area) for fully-independent ($\chi=0$) variables with return periods T_x and T_y	295
Table G.4 Joint return periods T (shaded area) for partially-dependent ($\chi=0.01$) variables with return periods T_x and T_y	295
Table G.5 Joint return periods T (shaded area) for partially-dependent ($\chi=0.1$) variables with return periods T_x and T_y	296
Table G.6 Joint return periods T (shaded area) for partially-dependent ($\chi=0.2$) variables with return periods T_x and T_y	296
Table G.7 Joint return periods T (shaded area) for partially-dependent ($\chi=0.3$) variables with return periods T_x and T_y	296

Table G.8 Joint return periods T (shaded area) for partially-dependent ($\chi=0.4$) variables with return periods T_x and T_y	297
Table G.9 Joint return periods T (shaded area) for partially-dependent ($\chi=0.5$) variables with return periods T_x and T_y	297
Table G.10 Joint return periods T (shaded area) for partially-dependent ($\chi=0.6$) variables with return periods T_x and T_y	297
Table G.11 Joint return periods T (shaded area) for partially-dependent ($\chi=0.7$) variables with return periods T_x and T_y	298
Table G.12 Joint return periods T (shaded area) for partially-dependent ($\chi=0.8$) variables with return periods T_x and T_y	298
Table G.13 Joint return periods T (shaded area) for partially-dependent ($\chi=0.9$) variables with return periods T_x and T_y	298
Table G.14 Joint return periods T (shaded area) for fully-dependent ($\chi=1$) variables with return periods T_x and T_y	299
Table G.15 Joint return periods T (shaded area) for partially-dependent ($\chi=0.045$) variables X (Barcombe Mills flow, m^3/s) and Y (Newhaven tide, mAOD) with return periods T_x and T_y . Flow / tide magnitudes corresponding to the return periods are shown in italics.....	300
Table G.16 Joint daily probabilities of exceedance $P(X > x^*, Y > y^*)$ (shaded area) for partially-dependent ($\chi=0.045$) variables X (Barcombe Mills flow, m^3/s) and Y (Newhaven tide, mAOD) with probabilities $P(X > x^*)$ and $P(Y > y^*)$. Flow / tide magnitudes corresponding to the daily probabilities are shown in italics.	301
Table G.17 Joint return periods T (shaded area) for partially-dependent ($\chi=0.338$) variables X (Barcombe Mills flow, m^3/s) and Y (Newhaven surge, m) with return periods T_x and T_y . Flow / surge magnitudes corresponding to the return periods are shown in italics.....	302
Table G.18 Joint return periods T (shaded area) for independent ($\chi=0$) variables X (Barcombe Mills flow, m^3/s) and Y (Newhaven tide, mAOD) with return periods T_x and T_z . Flow / tide magnitudes corresponding to the return periods are shown in italics.....	302
Table G.19 Joint daily probabilities of exceedance $P(X > x^*, Y > y^*)$ (shaded area) for partially-dependent ($\chi=0.338$) variables X (Barcombe Mills flow, m^3/s) and Y (Newhaven surge, m) with probabilities $P(X > x^*)$ and $P(Y > y^*)$. Flow / surge magnitudes corresponding to the daily probabilities are shown in italics.	303
Table G.20 Joint daily probabilities of exceedance $P(X > x^*, Y > y^*)$ (shaded area) for independent ($\chi=0$) variables X (Barcombe Mills flow, m^3/s) and Y (Newhaven tide, mAOD) with probabilities $P(X > x^*)$ and $P(Y > y^*)$. Flow / tide magnitudes corresponding to the daily probabilities are shown in italics.	304
Table G.21 Structure function matrix for resultant water levels at Lewes Corporation Yard (mAOD) $Z_{x,y}$ (shaded area) from combinations of variables X (Barcombe Mills flow, m^3/s) and Y (Newhaven tide, mAOD). return periods T_x and T_y corresponding to tide / flow magnitudes are shown in italics.	305
Table G.22 Structure function matrix for resultant water levels at Lewes Gas Works (mAOD) $Z_{x,y}$ (shaded area) from combinations of variables X (Barcombe Mills	

flow, m ³ /s) and <i>Y</i> (Newhaven tide, mAOD). Return periods T_x and T_y corresponding to tide / flow magnitudes are shown in italics.	305
Table G.23 Structure function matrix for resultant water levels at Lewes Corporation Yard (mAOD) $Z_{x,y}$ (shaded area) from combinations of variables <i>X</i> (Barcombe Mills flow, m ³ /s) and <i>Y</i> (Newhaven tide, mAOD). Daily probabilities of exceedance T_x and T_y corresponding to tide / flow magnitudes are shown in italics.	306
Table G.24 Structure function matrix for resultant water levels at Lewes Gas Works (mAOD) $Z_{x,y}$ (shaded area) from combinations of variables <i>X</i> (Barcombe Mills flow, m ³ /s) and <i>Y</i> (Newhaven tide, mAOD). Daily probabilities of exceedance T_x and T_y corresponding to tide / flow magnitudes are shown in italics.	307
Table G.25 Resultant water levels at Lewes Corporation Yard for combined Barcombe Mills flow and Newhaven tide events equating to the 1:2 year joint return periods. Highest stage at Lewes Corporation Yard (shaded area) selected as the maximum 1:2 year combined flow / tide event.	320
Table G.26 Resultant water levels at Lewes Corporation Yard for combined Barcombe Mills flow and Newhaven tide events equating to the 1:5 year joint return periods. Highest stage at Lewes Corporation Yard (shaded area) selected as the maximum 1:5 year combined flow / tide event.	320
Table G.27 Resultant water levels at Lewes Corporation Yard for combined Barcombe Mills flow and Newhaven tide events equating to the 1:10 year joint return periods. Highest stage at Lewes Corporation Yard (shaded area) selected as the maximum 1:10 year combined flow / tide event.	321
Table G.28 Resultant water levels at Lewes Corporation Yard for combined Barcombe Mills flow and Newhaven tide events equating to the 1:25 year joint return periods. Highest stage at Lewes Corporation Yard (shaded area) selected as the maximum 1:25 year combined flow / tide event.	322
Table G.29 Resultant water levels at Lewes Corporation Yard for combined Barcombe Mills flow and Newhaven tide events equating to the 1:50 year joint return periods. Highest stage at Lewes Corporation Yard (shaded area) selected as the maximum 1:50 year combined flow / tide event.	323
Table G.30 Resultant water levels at Lewes Corporation Yard for combined Barcombe Mills flow and Newhaven tide events equating to the 1:100 year joint return periods. Highest stage at Lewes Corporation Yard (shaded area) selected as the maximum 1:100 year combined flow / tide event.	325
Table G.31 Resultant water levels at Lewes Corporation Yard for combined Barcombe Mills flow and Newhaven tide events equating to the 1:200 year joint return periods. Highest stage at Lewes Corporation Yard (shaded area) selected as the maximum 1:200 year combined flow / tide event.	327
Table G.32 Resultant water levels at Lewes Gas Works for combined Barcombe Mills flow and Newhaven tide events equating to the 1:2 year joint return periods. Highest stage at Lewes Gas Works (shaded area) selected as the maximum 1:2 year combined flow / tide event.	329
Table G.33 Resultant water levels at Lewes Gas Works for combined Barcombe Mills flow and Newhaven tide events equating to the 1:5 year joint return periods. Highest stage at Lewes Gas Works (shaded area) selected as the maximum 1:5 year combined flow / tide event.	329
Table G.34 Resultant water levels at Lewes Gas Works for combined Barcombe Mills flow and Newhaven tide events equating to the 1:10 year joint return periods. Highest stage at Lewes Gas Works (shaded area) selected as the maximum 1:10 year combined flow / tide event.	330

Table G.35 Resultant water levels at Lewes Gas Works for combined Barcombe Mills flow and Newhaven tide events equating to the 1:25 year joint return periods. Highest stage at Lewes Gas Works (shaded area) selected as the maximum 1:25 year combined flow / tide event.	331
Table G.36 Resultant water levels at Lewes Gas Works for combined Barcombe Mills flow and Newhaven tide events equating to the 1:50 year joint return periods. Highest stage at Lewes Gas Works (shaded area) selected as the maximum 1:50 year combined flow / tide event.	332
Table G.37 Resultant water levels at Lewes Gas Works for combined Barcombe Mills flow and Newhaven tide events equating to the 1:100 year joint return periods. Highest stage at Lewes Gas Works (shaded area) selected as the maximum 1:100 year combined flow / tide event.	334
Table G.38 Resultant water levels at Lewes Gas Works for combined Barcombe Mills flow and Newhaven tide events equating to the 1:200 year joint return periods. Highest stage at Lewes Gas Works (shaded area) selected as the maximum 1:200 year combined flow / tide event.	336

APPENDIX A HYDROLOGICAL DATA

A.1 Upper Ouse & Uck Sub-Catchment Gauges

Table A.1 Gold Bridge river flow gauge, River Ouse

Location	Catchment Area	Total Series (including gaps)	Complete Series	
			AMAX	Daily
Gold Bridge TQ 429 214 (Ouse)	180.9 km ²	AMAX: 1959-2005 Daily: 1973-2005 15-min: 1981-2005	46 years (100%)	11703 days (98.6%)
Notes	Flow telemetry gauge operated by EA. All but exceptional flows contained, but gauge re-rated in 2005 with telemetry backdated to 1981. Releases from Ardingly reservoir provide baseflow in summer. Some flood structures and STW u/s. Artificial structures have a limited impact.			
Source: Environment Agency (2005a)				

Table A.2 Isfield Weir river flow gauge, River Uck

Location	Catchment Area	Total Series (including gaps)	Complete Series	
			AMAX	Daily
Isfield Weir TQ 459 190 (Uck)	87.8 km ²	AMAX: 1964-2005 Daily: 1973-2005 15-min: 1981-2005	41 years (100%)	12033 days (99.8%)
Notes	Flow telemetry gauge operated by EA. Well sited d/s of railway embankment, only very extreme flows bypass. No abstractions, but discharge from STW and opening of Uckfield Mill flood gates can produce abrupt flow changes. Gauge re-rated in 2005 with telemetry backdated to 1981.			
Source: Environment Agency (2005a)				

Table A.3 Clappers Bridge river flow gauge, Bevern Stream

Location	Catchment Area	Total Series (including gaps)	Complete Series	
			AMAX	Daily
Clappers Bridge TQ 423 161 (Bevern Stream)	34.6 km ²	AMAX: 1969-2005 Daily: 1973-2005 15-min: 1981-2005	35 years (97.2%)	11780 days (99.2%)
Notes	Flow telemetry gauge operated by EA. Most flows contained in structure, but stream is narrow d/s of gauge so some overtopping can occur. Negligible impact of artificial influences on flow.			
Source: Environment Agency (2005a)				

Table A.4 Old Ship river flow gauge, Clay Hill Stream

Location	Catchment Area	Total Series (including gaps)	Complete Series	
			AMAX	Daily
Old Ship TQ 448 153 (Clay Hill Stream)	7.1 km ²	AMAX: 1969-2005 Daily: 1973-2005 15-min: 1981-2005	36 years (100%)	11872 days (100%)
Notes	Flow telemetry gauge operated by EA. River flow understood to be modular throughout flow range, some overtopping can occur. Extended periods with zero flow, esp. in summer.			
Source: Environment Agency (2005a)				

A.2 Middle Ouse Sub-Catchment Gauges

Table A.5 Barcombe Mills river flow gauge, River Ouse

Location	Catchment Area	Total Series (including gaps)	Complete Series	
			AMAX	Daily
Barcombe Mills u/s Flow & Ultrasonic TQ 433 148 (Ouse)	395.7 km ²	AMAX: 1956-2005 Daily: 1973-2005 15-min: 1981-2005	49 years (100%)	10916 days (91.9%)
Notes	Flow telemetry gauge operated by EA. Long history of poor data recording due to a complex structure of weirs and sluices. 4-path ultrasonic gauge was subject to drowning and bypassing. Measurement complicated further by sluice gate operations and water abstraction u/s. New ultrasonic gauge (2003) u/s of abstraction still suffers from flow measurement problems, especially during extreme flows.			
Source: Environment Agency (2005a)				

Table A.6 Barcombe Mills river stage gauge, River Ouse

Location	Catchment Area	Total Series (including gaps)	Complete Series	
			AMAX	Daily
Barcombe Mills Weir TQ 433 148 (Ouse)	395.7 km ²	AMAX: 1952-2000 Daily: N/A 15-min: N/A	45 years (91.8%)	N/A
Notes	Stage chart gauge operated by EA. History of unreliable data recording due to a complex structure of weirs and sluices. Measurement complicated further by sluice gate operations and water abstraction u/s. Stages are calculated using rating curves and readings from flow gauges.			
Source: Environment Agency (2005a)				

A.3 Lower Ouse Sub-Catchment Gauges

Table A.7 Lewes Corporation Yard river stage gauge, River Ouse

Location	Catchment Area	Total Series (including gaps)	Complete Series	
			AMAX	Daily
Lewes Corporation Yard TQ 416 106 (Ouse)	N/A	AMAX: 1952-2006 Daily: 2000-2006 15-min: 2000-2006	6 years (100%)	1384 days (67.8%)
Notes	Stage float telemetry gauge operated by EA u/s of Phoenix Causeway. Originally a low-rated gauge, the gauge produced a reliable chart dataset. New telemetry gauge created an inconsistent record with datum shifts and missing periods caused by sticking floats and poor calibration. Upgraded in 2003 to a pressure transducer gauge but reliability issues remained. Corrected in November 2005 and now provides reliable stage recordings for Lewes.			
Source: Environment Agency (2005a)				

Table A.8 Lewes Gas Works river stage gauge, River Ouse

Location	Catchment Area	Total Series (including gaps)	Complete Series	
			AMAX	Daily
Lewes Gas Works TQ 420 101 (Ouse)	N/A	AMAX: 1952-2000 Daily: N/A Hourly: Oct 2000 15-min: N/A	44 years (89.8%)	N/A
Notes	Stage gauge operated by EA. Chart data only which has not been digitised. Fairly inconsistent dataset with numerous missing sections. October 2000 observations digitised for flood analysis only. Reasonable AMAX series checked against Corporation Yard and Newhaven observations.			
Source: Environment Agency (2005a)				

Table A.9 Southease Bridge river stage gauge, River Ouse

Location	Catchment Area	Total Series (including gaps)	Complete Series	
			AMAX	Daily
Southease Bridge TQ 427 053 (Ouse)	N/A	AMAX: 1999-2003 Daily: 1999-2003 15-min: 1999-2003	5 years (100%)	1583 days (99.4%)
Notes	Temporary stage telemetry gauge operated by EA. Gauge installed for EA project, decommissioned in 2003. Provides fairly consistent dataset with some datum shifts.			
Source: Environment Agency (2005a)				

Table A.10 Newhaven (EA) tide gauge, River Ouse

Location	Catchment Area	Total Series (including gaps)	Complete Series	
			AMAX	Daily
Newhaven (EA) TQ 4516 0002	N/A	AMAX: 1913-2005 Daily: 1990-2005 15-min: 1990-2005	83 years (89.2%)	3884 days (74.5%)
Notes	Telemetry station from 1990, chart only prior to this date. Data recorded and held by EA. Located at the river mouth in the vicinity of the cross-channel ferry terminal. Poor history of data recording since telemetry gauge was installed. Numerous missing sections and further error flagged observations. Long AMAX series back to 1913 but no precise recorded dates before 1990.			
Source: Environment Agency (2005a)				

Table A.11 Newhaven (Proudman) tide gauge, River Ouse

Location	Catchment Area	Total Series (including gaps)	Complete Series	
			AMAX	Daily
Newhaven (Proudman) TQ 4511 0005	N/A	AMAX: 1981-2005 Daily: 1981-2005 15-min: 1981-2005	21 years (84%)	6022 days (69.9%)
Notes	Grade-A Telemetry station since 1981. Data recorded and held by the Proudman . The gauge is located at the river mouth at the harbour master’s station. Reliable quality checked data but missing section from 1987-1990 due to gauge refurbishment.			
Source: Proudman (2006)				

A.4 Locations of the Ouse Catchment Gauges

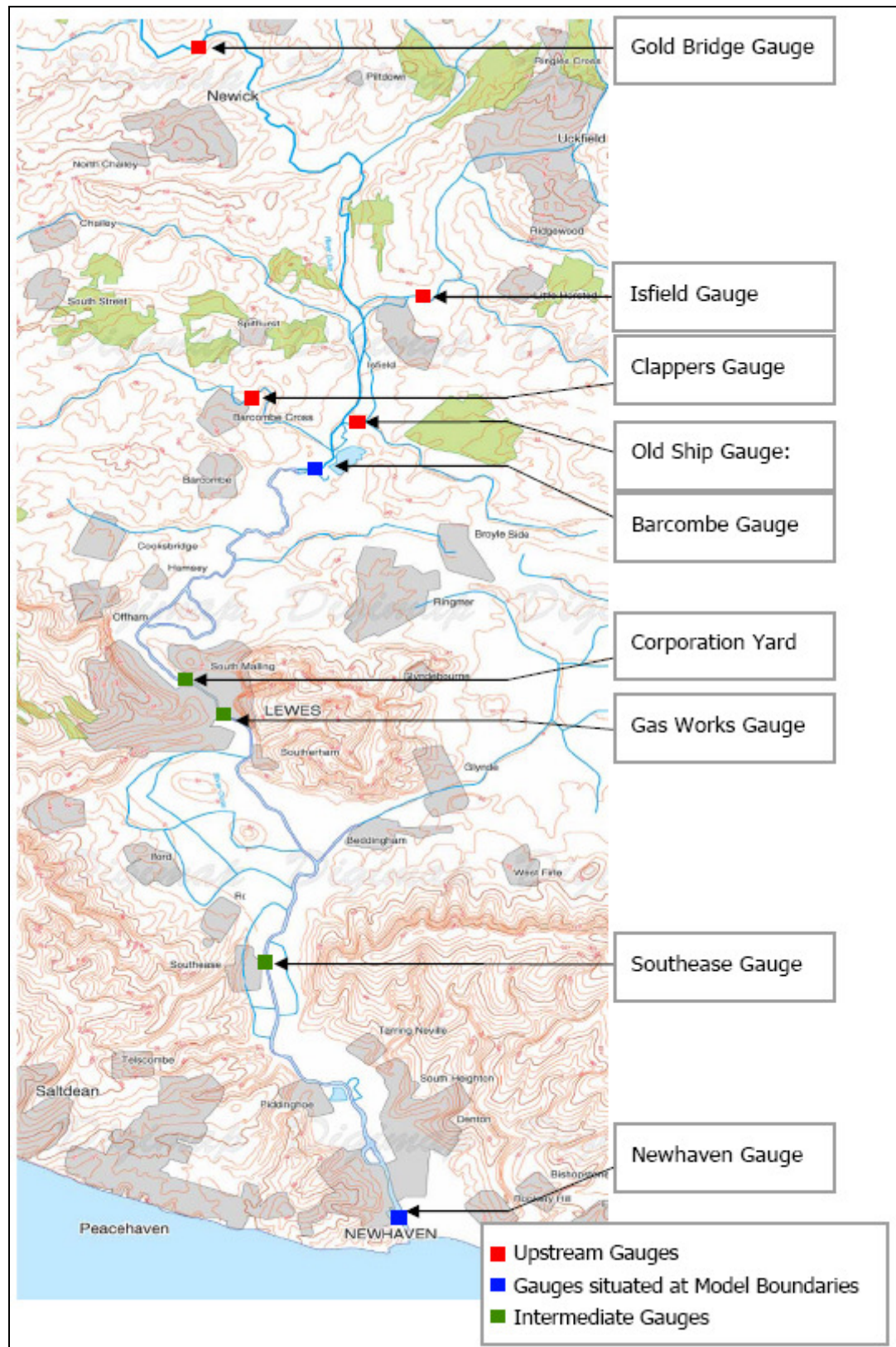


Figure A.1 Map of river flow, stage and tide gauges in the Ouse catchment

APPENDIX B MODELLING & SIMULATION

B.1 Synthesised Barcombe Mills Flow Series

B.1.1 Calibration with HYSIM Simulated Series

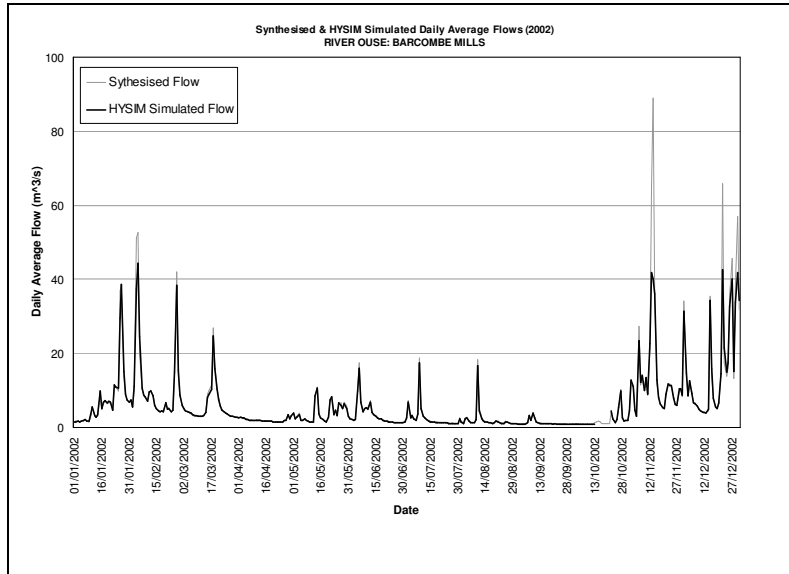


Figure B.1 Time-series plot of synthesised daily mean flow with HYSIM simulated daily mean flow at Barcombe Mills (2002)

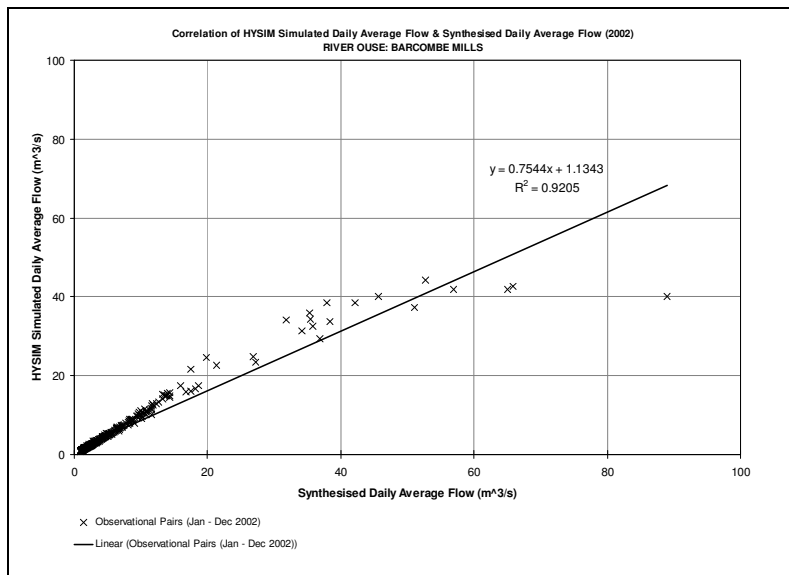


Figure B.2 Correlation of synthesised and HYSIM simulated daily mean flow magnitudes at Barcombe Mills (2002): complete series

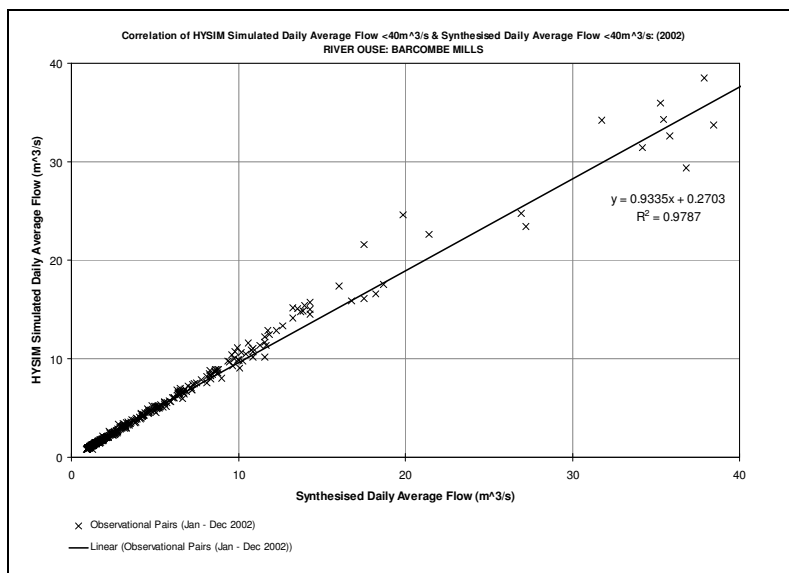


Figure B.3 Correlation of synthesised and HYSIM simulated daily mean flow magnitudes at Barcombe Mills (2002): <40m³/s only

B.1.2 Calibration with Barcombe Mills Recorded Series

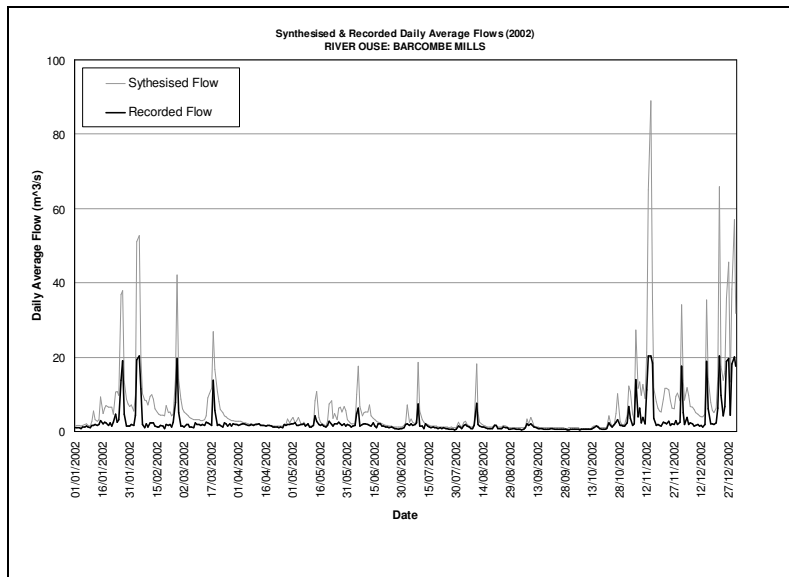


Figure B.4 Time-series plot of synthesised daily mean flow with recorded daily mean flow at Barcombe Mills (2002)

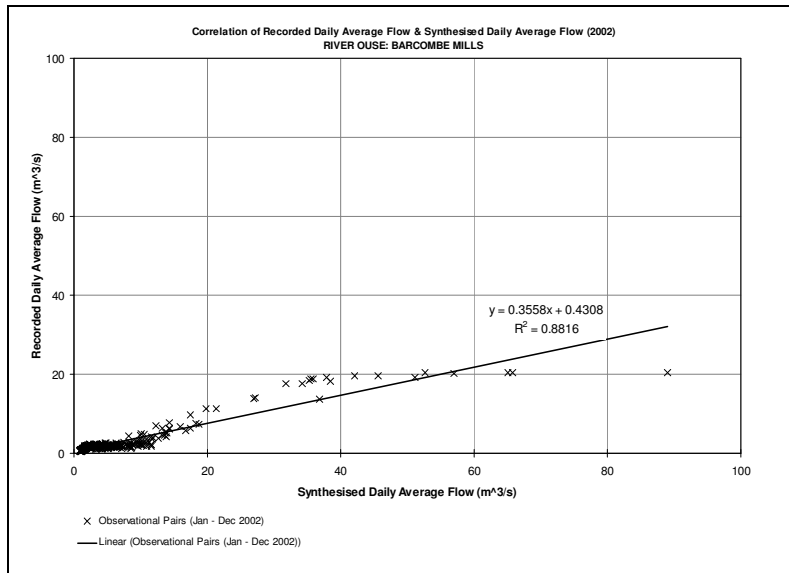


Figure B.5 Correlation of synthesised and recorded daily mean flow magnitudes at Barcombe Mills (2002): complete series

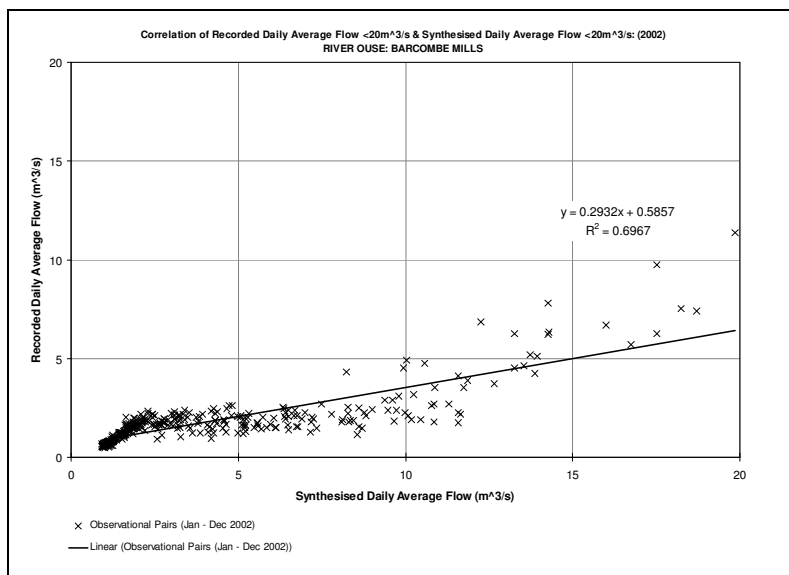


Figure B.6 Correlation of synthesised and recorded daily mean flow magnitudes at Barcombe Mills (2002): <20m³/s only

B.2 Hydraulic Modelling of the Lower Ouse

B.2.1 DGPS Survey of the Lower Ouse

A static survey was undertaken to determine a local network of GPS base stations in the lower Ouse catchment. This network was adjusted to the Ordnance Survey (OS) GPS network. There are two types of OS GPS points at key locations around the UK which are freely available for download by DGPS surveyors. The first are called Active Stations of which there are approximately thirty in the UK. These are fixed GPS stations which continuously log raw WGS-84 GPS data which surveyors can use to adjust a local network. This in effect corrects local networks by locking them into highly accurate known GPS points. Normally, four would be used for a network, but because Lewes's position on the south coast, it was only possible to use three due to the absence of one in a southerly position*. The three active stations used were OSHQ on the OS building in Southampton, LOND in London, and NFO1 at North Foreland near Dover (Figure B.7).

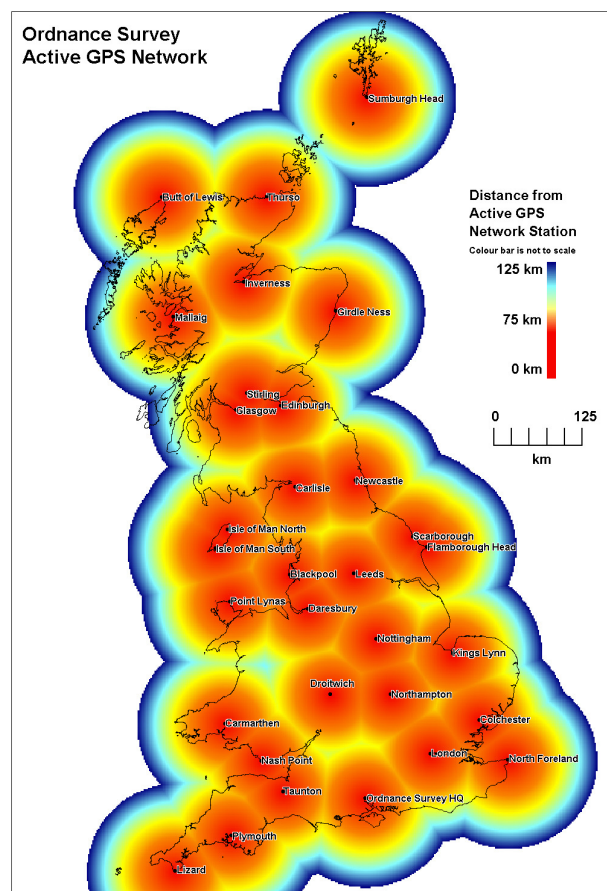


Figure B.7 Map of OS active GPS stations, UK

*OS Active GPS Network correct at time of survey, December 2003

The second type of points are called Passive Stations, which are traditionally old OS trig points from the triangulation of Britain that have been occupied by OS DGPS equipment in the last five years and have been given precise DGPS coordinates. There are about 300 of these in the UK. There was not one available in the immediate area around Lewes however, so Roedean near Brighton Marina, East Sussex was occupied and included in the local GPS network. Roedean was not used as a base station during the DGPS land Lewes survey, but it added a further layer of accuracy to the network adjustment at a more local scale than the Active Stations.

The local network consisted of...

The accuracy of the adjusted local DGPS network was measured by surveying one station DGPS whilst occupying another. This ideally would involve the Passive Station (Roedean) or a secondary recorded station within the network. For this test, the base station was set-up at Lewes Golf Course and the measured station was 'Kiri', above Rodmell. The baseline distance between them was 3.1 miles. The results of the accuracy tests are as follows:

Kiri (used in the network adjustment)

Easting	541469.405m
Northing	105264.352m
Elevation	69.433m

Measurements taken 21/22/23 October 2003

Error estimates (in adjustment):

Easting	0.0049m
Northing	0.0054m
Elevation	0.0000m

Confidence - 95%

Kiri (test measurement taken with base at Golf):

Easting	541469.385m
Northing	105264.370m
Elevation	69.466m

Measurement taken 17 November 2003

Differences between coordinates:

Easting **+/- 0.020m**

Northing **+/- 0.018m**

Elevation **+/- 0.033m**

These results were determined to be within acceptable bounds of accuracy, thus the network was accepted for use in the DGPS land survey.

B.2.2 Model Calibration Input Event Hydrographs

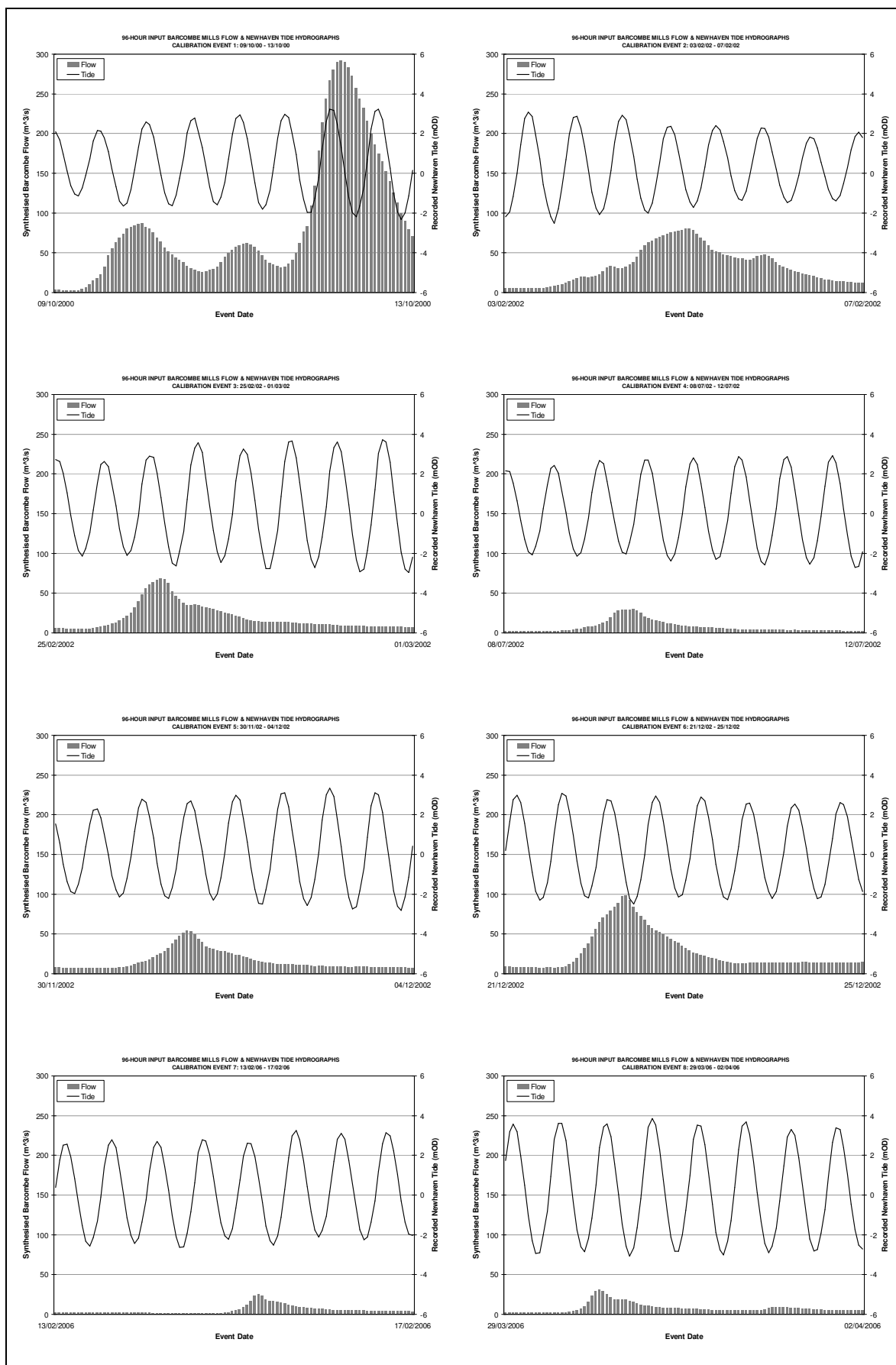


Figure B.8 Calibration input event hydrographs at Barcombe Mills & Newhaven (event no.'s 1 to 8)

B.2.3 HEC-RAS Model

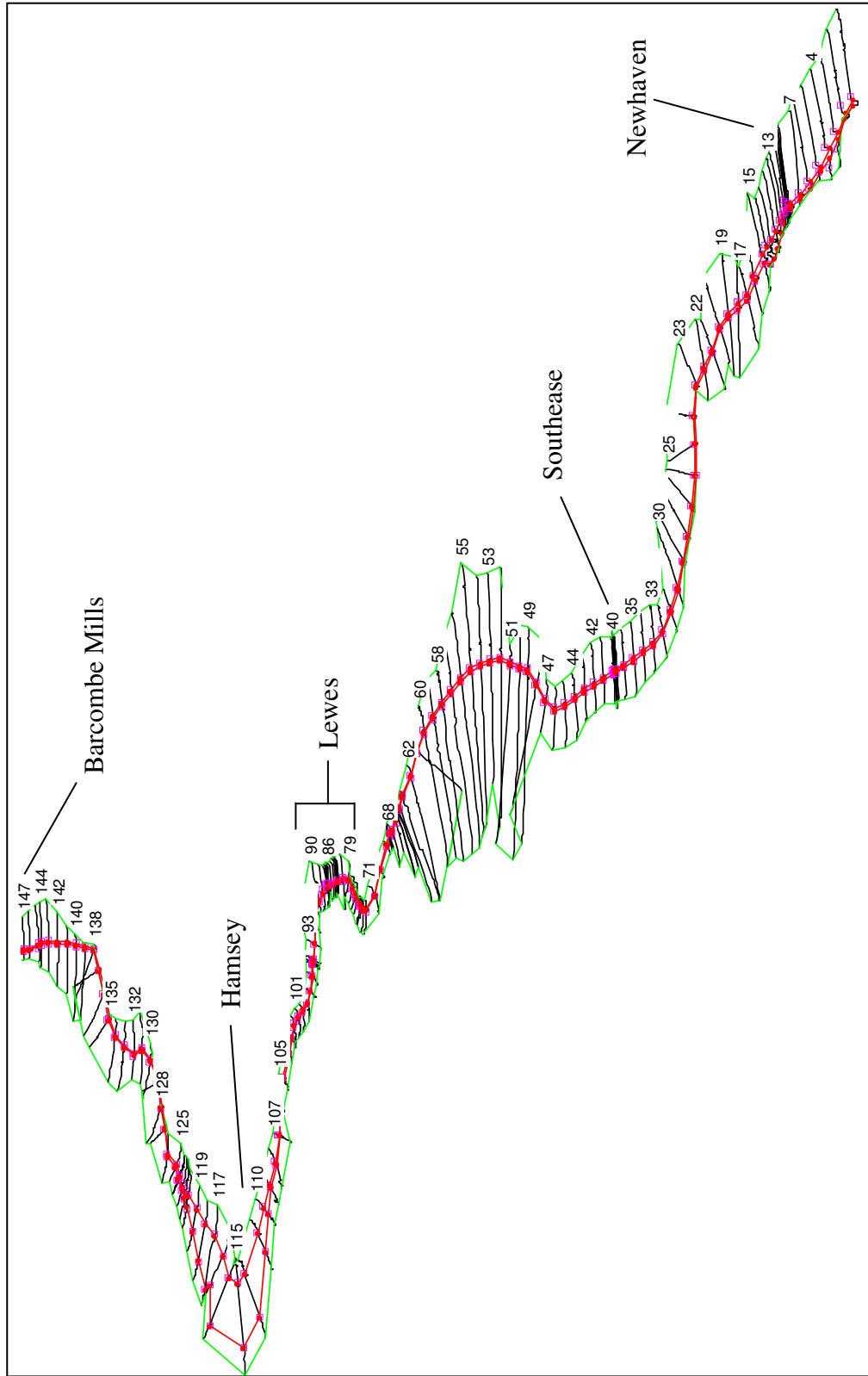


Figure B.9 3-dimensional map of the Lower Ouse hydraulic HEC-RAS model

B.3 Continuous Simulation

B.3.1 Simulated Stage at Lewes Corporation Yard & Lewes Gas Works

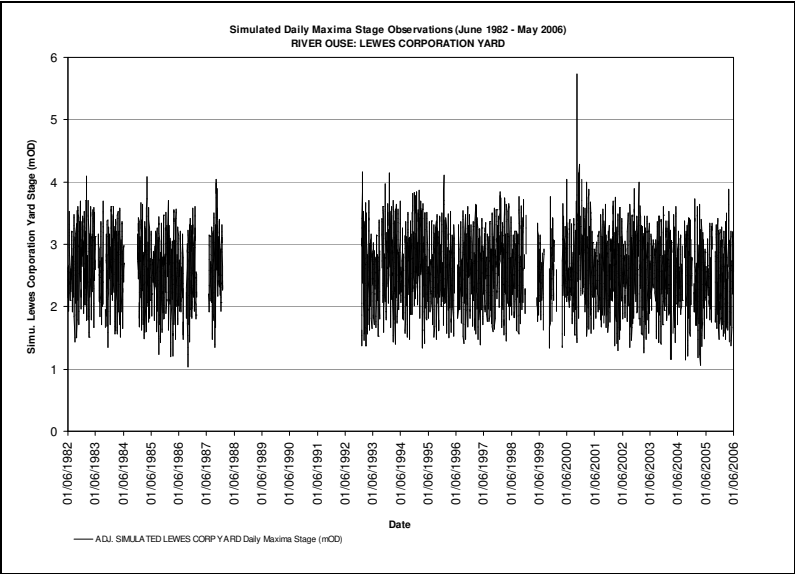


Figure B.10 Simulated stage at Lewes Corporation Yard (June 1982 - May 2006)

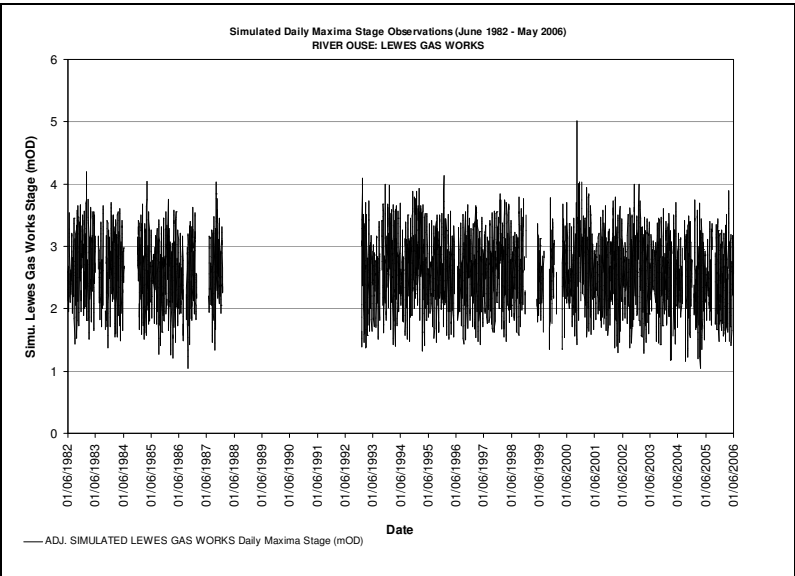


Figure B.11 Simulated stage at Lewes Gas Works (June 1982 - May 2006)

B.3.2 Calibration of Simulated Stage at Lewes Corporation Yard with 2000 - 2006 Recorded Series

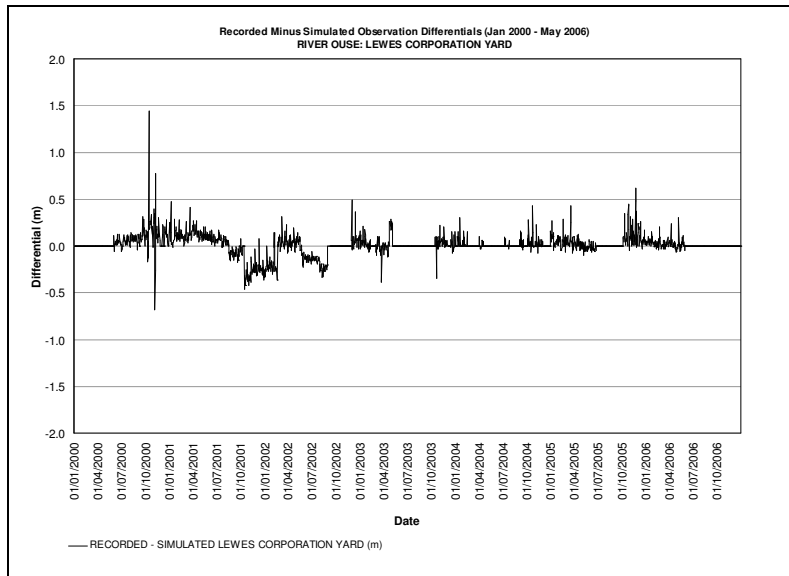


Figure B.12 Recorded minus model simulated stage differentials (Jun 2000 - May 2006)

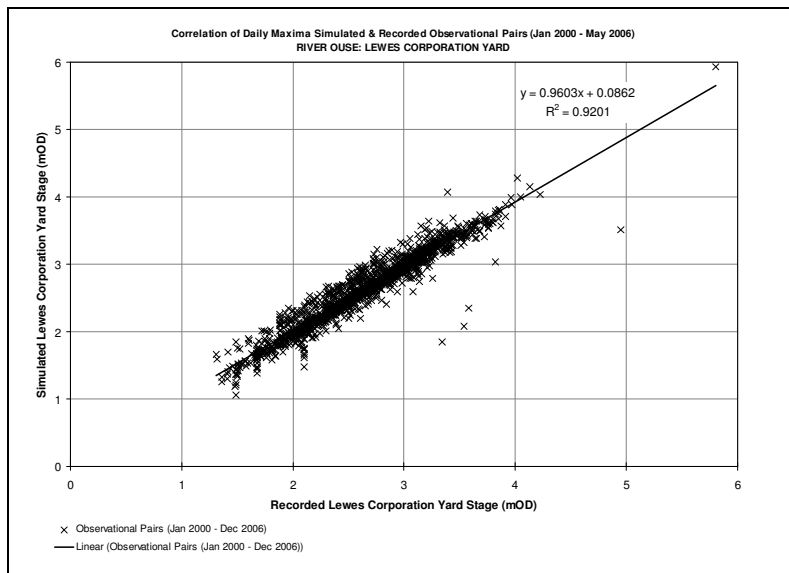


Figure B.13 Correlation of recorded & model simulated stage (Jun 2000 - May 2006)

B.3.3 Calibration of Simulated Series at Lewes Corporation Yard with 2005 - 2006 Recorded Series

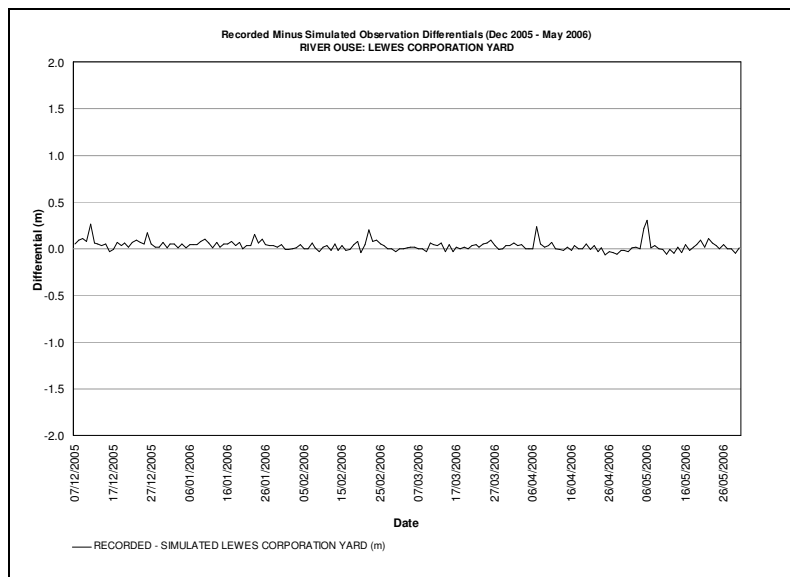


Figure B.14 Recorded minus model simulated stage differentials (Dec 2005 - May 2006)

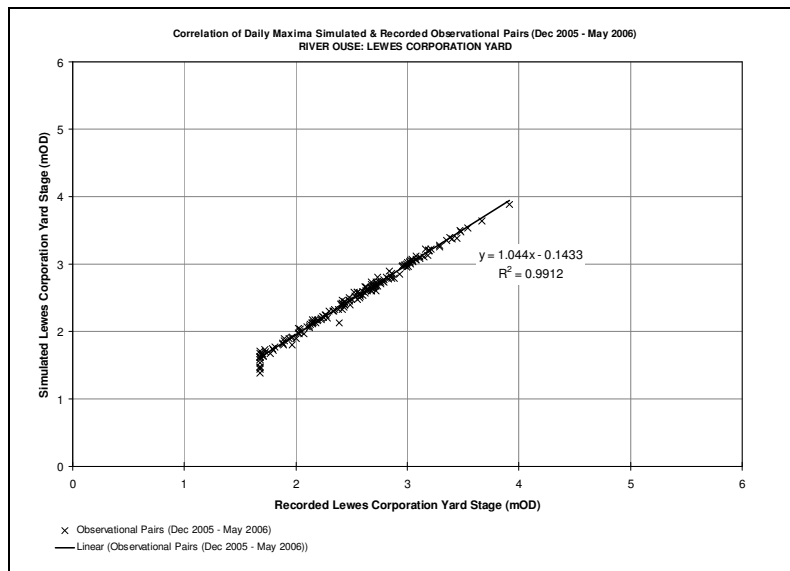


Figure B.15 Correlation of recorded & model simulated stage (Dec 2005 - May 2006)

B.4 Representative Hydrographs

B.4.1 Barcombe Mills Flow Representative Hydrographs

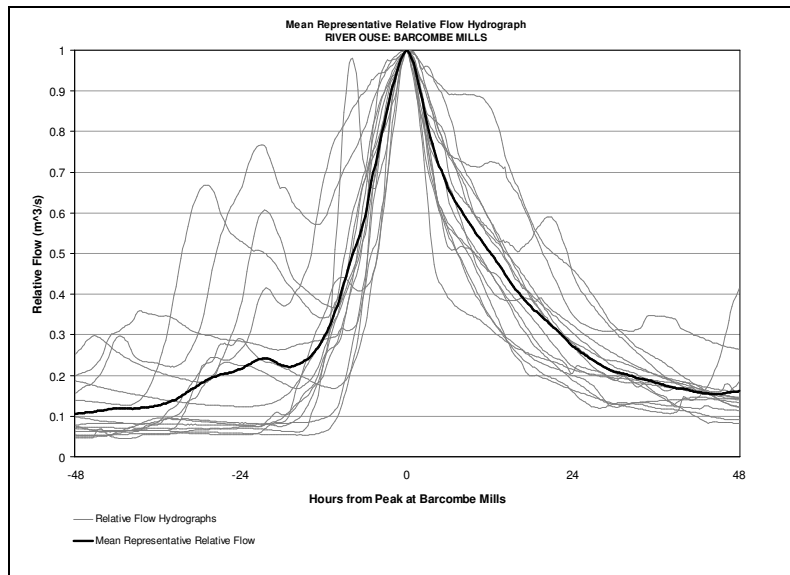


Figure B.16 Mean representative flow hydrograph at Barcombe Mills

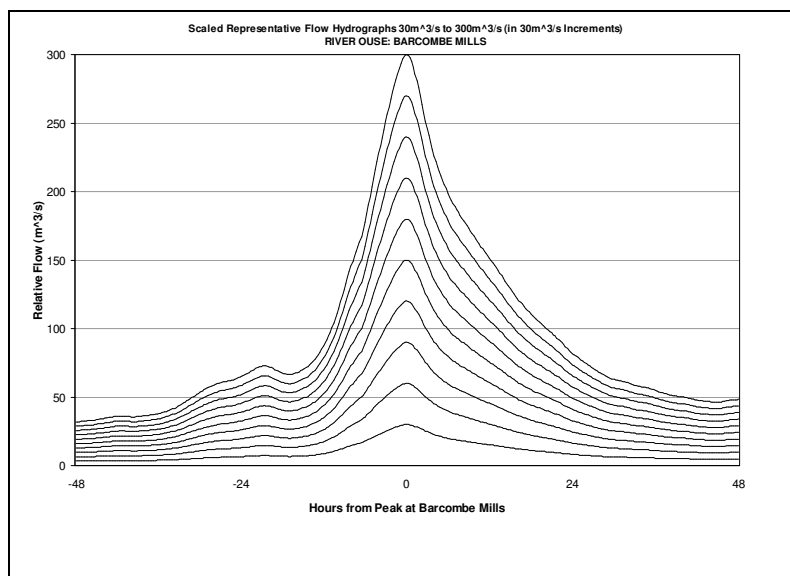


Figure B.17 Scaled representative flow hydrographs at Barcombe Mills ($30\text{m}^3/\text{s}$ to $300\text{m}^3/\text{s}$, in $30\text{m}^3/\text{s}$ increments)

B.4.2 Newhaven Tide Representative Hydrographs

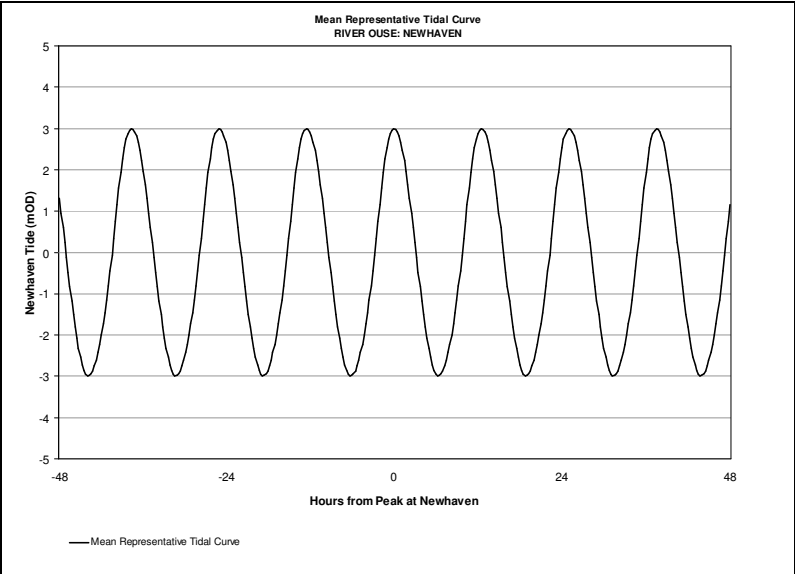


Figure B.18 Mean representative tide hydrograph at Newhaven

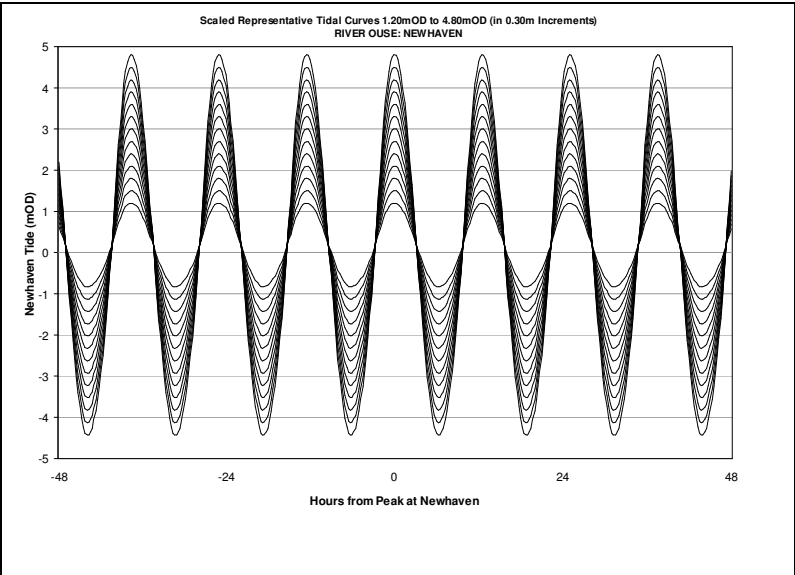


Figure B.19 Scaled representative tide hydrographs at Newhaven (1.20mAOD to 4.80mOD, in 0.30m increments)

B.4.3 Time-Lagged Analysis

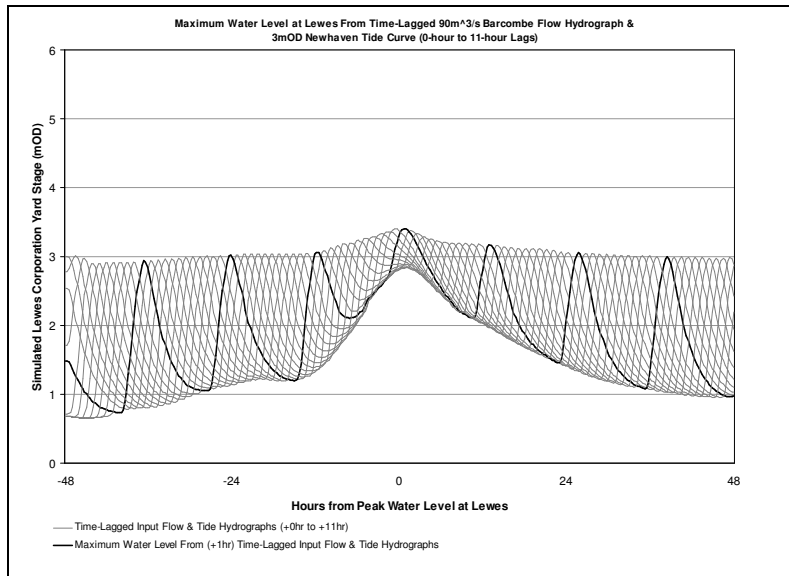


Figure B.20 Maximum water level at Lewes from time-lagged 90m³/s Barcombe Mills flow & 3mAOD Newhaven tide hydrographs (0-hour to 11-hour lags)

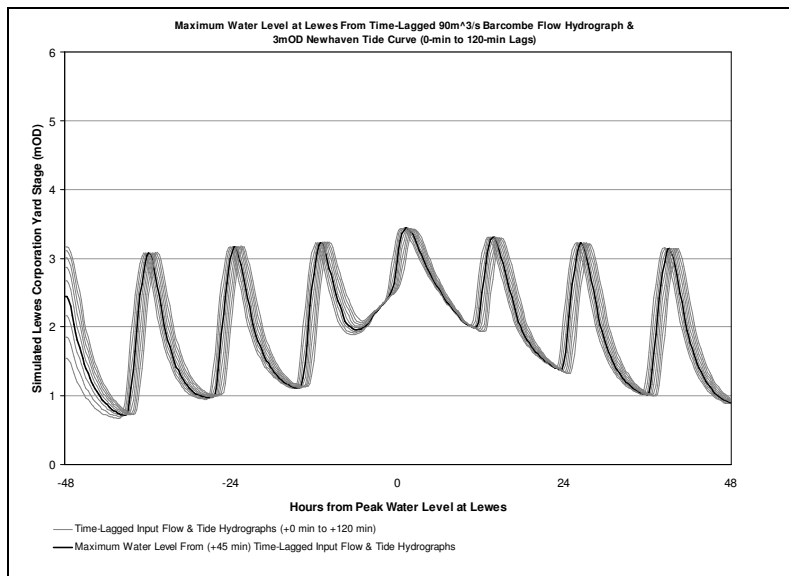


Figure B.21 Maximum water level at Lewes from time-lagged 90m³/s Barcombe Mills flow & 3mAOD Newhaven tide hydrographs (0-min to 120-min lags)

B.5 Structure Function Matrices

(see overleaf)

Table B.1 Structure function matrix for resultant simulated maximum water levels at Lewes Corporation Yard (mAOD) (shaded area) from the combinations of variables of Barcombe Mills flow (m^3/s) and Newhaven tide (mAOD).

Barcombe Mills Flow Magnitudes (m3/s)	Newhaven Tide Levels (mAOD)												
	1.20	1.50	1.80	2.10	2.40	2.70	3.00	3.30	3.60	3.90	4.20	4.50	4.80
1	1.07	1.33	1.60	1.87	2.14	2.40	2.70	3.00	3.27	3.52	3.76	3.98	4.17
30	1.64	1.80	2.02	2.30	2.58	2.85	3.10	3.36	3.60	3.83	4.05	4.25	4.43
60	2.36	2.42	2.50	2.63	2.79	2.99	3.23	3.50	3.74	3.97	4.20	4.43	4.62
90	2.89	2.92	2.97	3.04	3.13	3.24	3.40	3.59	3.81	4.05	4.29	4.54	4.76
120	3.35	3.37	3.40	3.44	3.49	3.57	3.66	3.78	3.94	4.13	4.38	4.63	4.86
150	3.71	3.73	3.74	3.77	3.81	3.85	3.92	4.01	4.13	4.28	4.51	4.72	4.97
180	4.03	4.04	4.05	4.07	4.10	4.14	4.20	4.30	4.39	4.52	4.69	4.87	5.04
210	4.33	4.34	4.35	4.37	4.44	4.50	4.58	4.66	4.75	4.84	4.95	5.06	5.21
240	4.80	4.80	4.81	4.82	4.85	4.91	4.95	5.01	5.06	5.12	5.20	5.31	5.39
270	5.28	5.28	5.29	5.29	5.30	5.31	5.34	5.38	5.42	5.46	5.52	5.61	5.71
300	5.77	5.77	5.78	5.78	5.79	5.80	5.81	5.82	5.86	5.90	5.98	6.06	6.13

Table B.2 Structure function matrix for resultant simulated maximum water levels at Lewes Gas Works (mAOD) (shaded area) from the combinations of variables of Barcombe Mills flow (m^3/s) and Newhaven tide (mAOD).

Barcombe Mills Flow Magnitudes (m3/s)	Newhaven Tide Levels (mAOD)												
	1.20	1.50	1.80	2.10	2.40	2.70	3.00	3.30	3.60	3.90	4.20	4.50	4.80
1	1.09	1.35	1.62	1.89	2.17	2.44	2.72	3.02	3.30	3.56	3.82	4.07	4.30
30	1.53	1.72	1.97	2.26	2.55	2.83	3.09	3.37	3.62	3.85	4.07	4.29	4.50
60	2.17	2.25	2.36	2.51	2.70	2.92	3.19	3.47	3.72	3.98	4.21	4.43	4.64
90	2.66	2.70	2.77	2.86	2.97	3.12	3.31	3.53	3.77	4.02	4.29	4.54	4.76
120	3.08	3.11	3.15	3.21	3.29	3.39	3.51	3.67	3.85	4.07	4.33	4.60	4.85
150	3.43	3.45	3.48	3.52	3.57	3.64	3.74	3.85	3.99	4.17	4.39	4.66	4.93
180	3.73	3.75	3.77	3.80	3.84	3.90	3.97	4.03	4.17	4.31	4.50	4.71	4.99
210	4.01	4.04	4.06	4.08	4.11	4.14	4.16	4.25	4.36	4.49	4.67	4.85	5.06
240	4.16	4.18	4.19	4.22	4.26	4.32	4.40	4.50	4.64	4.75	4.89	5.03	5.19
270	4.25	4.26	4.28	4.33	4.39	4.47	4.56	4.68	4.81	4.92	5.05	5.18	5.33
300	4.31	4.33	4.38	4.46	4.55	4.66	4.77	4.88	5.00	5.13	5.26	5.43	5.56

B.6 Simulated Longitudinal Sections

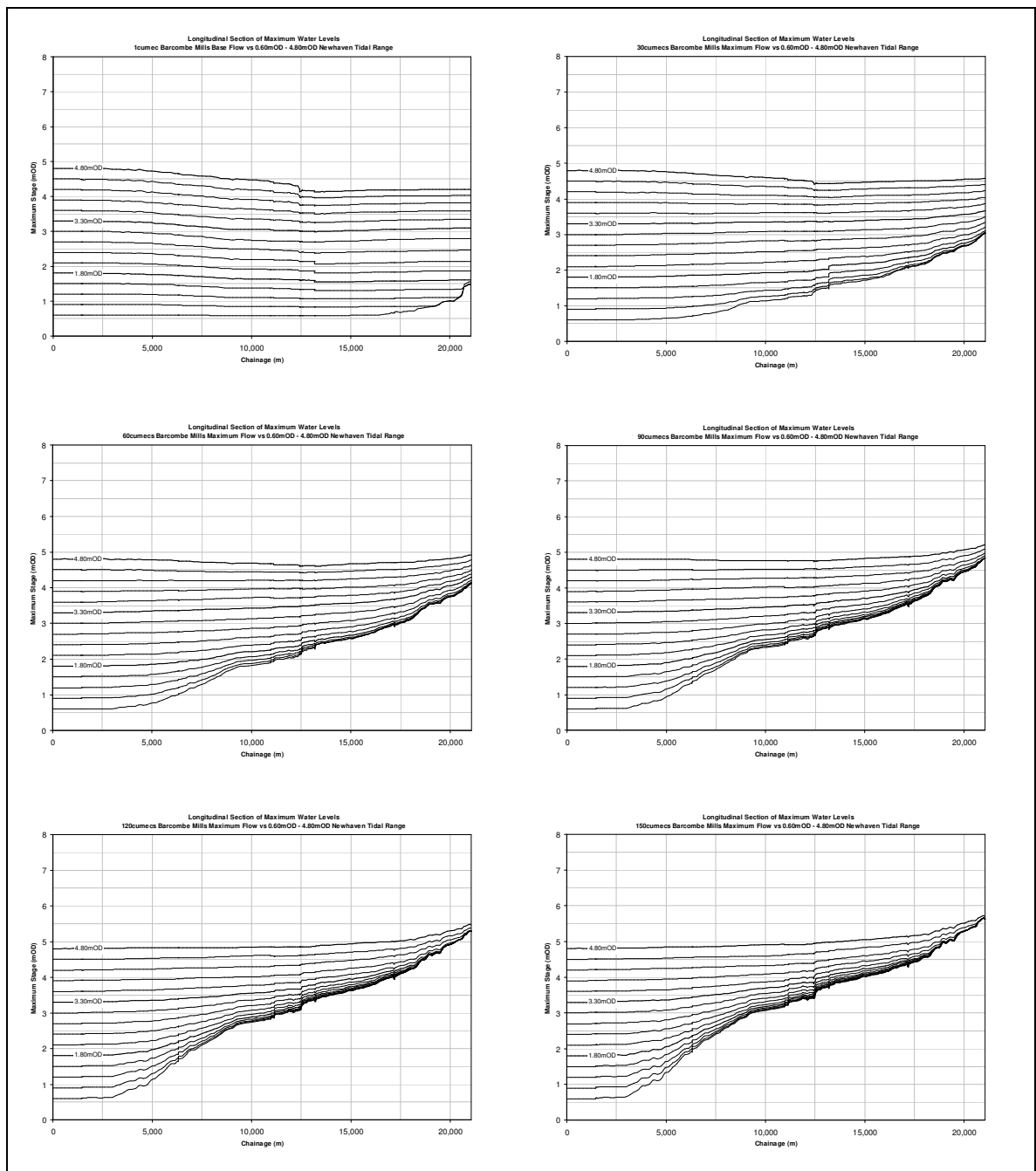
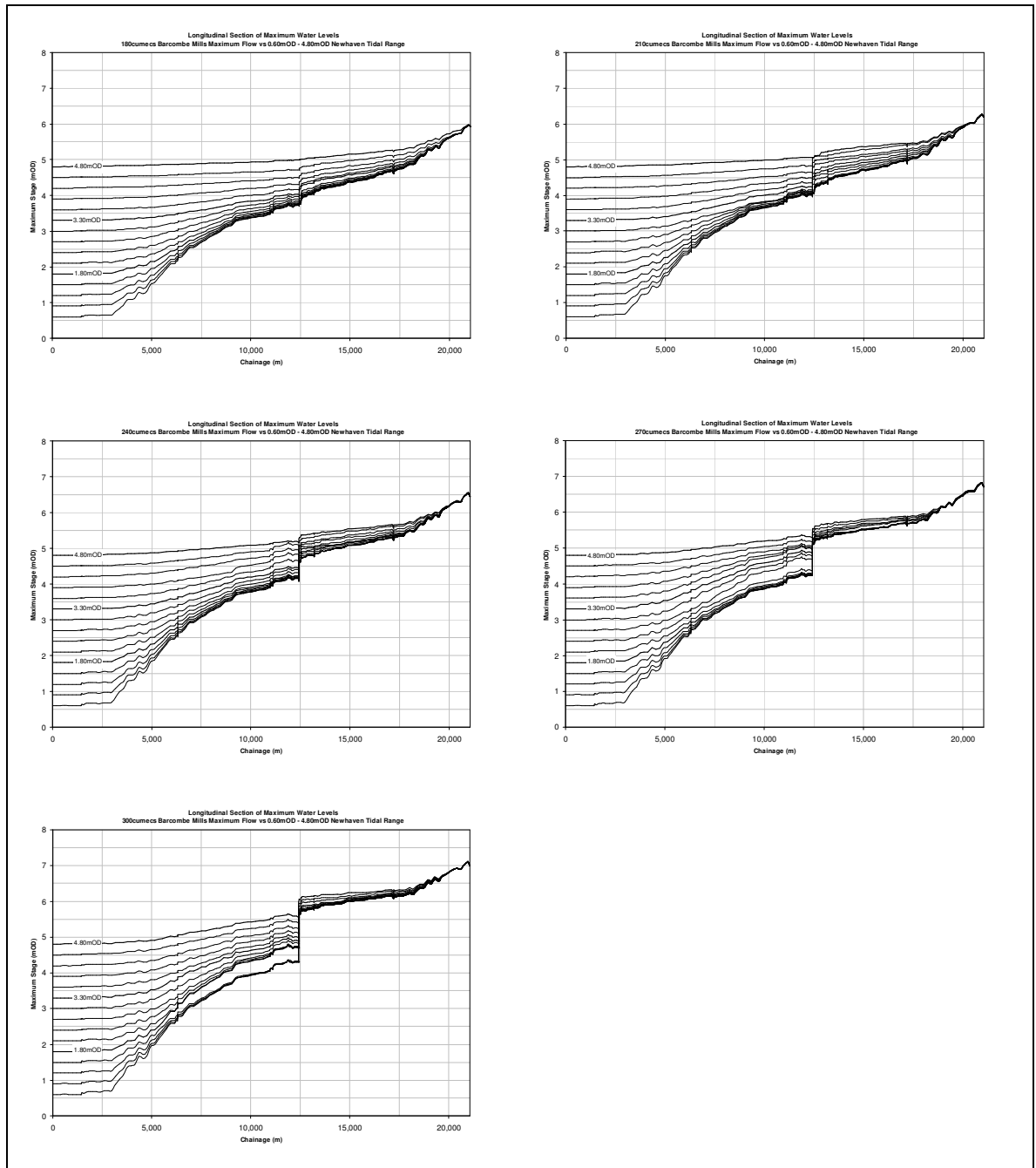


Figure B.22 Longitudinal sections of maximum water levels at for all combinations of flow and tide (1 to 300m³/s flow v 0.60 to 4.80mAOD tide)



Continued

B.7 Historical Emulation

B.7.1 Calibration of Emulated Series at Lewes Corporation Yard with 1982 - 2006 Simulated Series

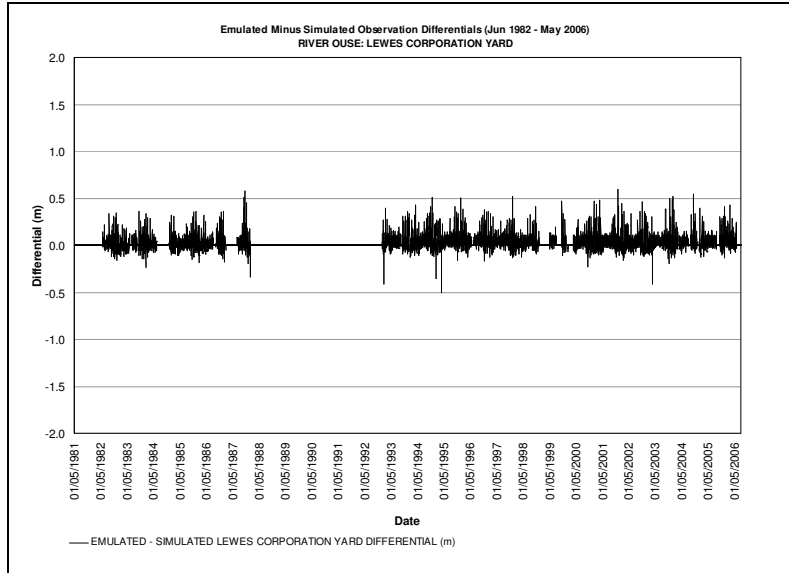


Figure B.23 Recorded minus model simulated stage differentials (Jun 2000 - May 2006)

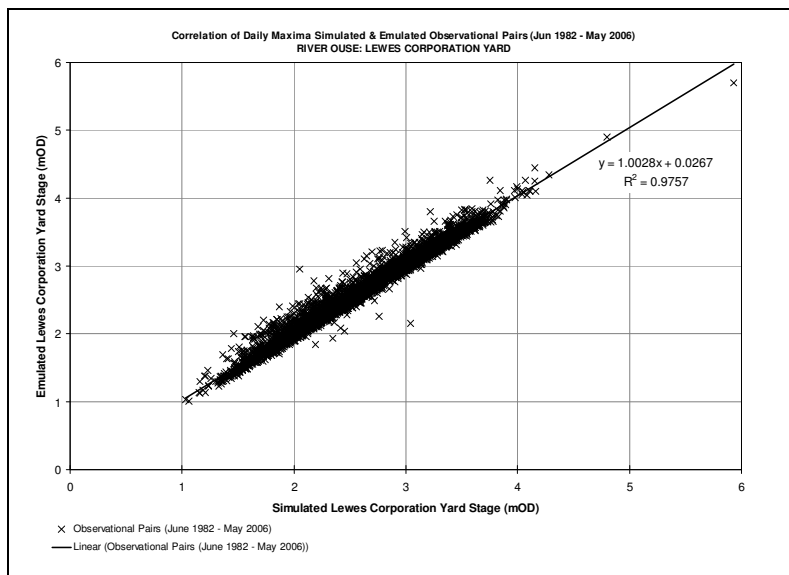


Figure B.24 Correlation of recorded & model simulated stage (Jun 2000 - May 2006)

B.7.2 Calibration of Emulated Series at Lewes Corporation Yard with 2000 - 2006 Recorded Series

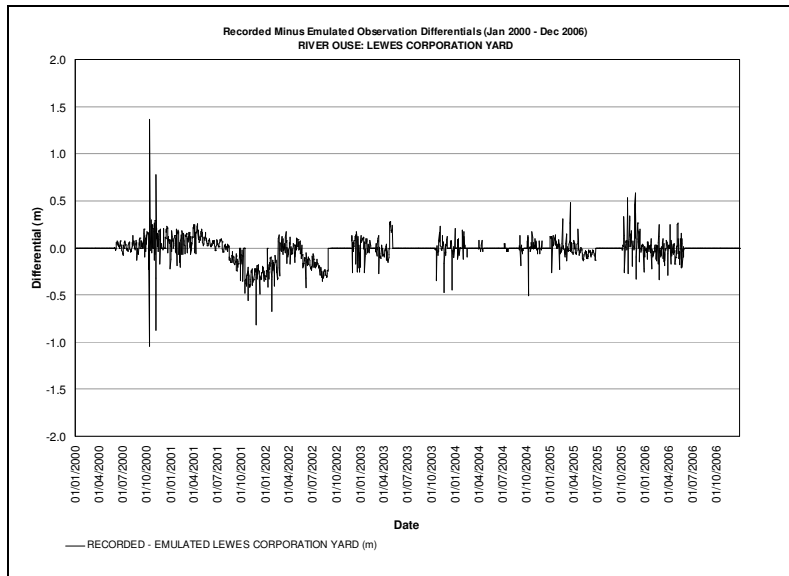


Figure B.25 Recorded minus structure function emulated stage differentials (Jun 2000 - May 2006)

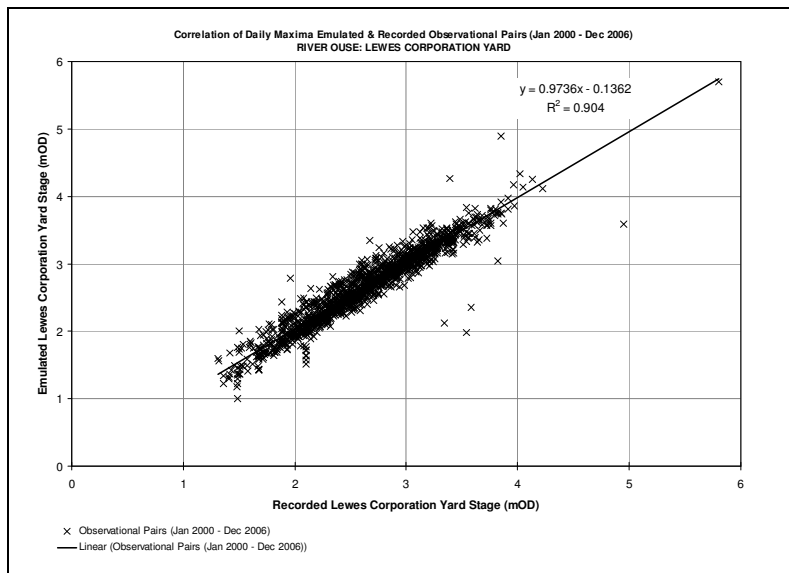


Figure B.26 Correlation of recorded & structure function emulated stage (Jun 2000 - May 2006)

B.7.3 Calibration of Emulated Series at Lewes Corporation Yard with 2005 - 2006 Recorded Series

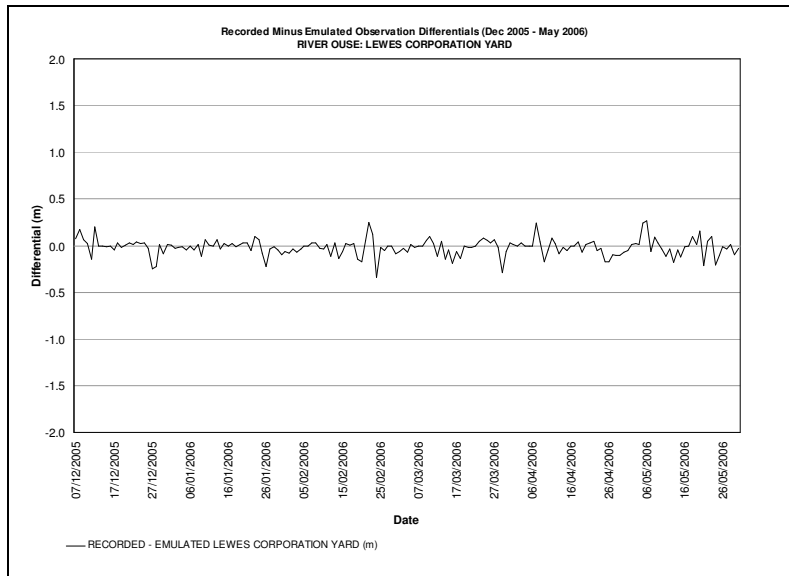


Figure B.27 Recorded minus structure function emulated stage differentials (Dec 2005 - May 2006)

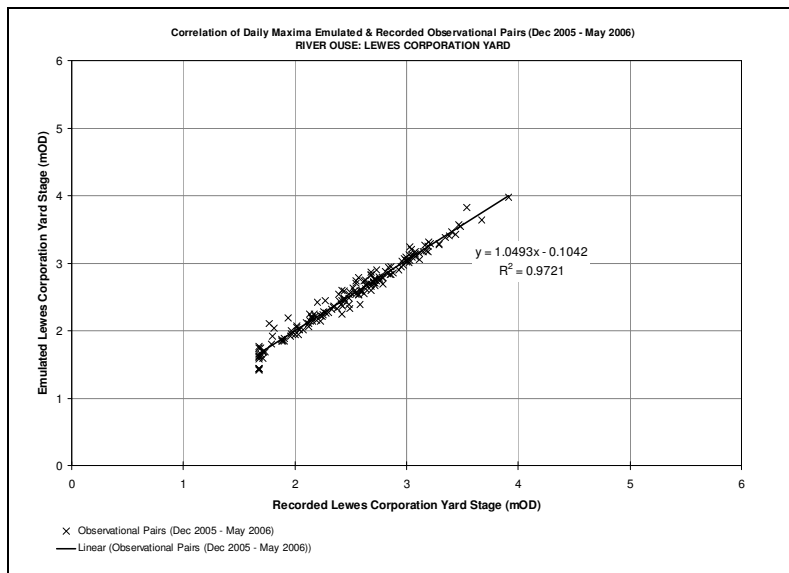


Figure B.28 Correlation of recorded & structure function emulated stage (Dec 2005 - May 2006)

APPENDIX C ANNUAL MAXIMA SERIES

C.1 Upper Ouse & Uck Sub-Catchments

C.1.1 Gold Bridge AMAX

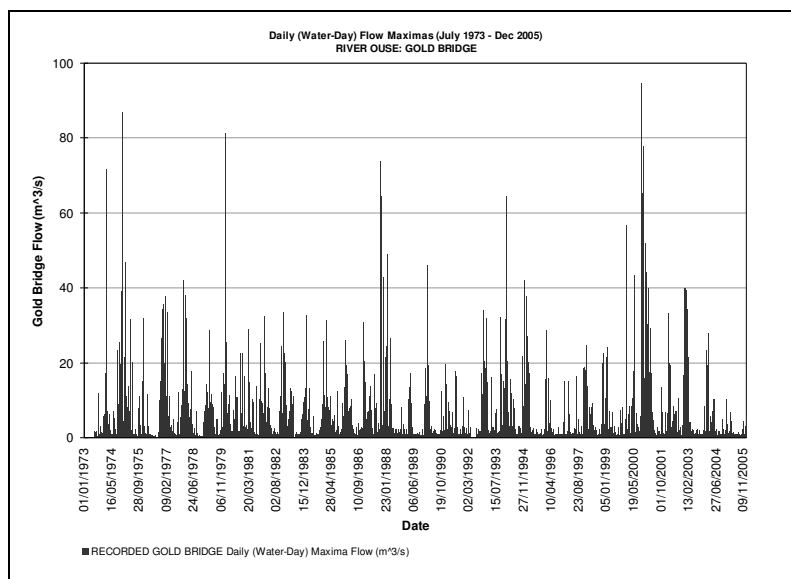


Figure C.1 Daily maxima flow observations at Gold Bridge (1973-2005)

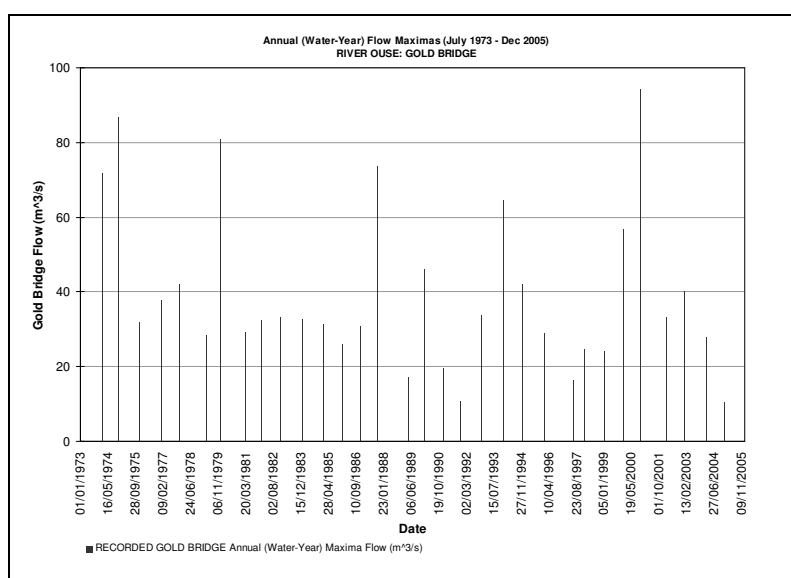


Figure C.2 Annual maxima flow observations at Gold Bridge (1973-2005)

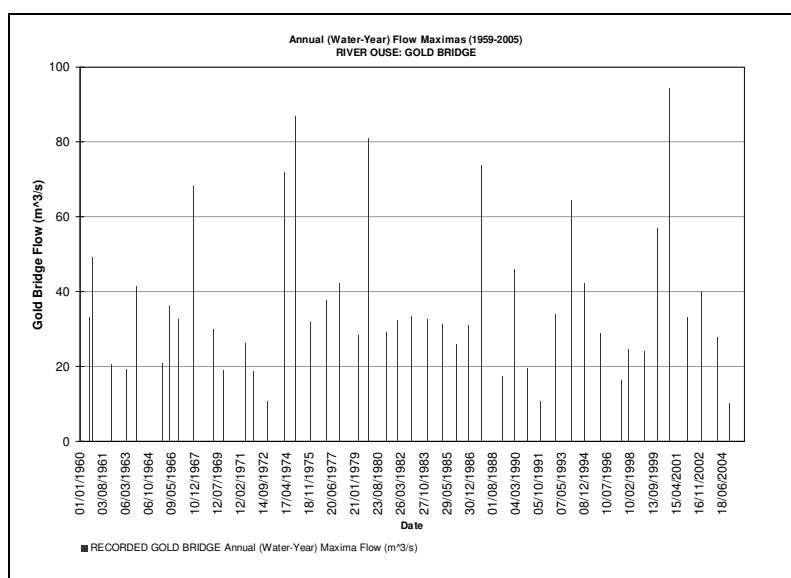


Figure C.3 Extended annual maxima flow observations at Gold Bridge (1959-2005)

Table C.1 Annual maxima flow observations at Gold Bridge (1959-2005)

Water Year	Date	Flow (m ³ /s)	Water Year	Date	Flow (m ³ /s)	Water Year	Date	Flow (m ³ /s)
1959/0	12/08/1960	33.10	1975/6	02/12/1975	31.80	1991/2	19/11/1991	10.80
1960/1	03/11/1960	49.30	1976/7	14/01/1977	37.70	1992/3	02/12/1992	33.80
1961/2	11/01/1962	20.70	1977/8	08/12/1977	42.20	1993/4	30/12/1993	64.50
1962/3	12/03/1963	19.30	1978/9	08/04/1979	28.50	1994/5	08/12/1994	42.10
1963/4	19/11/1963	41.40	1979/0	28/12/1979	81.10	1995/6	09/01/1996	28.80
1964/5	04/09/1965	21.10	1980/1	09/03/1981	29.10	1996/7	27/06/1997	16.40
1965/6	26/02/1966	36.30	1981/2	14/12/1981	32.40	1997/8	02/01/1998	24.70
1966/7	24/10/1966	32.60	1982/3	09/12/1982	33.40	1998/9	19/01/1999	24.10
1967/8	04/11/1967	68.30	1983/4	23/01/1984	32.70	1999/0	24/12/1999	56.80
1968/9	13/03/1969	29.90	1984/5	21/01/1985	31.40	2000/1	12/10/2000	94.40
1969/0	17/11/1969	19.00	1985/6	03/01/1986	26.00	2001/2	04/02/2002	33.30
1970/1	19/06/1971	26.20	1986/7	21/11/1986	30.90	2002/3	22/12/2002	40.10
1971/2	11/01/1972	18.80	1987/8	09/10/1987	73.70	2003/4	01/02/2004	27.80
1972/3	13/12/1972	10.80	1988/9	11/04/1989	17.40	2004/5	19/12/2004	10.30
1973/4	11/02/1974	71.90	1989/0	31/01/1990	46.20			
1974/5	22/11/1974	86.90	1990/1	08/01/1991	19.60			

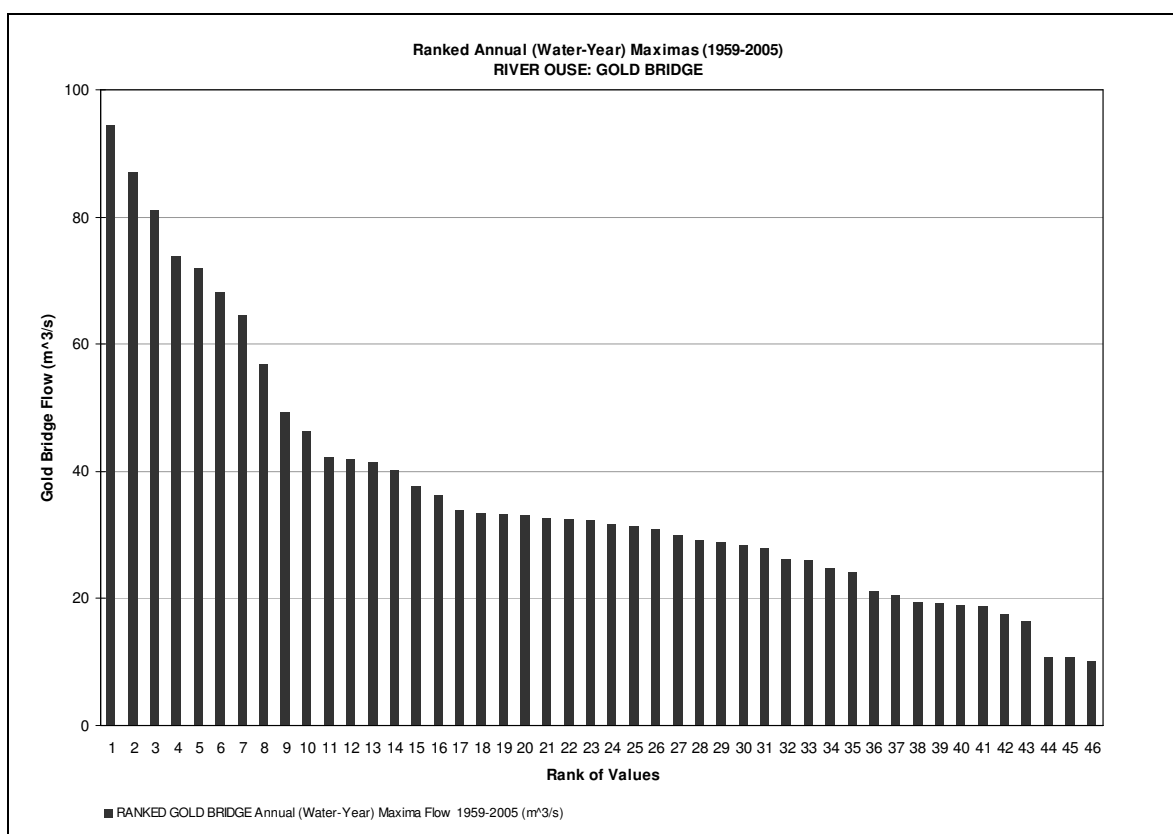


Figure C.4 Ranked annual maxima flow observations at Gold Bridge (1959-2005)

Table C.2 Return periods & flow magnitude estimates at Gold Bridge

Station	Gold Bridge	Mean	36.687	
River	River Ouse	Standard Error	2.991	
Data Period	1959-2005	Standard Deviation	20.287	
Complete Years	46	Skew	1.275	
Missing Years	0	Distribution	GEV	
Units	Flow (m ³ /s)	Anderson Darling	0.4292	
Max	94.40 (12/10/2000)	Parameters	μ	27.121
Min	10.30 (19/12/2004)		α	12.549
			k	-0.174

Location	Return Period (Years)	Estimated Magnitude	95% Confidence Interval		Standard Error
			lower	upper	
Gold Bridge TQ 429 214 (Ouse)	1	5.67	N/A		N/A
	2	31.87	27.42	37.33	2.53
	5	48.63	41.79	57.52	4.01
	10	61.69	50.86	76.36	6.50
	25	80.84	59.77	106.65	11.96
	50	97.23	65.27	136.06	18.06
	100	115.61	68.45	172.81	26.62
	200	136.28	71.88	219.94	37.77

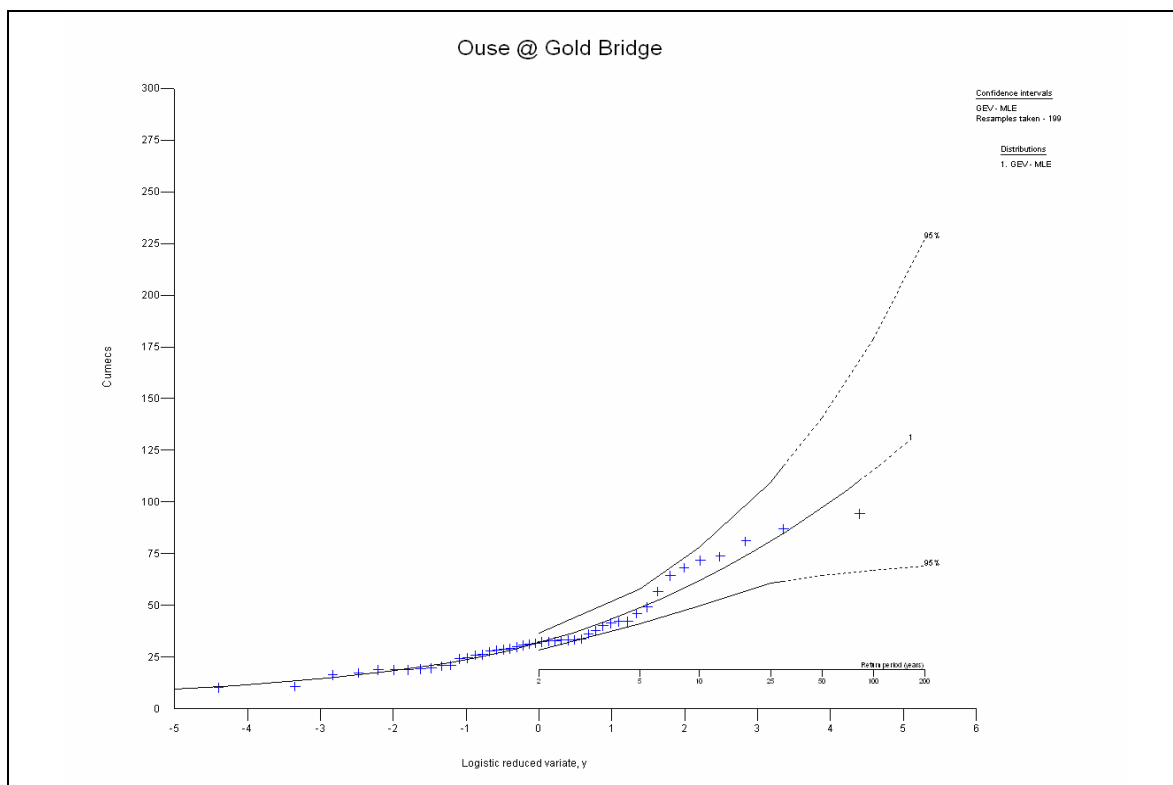


Figure C.5 GEV distribution plot at Gold Bridge (1959-2005)

C.1.2 Isfield Weir AMAX

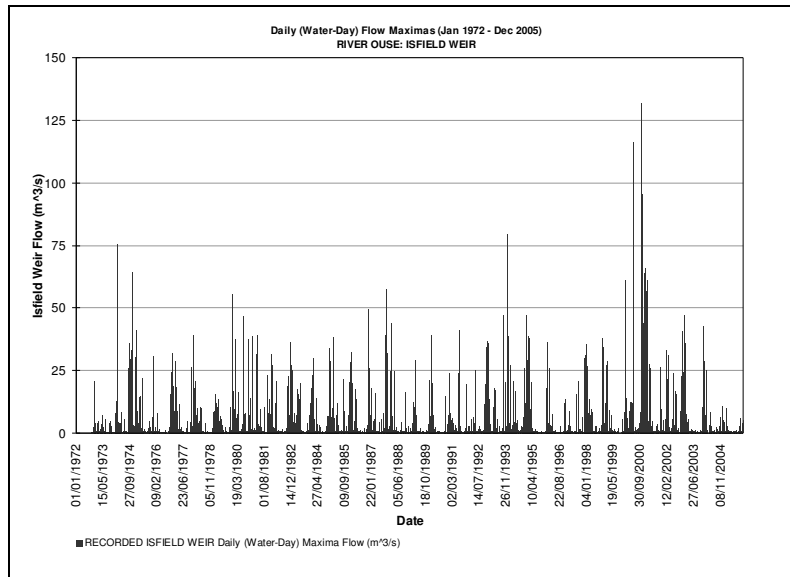


Figure C.6 Daily maxima flow observations at Isfield Weir (1972-2005)

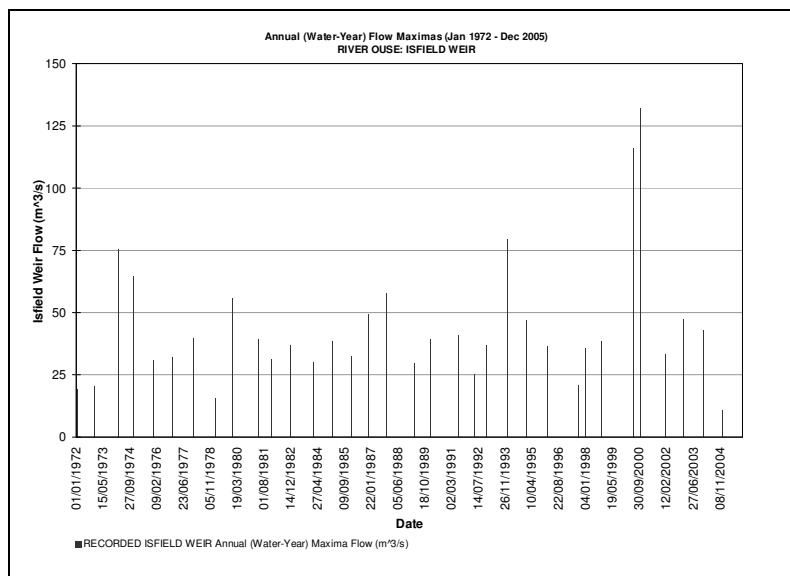


Figure C.7 Annual maxima flow observations at Isfield Weir (1972-2005)

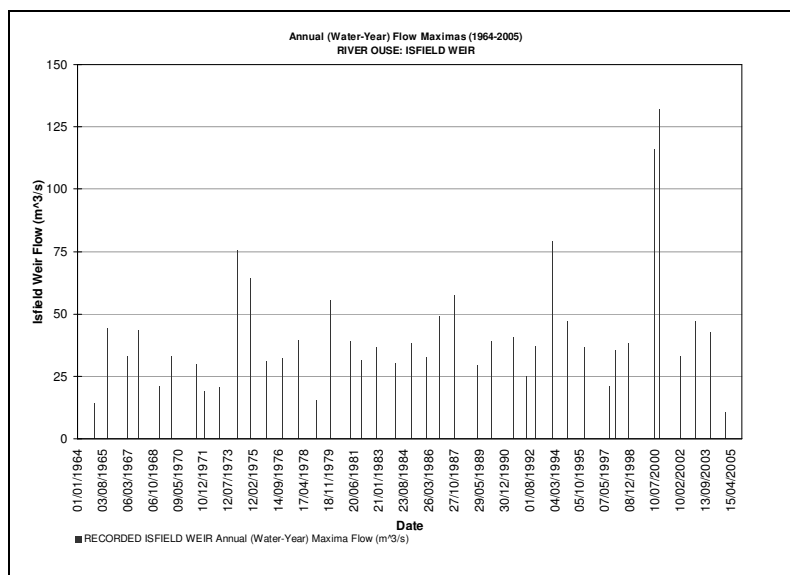


Figure C.8 Extended annual maxima flow observations at Isfield Weir (1964-2005)

Table C.3 Annual maxima flow observations at Isfield Weir (1964-2005)

Water Year	Date	Flow (m ³ /s)	Water Year	Date	Flow (m ³ /s)	Water Year	Date	Flow (m ³ /s)
1964/5	03/09/1965	21.50	1978/9	01/02/1979	15.40	1992/3	02/12/1992	36.80
1965/6	20/11/1965	44.20	1979/0	27/12/1979	55.60	1993/4	30/12/1993	79.40
1966/7	28/02/1967	33.10	1980/1	30/03/1981	39.10	1994/5	08/12/1994	46.90
1967/8	04/11/1967	43.30	1981/2	14/12/1981	31.40	1995/6	09/01/1996	36.50
1968/9	21/02/1969	20.80	1982/3	25/11/1982	36.60	1996/7	06/08/1997	20.80
1969/0	17/11/1969	33.10	1983/4	23/01/1984	30.20	1997/8	02/01/1998	35.50
1970/1	19/06/1971	29.60	1984/5	21/01/1985	38.30	1998/9	24/10/1998	38.20
1971/2	11/01/1972	19.00	1985/6	03/01/1986	32.40	1999/0	28/05/2000	116.00
1972/3	09/12/1972	20.50	1986/7	20/11/1986	49.40	2000/1	11/10/2000	132.00
1973/4	13/02/1974	75.60	1987/8	20/10/1987	57.50	2001/2	26/01/2002	33.20
1974/5	22/11/1974	64.40	1988/9	11/04/1989	29.30	2002/3	02/01/2003	47.10
1975/6	01/12/1975	30.90	1989/0	31/01/1990	39.30	2003/4	28/12/2003	42.70
1976/7	30/11/1976	32.10	1990/1	03/07/1991	40.80	2004/5	18/12/2004	10.70
1977/8	08/12/1977	39.40	1991/2	01/05/1992	24.90			

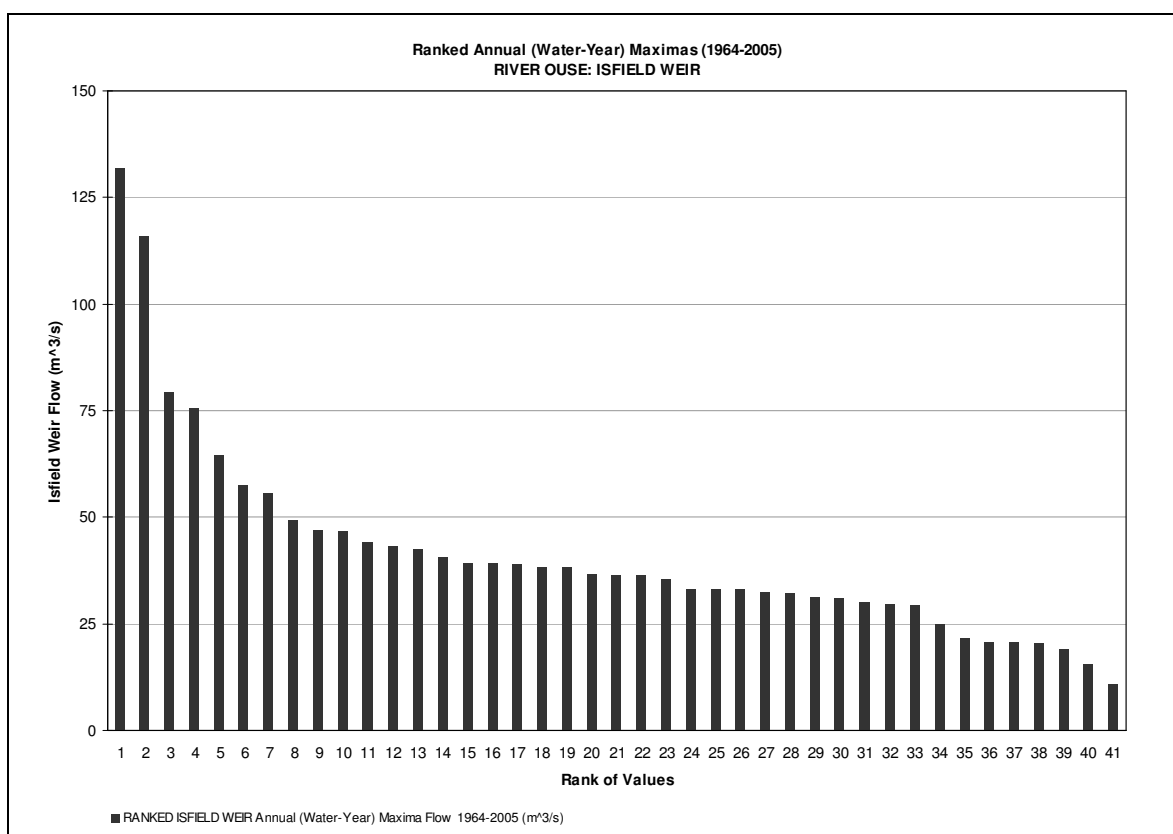


Figure C.9 Ranked annual maxima flow observations at Isfield Weir (1964-2005)

Table C.4 Return periods & flow magnitude estimates at Isfield Weir

Station	Isfield Weir	Mean	41.549		
River	River Uck	Standard Error	3.722		
Data Period	1964-2005	Standard Deviation	23.833		
Complete Years	41	Skew	2.244		
Missing Years	0	Distribution	GEV		
Units	Flow (m^3/s)	Anderson Darling	0.6626		
Max	132.00 (11/10/2000)	Parameters	μ	31.562	
Min	10.70 (18/12/2004)		α	13.646	
			k	-0.141	

Location	Return Period (Years)	Estimated Magnitude	95% Confidence Interval		Standard Error
			lower	upper	
Isfield Weir TQ 459 190 (Uck)	1	7.48	N/A		N/A
	2	36.69	32.35	41.93	2.44
	5	54.35	45.60	64.63	4.85
	10	67.69	51.96	86.14	8.72
	25	86.69	58.45	121.88	16.18
	50	102.51	60.27	156.17	24.46
	100	119.85	62.35	198.02	34.61
	200	138.90	62.62	248.60	47.44

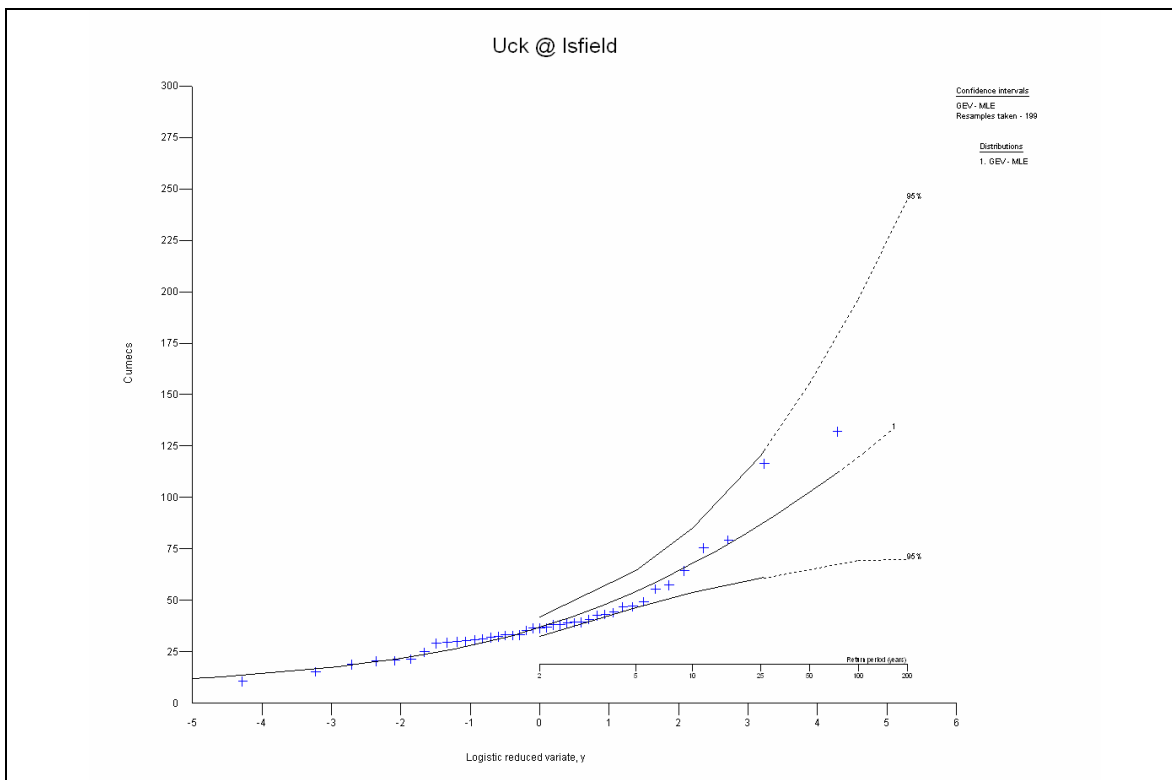


Figure C.10 GEV distribution plot at Isfield Weir (1964-2005)

C.1.3 Clappers Bridge AMAX

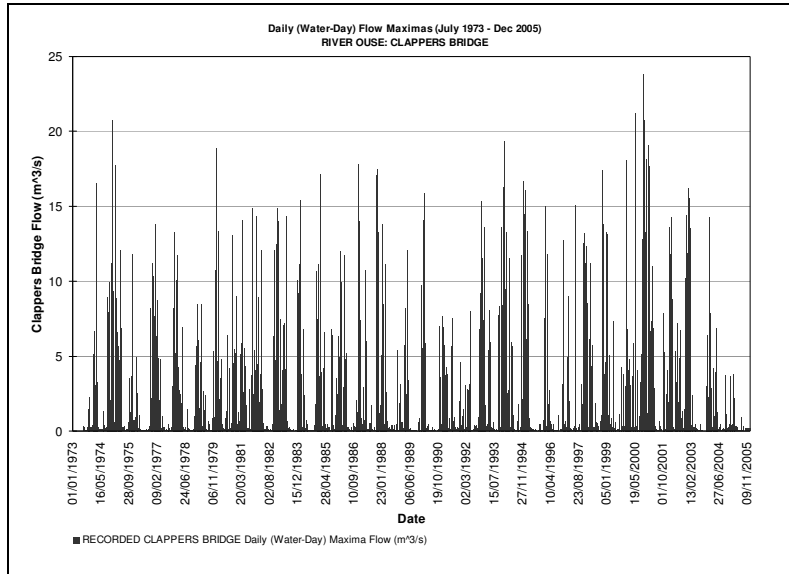


Figure C.11 Daily maxima flow observations at Clappers Bridge (1973-2005)

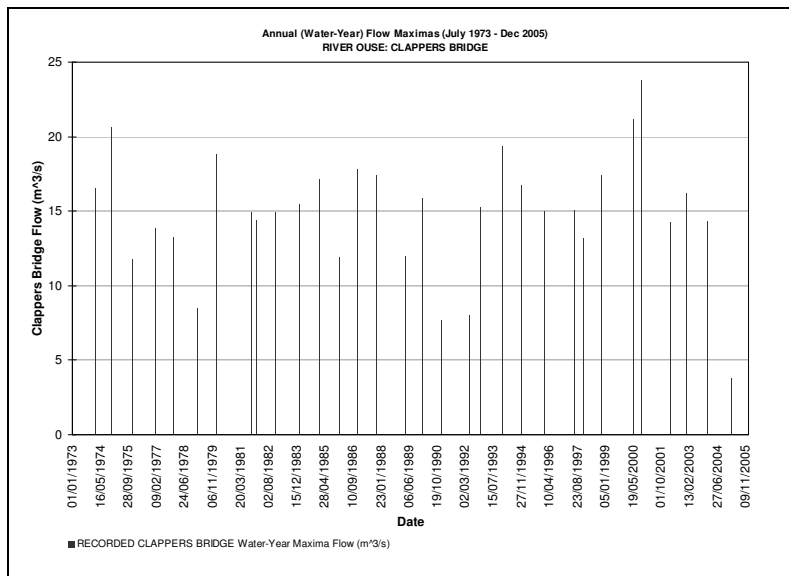


Figure C.12 Annual maxima flow observations at Clappers Bridge (1973-2005)

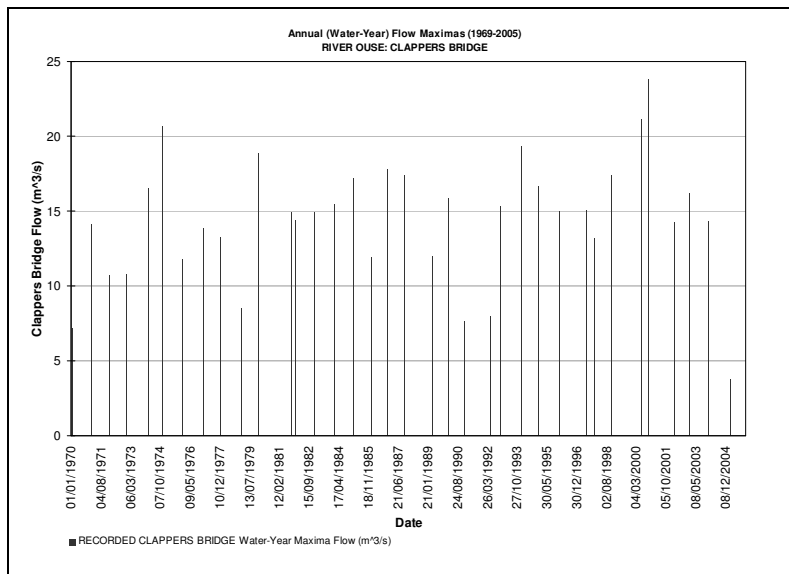


Figure C.13 Extended annual maxima flow observations at Clappers Bridge (1969-2005)

Table C.5 Annual maxima flow observations at Clappers Bridge (1969-2005)

Water Year	Date	Flow (m ³ /s)	Water Year	Date	Flow (m ³ /s)	Water Year	Date	Flow (m ³ /s)
1969/0	24/01/1970	7.18	1981/2	13/12/1981	14.38	1993/4	30/12/1993	19.34
1970/1	23/01/1971	14.10	1982/3	09/12/1982	14.88	1994/5	08/12/1994	16.68
1971/2	11/01/1972	10.70	1983/4	23/01/1984	15.44	1995/6	09/01/1996	15.01
1972/3	13/12/1972	10.80	1984/5	21/01/1985	17.14	1996/7	26/06/1997	15.07
1973/4	14/02/1974	16.52	1985/6	02/01/1986	11.96	1997/8	28/11/1997	13.18
1974/5	22/11/1974	20.69	1986/7	20/11/1986	17.80	1998/9	24/10/1998	17.38
1975/6	01/12/1975	11.81	1987/8	20/10/1987	17.45	1999/0	28/05/2000	21.18
1976/7	13/01/1977	13.83	1988/9	11/04/1989	12.02	2000/1	11/10/2000	23.78
1977/8	07/12/1977	13.28	1989/0	31/01/1990	15.86	2001/2	26/02/2002	14.26
1978/9	01/02/1979	8.49	1990/1	01/01/1991	7.65	2002/3	22/12/2002	16.22
1979/0	27/12/1979	18.84	1991/2	01/05/1992	8.01	2003/4	27/12/2003	14.30
1980/1	26/09/1981	14.88	1992/3	25/11/1992	15.30	2004/5	02/03/2005	

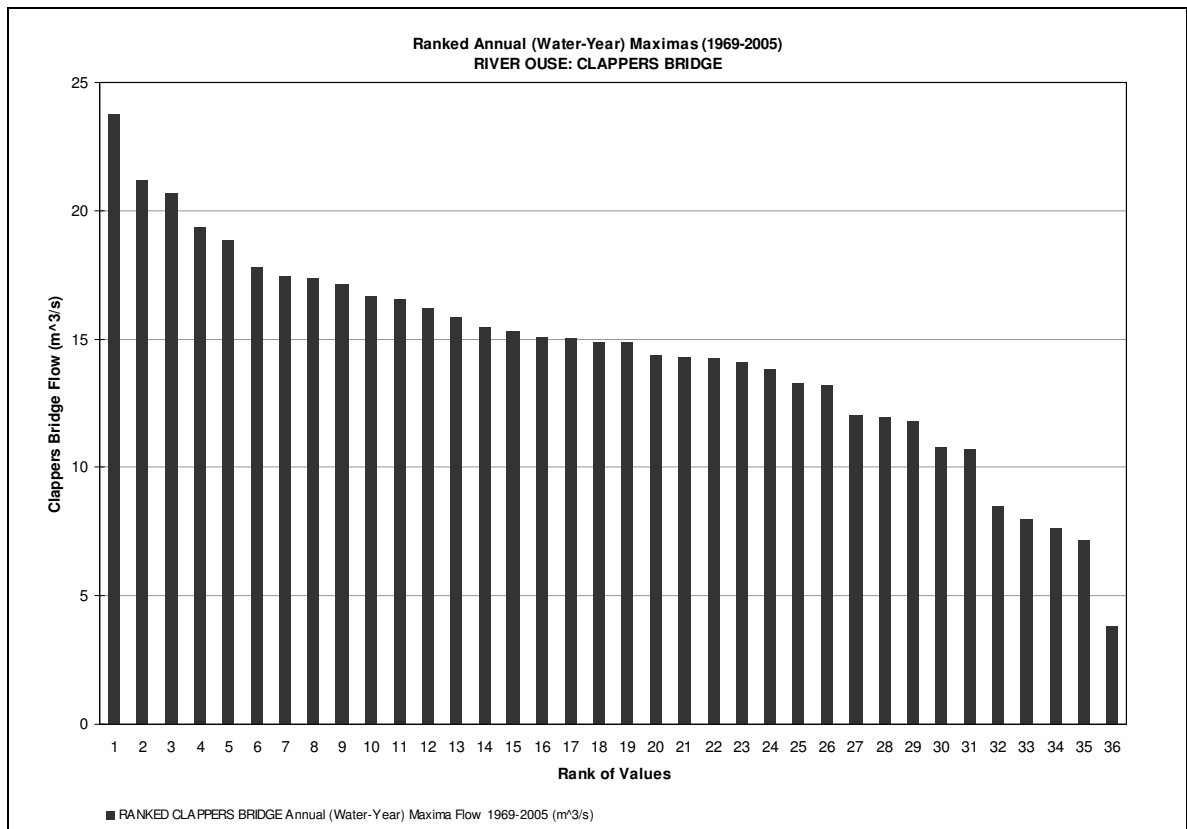


Figure C.14 Ranked annual maxima flow observations at Clappers Bridge (1969-2005)

Table C.6 Return periods & flow magnitude estimates at Clappers Bridge

Station	Clappers Bridge	Mean	14.726	
River	Bevern Stream	Standard Error	0.642	
Data Period	1969-2005	Standard Deviation	3.801	
Complete Years	35	Skew	-0.021	
Missing Years	1	Distribution	GEV	
Units	Flow (m ³ /s)	Anderson Darling	0.7033	
Max	23.78 (11/10/2000)	Parameters	μ	13.383
Min	7.18 (24/10/1970)		α	3.764
			k	0.271

Location	Return Period (Years)	Estimated Magnitude	95% Confidence Interval		Standard Error
			lower	upper	
Clappers Bridge TQ 423 161 (Bevern Stream)	1	3.20	N/A		N/A
	2	14.70	13.39	16.23	0.72
	5	18.02	16.76	19.92	0.81
	10	19.72	18.39	22.41	1.02
	25	21.43	20.02	25.38	1.37
	50	22.44	20.78	27.21	1.64
	100	23.28	21.28	28.95	1.96
	200	23.96	21.40	30.46	2.31

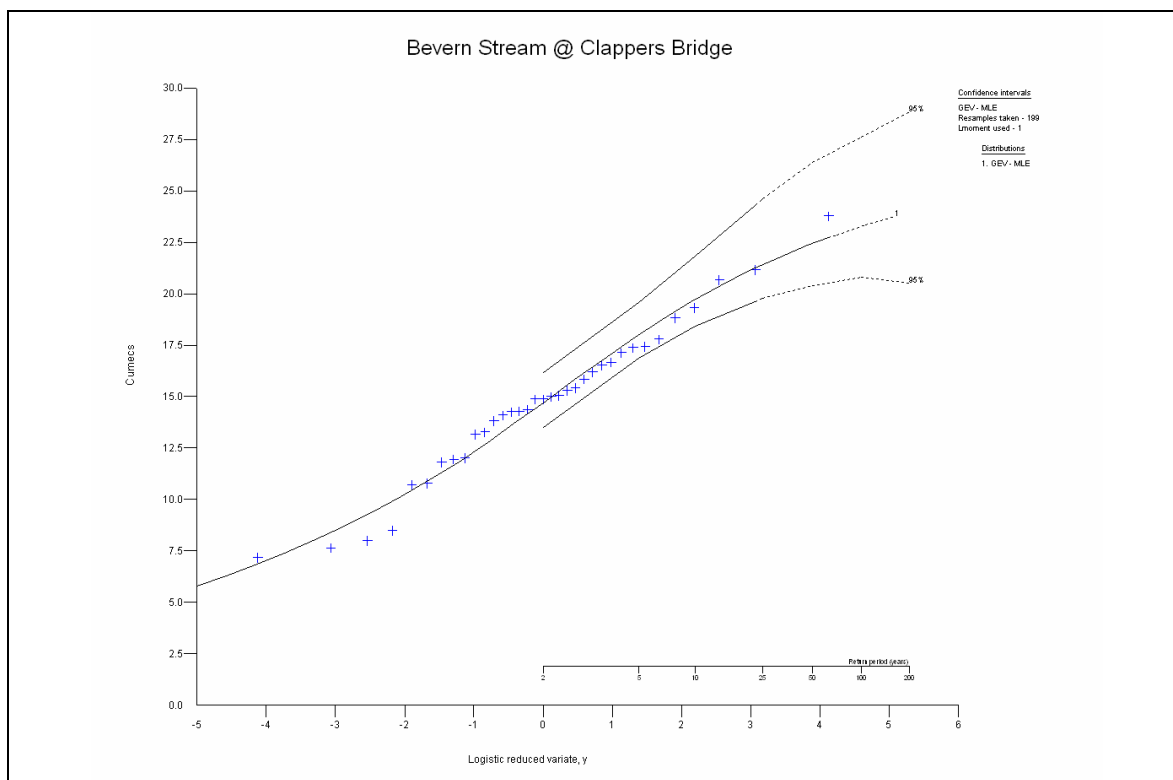


Figure C.15 GEV distribution plot at Clappers Bridge (1969-2005)

C.1.4 Old Ship AMAX

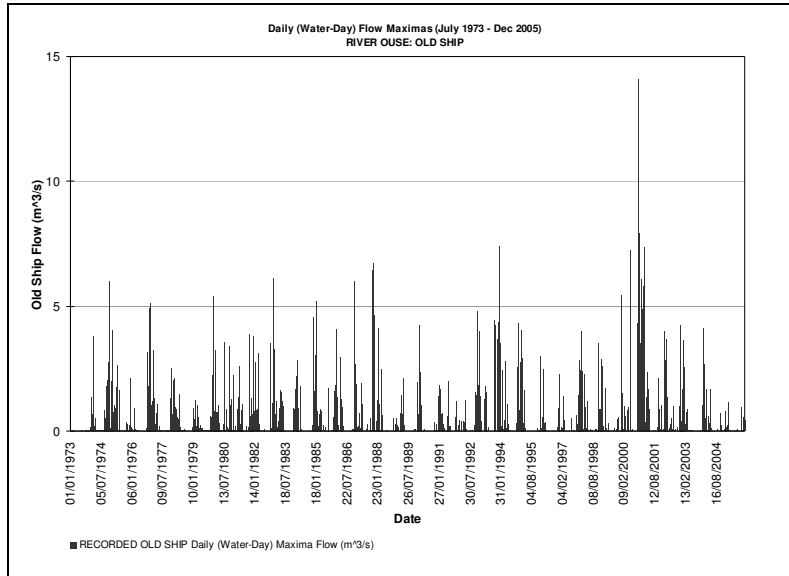


Figure C.16 Daily maxima flow observations at Old Ship (1973-2005)

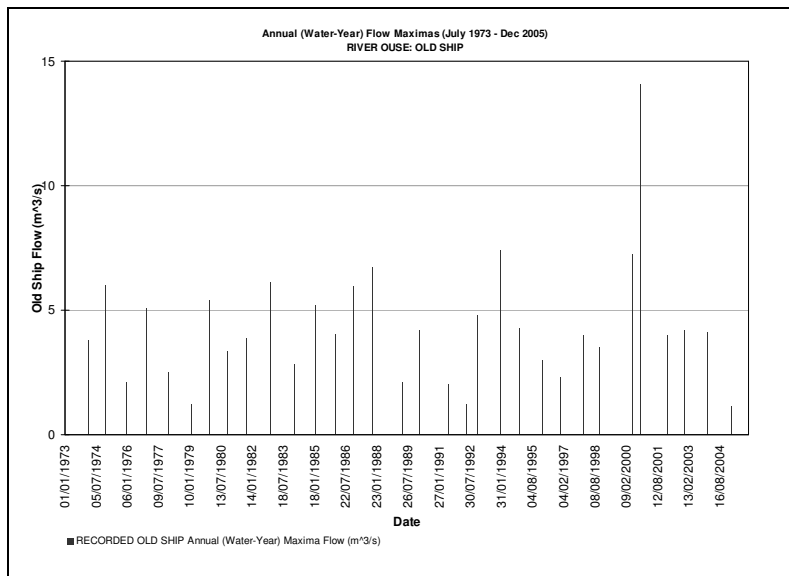


Figure C.17 Annual maxima flow observations at Old Ship (1973-2005)

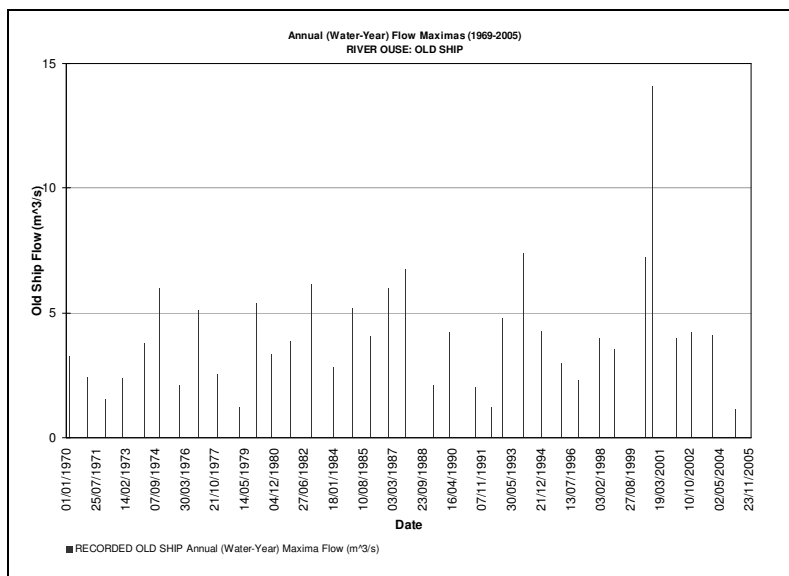


Figure C.18 Extended annual maxima flow observations at Old Ship (1969-2005)

Table C.7 Annual maxima flow observations at Old Ship (1969-2005)

Water Year	Date	Flow (m ³ /s)	Water Year	Date	Flow (m ³ /s)	Water Year	Date	Flow (m ³ /s)
1969/0	12/02/1970	3.28	1981/2	03/10/1981	3.87	1993/4	30/12/1993	7.40
1970/1	23/01/1971	2.42	1982/3	24/11/1982	6.11	1994/5	08/12/1994	4.28
1971/2	11/01/1972	1.52	1983/4	23/01/1984	2.82	1995/6	08/01/1996	3.00
1972/3	08/12/1972	2.39	1984/5	21/01/1985	5.20	1996/7	24/11/1996	2.30
1973/4	10/02/1974	3.79	1985/6	02/01/1986	4.06	1997/8	02/01/1998	3.99
1974/5	21/11/1974	6.02	1986/7	20/11/1986	5.98	1998/9	24/10/1998	3.53
1975/6	01/12/1975	2.09	1987/8	20/10/1987	6.73	1999/0	27/05/2000	7.24
1976/7	30/11/1976	5.10	1988/9	11/04/1989	2.08	2000/1	12/10/2000	14.07
1977/8	07/12/1977	2.51	1989/0	31/01/1990	4.22	2001/2	26/01/2002	3.98
1978/9	01/02/1979	1.25	1990/1	03/07/1991	2.01	2002/3	14/11/2002	4.22
1979/0	27/12/1979	5.41	1991/2	28/04/1992	1.23	2003/4	27/12/2003	4.10
1980/1	16/10/1980	3.36	1992/3	25/11/1992	4.79	2004/5	02/03/2005	1.13

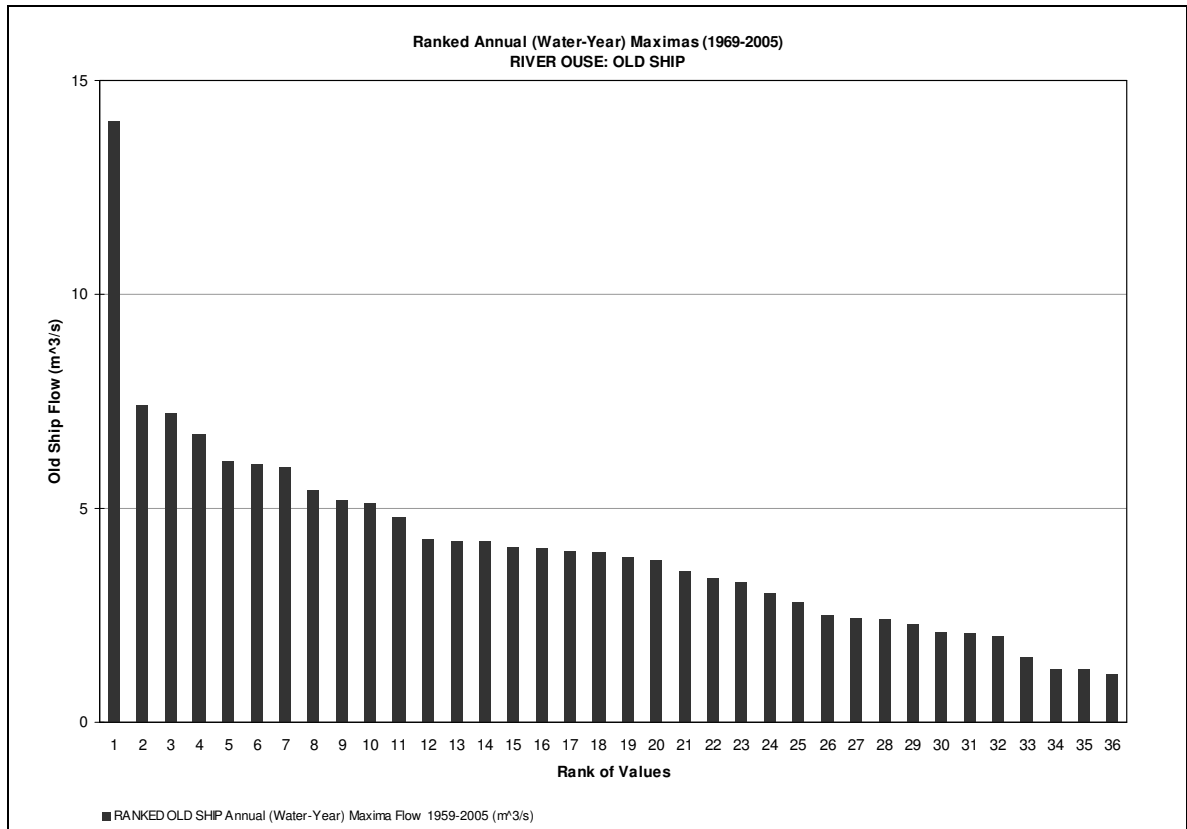


Figure C.19 Ranked annual maxima flow observations at Old Ship (1969-2005)

Table C.8 Return periods & flow magnitude estimates at Old Ship

Station	Old Ship	Mean	4.097		
River	Clayhill Stream	Standard Error	0.402		
Data Period	1969-2005	Standard Deviation	2.410		
Complete Years	36	Skew	2.085		
Missing Years	0	Distribution	GEV		
Units	Flow (m ³ /s)	Anderson Darling	0.2573		
Max	14.07 (12/10/2000)	Parameters	μ	3.012	
Min	1.13 (02/03/2005)		α	1.555	
			k	-0.111	

Location	Return Period (Years)	Estimated Magnitude	95% Confidence Interval		Standard Error
			lower	upper	
Old Ship TQ 448 153 (Clay Hill Stream)	1	0.55	N/A		N/A
	2	3.59	2.91	4.54	0.42
	5	5.55	4.55	7.13	0.66
	10	6.99	5.60	9.18	0.91
	25	8.98	6.71	13.00	1.61
	50	10.60	7.10	16.61	2.43
	100	12.34	7.53	20.88	3.40
	200	14.22	7.67	26.92	4.91

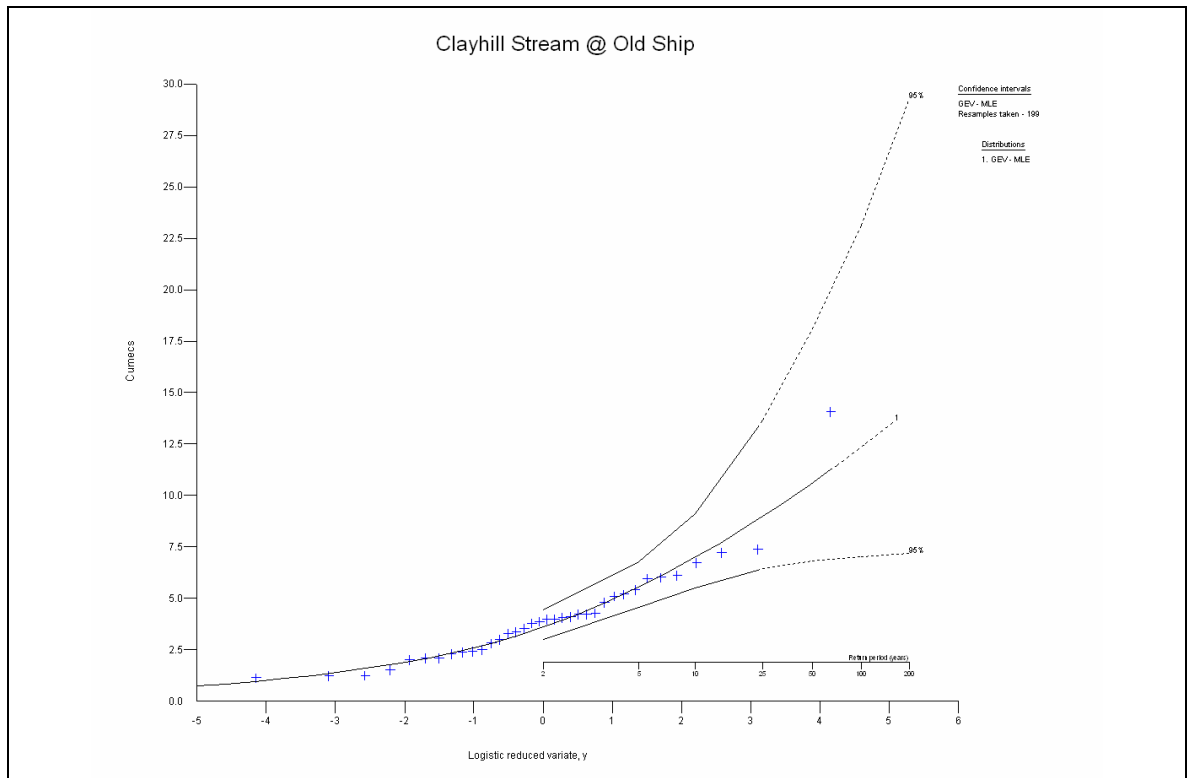


Figure C.20 GEV distribution plot at Old Ship (1969-2005)

C.2 Middle Ouse Sub-Catchment

C.2.1 Extending the Barcombe Mills Series

Table C.9 Linearly correlated Barcombe Mills total runoff, stage and flow AMAX series (1952-2000)

Water Year	Water-Day	AMAX Total 24-Hour Runoff Volume (Million m ³)	AMAX Stage (mAOD)	AMAX Flow (m ³ /s)
1952/3	28/11/1952	7.90	6.10	99.00
1953/4	03/03/1954	6.80	5.98	82.49
1954/5	30/11/1954	7.00	6.01	86.62
1955/6	11/01/1956	6.50	5.95	78.36
1956/7	08/02/1957	6.50	5.95	92.50
1957/8	05/11/1957	6.00	5.91	61.50
1958/9	14/12/1958	6.80	5.98	64.30
1959/0	12/08/1960			57.50
1960/1	03/11/1960	11.90	6.52	171.00
1961/2	11/01/1962	6.00	5.91	78.20
1962/3	12/03/1963			42.50
1963/4	03/11/1960	7.50	6.07	85.00
1964/5	04/09/1965			51.80
1965/6	20/11/1965			99.70
1966/7	30/12/1966			91.50
1967/8	05/11/1967	7.50	6.25	137.00
1968/9	13/03/1969	6.50	5.95	78.36
1969/0	16/11/1969	5.30	5.85	64.60
1970/1	19/06/1971	6.00	5.91	72.86
1971/2	11/01/1972	5.70	5.88	68.73
1972/3	02/04/1973	4.20	5.73	48.09
1973/4	11/02/1974	10.70	6.24	118.26
1974/5	22/11/1974	12.52	6.43	144.41
1975/6	02/12/1975	5.70	5.87	67.35
1976/7	01/12/1976	6.30	5.93	75.61
1977/8	08/12/1977	5.25	5.84	63.22
1978/9	02/02/1979	5.20	5.83	61.85
1979/0	28/12/1979	12.60	6.38	137.53
1980/1	27/09/1981			65.16
1981/2	14/12/1981	5.13	5.82	65.46
1982/3	09/12/1982	7.01	6.07	92.69
1983/4	23/01/1984	5.17	5.85	70.79
1984/5	21/01/1985	6.02	5.94	82.05
1985/6	03/01/1986	7.00	6.02	77.87
1986/7	21/11/1986	6.55	6.07	94.45
1987/8	21/10/1987			139.47
1988/9	11/04/1989	5.68	5.81	62.70
1989/0	31/01/1990	8.75	6.14	107.03
1990/1	03/07/1991			71.33
1991/2	19/11/1991			39.29
1992/3	02/12/1992			84.62
1993/4	30/12/1993			185.74
1994/5	08/12/1994			115.28
1995/6	09/01/1996			76.13
1996/7	27/06/1997	2.80	5.50	42.17
1997/8	02/01/1998	6.37	6.05	81.36
1998/9	24/10/1998			78.14
1999/0	28/05/2000			178.31
2000/1	12/10/2000	21.65	7.51	292.22

Table C.10 Analysis of extended Barcombe Mills flow AMAX series with concurrent upper catchment observations (1952-1980)

Water-Day	EXTENDED BARCOMBE MILLS AMAX Flow (m ³ /s)	GOLD BRIDGE Flow (m ³ /s)	ISFIELD WEIR Flow (m ³ /s)	CLAPPERS BRIDGE Flow (m ³ /s)	OLD SHIP Flow (m ³ /s)
28/11/1952	99.00				
03/03/1954	82.49				
30/11/1954	86.62				
11/01/1956	78.36				
08/02/1957	92.50				
05/11/1957	61.50				
14/12/1958	64.30				
12/08/1960	57.50				
03/11/1960	171.00	49.30			
11/01/1962	78.20	20.70			
12/03/1963	42.50	19.30			
03/11/1960	85.00	41.40			
04/09/1965	51.80	21.10			
20/11/1965	99.70	32.60	44.20		
30/12/1966	91.50	17.40	12.70		
05/11/1967	137.00	68.30	43.30		
13/03/1969	78.36	29.90			
16/11/1969	64.60	19.00	33.10	7.06	
19/06/1971	72.86	26.20	29.60	9.44	2.21
11/01/1972	68.73	18.80		10.70	1.52
02/04/1973	48.09	6.62	3.55	3.02	
11/02/1974	118.26	71.90	48.10	16.08	3.79
22/11/1974	144.41	86.90	64.40	20.69	6.02
02/12/1975	67.35	31.80	30.90	11.81	2.09
01/12/1976	75.61	35.50	32.10	10.30	5.10
08/12/1977	63.22	42.20	39.40	13.28	2.51
02/02/1979	61.85	14.30	15.40	8.49	1.25
28/12/1979	137.53	81.10	55.60	18.84	5.41
Key		No data available			
		Significant flow event recorded on same day as Barcombe AMAX			
		AMAX flow event recorded on same day as Barcombe AMAX			
		No significant flow event recorded on same day as Barcombe AMAX			

C.2.2 Barcombe Mills (Flow) AMAX

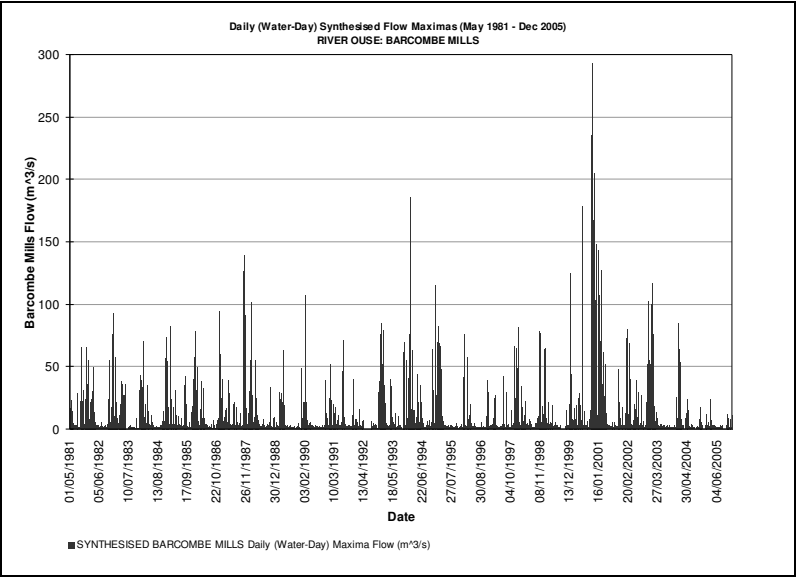


Figure C.21 Daily maxima flow observations at Barcombe Mills (1981-2005)

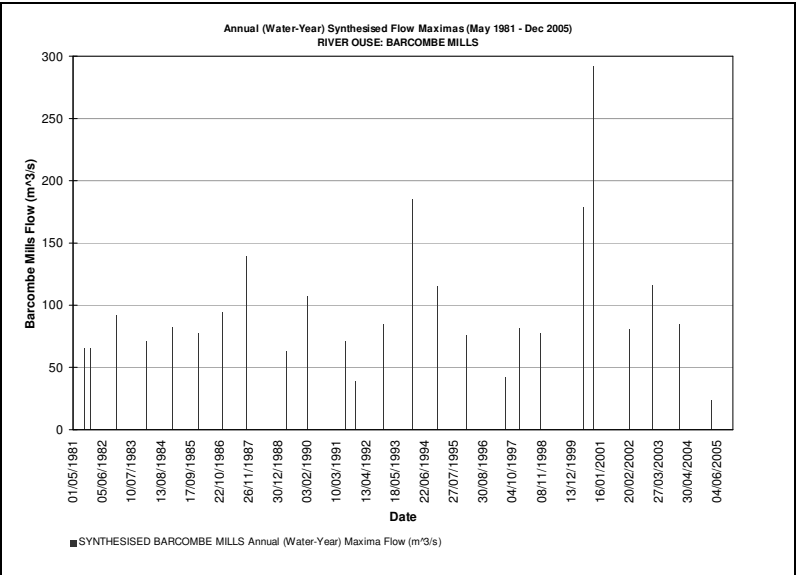


Figure C.22 Annual maxima flow observations at Barcombe Mills (1981-2005)

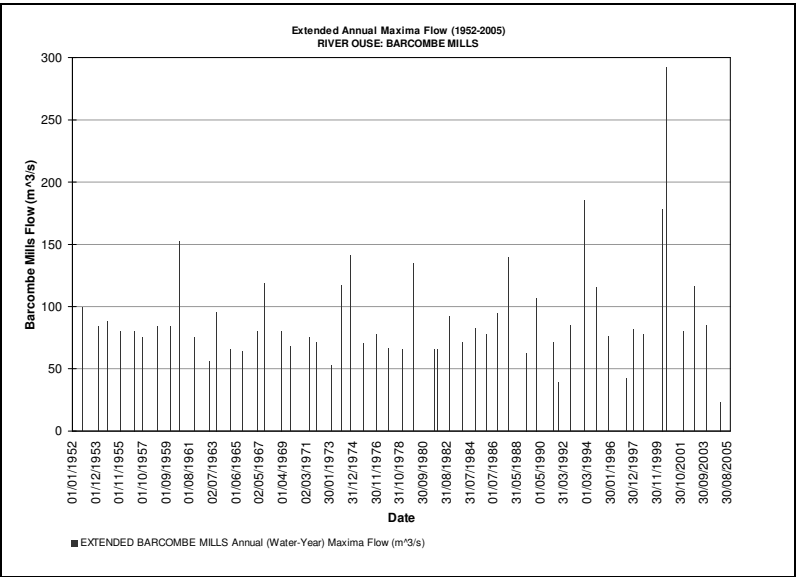


Figure C.23 Extended annual maxima flow observations at Barcombe Mills (1952-2005)

Table C.11 Annual maxima flow observations at Barcombe Mills (1952-2005)

Water Year	Date	Flow (m ³ /s)	Water Year	Date	Flow (m ³ /s)	Water Year	Date	Flow (m ³ /s)
1952/3	28/11/1952	99.00	1970/1	19/06/1971	72.86	1988/9	11/04/1989	62.70
1953/4	03/03/1954	82.49	1971/2	11/01/1972	68.73	1989/0	31/01/1990	107.03
1954/5	30/11/1954	86.62	1972/3	02/04/1973	48.09	1990/1	03/07/1991	71.33
1955/6	11/01/1956	78.36	1973/4	11/02/1974	118.26	1991/2	19/11/1991	39.29
1956/7	08/02/1957	92.50	1974/5	22/11/1974	144.41	1992/3	02/12/1992	84.62
1957/8	05/11/1957	61.50	1975/6	02/12/1975	67.35	1993/4	30/12/1993	185.74
1958/9	14/12/1958	64.30	1976/7	01/12/1976	75.61	1994/5	08/12/1994	115.28
1959/0	12/08/1960	57.50	1977/8	08/12/1977	63.22	1995/6	09/01/1996	76.13
1960/1	03/11/1960	171.00	1978/9	02/02/1979	61.85	1996/7	27/06/1997	42.17
1961/2	11/01/1962	78.20	1979/0	28/12/1979	137.53	1997/8	02/01/1998	81.36
1962/3	12/03/1963	42.50	1980/1	27/09/1981	65.16	1998/9	24/10/1998	78.14
1963/4	03/11/1960	85.00	1981/2	14/12/1981	65.46	1999/0	28/05/2000	178.31
1964/5	04/09/1965	51.80	1982/3	09/12/1982	92.69	2000/1	12/10/2000	292.22
1965/6	20/11/1965	99.70	1983/4	23/01/1984	70.79	2001/2	05/02/2002	80.40
1966/7	30/12/1966	91.50	1984/5	21/01/1985	82.05	2002/3	02/01/2003	116.10
1967/8	05/11/1967	137.00	1985/6	03/01/1986	77.87	2003/4	28/12/2003	84.82
1968/9	13/03/1969	78.36	1986/7	21/11/1986	94.45	2004/5	02/03/2005	23.50
1969/0	16/11/1969	64.60	1987/8	21/10/1987	139.47			

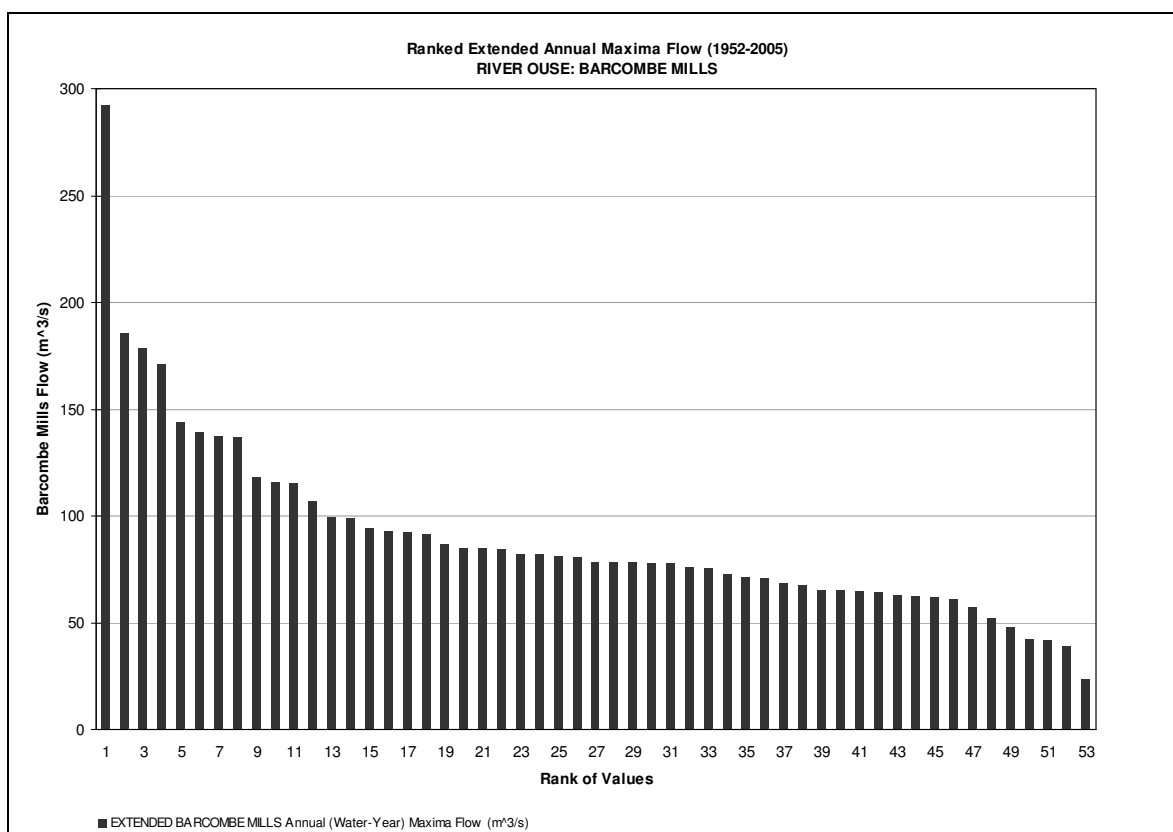


Figure C.24 Ranked annual maxima flow observations at Barcombe Mills (1952-2005)

Table C.12 Return periods & flow magnitude estimates at Barcombe Mills

Station	Barcombe Mills	Mean	90.319		
River	River Ouse	Standard Error	6.077		
Data Period	1952-2005	Standard Deviation	44.238		
Complete Years	53	Skew	2.266		
Missing Years	0	Distribution	GEV		
Units	Flow (m ³ /s)	Anderson Darling	1.546		
Max	292.22 (12/10/2000)	Parameters	μ	71.341	
Min	23.50 (02/03/2005)		α	27.731	
			k	-0.094	

Location	Return Period (Years)	Estimated Magnitude	95% Confidence Interval		Standard Error
			lower	upper	
Barcombe Mills u/s Flow & Ultrasonic TQ 433 148 (Ouse)	1	50.00	N/A		N/A
	2	81.68	74.05	90.40	4.17
	5	116.02	103.21	134.39	7.95
	10	140.86	118.83	170.79	13.26
	25	174.86	137.42	223.43	21.94
	50	202.13	147.37	273.74	32.24
	100	231.04	150.08	332.12	46.44
	200	261.80	157.06	403.20	62.79

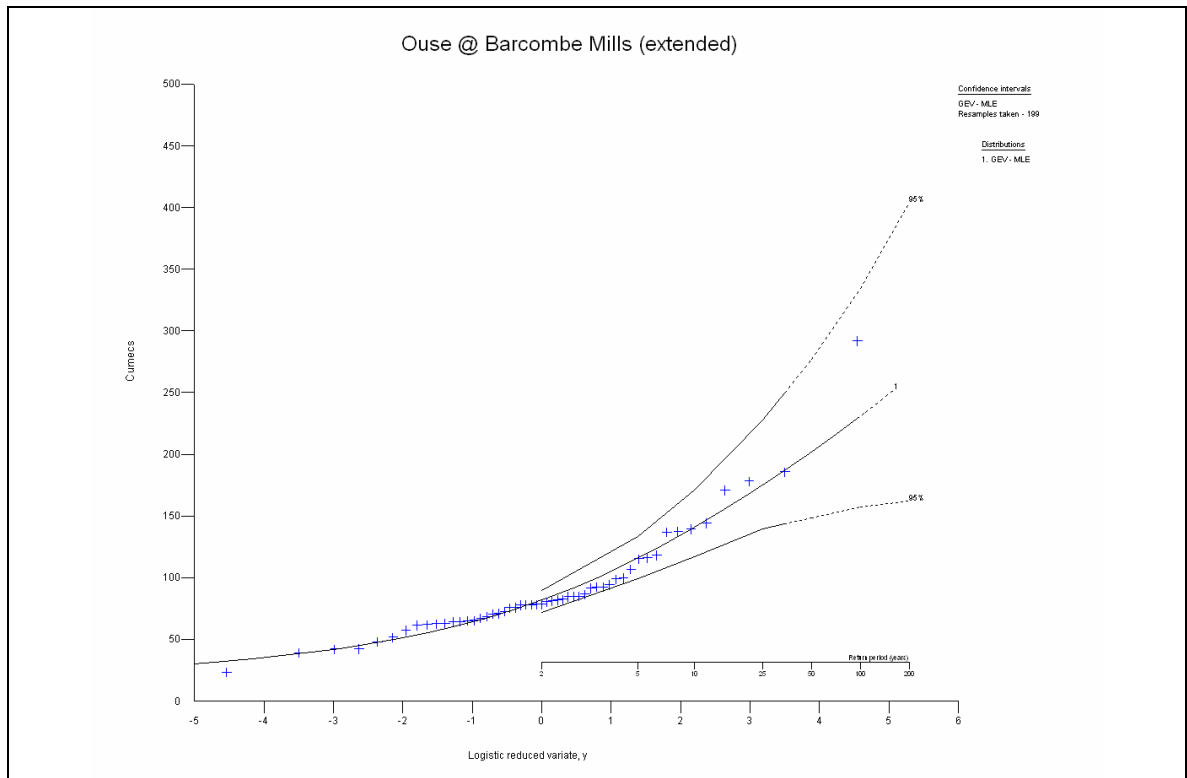


Figure C.25 GEV distribution plot at Barcombe Mills (Flow) (1952-2005)

C.3 Lower Ouse Sub-Catchment

C.3.1 Extending the Lewes Corporation Yard Series

Table C.13 Concurrent recorded and simulated Lewes Corporation Yard stage AMAX series differential (1982-2005)

Water Year	Water-Day	RECORDED LEWES CORP YARD AMAX Stage (mAOD)	Water-Day	SIMULATED LEWES CORP YARD AMAX Stage (mAOD)	RECORDED – SIMULATED DIFF. (m)
1982/3	01/02/1983	4.04	01/02/1983	4.10	-0.06
1983/4	23/01/1984	3.60	23/01/1984	3.61	-0.01
1984/5	23/11/1984	4.10	07/04/1985	4.08	
1985/6	11/01/1986	3.75	11/01/1986	3.71	0.04
1986/7	28/04/1987	3.76	01/01/1987	3.60	
1987/8	07/10/1987	4.01	08/10/1987	4.04	-0.03
1988/9					
1989/0					
1990/1					
1991/2	30/08/1992	3.67			
1992/3	10/01/1993	4.14	11/01/1993	4.16	-0.02
1993/4	30/12/1993	4.12	30/12/1993	4.15	-0.03
1994/5	01/02/1995	3.93	01/02/1995	3.87	0.06
1995/6	23/12/1995	4.08	23/12/1995	4.11	-0.03
1996/7	09/02/1997	3.46	09/02/1997	3.64	-0.18
1997/8	04/01/1998	3.85	04/01/1998	3.85	0.00
1998/9	06/11/1998	3.73	06/11/1998	3.72	0.01
1999/0	25/12/1999	4.14	28/05/2000	4.05	
2000/1	12/10/2000	5.80	12/10/2000	5.93	-0.13
2001/2	26/02/2002	3.65	26/02/2002	3.76	-0.11
2002/3	02/01/2003	3.96	02/01/2003	3.99	-0.03
2003/4	23/11/2003	3.60	24/11/2003	3.61	-0.01
2004/5	12/01/2005	3.68	12/01/2005	3.73	-0.05
Max		5.80		5.93	0.06
Min		3.46		3.60	-0.18
Mean					-0.04
Key		No data available			
		No concurrent recorded and simulated AMAX observations available			
		Concurrent recorded and simulated AMAX observations			

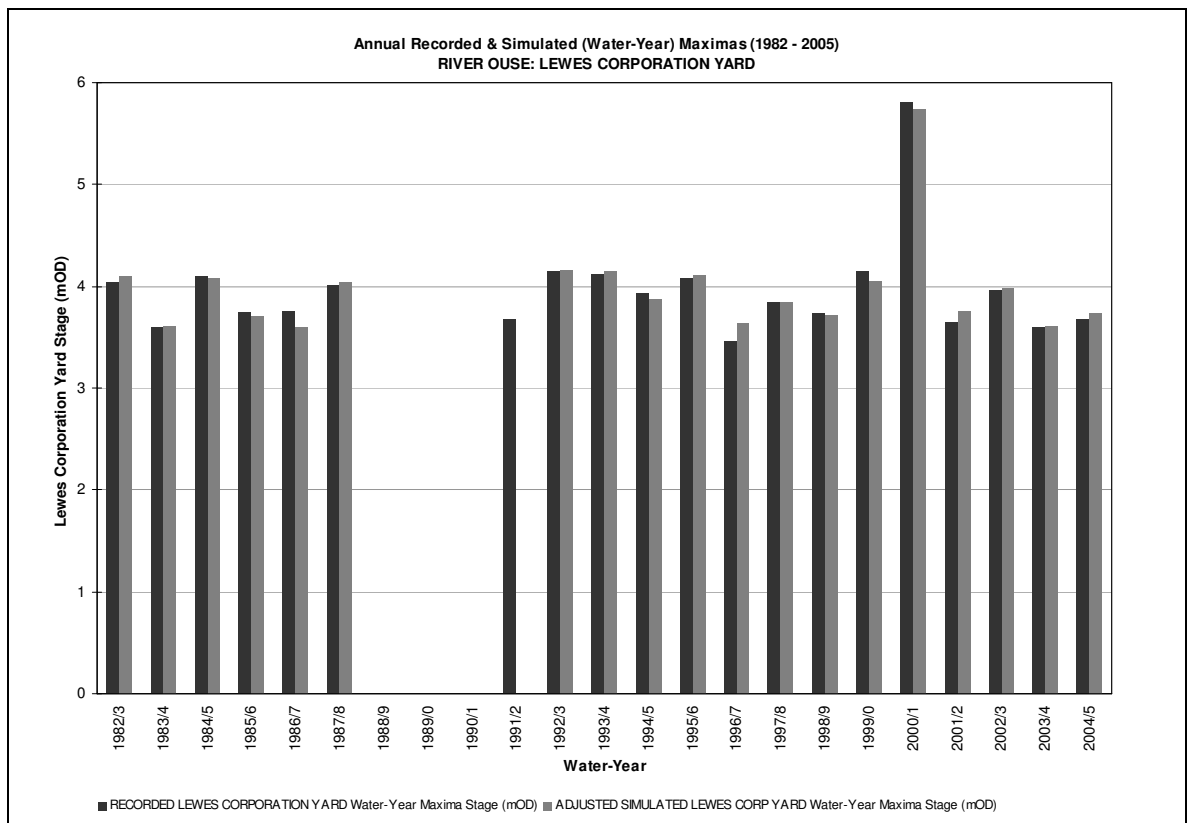


Figure C.26 Annual maxima recorded & simulated stage at Lewes Corporation Yard (1982-2005)

C.3.2 Lewes Corporation Yard AMAX

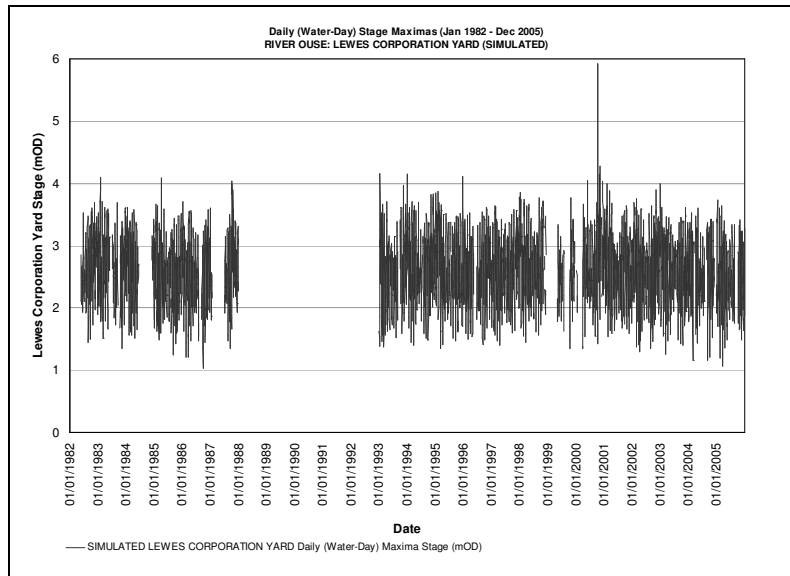


Figure C.27 Simulated daily maxima stage observations at Lewes Corporation Yard (1981-2005)

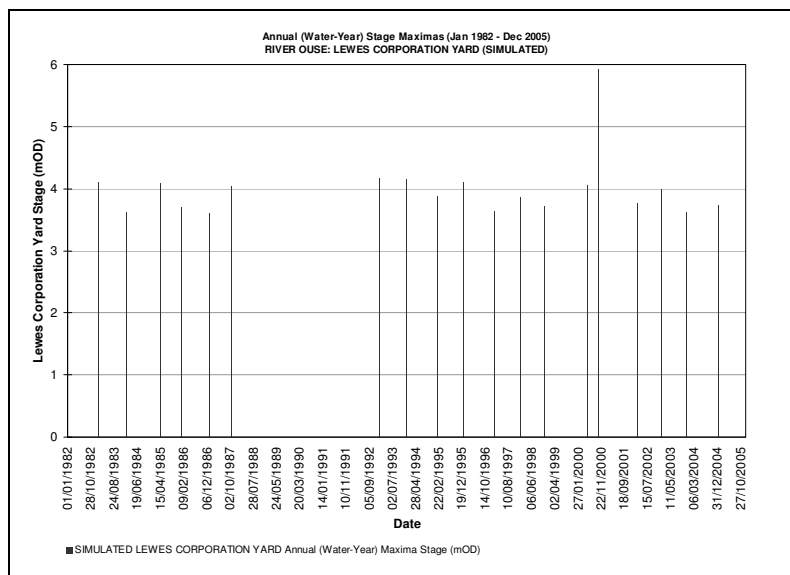


Figure C.28 Simulated annual maxima stage observations at Lewes Corporation Yard (1981-2005)

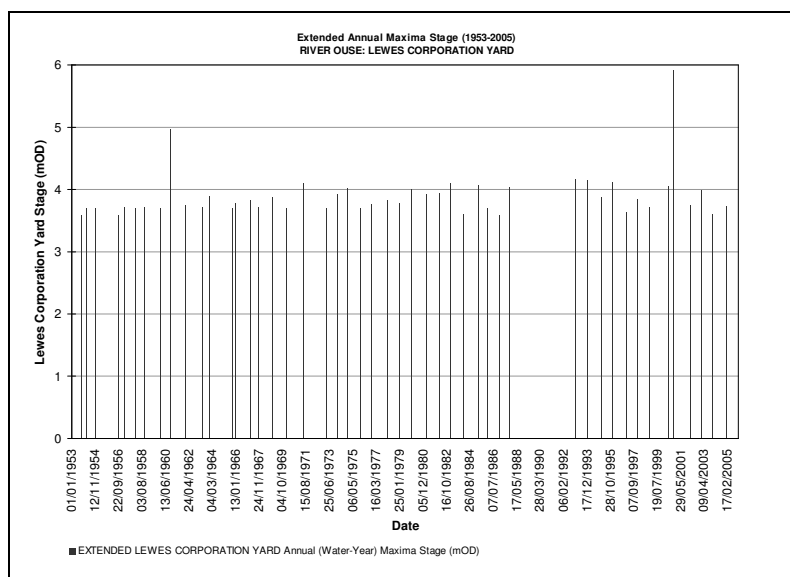


Figure C.29 Extended annual maxima stage observations at Lewes Corporation Yard (1953-2005)

Table C.14 Annual maxima stage observations at Lewes Corporation Yard (1953-2005)

Water Year	Date	Stage (mAOD)	Water Year	Date	Stage (mAOD)	Water Year	Date	Stage (mAOD)
1952/3	24/09/1953	3.60	1970/1	26/05/1971	4.10	1988/9		
1953/4	08/03/1954	3.69	1971/2			1989/0		
1954/5	11/11/1954	3.69	1972/3	02/04/1973	3.70	1990/1		
1955/6	06/09/1956	3.59	1973/4	11/02/1974	3.92	1991/2		
1956/7	15/02/1957	3.72	1974/5	22/11/1974	4.02	1992/3	11/01/1993	4.16
1957/8	06/01/1958	3.69	1975/6	02/12/1975	3.69	1993/4	30/12/1993	4.15
1958/9	14/10/1958	3.72	1976/7	23/10/1976	3.77	1994/5	01/02/1995	3.87
1959/0	31/12/1959	3.69	1977/8	12/01/1978	3.84	1995/6	23/12/1995	4.11
1960/1	04/11/1960	4.97	1978/9	30/01/1979	3.79	1996/7	09/02/1997	3.64
1961/2	11/01/1962	3.75	1979/0	28/12/1979	4.01	1997/8	04/01/1998	3.85
1962/3	25/04/1963	3.72	1980/1	10/03/1981	3.92	1998/9	06/11/1998	3.72
1963/4	19/11/1963	3.90	1981/2	11/03/1982	3.95	1999/0	28/05/2000	4.05
1964/5	26/09/1965	3.69	1982/3	01/02/1983	4.10	2000/1	12/10/2000	5.74
1965/6	10/12/1965	3.78	1983/4	23/01/1984	3.61	2001/2	26/02/2002	3.76
1966/7	28/02/1967	3.84	1984/5	07/04/1985	4.08	2002/3	02/01/2003	3.99
1967/8	05/11/1967	3.72	1985/6	11/01/1986	3.71	2003/4	24/11/2003	3.61
1968/9	21/12/1968	3.87	1986/7	01/01/1987	3.60	2004/5	12/01/2005	3.73
1969/0	11/01/1970	3.70	1987/8	08/10/1987	4.04			

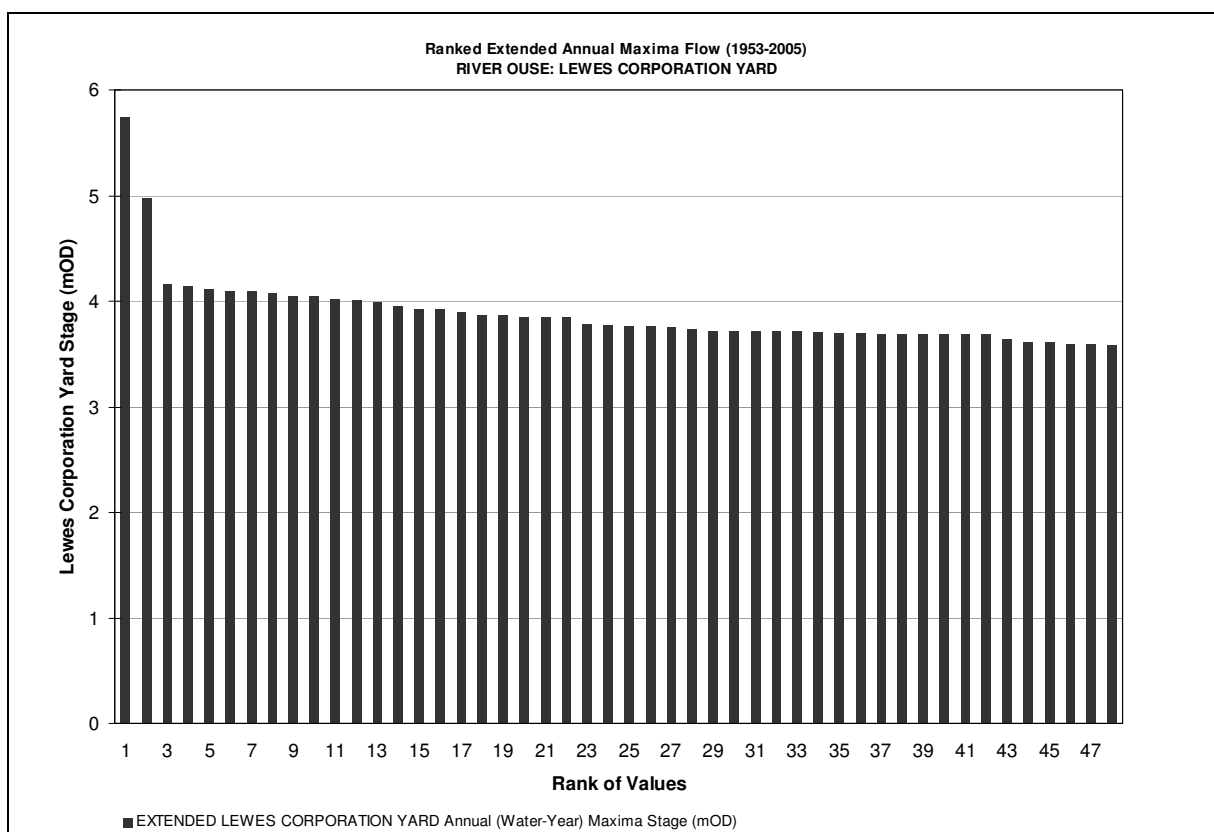


Figure C.30 Ranked annual maxima stage observations at Lewes Corporation Yard (1953-2005)

Table C.15 Return periods & stage magnitude estimates at Lewes Corporation Yard

Station	Lewes Corporation Yard	Mean	3.891		
River	River Ouse	Standard Error	0.055		
Data Period	1953-2005	Standard Deviation	0.381		
Complete Years	48	Skew	3.585		
Missing Years	5	Distribution	GEV		
Units	Stage (mAOD)	Anderson Darling	0.540		
Max	5.74 (12/10/2000)	Parameters	μ	3.734	
Min	3.59 (06/09/1956)		α	0.134	
			k	-0.379	

Location	Return Period (Years)	Estimated Magnitude	95% Confidence Interval		Standard Error
			lower	upper	
Lewes Corporation Yard TQ 416 106 (Ouse)	1	3.54	N/A		N/A
	2	3.79	3.72	3.83	0.03
	5	4.01	3.86	4.13	0.07
	10	4.21	3.94	4.44	0.13
	25	4.57	3.98	5.04	0.27
	50	4.93	3.97	5.79	0.46
	100	5.40	3.89	6.83	0.75
	200	6.01	3.77	8.28	1.15

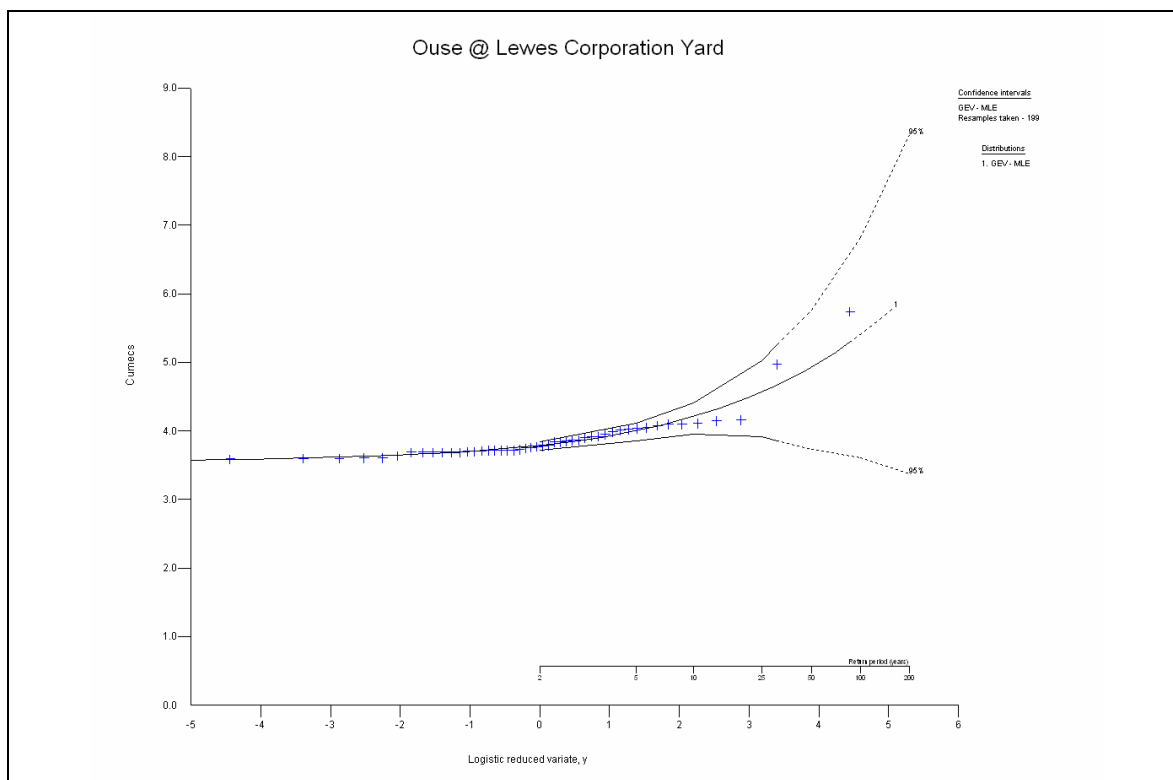


Figure C.31 GEV distribution plot at Lewes Corporation Yard (1953-2005)

C.3.3 Lewes Gas Works AMAX

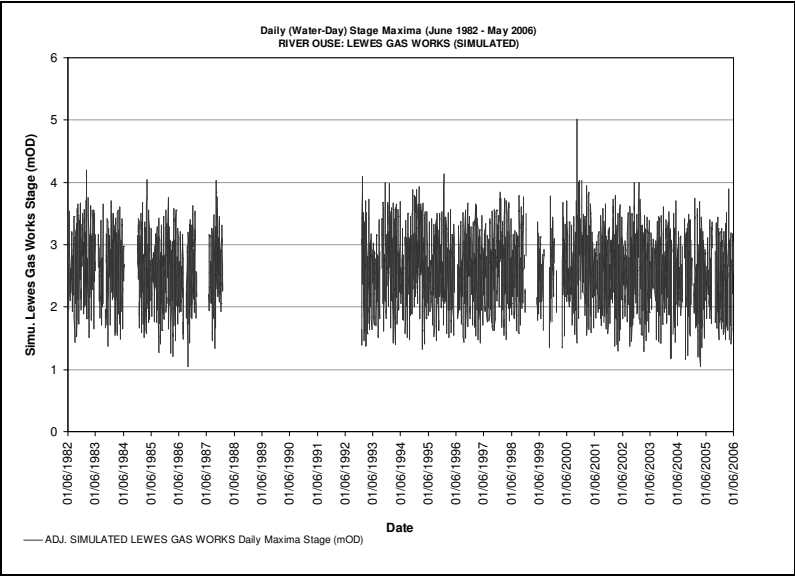


Figure C.32 Simulated daily maxima stage observations at Lewes Gas Works (1981-2005)

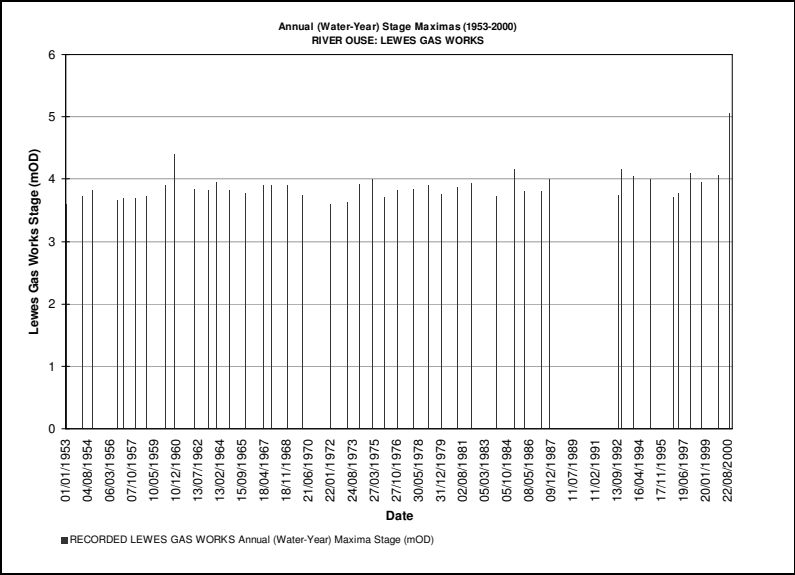


Figure C.33 Extended annual maxima stage observations at Lewes Gas Works (1953-2000)

Table C.16 Annual maxima stage observations at Lewes Gas Works (1953-2000)

Water Year	Date	Stage (mAOD)	Water Year	Date	Stage (mAOD)	Water Year	Date	Stage (mAOD)
1952/3	01/02/1953	3.60	1970/1			1988/9		
1953/4	08/03/1954	3.72	1971/2	20/01/1972	3.59	1989/0		
1954/5	26/11/1954	3.81	1972/3	02/04/1973	3.62	1990/1		
1955/6	06/09/1956	3.66	1973/4	09/02/1974	3.92	1991/2	30/09/1992	3.74
1956/7	14/02/1957	3.69	1974/5	28/01/1975	4.00	1992/3	11/01/1993	4.15
1957/8	06/01/1958	3.69	1975/6	02/12/1975	3.71	1993/4	14/11/1993	4.04
1958/9	14/10/1958	3.72	1976/7	23/10/1976	3.82	1994/5	02/02/1995	4.01
1959/0	26/02/1960	3.90	1977/8	12/01/1978	3.84	1995/6	28/09/1996	3.70
1960/1	03/10/1960	4.39	1978/9	02/02/1979	3.90	1996/7	10/02/1997	3.78
1961/2	05/04/1962	3.84	1979/0	28/12/1979	3.76	1997/8	04/01/1998	4.09
1962/3	26/03/1963	3.81	1980/1	10/03/1981	3.87	1998/9	06/10/1998	3.96
1963/4	03/11/1963	3.96	1981/2	10/03/1982	3.94	1999/0	25/12/1999	4.07
1964/5	23/10/1964	3.81	1982/3			2000/1	12/10/2000	5.06
1965/6	10/12/1965	3.78	1983/4	21/12/1983	3.73	2001/2		
1966/7	07/03/1967	3.90	1984/5	08/04/1985	4.15	2002/3		
1967/8	02/11/1967	3.90	1985/6	11/01/1986	3.80	2003/4		
1968/9	21/12/1968	3.90	1986/7	29/03/1987	3.80	2004/5		
1969/0	11/01/1970	3.75	1987/8	08/10/1987	3.99			

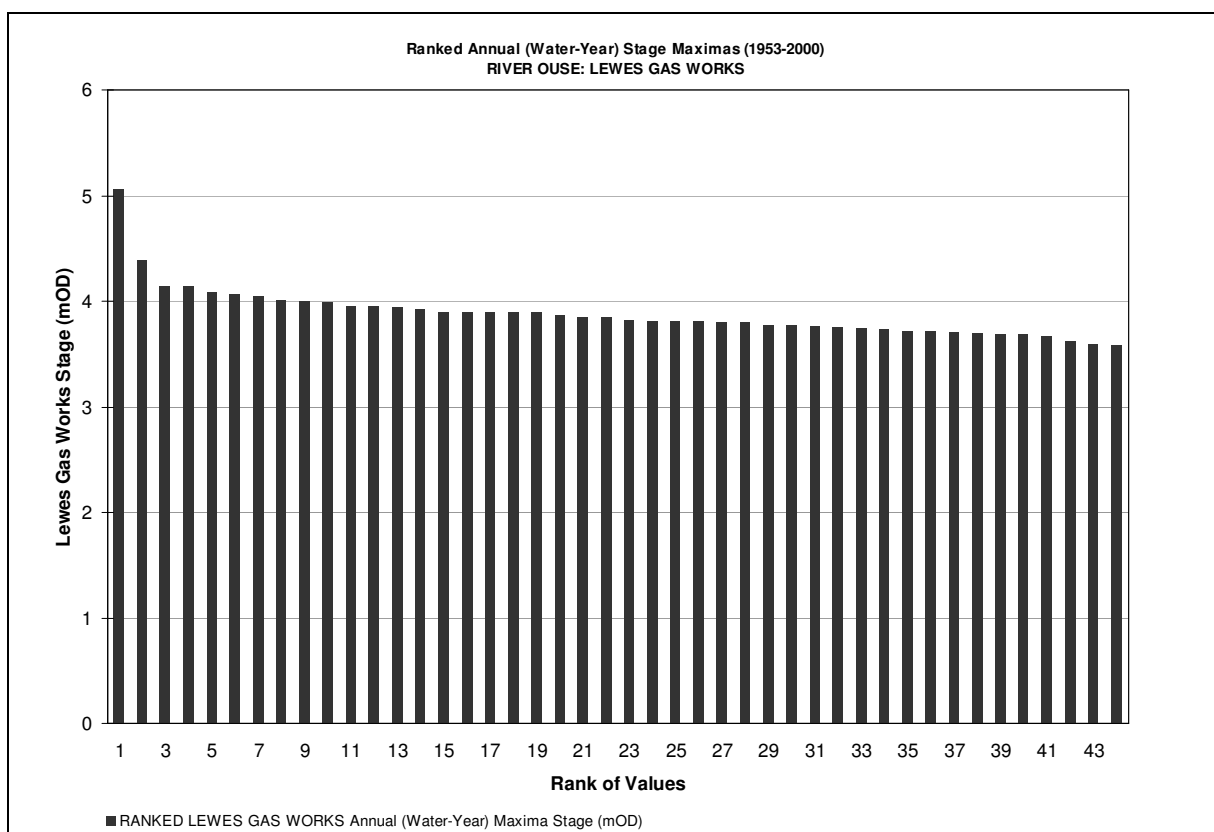


Figure C.34 Ranked annual maxima stage observations at Lewes Gas Works (1953-2000)

Table C.17 Return periods & stage magnitude estimates at Lewes Gas Works

Station	Lewes Gas Works	Mean	3.883		
River	River Ouse	Standard Error	0.037		
Data Period	1953-2000	Standard Deviation	0.244		
Complete Years	44	Skew	2.845		
Missing Years	5	Distribution	GEV		
Units	Stage (mAOD)	Anderson Darling	0.254		
Max	5.06 (12/10/2000)	Parameters	μ	3.779	
Min	3.59 (20/01/1972)		α	0.140	
			k	-0.141	

Location	Return Period (Years)	Estimated Magnitude	95% Confidence Interval		Standard Error
			lower	upper	
Lewes Gas Works TQ 420 101 (Ouse)	1	3.53	N/A		N/A
	2	3.83	3.78	3.88	0.03
	5	4.01	3.92	4.11	0.05
	10	4.15	3.98	4.31	0.08
	25	4.34	3.97	4.64	0.17
	50	4.51	3.94	4.94	0.26
	100	4.75	3.86	5.27	0.36
	200	4.99	3.73	5.66	0.49

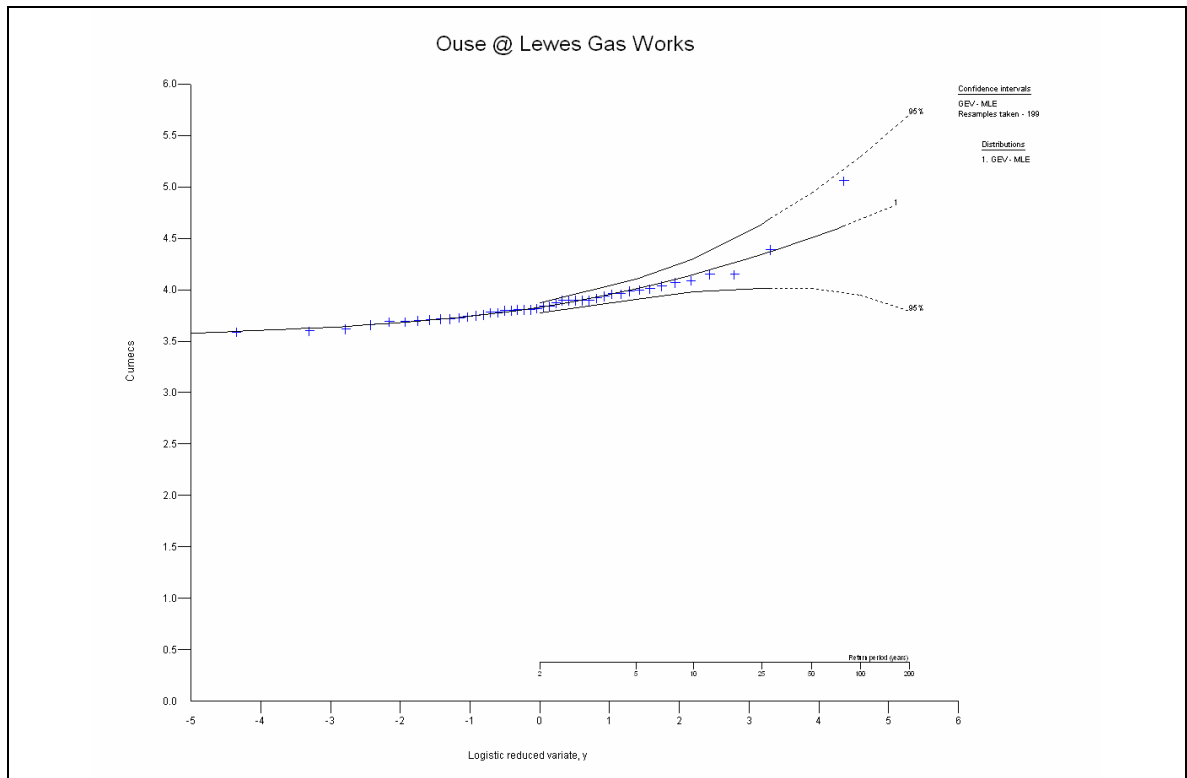


Figure C.35 GEV distribution plot at Lewes Gas Works (1953-2000)

C.4 Tide

C.4.1 Extending the Newhaven (Tide) Series

Table C.18 Extended annual maxima flow observations at Newhaven (1913-2006)

Year	Date	Tide (mAOD)	Year	Date	Tide (mAOD)	Year	Date	Tide (mAOD)
1913		3.76	1945		3.99	1977		
1914			1946		3.76	1978		
1915			1947		3.73	1979		
1916		3.51	1948		3.91	1980		
1917		3.66	1949		4.19	1981		
1918		4.04	1950		4.04	1982	21/08/1982	3.85
1919		3.76	1951		3.86	1983	01/02/1983	4.42
1920			1952		3.91	1984	15/04/1984	3.98
1921		3.86	1953		4.04	1985	07/04/1985	4.34
1922		3.94	1954		4.27	1986	02/12/1986	3.98
1923		3.96	1955		4.06	1987	07/10/1987	4.15
1924		3.76	1956		3.88	1988		4.13
1925			1957		4.03	1989		
1926		3.89	1958		4.12	1990		
1927		3.81	1959		4.12	1991	03/01/1991	4.00
1928		3.86	1960		3.97	1992	29/08/1992	4.05
1929		3.68	1961		4.21	1993	11/01/1993	4.16
1930		3.76	1962		4.09	1994	04/12/1994	4.10
1931		3.89	1963		4.12	1995	23/12/1995	4.25
1932		3.84	1964		3.94	1996	27/09/1996	3.98
1933		3.56	1965		4.15	1997	09/02/1997	4.01
1934		3.76	1966		4.03	1998	28/02/1998	4.17
1935		3.86	1967		4.21	1999	24/10/1999	4.09
1936		3.96	1968		4.03	2000	29/09/2000	3.96
1937		3.81	1969		3.97	2001	11/03/2001	4.09
1938		3.89	1970		3.94	2002	09/09/2002	4.01
1939		3.96	1971		3.88	2003	02/01/2003	3.96
1940		4.09	1972		3.91	2004	16/10/2004	3.85
1941		3.89	1973		4.00	2005	11/03/2005	4.08
1942		3.71	1974		4.03	2006	30/03/2006	4.10
1943		4.14	1975		4.12			
1944		3.89	1976		4.06			
Key								
		No data available						
		AMAX values extracted from Proudman Newhaven gauge (1991-2006)						
		AMAX values extracted from EA Newhaven gauge (1913-1990)						

C.4.2 Frequency of Tidal AMAX Events at Newhaven

Figure C.36 calculates the probability of exceedance of the highest astronomical tide (HAT), estimated to be 4.03mAOD at Newhaven (Proudman, 2006), to be 39% in any given year, taken from the AMAX observations (1913-2006).

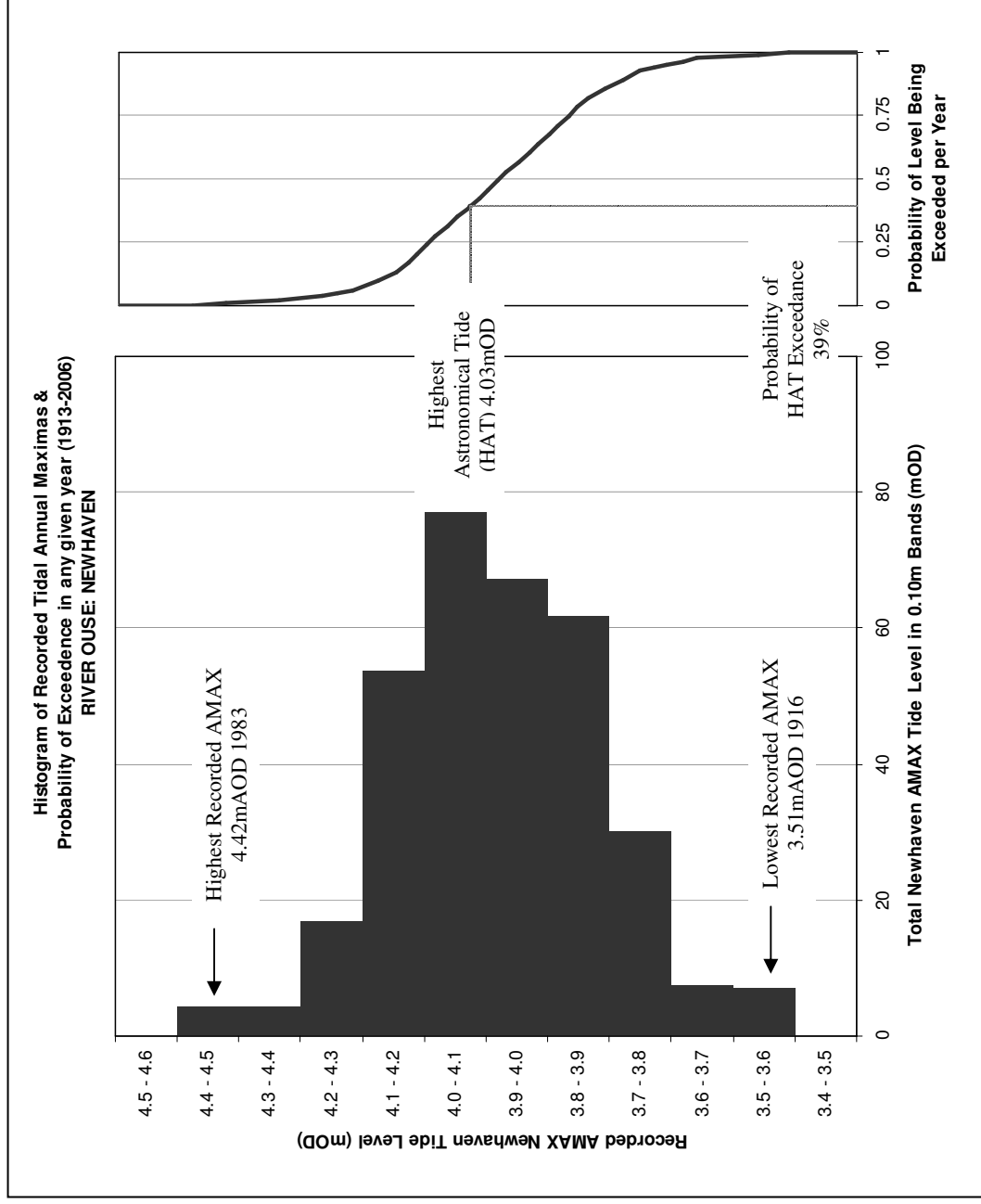


Figure C.36 Histogram of Newhaven recorded AMAX tide & probability of exceedance in any given year (1913-2006)

C.4.3 Newhaven (Tide) AMAX

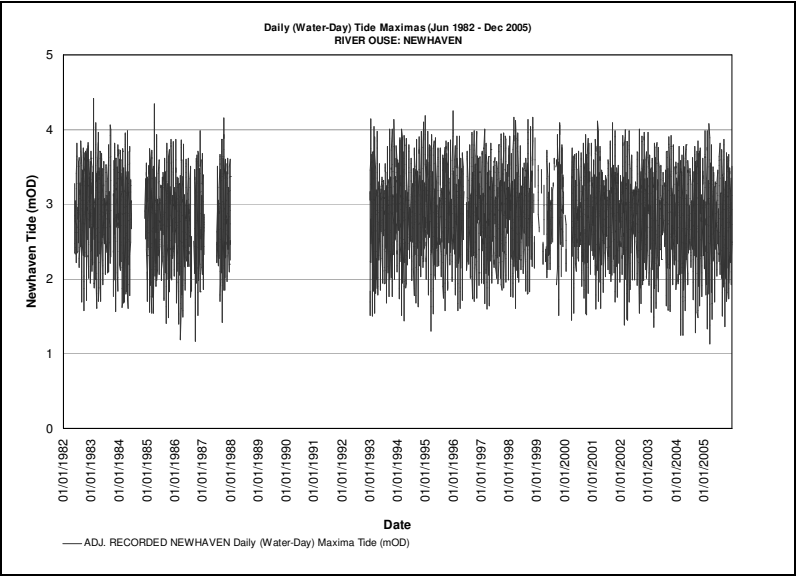


Figure C.37 Recorded daily maxima tide observations at Newhaven (1982-2005)

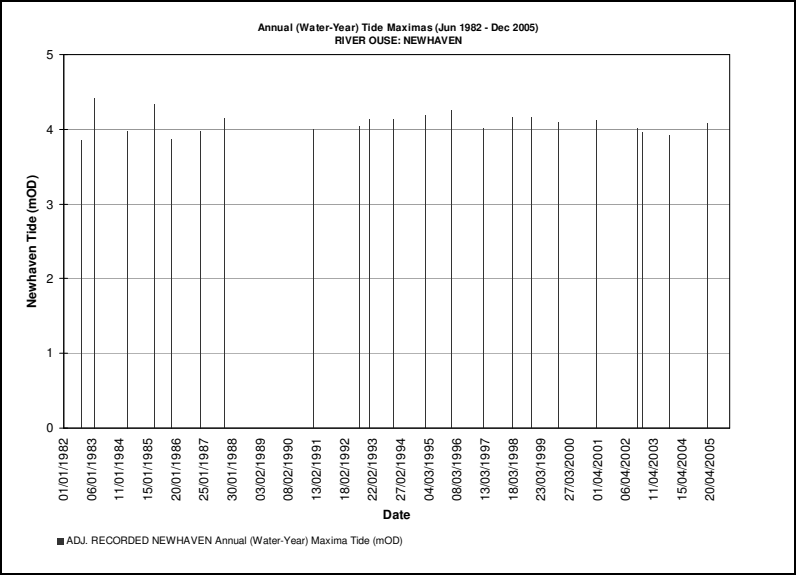


Figure C.38 Recorded annual maxima tide observations at Newhaven (1982-2005)

Table C.19 Annual maxima tide observations at Newhaven (1913-2006)

Water Year	Date	Tide (mAOD)	Water Year	Date	Tide (mAOD)	Water Year	Date	Tide (mAOD)
1913	-	3.76	1945	-	3.99	1977		
1914			1946	-	3.76	1978		
1915			1947	-	3.73	1979		
1916	-	3.51	1948	-	3.91	1980		
1917	-	3.66	1949	-	4.19	1981		
1918	-	4.04	1950	-	4.04	1982	21/08/1982	3.85
1919	-	3.76	1951	-	3.86	1983	01/02/1983	4.42
1920			1952	-	3.91	1984	15/04/1984	3.98
1921	-	3.86	1953	-	4.04	1985	07/04/1985	4.34
1922	-	3.94	1954	-	4.27	1986	02/12/1986	3.98
1923	-	3.96	1955	-	4.06	1987	07/10/1987	4.15
1924	-	3.76	1956	-	3.88	1988	-	4.13
1925			1957	-	4.03	1989		
1926	-	3.89	1958	-	4.12	1990		
1927	-	3.81	1959	-	4.12	1991	03/01/1991	4.00
1928	-	3.86	1960	-	3.97	1992	29/08/1992	4.05
1929	-	3.68	1961	-	4.21	1993	11/01/1993	4.16
1930	-	3.76	1962	-	4.09	1994	04/12/1994	4.10
1931	-	3.89	1963	-	4.12	1995	23/12/1995	4.25
1932	-	3.84	1964	-	3.94	1996	27/09/1996	3.98
1933	-	3.56	1965	-	4.15	1997	09/02/1997	4.01
1934	-	3.76	1966	-	4.03	1998	28/02/1998	4.17
1935	-	3.86	1967	-	4.21	1999	24/10/1999	4.09
1936	-	3.96	1968	-	4.03	2000	29/09/2000	3.96
1937	-	3.81	1969	-	3.97	2001	11/03/2001	4.09
1938	-	3.89	1970	-	3.94	2002	09/09/2002	4.01
1939	-	3.96	1971	-	3.88	2003	02/01/2003	3.96
1940	-	4.09	1972	-	3.91	2004	16/10/2004	3.85
1941	-	3.89	1973	-	4.00	2005	11/03/2005	4.08
1942	-	3.71	1974	-	4.03	2006	30/03/2006	4.10
1943	-	4.14	1975	-	4.12			
1944	-	3.89	1976	-	4.06			

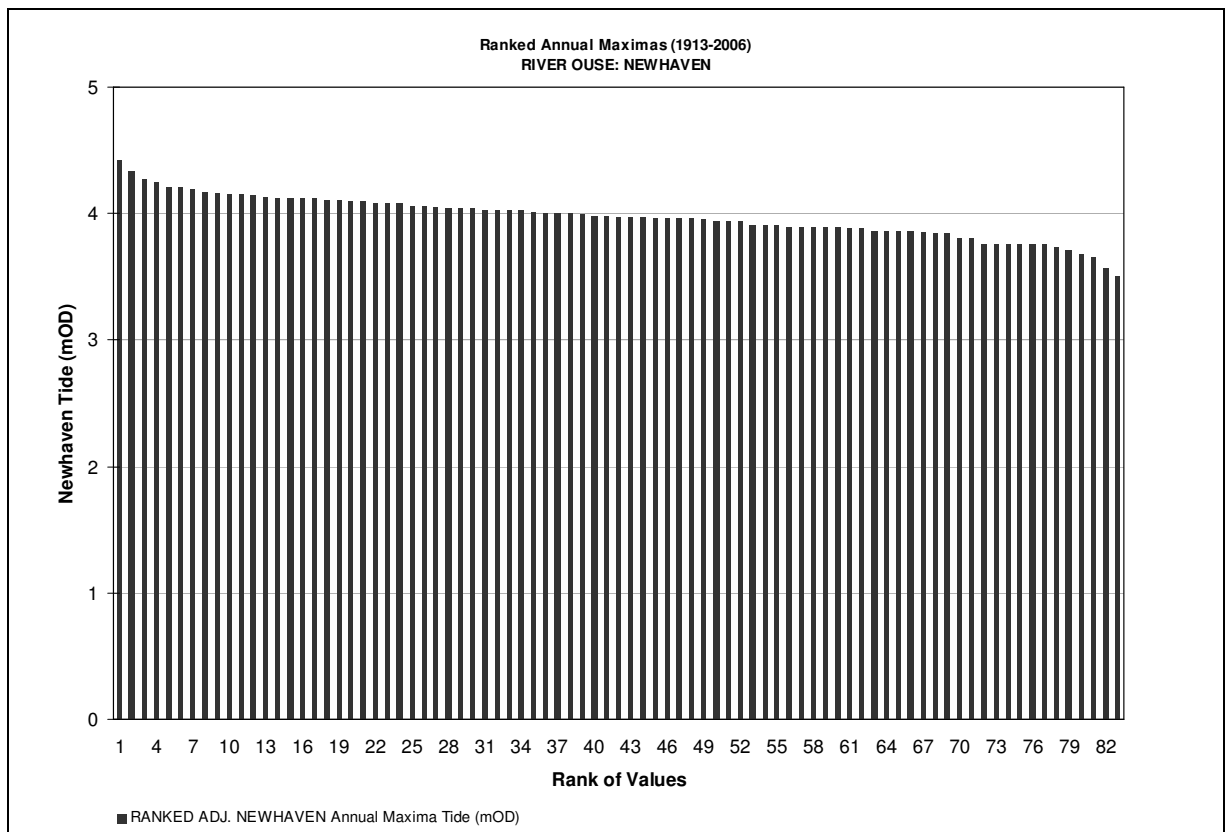


Figure C.39 Ranked annual maxima tide observations at Newhaven (1913-2006)

Table C.20 Return periods & tide magnitude estimates at Newhaven

Station	Newhaven	Mean	3.973	
River	River Ouse	Standard Error	0.018	
Data Period	1913-2006	Standard Deviation	0.166	
Complete Years	83	Skew	-0.159	
Missing Years	11	Distribution	GEV	
Units	Tide (mAOD)	Anderson Darling	0.233	
Max	4.42 (01/02/1983)	Parameters	μ	3.914
Min	3.51 (1916)		α	0.169
			k	0.281

Location	Return Period (Years)	Estimated Magnitude	95% Confidence Interval		Standard Error
			lower	upper	
Newhaven (Tide) TQ 4511 0005 (Ouse)	1	3.45	N/A		N/A
	2	3.97	3.94	4.00	0.02
	5	4.12	4.09	4.16	0.02
	10	4.20	4.15	4.25	0.02
	25	4.27	4.22	4.35	0.03
	50	4.32	4.26	4.41	0.04
	100	4.35	4.28	4.47	0.05
	200	4.38	4.29	4.52	0.06

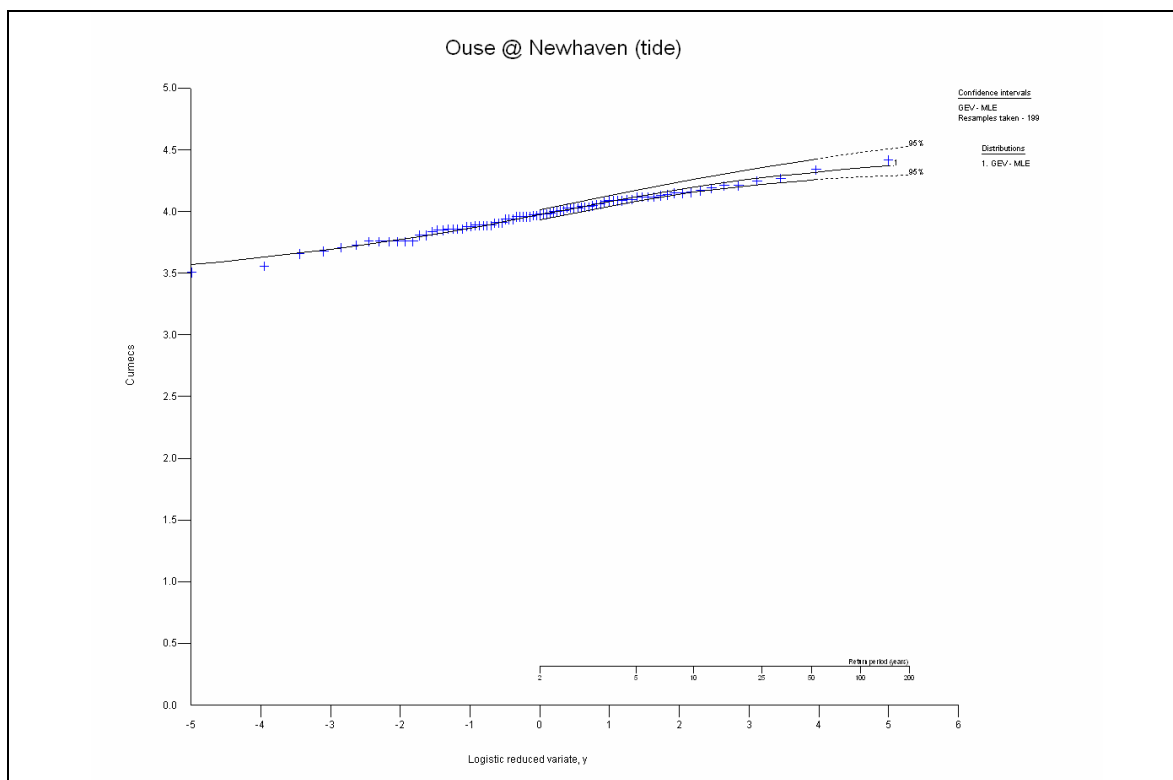


Figure C.40 GEV distribution plot at Newhaven (1913-2006)

C.4.4 Newhaven (Surge) AMAX

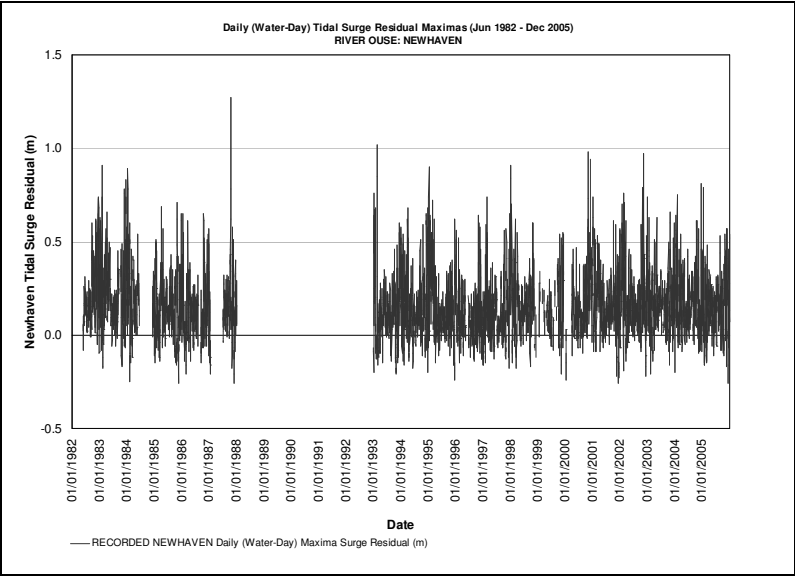


Figure C.41 Recorded daily maxima surge observations at Newhaven (1982-2005)

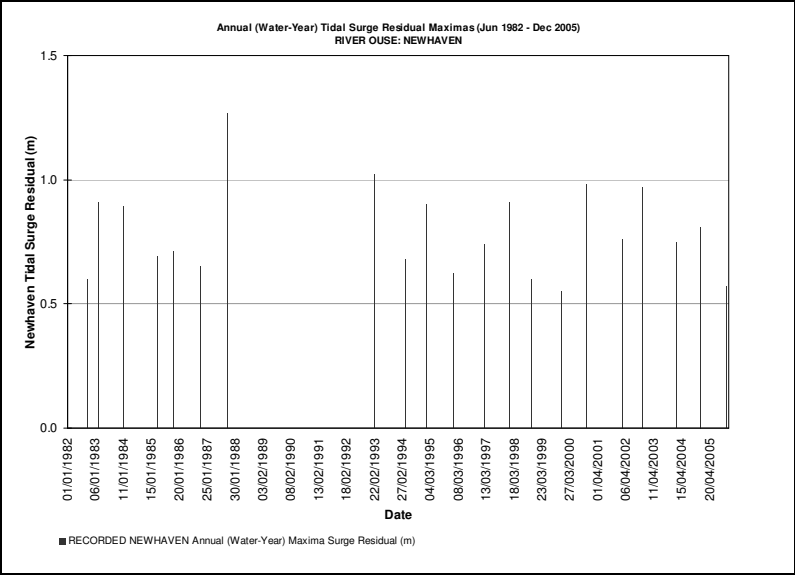


Figure C.42 Recorded annual maxima surge observations at Newhaven (1982-2005)

Table C.21 Annual maxima surge observations at Newhaven (1982-2005)

Water Year	Date	Surge (m)	Water Year	Date	Surge (m)	Water Year	Date	Surge (m)
1981/2	21/09/1982	0.60	1990/1			1999/0	30/11/1999	0.55
1982/3	01/02/1983	0.91	1991/2			2000/1	30/10/2000	0.98
1983/4	13/01/1984	0.89	1992/3	21/02/1993	1.02	2001/2	22/02/2002	0.76
1984/5	07/04/1985	0.69	1993/4	04/04/1994	0.68	2002/3	13/11/2002	0.97
1985/6	06/11/1985	0.71	1994/5	10/01/1995	0.90	2003/4	31/01/2004	0.75
1986/7	20/10/1986	0.65	1995/6	23/12/1995	0.62	2004/5	17/12/2004	0.81
1987/8	15/10/1987	1.27	1996/7	18/02/1997	0.74	2005/6	24/11/2005	0.57
1988/9			1997/8	04/01/1998	0.91			
1989/0			1998/9	25/10/1998	0.60			

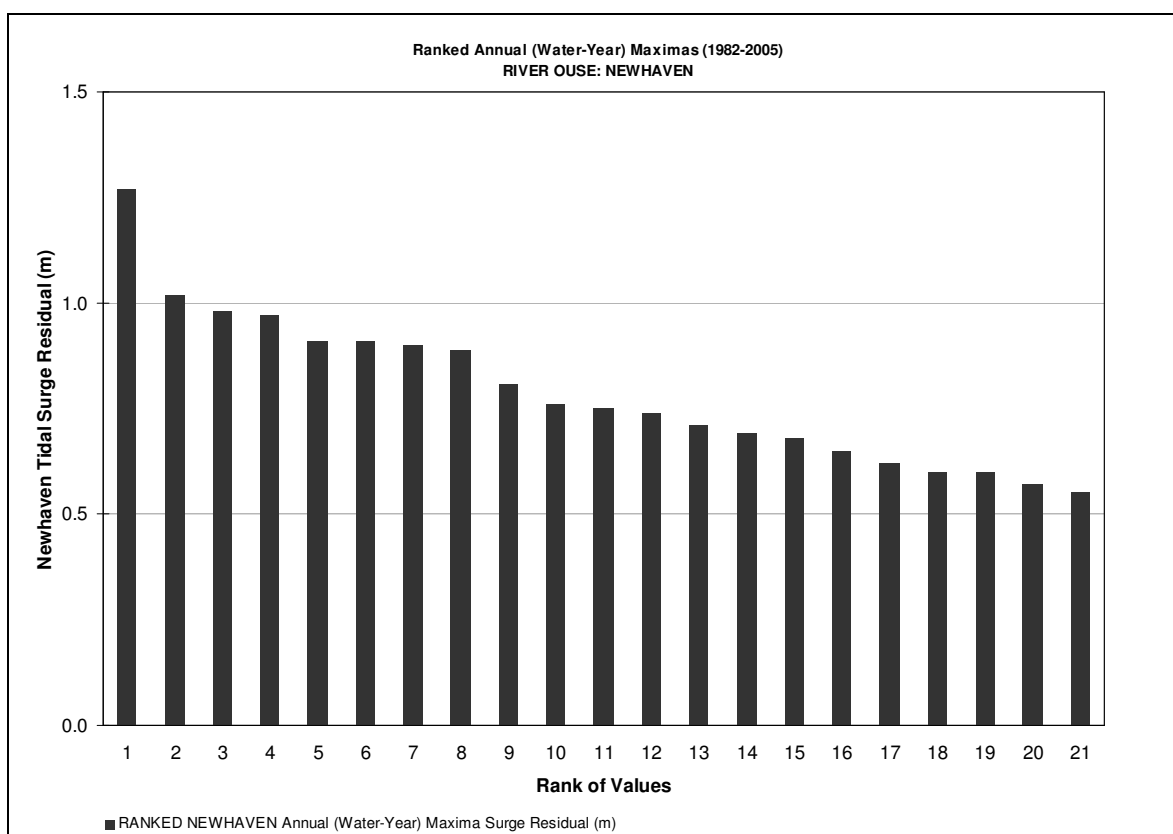


Figure C.43 Ranked annual maxima surge observations at Newhaven (1982-2005)

Table C.22 Return periods & surge magnitude estimates at Newhaven

Station	Newhaven	Mean	0.790		
River	River Ouse	Standard Error	0.040		
Data Period	1982-2005	Standard Deviation	0.182		
Complete Years	21	Skew	0.834		
Missing Years	4	Distribution	GEV		
Units	Surge (m)	Anderson Darling	0.239		
Max	1.27 (15/10/1987)	Parameters	μ	0.703	
Min	0.55 (30/11/1999)		α	0.135	
			k	-0.061	

Location	Return Period (Years)	Estimated Magnitude	95% Confidence Interval		Standard Error
			lower	upper	
Newhaven (Surge) TQ 4511 0005 (Ouse)	1	0.44	N/A		N/A
	2	0.75	0.66	0.88	0.05
	5	0.92	0.82	1.05	0.06
	10	1.03	0.90	1.18	0.07
	25	1.18	0.73	1.45	0.19
	50	1.30	0.61	1.72	0.28
	100	1.42	0.50	2.02	0.39
	200	1.55	0.40	2.36	0.50

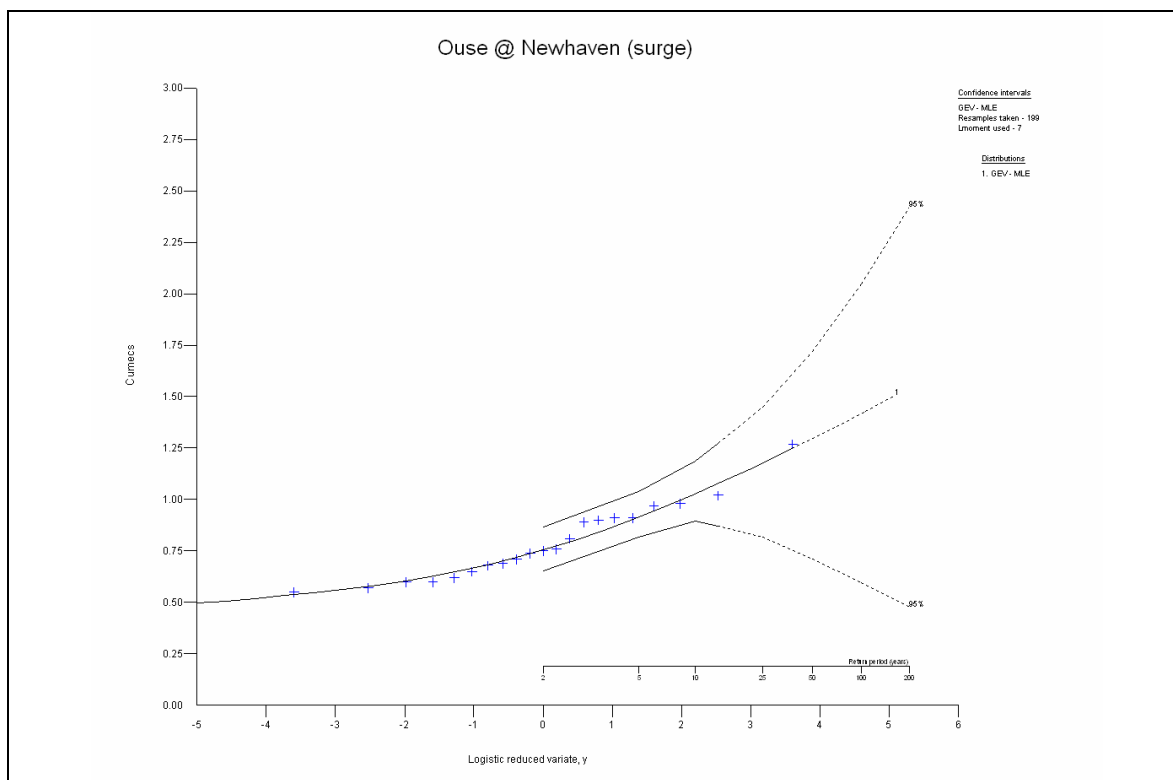


Figure C.44 GEV distribution plot at Newhaven (1982-2005)

C.4.5 Newhaven (Surge at High Tide) AMAX

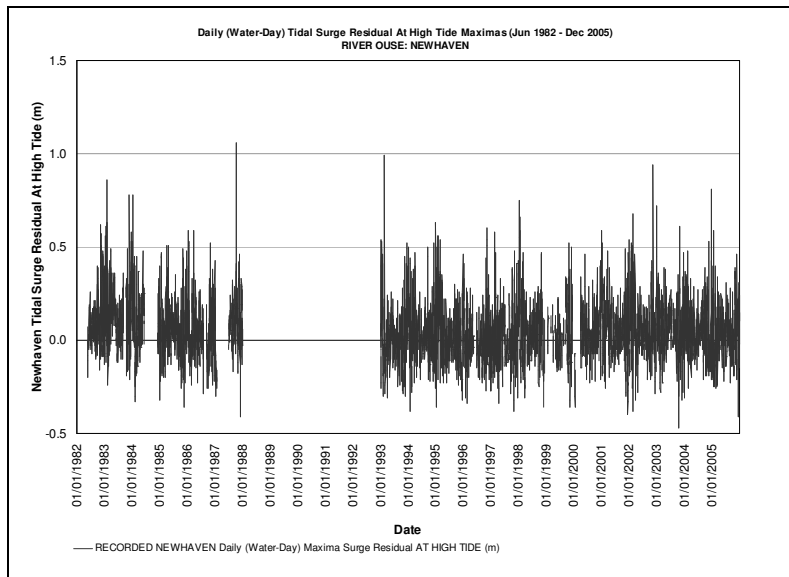


Figure C.45 Recorded daily surge at high tide observations at Newhaven (1982-2005)

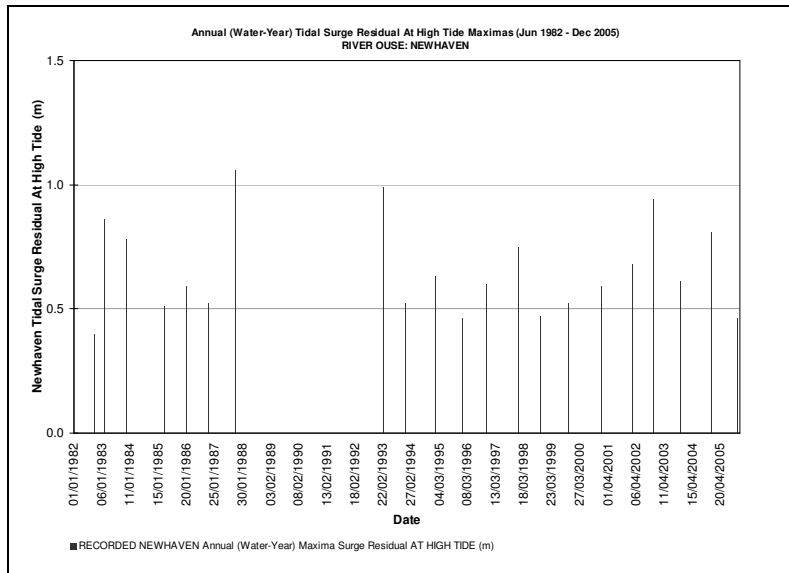


Figure C.46 Recorded annual maxima surge at high tide observations at Newhaven (1982-2005)

Table C.23 Annual maxima surge at high tide observations at Newhaven (1982-2005)

Water Year	Date	Surge (m)	Water Year	Date	Surge (m)	Water Year	Date	Surge (m)
1981/2	29/09/1982	0.40	1990/1			1999/0	24/10/1999	0.52
1982/3	01/02/1983	0.86	1991/2			2000/1	01/01/2001	0.59
1983/4	26/11/1983	0.78	1992/3	21/02/1993	0.99	2001/2	22/02/2002	0.68
1984/5	07/04/1985	0.51	1993/4	19/12/1993	0.52	2002/3	13/11/2002	0.94
1985/6	11/01/1986	0.59	1994/5	01/01/1995	0.63	2003/4	02/11/2003	0.61
1986/7	31/10/1986	0.52	1995/6	23/12/1995	0.46	2004/5	17/12/2004	0.81
1987/8	15/10/1987	1.06	1996/7	06/11/1996	0.60	2005/6	24/11/2005	0.46
1988/9			1997/8	04/01/1998	0.75			
1989/0			1998/9	27/10/1998	0.47			

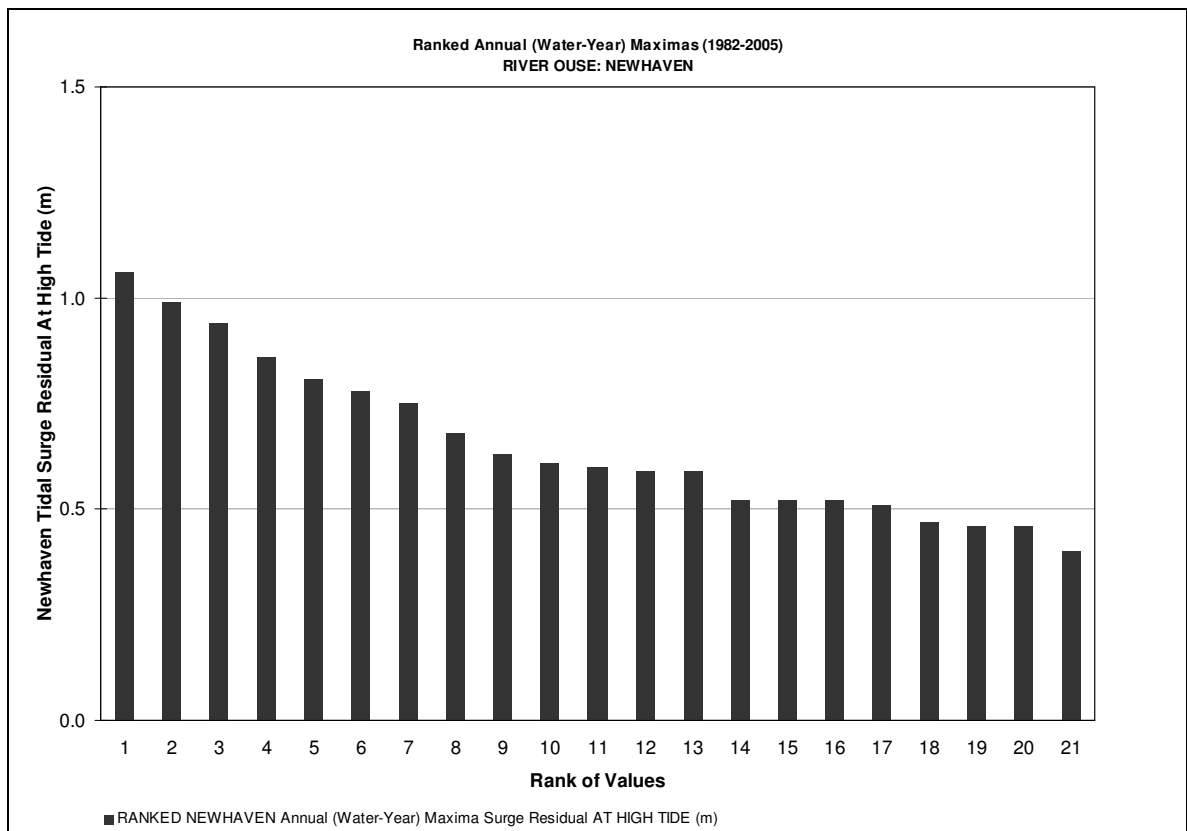


Figure C.47 Ranked annual maxima surge at high tide observations at Newhaven (1982-2005)

Table C.24 Return periods & surge at high tide magnitude estimates at Newhaven

Station	Newhaven	Mean	0.655		
River	River Ouse	Standard Error	0.041		
Data Period	1982-2005	Standard Deviation	0.189		
Complete Years	21	Skew	0.769		
Missing Years	4	Distribution	GEV		
Units	Surge at High Tide (m)	Anderson Darling	0.239		
Max	1.06 (15/10/1987)	Parameters	μ	0.560	
Min	0.40 (29/09/1982)		α	0.131	
			k	-0.144	

Location	Return Period (Years)	Estimated Magnitude	95% Confidence Interval		Standard Error
			lower	upper	
Newhaven (Surge at High Tide) TQ 4511 0005 (Ouse)	1	0.32	N/A		N/A
	2	0.61	0.50	0.70	0.05
	5	0.78	0.67	0.93	0.07
	10	0.91	0.77	1.12	0.09
	25	1.09	0.72	1.44	0.18
	50	1.24	0.66	1.77	0.28
	100	1.41	0.54	2.19	0.42
	200	1.60	0.41	2.70	0.58

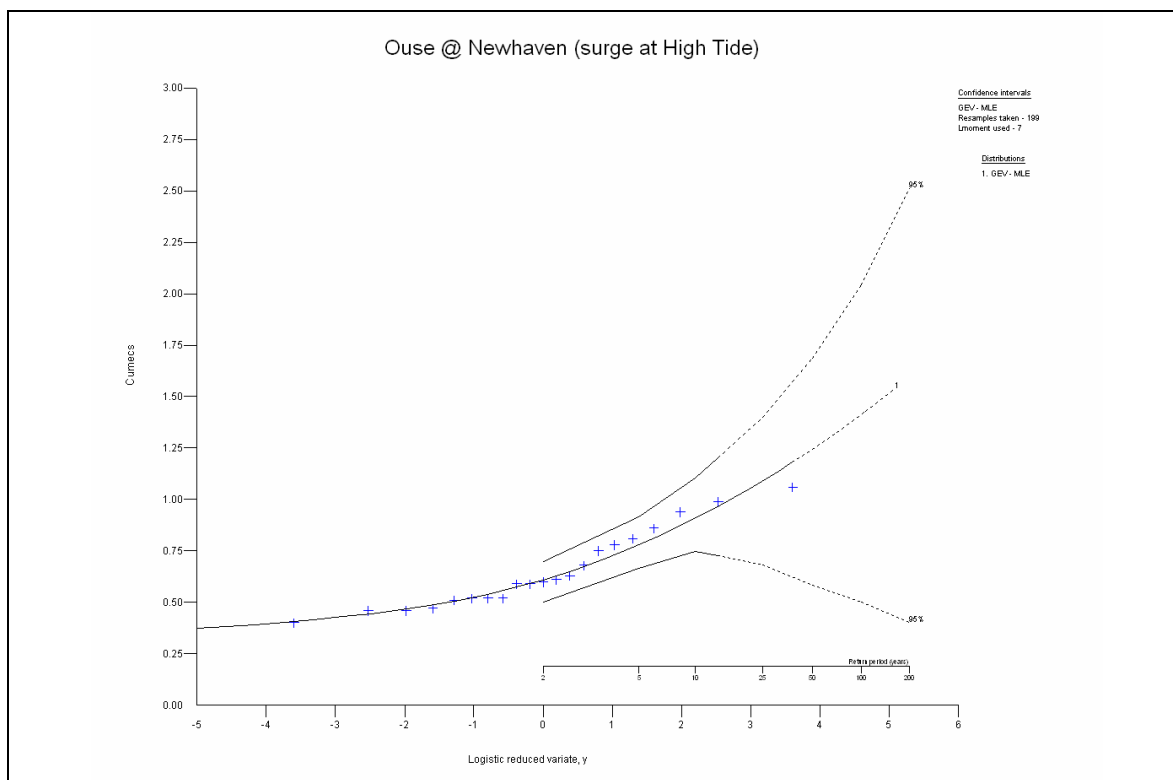


Figure C.48 GEV distribution plot at Newhaven (1982-2005)

C.5 Concurrent AMAX Events

C.5.1 Lewes Corporation Yard & Barcombe Mills

Table C.25 Concurrent AMAX Lewes Corporation Yard stage & Barcombe Mills flow series with estimated return periods

Water Year	Water-Day	LEWES CORP YARD AMAX Stage (mAOD)	Return Period (years)	BARCOMBE MILLS AMAX Flow (m ³ /s)	Return Period (years)
1960/1	04/11/1960	4.97	53	152.33	15
1961/2	11/01/1962	3.75	2	75.20	2
1963/4	19/11/1963	3.90	3	95.43	2
1965/6	10/12/1965	3.78	2	63.82	1
1966/7	28/02/1967	3.84	3	80.26	2
1967/8	05/11/1967	3.72	1	118.19	5
1972/3	02/04/1973	3.70	1	52.44	1
1973/4	11/02/1974	3.92	4	116.93	5
1974/5	22/11/1974	4.02	5	140.95	11
1975/6	02/12/1975	3.69	1	70.14	1
1979/0	28/12/1979	4.01	5	134.63	9
1983/4	23/01/1984	3.61	1	70.79	1
1993/4	30/12/1993	4.15	8	185.74	41
1999/0	28/05/2000	4.05	6	178.31	33
2000/1	12/10/2000	5.74	150	292.22	>200
2002/3	02/01/2003	3.99	5	116.10	5
Max		5.74	150		
Min		3.61	1		
Mean		4.05	25		

C.5.2 Lewes Corporation Yard & Newhaven (Tide)

Table C.26 Concurrent AMAX Lewes Corporation Yard stage & Newhaven tide series with estimated return periods

Water Year	Water-Day	LEWES CORP YARD AMAX Stage (mAOD)	Return Period (years)	NEWHAVEN AMAX Tide (mAOD)	Return Period (years)
1982/3	01/02/1983	4.10	7	4.42	>200
1984/5	07/04/1985	4.08	7	4.34	78
1987/8	08/10/1987	4.04	6	4.15	6
1992/3	11/01/1993	4.16	9	4.14	6
1995/6	23/12/1995	4.11	7	4.25	19
1996/7	09/02/1997	3.64	1	4.01	2
1998/9	06/11/1998	3.72	2	4.16	7
Max		4.16	9		
Min		3.64	1		
Mean		3.98	6		

APPENDIX D PEAKS-OVER-THRESHOLD SERIES

D.1 Independent POT Exceedance

D.1.1 Comparison of Threshold Selections

Table D.1 Synthesised flow POT exceedance occurrences at Barcombe Mills (1981-2005)

Gauge	Threshold Selection	Threshold Value (flow m ³ /s)	Complete Series (excluding gaps) (years)	Complete Series (excluding gaps) (%)	No. Exceedance (days)	No. Exceedance / Complete Series (%)	No. Exceedance / Year	Modal Month of POT Exceedance	Maximum Exceedance Value (m ³ /s)
Barcombe Mills Synthesised Flow 1981-2005	99%	74.84	23.7	95.9%	43	1.0%	1.8	JAN	
	98%	52.14	23.7	95.9%	86	2.0%	3.7	JAN	
	95%	23.73	23.7	95.9%	216	5.0%	9.1	JAN	292.22
	5/year	39.87	23.7	95.9%	118	2.7%	5.0	JAN	
	Low AMAX	23.50	23.7	95.9%	222	5.1%	9.4	JAN	

Table D.2 Simulated stage POT exceedance occurrences at Lewes Corporation Yard (1982-2005)

Gauge	Threshold Selection	Threshold Value (stage mAOD)	Complete Series (excluding gaps) (years)	Complete Series (excluding gaps) (%)	No. Exceedance (days)	No. Exceedance / Complete Series (%)	No. Exceedance / Year	Modal Month of POT Exceedance	Maximum Exceedance Value (mAOD)
Lewes Corporation Yard Simulated Stage 1982-2005	99%	3.74	15.8	67.1%	29	1.0%	1.8	JAN	
	98%	3.62	15.8	67.1%	58	2.0%	3.7	FEB	
	95%	3.43	15.8	67.1%	145	5.0%	9.1	JAN	5.74
	5/year	3.58	15.8	67.1%	79	2.7%	5.0	JAN	
	Low AMAX	3.60	15.8	67.1%	72	2.5%	4.5	JAN	

Table D.3 Recorded tide POT exceedance occurrences at Newhaven (1982-2005)

Gauge	Threshold Selection	Threshold Value (tide mAOD)	Complete Series (excluding gaps) (years)	Complete Series (excluding gaps) (%)	No. Exceedance (days)	No. Exceedance / Complete Series (%)	No. Exceedance / Year	Modal Month of POT Exceedance	Maximum Exceedance Value (mAOD)
Newhaven Recorded Tide 1982-2005	99%	3.95	16.5	69.9%	60	1.0%	3.6	FEB	
	98%	3.87	16.5	69.9%	120	2.0%	7.3	OCT	
	95%	3.74	16.5	69.9%	301	5.0%	18.3	SEP	4.42
	5/year	3.83	16.5	69.9%	165	2.7%	10.0	SEP	
	Low AMAX	3.85	16.5	69.9%	154	2.6%	9.3	SEP	

Table D.4 Predicted tide POT exceedance occurrences at Newhaven (1982-2005)

Gauge	Threshold Selection	Threshold Value (tide mAOD)	Complete Series (excluding gaps) (years)	Complete Series (excluding gaps) (%)	No. Exceedance (days)	No. Exceedance / Complete Series (%)	No. Exceedance / Year	Modal Month of POT Exceedance	Maximum Exceedance Value (mAOD)
Newhaven Predicted Tide 1982-2005	99%	3.87	16.5	69.9%	60	1.0%	3.6	OCT	
	98%	3.80	16.5	69.9%	120	2.0%	7.3	OCT	
	95%	3.67	16.5	69.9%	301	5.0%	18.3	SEP	
	90%	3.53	16.5	69.9%	602	10.0%	36.5	SEP	4.08
	80%	3.33	16.5	69.9%	1204	20.0%	73.0	SEP/OCT	
	66.6%	3.13	16.5	69.9%	2007	33.3%	121.7	OCT	
	50%	2.90	16.5	69.9%	3010	50.0%	182.6	OCT	
	5/year	3.76	16.5	69.9%	165	2.7%	10.0	SEP	

Table D.5 Recorded maximum surge POT exceedance occurrences at Newhaven (1982-2005)

Gauge	Threshold Selection	Threshold Value (surge m)	Complete Series (excluding gaps) (years)	Complete Series (excluding gaps) (%)	No. Exceedance (days)	No. Exceedance / Complete Series (%)	No. Exceedance / Year	Modal Month of POT Exceedance	Maximum Exceedance Value (m)
Newhaven Recorded Maximum Surge 1982-2005	99%	0.69	16.5	69.9%	30	1.0%	1.8	JAN	
	98%	0.61	16.5	69.9%	60	2.0%	3.7	JAN	
	95%	0.51	16.5	69.9%	151	5.0%	9.1	JAN	1.27
	5/year	0.59	16.5	69.9%	82	2.7%	5.0	JAN	
	Low AMAX	0.55	16.5	69.9%	119	4.0%	7.2	JAN	

Table D.6 Recorded surge at high tide POT exceedance occurrences at Newhaven (1982-2005)

Gauge	Threshold Selection	Threshold Value (surge m)	Complete Series (excluding gaps) (years)	Complete Series (excluding gaps) (%)	No. Exceedance (days)	No. Exceedance / Complete Series (%)	No. Exceedance / Year	Modal Month of POT Exceedance	Maximum Exceedance Value (m)
Newhaven Recorded Surge at High Tide 1982-2005	99%	0.54	16.5	69.9%	30	1.0%	1.8	JAN	
	98%	0.48	16.5	69.9%	60	2.0%	3.7	JAN	
	95%	0.36	16.5	69.9%	151	5.0%	9.1	JAN	1.07
	5/year	0.45	16.5	69.9%	82	2.7%	5.0	JAN	
	Low AMAX	0.40	16.5	69.9%	115	3.8%	7.0	JAN	

D.1.2 Upper Ouse Catchment POT Results Comparison

Table D.7 POT exceedance occurrences at the upper Ouse catchment gauges (1993 & 2007 Study Comparison)

Gauge	Threshold Value (flow m ³ /s)	Complete Series (excluding gaps) (years)		No. Exceedance (days)		No. Exceedance / Year		Modal Month of POT Exceedance	
		1993 Study	2007 Study	1993 Study	2007 Study	1993 Study	2007 Study	1993 Study	2007 Study
Gold Bridge	15.00	22.9	32.0	133	169	5.8	5.3	JAN	JAN
Isfield Weir	17.35	18.5	32.9	80	172	4.3	5.2	NOV	DEC/JAN
Clappers Bridge	5.90	13.2	32.3	82	253	6.2	7.8	DEC/JAN	JAN
Old Ship	1.50	5.0	32.5	28	178	5.6	5.5	NOV/JAN	JAN

D.1.3 Seasonality

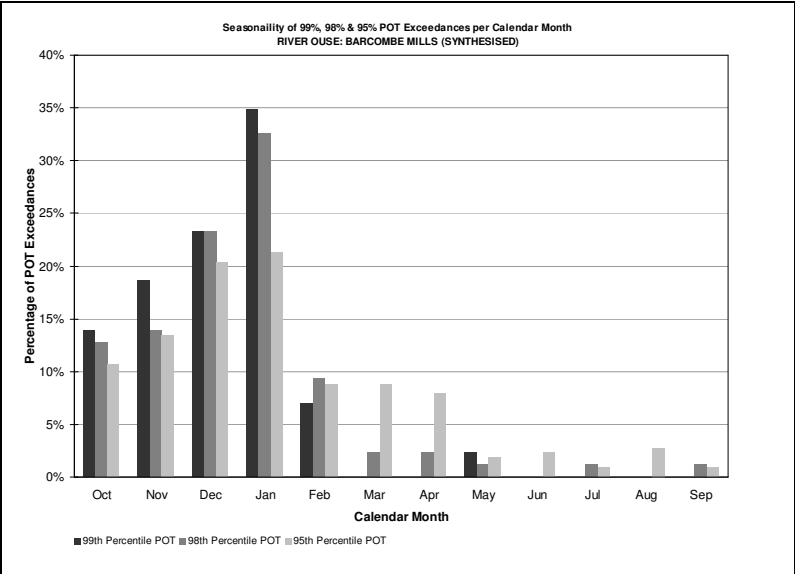


Figure D.1 Seasonality of 99th, 98th & 95th percentile POT exceedances per calendar month at Barcombe Mills

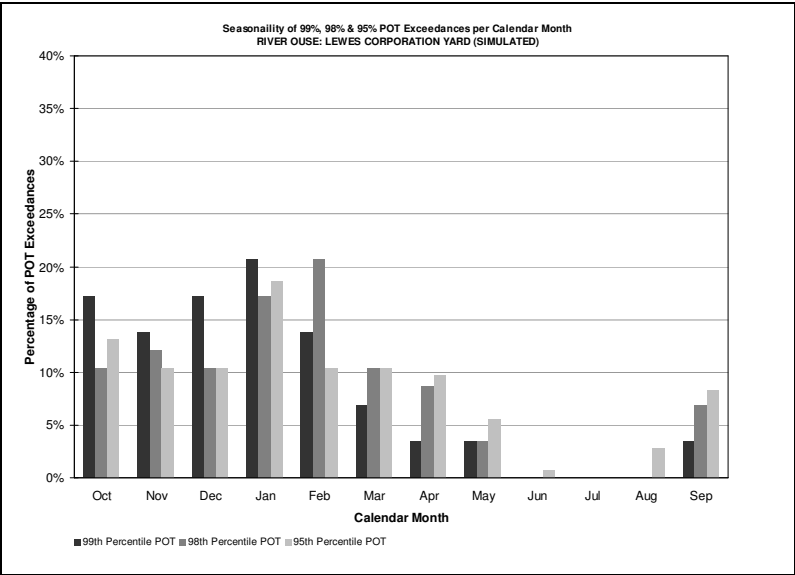


Figure D.2 Seasonality of 99th, 98th & 95th percentile POT exceedances per calendar month at Lewes Corporation Yard

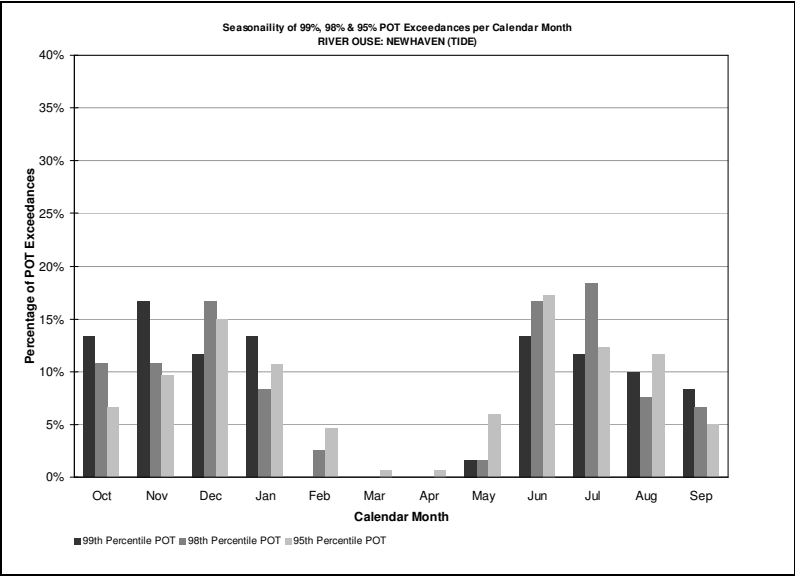


Figure D.3 Seasonality of 99th, 98th & 95th percentile POT exceedances per calendar month at Newhaven (recorded tide)

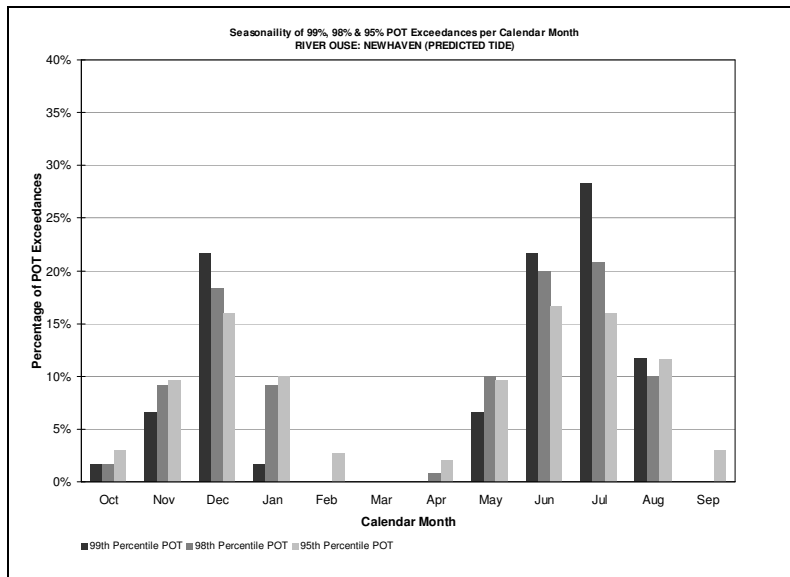


Figure D.4 Seasonality of 99th, 98th & 95th percentile POT exceedances per calendar month at Newhaven (predicted tide)

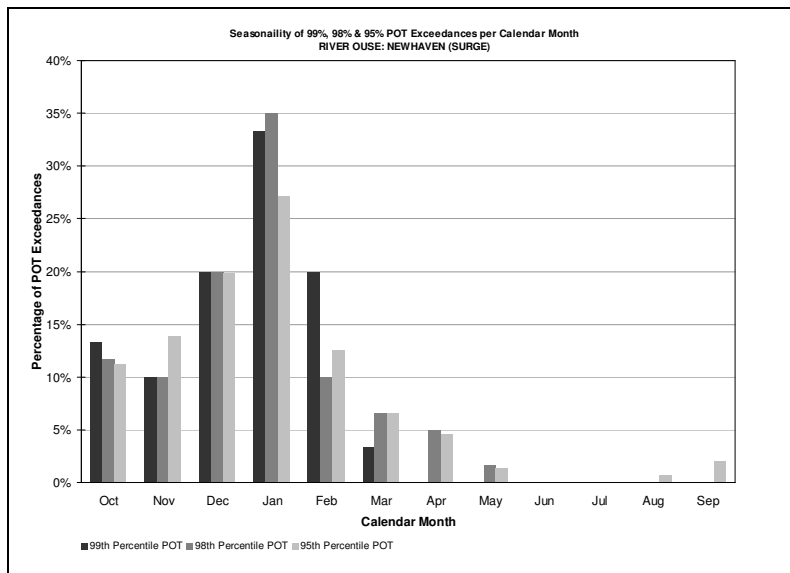


Figure D.5 Seasonality of 99th, 98th & 95th percentile POT exceedances per calendar month at Newhaven (maximum surge)

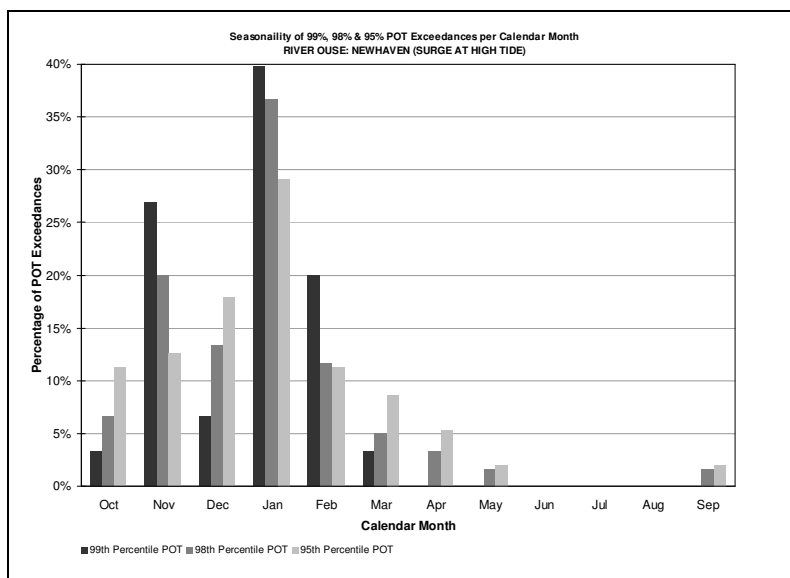


Figure D.6 Seasonality of 99th, 98th & 95th percentile POT exceedances per calendar month at Newhaven (surge at high tide)

D.2 Joint Occurrence of POT Events

D.2.1 Barcombe Mills & Lewes Corporation Yard

Table D.8 Joint POT exceedances at Barcombe Mills & Lewes Corporation Yard (1982-2005)

Gauge Pairing	Threshold Selection	Threshold Value	Concurrent Series (excluding gaps) (years)	Concurrent Series (excluding gaps) (%)	No. Independent Exceedance (days)	Same Day Joint POT Exceedances (days)	Same Day Joint POT (%)	±1 Day Joint POT Exceedances (days)	±1 Day Joint POT (%)
Barcombe Mills Lewes Corp Yard	99%	74.84 3.96	15.8	67.1%	35 29	9	25.7% 31.0%	11	31.4% 37.9%
Barcombe Mills Lewes Corp Yard	98%	52.14 3.72	15.8	67.1%	64 58	13	20.3% 22.4%	17	26.6% 29.3%
Barcombe Mills Lewes Corp Yard	95%	23.73 3.44	15.8	67.1%	156 145	38	24.4% 26.2%	53	34.0% 36.6%
Barcombe Mills Lewes Corp Yard	5/year	39.87 3.63	15.8	67.1%	89 79	17	19.1% 21.5%	24	27.0% 30.4%
Barcombe Mills Lewes Corp Yard	Low AMAX	23.50 3.60	15.8	67.1%	161 72	27	16.8% 37.5%	37	23.0% 51.4%

D.2.2 Barcombe Mills & Newhaven (Tide)

Table D.9 Joint POT exceedances at Barcombe Mills & Newhaven (tide) (1982-2005)

Gauge Pairing	Threshold Selection	Threshold Value	Concurrent Series (excluding gaps) (years)	Concurrent Series (excluding gaps) (%)	No. Independent Exceedance (days)	Same Day Joint POT Exceedances (days)	(%)	±1 Day Joint POT Exceedances (days)	(%)
Barcombe Mills Newhaven (Tide)	99%	74.84	15.9	67.3%	35	2	5.7%	2	5.7%
		3.95					3.4%		3.4%
Barcombe Mills Newhaven (Tide)	98%	52.14	15.9	67.3%	65	5	7.7%	7	10.8%
		3.87					4.4%		6.1%
Barcombe Mills Newhaven (Tide)	95%	23.73	15.9	67.3%	157	19	12.1%	24	15.3%
		3.74					6.5%		8.2%
Barcombe Mills Newhaven (Tide)	5/year	39.87	15.9	67.3%	90	6	6.7%	8	8.9%
		3.83					3.8%		5.1%
Barcombe Mills Newhaven (Tide)	Low AMAX	23.50	15.9	67.3%	162	9	5.6%	15	9.3%
		3.85					6.1%		10.2%

D.2.3 Barcombe Mills & Newhaven (Maximum Surge)

Table D.10 Joint POT exceedances at Barcombe Mills & Newhaven (maximum surge) (1982-2005)

Gauge Pairing	Threshold Selection	Threshold Value	Concurrent Series (excluding gaps) (years)	Concurrent Series (excluding gaps) (%)	No. Independent Exceedance (days)	Same Day Joint POT Exceedances (days)	(%)	±1 Day Joint POT Exceedances (days)	(%)
Barcombe Mills Newhaven (Surge)	99%	74.84	15.9	67.3%	35	5	14.3%	7	20.0%
		0.69			29		17.2%		24.1%
Barcombe Mills Newhaven (Surge)	98%	52.14	15.9	67.3%	65	12	18.5%	20	30.8%
		0.61			59		20.3%		33.9%
Barcombe Mills Newhaven (Surge)	95%	23.73	15.9	67.3%	157	37	23.6%	60	38.2%
		0.51			149		24.8%		40.3%
Barcombe Mills Newhaven (Surge)	5/year	39.87	15.9	67.3%	90	17	18.9%	29	32.2%
		0.59			81		21.0%		35.8%
Barcombe Mills Newhaven (Surge)	Low AMAX	23.50	15.9	67.3%	162	31	19.1%	53	32.7%
		0.55			118		26.3%		44.9%

D.2.4 Lewes Corporation Yard & Newhaven (Tide)

Table D.11 Joint POT exceedances at Lewes Corporation Yard & Newhaven (tide) (1982-2005)

Gauge Pairing	Threshold Selection	Threshold Value	Concurrent Series (excluding gaps) (years)	Concurrent Series (excluding gaps) (%)	No. Independent Exceedance (days)	Same Day Joint POT Exceedances (days)	(%)	±1 Day Joint POT Exceedances (days)	(%)
Lewes Corp Yard Newhaven (Tide)	99%	3.96	15.8	67.0%	29	15	51.7%	16	55.2%
		3.95			59		25.4%		27.1%
Lewes Corp Yard Newhaven (Tide)	98%	3.72	15.8	67.0%	58	35	60.3%	37	63.8%
		3.87			114		30.7%		32.5%
Lewes Corp Yard Newhaven (Tide)	95%	3.44	15.8	67.0%	145	102	70.3%	106	73.1%
		3.74			291		35.1%		36.4%
Lewes Corp Yard Newhaven (Tide)	5/year	3.63	15.8	67.0%	79	45	57.0%	47	59.5%
		3.83			158		28.5%		29.7%
Lewes Corp Yard Newhaven (Tide)	Low AMAX	3.60	15.8	67.0%	72	42	58.3%	44	61.1%
		3.85			147		28.6%		29.9%

D.2.5 Lewes Corporation Yard & Newhaven (Maximum Surge)

Table D.12 Joint POT exceedances at Lewes Corporation Yard & Newhaven (maximum surge) (1982-2005)

Gauge Pairing	Threshold Selection	Threshold Value	Concurrent Series (excluding gaps) (years)	Concurrent Series (excluding gaps) (%)	No. Independent Exceedance (days)	Same Day Joint POT Exceedances (days)	(%)	±1 Day Joint POT Exceedances (days)	(%)
Lewes Corp Yard Newhaven (Surge)	99%	3.96 0.69	15.8	67.0%	29 29	6	20.7% 20.7%	6	20.7% 20.7%
Lewes Corp Yard Newhaven (Surge)	98%	3.72 0.61	15.8	67.0%	58 59	16	27.6% 27.1%	16	27.6% 27.1%
Lewes Corp Yard Newhaven (Surge)	95%	3.44 0.51	15.8	67.0%	145 149	32	22.1% 21.5%	39	26.9% 26.2%
Lewes Corp Yard Newhaven (Surge)	5/year	3.63 0.59	15.8	67.0%	79 81	21	26.6% 25.9%	24	30.4% 29.6%
Lewes Corp Yard Newhaven (Surge)	Low AMAX	3.60 0.55	15.8	67.0%	72 118	23	31.9% 19.5%	27	37.5% 22.9%

D.2.6 Newhaven (Tide) & Newhaven (Maximum Surge)

Table D.13 Joint POT exceedances at Newhaven (tide) & Newhaven (maximum surge) (1982-2005)

Gauge Pairing	Threshold Selection	Threshold Value	Concurrent Series (excluding gaps) (years)	Concurrent Series (excluding gaps) (%)	No. Independent Exceedance (days)	Same Day Joint POT Exceedances (days)	(%)	±1 Day Joint POT Exceedances (days)	(%)
Newhaven (Tide)	99%	3.95	16.5	69.9%	60	4	6.7%	4	6.7%
Newhaven (Surge)		0.69			30		13.3%		13.3%
Newhaven (Tide)	98%	3.87	16.5	69.9%	120	9	7.5%	11	9.2%
Newhaven (Surge)		0.61			60		15.0%		18.3%
Newhaven (Tide)	95%	3.74	16.5	69.9%	301	27	9.0%	32	10.6%
Newhaven (Surge)		0.51			151		17.9%		21.2%
Newhaven (Tide)	5/year	3.83	16.5	69.9%	165	13	7.9%	15	9.1%
Newhaven (Surge)		0.59			82		15.9%		18.3%
Newhaven (Tide)	Low AMAX	3.85	16.5	69.9%	154	13	8.4%	15	9.7%
Newhaven (Surge)		0.55			119		10.9%		12.6%

D.2.7 Newhaven (Maximum Surge) & Newhaven (Surge at High Tide)

Table D.14 Joint POT exceedances at Newhaven (maximum surge) & Newhaven (surge at high tide) (1982-2005)

Gauge Pairing	Threshold Selection	Threshold Value	Concurrent Series (excluding gaps) (years)	Concurrent Series (excluding gaps) (%)	No. Independent Exceedance (days)	Same Day Joint POT Exceedances (days)	(%)	±1 Day Joint POT Exceedances (days)	(%)
Newhaven (Surge) (Surge / High Tide)	99%	0.69 0.54	16.5	69.8%	30 30	15	50.0% 50.0%	15	50.0% 50.0%
Newhaven (Surge) (Surge / High Tide)	98%	0.61 0.48	16.5	69.8%	60 60	25	41.7% 41.7%	29	48.3% 48.3%
Newhaven (Surge) (Surge / High Tide)	95%	0.51 0.36	16.5	69.8%	151 151	81	53.6% 53.6%	99	65.6% 65.6%
Newhaven (Surge) (Surge / High Tide)	5/year	0.59 0.45	16.5	69.8%	82 82	43	52.4% 52.4%	49	59.8% 59.8%
Newhaven (Surge) (Surge / High Tide)	Low AMAX	0.55 0.40	16.5	69.8%	119 115	68	57.1% 59.1%	80	67.2% 69.6%

D.3 Joint POT Correlation

D.3.1 Barcombe Mills & Lewes Corporation Yard

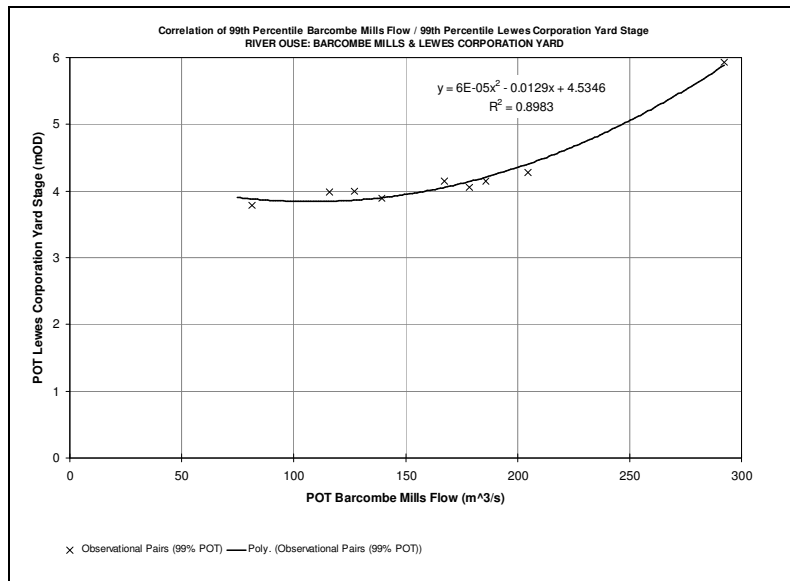


Figure D.7 Correlation of 99th percentile joint POT exceedances at Barcombe Mills & Lewes Corporation Yard (1982-2005)

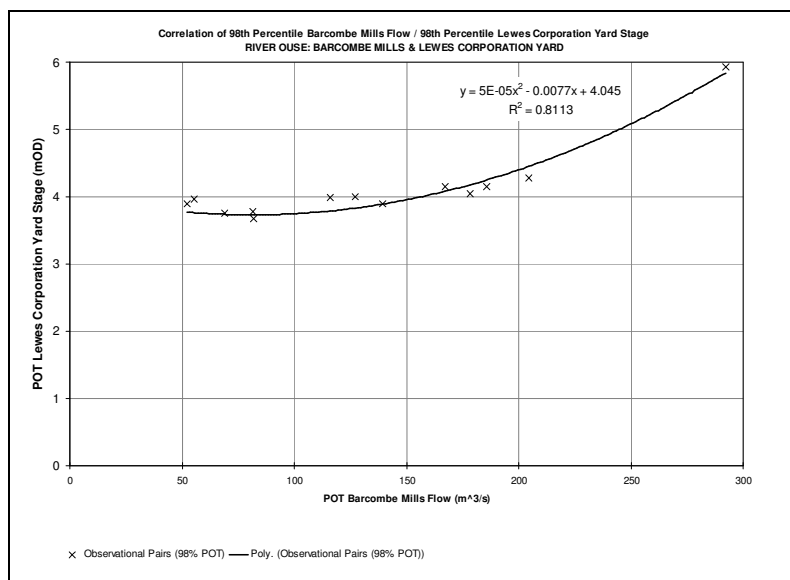


Figure D.8 Correlation of 98th percentile joint POT exceedances at Barcombe Mills & Lewes Corporation Yard (1982-2005)

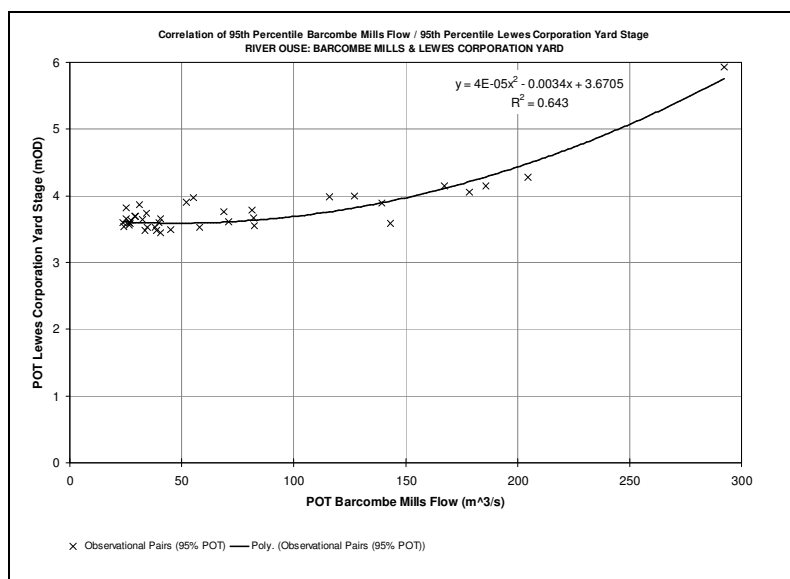


Figure D.9 Correlation of 95th percentile joint POT exceedances at Barcombe Mills & Lewes Corporation Yard (1982-2005)

D.3.2 Barcombe Mills & Newhaven (Tide)

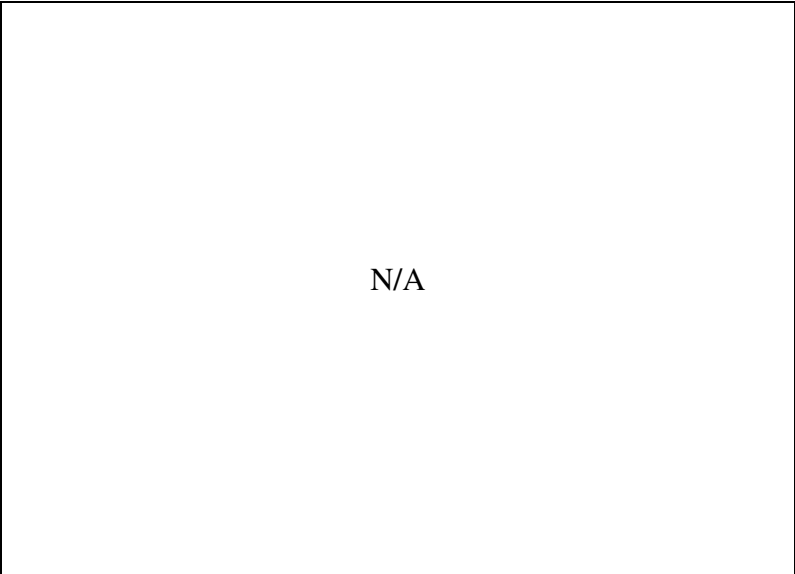


Figure D.10 Correlation of 99th percentile joint POT exceedances at Barcombe Mills & Newhaven (tide) (1982-2005)

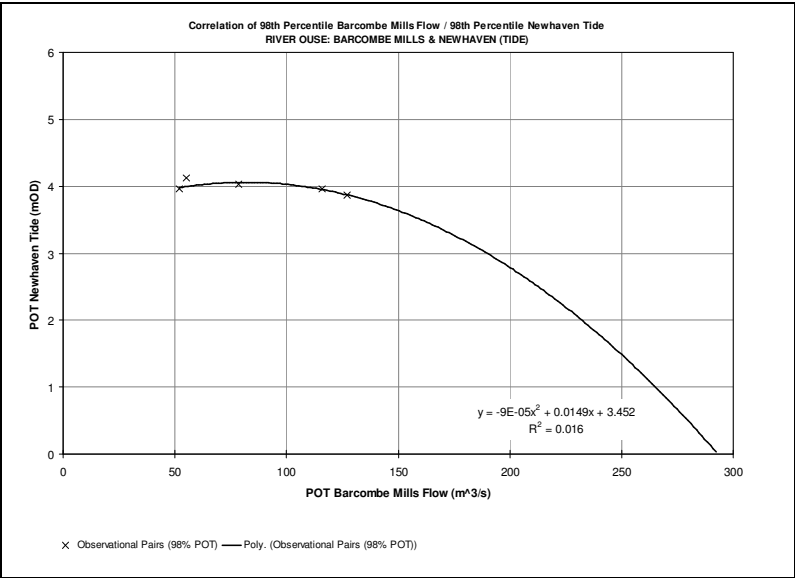


Figure D.11 Correlation of 98th percentile joint POT exceedances at Barcombe Mills & Newhaven (tide) (1982-2005)

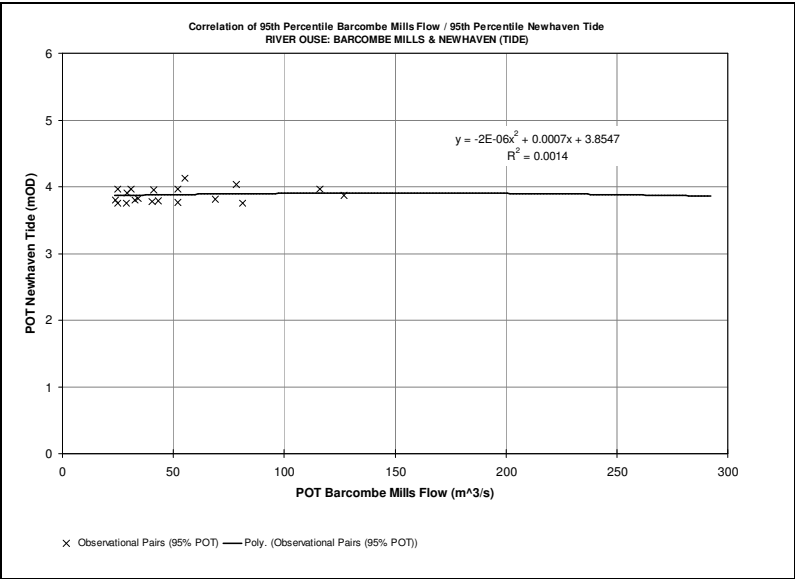


Figure D.12 Correlation of 95th percentile joint POT exceedances at Barcombe Mills & Newhaven (tide) (1982-2005)

D.3.3 Barcombe Mills & Newhaven (Surge)

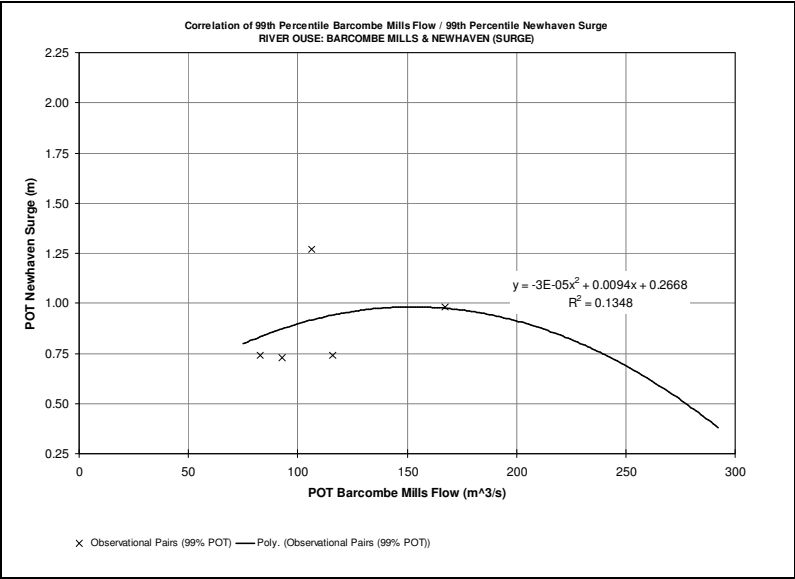


Figure D.13 Correlation of 99th percentile joint POT exceedances at Barcombe Mills & Newhaven (maximum surge) (1982-2005)

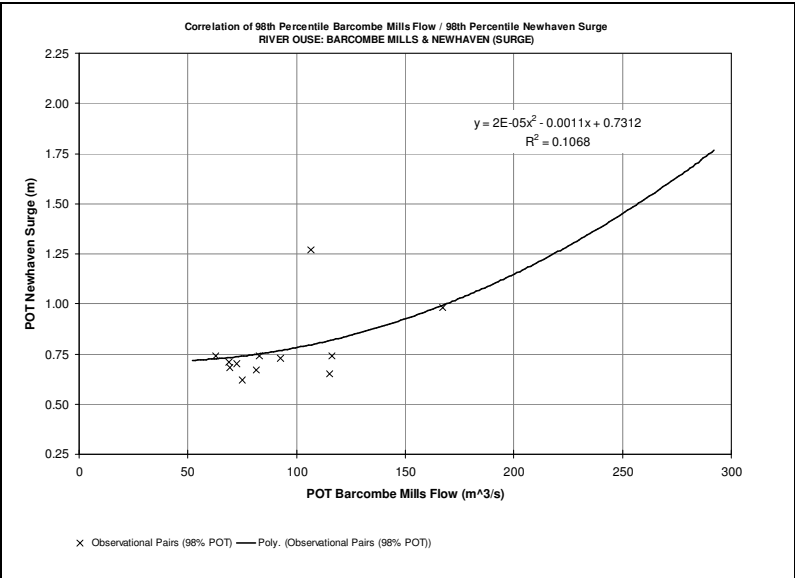


Figure D.14 Correlation of 98th percentile joint POT exceedances at Barcombe Mills & Newhaven (maximum surge) (1982-2005)

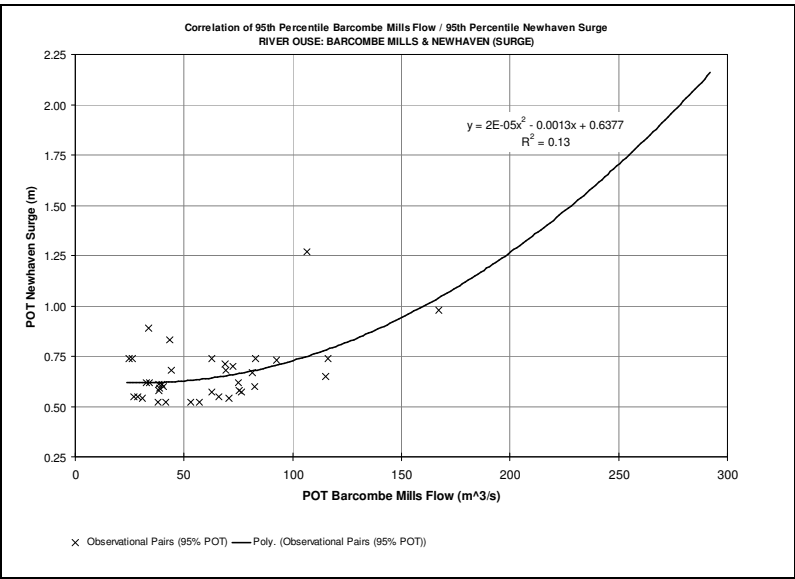


Figure D.15 Correlation of 95th percentile joint POT exceedances at Barcombe Mills & Newhaven (maximum surge) (1982-2005)

D.3.4 Lewes Corporation Yard & Newhaven (Tide)

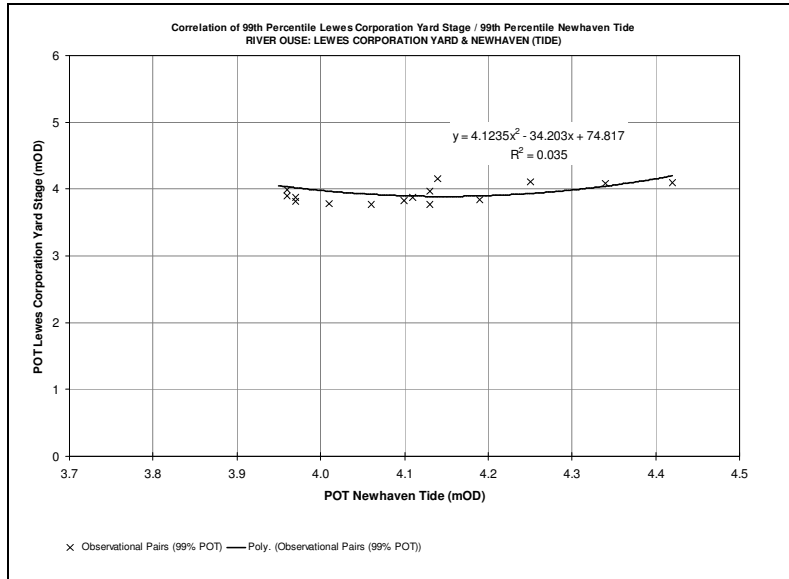


Figure D.16 Correlation of 99th percentile joint POT exceedances at Lewes Corporation Yard & Newhaven (tide) (1982-2005)

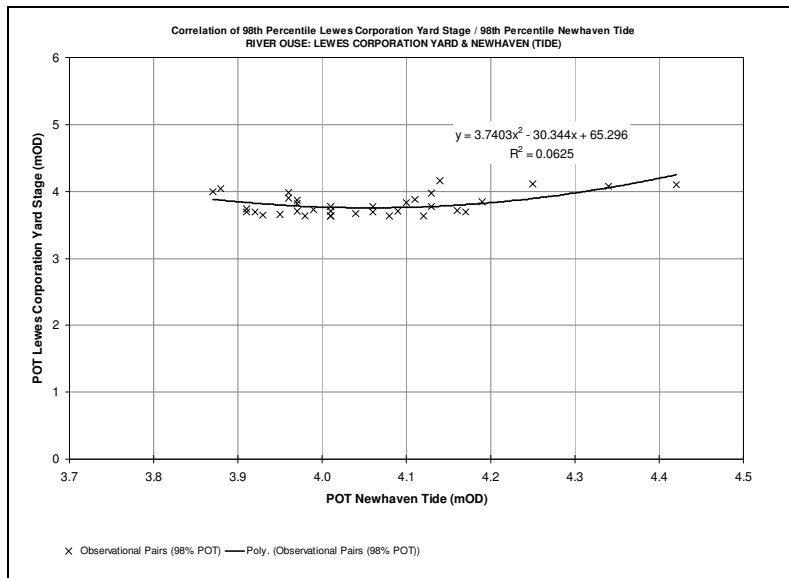


Figure D.17 Correlation of 98th percentile joint POT exceedances at Lewes Corporation Yard & Newhaven (tide) (1982-2005)

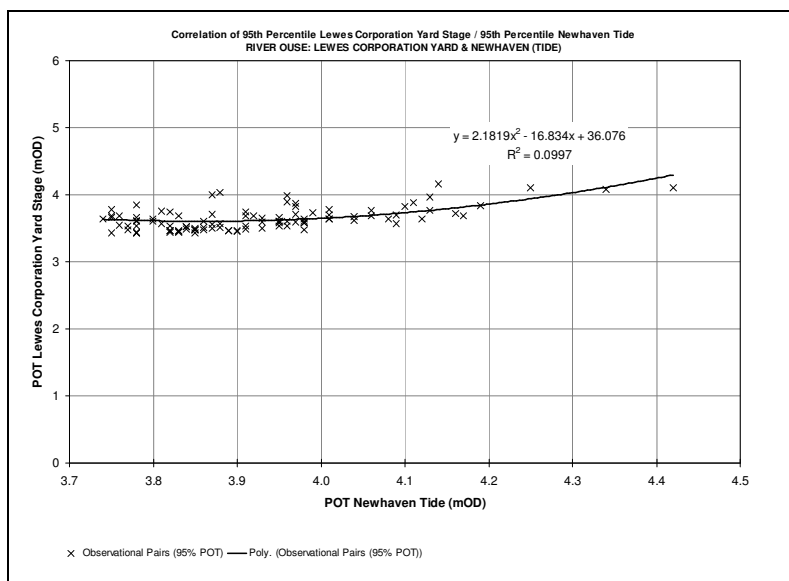


Figure D.18 Correlation of 95th percentile joint POT exceedances at Lewes Corporation Yard & Newhaven (tide) (1982-2005)

D.3.5 Lewes Corporation Yard & Newhaven (Surge)

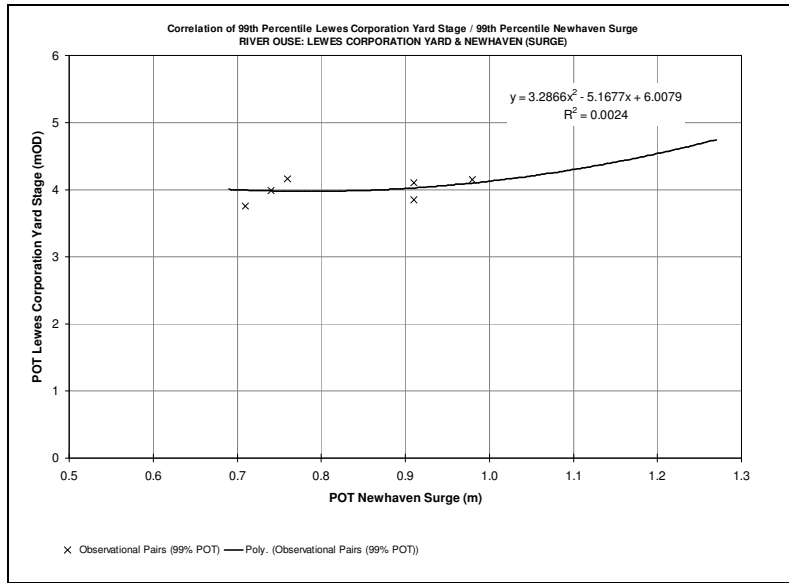


Figure D.19 Correlation of 99th percentile joint POT exceedances at Lewes Corporation Yard & Newhaven (maximum surge) (1982-2005)

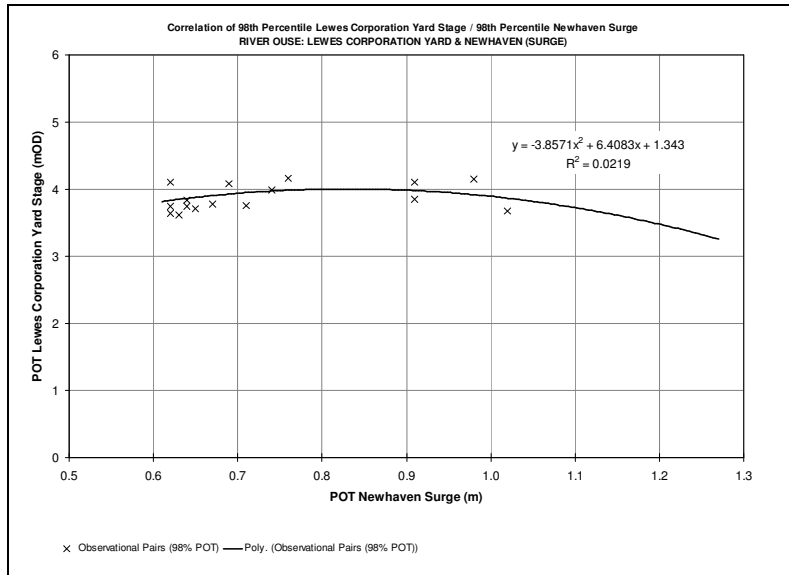


Figure D.20 Correlation of 98th percentile joint POT exceedances at Lewes Corporation Yard & Newhaven (maximum surge) (1982-2005)

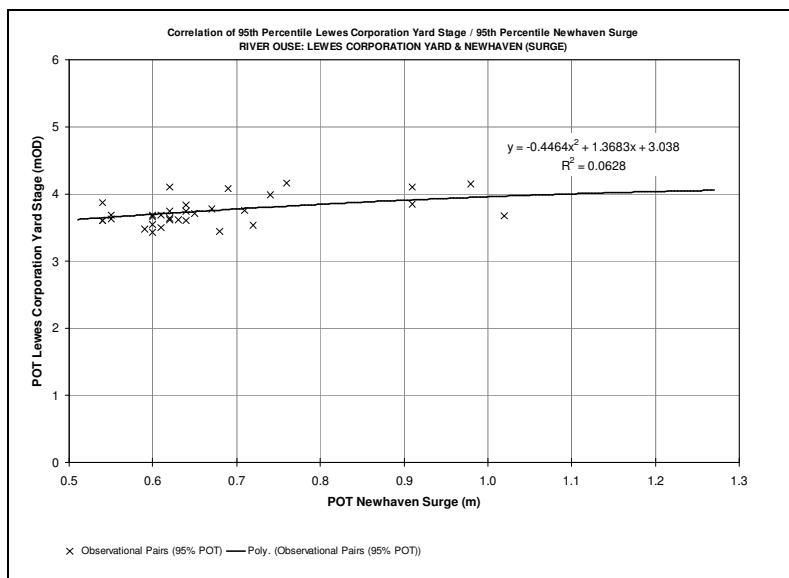


Figure D.21 Correlation of 95th percentile joint POT exceedances at Lewes Corporation Yard & Newhaven (maximum surge) (1982-2005)

APPENDIX E HISTORICAL FLOOD EVENTS

E.1 Historical Flooding in the Ouse Catchment

Table E.1 Record of flood events at Uckfield (River Uck) & Lewes (River Ouse)

Flood Event	Uckfield (Uck)	Lewes (Ouse)	Flood Event	Uckfield (Uck)	Lewes (Ouse)
1671		E	4th–6th Nov. 1957	M	M
January 1726		E	27th January 1958	S	M
January 1772		E	27th June 1958	M	
1801		E	16th Dec. 1958	S	
29th January 1814		E	16th January 1959		
19th Sept. 1829		S	14th October 1959		M
4th October 1852		S	3rd November 1960		
23rd October 1852	E	E	December 1960	E	E
31st October 1852		S	4th January 1961		
1st Dec. 1852			30th January 1961		
31st October 1865	E	E	9th March 1961		
11th Nov. 1875	E		2nd Sept. 1963		
December 1876			5th–12th Nov. 1963	M	
January 1877			18th Nov. 1963		
October 1880			27th Nov. 1963		
17th Nov. 1894		S	March 1964	M	
January 1904		S	19th June 1964		
19th Nov. 1911		E	20th Nov. 1965	M	M
December 1915		S	December 1965		M
1916	M		28th February 1967		
16th January 1918	S		8th March 1967	M	
28th Dec. 1924		S	5th October 1967	M	
16th Nov. 1929	S		16th Sept. 1968		M
29th Nov. 1935			October 1968		M
25th January 1939	S		13th March 1969		M
11th Nov. 1950	S		11 February 1974		M
28th Nov. 1950		M	22 November 1974		
21st Feb. 1951		M	27th January 1975	M	
8th Nov. 1951		M	28th Dec. 1979	M	
28th Feb. 1952	S		25th Nov. 1982	S	M
28th Nov. 1952	M		21st Nov. 1986	S	S
21st Feb. 1953			9th–10th Oct. 1987		
7th March 1954	M		31st January 1990	S	S
15th January 1955		M	30th–31st Dec. 1993		
12th January 1956	M		25th–26th Dec. 1999		
28th Dec. 1956	M		28th May 2000		
2nd February 1957		M	9th–12th Oct. 2000	E	E
4th February 1957		M			
8th February 1957		M			
15th Feb. 1957		M			
14th March 1957	M				

‘E’ represents an ‘Extreme’ event. A very rare flood event characterised by serious flooding of urban areas and probably widely reported as being ‘the worst in living memory’, ‘worst recorded’, or a similar description.

‘S’ represents a ‘Serious’ event. A rare flood event, characterised by serious flooding of urban areas, but less serious than an identified ‘Extreme Flood Event’ to which this serious event is probably compared.

‘M’ represents a ‘Moderate’ or ‘Minor’ event. The remaining flood events that cover a wide range, including those in which only individual low lying properties or surrounding rural areas are flooded.

A level of severity of a flood event is subjective and can be applied to numerous flooding impacts, such as cost, number of properties damaged, area flooded, and so on. In engineering terms, this may equally be peak flood height, peak flow, flood duration or cost of redevelopment. Table E.1 demonstrates this problem. Historical flood events in the Ouse catchment have been given labels as being either 'Extreme', 'Serious' or 'Moderate'. However, there is no reference to any one particular impact (e.g. number of properties flooded). Instead, the data is reliant upon individual's interpretations on what constitutes a serious flood. The problem is increased by the change in people's perceptions of what the impact labels actually mean. The rapid urbanisation of Lewes in the 1960's noticeably increased the potential impact of a flood - there were now more properties to flood and people to affect.

Indeed, Table E.1 appears to show that there are more flood events in recent years, suggesting that the problem of flooding is getting worse, with the last 50 years filling three-quarters of the table. This is perhaps an inaccurate portrayal of the flooding history in the catchment. Changes in people's perception of what a severe flood event is, expansion of the town and better data recording all contribute to more floods being recorded in recent years. Smaller flood events, which historically may not have been recorded, now have been, giving the appearance of increased flooding frequency.

Historically, only the most severe events which put the town at risk would probably have been considered worthy of being recorded; many of the flood events may actually have been severe enough to flood the modern day town of Lewes but which at the time may only have flooded fields, thus they weren't recorded. It could be disputed that given the background of continuous flooding in the region, events of similar or greater magnitude may well have taken place in Lewes prior to the rapid expansion of the town in the 1960's. It is perhaps understandable however that the October 2000 flood event in the area has the label of being the 'worst in living memory', because it satisfies many of the impact statements. But the label is both misleading and masks the true impact.

The term is often used when comparison between events is difficult, often because events occur over irregular and long periods. But events are quickly forgotten or exaggerated over time, leading to underestimation of historical events. This makes each new flood appear worse than the last, when the reality may be quite different. This is not to say however that flooding may indeed be more prevalent today than 50 years ago. Changes in the urban extent of the town, alterations to land use around Lewes and newer river

defences may have actually increased the risk of flooding, but this cannot be determined from the type of historical analytical approach used here.

A different approach may list some of the historic flood events in Lewes by ranking peak flood levels. However, there are also problems associated with using such a methodology to calculate risk. In many cases, recording may have been limited and anecdotal. Historical flood levels may not be directly comparable due to changes in channel capacities, dredging activities, and flood defence works; like-for-like events are not necessarily being compared. Inevitably, there will also be missing years in the data records. For example, there is no record of the North Sea flood in January 1953 affecting the Lewes area. It is not clear whether its omission from the records is because it didn't actually affect the area, or simply that the dataset is incomplete.

By selecting one particular flood impact category such as peak flood levels, the actual severity of different flood events is comparable, but historical changes (i.e. to river defences) also needs to be taken in consideration, and attention paid to the original recorded datasets. Historical records can suggest the frequency and indicate some level of severity, but it should be remembered that it is speculative at best. As such, analysis needs to be event specific, focusing on the input variables rather than just the output flood levels.

E.2 Extreme Event Analysis of the 12th October 2000 Flood

E.2.1 Flood Account

The 12th October 2000 Ouse flood of the towns of Uckfield and Lewes is the best documented flood event in the catchment. MORECS data (Met Office, 2000) for grids 172 & 173, which cover the Ouse catchment, suggests that at the end of August 2000 the catchment had a soil moisture deficit of 100mm. This followed almost average rainfalls for the period of January to August of that year. September was then wet, and early October saw some modest rainfalls which reduced the soil moisture deficit to around 35mm. This was above the long-term average, but was not particularly noteworthy.

The rainfall in the Ouse catchment in early part of October 2000 was also nothing exceptional. The first eight days of October saw a range of between 8mm and 14mm total daily rainfall levels. By contrast, the 96 hours preceding the 12th October flood event

were extraordinarily wet, caused by three distinct and intense rainfall events from the 9th to the 12th October. The third, over the night of the 11th/12th, saw the most intense rainfall and the lowest pressure (965Mb). These three rainfall events individually made up 39%, 25% and 95% respectively of the average expected monthly rainfall values for October in the Ouse Catchment (Met Office, 2000).

Over the 96 hours preceding the flooding on the 12th, the catchment had an average rainfall of between 150mm and 160mm, with the central part of the Ouse having the highest totals of 200mm. The 16 hours from 18:00GMT on the 11th October to 10:00GMT on the 12th October saw the bulk of the recorded rainfall during the 24 hour Rain Day, from 09:00GMT on the 11th to 09:00GMT on the 12th. This was the third distinct rainfall event preceding the flood on the 12th.

The first two rainfalls eliminated the remaining soil moisture deficit. MORECS shows that after the first rainfall event on the 9th/10th, the average soil moisture deficit would have reduced to approximately 10mm. A further 22mm of rainfall from the second event on the night of the 10th/11th would have reduced this to zero as the soil reached field capacity. However, it was the third and most intense rainfall event on the night of the 11th/12th October which ultimately led to the severe flooding in Uckfield and Lewes.

River levels responded almost immediately to the third heavy rainfall on the already saturated basin. The town of Uckfield flooded dramatically from approximately 04:00GMT, with a peak at the High Street between 08:00 and 09:00GMT. Water levels continued to rise at the Barcombe Mills gauge during the morning, with an estimated peak time of 11:00GMT. River levels rose quickly in the centre of Lewes, but were still in bank at 09:00GMT. By this time however, the floodplain was now almost full with the embankments breached to below Hamsey.

By 11:00GMT, some peripheral parts of Lewes were starting to flood, and by 12:00GMT water started to back up behind the narrow Cliffe Bridge and the surrounding river defences were overtopped. Floodwaters began to weir the main Lewes river defence walls, inundating all of the low lying urban areas of Lewes at an estimated rate of 1m in half an hour at its peak. The flood waters had overwhelmed the defences completely by 13:00GMT, leading to the catastrophic flooding of the town, peaking at approximately 20:30GMT on the evening of the 12th.

E.2.2 Peak Flood Magnitudes & Estimated Return Periods

Although the 12th October 2000 flood was primarily fluvial, it provides a unique opportunity to study the hydrodynamics of the catchment and the interaction between tides and fluvial flows at Lewes during an extreme event. Table E.2 details recorded peak magnitudes from the flood event with return periods estimated using the GEV distributions for each gauge. Peak levels and flows have been taken from recorded, synthesised and continuously simulated series throughout the catchment.

Using the recorded data from the 12th October 2000 flood event, conclusions can be drawn about how the catchment reacted under extreme flow conditions. EA trigger times show that the rainfall over the night of the 11th/12th produced an almost instance runoff response which was catchment-wide. This is reflected in the high flow magnitudes recorded at the four upper catchment gauges within 2 ½ hours of each other on the morning of the 12th. However, significant variability exists between the estimated return periods and the peak flow magnitudes at the upper catchment gauges, with Gold Bridge returning a substantially lower return period than the other three gauges. This is largely due to the Gold Bridge AMAX series containing several similarly high peaks to the 2000 event compared with the peak flows observed at the other three gauges which are significantly higher than any previously recorded AMAX observation.

Table E.2 Peak flood magnitudes for the 11th / 12th October 2000 Ouse catchment flood event & estimated return periods

Gauge	Time (GMT)	Peak Stage (mAOD)	Peak Flow (m ³ /s)	Return Period (years)
Gold Bridge	09:45	13.96	94.40	44
Isfield Weir	09:00	14.06	132.00	157
Clappers Bridge	08:30	11.04	23.78	164
Old Ship	11:00	8.12	14.07	190
Barcombe Mills	11:00	7.76 (estimated)	292.22 (synthesised)	>200
Lewes Corp Yard	20:30	5.74 (simulated)	-	172
Lewes Gas Works	20:30	5.07	-	>200
Southeast Gauge	22:45	3.86	-	-
Newhaven (Tide)	10:15	3.29	-	<1
Newhaven (Surge)	20:00 (11/10/00)	0.30	-	<1

The peak flow of $132\text{m}^3/\text{s}$ at Isfield Weir suggests that the approximate $60\text{m}^3/\text{s}$ channel capacity through the town of Uckfield (3.5km upstream from the gauge) was less than 50% of the peak river flow on the morning of the 12th, so the flooding of the town during the event was inevitable.

The pattern of events during the October 12th flood event saw river flows rise all morning at Barcombe Mills due to the catchment-wide response to the rainfall and runoff. This process quickly surpassed the $85\text{m}^3/\text{s}$ channel capacity at the site, overtopping the defences, causing the low lying areas to quickly fill with floodwaters and completely drowning the gauging station (Figure E.3 & Figure E.4). The continuous simulation exercise (section 4.4) generated a peak flow of $292\text{m}^3/\text{s}$ at Barcombe Mills which was estimated to be well in exceedance of the 1:200 year return period. An exact return period estimation was not possible as the extreme magnitude was outside of the limits of the extrapolated GEV distribution.

As the flood waters entered the Lower Ouse, defences were overtopped and the floodplains inundated. The natural constriction in the floodplain in the upstream approaches to Lewes combined with the lack of offstream storage caused flow velocities to increase and river levels to rise, overwhelming the $170\text{m}^3/\text{s}$ channel capacity in Lewes and overtopping the town's defences. Recorded stage at the Lewes Corporation Yard gauge topped out at 4.95mAOD during the flood (peak estimated at 5.8mAOD). The continuous simulation exercise (section 4.4) produced a peak stage at Lewes on the 12th October 2000 at 20.30GMT with a corresponding height of 5.74mAOD (Figure E.5 & Figure E.6) with an estimate return period of 1:150 years using the GEV distribution.

The continuous simulation indicated a 0.2m head loss under the Phoenix Causeway bridge structure. Below the crossing, the simulated stages peaked at around 5.57mOD. Further downstream, the maximum head difference either side of Cliffe Bridge at the peak of the flood was estimated to be 0.53m, which is corroborated by the peak water level of 5.07mAOD recorded downstream at the Lewes Gas Works gauge and a corresponding return period exceeding the 1:200 year limit of the extrapolated GEV distribution.

This amount of head loss suggests there was an average flow velocity of $3\text{m}^3/\text{s}$ during the peak of the flood. The waterway through Cliffe Bridge is calculated as 65m^2 , providing a flow capacity of $195\text{m}^3/\text{s}$ under Cliffe Bridge. Cliffe Bridge seriously impeded the river flow during the flood event, and as such significant flow volumes bypassed it. This

suggests that the peak flow was well in excess of 200m³/s in the centre of Lewes. Table E.3 shows how the recorded and simulated peak stage corresponded to the existing flood defence levels in the centre of Lewes, illustrating overtopping depths and head loss at the structures of Phoenix Causeway and Cliffe Bridge.

Table E.3 Peak 12th October 2000 Lewes flood magnitudes at key river structures & corresponding overtopping levels

Location / Structure	Peak Flood Stage (mAOD)	Flood Defence Design Level (mAOD)	Depth of Overtopping (m)
u/s of Phoenix Causeway	5.74	4.95	0.79
u/s of Cliffe Bridge	5.57	4.95	0.62
d/s of Cliffe Bridge	5.07	4.73	0.34

During the 12th October 2000 flood events, the tide at Newhaven was a medium-high ‘high tide’ with a predicted height of 3.25mOD, but was exceeded by 30% of that year’s tides (Figure E.9 & Figure E.10). For the same period, the Met Office forecasted a slight positive meteorological surge which produced a maximum positive value of 0.30m at 20:00GMT on the 11th, but which has dropped to 0.04m at the time of the high tide on the morning of the 12th at 10:15GMT (Figure E.11 & Figure E.12).

Both tide and surge magnitudes are below the 1:1 year return period estimates for the duration of the flood. The series of exceptional rainfalls between the 9th & 12th October did not have an adverse effect on the tidal levels.

E.2.3 Interaction of Fluvial Flow & Tide at Lewes

During the flood event on the morning of the 12th October 2000, the lag time from the high tide at Newhaven at 10:15GMT with a predicted height of 3.25mAOD should have meant that the high tide at Lewes would be around 11:15GMT, with a peak of approximately 3.02mAOD under low flow conditions. After high tide, water levels at Lewes would also have been expected to start dropping.

Recordings from the Lewes Corporation Yard gauge suggest however that from the early hours of the 12th, the extreme fluvial flows effectively drowned out the incoming tide (Figure E.14). From approximately 02:30GMT, water levels in Lewes started rising, two

hours before the early morning low tide. At 06:30GMT, five hours before the expected high tide level, water levels in Lewes had surpassed the predicted level and continued to rise. By the time the high tide should have been recorded at Lewes around 11:15GMT, the recorded tide of 3.29mAOD at Newhaven is barely visible in the level hydrographs taken from the Lewes Corporation Yard gauge. Two consecutive tidal cycles are then not visible in the simulated stage at Lewes. Figure E.13 & Figure E.14 show comparison hydrographs of stage at Lewes with Barcombe Mills flow and Newhaven tide for the period of the flood, demonstrating the relative impacts of both on the timing and magnitude of water levels at Lewes.

As the defences had been breached both above and within Lewes, the flow characteristics below Lewes were altered. During its peak, a potentially significant proportion of the flood waters left the river channel when the defences were breached and the town centre inundated. This reduced the volume of water flowing downstream towards Newhaven, producing an energy head loss. The result was a dampening effect on the tidal levels further downstream, which was significant enough to retain the river in bank down to Newhaven.

E.2.4 Calibration Hydrographs

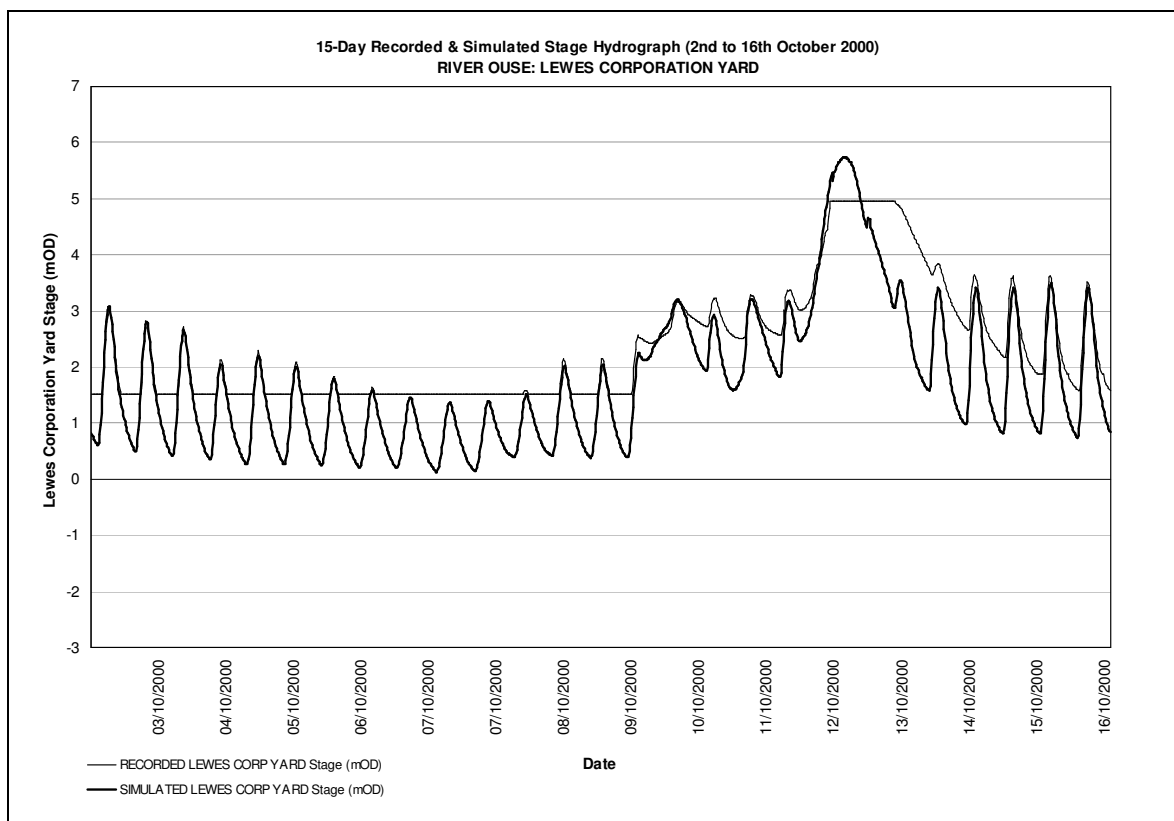


Figure E.1 15-Day recorded & simulated stage hydrographs (2nd – 16th October 2000) at Lewes Corporation Yard

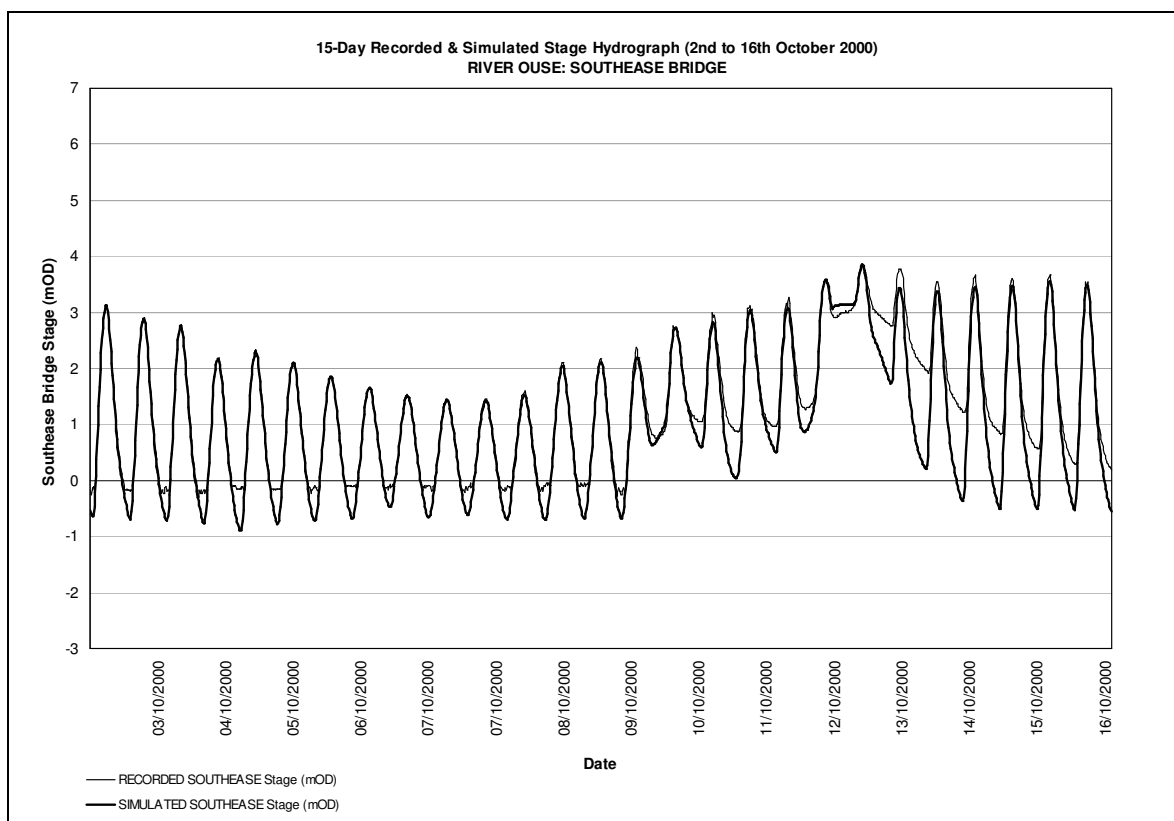


Figure E.2 15-Day recorded & simulated stage hydrographs (2nd – 16th October 2000) at Southeast Bridge

E.2.5 Flood Hydrographs

E.2.5.1 Barcombe Mills

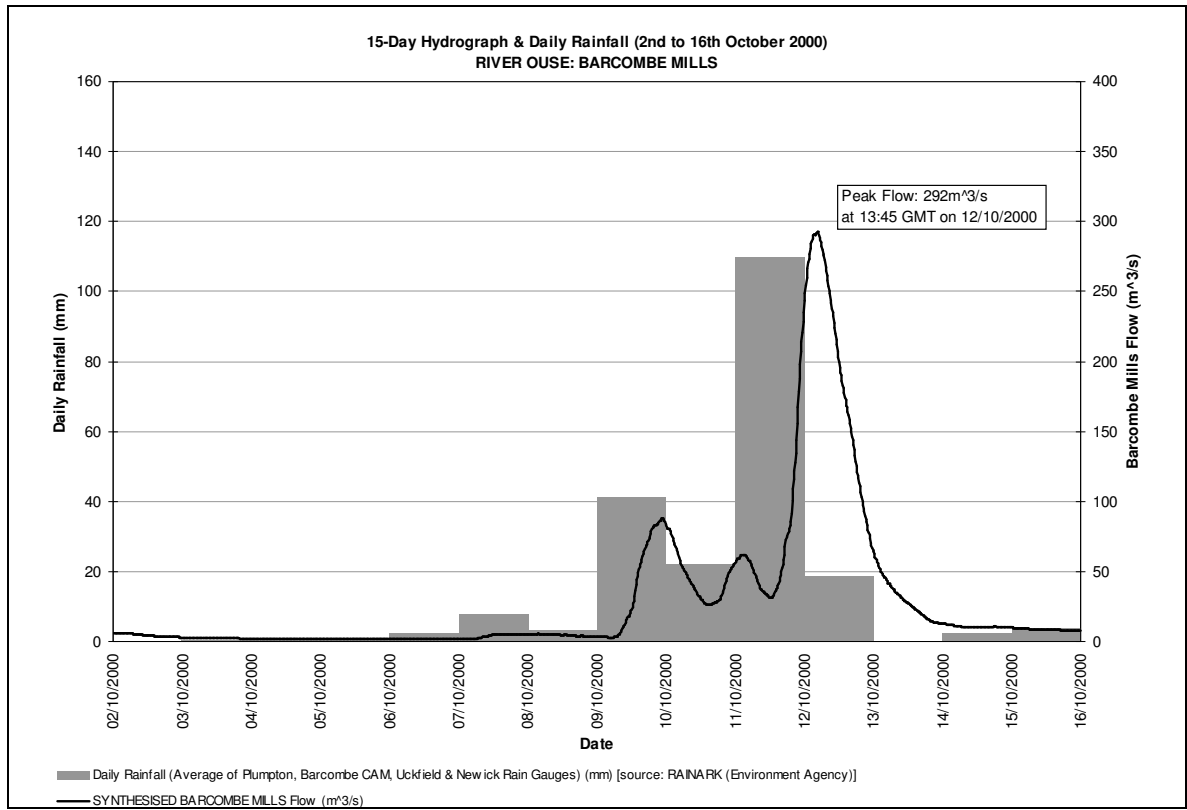


Figure E.3 15-Day flow hydrograph & daily rainfall (2nd – 16th October 2000) at Barcombe Mills

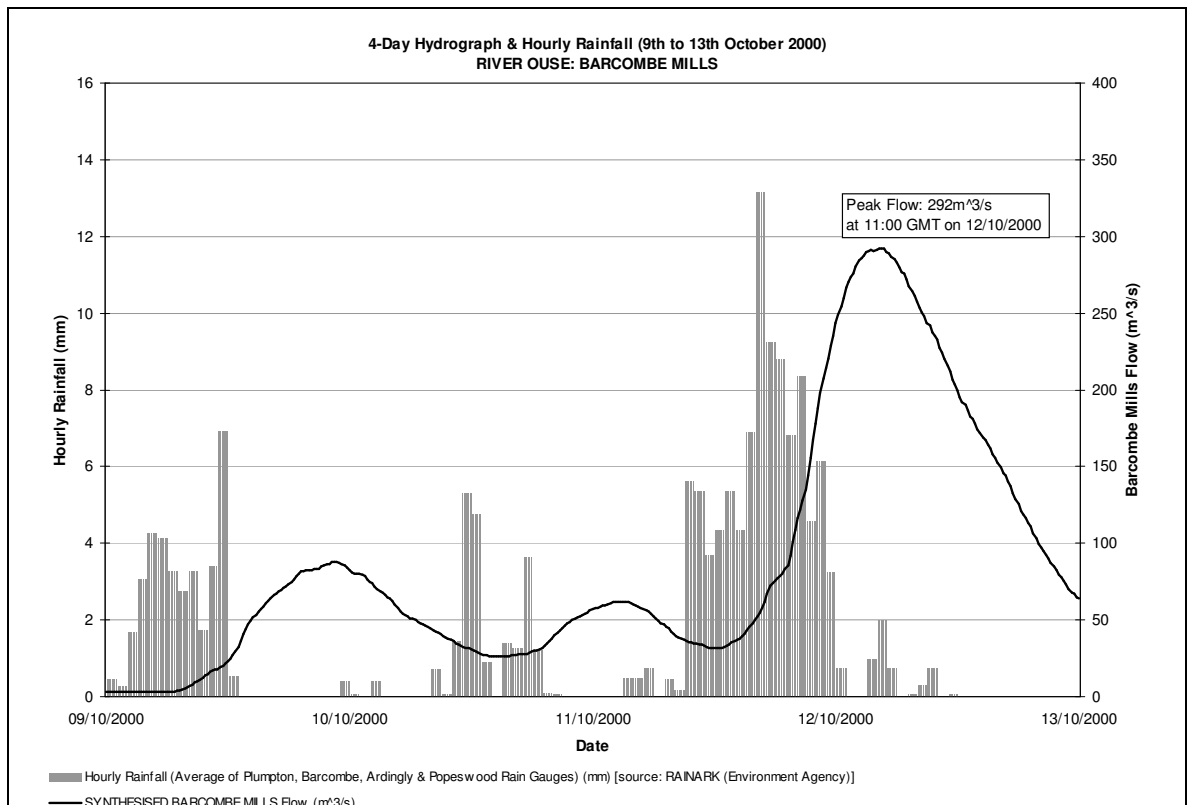


Figure E.4 4-Day flow hydrograph & hourly rainfall (9th - 13th October 2000) at Barcombe Mills

E.2.5.2 Lewes Corporation Yard

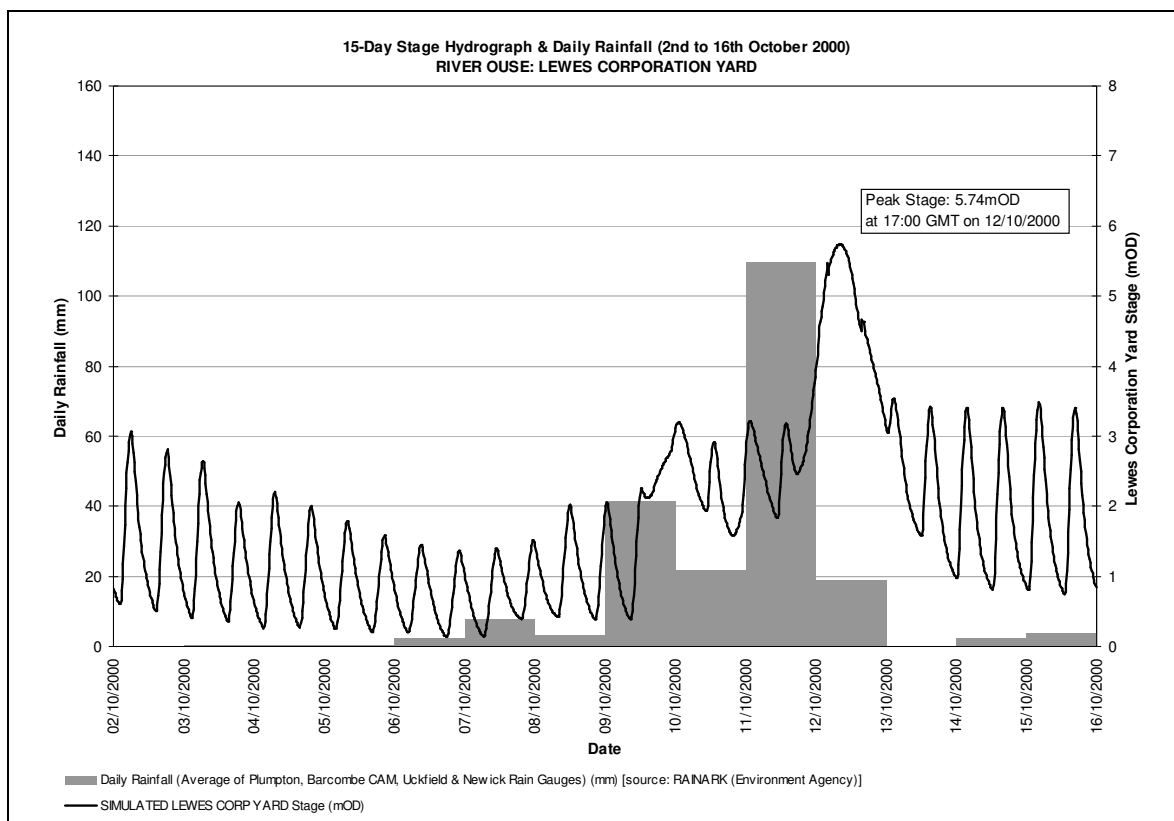


Figure E.5 15-Day stage hydrograph & daily rainfall (2nd – 16th October 2000) at Lewes Corporation Yard

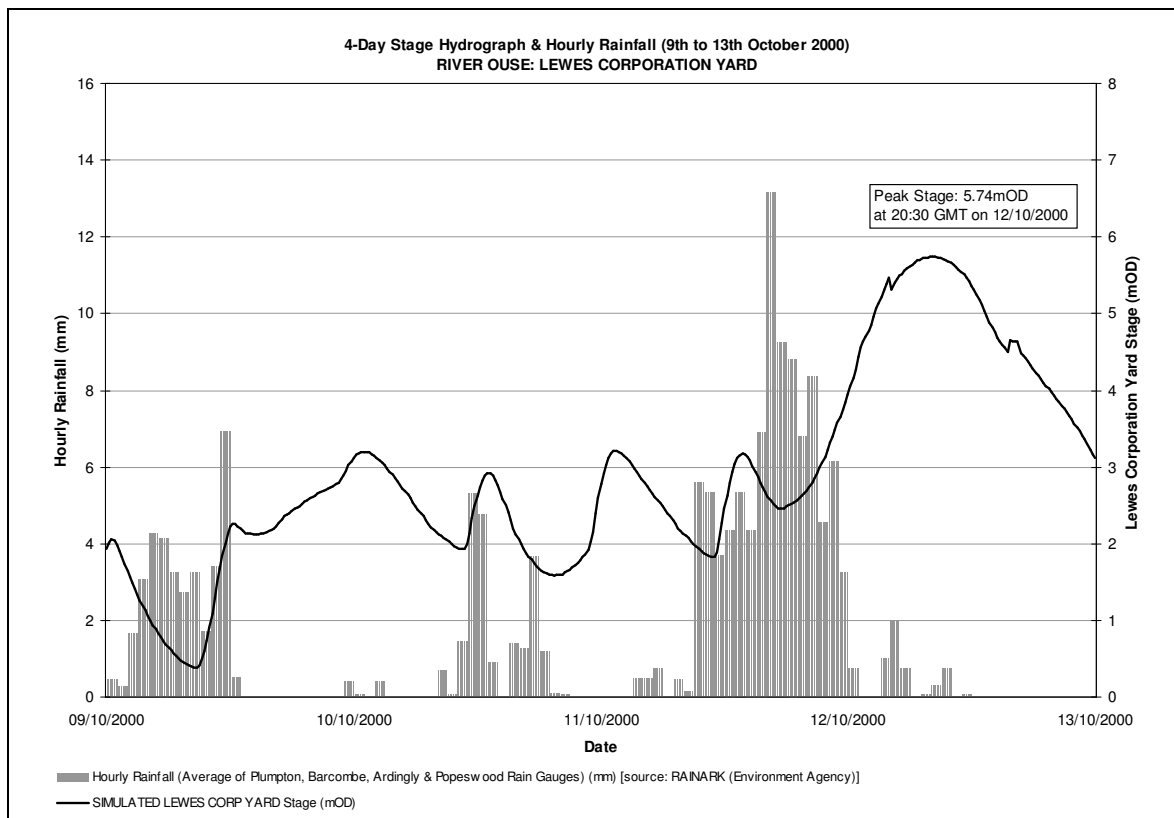


Figure E.6 4-Day stage hydrograph & hourly rainfall (9th - 13th October 2000) at Lewes Corporation Yard

E.2.5.3 Southease Bridge

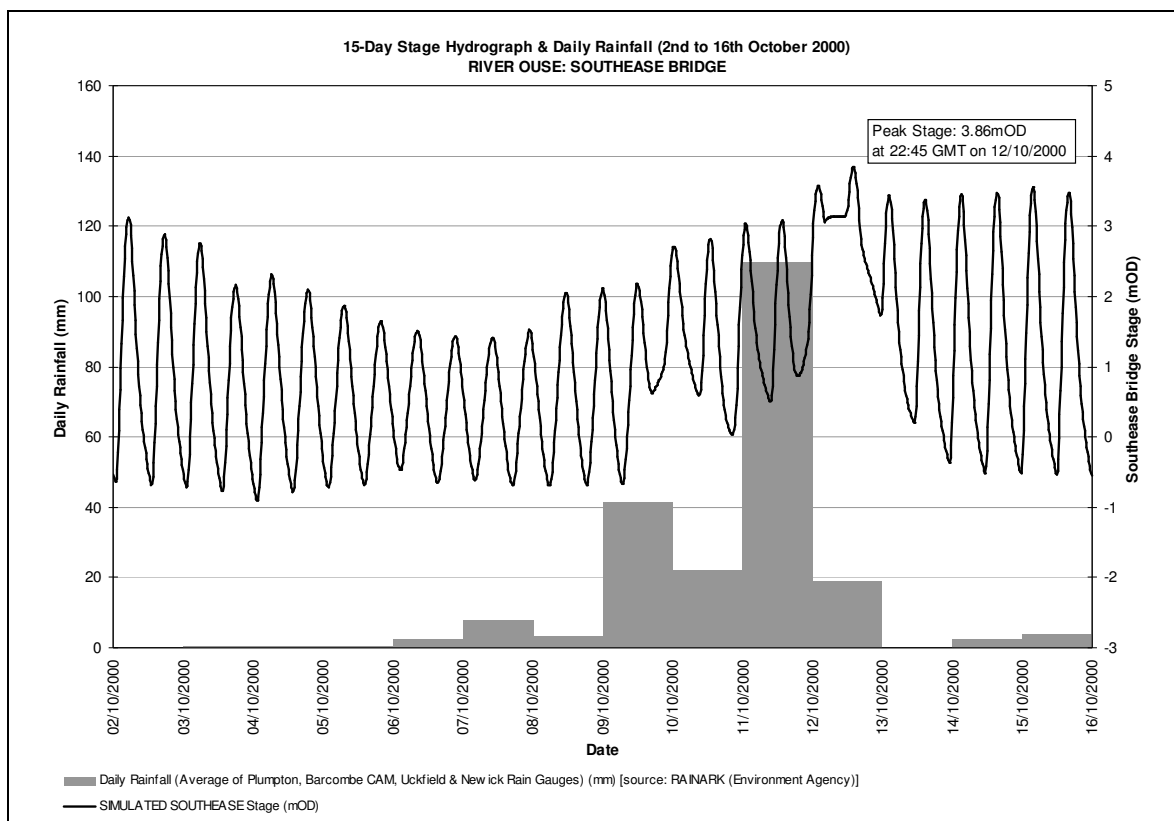


Figure E.7 15-Day stage hydrograph & daily rainfall (2nd – 16th October 2000) at Southease Bridge

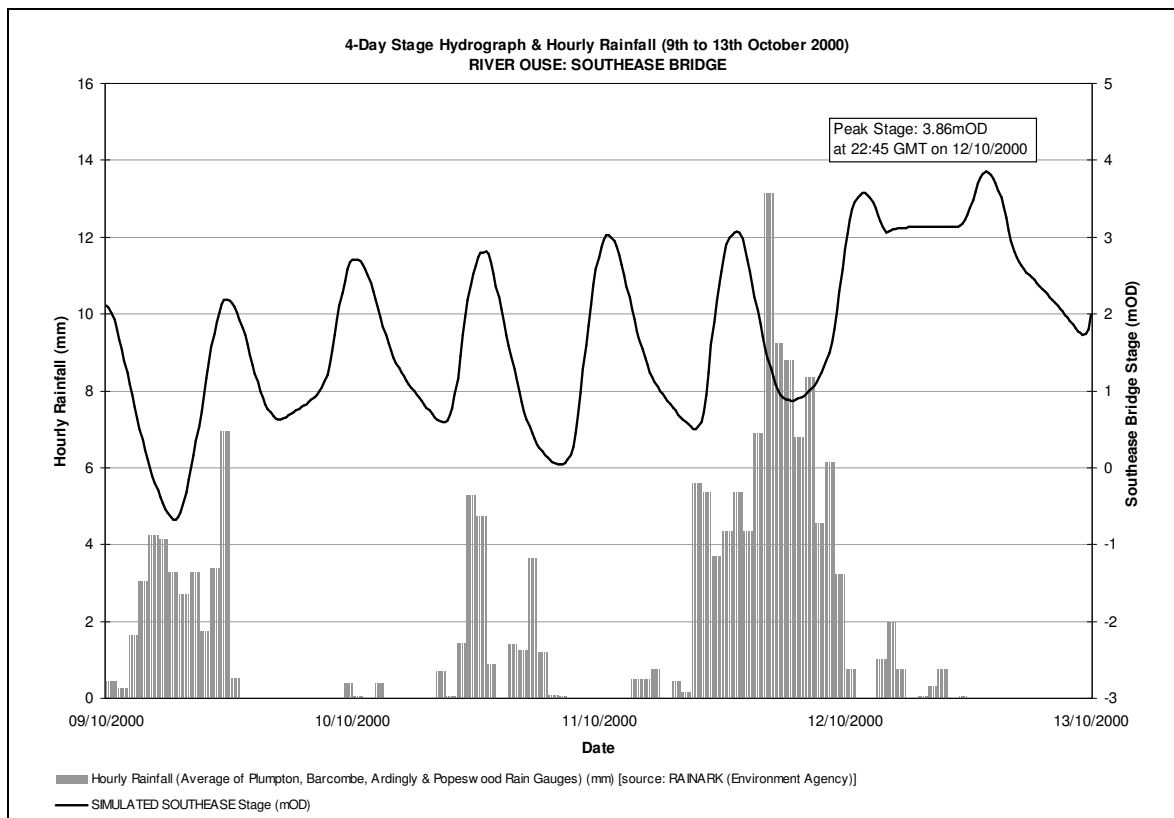


Figure E.8 4-Day stage hydrograph & hourly rainfall (9th - 13th October 2000) at Southease Bridge

E.2.5.4 Newhaven (Tide)

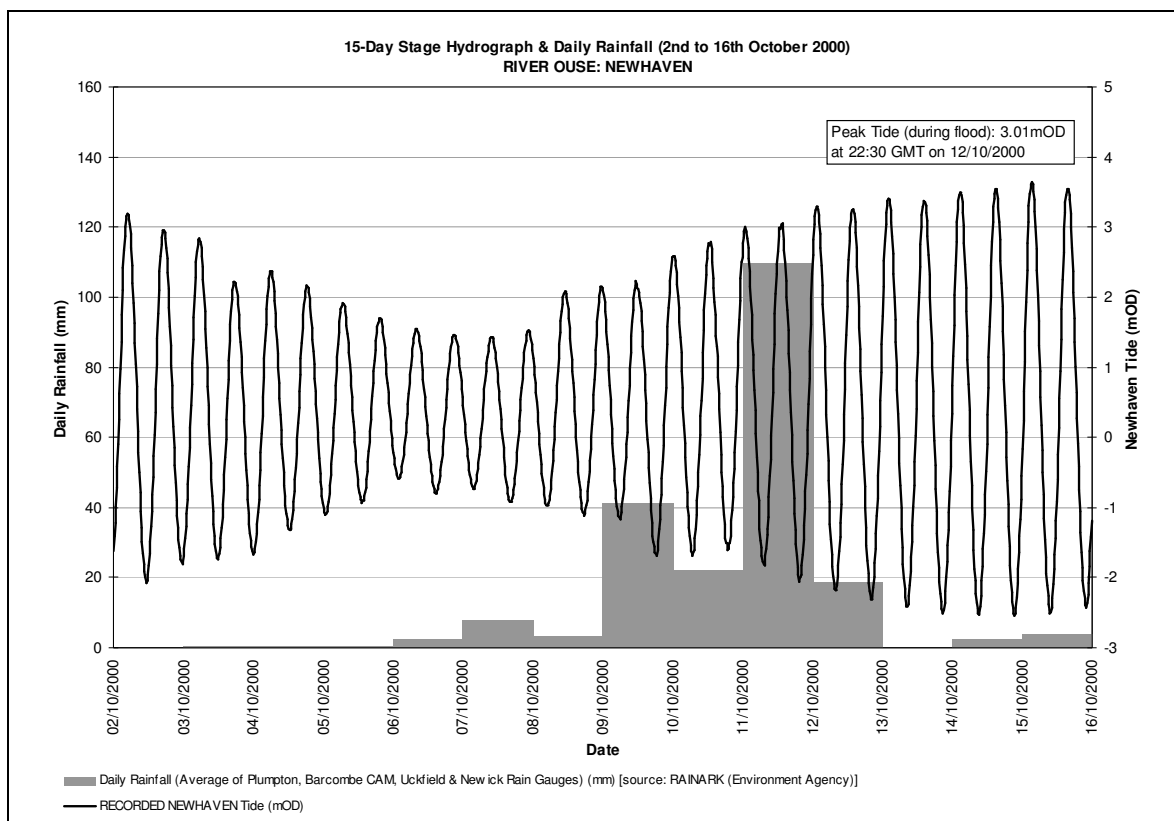


Figure E.9 15-Day tide hydrograph & daily rainfall (2nd – 16th October 2000) at Newhaven

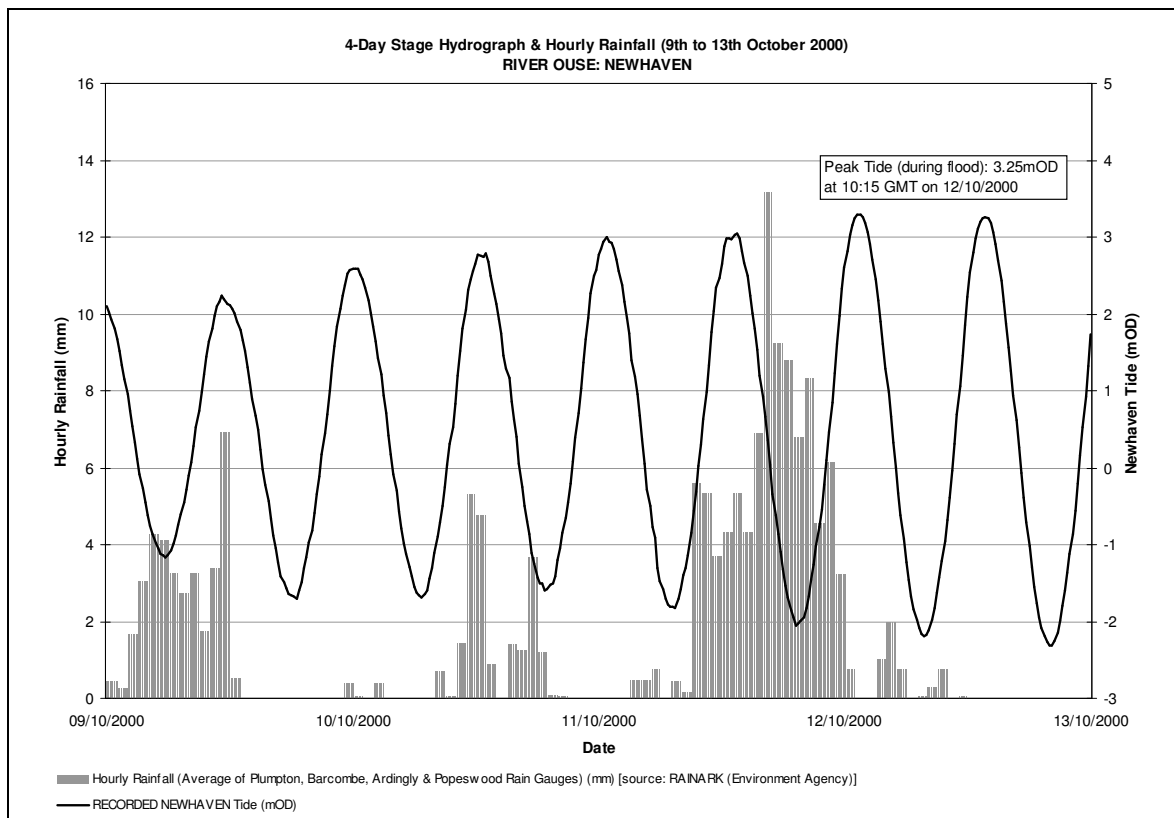


Figure E.10 4-Day tide hydrograph & hourly rainfall (9th - 13th October 2000) at Newhaven

E.2.5.5 Newhaven (Surge)

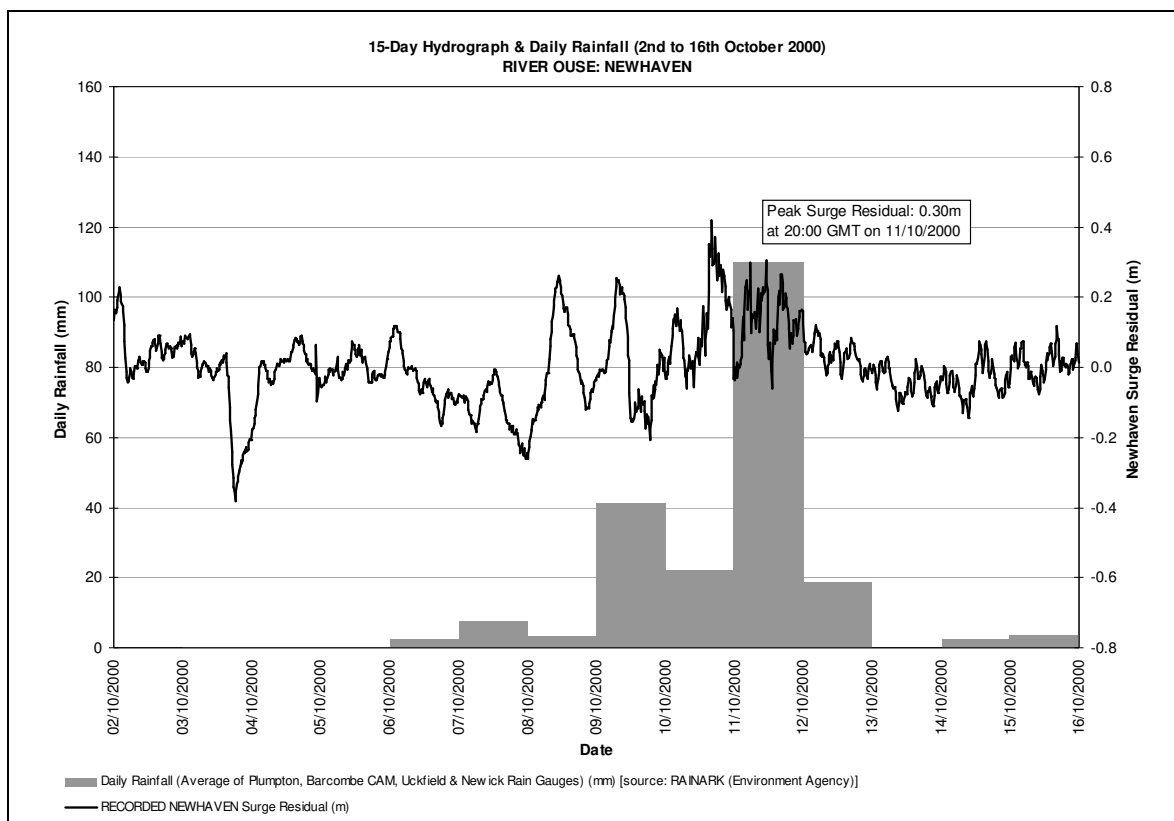


Figure E.11 15-Day surge hydrograph & daily rainfall (2nd – 16th October 2000) at Newhaven

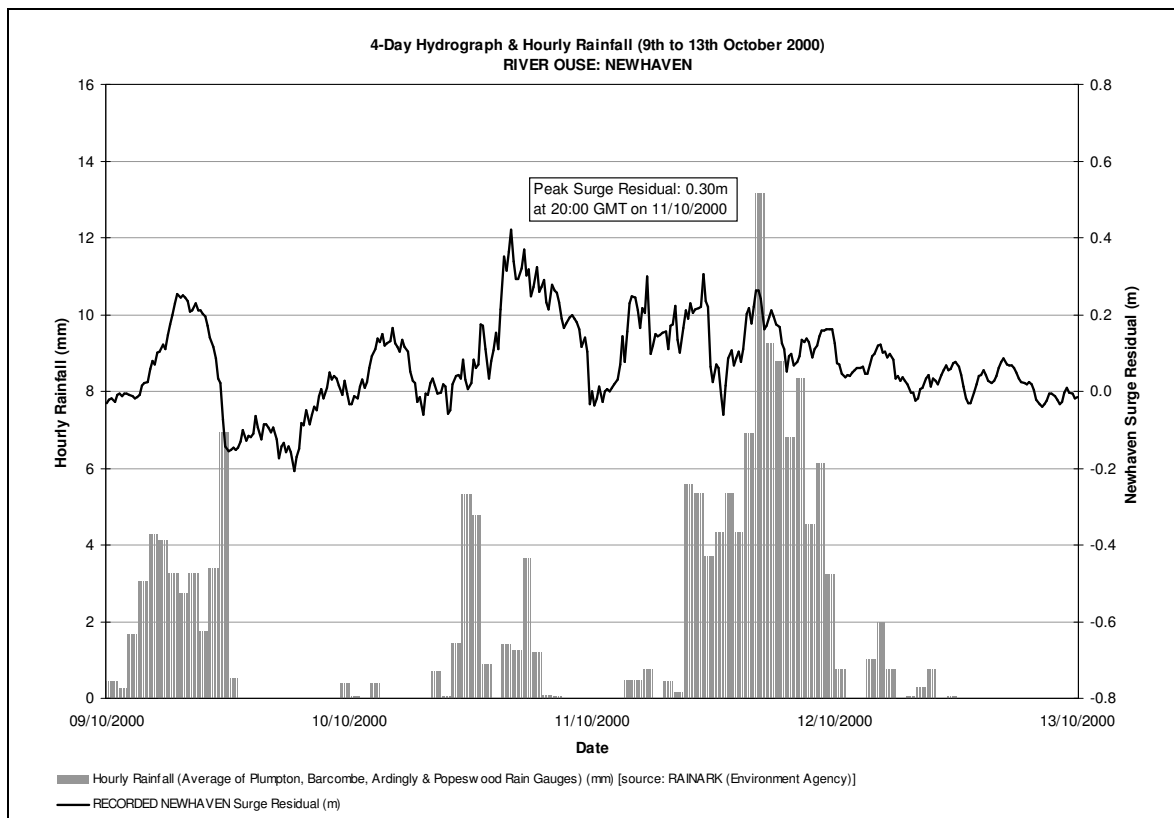


Figure E.12 4-Day surge hydrograph & hourly rainfall (9th - 13th October 2000) at Newhaven

E.2.6 Hydrographs of Flow & Tide Interaction at Lewes

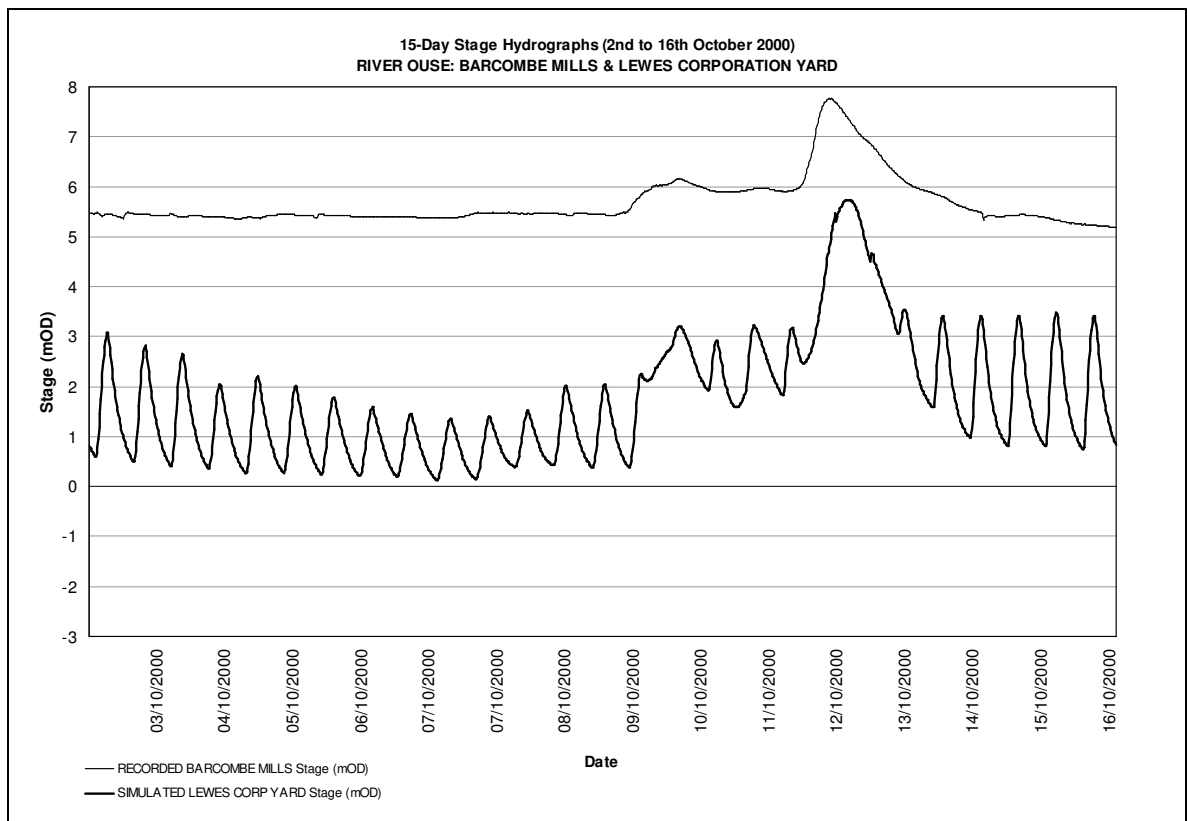


Figure E.13 15-Day stage hydrographs (2nd – 16th October 2000) at Barcombe Mills & Lewes Corporation Yard

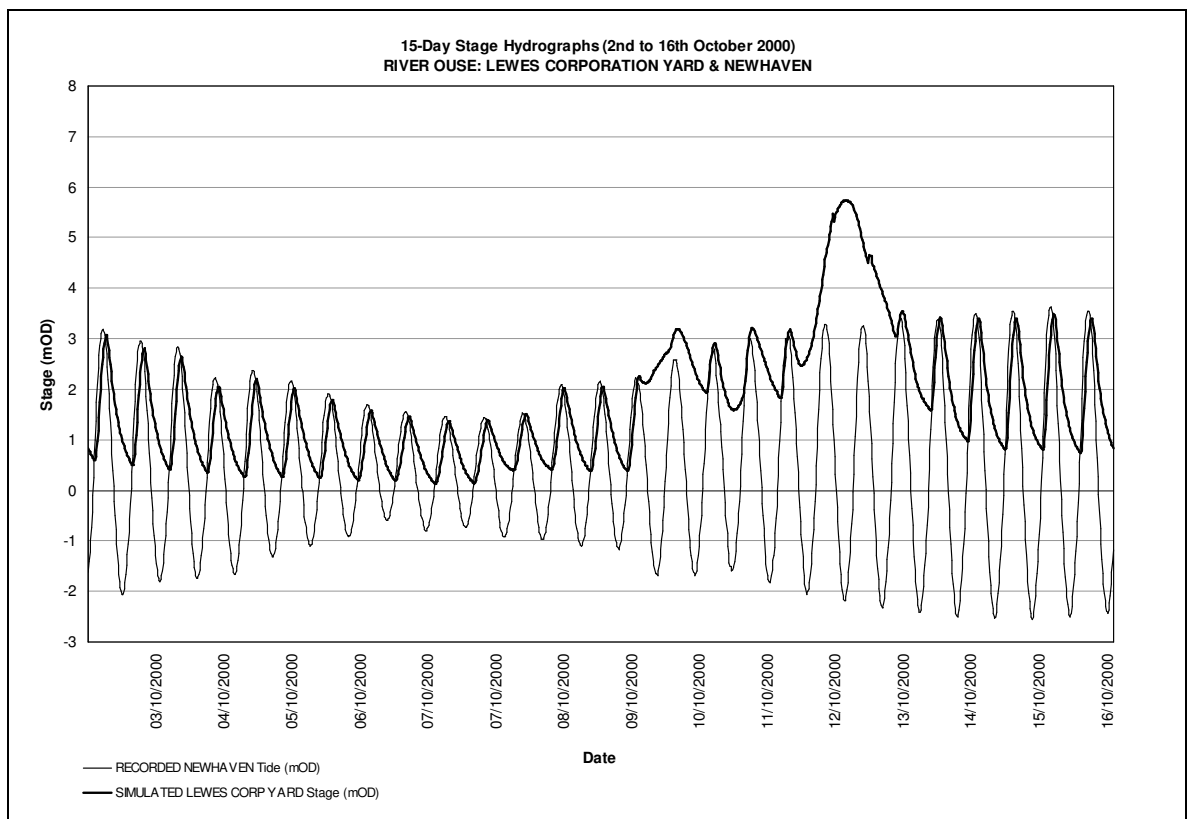


Figure E.14 15-Day stage hydrographs (2nd – 16th October 2000) at Lewes Corporation Yard & Newhaven

APPENDIX F STATISTICAL DEPENDENCE

F.1 Dependence Worked Example

F.1.1 Data Preparation

A dependence analysis is based on two simultaneously recorded variables of interest, known as observational pairs. For the purposes of this example, a short dataset was used, consisting of two concurrently recorded 40-day daily maxima records from the two boundary sites for the tidal reach of the Lower Ouse of Barcombe Mills flow and Newhaven tide. In practice, this dataset is too short to accurately calculate a value of dependence; Hawkes & Svensson (2003) suggest that a minimum of five years of concurrent observational pairs are required to accurately obtain a value of dependence.

A daily maxima series of river flow and tide was extracted from the available 15-minute data series for Barcombe Mills and Newhaven, for the 24-hour water day 09:00-09:00GMT. This process produced a series of 40 observational pairs of daily maxima recordings (Table F.1). The dataset did not include any missing data points, and was quality checked for any inaccurate or suspect recordings. In practice, the problem of missing or inaccurate data can have a profound effect on the dependence function, thus a rigorous data preparation regime prior to the calculation phase is normally required.

F.1.2 Threshold Selection

The basis of dependence theory is the probability of exceedance of a threshold level (x^*, y^*) for each variable (X, Y) , determining which of the observed values can be classed as extreme. The dependence measure χ can be estimated from any threshold level. The selection of x^* and y^* however is determined by two requirements: firstly to have enough data points above the threshold to be able to determine dependence, and secondly for the threshold to be high enough to regard the values as extreme. The threshold values are also selected for each variable independently from the other and from the point of interest.

For the Barcombe Mills flow series, the threshold was based upon the observed data from the Barcombe gauge, rather than from the point of interest (in this case Lewes). Similarly, the threshold value for the Newhaven series was selected from historic occurrence of extreme values at the Newhaven gauge.

Table F.1 Example observational pairs of daily maxima Barcombe Mills flow and Newhaven tide

Water Day Series No	X Daily Maxima Flow (m³/s)	Y Daily Maxima Tide (mCD)
1	0.186	5.105
2	0.182	4.957
3	0.164	5.121
4	0.164	5.498
5	3.360	6.424
6	6.680	6.441
7	3.600	6.320
8	1.600	6.732
9	2.070	6.866
10	12.100	7.297
11	4.580	6.987
12	2.420	7.005
13	1.830	7.405
14	0.977	6.541
15	1.010	6.308
16	0.561	5.736
17	0.490	6.074
18	0.635	5.493
19	0.387	6.077
20	2.060	6.134
21	2.350	6.304
22	6.600	7.222
23	1.700	6.466
24	1.100	6.940
25	0.635	6.831
26	1.090	6.565
27	0.945	6.337
28	1.290	6.097
29	1.590	5.748
30	0.807	5.469
31	0.534	5.177
32	0.434	4.771
33	0.387	4.994
34	0.293	5.473
35	0.293	5.893
36	0.268	6.290
37	0.304	6.710
38	0.262	6.832
39	0.252	7.012
40	0.223	6.981

Figure F.1 shows a scatter plot of pairs of daily maxima values from the Barcombe Mills and Newhaven datasets, with selected threshold levels for each variable. From the observational pairs, the threshold values were selected as $x^* = 6.0 \text{ m}^3/\text{s}$ for variable X , and $y^* = 7.0 \text{ mCD}$ for variable Y . The values located in the shaded upper right-hand section of the chart exceed *both* of the selected x^* and y^* thresholds, and thus satisfied the extreme criteria required to calculate the dependence measure χ .

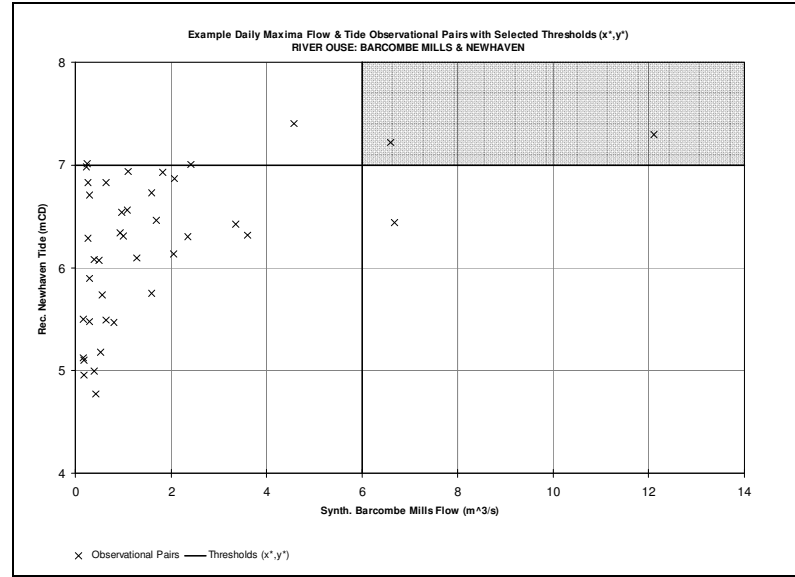


Figure F.1 Scatter plot of example threshold levels for daily maxima flow at Barcombe Mills and daily maxima tide at Newhaven

The threshold selection is a result of discretion and experience, provided that the threshold requirements are met. For example, setting the threshold value above the maximum value in the series would produce a zero dependence answer; setting the value to select only the extreme values provides enough points to successfully calculate a value of dependence. In practice, for an accurate calculation of dependence using a larger dataset (minimum of five years concurrent data), the selection of threshold values is best determined using a peaks-over-threshold (POT) approach, which selects extreme values based on a percentage of non-exceedance threshold level. This process eliminates the non-extreme peaks (i.e. the everyday maximum values), and produces a set of the most extreme peaks.

F.1.3 Calculation of the Dependence Measure χ

Recall from Chapter 6 that the dependence measure χ is defined by the following equation, for a selected threshold of u , with limits of $0 \leq u \leq 1$:

$$\chi(u) = 2 - \frac{\ln P(U \leq u, V \leq u)}{\ln P(U \leq u)} \text{ for } 0 \leq u \leq 1 \quad (F.1)$$

The basis of dependence theory is the probability of exceedance of a selected threshold level u . In practice however, the threshold u corresponds to the selected threshold levels (x^*, y^*) for the two observed series (X, Y) . The level of dependence is then calculated not just from the extremes of one variable, but also from the simultaneous occurrence of extreme values from *both* variables. This can be achieved by counting the observational pairs of (X, Y) where *only one* variable exceeds its individual threshold level x^* or y^* when the other does not, and where *neither* variable simultaneously exceed their individual threshold levels. This can be undertaken by substituting for equation F.1:

$$P(U \leq u, V \leq u) = \frac{\text{Number of } (X, Y) \text{ such that } X \leq x^* \text{ and } Y \leq y^*}{\text{Total number of } (X, Y)} \quad (F.2)$$

and:

$$\ln P(U \leq u) = \frac{1}{2} \ln \left[\frac{\text{Number of } X \leq x^*}{\text{Total number of } X} \cdot \frac{\text{Number of } Y \leq y^*}{\text{Total number of } Y} \right] \quad (F.3)$$

Firstly, to calculate $P(U \leq u, V \leq u)$ from equation F.2, the initial step is to count the total number of (X, Y) observation pairs, together with the number of pairs of (X, Y) which satisfy $X \leq x^*$ and $Y \leq y^*$ simultaneously. From the example dataset, there were 40 pairs of (X, Y) , and 34 pairs of (X, Y) which satisfied $X \leq x^*$ and $Y \leq y^*$. It is important to highlight that this number of 34 pairs included only the observation pairs of (X, Y) which satisfied the simultaneous criteria $X \leq x^*$ and $Y \leq y^*$, as dependence is calculated not just from the extremes of one variable, but from the occurrence of extreme values from both variables at the same time. Therefore, at this stage the calculation does not include any of the other possible combination pairs of $X \geq x^*$ and $Y \geq y^*$, $X \leq x^*$ and $Y \geq y^*$, or $X \geq x^*$ and $Y \leq y^*$.

This can be demonstrated through the example data reproduced in Table F.2 where the observational pairs are displayed that satisfy all possible criteria. There are 2 observational pairs where both variables simultaneously exceeded their thresholds ($X \geq x^*$ and $Y \geq y^*$), and 4 pairs where only one variable exceeded their threshold but the other did not (either $X \leq x^*$ and $Y \geq y^*$, or $X \geq x^*$ and $Y \leq y^*$). This left 34

observational pairs where neither variable simultaneously exceeded their threshold ($X \leq x^*$ and $Y \leq y^*$). Thus:

$$P(U \leq u, V \leq u) = \frac{\text{Number of } (X, Y) \text{ such that } X \leq x^* \text{ and } Y \leq y^*}{\text{Total number of } (X, Y)}$$

$$= \frac{34}{40} = 0.85$$

Secondly, to calculate $\ln P(U \leq u)$ from equation F.3, the number of observation pairs of (X, Y) , from a total number of 40, which satisfied $X \leq x^*$ and $Y \leq y^*$ independently from each other were similarly counted. From the example dataset, it can be shown that there were 37 values of X such that $X \leq x^*$, and 35 values of Y such that $Y \leq y^*$. Thus:

$$\ln P(U \leq u) = \frac{1}{2} \ln \left[\frac{\text{Number of } X \leq x}{\text{Total number of } X} \cdot \frac{\text{Number of } Y \leq y^*}{\text{Total number of } Y} \right]$$

$$= \frac{1}{2} \ln \left[\frac{37}{40} \cdot \frac{35}{40} \right] = -0.106$$

Substituting into equation F.1 provided:

$$\chi = 2 - \frac{\ln P(U \leq u, V \leq u)}{\ln P(U \leq u)} = 2 - \frac{\ln 0.85}{-0.106} = 0.467$$

Table F.2 Example threshold exceedance of observational pairs

Water Day Series No	X Daily Maxima Flow (m ³ /s)	Y Daily Maxima Tide (mCD)
1	0.186	5.105
2	0.182	4.957
3	0.164	5.121
4	0.164	5.498
5	3.360	6.424
6	6.680	6.441
7	3.600	6.320
8	1.600	6.732
9	2.070	6.866
10	12.100	7.297
11	4.580	6.987
12	2.420	7.005
13	1.830	7.405
14	0.977	6.541
15	1.010	6.308
16	0.561	5.736
17	0.490	6.074
18	0.635	5.493
19	0.387	6.077
20	2.060	6.134
21	2.350	6.304
22	6.600	7.222
23	1.700	6.466
24	1.100	6.940
25	0.635	6.831
26	1.090	6.565
27	0.945	6.337
28	1.290	6.097
29	1.590	5.748
30	0.807	5.469
31	0.534	5.177
32	0.434	4.771
33	0.387	4.994
34	0.293	5.473
35	0.293	5.893
36	0.268	6.290
37	0.304	6.710
38	0.262	6.832
39	0.252	7.012
40	0.223	6.981

Observed pair (X,Y) where only one variable exceeds their respective threshold x^* or y^* .

Observed pair (X,Y) where both variables exceed their respective thresholds x^* and y^* .

F.1.4 Interpreting χ

The dependence measure χ can be used as a percentage risk of occurrence. The value of $\chi = 0.467$ calculated from the example dataset (X, Y) means that if one of the variables (i.e. X) exceeds its (extreme) threshold (x^*) , there is a 46.7% chance that the other variable (i.e. Y) will simultaneously exceed its extreme threshold (y^*) . If each of the variables were to approach extreme levels, $\chi = 1$ would indicate total (100%) dependence and $\chi = 0$ total (0%) independence.

This example produced a high level of dependence between the two variables. This interprets as when an extreme river flow event occurs, there is nearly a 50% chance that the tide will also produce extreme levels. This high level of dependence suggests that dependence should be used to calculate the joint probability of occurrence of water levels from the combination of river flows and tides rather than just river flows or tides alone. However, as this is a sample dataset, the results are extremely unlikely to be accurate. Such a high level of dependence between tides and river flows would be unusual as they are not governed by the same drivers; tides are predominantly generated by astronomical movements of the earth, sun and moon, whereas extreme river flows are predominantly generated by meteorological events. Dependence instead is more likely to exist between river flow and the meteorological component of the tide (i.e. surge) which may both be caused by the same low pressure weather system.

F.2 Daily Maxima Dependence Datasets

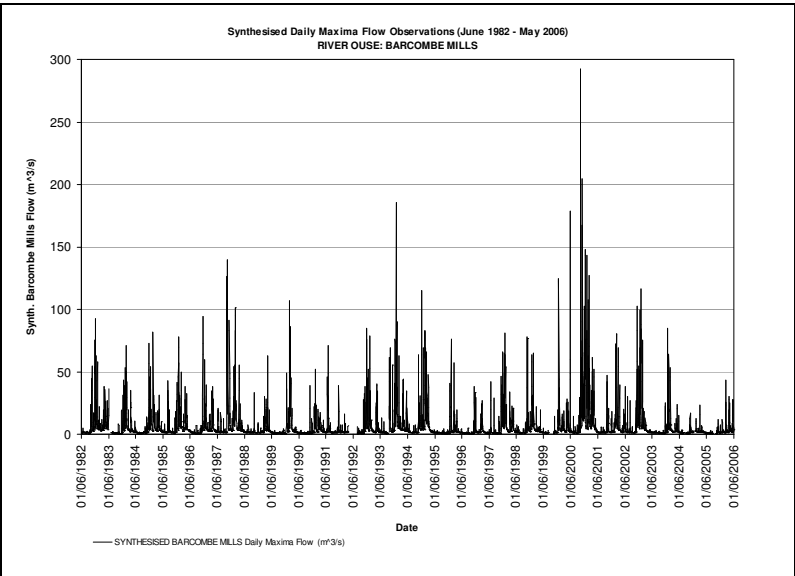


Figure F.2 Synthesised daily maxima flow observations at Barcombe Mills (May 1982 - June 2006)

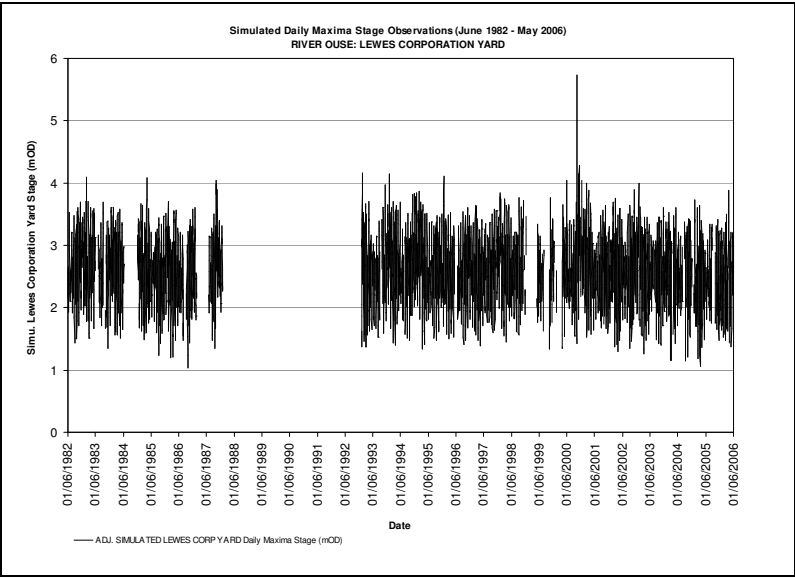


Figure F.3 Simulated daily maxima stage observations at Lewes Corporation Yard (May 1982 - June 2006)

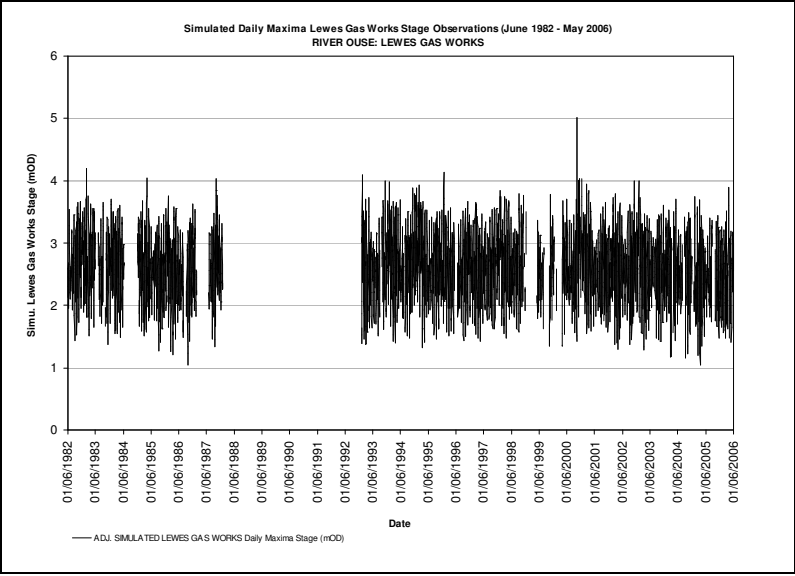


Figure F.4 Simulated daily maxima stage observations at Lewes Gas Works (May 1982 - June 2006)

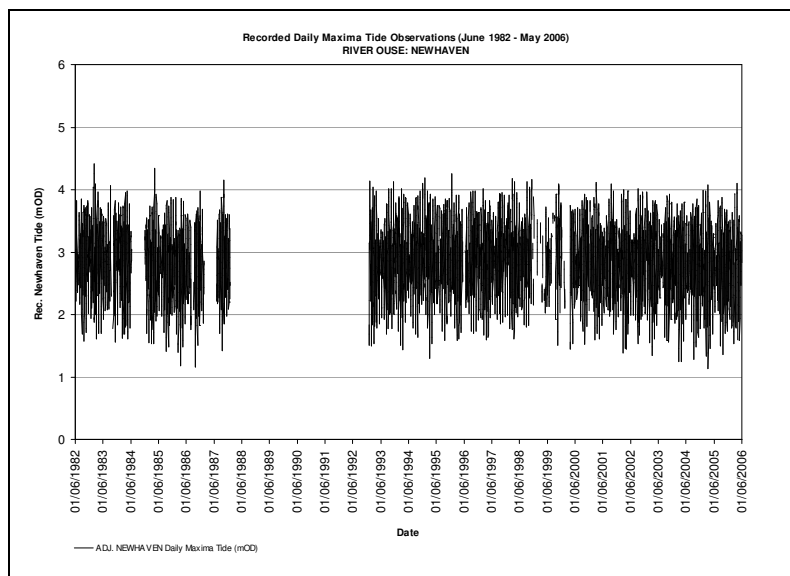


Figure F.5 Recorded daily maxima tide observations at Newhaven (May 1982 - June 2006)

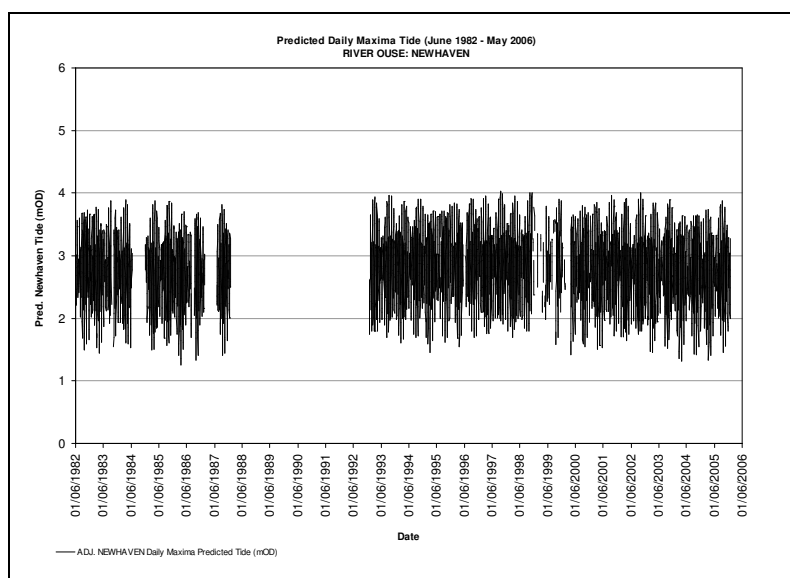


Figure F.6 Predicted daily maxima tide at Newhaven (May 1982 - June 2006)

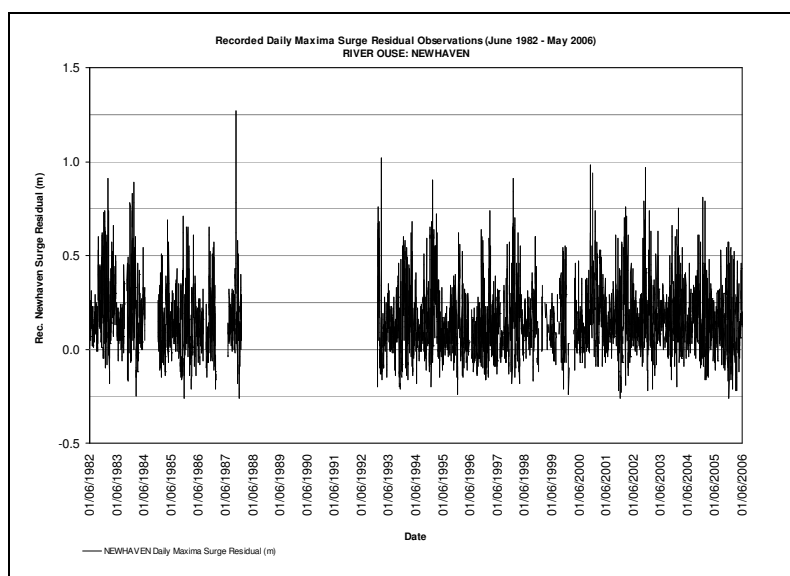


Figure F.7 Recorded daily maxima surge observations at Newhaven (May 1982 - June 2006)

APPENDIX G JOINT PROBABILITY

G.1 Daily Exceedance Probabilities

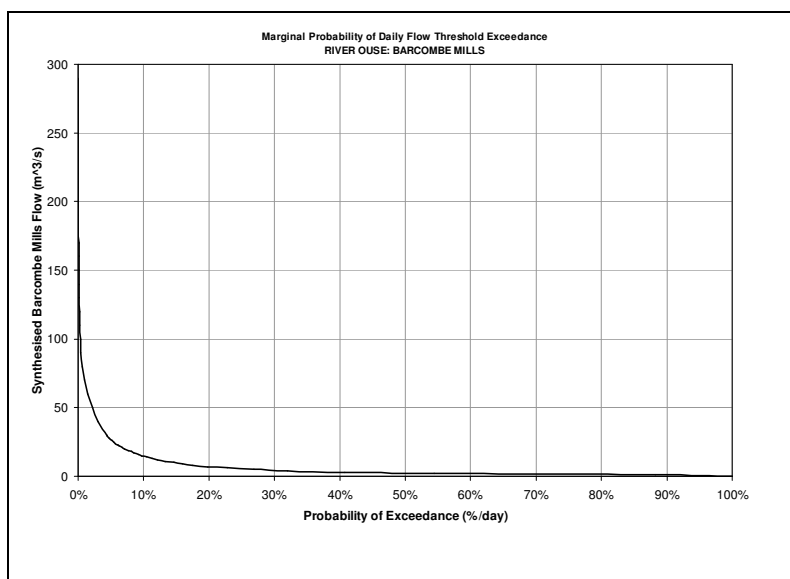


Figure G.1 Daily probability of synthesised flow threshold exceedance at Barcombe Mills (1981-2006)

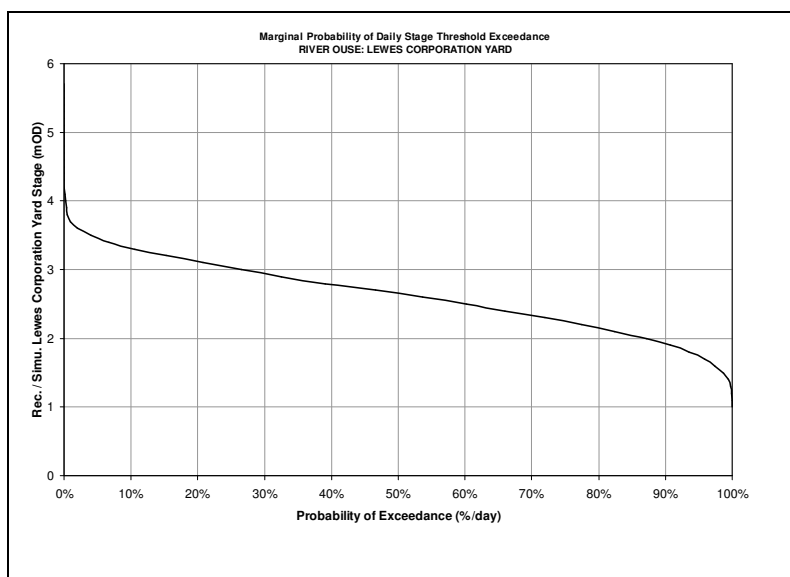


Figure G.2 Daily probability of simulated stage threshold exceedance at Lewes Corporation Yard (1982-2006)

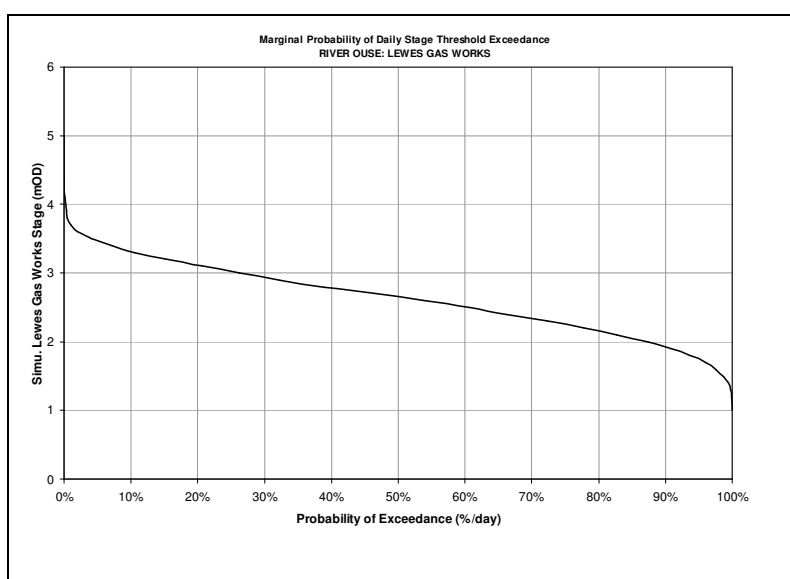


Figure G.3 Daily probability of simulated stage threshold exceedance at Lewes Gas Works (1982-2006)

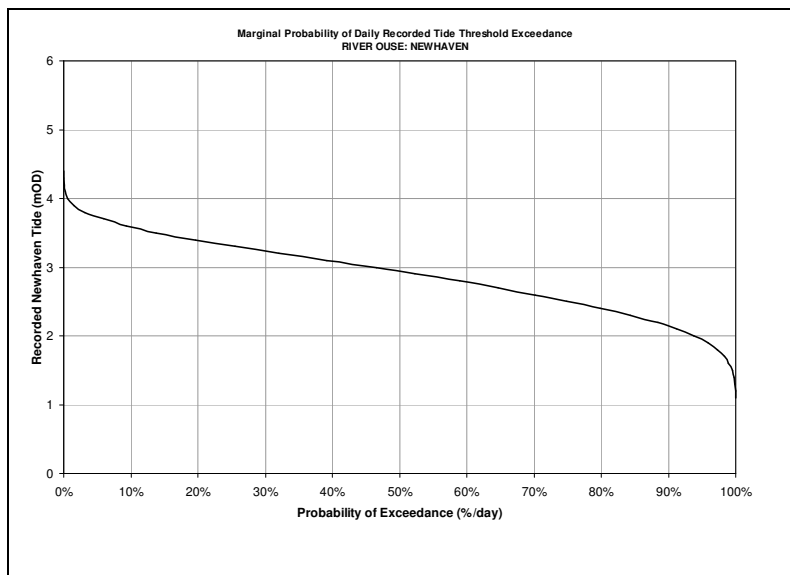


Figure G.4 Daily probability of recorded tide threshold exceedance at Newhaven (1982-2006)

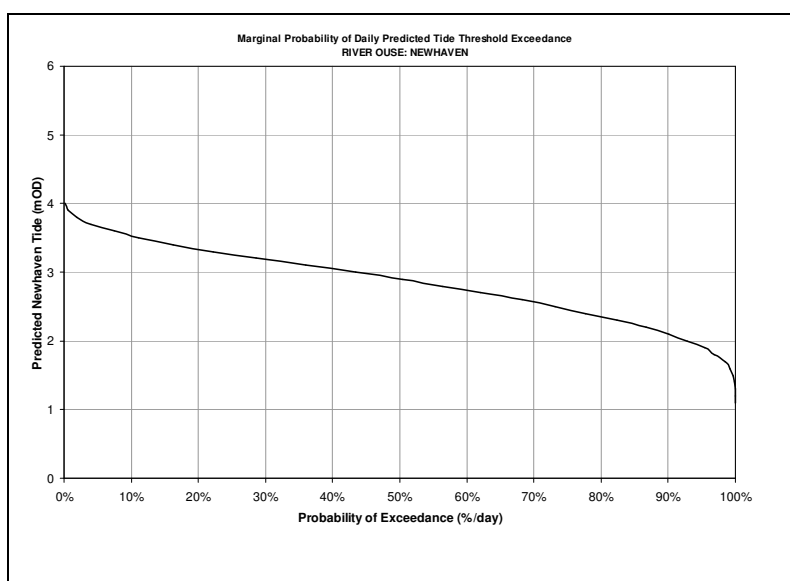


Figure G.5 Daily probability of predicted tide threshold exceedance at Newhaven (1982-2006)

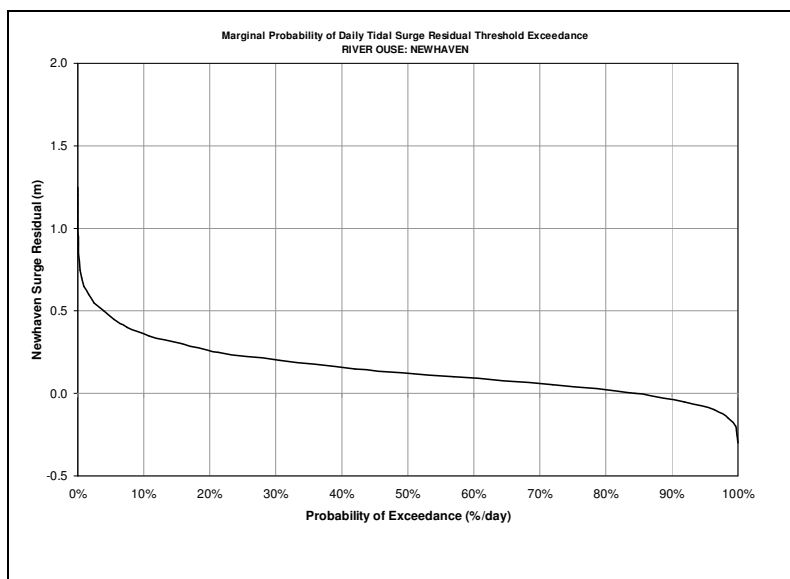


Figure G.6 Daily probability of tidal surge threshold exceedance at Newhaven (1982-2006)

G.2 Comparison of Joint Return Period Methods

Table G.1 shows joint return periods T (in the shaded area) of the threshold u for variables with identical return periods T_u and different levels of dependence χ , calculated using equation 7.6 (Svensson and Jones, 2000).

$$T = \frac{1}{\left(1 - \frac{1}{T_u}\right)^{2-\chi} + \left(\frac{2}{T_u}\right) - 1} \quad (7.6)$$

Table G.1 Joint return periods T (shaded area) for combined events with identical return periods T_u with different levels of dependence χ , calculated using equation 7.6

T_u	Dependence χ										
	0	0.1	0.2	0.3	0.4	0.5	0.6	0.7	0.8	0.9	1
2	4	3.7	3.5	3.2	3	2.8	2.6	2.5	2.3	2.1	2
5	25	18.4	14.4	11.9	10	8.7	7.6	6.7	6.1	5.5	5
10	100	53.8	36.7	27.8	22.3	18.6	15.9	13.9	12.3	11	10
25	625	186.2	109.2	77.2	59.6	48.5	40.9	35.3	31.1	27.7	25
50	2500	426.9	233.2	160.3	122.1	98.5	82.6	71	62.3	55.5	50
100	10000	921.2	482.6	326.8	247	198.5	165.9	142.5	124.8	111	100
200	40000	1918	982.3	660.1	497	398.5	332.6	285.3	249.8	222.2	200

Table G.2 shows joint return periods T (in the shaded area) of the threshold u for variables with identical return periods T_u and different levels of dependence χ , calculated using equation 7.7 (e.g. Hawkes, 2004).

$$T = \frac{T_u}{\chi} \quad (7.7)$$

Table G.2 Joint return periods T (shaded area) for combined events with identical return periods T_u with different levels of dependence χ , calculated using equation 7.7

T_u	Dependence χ										
	0	0.1	0.2	0.3	0.4	0.5	0.6	0.7	0.8	0.9	1
2	-	20	10	6.7	5	4	3.3	2.9	2.5	2.2	2
5	-	50	25	16.7	12.5	10	8.3	7.1	6.3	5.6	5
10	-	100	50	33.3	25	20	16.7	14.3	12.5	11.1	10
25	-	250	125	83.3	62.5	50	41.7	35.7	31.3	27.8	25
50	-	500	250	166.7	125	100	83.3	71.4	62.5	55.6	50
100	-	1000	500	333.3	250	200	166.7	142.9	125	111.1	100
200	-	2000	1000	666.7	500	400	333.3	285.7	250	222.2	200

G.3 Interpretation of the Dependence Measure

G.3.1 Calculation of Extreme Joint Return Periods using χ

The following tables (Table G.3 to Table G.14) illustrate the relative effects of the dependence measure χ on the calculation of the joint return period T using equation 7.11 for non-identical return periods (T_x, T_y) , ranging from fully-independent to fully-dependent variables (X, Y) :

$$T = \frac{1}{\left(1 - \frac{1}{\sqrt{T_x \cdot T_y}}\right)^{2-\chi} + \left(\frac{2}{\sqrt{T_x \cdot T_y}}\right) - 1} \quad (7.11)$$

It was assumed that a joint event could be classed as extreme if both variables exceeded their given thresholds, and that the dependence measure χ could be applied to all threshold levels.

Table G.3 Joint return periods T (shaded area) for fully-independent ($\chi=0$) variables with return periods T_x and T_y

		Return Periods T_y (Years)						
		2	5	10	25	50	100	200
Return Periods T_x (Years)	2	4.00	10.00	20.00	50.00	100.00	200.00	400.00
	5	10.00	25.00	50.00	125.00	250.00	500.00	1000.00
	10	20.00	50.00	100.00	250.00	500.00	1000.00	2000.00
	25	50.00	125.00	250.00	625.00	1250.00	2500.00	5000.00
	50	100.00	250.00	500.00	1250.00	2500.00	5000.00	10000.00
	100	200.00	500.00	1000.00	2500.00	5000.00	10000.00	20000.00
	200	400.00	1000.00	2000.00	5000.00	10000.00	20000.00	40000.00

Table G.4 Joint return periods T (shaded area) for partially-dependent ($\chi=0.01$) variables with return periods T_x and T_y

		Return Periods T_y (Years)						
		2	5	10	25	50	100	200
Return Periods T_x (Years)	2	3.97	9.83	19.41	47.34	92.13	177.51	337.49
	5	9.83	24.14	47.34	113.93	218.65	413.63	768.41
	10	19.41	47.34	92.13	218.65	413.63	768.41	1396.32
	25	47.34	113.93	218.65	506.00	933.74	1683.37	2954.73
	50	92.13	218.65	413.63	933.74	1683.37	2954.73	5037.57
	100	177.51	413.63	768.41	1683.37	2954.73	5037.57	8335.81
	200	337.49	768.41	1396.32	2954.73	5037.57	8335.81	13400.04

Table G.5 Joint return periods T (shaded area) for partially-dependent ($\chi=0.1$) variables with return periods T_x and T_y

		Return Periods T_y (Years)						
		2	5	10	25	50	100	200
Return Periods T_x (Years)	2	3.73	8.47	15.28	31.92	53.82	88.06	140.03
	5	8.47	18.37	31.92	63.27	102.54	161.69	248.87
	10	15.28	31.92	53.82	102.54	161.69	248.87	375.39
	25	31.92	63.27	102.54	186.23	284.65	426.94	630.80
	50	53.82	102.54	161.69	284.65	426.94	630.80	921.21
	100	88.06	161.69	248.87	426.94	630.80	921.21	1333.57
	200	140.03	248.87	375.39	630.80	921.21	1333.57	1917.99

Table G.6 Joint return periods T (shaded area) for partially-dependent ($\chi=0.2$) variables with return periods T_x and T_y

		Return Periods T_y (Years)						
		2	5	10	25	50	100	200
Return Periods T_x (Years)	2	3.48	7.30	12.30	23.35	36.70	56.31	84.70
	5	7.30	14.45	23.35	42.22	64.34	96.26	141.92
	10	12.30	23.35	36.70	64.34	96.26	141.92	206.92
	25	23.35	42.22	64.34	109.23	160.41	233.19	336.41
	50	36.70	64.34	96.26	160.41	233.19	336.41	482.61
	100	56.31	96.26	141.92	233.19	336.41	482.61	689.55
	200	84.70	141.92	206.92	336.41	482.61	689.55	982.31

Table G.7 Joint return periods T (shaded area) for partially-dependent ($\chi=0.3$) variables with return periods T_x and T_y

		Return Periods T_y (Years)						
		2	5	10	25	50	100	200
Return Periods T_x (Years)	2	3.25	6.39	10.25	18.35	27.77	41.31	60.62
	5	6.39	11.86	18.35	31.61	46.80	68.44	99.17
	10	10.25	18.35	27.77	46.80	68.44	99.17	142.73
	25	18.35	31.61	46.80	77.19	111.57	160.30	229.26
	50	27.77	46.80	68.44	111.57	160.30	229.26	326.84
	100	41.31	68.44	99.17	160.30	229.26	326.84	464.88
	200	60.62	99.17	142.73	229.26	326.84	464.88	660.12

Table G.8 Joint return periods T (shaded area) for partially-dependent ($\chi=0.4$) variables with return periods T_x and T_y

		Marginal Return Periods T_y (Years)						
		2	5	10	25	50	100	200
Marginal Return Periods T_x (Years)	2	3.03	5.66	8.75	15.07	22.29	32.57	47.15
	5	5.66	10.02	15.07	25.21	36.72	53.04	76.15
	10	8.75	15.07	22.29	36.72	53.04	76.15	108.87
	25	15.07	25.21	36.72	59.62	85.48	122.06	173.82
	50	22.29	36.72	53.04	85.48	122.06	173.82	247.03
	100	32.57	53.04	76.15	122.06	173.82	247.03	350.58
	200	47.15	76.15	108.87	173.82	247.03	350.58	497.02

Table G.9 Joint return periods T (shaded area) for partially-dependent ($\chi=0.5$) variables with return periods T_x and T_y

		Return Periods T_y (Years)						
		2	5	10	25	50	100	200
Return Periods T_x (Years)	2	2.83	5.05	7.62	12.76	18.58	26.84	38.54
	5	5.05	8.65	12.76	20.93	30.18	43.26	61.77
	10	7.62	12.76	18.58	30.18	43.26	61.77	87.96
	25	12.76	20.93	30.18	48.53	69.23	98.52	139.93
	50	18.58	30.18	43.26	69.23	98.52	139.93	198.51
	100	26.84	43.26	61.77	98.52	139.93	198.51	281.35
	200	38.54	61.77	87.96	139.93	198.51	281.35	398.50

Table G.10 Joint return periods T (shaded area) for partially-dependent ($\chi=0.6$) variables with return periods T_x and T_y

		Return Periods T_y (Years)						
		2	5	10	25	50	100	200
Return Periods T_x (Years)	2	2.64	4.55	6.72	11.03	15.91	22.81	32.57
	5	4.55	7.59	11.03	17.87	25.59	36.50	51.93
	10	6.72	11.03	15.91	25.59	36.50	51.93	73.76
	25	11.03	17.87	25.59	40.90	58.15	82.56	117.08
	50	15.91	25.59	36.50	58.15	82.56	117.08	165.89
	100	22.81	36.50	51.93	82.56	117.08	165.89	234.93
	200	32.57	51.93	73.76	117.08	165.89	234.93	332.56

Table G.11 Joint return periods T (shaded area) for partially-dependent ($\chi=0.7$) variables with return periods T_x and T_y

		Return Periods T_y (Years)						
		2	5	10	25	50	100	200
Return Periods T_x (Years)	2	2.46	4.12	5.99	9.71	13.89	19.81	28.17
	5	4.12	6.75	9.71	15.58	22.19	31.55	44.78
	10	5.99	9.71	13.89	22.19	31.55	44.78	63.49
	25	9.71	15.58	22.19	35.32	50.11	71.03	100.62
	50	13.89	22.19	31.55	50.11	71.03	100.62	142.46
	100	19.81	31.55	44.78	71.03	100.62	142.46	201.63
	200	28.17	44.78	63.49	100.62	142.46	201.63	285.32

Table G.12 Joint return periods T (shaded area) for partially-dependent ($\chi=0.8$) variables with return periods T_x and T_y

		Return Periods T_y (Years)						
		2	5	10	25	50	100	200
Return Periods T_x (Years)	2	2.30	3.76	5.40	8.65	12.31	17.49	24.81
	5	3.76	6.06	8.65	13.79	19.58	27.76	39.34
	10	5.40	8.65	12.31	19.58	27.76	39.34	55.71
	25	8.65	13.79	19.58	31.06	44.01	62.31	88.20
	50	12.31	19.58	27.76	44.01	62.31	88.20	124.81
	100	17.49	27.76	39.34	62.31	88.20	124.81	176.59
	200	24.81	39.34	55.71	88.20	124.81	176.59	249.81

Table G.13 Joint return periods T (shaded area) for partially-dependent ($\chi=0.9$) variables with return periods T_x and T_y

		Return Periods T_y (Years)						
		2	5	10	25	50	100	200
Return Periods T_x (Years)	2	2.14	3.44	4.90	7.79	11.04	15.64	22.15
	5	3.44	5.48	7.79	12.35	17.50	24.78	35.07
	10	4.90	7.79	11.04	17.50	24.78	35.07	49.62
	25	7.79	12.35	17.50	27.71	39.22	55.49	78.50
	50	11.04	17.50	24.78	39.22	55.49	78.50	111.04
	100	15.64	24.78	35.07	55.49	78.50	111.04	157.07
	200	22.15	35.07	49.62	78.50	111.04	157.07	222.15

Table G.14 Joint return periods T (shaded area) for fully-dependent ($\chi=1$) variables with return periods T_x and T_y

		Return Periods T_y (Years)						
		2	5	10	25	50	100	200
Return Periods T_x (Years)	2	2.00	3.16	4.47	7.07	10.00	14.14	20.00
	5	3.16	5.00	7.07	11.18	15.81	22.36	31.62
	10	4.47	7.07	10.00	15.81	22.36	31.62	44.72
	25	7.07	11.18	15.81	25.00	35.36	50.00	70.71
	50	10.00	15.81	22.36	35.36	50.00	70.71	100.00
	100	14.14	22.36	31.62	50.00	70.71	100.00	141.42
	200	20.00	31.62	44.72	70.71	100.00	141.42	200.00

G.3.2 Calculation of Daily Joint Probabilities using χ

A similar analysis to assess the relative effects of the dependence measure χ on the calculation of the joint probabilities was undertaken using equation 7.15 for non-identical probabilities $P(X > x^*)$ and $P(Y > y^*)$, ranging from fully-independent to fully-dependent variables (X, Y) :

$$P(U > u, V > u) =$$

$$\left[1 - \sqrt{P(X > x^*) \cdot P(Y > y^*)}\right]^{2-\chi} + 2\left[\sqrt{P(X > x^*) \cdot P(Y > y^*)}\right] - 1 \quad (7.15)$$

The resultant graphs are too large to be reproduced here. Please refer to the accompanying CD, under ‘Joint Probability Analysis’.

G.4 Bivariate Joint Probability Tables

G.4.1 Bivariate Joint Return Periods

Table G.15 Joint return periods T (shaded area) for partially-dependent ($\chi=0.045$) variables X (Barcombe Mills flow, m³/s) and Y (Newhaven tide, mAOD) with return periods T_x and T_y . Flow / tide magnitudes corresponding to the return periods are shown in italics.

Variable X (Barcombe Mills Flow) with Return Periods T_x (years) & Flow Magnitudes (m ³ /s)		Variable Y (Newhaven Tide) with Return Periods T_y (years) & Tide Levels (mAOD)							
		1	2	5	10	25	50	100	200
		<i>3.86</i>	<i>3.97</i>	<i>4.12</i>	<i>4.20</i>	<i>4.27</i>	<i>4.32</i>	<i>4.35</i>	<i>4.38</i>
1	<i>50.00</i>	1.00	1.98	4.80	9.25	21.52	39.88	72.20	127.31
2	<i>81.68</i>	1.98	3.88	9.25	17.57	39.88	72.20	127.31	218.08
5	<i>116.02</i>	4.80	9.25	21.52	39.88	86.93	151.89	257.68	424.27
10	<i>140.86</i>	9.25	17.57	39.88	72.20	151.89	257.68	424.27	678.82
25	<i>174.86</i>	21.52	39.88	86.93	151.89	303.53	495.07	785.23	1214.86
50	<i>202.13</i>	39.88	72.20	151.89	257.68	495.07	785.23	1214.86	1840.38
100	<i>231.04</i>	72.20	127.31	257.68	424.27	785.23	1214.86	1840.38	2740.64
200	<i>261.80</i>	127.31	218.08	424.27	678.82	1214.86	1840.38	2740.64	4026.74

G.4.2 Bivariate Daily Joint Probabilities

(see overleaf)

Table G.16 Joint daily probabilities of exceedance $P(X > x^*, Y > y^*)$ (shaded area) for partially-dependent ($\chi=0.045$) variables X (Barcombe Mills flow, m³/s) and Y (Newhaven tide, mAOD) with probabilities $P(X > x^*)$ and $P(Y > y^*)$. Flow / tide magnitudes corresponding to the daily probabilities are shown in italics.

Variable X (Barcombe Mills Flow) with Daily Probabilities of Exceedance & Flow Magnitudes (m ³ /s)		Variable Y (Newhaven Tide) with Daily Probabilities of Exceedance & Tide Levels (mAOD)													
		0.9995	0.9957	0.9729	0.9125	0.7989	0.6465	0.4651	0.2552	0.0937	0.0158	0.0007	0.0001	<0.0001	
		1.20	1.50	1.80	2.10	2.40	2.70	3.00	3.30	3.60	3.90	4.20	4.50	4.80	
0.9999	1	0.9994	0.9956	0.9729	0.9127	0.8000	0.6493	0.4704	0.2631	0.1016	0.0204	0.0018	0.0005	0.0005	
0.0432	30	0.0498	0.0496	0.0486	0.0458	0.0406	0.0336	0.0252	0.0150	0.0066	0.0018	0.0003	0.0001	0.0001	
0.0146	60	0.0191	0.0190	0.0186	0.0176	0.0157	0.0132	0.0100	0.0062	0.0029	0.0009	0.0001	0.0001	0.0001	
0.0042	90	0.0068	0.0068	0.0067	0.0063	0.0057	0.0049	0.0038	0.0025	0.0013	0.0004	0.0001	<0.0001	<0.0001	
0.0019	120	0.0037	0.0037	0.0036	0.0035	0.0032	0.0027	0.0022	0.0014	0.0008	0.0003	0.0001	<0.0001	<0.0001	
0.0010	150	0.0023	0.0023	0.0023	0.0022	0.0020	0.0017	0.0014	0.0010	0.0005	0.0002	<0.0001	<0.0001	<0.0001	
0.0006	180	0.0017	0.0017	0.0017	0.0016	0.0014	0.0013	0.0010	0.0007	0.0004	0.0001	<0.0001	<0.0001	<0.0001	
0.0002	210	0.0007	0.0007	0.0007	0.0007	0.0006	0.0006	0.0005	0.0003	0.0002	0.0001	<0.0001	<0.0001	<0.0001	
0.0001	240	0.0005	0.0005	0.0005	0.0005	0.0005	0.0004	0.0004	0.0003	0.0001	0.0001	<0.0001	<0.0001	<0.0001	
<0.0001	270	0.0005	0.0005	0.0005	0.0005	0.0005	0.0004	0.0004	0.0003	0.0001	0.0001	<0.0001	<0.0001	<0.0001	
<0.0001	300	0.0005	0.0005	0.0005	0.0005	0.0005	0.0004	0.0004	0.0003	0.0001	0.0001	<0.0001	<0.0001	<0.0001	

G.5 Trivariate Joint Probability Tables

G.5.1 Trivariate Joint Return Periods

Table G.17 Joint return periods T (shaded area) for partially-dependent ($\chi=0.338$) variables X (Barcombe Mills flow, m³/s) and Y (Newhaven surge, m) with return periods T_x and T_y . Flow / surge magnitudes corresponding to the return periods are shown in italics.

Variable X (Barcombe Mills Flow) with Return Periods T_x (years) & Flow Magnitudes (m ³ /s)		Variable Y (Newhaven Surge) with Return Periods T_y (years) & Surge Levels (m)							
		1	2	5	10	25	50	100	200
		<i>0.60</i>	<i>0.75</i>	<i>0.92</i>	<i>1.03</i>	<i>1.18</i>	<i>1.3</i>	<i>1.42</i>	<i>1.55</i>
1	<i>50.00</i>	1	1.84	3.73	6.09	11.09	16.95	25.40	37.49
2	<i>81.68</i>	1.84	3.16	6.09	9.63	16.95	25.40	37.49	54.70
5	<i>116.02</i>	3.73	6.09	11.09	16.95	28.84	42.38	61.65	88.96
10	<i>140.86</i>	6.09	9.63	16.95	25.40	42.38	61.65	88.96	127.65
25	<i>174.86</i>	11.09	16.95	28.84	42.38	69.42	99.98	143.26	204.49
50	<i>202.13</i>	16.95	25.40	42.38	61.65	99.98	143.26	204.49	291.11
100	<i>231.04</i>	25.40	37.49	61.65	88.96	143.26	204.49	291.11	413.64
200	<i>261.80</i>	37.49	54.70	88.96	127.65	204.49	291.11	413.64	586.94

Table G.18 Joint return periods T (shaded area) for independent ($\chi=0$) variables X (Barcombe Mills flow, m³/s) and Y (Newhaven tide, mAOD) with return periods T_x and T_z . Flow / tide magnitudes corresponding to the return periods are shown in italics.

Variable X (Barcombe Mills Flow) with Return Periods T_x (years) & Flow Magnitudes (m ³ /s)		Variable Y (Newhaven Tide) with Return Periods T_z (years) & Tide Levels (mAOD)							
		1	2	5	10	25	50	100	200
		<i>3.86</i>	<i>3.97</i>	<i>4.12</i>	<i>4.20</i>	<i>4.27</i>	<i>4.32</i>	<i>4.35</i>	<i>4.38</i>
1	<i>50.00</i>	1	2	5	10	25	50	100	200
2	<i>81.68</i>	2	4	10	20	50	100	200	400
5	<i>116.02</i>	5	10	25	50	125	250	500	1000
10	<i>140.86</i>	10	20	50	100	250	500	1000	2000
25	<i>174.86</i>	25	50	125	250	625	1250	2500	5000
50	<i>202.13</i>	50	100	250	500	1250	2500	5000	10000
100	<i>231.04</i>	100	200	500	1000	2500	5000	10000	20000
200	<i>261.80</i>	200	400	1000	2000	5000	10000	20000	40000

G.5.2 Trivariate Daily Joint Probabilities

(see overleaf)

Table G.19 Joint daily probabilities of exceedance $P(X > x^*, Y > y^*)$ (shaded area) for partially-dependent ($\chi=0.338$) variables X (Barcombe Mills flow, m³/s) and Y (Newhaven surge, m) with probabilities $P(X > x^*)$ and $P(Y > y^*)$. Flow / surge magnitudes corresponding to the daily probabilities are shown in italics.

Variable X (Barcombe Mills Flow) with Daily Probabilities of Exceedance & Flow Magnitudes (m ³ /s)		Variable Y (Newhaven Surge) with Daily Probabilities of Exceedance & Surge Levels (m)													
		0.8442	0.5686	0.3054	0.1578	0.0754	0.0390	0.0166	0.0056	0.0022	0.0012	0.0003	0.0002	0.0001	
		0.00	0.10	0.20	0.30	0.40	0.50	0.60	0.70	0.80	0.90	1.00	1.10	1.20	
0.9999	1	0.8530	0.6052	0.3679	0.2255	0.1357	0.0887	0.0528	0.0285	0.0169	0.0122	0.0063	0.0044	0.0034	
0.0432	30	0.0850	0.0667	0.0462	0.0317	0.0211	0.0148	0.0094	0.0054	0.0033	0.0024	0.0013	0.0009	0.0007	
0.0146	60	0.0444	0.0354	0.0250	0.0175	0.0118	0.0084	0.0054	0.0031	0.0019	0.0014	0.0007	0.0005	0.0004	
0.0042	90	0.0220	0.0178	0.0128	0.0090	0.0062	0.0044	0.0028	0.0017	0.0010	0.0007	0.0004	0.0003	0.0002	
0.0019	120	0.0144	0.0117	0.0084	0.0060	0.0041	0.0029	0.0019	0.0011	0.0007	0.0005	0.0003	0.0002	0.0001	
0.0010	150	0.0103	0.0083	0.0061	0.0043	0.0030	0.0021	0.0014	0.0008	0.0005	0.0004	0.0002	0.0001	0.0001	
0.0006	180	0.0080	0.0065	0.0047	0.0034	0.0023	0.0017	0.0011	0.0006	0.0004	0.0003	0.0002	0.0001	0.0001	
0.0002	210	0.0040	0.0033	0.0024	0.0017	0.0012	0.0008	0.0006	0.0003	0.0002	0.0001	0.0001	0.0001	<0.0001	
0.0001	240	0.0032	0.0026	0.0019	0.0014	0.0009	0.0007	0.0004	0.0003	0.0002	0.0001	0.0001	<0.0001	<0.0001	
<0.0001	270	0.0032	0.0026	0.0019	0.0014	0.0009	0.0007	0.0004	0.0003	0.0002	0.0001	0.0001	<0.0001	<0.0001	
<0.0001	300	0.0032	0.0026	0.0019	0.0014	0.0009	0.0007	0.0004	0.0003	0.0002	0.0001	0.0001	<0.0001	<0.0001	

Table G.20 Joint daily probabilities of exceedance $P(X > x^*, Y > y^*)$ (shaded area) for independent ($\chi=0$) variables X (Barcombe Mills flow, m³/s) and Y (Newhaven tide, mAOD) with probabilities $P(X > x^*)$ and $P(Y > y^*)$. Flow / tide magnitudes corresponding to the daily probabilities are shown in italics.

Variable X (Barcombe Mills Flow) with Daily Probabilities of Exceedance & Flow Magnitudes (m ³ /s)	Variable Y (Newhaven Tide) with Daily Probabilities of Exceedance & Tide Levels (mAOD)													
	0.9995	0.9957	0.9729	0.9125	0.7989	0.6465	0.4651	0.2552	0.0937	0.0158	0.0007	0.0001	<0.0001	
1.20	1.50	1.80	2.10	2.40	2.70	3.00	3.30	3.60	3.90	4.20	4.50	4.80		
0.9999	1	0.9994	0.9956	0.9728	0.9124	0.7988	0.6464	0.4651	0.2552	0.0936	0.0158	0.0007	0.0001	0.0001
0.0432	30	0.0431	0.0430	0.0420	0.0394	0.0345	0.0279	0.0201	0.0110	0.0040	0.0007	<0.0001	<0.0001	<0.0001
0.0146	60	0.0146	0.0145	0.0142	0.0133	0.0116	0.0094	0.0068	0.0037	0.0014	0.0002	<0.0001	<0.0001	<0.0001
0.0042	90	0.0042	0.0041	0.0041	0.0038	0.0033	0.0027	0.0019	0.0011	0.0004	0.0001	<0.0001	<0.0001	<0.0001
0.0019	120	0.0019	0.0019	0.0018	0.0017	0.0015	0.0012	0.0009	0.0005	0.0002	<0.0001	<0.0001	<0.0001	<0.0001
0.0010	150	0.0010	0.0010	0.0010	0.0009	0.0008	0.0006	0.0005	0.0003	0.0001	<0.0001	<0.0001	<0.0001	<0.0001
0.0006	180	0.0006	0.0006	0.0006	0.0006	0.0005	0.0004	0.0003	0.0002	0.0001	<0.0001	<0.0001	<0.0001	<0.0001
0.0002	210	0.0002	0.0002	0.0002	0.0001	0.0001	0.0001	0.0001	<0.0001	<0.0001	<0.0001	<0.0001	<0.0001	<0.0001
0.0001	240	0.0001	0.0001	0.0001	0.0001	0.0001	0.0001	<0.0001	<0.0001	<0.0001	<0.0001	<0.0001	<0.0001	<0.0001
<0.0001	270	0.0001	0.0001	0.0001	0.0001	0.0001	0.0001	<0.0001	<0.0001	<0.0001	<0.0001	<0.0001	<0.0001	<0.0001
<0.0001	300	0.0001	0.0001	0.0001	0.0001	0.0001	0.0001	<0.0001	<0.0001	<0.0001	<0.0001	<0.0001	<0.0001	<0.0001

G.6 Structure Function Tables

G.6.1 Structure Functions for Return Period Conversions

Table G.21 Structure function matrix for resultant water levels at Lewes Corporation Yard (mAOD) $Z_{x,y}$ (shaded area) from combinations of variables X (Barcombe Mills flow, m³/s) and Y (Newhaven tide, mAOD). return periods T_x and T_y corresponding to tide / flow magnitudes are shown in italics.

Variable X (Barcombe Mills Flow) with Return Periods T_x (years) & Flow Magnitudes (m ³ /s)		Variable Y (Newhaven Tide) with Return Periods T_y (years) & Tide Levels (mAOD)							
		<i>1</i>	<i>2</i>	<i>5</i>	<i>10</i>	<i>25</i>	<i>50</i>	<i>100</i>	<i>200</i>
		3.86	3.97	4.12	4.20	4.27	4.32	4.35	4.38
<i>1</i>	50.00	3.89	3.97	4.09	4.15	4.19	4.24	4.25	4.28
<i>2</i>	81.68	4.00	4.08	4.20	4.27	4.31	4.36	4.38	4.41
<i>5</i>	116.02	4.09	4.17	4.30	4.37	4.42	4.47	4.48	4.52
<i>10</i>	140.86	4.21	4.28	4.41	4.47	4.52	4.56	4.57	4.60
<i>25</i>	174.86	4.46	4.52	4.61	4.66	4.70	4.73	4.75	4.77
<i>50</i>	202.13	4.74	4.78	4.85	4.88	4.91	4.93	4.94	4.96
<i>100</i>	231.04	5.03	5.05	5.10	5.13	5.15	5.17	5.18	5.19
<i>200</i>	261.80	5.36	5.38	5.42	5.43	5.45	5.47	5.48	5.49

Table G.22 Structure function matrix for resultant water levels at Lewes Gas Works (mAOD) $Z_{x,y}$ (shaded area) from combinations of variables X (Barcombe Mills flow, m³/s) and Y (Newhaven tide, mAOD). Return periods T_x and T_y corresponding to tide / flow magnitudes are shown in italics.

Variable X (Barcombe Mills Flow) with Return Periods T_x (years) & Flow Magnitudes (m ³ /s)		Variable Y (Newhaven Tide) with Return Periods T_y (years) & Tide Levels (mAOD)							
		<i>1</i>	<i>2</i>	<i>5</i>	<i>10</i>	<i>25</i>	<i>50</i>	<i>100</i>	<i>200</i>
		3.86	3.97	4.12	4.20	4.27	4.32	4.35	4.38
<i>1</i>	50.00	3.90	3.98	4.10	4.16	4.21	4.25	4.28	4.30
<i>2</i>	81.68	3.98	4.06	4.20	4.27	4.32	4.37	4.40	4.41
<i>5</i>	116.02	4.03	4.12	4.25	4.32	4.38	4.43	4.47	4.49
<i>10</i>	140.86	4.11	4.19	4.31	4.37	4.43	4.48	4.52	4.53
<i>25</i>	174.86	4.27	4.33	4.43	4.48	4.53	4.57	4.60	4.61
<i>50</i>	202.13	4.42	4.48	4.58	4.62	4.66	4.70	4.72	4.74
<i>100</i>	231.04	4.66	4.70	4.78	4.82	4.85	4.88	4.91	4.92
<i>200</i>	261.80	4.86	4.90	4.97	5.01	5.03	5.06	5.08	5.09

G.6.2 Structure Functions for Daily Probability Conversions

(see overleaf)

Table G.23 Structure function matrix for resultant water levels at Lewes Corporation Yard (mAOD) $Z_{x,y}$ (shaded area) from combinations of variables X (Barcombe Mills flow, m^3/s) and Y (Newhaven tide, mAOD). Daily probabilities of exceedance T_x and T_y corresponding to tide / flow magnitudes are shown in italics.

Variable X (Barcombe Mills Flow) with Daily Probabilities of Exceedance & Flow Magnitudes (m^3/s)		Variable Y (Newhaven Tide) with Daily Probabilities of Exceedance & Tide Levels (mAOD)															
		<i>0.9995</i>	<i>0.9957</i>	<i>0.9729</i>	<i>0.9125</i>	<i>0.7989</i>	<i>0.6465</i>	<i>0.4651</i>	<i>0.2552</i>	<i>0.0937</i>	<i>0.0158</i>	<i>0.0007</i>	<i>0.0001</i>	<i><0.0001</i>			
		1.20	1.50	1.80	2.10	2.40	2.70	3.00	3.30	3.60	3.90	4.20	4.50	4.80			
<i>0.9999</i>	1	1.07	1.33	1.60	1.87	2.14	2.40	2.70	3.00	3.27	3.52	3.76	3.98	4.17			
<i>0.0432</i>	30	1.64	1.80	2.02	2.30	2.58	2.85	3.10	3.36	3.60	3.83	4.05	4.25	4.43			
<i>0.0146</i>	60	2.36	2.42	2.50	2.63	2.79	2.99	3.23	3.50	3.74	3.97	4.20	4.43	4.62			
<i>0.0042</i>	90	2.89	2.92	2.97	3.04	3.13	3.24	3.40	3.59	3.81	4.05	4.29	4.54	4.76			
<i>0.0019</i>	120	3.35	3.37	3.40	3.44	3.49	3.57	3.66	3.78	3.94	4.13	4.38	4.63	4.86			
<i>0.0010</i>	150	3.71	3.73	3.74	3.77	3.81	3.85	3.92	4.01	4.13	4.28	4.51	4.72	4.97			
<i>0.0006</i>	180	4.03	4.04	4.05	4.07	4.10	4.14	4.20	4.30	4.39	4.52	4.69	4.87	5.04			
<i>0.0002</i>	210	4.33	4.34	4.35	4.37	4.44	4.50	4.58	4.66	4.75	4.84	4.95	5.06	5.21			
<i>0.0001</i>	240	4.80	4.80	4.81	4.82	4.85	4.91	4.95	5.01	5.06	5.12	5.20	5.31	5.39			
<i><0.0001</i>	270	5.28	5.28	5.29	5.29	5.30	5.31	5.34	5.38	5.42	5.46	5.52	5.61	5.71			
<i><0.0001</i>	300	5.77	5.77	5.78	5.78	5.79	5.80	5.81	5.82	5.86	5.90	5.98	6.06	6.13			

Table G.24 Structure function matrix for resultant water levels at Lewes Gas Works (mAOD) $Z_{x,y}$ (shaded area) from combinations of variables X (Barcombe Mills flow, m^3/s) and Y (Newhaven tide, mAOD). Daily probabilities of exceedance T_x and T_y corresponding to tide / flow magnitudes are shown in italics.

Variable X (Barcombe Mills Flow) with Daily Probabilities of Exceedance & Flow Magnitudes (m³/s)			Variable Y (Newhaven Tide) with Daily Probabilities of Exceedance & Tide Levels (mAOD)																																																																																																																																																																																																																																																																																																																																																																																																																																											
			0.9995				0.9957				0.9729				0.9125				0.7989				0.6465				0.4651				0.2552				0.0937				0.0158				0.0007				0.0001				<0.0001																																																																																																																																																																																																																																																																																																																																																																																											
			1.20	1.50	1.80	2.10	2.40	2.70	3.00	3.30	3.60	3.90	4.20	4.50	4.80	5.10	5.40	5.70	6.00	6.30	6.60	6.90	7.20	7.50	7.80	8.10	8.40	8.70	9.00	9.30	9.60	9.90	10.20	10.50	10.80	11.10	11.40	11.70	12.00																																																																																																																																																																																																																																																																																																																																																																																																							
0.9999	1	1.09	1.35	1.62	1.89	2.17	2.44	2.72	3.02	3.30	3.56	3.82	4.07	4.30	4.53	4.76	5.00	5.23	5.46	5.69	5.92	6.15	6.38	6.61	6.84	7.07	7.30	7.53	7.76	7.99	8.22	8.45	8.68	8.91	9.14	9.37	9.60	9.83	10.06	10.29	10.52	10.75	10.98	11.21	11.44	11.67	11.90	12.13	12.36	12.59	12.82	13.05	13.28	13.51	13.74	13.97	14.20	14.43	14.66	14.89	15.12	15.35	15.58	15.81	16.04	16.27	16.50	16.73	16.96	17.19	17.42	17.65	17.88	18.11	18.34	18.57	18.80	19.03	19.26	19.49	19.72	19.95	20.18	20.41	20.64	20.87	21.10	21.33	21.56	21.79	22.02	22.25	22.48	22.71	22.94	23.17	23.40	23.63	23.86	24.09	24.32	24.55	24.78	25.01	25.24	25.47	25.70	25.93	26.16	26.39	26.62	26.85	27.08	27.31	27.54	27.77	28.00	28.23	28.46	28.69	28.92	29.15	29.38	29.61	29.84	30.07	30.30	30.53	30.76	30.99	31.22	31.45	31.68	31.91	32.14	32.37	32.60	32.83	33.06	33.29	33.52	33.75	33.98	34.21	34.44	34.67	34.90	35.13	35.36	35.59	35.82	36.05	36.28	36.51	36.74	36.97	37.20	37.43	37.66	37.89	38.12	38.35	38.58	38.81	39.04	39.27	39.50	39.73	39.96	40.19	40.42	40.65	40.88	41.11	41.34	41.57	41.80	42.03	42.26	42.49	42.72	42.95	43.18	43.41	43.64	43.87	44.10	44.33	44.56	44.79	45.02	45.25	45.48	45.71	45.94	46.17	46.40	46.63	46.86	47.09	47.32	47.55	47.78	48.01	48.24	48.47	48.70	48.93	49.16	49.39	49.62	49.85	50.08	50.31	50.54	50.77	51.00	51.23	51.46	51.69	51.92	52.15	52.38	52.61	52.84	53.07	53.30	53.53	53.76	53.99	54.22	54.45	54.68	54.91	55.14	55.37	55.60	55.83	56.06	56.29	56.52	56.75	56.98	57.21	57.44	57.67	57.90	58.13	58.36	58.59	58.82	59.05	59.28	59.51	59.74	59.97	60.20	60.43	60.66	60.89	61.12	61.35	61.58	61.81	62.04	62.27	62.50	62.73	62.96	63.19	63.42	63.65	63.88	64.11	64.34	64.57	64.80	65.03	65.26	65.49	65.72	65.95	66.18	66.41	66.64	66.87	67.10	67.33	67.56	67.79	68.02	68.25	68.48	68.71	68.94	69.17	69.40	69.63	69.86	70.09	70.32	70.55	70.78	71.01	71.24	71.47	71.70	71.93	72.16	72.39	72.62	72.85	73.08	73.31	73.54	73.77	74.00	74.23	74.46	74.69	74.92	75.15	75.38	75.61	75.84	76.07	76.30	76.53	76.76	76.99	77.22	77.45	77.68	77.91	78.14	78.37	78.60	78.83	79.06	79.29	79.52	79.75	79.98	80.21	80.44	80.67	80.90	81.13	81.36	81.59	81.82	82.05	82.28	82.51	82.74	82.97	83.20	83.43	83.66	83.89	84.12	84.35	84.58	84.81	85.04	85.27	85.50	85.73	85.96	86.19	86.42	86.65	86.88	87.11	87.34	87.57	87.80	88.03	88.26	88.49	88.72	88.95	89.18	89.41	89.64	89.87	90.10	90.33	90.56	90.79	91.02	91.25	91.48	91.71	91.94	92.17	92.40	92.63	92.86	93.09	93.32	93.55	93.78	94.01	94.24	94.47	94.70	94.93	95.16	95.39	95.62	95.85	96.08	96.31	96.54	96.77	97.00	97.23	97.46	97.69	97.92	98.15	98.38	98.61	98.84	99.07	99.30	99.53	99.76	99.99

G.7 Extreme Joint Return Periods

G.7.1 Extreme Joint Return Periods at Lewes Corporation Yard

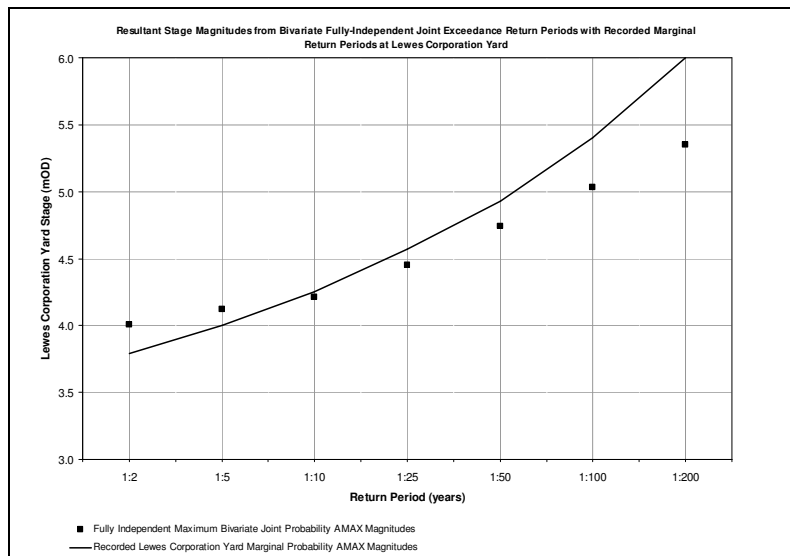


Figure G.7 Resultant stage magnitudes from bivariate (flow & tide) fully-independent joint return periods with recorded return periods at Lewes Corporation Yard

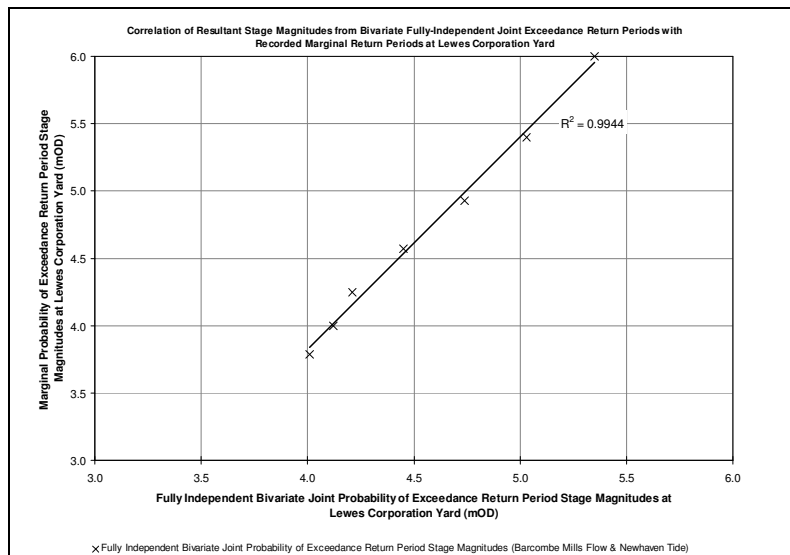


Figure G.8 Correlation of resultant stage magnitudes from bivariate (flow & tide) fully-independent joint return periods with recorded return periods at Lewes Corporation Yard

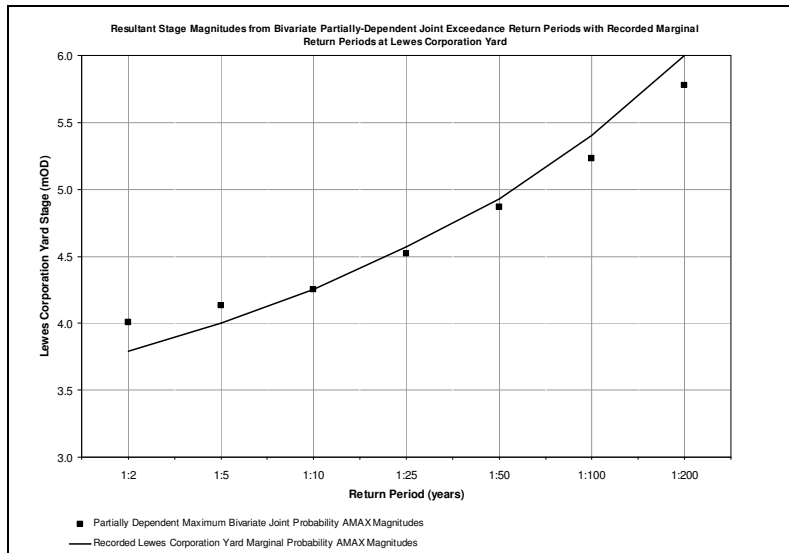


Figure G.9 Resultant stage magnitudes from bivariate (flow & tide) partially-dependent joint return periods with recorded return periods at Lewes Corporation Yard

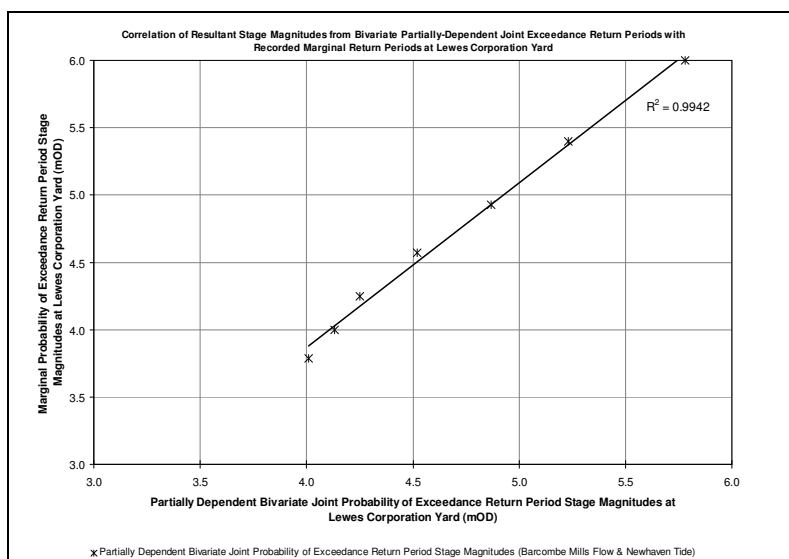


Figure G.10 Correlation of resultant stage magnitudes from bivariate (flow & tide) partially-dependent joint return periods with recorded return periods at Lewes Corporation Yard

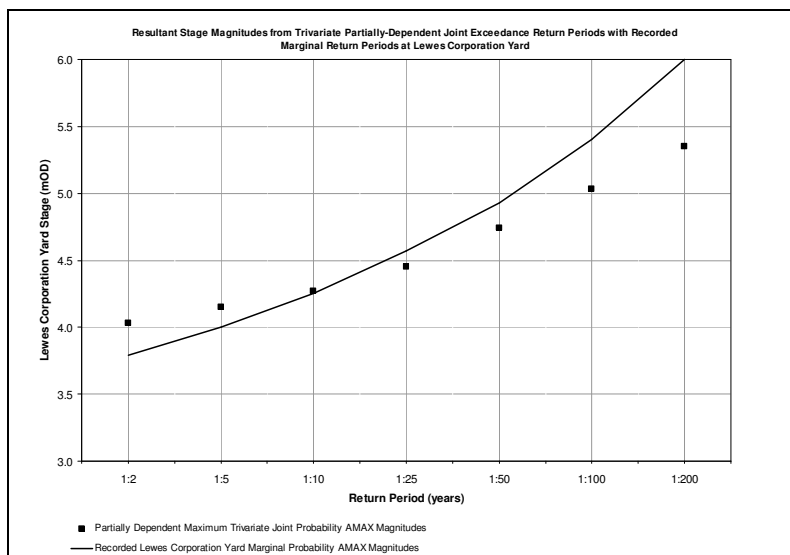


Figure G.11 Resultant stage magnitudes from trivariate (flow, tide & surge) partially-dependent joint return periods with recorded return periods at Lewes Corporation Yard

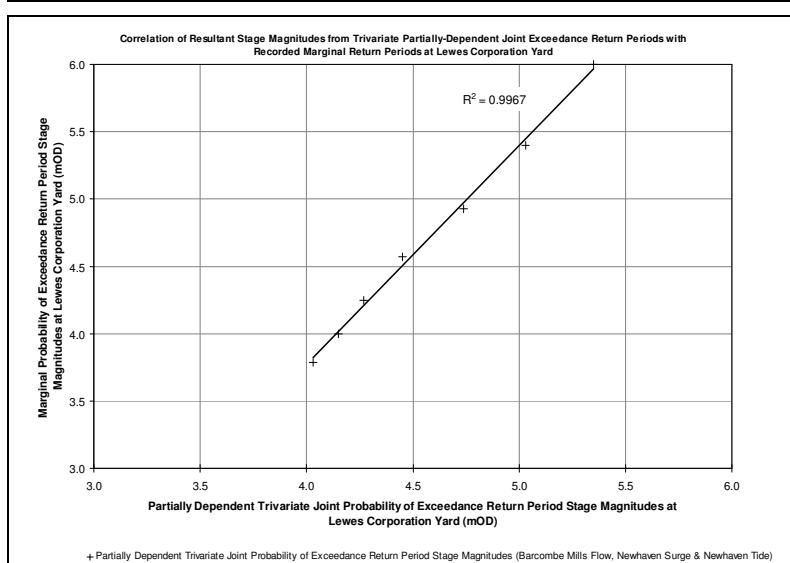


Figure G.12 Correlation of resultant stage magnitudes from trivariate (flow, tide & surge) partially-dependent joint return periods with recorded return periods at Lewes Corporation Yard

G.7.2 Extreme Joint Return Periods at Lewes Gas Works

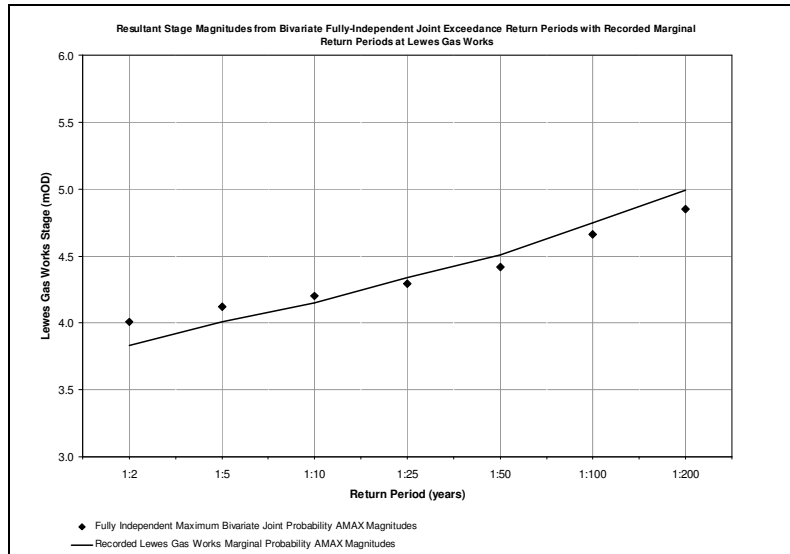


Figure G.13 Resultant stage magnitudes from bivariate (flow & tide) fully-independent joint return periods with recorded return periods at Lewes Gas Works

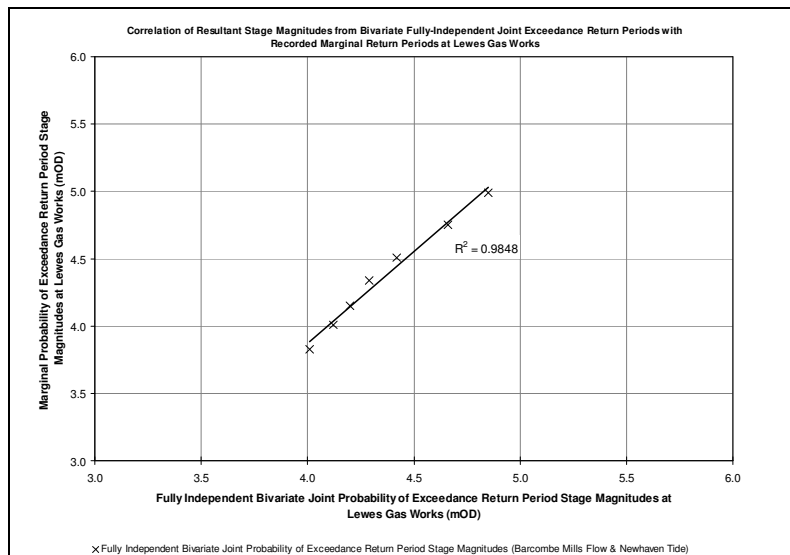


Figure G.14 Correlation of resultant stage magnitudes from bivariate (flow & tide) fully-independent joint return periods with recorded return periods at Lewes Gas Works

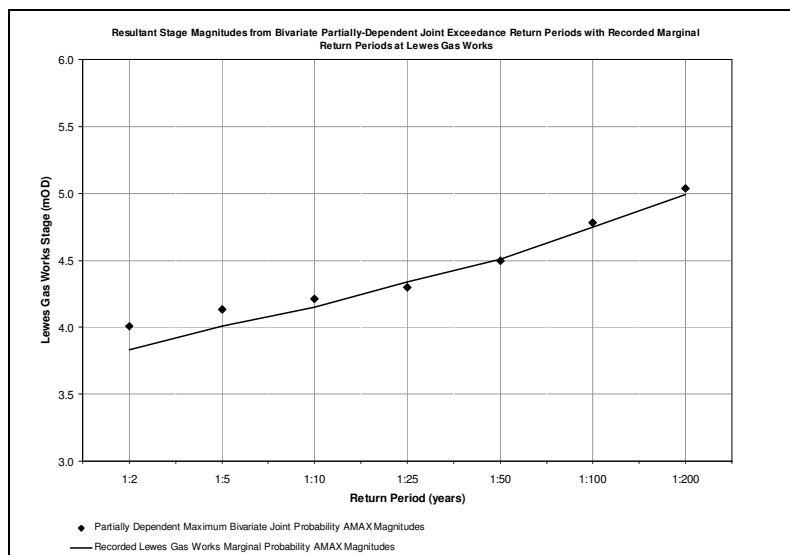


Figure G.15 Resultant stage magnitudes from bivariate (flow & tide) partially-dependent joint return periods with recorded return periods at Lewes Gas Works

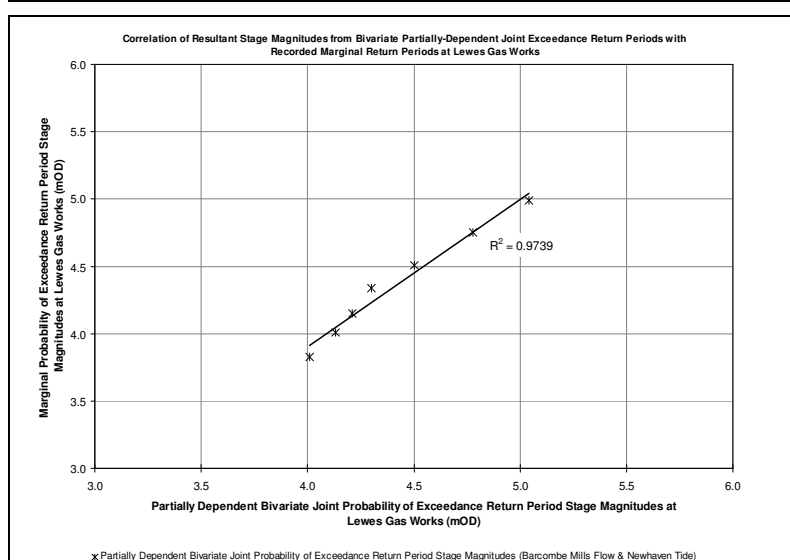


Figure G.16 Correlation of resultant stage magnitudes from bivariate (flow & tide) partially-dependent joint return periods with recorded return periods at Lewes Gas Works

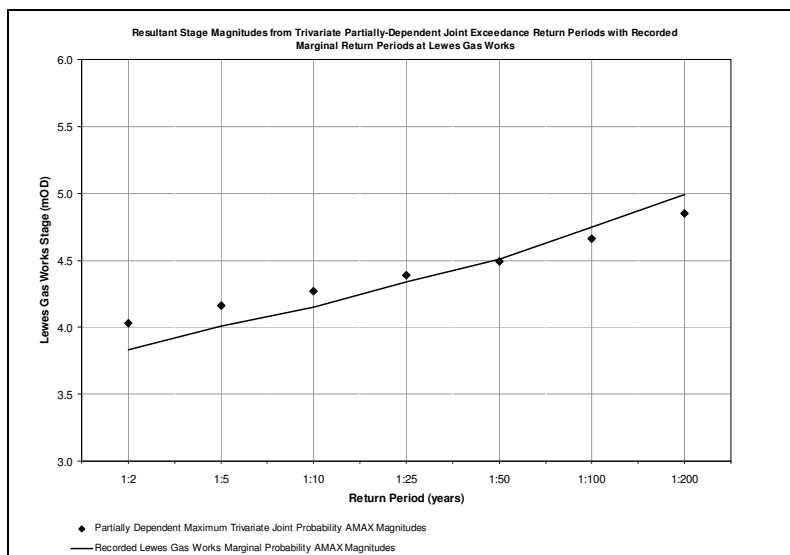


Figure G.17 Resultant stage magnitudes from trivariate (flow, tide & surge) partially-dependent joint return periods with recorded return periods at Lewes Gas Works

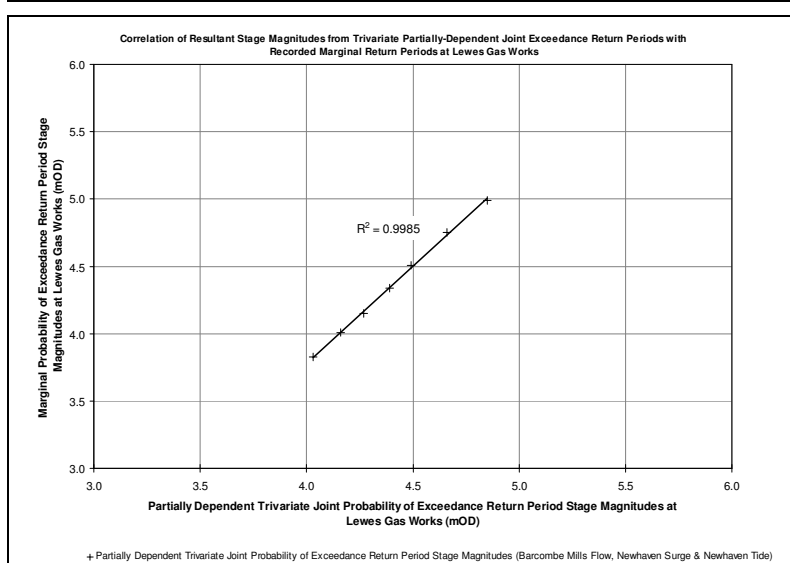


Figure G.18 Correlation of resultant stage magnitudes from trivariate (flow, tide & surge) partially-dependent joint return periods with recorded return periods at Lewes Gas Works

G.8 Daily Joint Probabilities

G.8.1 Daily Joint Probabilities at Lewes Corporation Yard

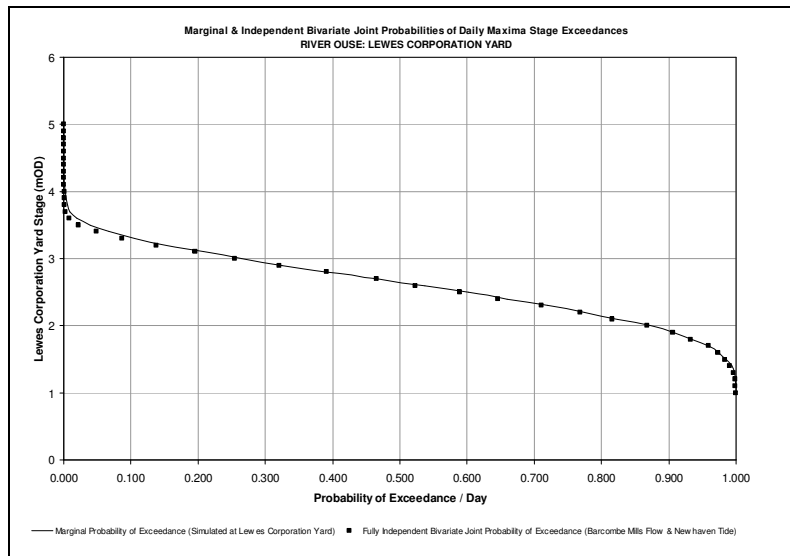


Figure G.19 & fully-independent bivariate (flow & tide) joint probabilities of daily maxima stage exceedances at Lewes Corporation Yard

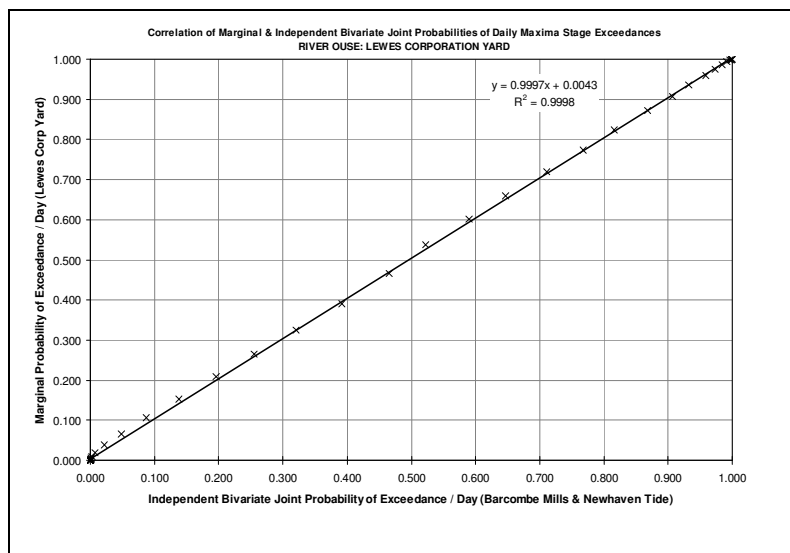


Figure G.20 Correlation of single & fully-independent bivariate (flow & tide) joint probabilities of daily maxima stage exceedances at Lewes Corporation Yard: complete series

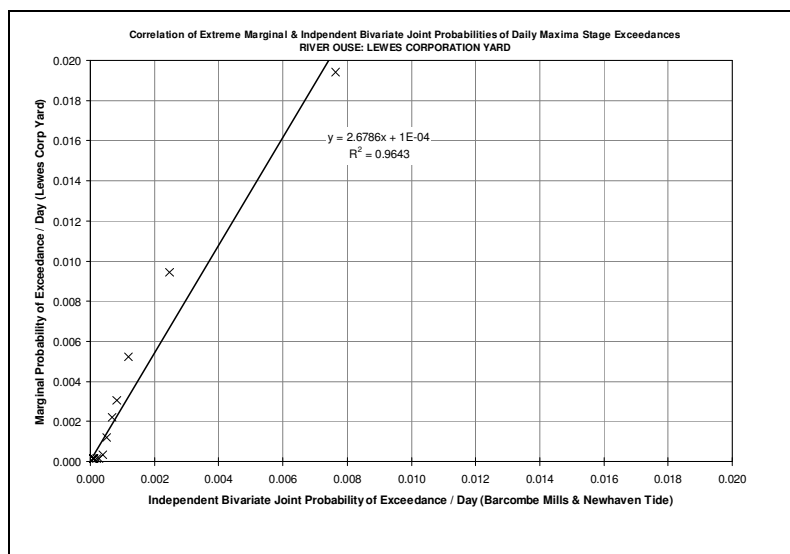


Figure G.21 Correlation of single & fully-independent bivariate (flow & tide) joint probabilities of daily maxima stage exceedances at Lewes Corporation Yard: extreme values (top 2%) only

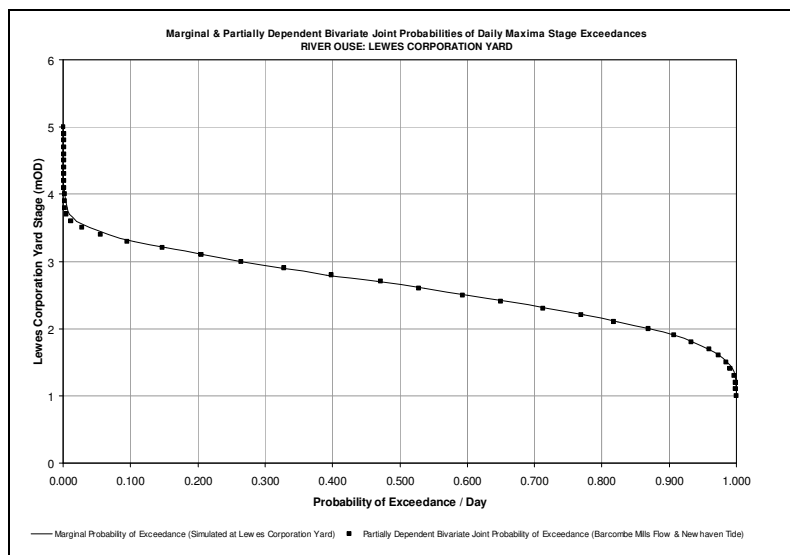


Figure G.22 Single & partially-dependent bivariate (flow & tide) joint probabilities of daily maxima stage exceedances at Lewes Corporation Yard

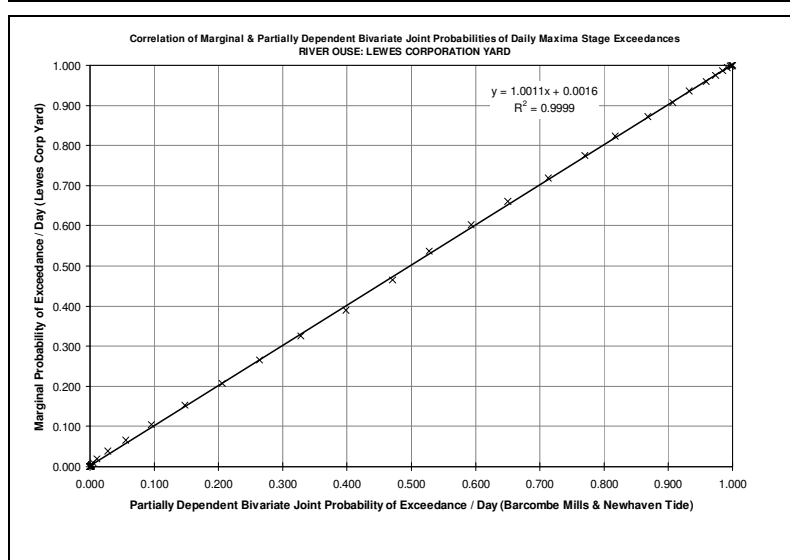


Figure G.23 Correlation of single & partially-dependent bivariate (flow & tide) joint probabilities of daily maxima stage exceedances at Lewes Corporation Yard: complete series

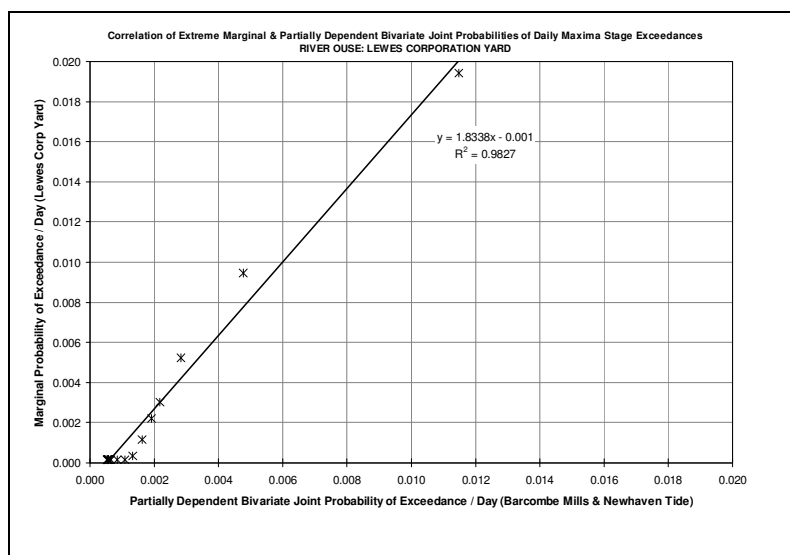


Figure G.24 Correlation of single & partially-dependent bivariate (flow & tide) joint probabilities of daily maxima stage exceedances at Lewes Corporation Yard: extreme values (top 2%) only

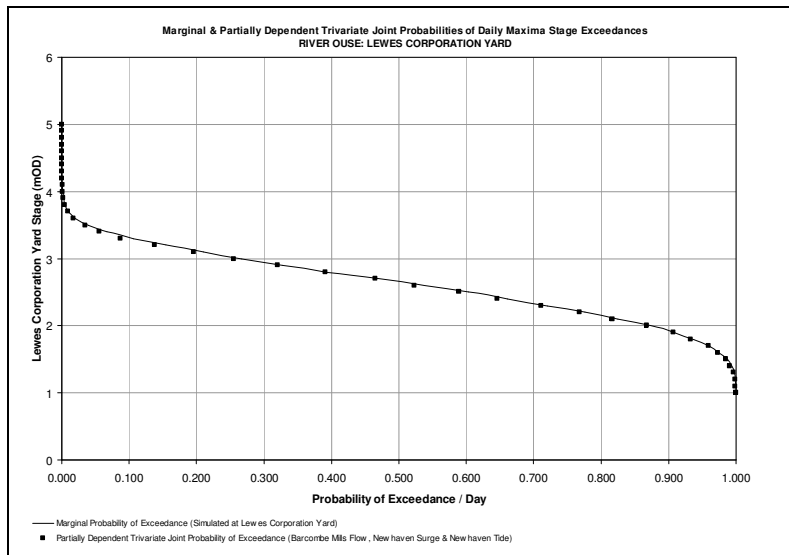


Figure G.25 Single & partially-dependent trivariate (flow, tide & surge) joint probabilities of daily maxima stage exceedances at Lewes Corporation Yard

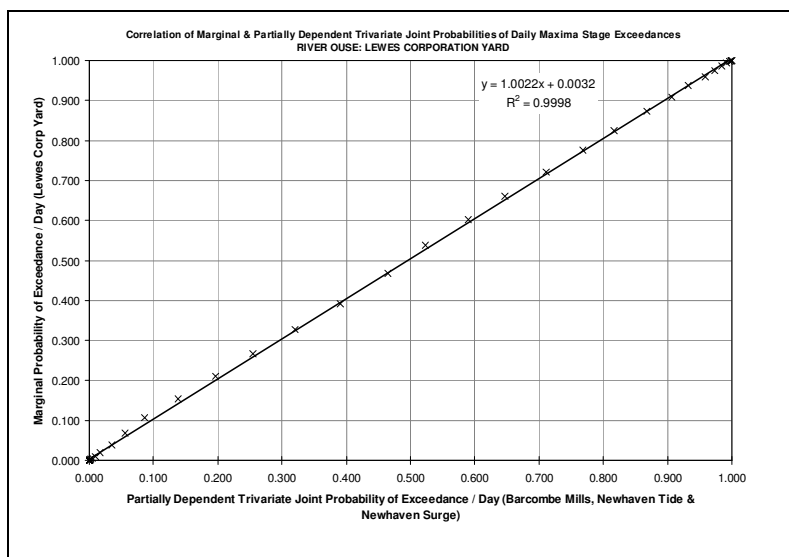


Figure G.26 Correlation of single & partially-dependent trivariate (flow, tide & surge) joint probabilities of daily maxima stage exceedances at Lewes Corporation Yard: complete series

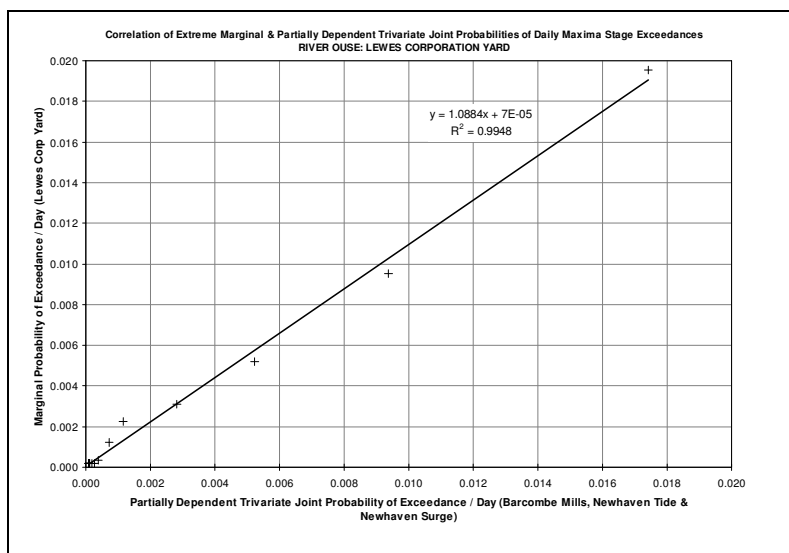


Figure G.27 Correlation of single & partially- trivariate (flow, tide & surge) joint probabilities of daily maxima stage exceedances at Lewes Corporation Yard: extreme values (top 2%) only

G.8.2 Daily Joint Probabilities at Lewes Gas Works

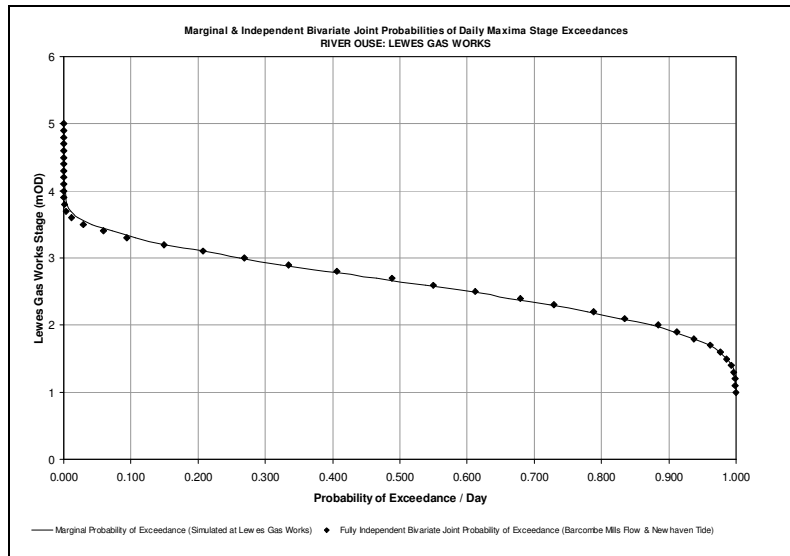


Figure G.28 Single & fully-independent bivariate (flow & tide) joint probabilities of daily maxima stage exceedances at Lewes Gas Works

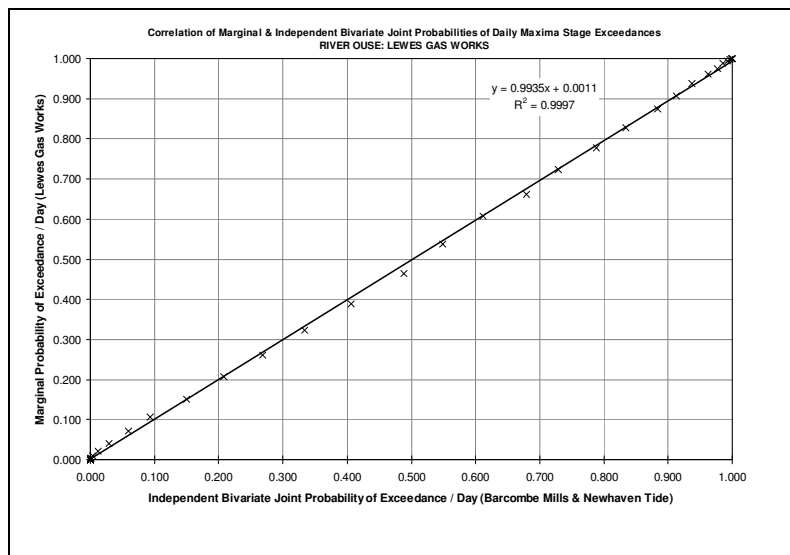


Figure G.29 Correlation of single & fully-independent bivariate (flow & tide) joint probabilities of daily maxima stage exceedances at Lewes Gas Works: complete series

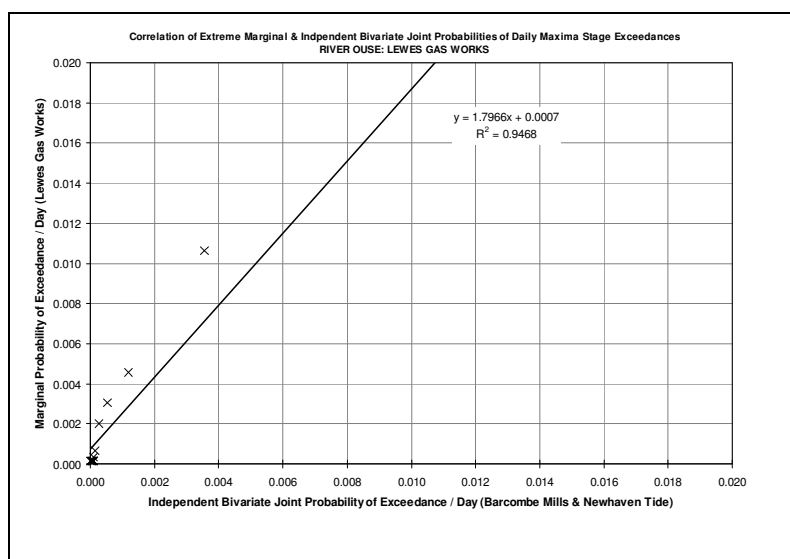


Figure G.30 Correlation of single & fully-independent bivariate (flow & tide) joint probabilities of daily maxima stage exceedances at Lewes Gas Works: extreme values (top 2%) only

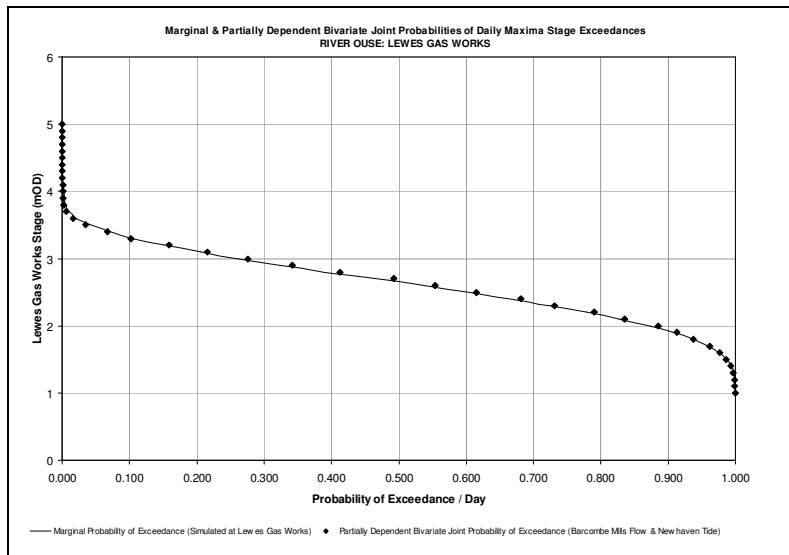


Figure G.31 Single & partially-dependent bivariate (flow & tide) joint probabilities of daily maxima stage exceedances at Lewes Gas Works

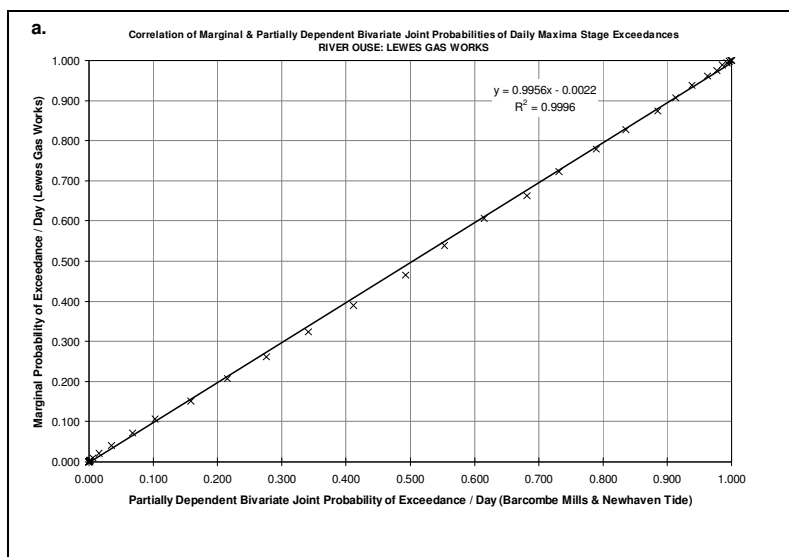


Figure G.32 Correlation of single & partially-dependent bivariate (flow & tide) joint probabilities of daily maxima stage exceedances at Lewes Gas Works: complete series

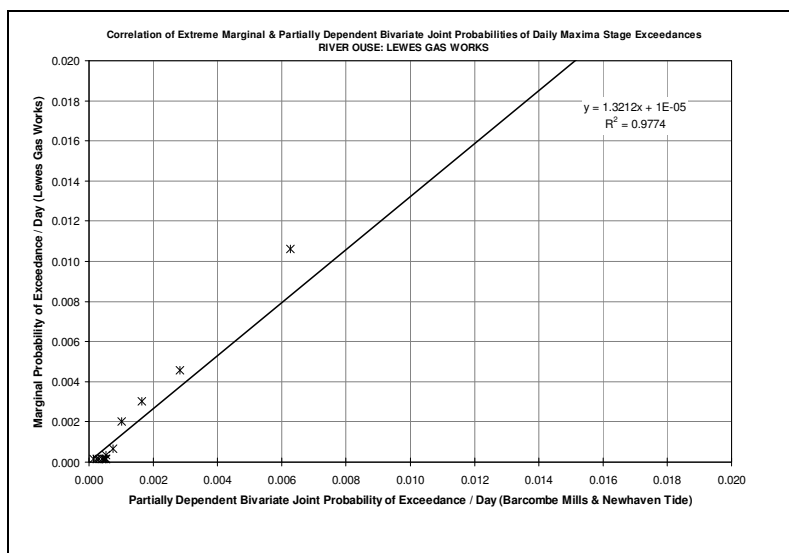


Figure G.33 Correlation of single & partially-dependent bivariate (flow & tide) joint probabilities of daily maxima stage exceedances at Lewes Gas Works: extreme values (top 2%) only

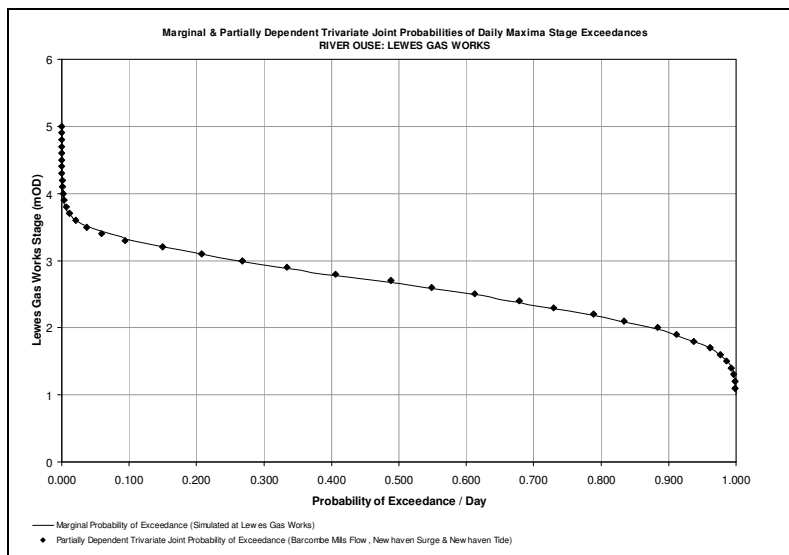


Figure G.34 Single & partially-dependent trivariate (flow, tide & surge) joint probabilities of daily maxima stage exceedances at Lewes Gas Works

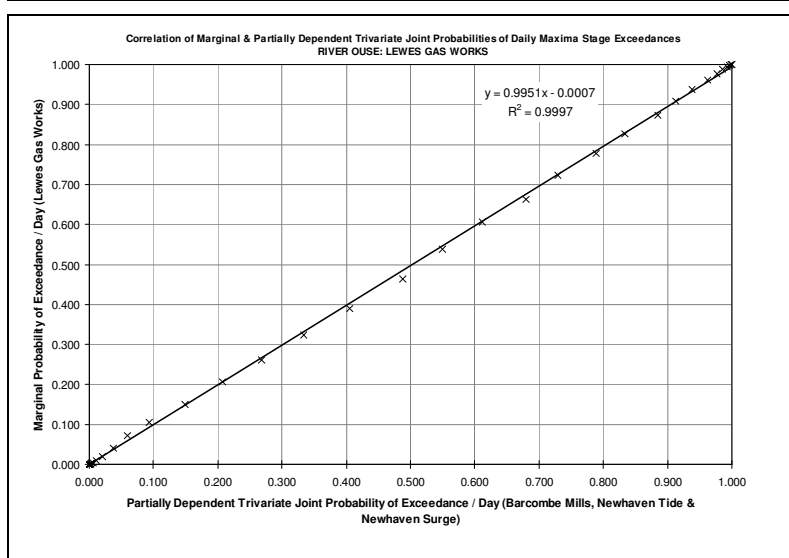


Figure G.35 Correlation of single & partially-dependent trivariate (flow, tide & surge) joint probabilities of daily maxima stage exceedances at Lewes Gas Works: complete series

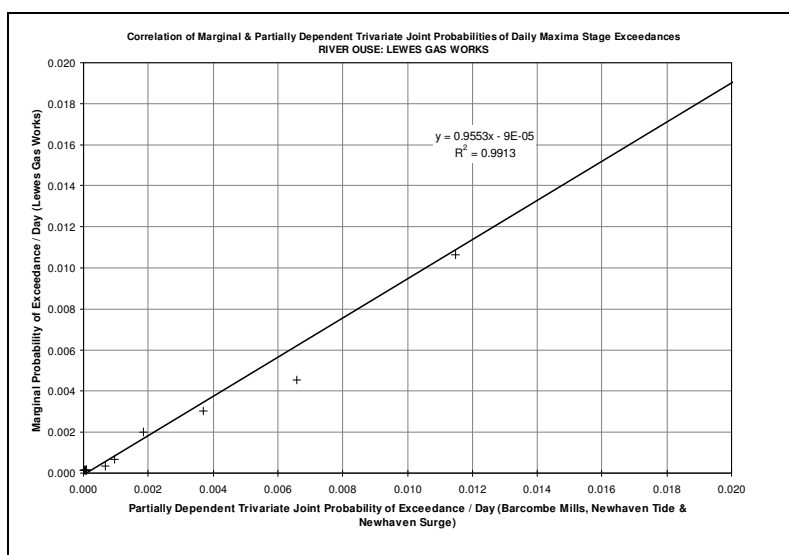


Figure G.36 Correlation of single & partially- trivariate (flow, tide & surge) joint probabilities of daily maxima stage exceedances at Lewes Gas Works: extreme values (top 2%) only

G.9 Extreme Joint Return Periods & Resultant Water Levels

G.9.1 Joint Return Periods at Lewes Corporation Yard

Table G.25 Resultant water levels at Lewes Corporation Yard for combined Barcombe Mills flow and Newhaven tide events equating to the 1:2 year joint return periods. Highest stage at Lewes Corporation Yard (shaded area) selected as the maximum 1:2 year combined flow / tide event.

Barc. Mills Flow (m ³ /s)	Newh'n Tide (mAOD)	Lewes Corp. Yard Stage (mAOD)	Barc. Mills Flow (m ³ /s)	Newh'n Tide (mAOD)	Lewes Corp. Yard Stage (mAOD)	Barc. Mills Flow (m ³ /s)	Newh'n Tide (mAOD)	Lewes Corp. Yard Stage (mAOD)
50	3.96	3.97	61	3.94	4.00	72	3.90	4.00
51	3.96	3.97	62	3.94	4.01	73	3.90	4.00
52	3.96	3.98	63	3.92	3.99	74	3.90	4.01
53	3.96	3.98	64	3.92	4.00	75	3.88	3.99
54	3.96	3.99	65	3.92	4.00	76	3.88	4.00
55	3.94	3.98	66	3.92	4.00	77	3.88	4.00
56	3.94	3.98	67	3.92	4.00	78	3.88	4.00
57	3.94	3.99	68	3.92	4.01	79	3.86	3.99
58	3.94	3.99	69	3.90	3.99	80	3.86	3.99
59	3.94	4.00	70	3.90	4.00	81	3.86	3.99
60	3.94	4.00	71	3.90	4.00	82	3.86	4.00

Table G.26 Resultant water levels at Lewes Corporation Yard for combined Barcombe Mills flow and Newhaven tide events equating to the 1:5 year joint return periods. Highest stage at Lewes Corporation Yard (shaded area) selected as the maximum 1:5 year combined flow / tide event.

Barc. Mills Flow (m ³ /s)	Newh'n Tide (mAOD)	Lewes Corp. Yard Stage (mAOD)	Barc. Mills Flow (m ³ /s)	Newh'n Tide (mAOD)	Lewes Corp. Yard Stage (mAOD)	Barc. Mills Flow (m ³ /s)	Newh'n Tide (mAOD)	Lewes Corp. Yard Stage (mAOD)
50	4.12	4.09	73	4.04	4.11	96	3.96	4.11
51	4.12	4.09	74	4.04	4.12	97	3.96	4.12
52	4.10	4.08	75	4.04	4.12	98	3.94	4.10
53	4.10	4.09	76	4.04	4.12	99	3.94	4.11
54	4.10	4.09	77	4.04	4.13	100	3.94	4.11
55	4.10	4.10	78	4.04	4.13	101	3.94	4.11
56	4.10	4.10	79	4.02	4.12	102	3.94	4.11
57	4.10	4.11	80	4.02	4.12	103	3.92	4.10
58	4.08	4.10	81	4.02	4.12	104	3.92	4.10
59	4.08	4.10	82	4.02	4.12	105	3.92	4.11
60	4.08	4.11	83	4.02	4.13	106	3.92	4.11
61	4.08	4.11	84	4.00	4.11	107	3.92	4.11
62	4.08	4.11	85	4.00	4.12	108	3.90	4.10
63	4.08	4.12	86	4.00	4.12	109	3.90	4.10
64	4.08	4.12	87	4.00	4.12	110	3.90	4.10
65	4.08	4.12	88	3.98	4.11	111	3.90	4.11
66	4.08	4.13	89	3.98	4.11	112	3.88	4.10
67	4.06	4.11	90	3.98	4.11	113	3.88	4.10
68	4.06	4.12	91	3.98	4.12	114	3.88	4.10
69	4.06	4.12	92	3.96	4.10	115	3.86	4.09
70	4.06	4.12	93	3.96	4.11	116	3.86	4.09
71	4.06	4.12	94	3.96	4.11	117	3.86	4.10
72	4.06	4.13	95	3.96	4.11			

Table G.27 Resultant water levels at Lewes Corporation Yard for combined Barcombe Mills flow and Newhaven tide events equating to the 1:10 year joint return periods. Highest stage at Lewes Corporation Yard (shaded area) selected as the maximum 1:10 year combined flow / tide event.

Barc. Mills Flow (m³/s)	Newh'n Tide (mAOD)	Lewes Corp. Yard Stage (mAOD)	Barc. Mills Flow (m³/s)	Newh'n Tide (mAOD)	Lewes Corp. Yard. Stage (mAOD)	Barc. Mills Flow (m³/s)	Newh'n Tide (mAOD)	Lewes Corp. Yard. Stage (mAOD)
50	4.20	4.15	82	4.12	4.20	114	4.00	4.20
51	4.20	4.16	83	4.12	4.21	115	3.98	4.18
52	4.18	4.14	84	4.12	4.21	116	3.98	4.19
53	4.18	4.15	85	4.12	4.21	117	3.98	4.19
54	4.18	4.15	86	4.12	4.21	118	3.98	4.19
55	4.18	4.16	87	4.10	4.20	119	3.96	4.18
56	4.18	4.16	88	4.10	4.20	120	3.96	4.18
57	4.18	4.17	89	4.10	4.21	121	3.96	4.18
58	4.18	4.17	90	4.10	4.21	122	3.96	4.19
59	4.18	4.18	91	4.10	4.21	123	3.96	4.19
60	4.18	4.18	92	4.10	4.22	124	3.96	4.20
61	4.18	4.19	93	4.08	4.20	125	3.94	4.19
62	4.16	4.18	94	4.08	4.21	126	3.94	4.19
63	4.16	4.18	95	4.08	4.21	127	3.94	4.20
64	4.16	4.18	96	4.08	4.21	128	3.94	4.20
65	4.16	4.18	97	4.08	4.21	129	3.94	4.21
66	4.16	4.19	98	4.06	4.20	130	3.92	4.20
67	4.16	4.19	99	4.06	4.20	131	3.92	4.20
68	4.16	4.19	100	4.06	4.21	132	3.92	4.21
69	4.16	4.20	101	4.06	4.21	133	3.92	4.21
70	4.16	4.20	102	4.06	4.21	134	3.90	4.20
71	4.16	4.20	103	4.04	4.20	135	3.90	4.21
72	4.14	4.19	104	4.04	4.20	136	3.90	4.21
73	4.14	4.19	105	4.04	4.20	137	3.90	4.22
74	4.14	4.20	106	4.04	4.21	138	3.88	4.21
75	4.14	4.20	107	4.02	4.19	139	3.88	4.21
76	4.14	4.20	108	4.02	4.20	140	3.88	4.22
77	4.14	4.20	109	4.02	4.20	141	3.86	4.21
78	4.14	4.21	110	4.02	4.20	142	3.86	4.22
79	4.14	4.21	111	4.02	4.20	143	3.86	4.22
80	4.12	4.20	112	4.00	4.19	144	3.86	4.23
81	4.12	4.20	113	4.00	4.19			

Table G.28 Resultant water levels at Lewes Corporation Yard for combined Barcombe Mills flow and Newhaven tide events equating to the 1:25 year joint return periods. Highest stage at Lewes Corporation Yard (shaded area) selected as the maximum 1:25 year combined flow / tide event.

Barc. Mills Flow (m ³ /s)	Newh'n Tide (mAOD)	Lewes Corp. Yard Stage (mAOD)	Barc. Mills Flow (m ³ /s)	Newh'n Tide (mAOD)	Lewes Corp. Yard. Stage (mAOD)	Barc. Mills Flow (m ³ /s)	Newh'n Tide (mAOD)	Lewes Corp. Yard. Stage (mAOD)
50	4.28	4.21	95	4.20	4.31	140	4.04	4.34
51	4.28	4.21	96	4.20	4.31	141	4.04	4.35
52	4.28	4.22	97	4.18	4.29	142	4.04	4.35
53	4.26	4.21	98	4.18	4.30	143	4.04	4.35
54	4.26	4.21	99	4.18	4.30	144	4.02	4.34
55	4.26	4.22	100	4.18	4.30	145	4.02	4.35
56	4.26	4.23	101	4.18	4.31	146	4.02	4.35
57	4.26	4.23	102	4.18	4.31	147	4.02	4.36
58	4.26	4.24	103	4.18	4.31	148	4.00	4.35
59	4.26	4.24	104	4.18	4.32	149	4.00	4.35
60	4.26	4.25	105	4.16	4.30	150	4.00	4.36
61	4.26	4.25	106	4.16	4.31	151	4.00	4.36
62	4.26	4.25	107	4.16	4.31	152	3.98	4.36
63	4.26	4.26	108	4.16	4.31	153	3.98	4.36
64	4.26	4.26	109	4.16	4.31	154	3.98	4.37
65	4.26	4.26	110	4.16	4.32	155	3.96	4.36
66	4.24	4.25	111	4.14	4.30	156	3.96	4.37
67	4.24	4.25	112	4.14	4.31	157	3.96	4.38
68	4.24	4.26	113	4.14	4.31	158	3.96	4.39
69	4.24	4.26	114	4.14	4.31	159	3.96	4.39
70	4.24	4.26	115	4.14	4.32	160	3.96	4.40
71	4.24	4.26	116	4.14	4.32	161	3.94	4.40
72	4.24	4.27	117	4.14	4.32	162	3.94	4.40
73	4.24	4.27	118	4.12	4.31	163	3.94	4.41
74	4.24	4.27	119	4.12	4.31	164	3.94	4.42
75	4.24	4.28	120	4.12	4.31	165	3.94	4.43
76	4.24	4.28	121	4.12	4.32	166	3.92	4.42
77	4.24	4.28	122	4.12	4.32	167	3.92	4.43
78	4.24	4.29	123	4.12	4.33	168	3.92	4.44
79	4.22	4.27	124	4.10	4.31	169	3.92	4.44
80	4.22	4.28	125	4.10	4.32	170	3.92	4.45
81	4.22	4.28	126	4.10	4.32	171	3.90	4.45
82	4.22	4.28	127	4.10	4.33	172	3.90	4.46
83	4.22	4.29	128	4.10	4.33	173	3.90	4.46
84	4.22	4.29	129	4.08	4.32	174	3.90	4.47
85	4.22	4.29	130	4.08	4.33	175	3.88	4.47
86	4.22	4.29	131	4.08	4.33	176	3.88	4.48
87	4.22	4.30	132	4.08	4.34	177	3.88	4.49
88	4.22	4.30	133	4.08	4.34	178	3.88	4.50
89	4.20	4.29	134	4.06	4.33	179	3.86	4.49
90	4.20	4.29	135	4.06	4.33	180	3.86	4.50
91	4.20	4.29	136	4.06	4.34	181	3.86	4.51
92	4.20	4.30	137	4.06	4.34	182	3.86	4.52
93	4.20	4.30	138	4.06	4.35			
94	4.20	4.30	139	4.04	4.34			

Table G.29 Resultant water levels at Lewes Corporation Yard for combined Barcombe Mills flow and Newhaven tide events equating to the 1:50 year joint return periods. Highest stage at Lewes Corporation Yard (shaded area) selected as the maximum 1:50 year combined flow / tide event.

Barc. Mills Flow (m ³ /s)	Newh'n Tide (mAOD)	Lewes Corp. Yard Stage (mAOD)	Barc. Mills Flow (m ³ /s)	Newh'n Tide (mAOD)	Lewes Corp. Yard. Stage (mAOD)	Barc. Mills Flow (m ³ /s)	Newh'n Tide (mAOD)	Lewes Corp. Yard. Stage (mAOD)
50	4.32	4.24	98	4.26	4.36	146	4.12	4.43
51	4.32	4.24	99	4.26	4.37	147	4.12	4.44
52	4.32	4.25	100	4.24	4.35	148	4.12	4.44
53	4.32	4.25	101	4.24	4.36	149	4.12	4.44
54	4.32	4.26	102	4.24	4.36	150	4.12	4.45
55	4.32	4.27	103	4.24	4.36	151	4.12	4.46
56	4.32	4.27	104	4.24	4.37	152	4.12	4.46
57	4.32	4.28	105	4.24	4.37	153	4.10	4.45
58	4.32	4.28	106	4.24	4.37	154	4.10	4.46
59	4.30	4.27	107	4.24	4.37	155	4.10	4.47
60	4.30	4.28	108	4.24	4.38	156	4.10	4.47
61	4.30	4.28	109	4.22	4.36	157	4.10	4.48
62	4.30	4.28	110	4.22	4.37	158	4.08	4.47
63	4.30	4.29	111	4.22	4.37	159	4.08	4.48
64	4.30	4.29	112	4.22	4.37	160	4.08	4.49
65	4.30	4.29	113	4.22	4.38	161	4.08	4.49
66	4.30	4.30	114	4.22	4.38	162	4.08	4.50
67	4.30	4.30	115	4.22	4.38	163	4.08	4.51
68	4.30	4.30	116	4.22	4.38	164	4.06	4.50
69	4.30	4.31	117	4.22	4.39	165	4.06	4.51
70	4.30	4.31	118	4.20	4.37	166	4.06	4.51
71	4.30	4.31	119	4.20	4.38	167	4.06	4.52
72	4.30	4.32	120	4.20	4.38	168	4.06	4.53
73	4.30	4.32	121	4.20	4.38	169	4.04	4.52
74	4.30	4.32	122	4.20	4.39	170	4.04	4.53
75	4.30	4.33	123	4.20	4.39	171	4.04	4.54
76	4.30	4.33	124	4.20	4.40	172	4.04	4.54
77	4.28	4.32	125	4.20	4.40	173	4.02	4.54
78	4.28	4.32	126	4.18	4.39	174	4.02	4.54
79	4.28	4.32	127	4.18	4.39	175	4.02	4.55
80	4.28	4.32	128	4.18	4.40	176	4.02	4.56
81	4.28	4.33	129	4.18	4.40	177	4.02	4.57
82	4.28	4.33	130	4.18	4.41	178	4.00	4.56
83	4.28	4.33	131	4.18	4.41	179	4.00	4.57
84	4.28	4.34	132	4.18	4.42	180	4.00	4.58
85	4.28	4.34	133	4.16	4.40	181	4.00	4.59
86	4.28	4.34	134	4.16	4.41	182	3.98	4.59
87	4.28	4.35	135	4.16	4.41	183	3.98	4.60
88	4.28	4.35	136	4.16	4.42	184	3.98	4.61
89	4.26	4.34	137	4.16	4.42	185	3.98	4.62
90	4.26	4.34	138	4.16	4.43	186	3.96	4.62
91	4.26	4.34	139	4.16	4.43	187	3.96	4.63
92	4.26	4.35	140	4.14	4.42	188	3.96	4.64
93	4.26	4.35	141	4.14	4.42	189	3.96	4.65
94	4.26	4.35	142	4.14	4.43	190	3.96	4.66
95	4.26	4.36	143	4.14	4.43	191	3.96	4.67
96	4.26	4.36	144	4.14	4.44	192	3.94	4.67
97	4.26	4.36	145	4.14	4.44	193	3.94	4.68

Continued

Barc. Mills Flow (m³/s)	Newh'n Tide (mAOD)	Lewes Corp. Yard Stage (mAOD)	Barc. Mills Flow (m³/s)	Newh'n Tide (mAOD)	Lewes Corp. Yard. Stage (mAOD)	Barc. Mills Flow (m³/s)	Newh'n Tide (mAOD)	Lewes Corp. Yard. Stage (mAOD)
194	3.94	4.69	201	3.92	4.75	208	3.88	4.81
195	3.94	4.70	202	3.90	4.75	209	3.88	4.82
196	3.94	4.71	203	3.90	4.77	210	3.88	4.83
197	3.94	4.72	204	3.90	4.78	211	3.86	4.84
198	3.92	4.72	205	3.90	4.79	212	3.86	4.85
199	3.92	4.73	206	3.90	4.80	213	3.86	4.86
200	3.92	4.74	207	3.88	4.80	214	3.86	4.87

Table G.30 Resultant water levels at Lewes Corporation Yard for combined Barcombe Mills flow and Newhaven tide events equating to the 1:100 year joint return periods. Highest stage at Lewes Corporation Yard (shaded area) selected as the maximum 1:100 year combined flow / tide event.

Barc. Mills Flow (m ³ /s)	Newh'n Tide (mAOD)	Lewes Corp. Yard Stage (mAOD)	Barc. Mills Flow (m ³ /s)	Newh'n Tide (mAOD)	Lewes Corp. Yard. Stage (mAOD)	Barc. Mills Flow (m ³ /s)	Newh'n Tide (mAOD)	Lewes Corp. Yard. Stage (mAOD)
50	4.36	4.27	98	4.30	4.40	146	4.22	4.51
51	4.36	4.27	99	4.30	4.40	147	4.22	4.51
52	4.36	4.28	100	4.30	4.40	148	4.20	4.50
53	4.36	4.28	101	4.30	4.41	149	4.20	4.51
54	4.36	4.29	102	4.30	4.41	150	4.20	4.51
55	4.36	4.30	103	4.30	4.41	151	4.20	4.52
56	4.36	4.30	104	4.30	4.42	152	4.20	4.52
57	4.36	4.31	105	4.30	4.42	153	4.20	4.53
58	4.36	4.31	106	4.30	4.42	154	4.20	4.53
59	4.36	4.32	107	4.30	4.42	155	4.20	4.54
60	4.36	4.32	108	4.30	4.43	156	4.18	4.53
61	4.34	4.31	109	4.28	4.41	157	4.18	4.54
62	4.34	4.31	110	4.28	4.42	158	4.18	4.54
63	4.34	4.32	111	4.28	4.42	159	4.18	4.55
64	4.34	4.32	112	4.28	4.42	160	4.18	4.56
65	4.34	4.32	113	4.28	4.43	161	4.18	4.56
66	4.34	4.33	114	4.28	4.43	162	4.18	4.57
67	4.34	4.33	115	4.28	4.43	163	4.18	4.57
68	4.34	4.33	116	4.28	4.43	164	4.16	4.57
69	4.34	4.34	117	4.28	4.44	165	4.16	4.57
70	4.34	4.34	118	4.28	4.44	166	4.16	4.58
71	4.34	4.34	119	4.28	4.44	167	4.16	4.59
72	4.34	4.35	120	4.26	4.43	168	4.16	4.59
73	4.34	4.35	121	4.26	4.43	169	4.16	4.60
74	4.34	4.35	122	4.26	4.44	170	4.16	4.60
75	4.34	4.36	123	4.26	4.44	171	4.14	4.60
76	4.34	4.36	124	4.26	4.45	172	4.14	4.60
77	4.34	4.36	125	4.26	4.45	173	4.14	4.61
78	4.34	4.37	126	4.26	4.45	174	4.14	4.62
79	4.34	4.37	127	4.26	4.46	175	4.14	4.62
80	4.34	4.37	128	4.26	4.46	176	4.14	4.63
81	4.34	4.38	129	4.26	4.47	177	4.14	4.64
82	4.32	4.36	130	4.24	4.45	178	4.12	4.63
83	4.32	4.37	131	4.24	4.46	179	4.12	4.64
84	4.32	4.37	132	4.24	4.46	180	4.12	4.64
85	4.32	4.37	133	4.24	4.47	181	4.12	4.65
86	4.32	4.38	134	4.24	4.47	182	4.12	4.66
87	4.32	4.38	135	4.24	4.48	183	4.12	4.67
88	4.32	4.38	136	4.24	4.48	184	4.12	4.68
89	4.32	4.39	137	4.24	4.48	185	4.10	4.68
90	4.32	4.39	138	4.24	4.49	186	4.10	4.69
91	4.32	4.39	139	4.22	4.48	187	4.10	4.70
92	4.32	4.40	140	4.22	4.48	188	4.10	4.71
93	4.32	4.40	141	4.22	4.49	189	4.10	4.72
94	4.32	4.40	142	4.22	4.49	190	4.08	4.72
95	4.32	4.41	143	4.22	4.49	191	4.08	4.73
96	4.32	4.41	144	4.22	4.50	192	4.08	4.74
97	4.30	4.39	145	4.22	4.50	193	4.08	4.75

Continued

Barc. Mills Flow (m ³ /s)	Newh'n Tide (mAOD)	Lewes Corp. Yard Stage (mAOD)	Barc. Mills Flow (m ³ /s)	Newh'n Tide (mAOD)	Lewes Corp. Yard. Stage (mAOD)	Barc. Mills Flow (m ³ /s)	Newh'n Tide (mAOD)	Lewes Corp. Yard. Stage (mAOD)
194	4.08	4.75	213	4.00	4.90	232	3.92	5.05
195	4.08	4.76	214	4.00	4.91	233	3.92	5.06
196	4.06	4.76	215	4.00	4.92	234	3.92	5.07
197	4.06	4.77	216	3.98	4.92	235	3.92	5.08
198	4.06	4.78	217	3.98	4.93	236	3.92	5.09
199	4.06	4.79	218	3.98	4.94	237	3.92	5.10
200	4.06	4.80	219	3.98	4.95	238	3.90	5.10
201	4.04	4.80	220	3.96	4.95	239	3.90	5.11
202	4.04	4.81	221	3.96	4.96	240	3.90	5.12
203	4.04	4.82	222	3.96	4.97	241	3.90	5.13
204	4.04	4.83	223	3.96	4.98	242	3.90	5.14
205	4.04	4.84	224	3.96	4.99	243	3.88	5.15
206	4.04	4.85	225	3.96	5.00	244	3.88	5.16
207	4.02	4.85	226	3.96	5.01	245	3.88	5.17
208	4.02	4.86	227	3.94	5.01	246	3.88	5.18
209	4.02	4.87	228	3.94	5.02	247	3.86	5.19
210	4.02	4.88	229	3.94	5.03	248	3.86	5.20
211	4.00	4.89	230	3.94	5.04	249	3.86	5.21
212	4.00	4.89	231	3.94	5.05	250	3.86	5.23

Table G.31 Resultant water levels at Lewes Corporation Yard for combined Barcombe Mills flow and Newhaven tide events equating to the 1:200 year joint return periods. Highest stage at Lewes Corporation Yard (shaded area) selected as the maximum 1:200 year combined flow / tide event.

Barc. Mills Flow (m ³ /s)	Newh'n Tide (mAOD)	Lewes Corp. Yard Stage (mAOD)	Barc. Mills Flow (m ³ /s)	Newh'n Tide (mAOD)	Lewes Corp. Yard. Stage (mAOD)	Barc. Mills Flow (m ³ /s)	Newh'n Tide (mAOD)	Lewes Corp. Yard. Stage (mAOD)
50	4.40	4.30	98	4.36	4.45	146	4.28	4.55
51	4.40	4.30	99	4.36	4.45	147	4.28	4.55
52	4.40	4.31	100	4.34	4.44	148	4.28	4.56
53	4.40	4.31	101	4.34	4.44	149	4.28	4.56
54	4.38	4.30	102	4.34	4.44	150	4.28	4.57
55	4.38	4.31	103	4.34	4.45	151	4.28	4.57
56	4.38	4.32	104	4.34	4.45	152	4.28	4.58
57	4.38	4.32	105	4.34	4.45	153	4.26	4.57
58	4.38	4.33	106	4.34	4.45	154	4.26	4.58
59	4.38	4.33	107	4.34	4.46	155	4.26	4.58
60	4.38	4.34	108	4.34	4.46	156	4.26	4.59
61	4.38	4.34	109	4.34	4.46	157	4.26	4.59
62	4.38	4.34	110	4.34	4.47	158	4.26	4.60
63	4.38	4.35	111	4.34	4.47	159	4.26	4.60
64	4.38	4.35	112	4.34	4.47	160	4.26	4.61
65	4.38	4.36	113	4.34	4.48	161	4.26	4.62
66	4.38	4.36	114	4.34	4.48	162	4.26	4.62
67	4.38	4.36	115	4.34	4.48	163	4.24	4.61
68	4.38	4.37	116	4.32	4.47	164	4.24	4.62
69	4.38	4.37	117	4.32	4.47	165	4.24	4.63
70	4.38	4.37	118	4.32	4.47	166	4.24	4.63
71	4.38	4.38	119	4.32	4.48	167	4.24	4.64
72	4.38	4.38	120	4.32	4.48	168	4.24	4.64
73	4.38	4.38	121	4.32	4.48	169	4.24	4.65
74	4.38	4.39	122	4.32	4.49	170	4.24	4.66
75	4.38	4.39	123	4.32	4.49	171	4.24	4.66
76	4.38	4.39	124	4.32	4.50	172	4.24	4.67
77	4.38	4.40	125	4.32	4.50	173	4.22	4.66
78	4.38	4.40	126	4.32	4.50	174	4.22	4.67
79	4.38	4.40	127	4.32	4.51	175	4.22	4.67
80	4.38	4.41	128	4.32	4.51	176	4.22	4.68
81	4.38	4.41	129	4.30	4.50	177	4.22	4.68
82	4.36	4.40	130	4.30	4.50	178	4.22	4.69
83	4.36	4.40	131	4.30	4.51	179	4.22	4.70
84	4.36	4.40	132	4.30	4.51	180	4.22	4.70
85	4.36	4.41	133	4.30	4.51	181	4.22	4.71
86	4.36	4.41	134	4.30	4.52	182	4.20	4.71
87	4.36	4.41	135	4.30	4.52	183	4.20	4.72
88	4.36	4.42	136	4.30	4.53	184	4.20	4.72
89	4.36	4.42	137	4.30	4.53	185	4.20	4.73
90	4.36	4.42	138	4.30	4.53	186	4.20	4.74
91	4.36	4.43	139	4.30	4.54	187	4.20	4.75
92	4.36	4.43	140	4.30	4.54	188	4.20	4.76
93	4.36	4.43	141	4.28	4.53	189	4.20	4.77
94	4.36	4.44	142	4.28	4.53	190	4.18	4.77
95	4.36	4.44	143	4.28	4.54	191	4.18	4.78
96	4.36	4.44	144	4.28	4.54	192	4.18	4.78
97	4.36	4.44	145	4.28	4.55	193	4.18	4.79

Continued

Barc. Mills Flow (m ³ /s)	Newh'n Tide (mAOD)	Lewes Corp. Yard Stage (mAOD)	Barc. Mills Flow (m ³ /s)	Newh'n Tide (mAOD)	Lewes Corp. Yard. Stage (mAOD)	Barc. Mills Flow (m ³ /s)	Newh'n Tide (mAOD)	Lewes Corp. Yard. Stage (mAOD)
194	4.18	4.80	227	4.08	5.05	260	3.96	5.36
195	4.18	4.81	228	4.08	5.06	261	3.96	5.37
196	4.18	4.82	229	4.08	5.07	262	3.96	5.38
197	4.18	4.83	230	4.08	5.08	263	3.96	5.39
198	4.18	4.84	231	4.08	5.09	264	3.96	5.40
199	4.16	4.84	232	4.08	5.10	265	3.96	5.42
200	4.16	4.85	233	4.06	5.10	266	3.94	5.42
201	4.16	4.85	234	4.06	5.11	267	3.94	5.43
202	4.16	4.86	235	4.06	5.12	268	3.94	5.45
203	4.16	4.87	236	4.06	5.13	269	3.94	5.46
204	4.16	4.88	237	4.06	5.14	270	3.94	5.47
205	4.16	4.89	238	4.06	5.15	271	3.94	5.48
206	4.16	4.90	239	4.04	5.15	272	3.94	5.50
207	4.14	4.90	240	4.04	5.16	273	3.92	5.51
208	4.14	4.91	241	4.04	5.17	274	3.92	5.52
209	4.14	4.92	242	4.04	5.18	275	3.92	5.54
210	4.14	4.93	243	4.04	5.19	276	3.92	5.55
211	4.14	4.94	244	4.04	5.20	277	3.92	5.57
212	4.14	4.95	245	4.02	5.21	278	3.92	5.58
213	4.14	4.95	246	4.02	5.22	279	3.90	5.59
214	4.12	4.96	247	4.02	5.23	280	3.90	5.61
215	4.12	4.96	248	4.02	5.24	281	3.90	5.62
216	4.12	4.97	249	4.02	5.25	282	3.90	5.64
217	4.12	4.98	250	4.00	5.26	283	3.90	5.65
218	4.12	4.99	251	4.00	5.27	284	3.88	5.66
219	4.12	5.00	252	4.00	5.28	285	3.88	5.68
220	4.12	5.01	253	4.00	5.29	286	3.88	5.69
221	4.10	5.01	254	4.00	5.30	287	3.88	5.71
222	4.10	5.02	255	3.98	5.31	288	3.86	5.72
223	4.10	5.03	256	3.98	5.32	289	3.86	5.73
224	4.10	5.03	257	3.98	5.33	290	3.86	5.75
225	4.10	5.04	258	3.98	5.34	291	3.86	5.76
226	4.10	5.05	259	3.96	5.35	292	3.86	5.78

G.9.2 Joint Return Periods at Lewes Gas Works

Table G.32 Resultant water levels at Lewes Gas Works for combined Barcombe Mills flow and Newhaven tide events equating to the 1:2 year joint return periods. Highest stage at Lewes Gas Works (shaded area) selected as the maximum 1:2 year combined flow / tide event.

Barc. Mills Flow (m ³ /s)	Newh'n Tide (mAOD)	Lewes Gas Works Stage (mAOD)	Barc. Mills Flow (m ³ /s)	Newh'n Tide (mAOD)	Lewes Gas Works. Stage (mAOD)	Barc. Mills Flow (m ³ /s)	Newh'n Tide (mAOD)	Lewes Gas Works. Stage (mAOD)
50	3.96	3.98	61	3.94	4.01	72	3.90	4.00
51	3.96	3.99	62	3.94	4.01	73	3.90	4.00
52	3.96	3.99	63	3.92	4.00	74	3.88	3.98
53	3.96	4.00	64	3.92	4.00	75	3.88	3.98
54	3.96	4.00	65	3.92	4.00	76	3.88	3.98
55	3.94	3.99	66	3.92	4.00	77	3.88	3.99
56	3.94	3.99	67	3.92	4.01	78	3.88	3.99
57	3.94	4.00	68	3.92	4.01	79	3.86	3.97
58	3.94	4.00	69	3.90	3.99	80	3.86	3.97
59	3.94	4.01	70	3.90	3.99	81	3.86	3.97
60	3.94	4.01	71	3.90	3.99	82	3.86	3.98

Table G.33 Resultant water levels at Lewes Gas Works for combined Barcombe Mills flow and Newhaven tide events equating to the 1:5 year joint return periods. Highest stage at Lewes Gas Works (shaded area) selected as the maximum 1:5 year combined flow / tide event.

Barc. Mills Flow (m ³ /s)	Newh'n Tide (mAOD)	Lewes Gas Works Stage (mAOD)	Barc. Mills Flow (m ³ /s)	Newh'n Tide (mAOD)	Lewes Gas Works. Stage (mAOD)	Barc. Mills Flow (m ³ /s)	Newh'n Tide (mAOD)	Lewes Gas Works. Stage (mAOD)
50	4.12	4.10	73	4.04	4.11	96	3.96	4.08
51	4.12	4.11	74	4.04	4.11	97	3.96	4.09
52	4.10	4.10	75	4.04	4.12	98	3.94	4.07
53	4.10	4.10	76	4.04	4.12	99	3.94	4.07
54	4.10	4.11	77	4.04	4.12	100	3.94	4.07
55	4.10	4.11	78	4.04	4.12	101	3.94	4.07
56	4.10	4.12	79	4.02	4.11	102	3.94	4.08
57	4.10	4.12	80	4.02	4.11	103	3.92	4.06
58	4.08	4.11	81	4.02	4.11	104	3.92	4.06
59	4.08	4.11	82	4.02	4.11	105	3.92	4.06
60	4.08	4.12	83	4.02	4.11	106	3.92	4.06
61	4.08	4.12	84	4.00	4.10	107	3.90	4.05
62	4.08	4.12	85	4.00	4.10	108	3.90	4.05
63	4.08	4.12	86	4.00	4.10	109	3.90	4.05
64	4.08	4.13	87	4.00	4.10	110	3.90	4.05
65	4.08	4.13	88	3.98	4.09	111	3.88	4.04
66	4.08	4.13	89	3.98	4.09	112	3.88	4.04
67	4.06	4.12	90	3.98	4.09	113	3.88	4.04
68	4.06	4.12	91	3.98	4.09	114	3.88	4.04
69	4.06	4.12	92	3.96	4.08	115	3.86	4.03
70	4.06	4.12	93	3.96	4.08	116	3.86	4.03
71	4.06	4.13	94	3.96	4.08	117	3.86	4.04
72	4.06	4.13	95	3.96	4.08	96	3.96	4.08

Table G.34 Resultant water levels at Lewes Gas Works for combined Barcombe Mills flow and Newhaven tide events equating to the 1:10 year joint return periods. Highest stage at Lewes Gas Works (shaded area) selected as the maximum 1:10 year combined flow / tide event.

Barc. Mills Flow (m ³ /s)	Newh'n Tide (mAOD)	Lewes Gas Works Stage (mAOD)	Barc. Mills Flow (m ³ /s)	Newh'n Tide (mAOD)	Lewes Gas Works. Stage (mAOD)	Barc. Mills Flow (m ³ /s)	Newh'n Tide (mAOD)	Lewes Gas Works. Stage (mAOD)
50	4.20	4.16	82	4.12	4.20	114	4.00	4.15
51	4.20	4.17	83	4.12	4.20	115	3.98	4.13
52	4.18	4.16	84	4.12	4.20	116	3.98	4.13
53	4.18	4.16	85	4.12	4.21	117	3.98	4.13
54	4.18	4.17	86	4.10	4.19	118	3.96	4.12
55	4.18	4.17	87	4.10	4.19	119	3.96	4.12
56	4.18	4.18	88	4.10	4.20	120	3.96	4.12
57	4.18	4.18	89	4.10	4.20	121	3.96	4.13
58	4.18	4.19	90	4.10	4.20	122	3.96	4.13
59	4.18	4.19	91	4.10	4.20	123	3.96	4.13
60	4.18	4.19	92	4.08	4.18	124	3.94	4.12
61	4.16	4.18	93	4.08	4.19	125	3.94	4.12
62	4.16	4.18	94	4.08	4.19	126	3.94	4.12
63	4.16	4.19	95	4.08	4.19	127	3.94	4.13
64	4.16	4.19	96	4.08	4.19	128	3.94	4.13
65	4.16	4.19	97	4.08	4.19	129	3.92	4.12
66	4.16	4.19	98	4.06	4.18	130	3.92	4.12
67	4.16	4.20	99	4.06	4.18	131	3.92	4.12
68	4.16	4.20	100	4.06	4.18	132	3.92	4.13
69	4.16	4.20	101	4.06	4.18	133	3.92	4.13
70	4.16	4.20	102	4.06	4.18	134	3.90	4.12
71	4.14	4.19	103	4.04	4.17	135	3.90	4.12
72	4.14	4.19	104	4.04	4.17	136	3.90	4.12
73	4.14	4.20	105	4.04	4.17	137	3.90	4.13
74	4.14	4.20	106	4.04	4.17	138	3.88	4.12
75	4.14	4.20	107	4.02	4.15	139	3.88	4.12
76	4.14	4.20	108	4.02	4.16	140	3.88	4.12
77	4.14	4.20	109	4.02	4.16	141	3.86	4.11
78	4.14	4.21	110	4.02	4.16	142	3.86	4.12
79	4.12	4.19	111	4.00	4.14	143	3.86	4.12
80	4.12	4.19	112	4.00	4.14			
81	4.12	4.20	113	4.00	4.15			

Table G.35 Resultant water levels at Lewes Gas Works for combined Barcombe Mills flow and Newhaven tide events equating to the 1:25 year joint return periods. Highest stage at Lewes Gas Works (shaded area) selected as the maximum 1:25 year combined flow / tide event.

Barc. Mills Flow (m ³ /s)	Newh'n Tide (mAOD)	Lewes Gas Works Stage (mAOD)	Barc. Mills Flow (m ³ /s)	Newh'n Tide (mAOD)	Lewes Gas Works Stage (mAOD)	Barc. Mills Flow (m ³ /s)	Newh'n Tide (mAOD)	Lewes Gas Works Stage (mAOD)
50	4.28	4.22	94	4.20	4.30	138	4.04	4.24
51	4.28	4.23	95	4.20	4.30	139	4.04	4.24
52	4.26	4.22	96	4.18	4.28	140	4.04	4.25
53	4.26	4.22	97	4.18	4.28	141	4.04	4.25
54	4.26	4.23	98	4.18	4.28	142	4.04	4.25
55	4.26	4.23	99	4.18	4.28	143	4.02	4.24
56	4.26	4.24	100	4.18	4.29	144	4.02	4.24
57	4.26	4.24	101	4.18	4.29	145	4.02	4.24
58	4.26	4.24	102	4.18	4.29	146	4.02	4.25
59	4.26	4.25	103	4.18	4.29	147	4.00	4.23
60	4.26	4.25	104	4.16	4.27	148	4.00	4.24
61	4.26	4.26	105	4.16	4.27	149	4.00	4.24
62	4.26	4.26	106	4.16	4.28	150	4.00	4.24
63	4.26	4.26	107	4.16	4.28	151	3.98	4.23
64	4.26	4.27	108	4.16	4.28	152	3.98	4.24
65	4.24	4.25	109	4.16	4.28	153	3.98	4.24
66	4.24	4.26	110	4.16	4.28	154	3.98	4.25
67	4.24	4.26	111	4.14	4.27	155	3.96	4.24
68	4.24	4.26	112	4.14	4.27	156	3.96	4.24
69	4.24	4.26	113	4.14	4.27	157	3.96	4.25
70	4.24	4.27	114	4.14	4.27	158	3.96	4.25
71	4.24	4.27	115	4.14	4.27	159	3.96	4.25
72	4.24	4.27	116	4.14	4.27	160	3.94	4.24
73	4.24	4.28	117	4.12	4.26	161	3.94	4.25
74	4.24	4.28	118	4.12	4.26	162	3.94	4.25
75	4.24	4.28	119	4.12	4.26	163	3.94	4.26
76	4.24	4.28	120	4.12	4.26	164	3.94	4.26
77	4.24	4.29	121	4.12	4.26	165	3.94	4.27
78	4.22	4.27	122	4.12	4.27	166	3.92	4.26
79	4.22	4.28	123	4.10	4.25	167	3.92	4.26
80	4.22	4.28	124	4.10	4.25	168	3.92	4.27
81	4.22	4.28	125	4.10	4.26	169	3.92	4.27
82	4.22	4.28	126	4.10	4.26	170	3.90	4.26
83	4.22	4.29	127	4.10	4.26	171	3.90	4.27
84	4.22	4.29	128	4.10	4.26	172	3.90	4.27
85	4.22	4.29	129	4.08	4.25	173	3.90	4.28
86	4.22	4.30	130	4.08	4.25	174	3.90	4.28
87	4.22	4.30	131	4.08	4.25	175	3.88	4.28
88	4.20	4.28	132	4.08	4.26	176	3.88	4.28
89	4.20	4.29	133	4.08	4.26	177	3.88	4.29
90	4.20	4.29	134	4.06	4.25	178	3.86	4.28
91	4.20	4.29	135	4.06	4.25	179	3.86	4.29
92	4.20	4.29	136	4.06	4.25	180	3.86	4.29
93	4.20	4.29	137	4.06	4.25	181	3.86	4.30

Table G.36 Resultant water levels at Lewes Gas Works for combined Barcombe Mills flow and Newhaven tide events equating to the 1:50 year joint return periods. Highest stage at Lewes Gas Works (shaded area) selected as the maximum 1:50 year combined flow / tide event.

Barc. Mills Flow (m ³ /s)	Newh'n Tide (mAOD)	Lewes Gas Works Stage (mAOD)	Barc. Mills Flow (m ³ /s)	Newh'n Tide (mAOD)	Lewes Gas Works. Stage (mAOD)	Barc. Mills Flow (m ³ /s)	Newh'n Tide (mAOD)	Lewes Gas Works. Stage (mAOD)
50	4.32	4.25	98	4.26	4.35	146	4.12	4.32
51	4.32	4.26	99	4.24	4.34	147	4.12	4.32
52	4.32	4.26	100	4.24	4.34	148	4.12	4.33
53	4.32	4.27	101	4.24	4.34	149	4.12	4.33
54	4.32	4.27	102	4.24	4.34	150	4.12	4.33
55	4.32	4.27	103	4.24	4.34	151	4.10	4.32
56	4.32	4.28	104	4.24	4.34	152	4.10	4.32
57	4.30	4.27	105	4.24	4.34	153	4.10	4.33
58	4.30	4.27	106	4.24	4.35	154	4.10	4.33
59	4.30	4.28	107	4.24	4.35	155	4.10	4.34
60	4.30	4.28	108	4.22	4.33	156	4.10	4.34
61	4.30	4.29	109	4.22	4.33	157	4.08	4.33
62	4.30	4.29	110	4.22	4.33	158	4.08	4.33
63	4.30	4.29	111	4.22	4.34	159	4.08	4.34
64	4.30	4.30	112	4.22	4.34	160	4.08	4.34
65	4.30	4.30	113	4.22	4.34	161	4.08	4.35
66	4.30	4.30	114	4.22	4.34	162	4.06	4.34
67	4.30	4.30	115	4.22	4.34	163	4.06	4.34
68	4.30	4.31	116	4.22	4.34	164	4.06	4.35
69	4.30	4.31	117	4.20	4.33	165	4.06	4.35
70	4.30	4.31	118	4.20	4.33	166	4.06	4.35
71	4.30	4.32	119	4.20	4.33	167	4.04	4.34
72	4.30	4.32	120	4.20	4.33	168	4.04	4.35
73	4.30	4.32	121	4.20	4.33	169	4.04	4.35
74	4.30	4.33	122	4.20	4.33	170	4.04	4.36
75	4.28	4.31	123	4.20	4.34	171	4.04	4.36
76	4.28	4.32	124	4.20	4.34	172	4.02	4.35
77	4.28	4.32	125	4.18	4.32	173	4.02	4.36
78	4.28	4.32	126	4.18	4.33	174	4.02	4.36
79	4.28	4.32	127	4.18	4.33	175	4.02	4.36
80	4.28	4.33	128	4.18	4.33	176	4.00	4.36
81	4.28	4.33	129	4.18	4.33	177	4.00	4.36
82	4.28	4.33	130	4.18	4.33	178	4.00	4.36
83	4.28	4.34	131	4.18	4.34	179	4.00	4.37
84	4.28	4.34	132	4.16	4.32	180	3.98	4.36
85	4.28	4.34	133	4.16	4.32	181	3.98	4.37
86	4.28	4.34	134	4.16	4.33	182	3.98	4.37
87	4.28	4.35	135	4.16	4.33	183	3.98	4.38
88	4.26	4.33	136	4.16	4.33	184	3.98	4.38
89	4.26	4.34	137	4.16	4.33	185	3.96	4.38
90	4.26	4.34	138	4.16	4.33	186	3.96	4.38
91	4.26	4.34	139	4.14	4.32	187	3.96	4.39
92	4.26	4.34	140	4.14	4.32	188	3.96	4.40
93	4.26	4.34	141	4.14	4.33	189	3.96	4.40
94	4.26	4.35	142	4.14	4.33	190	3.96	4.41
95	4.26	4.35	143	4.14	4.33	191	3.94	4.40
96	4.26	4.35	144	4.14	4.33	192	3.94	4.41
97	4.26	4.35	145	4.12	4.32	193	3.94	4.41

Continued

Barc. Mills Flow (m³/s)	Newh'n Tide (mAOD)	Lewes Gas Works Stage (mAOD)	Barc. Mills Flow (m³/s)	Newh'n Tide (mAOD)	Lewes Gas Works. Stage (mAOD)	Barc. Mills Flow (m³/s)	Newh'n Tide (mAOD)	Lewes Gas Works. Stage (mAOD)
194	3.94	4.42	201	3.90	4.44	208	3.88	4.47
195	3.94	4.42	202	3.90	4.44	209	3.88	4.48
196	3.94	4.43	203	3.90	4.45	210	3.86	4.47
197	3.92	4.42	204	3.90	4.45	211	3.86	4.48
198	3.92	4.43	205	3.90	4.46	212	3.86	4.49
199	3.92	4.44	206	3.88	4.46	213	3.86	4.50
200	3.92	4.44	207	3.88	4.46			

Table G.37 Resultant water levels at Lewes Gas Works for combined Barcombe Mills flow and Newhaven tide events equating to the 1:100 year joint return periods. Highest stage at Lewes Gas Works (shaded area) selected as the maximum 1:100 year combined flow / tide event.

Barc. Mills Flow (m ³ /s)	Newh'n Tide (mAOD)	Lewes Gas Works Stage (mAOD)	Barc. Mills Flow (m ³ /s)	Newh'n Tide (mAOD)	Lewes Gas Works. Stage (mAOD)	Barc. Mills Flow (m ³ /s)	Newh'n Tide (mAOD)	Lewes Gas Works. Stage (mAOD)
50	4.36	4.28	98	4.30	4.39	146	4.22	4.40
51	4.36	4.29	99	4.30	4.39	147	4.20	4.38
52	4.36	4.29	100	4.30	4.39	148	4.20	4.39
53	4.36	4.29	101	4.30	4.39	149	4.20	4.39
54	4.36	4.30	102	4.30	4.39	150	4.20	4.39
55	4.36	4.30	103	4.30	4.39	151	4.20	4.39
56	4.36	4.31	104	4.30	4.40	152	4.20	4.40
57	4.36	4.31	105	4.30	4.40	153	4.20	4.40
58	4.34	4.30	106	4.30	4.40	154	4.20	4.40
59	4.34	4.31	107	4.28	4.38	155	4.18	4.39
60	4.34	4.31	108	4.28	4.38	156	4.18	4.40
61	4.34	4.32	109	4.28	4.39	157	4.18	4.40
62	4.34	4.32	110	4.28	4.39	158	4.18	4.41
63	4.34	4.32	111	4.28	4.39	159	4.18	4.41
64	4.34	4.33	112	4.28	4.39	160	4.18	4.41
65	4.34	4.33	113	4.28	4.39	161	4.18	4.42
66	4.34	4.33	114	4.28	4.39	162	4.16	4.41
67	4.34	4.33	115	4.28	4.39	163	4.16	4.41
68	4.34	4.34	116	4.28	4.40	164	4.16	4.41
69	4.34	4.34	117	4.28	4.40	165	4.16	4.42
70	4.34	4.34	118	4.28	4.40	166	4.16	4.42
71	4.34	4.35	119	4.26	4.38	167	4.16	4.43
72	4.34	4.35	120	4.26	4.38	168	4.16	4.43
73	4.34	4.35	121	4.26	4.39	169	4.14	4.42
74	4.34	4.36	122	4.26	4.39	170	4.14	4.42
75	4.34	4.36	123	4.26	4.39	171	4.14	4.43
76	4.34	4.36	124	4.26	4.39	172	4.14	4.43
77	4.34	4.37	125	4.26	4.39	173	4.14	4.43
78	4.34	4.37	126	4.26	4.40	174	4.14	4.44
79	4.34	4.37	127	4.26	4.40	175	4.14	4.44
80	4.32	4.36	128	4.26	4.40	176	4.12	4.43
81	4.32	4.36	129	4.24	4.38	177	4.12	4.44
82	4.32	4.37	130	4.24	4.39	178	4.12	4.44
83	4.32	4.37	131	4.24	4.39	179	4.12	4.45
84	4.32	4.37	132	4.24	4.39	180	4.12	4.45
85	4.32	4.37	133	4.24	4.39	181	4.12	4.46
86	4.32	4.38	134	4.24	4.39	182	4.12	4.46
87	4.32	4.38	135	4.24	4.40	183	4.10	4.45
88	4.32	4.38	136	4.24	4.40	184	4.10	4.46
89	4.32	4.39	137	4.24	4.40	185	4.10	4.47
90	4.32	4.39	138	4.22	4.38	186	4.10	4.47
91	4.32	4.39	139	4.22	4.39	187	4.10	4.48
92	4.32	4.39	140	4.22	4.39	188	4.10	4.48
93	4.32	4.39	141	4.22	4.39	189	4.08	4.48
94	4.32	4.40	142	4.22	4.39	190	4.08	4.48
95	4.30	4.38	143	4.22	4.39	191	4.08	4.49
96	4.30	4.38	144	4.22	4.40	192	4.08	4.49
97	4.30	4.38	145	4.22	4.40	193	4.08	4.50

Continued

Barc. Mills Flow (m ³ /s)	Newh'n Tide (mAOD)	Lewes Gas Works Stage (mAOD)	Barc. Mills Flow (m ³ /s)	Newh'n Tide (mAOD)	Lewes Gas Works. Stage (mAOD)	Barc. Mills Flow (m ³ /s)	Newh'n Tide (mAOD)	Lewes Gas Works. Stage (mAOD)
194	4.06	4.49	213	4.00	4.57	232	3.92	4.69
195	4.06	4.50	214	3.98	4.57	233	3.92	4.70
196	4.06	4.50	215	3.98	4.58	234	3.92	4.71
197	4.06	4.51	216	3.98	4.59	235	3.92	4.72
198	4.06	4.52	217	3.98	4.60	236	3.90	4.72
199	4.06	4.52	218	3.96	4.59	237	3.90	4.72
200	4.04	4.52	219	3.96	4.60	238	3.90	4.73
201	4.04	4.52	220	3.96	4.61	239	3.90	4.74
202	4.04	4.53	221	3.96	4.62	240	3.88	4.74
203	4.04	4.53	222	3.96	4.63	241	3.88	4.75
204	4.04	4.54	223	3.96	4.64	242	3.88	4.75
205	4.02	4.53	224	3.96	4.64	243	3.88	4.76
206	4.02	4.54	225	3.94	4.64	244	3.88	4.77
207	4.02	4.54	226	3.94	4.65	245	3.86	4.76
208	4.02	4.55	227	3.94	4.66	246	3.86	4.77
209	4.00	4.54	228	3.94	4.67	247	3.86	4.78
210	4.00	4.55	229	3.94	4.68	248	3.86	4.78
211	4.00	4.56	230	3.92	4.67			
212	4.00	4.57	231	3.92	4.68			

Table G.38 Resultant water levels at Lewes Gas Works for combined Barcombe Mills flow and Newhaven tide events equating to the 1:200 year joint return periods. Highest stage at Lewes Gas Works (shaded area) selected as the maximum 1:200 year combined flow / tide event.

Barc. Mills Flow (m ³ /s)	Newh'n Tide (mAOD)	Lewes Gas Works Stage (mAOD)	Barc. Mills Flow (m ³ /s)	Newh'n Tide (mAOD)	Lewes Gas Works. Stage (mAOD)	Barc. Mills Flow (m ³ /s)	Newh'n Tide (mAOD)	Lewes Gas Works. Stage (mAOD)
50	4.40	4.31	98	4.34	4.42	146	4.28	4.45
51	4.40	4.31	99	4.34	4.42	147	4.28	4.46
52	4.38	4.30	100	4.34	4.42	148	4.28	4.46
53	4.38	4.31	101	4.34	4.42	149	4.28	4.46
54	4.38	4.31	102	4.34	4.43	150	4.26	4.44
55	4.38	4.32	103	4.34	4.43	151	4.26	4.45
56	4.38	4.32	104	4.34	4.43	152	4.26	4.45
57	4.38	4.33	105	4.34	4.43	153	4.26	4.45
58	4.38	4.33	106	4.34	4.43	154	4.26	4.46
59	4.38	4.34	107	4.34	4.43	155	4.26	4.46
60	4.38	4.34	108	4.34	4.44	156	4.26	4.46
61	4.38	4.35	109	4.34	4.44	157	4.26	4.47
62	4.38	4.35	110	4.34	4.44	158	4.26	4.47
63	4.38	4.35	111	4.34	4.44	159	4.26	4.47
64	4.38	4.36	112	4.34	4.44	160	4.24	4.46
65	4.38	4.36	113	4.32	4.43	161	4.24	4.46
66	4.38	4.36	114	4.32	4.43	162	4.24	4.47
67	4.38	4.36	115	4.32	4.43	163	4.24	4.47
68	4.38	4.37	116	4.32	4.43	164	4.24	4.47
69	4.38	4.37	117	4.32	4.43	165	4.24	4.48
70	4.38	4.37	118	4.32	4.43	166	4.24	4.48
71	4.38	4.38	119	4.32	4.44	167	4.24	4.48
72	4.38	4.38	120	4.32	4.44	168	4.24	4.49
73	4.38	4.38	121	4.32	4.44	169	4.24	4.49
74	4.38	4.39	122	4.32	4.44	170	4.22	4.48
75	4.38	4.39	123	4.32	4.44	171	4.22	4.48
76	4.38	4.39	124	4.32	4.45	172	4.22	4.49
77	4.38	4.40	125	4.32	4.45	173	4.22	4.49
78	4.38	4.40	126	4.32	4.45	174	4.22	4.49
79	4.36	4.39	127	4.30	4.43	175	4.22	4.50
80	4.36	4.39	128	4.30	4.44	176	4.22	4.50
81	4.36	4.39	129	4.30	4.44	177	4.22	4.50
82	4.36	4.40	130	4.30	4.44	178	4.22	4.51
83	4.36	4.40	131	4.30	4.44	179	4.20	4.50
84	4.36	4.40	132	4.30	4.44	180	4.20	4.50
85	4.36	4.41	133	4.30	4.45	181	4.20	4.51
86	4.36	4.41	134	4.30	4.45	182	4.20	4.51
87	4.36	4.41	135	4.30	4.45	183	4.20	4.52
88	4.36	4.42	136	4.30	4.45	184	4.20	4.52
89	4.36	4.42	137	4.30	4.45	185	4.20	4.53
90	4.36	4.42	138	4.30	4.46	186	4.20	4.53
91	4.36	4.43	139	4.28	4.44	187	4.20	4.54
92	4.36	4.43	140	4.28	4.44	188	4.18	4.53
93	4.36	4.43	141	4.28	4.44	189	4.18	4.54
94	4.36	4.43	142	4.28	4.45	190	4.18	4.54
95	4.36	4.43	143	4.28	4.45	191	4.18	4.55
96	4.36	4.43	144	4.28	4.45	192	4.18	4.56
97	4.36	4.44	145	4.28	4.45	193	4.18	4.56

Continued

Barc. Mills Flow (m ³ /s)	Newh'n Tide (mAOD)	Lewes Corp. Yard Stage (mAOD)	Barc. Mills Flow (m ³ /s)	Newh'n Tide (mAOD)	Lewes Corp. Yard. Stage (mAOD)	Barc. Mills Flow (m ³ /s)	Newh'n Tide (mAOD)	Lewes Corp. Yard. Stage (mAOD)
194	4.18	4.57	226	4.08	4.72	258	3.96	4.88
195	4.18	4.57	227	4.08	4.73	259	3.96	4.88
196	4.16	4.57	228	4.08	4.74	260	3.96	4.89
197	4.16	4.57	229	4.08	4.75	261	3.96	4.90
198	4.16	4.58	230	4.06	4.75	262	3.96	4.90
199	4.16	4.58	231	4.06	4.75	263	3.94	4.90
200	4.16	4.59	232	4.06	4.76	264	3.94	4.90
201	4.16	4.59	233	4.06	4.77	265	3.94	4.91
202	4.16	4.60	234	4.06	4.78	266	3.94	4.91
203	4.16	4.61	235	4.06	4.78	267	3.94	4.92
204	4.14	4.60	236	4.04	4.78	268	3.94	4.93
205	4.14	4.61	237	4.04	4.79	269	3.94	4.93
206	4.14	4.61	238	4.04	4.80	270	3.92	4.93
207	4.14	4.62	239	4.04	4.81	271	3.92	4.94
208	4.14	4.62	240	4.04	4.82	272	3.92	4.94
209	4.14	4.63	241	4.04	4.82	273	3.92	4.95
210	4.14	4.63	242	4.02	4.82	274	3.92	4.96
211	4.12	4.63	243	4.02	4.82	275	3.92	4.96
212	4.12	4.64	244	4.02	4.83	276	3.90	4.96
213	4.12	4.65	245	4.02	4.83	277	3.90	4.97
214	4.12	4.65	246	4.02	4.84	278	3.90	4.98
215	4.12	4.66	247	4.00	4.84	279	3.90	4.98
216	4.12	4.67	248	4.00	4.84	280	3.90	4.99
217	4.12	4.68	249	4.00	4.85	281	3.88	4.99
218	4.10	4.67	250	4.00	4.85	282	3.88	5.00
219	4.10	4.68	251	3.98	4.85	283	3.88	5.00
220	4.10	4.69	252	3.98	4.85	284	3.88	5.01
221	4.10	4.70	253	3.98	4.86	285	3.88	5.02
222	4.10	4.70	254	3.98	4.87	286	3.86	5.02
223	4.10	4.71	255	3.98	4.87	287	3.86	5.02
224	4.10	4.72	256	3.96	4.87	288	3.86	5.03
225	4.08	4.72	257	3.96	4.87	289	3.86	5.04

G.10 Joint Exceedance Curves for Extreme Return Periods

G.10.1 Joint Exceedance Curves at Lewes Corporation Yard

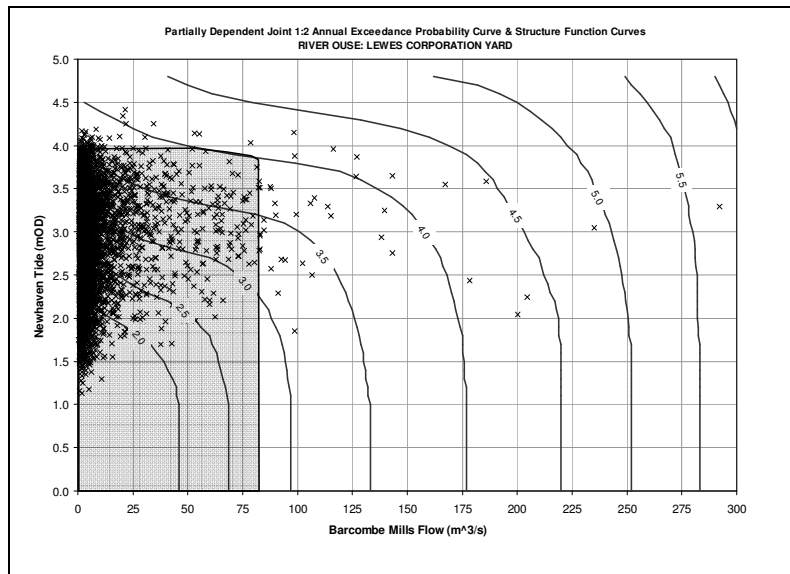


Figure G.37 Bivariate partially-dependent Barcombe Mills flow and Newhaven tide joint 1:2 year return period exceedance curve at Lewes Corporation Yard, with structure function curves and concurrent Barcombe Mills flow and Newhaven tide observations (1982 - 2005)

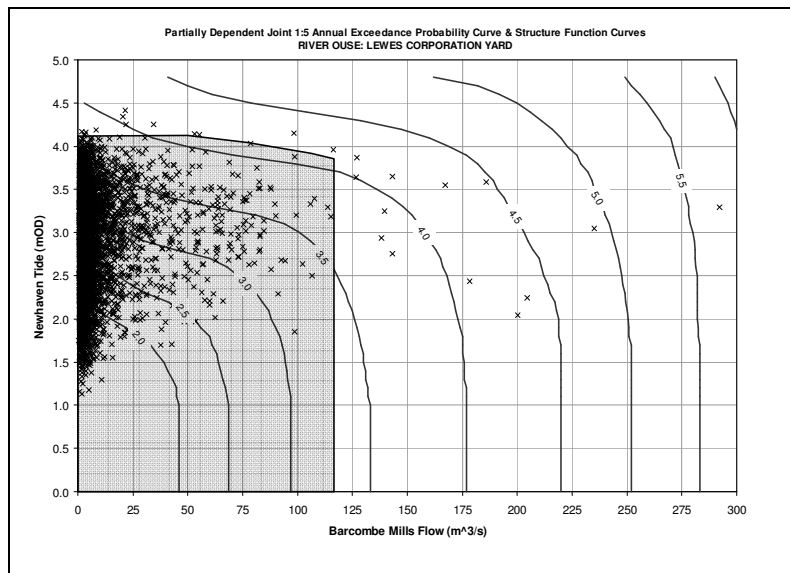


Figure G.38 Bivariate partially-dependent Barcombe Mills flow and Newhaven tide joint 1:5 year return period exceedance curve at Lewes Corporation Yard, with structure function curves and concurrent Barcombe Mills flow and Newhaven tide observations (1982 - 2005)

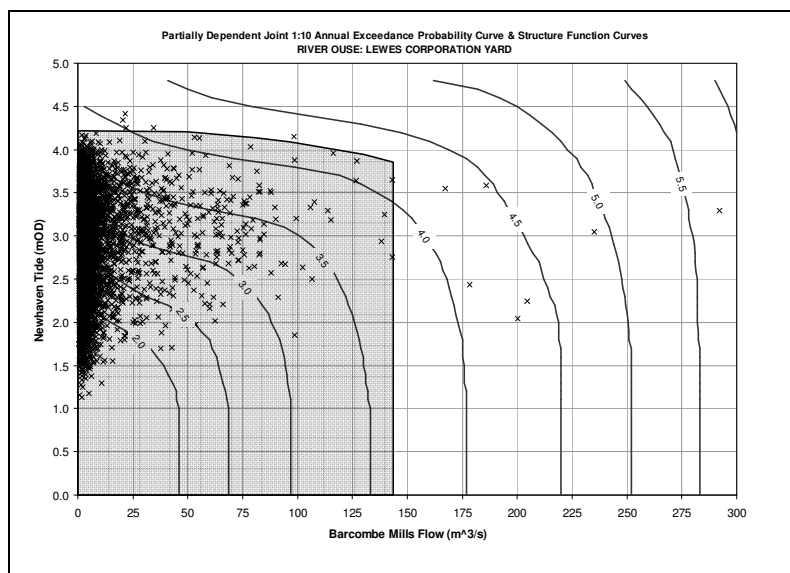


Figure G.39 Bivariate partially-dependent Barcombe Mills flow and Newhaven tide joint 1:10 year return period exceedance curve at Lewes Corporation Yard, with structure function curves and concurrent Barcombe Mills flow and Newhaven tide observations (1982 - 2005)

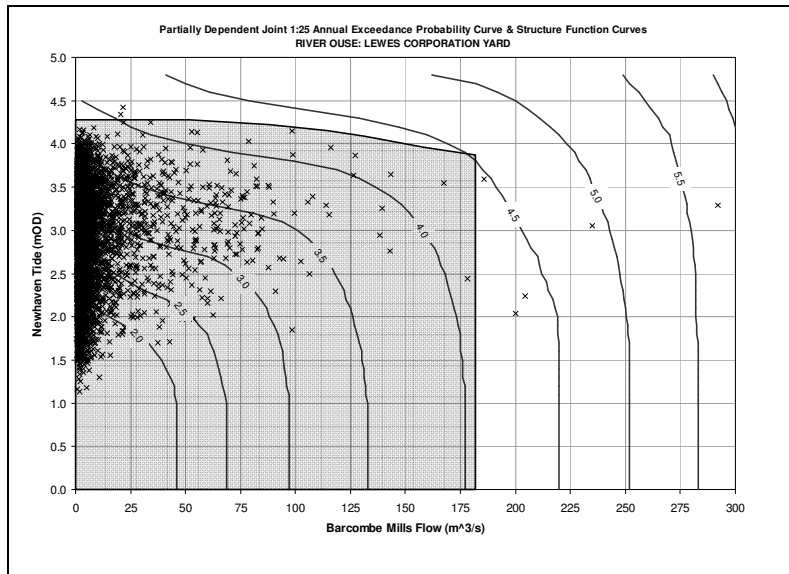


Figure G.40 Bivariate partially-dependent Barcombe Mills flow and Newhaven tide joint 1:2 year return period exceedance curve at Lewes Corporation Yard, with structure function curves and concurrent Barcombe Mills flow and Newhaven tide observations (1982 - 2005)

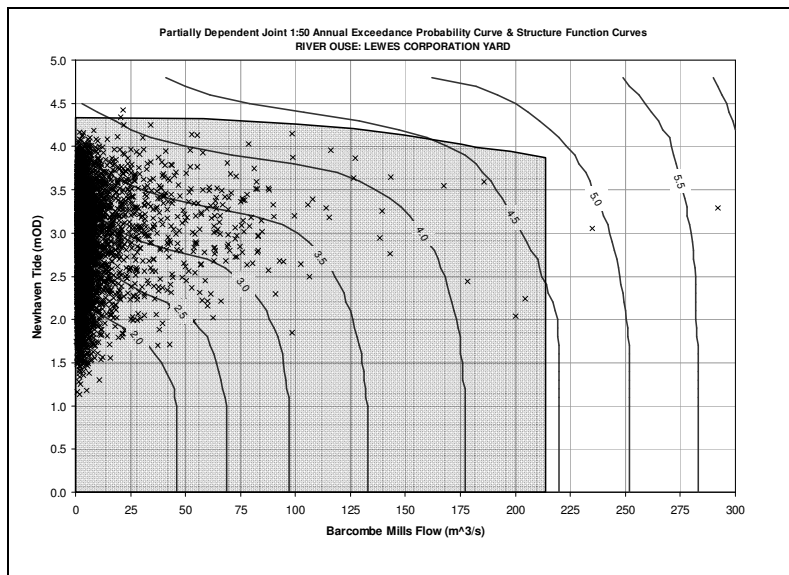


Figure G.41 Bivariate partially-dependent Barcombe Mills flow and Newhaven tide joint 1:50 year return period exceedance curve at Lewes Corporation Yard, with structure function curves and concurrent Barcombe Mills flow and Newhaven tide observations (1982 - 2005)

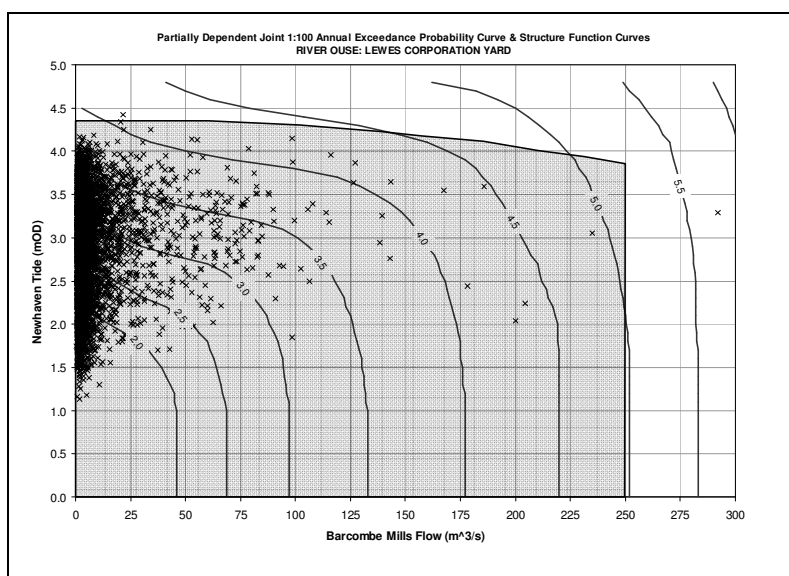


Figure G.42 Bivariate partially-dependent Barcombe Mills flow and Newhaven tide joint 1:100 year return period exceedance curve at Lewes Corporation Yard, with structure function curves and concurrent Barcombe Mills flow and Newhaven tide observations (1982 - 2005)

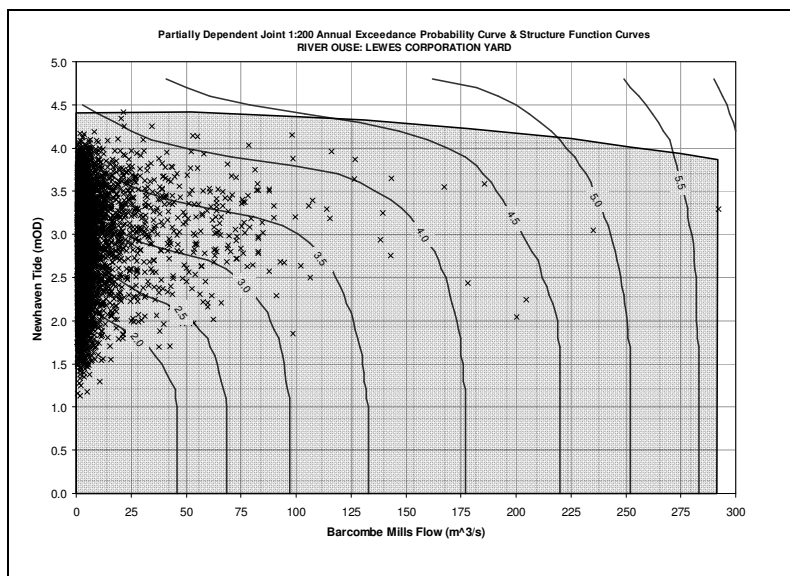


Figure G.43 Bivariate partially-dependent Barcombe Mills flow and Newhaven tide joint 1:200 year return period exceedance curve at Lewes Corporation Yard, with structure function curves and concurrent Barcombe Mills flow and Newhaven tide observations (1982 - 2005)

G.10.2 Joint Exceedance Curves at Lewes Gas Works

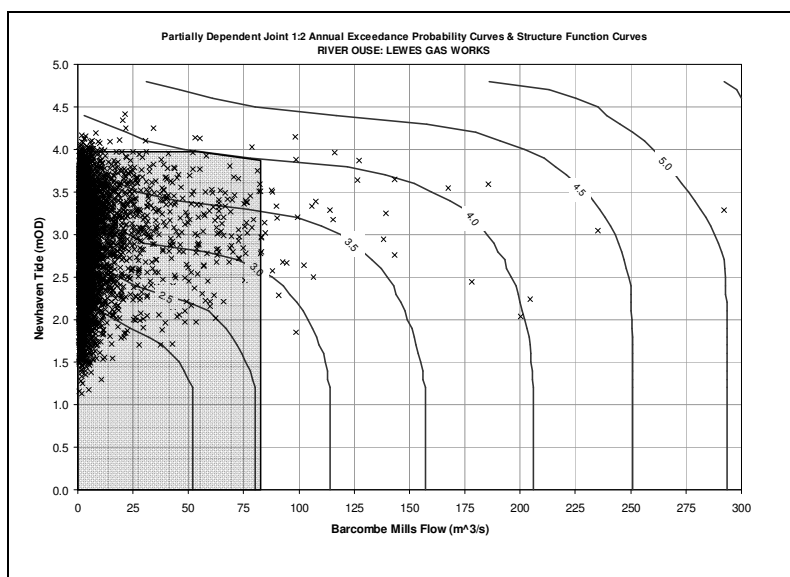


Figure G.44 Bivariate partially-dependent Barcombe Mills flow and Newhaven tide joint 1:2 year return period exceedance curve at Lewes Gas Works, with structure function curves and concurrent Barcombe Mills flow and Newhaven tide observations (1982 - 2005)

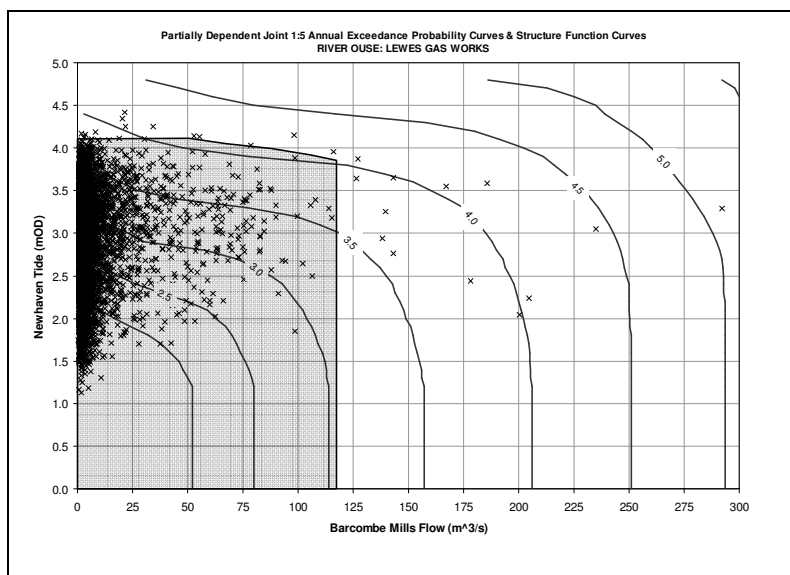


Figure G.45 Bivariate partially-dependent Barcombe Mills flow and Newhaven tide joint 1:5 year return period exceedance curve at Lewes Gas Works, with structure function curves and concurrent Barcombe Mills flow and Newhaven tide observations (1982 - 2005)

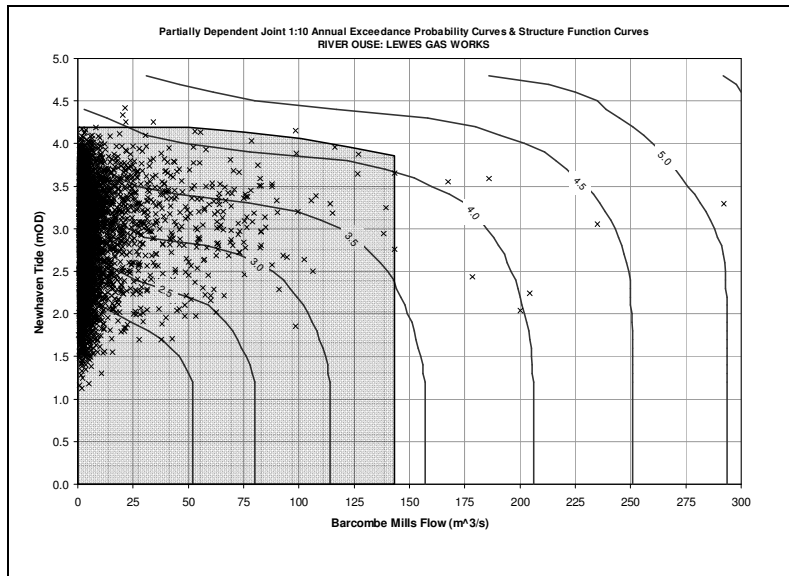


Figure G.46 Bivariate partially-dependent Barcombe Mills flow and Newhaven tide joint 1:10 year return period exceedance curve at Lewes Gas Works, with structure function curves and concurrent Barcombe Mills flow and Newhaven tide observations (1982 - 2005)

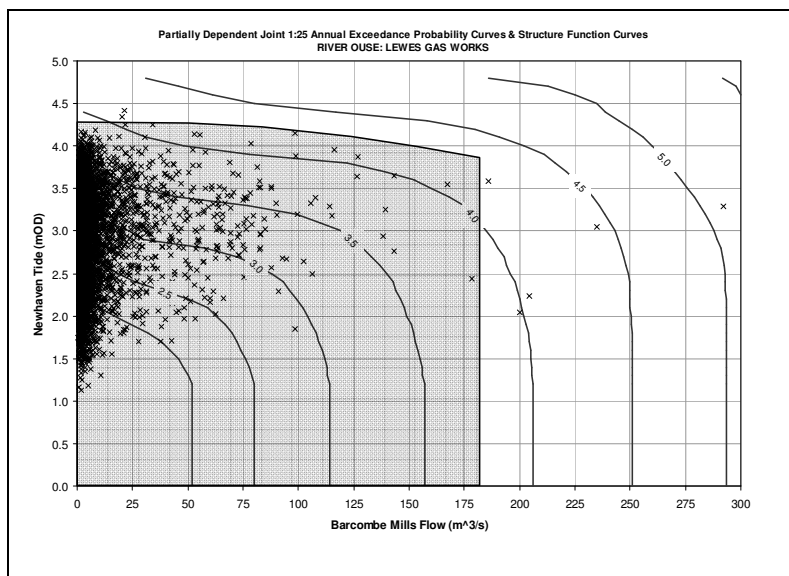


Figure G.47 Bivariate partially-dependent Barcombe Mills flow and Newhaven tide joint 1:25 year return period exceedance curve at Lewes Gas Works, with structure function curves and concurrent Barcombe Mills flow and Newhaven tide observations (1982 - 2005)

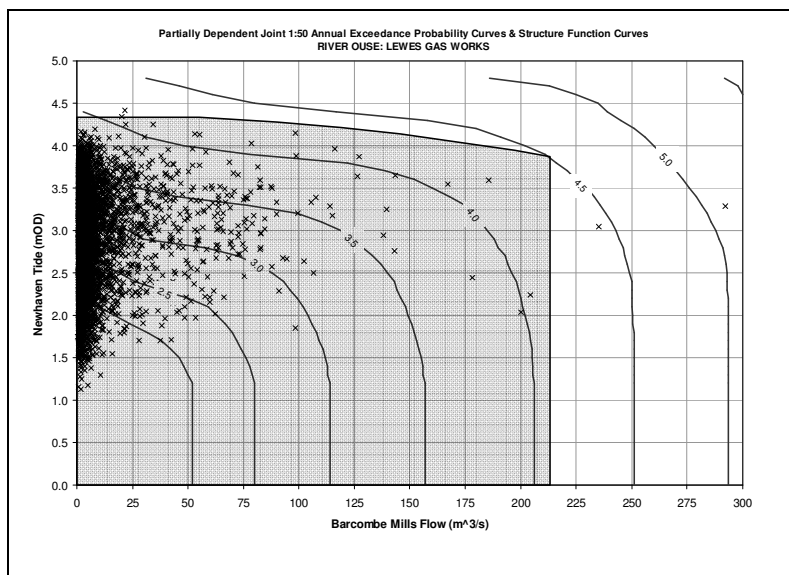


Figure G.48 Bivariate partially-dependent Barcombe Mills flow and Newhaven tide joint 1:50 year return period exceedance curve at Lewes Gas Works, with structure function curves and concurrent Barcombe Mills flow and Newhaven tide observations (1982 - 2005)

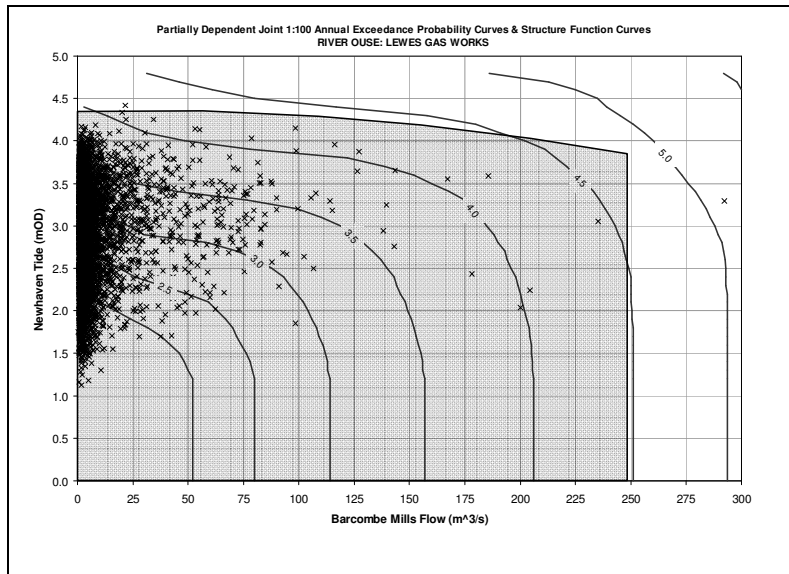


Figure G.49 Bivariate partially-dependent Barcombe Mills flow and Newhaven tide joint 1:100 year return period exceedance curve at Lewes Gas Works, with structure function curves and concurrent Barcombe Mills flow and Newhaven tide observations (1982 - 2005)

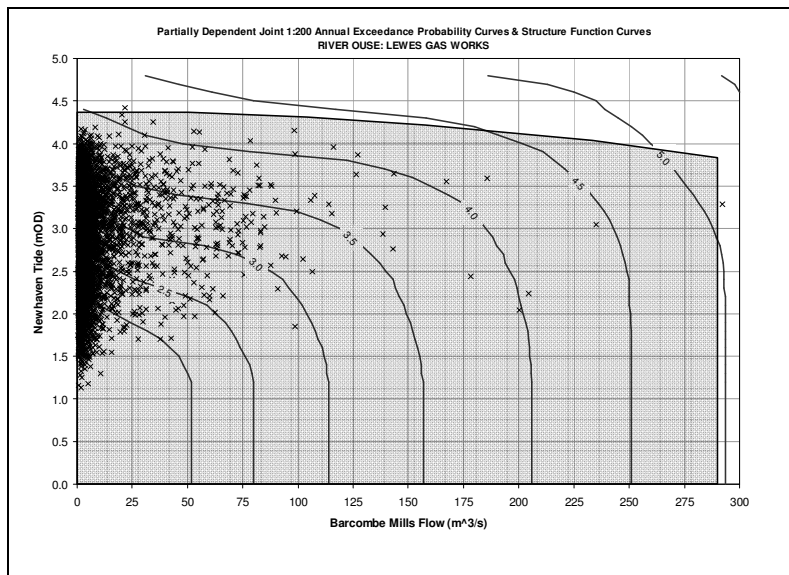


Figure G.50 Bivariate partially-dependent Barcombe Mills flow and Newhaven tide joint 1:200 year return period exceedance curve at Lewes Gas Works, with structure function curves and concurrent Barcombe Mills flow and Newhaven tide observations (1982 - 2005)

}